

AD _____

Award Number: DAMD17-02-1-0667

TITLE: Pathogenesis of Ovarian Serous Carcinoma as the Basis for Immunologic Directed Diagnosis and Treatment

PRINCIPAL INVESTIGATOR: Robert J. Kurman, M.D.

CONTRACTING ORGANIZATION: Johns Hopkins University
Baltimore, MD 21287

REPORT DATE: August 2006

TYPE OF REPORT: Final

PREPARED FOR: U.S. Army Medical Research and Materiel Command
Fort Detrick, Maryland 21702-5012

DISTRIBUTION STATEMENT: Approved for Public Release;
Distribution Unlimited

The views, opinions and/or findings contained in this report are those of the author(s) and should not be construed as an official Department of the Army position, policy or decision unless so designated by other documentation.

REPORT DOCUMENTATION PAGE

Form Approved
OMB No. 0704-0188

Public reporting burden for this collection of information is estimated to average 1 hour per response, including the time for reviewing instructions, searching existing data sources, gathering and maintaining the data needed, and completing and reviewing this collection of information. Send comments regarding this burden estimate or any other aspect of this collection of information, including suggestions for reducing this burden to Department of Defense, Washington Headquarters Services, Directorate for Information Operations and Reports (0704-0188), 1215 Jefferson Davis Highway, Suite 1204, Arlington, VA 22202-4302. Respondents should be aware that notwithstanding any other provision of law, no person shall be subject to any penalty for failing to comply with a collection of information if it does not display a currently valid OMB control number. **PLEASE DO NOT RETURN YOUR FORM TO THE ABOVE ADDRESS.**

1. REPORT DATE (DD-MM-YYYY) 01/08/06		2. REPORT TYPE Final		3. DATES COVERED (From - To) 1 Aug 2006 – 31 Jul 2006	
4. TITLE AND SUBTITLE Pathogenesis of Ovarian Serous Carcinoma as the Basis for Immunologic Directed Diagnosis and Treatment				5a. CONTRACT NUMBER	
				5b. GRANT NUMBER DAMD17-02-1-0667	
				5c. PROGRAM ELEMENT NUMBER	
6. AUTHOR(S) Robert J. Kurman, M.D. E-Mail: rkurman@jhmi.edu				5d. PROJECT NUMBER	
				5e. TASK NUMBER	
				5f. WORK UNIT NUMBER	
7. PERFORMING ORGANIZATION NAME(S) AND ADDRESS(ES) Johns Hopkins University Baltimore, MD 21287				8. PERFORMING ORGANIZATION REPORT NUMBER	
9. SPONSORING / MONITORING AGENCY NAME(S) AND ADDRESS(ES) U.S. Army Medical Research and Materiel Command Fort Detrick, Maryland 21702-5012				10. SPONSOR/MONITOR'S ACRONYM(S)	
				11. SPONSOR/MONITOR'S REPORT NUMBER(S)	
12. DISTRIBUTION / AVAILABILITY STATEMENT Approved for Public Release; Distribution Unlimited					
13. SUPPLEMENTARY NOTES					
14. ABSTRACT: The purpose of this study is to elucidate the pathogenesis of serous carcinoma by identifying the molecular genetic changes and preferentially expressed genes of different histological types of serous neoplasms. We hypothesize that the development of serous carcinoma proceeds along two main pathways: one is rapid progression from ovarian surface epithelium to high-grade serous carcinoma without well-established morphological precursors ("de novo" pathway) and the other is a gradual development from borderline tumors, to non-invasive micropapillary serous carcinomas then to low-grade carcinomas (stepwise pathway). The first pathway results in a high-grade neoplasm (conventional serous carcinoma) and the second leads to the development of a low-grade indolent tumor. Both types of carcinomas and the putative precursor lesions of invasive MPSC are characterized by distinctive molecular genetic alterations and specific gene expression. We identified that mutations in KRAS/BRAF/ERRB2 genes characterized the development of low-grade serous carcinomas. Expression of HLA-G, apoE and membralin molecules were confined to high-grade serous carcinomas. This project, designed to test our proposed model of diverse pathways in the pathogenesis of ovarian serous carcinoma, provides an etiologic basis for the other two projects.					
15. SUBJECT TERMS ovary, carcinoma, development, pathway, molecular genetics					
16. SECURITY CLASSIFICATION OF:			17. LIMITATION OF ABSTRACT	18. NUMBER OF PAGES	19a. NAME OF RESPONSIBLE PERSON
a. REPORT	b. ABSTRACT	c. THIS PAGE			USAMRMC
U	U	U	UU	249	19b. TELEPHONE NUMBER (include area code)

Table of Contents

Cover.....	1
SF 298.....	2
Table of Contents.....	3
Introduction.....	4
Body.....	5-9
Key Research Accomplishments.....	10
Reportable Outcomes.....	11-13
Conclusions.....	14
References.....	15-16
Appendices.....	attached

INTRODUCTION

The objective of this proposal is to elucidate the pathogenesis of serous carcinoma by identifying the molecular genetic changes and preferentially expressed genes of different histological types of serous neoplasms. We hypothesize that the development of serous carcinoma proceeds along two main pathways: one is rapid progression from ovarian surface epithelium to conventional serous carcinoma without well-established morphological precursors (“de novo” pathway) and the other is a gradual development from serous borderline tumor (atypical proliferative tumor), to non-invasive micropapillary serous carcinoma then to invasive micropapillary serous carcinoma (stepwise pathway). The first pathway results in a high-grade neoplasm (conventional serous carcinoma) and the second leads to the development of a low-grade indolent tumor (invasive micropapillary serous carcinoma). Both types of carcinomas and the putative precursor lesions of invasive micropapillary serous carcinoma are characterized by distinctive molecular genetic alterations and specific gene expression. This project, designed to test our proposed model of diverse pathways in the pathogenesis of ovarian serous carcinoma, provides an etiologic basis for the other two projects in this proposal. Although many genes are altered during tumorigenesis, only a few are truly critical for tumor progression. Identifying these genes holds promise for the development of new diagnostic assays and immunology-directed treatment for patients with different types of serous carcinoma.

BODY

There are no substantial changes or modifications of the original statements. The accomplishments associated with each task outlined in the approved statement of work are detailed, point by point in the followings. **Please be advised that** the research results from this study are substantial and they are published in 32 papers. Therefore, the following discussion is the succinct summary of the study outcome. Please refer to the published papers (listed) for details of study results. Representative reprints from the 32 papers are attached in the appendices of the progress report.

Task 1: To characterize the molecular genetic alterations of ovarian serous tumors developing along two different pathways.

In the grand funding period, we have conducted a systematic clinicopathologic and molecular analysis of a large number of ovarian serous borderline tumors (SBTs) and invasive epithelial ovarian tumors of all

Table 1. *TP53* mutation status in high-grade ovarian serous carcinomas.

case #	mutated exon	nucleotide change	amino acid change
HG1	E4	3' Intron-1st bp G to A	Splicing site
HG2	E4	136-1 bp insertion	46; Insertion
HG3	E4	159; TGG to TGA	53; W to stop
HG4	E4	159; TGG to TGA	53; W to stop
HG5	E4	264-1 bp deletion	89; Deletion
HG6	E4	400; TTT to GTT	134; F to V
HG7	E5	5' Intron-1st bp G to T	Splicing site
HG8	E5	416-1 bp deletion	139; Deletion
HG9	E5	434; CTG to CCG	145; L to R
HG10	E5	438; TGG to TGA	147; W to stop
HG11	E5	452; CCG to CAC	151; P to H
HG12	E5	468-469-2 bp deletion	156; Deletion
HG13	E5	466-486-21 bp deletion	156-172; Deletion
HG14	E5	488; TAC to TGC*	163; Y to C
HG15	E5	488; TAC to TGC	163; Y to C
HG16	E5	517; GTG to ATG	173; V to M
HG17	E5	524; CCG to CAC	175; R to H
HG18	E5	524; CCG to CAC	175; R to H
HG19	E5	524; CCG to CAC	175; R to H
HG20	E5	524; CCG to CAC	175; R to H
HG21	E6	566-581-16 bp deletion	189-194; Deletion
HG22	E6	568; CCG to TGG	190; R to W
HG23	E6	568; CCG to TGG	190; R to W
HG24	E6	578; CAT to CGT*	193; H to R
HG25	E6	581; CTT to CGT	194; L to R
HG26	E6	584; ATC to ACC	195; I to T
HG27	E6	596; ACG to ATG	199; R to M
HG28	E6	614; TAT to TGT	205; Y to C
HG29	E6	625-626-2 bp deletion	209; Deletion
HG30	E6	637; CGA to TGA	213; R to stop
HG31	E6	638; CGA to CTA	213; R to L
HG32	E6	641; CAT to CGT	213; H to R
HG33	E6	643; AGT to CGT	215; S to R
HG34	E6	647-1 bp deletion	216; Deletion
HG35	E6	653; GTG to CAG	218; V to Q
HG36	E6	659; TAT to TGT	220; Y to C
HG37	E7	5' Intron-2nd bp A to G	Splicing site
HG38	E7	686-687-2 bp deletion	229; Deletion
HG39	E7	712; TGT to AGT*	238; C to S
HG40	E7	715; AAC to TAC*	239; N to Y
HG41	E7	722; TCC to TTC	240; S to F
HG42	E7	723-1 bp deletion	241; Deletion
HG43	E7	742; CCG to TGG	248; R to W
HG44	E7	742; CCG to TGG	248; R to W
HG45	E7	743; CCG to CAG	248; R to Q
HG46	E7	742; CCG to TGG	248; R to W
HG47	E7	742; CCG to TGG	248; R to W
HG48	E7	747; AGG to AGT	249; R to S
HG49	E7	772-782-11 bp deletion	258-261; Deletion
HG50	E7	777; GAT to GAT	259; D to V
HG51	E8	783-791-9 bp deletion	262-264; Deletion
HG52	E8	809; TTT to TGT	270; F to C
HG53	E8	818; CGT to CAT	272; R to H
HG54	E8	880; GAG to TAG	293; E to stop
HG55	E8	880; GAG to TAG	293; E to stop
HG56	E8	916; CGA to TGA	306; R to stop
HG57	E9	964-1 bp deletion	322; Deletion
HG58		WT	
HG59		WT	
HG60		WT	
HG61		WT	
HG62		WT	
HG63		WT	
HG64		WT	
HG65		WT	
HG66		WT	
HG67		WT	
HG68		WT	
HG69		WT	
HG70		WT	
HG71		WT	

histologic types in an effort to delineate their pathogenesis and behavior¹. By careful examination of histopathology of SBTs, we identify a unique “variant” of SBTs- non-invasive micropapillary serous carcinoma (or intraepithelial low-grade serous carcinoma) which are more frequently associated with extraovarian disease (implant) and poor clinical outcome as compared to the conventional SBT (called atypical proliferative tumor)²⁻⁵. We define the morphological criteria of “good” versus “bad” implants to predict the clinical outcome in SBT patients⁶. Based on mutational analysis and the patterns of allelic imbalance, we provide the molecular evidence of tumor progression from cystadenoma to atypical proliferative tumor, intraepithelial low-grade serous carcinoma (or non-invasive micropapillary serous carcinoma) then to invasive low-grade serous carcinoma⁷. We demonstrate that mutations in BRAF and KRAS characterize SBT and low-grade serous carcinoma^{7,8} and that mutations in both genes occur early in the tumor progression, i.e., the cystadenoma stage, preceding the development of SBTs⁹. We are pleased that our original findings were validated by the subsequent independent studies by other research groups^{10,11}. We show that mutations of BRAF and KRAS correlate with the activation of mitogen activated protein kinase (MAPK), the downstream target of KRAS-BRAF signaling pathway, in SBT and low-grade serous carcinomas¹² and have defined the downstream molecular targets regulated by activated MAPK in SBT using serial analysis of gene expression¹³. More recently, we demonstrated that 12-bp insertion (nucleotide 2313-2324) occurred in approximately 10% of MPSCs and atypical proliferative (borderline) serous tumors¹⁴. Mutations in *KRAS*, *BRAF* and *ERBB2* were found mutually exclusive and accordingly, mutations in either of the genes were found in about at least two third of MPSCs and atypical proliferative (borderline) serous tumors. We further show

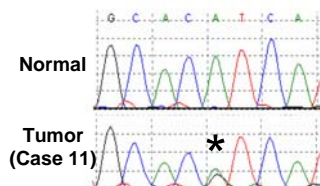
that in contrast to BRAF and KRAS, mutations in p53 gene are significantly less frequent in SBTs and low-grade serous carcinoma than in conventional high-grade serous carcinoma¹⁵. Using affinity purified tumor samples, we were able to demonstrate the p53 mutation frequency as high as 80% (Table 1). Furthermore, we have reported the distinct pattern in sequence mutations and amplification of PIK3CA and AKT2 genes in purified ovarian serous high-grade and low-grade tumors. We are the first research group reporting that ERBB2 somatic mutations in serous borderline tumors (Table 2 and Fig. 1). We have studied the chromosomal imbalance in SBTs using CGH and demonstrated that the pattern of chromosomal imbalance was similar between APST and non-invasive MPSC (intraepithelial low-grade serous carcinoma) but distinct from conventional high-grade serous carcinoma¹⁶. Based on our studies, we have extended our “dualistic pathway” model into a modified hypothesis in the development of ovarian cancer¹. Besides, we have developed a new technology to detect KRAS mutations based on homogeneous point mutation detection by quantum dot-mediated two-color fluorescence coincidence analysis.

Case No.	Tumor	PIK3CA	AKT2	ERBB2	KRAS	BRAF
1	SBT	WT	WT	12 bp ins*	WT	WT
2	SBT	WT	WT	WT	WT	T1976A:V600E
3	SBT	WT	WT	WT	G35T:G12V	WT
4	SBT	WT	WT	WT	G35A:G12D	WT
5	SBT	WT	WT	WT	G35A:G12D	WT
6	SBT	WT	WT	WT	WT	T1976A:V600E
7	SBT	WT	WT	WT	WT	WT
8	SBT	WT	WT	WT	WT	WT
9	SBT	WT	WT	WT	WT	WT
10	SBT	WT	WT	WT	WT	T1976A:V600E
11	SBT	A3140G:H1047R	WT	WT	G35T:G12V	WT
12	SBT	WT	WT	WT	G38T:G13V	WT
13	SBT	WT	WT	WT	WT	WT
14	SBT	WT	WT	WT	G35T:G12V	WT
15	SBT	WT	WT	WT	WT	WT
16	SBT	WT	WT	WT	WT	T1976A:V600E
17	SBT	WT	WT	12 bp ins*	WT	WT
18	SBT	WT	WT	WT	WT	T1976A:V600E
19	SBT	WT	WT	WT	WT	WT
20	SBT	WT	WT	WT	WT	WT
21	SBT	WT	WT	WT	G35T:G12V	WT

SBT: serous borderline tumor; * 12 bp insertion at 2313-2324 bp

Table 2. Somatic mutations in 5 kinases in a pilot set of serous borderline tumors (SBT). Nucleotide sequencing was performed on purified tumor cells (by dymal beads sorting from fresh tumors or laser capture microdissection from paraffin sections). Many of the specimens show somatic mutation (black boxes) in those genes except AKT2. Both ERBB2 mutations show a 12-bp insertion at 2313-2324 which has been reported as an activating mutation in lung cancer^{17, 18}. The PI3CA mutation is located in the kinase domain. This preliminary finding has been recently published¹⁴. NOTE: In this new set of SBTs, the mutation frequency in KRAS and BRAF was slightly lower than that we previously reported probably because of limited sample size.

PIK3CA



ERBB2

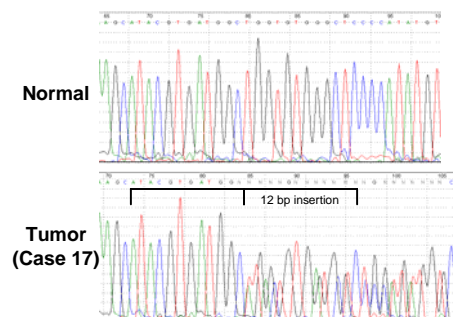


Fig. 1. Chromatograms of *PIK3CA* and *ERBB2* mutational status in two representative serous borderline tumors (case number 11 and 17). Case 11 shows a heterozygous somatic mutation at the nucleotide 3140 (A to G). Case 17 demonstrates a heterozygous 12 bp in-frame insertion mutation at the nucleotide of 2313-2324.

Task 2: To identify the genes preferentially expressed in the serous carcinomas.

Based on serial analysis of gene expression (SAGE), we have identified and characterized differential genes expressed in either low-grade (micropapillary) or high-grade serous carcinomas. We have finished SAGE

library construction, sequencing and analysis in 5 high-grade and 3 low-grade ovarian serous carcinomas. We then combined the SAGE results and Affymetrix microarray analysis (as an alternative approach to complement SAGE as described in the original aim), we have identified several high-grade associated and low-grade associated genes in ovarian cancer. More specifically, we have identified HLA-G, membralin and apolipoprotein E overexpression in high-grade but not in low-grade serous carcinoma. The validation and clinical application of HLA-G and apolipoprotein E expression will be described in the next section (Task 3). Besides, we have identified two low-grade associated genes, p21 and anti-trypsin, based on analysis of SAGE data we have collected. In addition, we have identified mesothelin as an ovarian cancer associated gene and the expression levels of mesothelin correlated with patient's overall survival. In the following, we have summarized the major findings.

In the funding period, we have identified a novel gene, membralin, based on SAGE analysis¹⁹. We have cloned the gene and deposited the nucleotide sequence into NCBI public database (GeneBank accession number: DQ005958). In our analysis, human membralin is unique and does not share significant sequence homology with other human genes, only membralins of other species. The gene contains 11-exons which encode at least two spliced variants in human cancer. The long form of membralin (membralin-1) comprises all 11-exons, encoding a protein of 620-amino acids long and the short form of membralin (membralin-3) contains all exons except for exon 10, encoding a protein of 408 amino acids. Expression of different membralin isoforms depends on tissue type. The long form, membralin-1, is expressed in ovarian and colorectal carcinomas but not in breast or pancreatic carcinomas, which express only the short splice form, membralin-3. Membralin-1-GFP fusion protein demonstrates exclusive cytoplasmic localization. Based on quantitative real-time PCR, *in situ* hybridization and Western blot analysis, membralin was highly expressed in ovarian serous carcinomas as compared to ovarian surface epithelium ($p < 0.001$) (Fig. 2). Ovarian carcinomas in effusions demonstrated a significantly higher level of membralin expression than in solid tumors ($p < 0.001$). In conclusion, these findings represent the first characterization of human membralin and suggest that membralin is a novel tumor-associated marker in ovarian serous carcinomas.

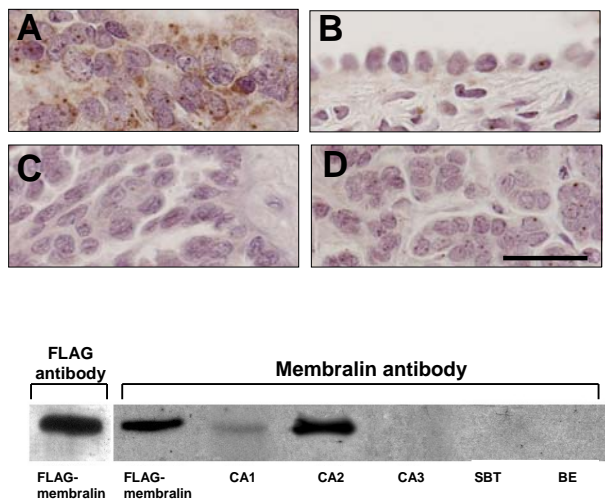


Fig. 2. Expression of membralin in ovarian cancer. *In situ* hybridization demonstrates that membralin signal is located in ovarian serous carcinoma tissue (A) but not in benign ovarian surface epithelium (B) or in serous borderline tumor (C). The sense (control) probe does not show detectable signal (D). Bar = 50 μ m. Western blot analysis shows that the membralin antibody reacts with the FLAG-membralin-1 fusion protein with a molecular mass of 68 kD in HEK293 cells transfected by the pCMV-Tag-2c-membralin (E). Membralin-1 protein is detected in two ovarian serous carcinomas (CA1 and CA2) that also show membralin signal based on *in situ* hybridization but not in another ovarian serous carcinoma (CA3), serous borderline tumor (SBT) or benign ovarian epithelium (BE), which did not show detectable signals.

Tumor-associated extracellular matrix proteins are essential for tumor development and are potential diagnostic markers. In the funding period, we have performed analysis of gene expression of extracellular matrix genes in ovarian serous neoplasms. Gene expression of 16 different extracellular matrix proteins was first analyzed in ovarian serous epithelium and tumors based on SAGE database as proposed in the Aim and validated by semiquantitative RT-PCR. As compared to normal ovarian surface epithelium, we found

overexpression of syndecan-1, collagen type IV alpha 2, emilin-1, and laminin-5 in ovarian serous carcinomas. Among them, syndecan-1 was selected for further study as it has not been well characterized in ovarian cancer and the syndecan-1 antibody was available for immunostaining in ovarian tumor tissue microarrays. We demonstrated that syndecan-1 was expressed in 30.4% of high-grade serous carcinomas, 29.7% of low-grade carcinomas and serous borderline tumors, but not in serous cystadenomas and ovarian surface epithelium. Syndecan-1 was strongly expressed in high-grade compared to low-grade serous carcinomas and serous borderline tumors ($p=0.007$). In summary, ovarian carcinomas exhibit upregulated expression of several extracellular matrix proteins including syndecan-1 which may represent a novel tumor-associated marker in ovarian serous carcinomas.

We further expand the proposed study in the last (no cost extension) year to look into the unique ovarian cancer signatures by comparing Ovarian/primary peritoneal serous carcinoma (OC/PPC) and diffuse peritoneal malignant mesothelioma (DMPM). This is because both tumor types are highly aggressive tumors that are closely related morphologically and histogenetically. It remains unclear whether both tumors are molecularly distinct neoplasms. The current study compared global gene expression patterns in OC/PPC and DMPM. Ten OC/PPC and five DMPM effusions were analyzed for gene expression profiles using the Affymetrix U133 Plus 2 arrays and the dCHIP analysis program. Differentially expressed candidate genes were validated using quantitative real-time PCR and immunohistochemistry. Unsupervised hierarchical clustering using all 54,675 genes in the array classified the samples into two groups, DMPM specimens vs. OC/PPC specimens. A total of 189 genes that were differentially expressed in these two groups were selected based on statistical significance. Genes overexpressed in DMPM included calretinin, vitronectin, claudin 15, $\alpha 4$ laminin, hyaluronan synthase 1, cadherin 11, RAB7, v-maf and the EGF-containing fibulin-like extracellular matrix protein 1. Genes overexpressed in OC/PPC included insulin-like growth factor II (IGF-II), IGF-II binding protein 3, cyclin E1, folate receptors 1 and 3, RAB25, MUC4, endothelin-1, CD24, kallikreins 6/7/8, claudins 3/4/6, Notch3 and MMP-7. Quantitative real-time PCR validated the differential expression of 13 genes, and immunohistochemistry confirmed the differences for 4 gene products. Our conclusion from this study is following. Expression profiling separates OC/PPC from DMPM and identifies a number of genes that are differentially expressed in these tumors. The molecular signatures unique to OC/PPC and DMPM should provide a molecular basis to study both tumors and new potential markers for facilitating their differential diagnosis.

Task 3: To validate the candidate genes and assess their biological significance in the development of serous carcinoma.

A total of four genes among many candidate genes were validated and characterized for their clinical significance and they include HLA-G^{20,21}, apolipoprotein E²², mesothelin²³ and membralin¹⁹. The summary of these three studies are summarized as follows.

The HLA-G immunoreactivity ranging from focal to diffuse was detected in 45 of 74 (61%) high-grade ovarian serous carcinomas but in none of the 18 low-grade serous carcinomas or 26 serous borderline tumors (atypical proliferative tumors and non-invasive micropapillary serous carcinomas) that were studied. The differential expression of HLA-G in high-grade but not low-grade serous carcinomas may have biological significance as HLA-G appears to facilitate tumor cell evasion of the immune system by protecting the malignant cells from lysis by natural killer cells. This finding is similar to the HLA-G expression observed in large cell carcinoma of the lung that is associated with a poor outcome as compared with absence of expression in carcinomas with a better prognosis. HLA-G staining was not detected in a wide variety of normal tissues including ovarian surface epithelium and normal breast tissue. RT-PCR demonstrated the presence of HLA-G5 isoform in all tumor samples expressing HLA-G. ELISA was performed to measure the sHLA-G in 42 malignant and 18 benign ascites supernatants. sHLA-G levels were significantly higher in malignant ascites than in benign controls ($p<0.001$). We found that the area under the receiver-operating characteristic (ROC) curve for sHLA-G was 0.95 for malignant versus benign ascites specimens. At 100% specificity, the highest sensitivity to detect a malignant ascites was 78% (95% CI, 68%

- 88%) at a cutoff of 13 ng/ml. In summary, our findings suggest that measurement of sHLA-G is a useful molecular adjunct to cytology in the differential diagnosis of malignant versus benign peritoneal ascites.

Apolipoprotein (Apo) E has been recently identified as a potential tumor-associated marker in ovarian cancer by serial analysis of gene expression. ApoE has long been known to play a key role in lipid transport and its specific isoforms participate in the atherosclerogenesis. However, its role in human cancer is not known. In this study, apoE expression was frequently detected in ovarian serous carcinomas, the most common and lethal type of ovarian cancer. It was not detected in serous borderline tumors and normal ovarian surface epithelium. Inhibition of apoE expression using an apoE specific siRNA led to G₂ cell cycle arrest and apoptosis in an apoE expressing ovarian cancer cell line, OVCAR3, but not in an apoE negative cell line, SKOV3²². Furthermore, the phenotype of apoE-siRNA treated OVCAR3 cells was not reversed by exogenous apoE in the culture medium. Expression of apoE in nuclei was significantly associated with a better patient survival who had advanced stage serous carcinomas at the 5-year follow-up (p=0.004). This study suggests a new role of apoE in cancer as apoE expression is important for the survival in apoE expressing ovarian cancer cells and its expression is associated with a favorable clinical outcome in ovarian cancer patients²².

Mesothelin expression levels were compared among 81 publicly available SAGE libraries of various carcinoma and normal tissue types. Immunohistochemistry using a well-characterized mesothelin monoclonal antibody (5B2) was performed to evaluate mesothelin expression in 167 high-grade and 31 low-grade ovarian serous carcinomas²³. Immunohistochemistry staining scores were correlated with patient survival, tumor site, tumor grade, *in vitro* drug resistance and differentiation status of tumor cells. SAGE analysis demonstrated that mesothelin was overexpressed in 50% of ovarian and pancreatic carcinomas but rarely in other cancer types including liver, colon, kidney, prostate and breast. Mesothelin immunoreactivity (>5% of tumor cells) was present in 55% of ovarian serous carcinomas with no difference in expression between high-grade and low-grade serous tumors (p = 0.82). Based on Kaplan-Meier analysis, we found that a diffuse mesothelin staining (> 50% of tumor cells) in primary high-grade ovarian carcinomas correlated significantly with prolonged survival in patients who had advanced stage disease and had received optimal debulking surgery followed by chemotherapy (p = 0.023) (Fig. 3). Mesothelin expression did not correlate significantly with patient age, tumor site, *in vitro* drug resistance or tumor differentiation status (p > 0.10). Our results provided new evidence that mesothelin expression is associated with prolonged survival in patients with high-grade ovarian serous carcinoma.

Membralin has been described above (Task 2) and will not be reiterated here.

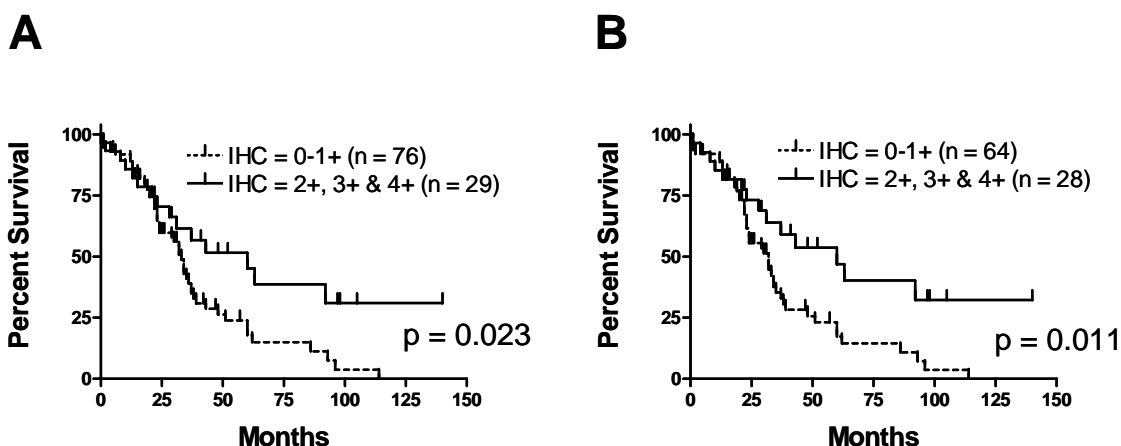


Fig 3. Kaplan-Meier survival curves comparing tumors with negative or focal mesothelin staining (scores of 0-1 or < 50% positive cells) to tumors with diffuse mesothelin staining (scores of 2+, 3+ and 4+) in (A) both stage III and stage IV high-grade primary ovarian serous carcinomas and (B) only stage III high-grade primary ovarian serous carcinoma.

KEY RESEARCH ACCOMPLISHMENTS

1. Molecular genetic analysis of ovarian carcinomas.

Based on the results from Project 1, we have provided cogent molecular genetic evidence to support the main hypothesis of the dualistic pathway in the development of ovarian serous carcinoma as proposed in this program project. We further modify and extend our hypothesis to include all the major types of ovarian carcinomas. The key finding is illustrated in Fig. 4. It is our pleasure to know that this model generated by the funding of DoD has gained wide attention and acceptance in the cancer research field as our papers related to this subject have been frequently cited in the literature (the hypothesis has been cited in 249 papers till Nov. 30, 2006 based on ISI web).

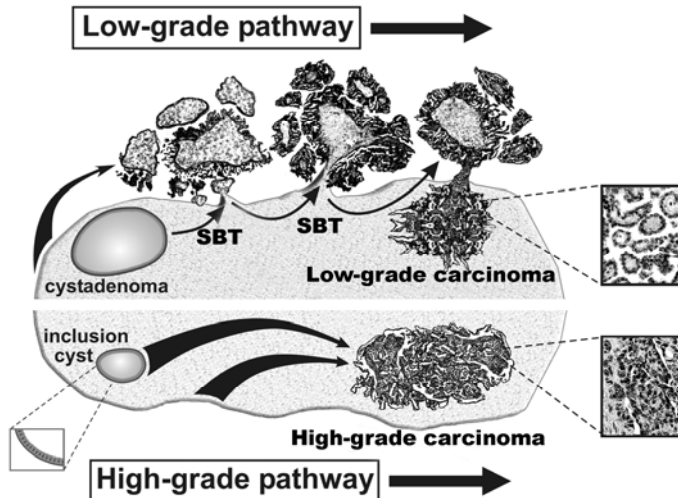


Fig. 4. Proposed model in the development of ovarian serous carcinoma. Low-grade serous carcinoma develops in a stepwise fashion from a serous borderline tumor (SBT) which may arise from the surface epithelium or from serous cystadenomas. High-grade serous carcinomas develop from the ovarian surface epithelium or inclusion cysts without morphologically recognizable intermediate stages. Low-grade carcinoma is a clinically indolent disease but patients will ultimately die of the disease. In contrast, high-grade carcinoma is very aggressive and most patients will succumb to the disease in a short period of time. Both low-grade and high-grade tumors are characterized by distinct molecular signatures.

2. We have identified several genes that are differentially expressed in high-grade serous carcinomas, based on gene expression analysis using SAGE or microarrays. We further demonstrate their biological and clinical significance as described in the previous section. The markers may provide the new molecular targets for future development of cancer targeted therapy.

3. We have completed the generations of ovarian tumor tissue arrays including a whole spectrum of lesions and normal tissues that could serve as an important research tool for this program project and others in ovarian cancer research. The tissue microarray set is currently ready to be used in the entire program project. They include:

- 10 TMAs of high-grade serous carcinomas
- 2 TMAs of low-grade serous carcinoma + serous borderline tumors
- 3 TMAs of clear cell ovarian carcinomas
- 2 TMAs of endometrioid ovarian carcinomas

REPORTABLE OUTCOMES

Articles published or in press in the funding period:

(A total of 32 peer-reviewed papers related to Project 1)

Singer G, Kurman RJ, Chang H-W, Cho SKR, Shih IM. Diverse tumorigenic pathways in ovarian serous carcinoma. *Am J Pathol*, 160:1223-1228, 2002.

Chang H-W, Ali SZ, Cho SR, Kurman RJ, Shih IM. Detection of allelic imbalance in ascitic supernatant by digital SNP analysis. *Clin Cancer Res*, 8:2580-2585, 2002.

Chang H-W, Singer G, Cho SR, Sokoll L, Montz F, Roden R, Zhang Z, Chan DW, Kurman RJ, Shih IM. Assessment of plasma DNA levels, allelic imbalance and CA 125 as diagnostic tests for cancer. *J Natl Can Inst*, 94:1697-1703, 2002.

Singer G, Shih IM, Truskinovsky A, Umudum H, Kurman RJ. Mutational analysis of K-ras segregates ovarian serous carcinomas into two types: Invasive MPSC (a low-grade tumor) and conventional serous carcinoma (a high-grade tumor). *Int J Gynecol Pathol*, 22:37-41, 2003.

Singer G, Oldt 3rd R, Cohen Y, Wang B, Sidransky D, Kurman RJ, Shih IM. Mutations in BRAF and KRAS Ras characterize the development of low-grade ovarian serous carcinoma. *J Natl Can Inst*, 95:484-486, 2003.

Buckhaults P, Zhang Z, Chen Y-C, Wang T-L, St. Croix B, Saha S, Bardelli A, Morin PJ, Polyak K, Hruban RH, Velculescu VE, Shih IM. Identifying tumor origin using a gene expression based classification map. *Cancer Res*, 63:4144-4149, 2003 (with cover illustration).

Singer G, Rebmann V, Chen Y-C, Cheng C-C, Liu H-T, Ali SZ, Reinsberg J, McMaster MT, Pfeiffer K, Chan DW, Wardelmann E, Grosse-Wilde H, Cheng CC, Kurman RJ, Shih I-M. HLA-G is a potential tumor marker in malignant effusion. *Clin Cancer Res*, 9: 4460-4466, 2003.

Pohl G and Shih IM. Principle and applications of digital PCR. *Expert Rev Mol Diagn*, 4:89-95, 2004.

Shih IM and Kurman RJ. Ovarian tumorigenesis - a proposed model based on morphological and molecular genetic analysis. *Am J Pathol*, 164: 1511-1518, 2004.

Cheng EJ, Kurman RJ, Wang M, Oldt III R, Wang BG, Berman DM, Shih IM. Molecular genetic analysis of ovarian serous cystadenoma. *Lab Invest*, 84:778-784, 2004.

Hsu C-Y, Bristow R, Cha MS, Wang BG, Ho C-L, Kurman RJ, Wang TL, Shih IM. Characterization of Active Mitogen-activated Protein Kinase in Ovarian Serous Carcinomas. *Clin Cancer Res*, 10:6432-6436, 2004.

Ho C-L, Kurman RJ, Dehari R, Wang T-L, Shih IM. Mutations of BRAF and KRAS precede the development of ovarian serous borderline tumors. *Cancer Res*, 64:6915-6918, 2004.

Davidson B, Elstrand MV, McMaster MT, Berner A, Kurman RJ, Risberg B, Trope CG, Shih IM. HLA-G expression in effusions is a possible marker of tumor susceptibility to chemotherapy in ovarian carcinoma. *Gyn Oncol*, 96:42-47, 2005.

Singer G, Stohr R, Cope L, Dehari R, Hartmann A, Cao D-F, Wang TL, Kurman RJ, Shih IM. Patterns of p53 mutations separate ovarian serous borderline tumors, low and high-grade carcinomas and provide support for a new model of ovarian carcinogenesis. *Am J Surg Pathol*, 29:218-224, 2005.

Chen Y-C, Pohl G, Wang TL, Morin PJ, Risberg B, Christesen GB, Yu A, Davidson B, Shih IM. Apolipoprotein E is required for cell proliferation and survival in ovarian cancer. *Cancer Res*, 65:331-337, 2005.

Pohl G, Ho C-L, Kurman RJ, Bristow R, Wang T-L, Shih IM. Inactivation of the MAPK pathway as a potential target-based therapy in ovarian serous tumors with KRAS or BRAF mutations. *Cancer Res*, 65:1994-2000, 2005.

Kurman RJ, Seidman JD, Shih IM. Commentary: Serous borderline tumors of the ovary, classifications, concepts and conundrums. *Histopathol*, 47:310-315, 2005.

Chen YC, Davidson B, Cheng CC, Maitra A, Giuntoli RL 2nd, Hruban RH, Wang T-L, Shih IM. Identification and characterization of membralin, a novel tumor-associated gene, in ovarian carcinoma. *Biochem Biophys Acta*, 1730:96-102, 2005.

Shih IM and Kurman RJ. Molecular pathogenesis of ovarian borderline tumors- new insights and old challenges. *Clin Cancer Res*, 11:7273-7279, 2005.

Hsu C-Y, Kurman RJ, Vang R, Wang T-L, Baak J, Shih IM. Nuclear size distinguishes low-grade from high-grade ovarian serous carcinoma and predicts outcome. *Human Pathol*, 36:1049-1054, 2005.

Shih IM, Sheu J, Yu CH, Santillan A, Yen MJ, Nakayama K, Bristow RE, Vang R, Parmigiani G, Kurman RJ, Trope CG, Davidson B and Wang T-L. Amplification of a chromatin remodeling gene, Rsf-1/HBXAP, in ovarian carcinoma. *Proc Natl Acad Sci USA*, 102:14004-14009, 2005.

Yen JM, Hsu C-Y, Mao T-L, Wu, TC, Roden R, Wang T-L, Shih IM. Diffuse mesothelin expression correlates with prolonged patient Survival in ovarian serous carcinoma. *Clin Cancer Res*, 12:827-831, 2006.

Yeh H-C, Ho Y-P, Shih IM, Wang Z-H. Homogeneous point mutation detection by quantum dot-mediated two-color fluorescence coincidence analysis. *Nucleic Acid Res*, 34:e35, 2006.

Nakayama K, Nakayama N, Kurman RJ, Cope L, Pohl G, Samuels Y, Velculescu VE, Wang TL, Shih IM. Sequence mutations and amplification of PIK3CA and AKT2 genes in purified ovarian serous neoplasms. *Cancer Biol Therapy*, 5:779-785, 2006.

Nakayama K, Nakayama N, Davidson B, Katabuchi H, Kurman RJ, Velculescu VE, Shih IM, Wang TL. Homozygous deletion of MKK4 in ovarian serous carcinoma. *Cancer Biol Therapy*, 6:630-634, 2006.

Park, JT, Li M, Nakayama K, Mao T-L, Davidson B, Zheng Z, Kurman RJ, Eberhart CG, Shih IM, Wang TL. Notch-3 gene amplification in ovarian cancer. *Cancer Res*, 66:6312-6318, 2006.

Mao T-L, Hsu C-Y, Yen MJ, Gilks B, Sheu JC, Gabrielson E, Vang R, Cope L, Kurman RJ, Wang TL, Shih IM. Expression of Rsf-1, a chromatin-remodeling gene, in ovarian and breast carcinoma. *Human Pathol*, 37:1169-1175, 2006.

Davidson B, Trope G, Wang T-L, Shih IM. Expression of the chromatin remodeling factor, Rsf-1, in effusions is a novel predictor of poor survival in ovarian carcinoma. *Gyn Oncol*, July 14, 2006, [Epub ahead of print].

Salani R, Neuberger I, Kurman RJ, Bristow R, Chang HW, Wang TL, Shih IM. Expression of extracellular matrix proteins in ovarian serous tumors. *Int J Gynecol Pathol*, in press.

Davidson B, Kleinberg L, Forences VA, Zhang Z, Wang TL, Shih IM. Gene expression signatures differentiate ovarian/peritoneal serous carcinoma from diffuse peritoneal malignant mesothelioma. Clin Cancer Res, 12:5944-5950, 2006.

Nakayama K, Nakayama N, Davidson B, Sheu J, Natini Jinawath, Santillan A, Salani R, Bristow RE, Morin PJ, Kurman RJ, Wang TL, Shih IM. A BTB/POZ protein, NAC-1, is related to tumor recurrence and is essential for tumor growth and survival. Proc Natl Acad Sci USA, 103:18739-18744, 2006.

Reiko D, Kurman RJ, Logani S, Shih IM. The development of high-grade serous carcinoma from atypical proliferative (borderline) serous tumors and low-grade micropapillary serous carcinoma- a morphologic and molecular genetic analysis. Am J Surg Pathol, in press.

Article submitted for review:

Research resource:

Ovarian tumor tissue microarrays- 17 tissue microarrays comprising more than 500 tissues. Protocols of digital PCR analysis for allelic imbalance.

Trainees who received awards using this funding resource:

- **HERA Research Award**, 2005, Kentaro Nakayama, MD, PhD, a research fellow
- **First Place Award for Research Fellow in Basic Research, Johns Hopkins Oncology**, 2005, Jim Sheu, PhD, a research fellow
- **International Union Against Cancer Technology Transfer Fellowship**, 2004, Gudun Pohl, MD, a research fellow
- **HERA Research Award**, 2003, Brant Wang, MD, PhD, a research fellow
- **Yong Investigator Award of the International Society of Gynecologic Pathologists**, 2004, Gad Singer, MD, a clinical fellow
- **Howard Hughes Undergraduate Research Award**, 2003, Robert J. Oldt III, JHU undergraduate student

CONCLUSIONS

Summary of the accomplished research findings: Ovarian epithelial tumors are the most common type of ovarian cancer and are the most lethal gynecologic malignancy. The main purpose of the Project 1 is to delineate the molecular basis of ovarian serous tumors and identify the genes that are associated with tumors that develop along different pathways in tumor progression. The overall DoD project 1 has made progress to meet the objectives of the proposal as we have finished all the tasks proposed in the specific aims.

Furthermore, we have extended the aims and have obtained new and related findings to the Project 1. Based on clinicopathological and molecular observations, we propose a new model for their development. In this model, ovarian serous tumors are divided into two categories designated low-grade and high-grade tumors which correspond to two main pathways of tumorigenesis. Low-grade neoplasms arise in a stepwise fashion from borderline tumors whereas high-grade tumors arise from ovarian surface epithelium or inclusion cysts for which morphologically recognizable precursor lesions have not been identified, so-called “de novo” development. Low-grade tumors are associated with distinct molecular changes that are rarely found in high-grade tumors, such as *BRAF*, *KRAS* and *ERBB2* mutations. Gene expression profiling has shown that the two types of ovarian serous tumors are characterized by distinct gene expression patterns. Some of the genes have been selected for further study to reveal their clinical and biological significance. As a result of DoD funding, we have generated a total of 32 peer-reviewed papers related to the aims of the Project 1.

Implications and significance of the accomplished research findings: Our proposed model of carcinogenesis in ovarian serous tumors reconciles the relationship of borderline tumors to invasive carcinoma and provides a morphologic and molecular framework for studies aimed at elucidating the pathogenesis of ovarian cancer. Identification and characterization of the panoply of molecular changes associated with ovarian carcinogenesis will facilitate development of diagnostic tests for early detection of ovarian cancer and for the development of novel therapies aimed at blocking key growth-signaling pathways.

REFERENCES

1. Shih I-M and Kurman RJ. Ovarian tumorigenesis- a proposed model based on morphological and molecular genetic analysis. *Am J Pathol* 2004; 164: 1511-8.
2. Burks RT, Sherman ME, and Kurman RJ. Micropapillary serous carcinoma of the ovary. A distinctive low-grade carcinoma related to serous borderline tumors. *Am J Surg Pathol* 1996; 20: 1319-30.
3. Riopel MA, Ronnett BM, and Kurman RJ. Evaluation of diagnostic criteria and behavior of ovarian intestinal- type mucinous tumors: atypical proliferative (borderline) tumors and intraepithelial, microinvasive, invasive, and metastatic carcinomas. *Am J Surg Pathol* 1999; 23: 617-35.
4. Seidman JD, Russell P, and Kurman RJ. Surface epithelial tumors of the ovary. *In: R. J. Kurman (ed.), Blaustein's Pathology of the Female Genital Tract, 5th edition, pp. 791-904. New York: Springer Verlag, 2002.*
5. Seidman JD and Kurman RJ. Subclassification of serous borderline tumors of the ovary into benign and malignant types. A clinicopathologic study of 65 advanced stage cases. *Am J Surg Pathol* 1996; 20: 1331-45.
6. Sehdev AES, Sehdev PS, and Kurman RJ. Noninvasive and invasive micropapillary serous carcinoma of the ovary: a clinicopathologic analysis of 135 cases. *Am J Surg Pathol* 2003; 27: 725-36.
7. Singer G, Kurman RJ, Chang H-W, Cho SKR, and Shih I-M. Diverse tumorigenic pathways in ovarian serous carcinoma. *Am J Pathol* 2002; 160: 1223-8.
8. Singer G, Oldt R, 3rd, Cohen Y, Wang BG, Sidransky D, Kurman RJ, and Shih Ie M. Mutations in BRAF and KRAS characterize the development of low-grade ovarian serous carcinoma. *J Natl Cancer Inst* 2003; 95: 484-6.
9. Ho C-L, Kurman RJ, Dehari R, Wang T-L, and Shih I-M. Mutations of BRAF and KRAS precede the development of ovarian serous borderline tumors. *Cancer Res* 2004; 64: 6915-8.
10. Sieben NL, Macropoulos P, Roemen GM, Kolkman-Uljee SM, Jan Fleuren G, Houmadi R, Diss T, Warren B, Al Adnani M, De Goeij AP, Krausz T, and Flanagan AM. In ovarian neoplasms, BRAF, but not KRAS, mutations are restricted to low-grade serous tumours. *J Pathol* 2004; 202: 336-40.
11. Mayr D, Hirschmann A, Lohrs U, and Diebold J. KRAS and BRAF mutations in ovarian tumors: A comprehensive study of invasive carcinomas, borderline tumors and extraovarian implants. *Gynecol Oncol* 2006;
12. Hsu C-Y, Bristow R, Cha M, Wang BG, Ho C-L, Kurman RJ, Wang T-L, and Shih I-M. Characterization of active mitogen-activated protein kinase in ovarian serous carcinomas. *Clin Cancer Res* 2004; 10: 6432-6.
13. Pohl G, Ho CL, Kurman RJ, Bristow R, Wang TL, and Shih Ie M. Inactivation of the mitogen-activated protein kinase pathway as a potential target-based therapy in ovarian serous tumors with KRAS or BRAF mutations. *Cancer Res* 2005; 65: 1994-2000.
14. Nakayama K, Nakayama N, Kurman RJ, Cope L, Pohl G, Samuels Y, Velculescu VE, Wang TL, and Shih Ie M. Sequence mutations and amplification of PIK3CA and AKT2 genes in purified ovarian serous neoplasms. *Cancer Biol Ther* 2006; 5: 779-85.
15. Singer G, Stohr R, Cope L, Dehari R, Hartmann A, Cao DF, Wang TL, Kurman RJ, and Shih IM. Patterns of p53 Mutations Separate Ovarian Serous Borderline Tumors and Low- and High-grade Carcinomas and Provide Support for a New Model of Ovarian Carcinogenesis: A Mutational Analysis With Immunohistochemical Correlation. *Am J Surg Pathol* 2005; 29: 218-24.
16. Staebler A, Heselmeyer-Haddad K, Bell K, Riopel M, Perlman E, Ried T, and Kurman RJ. Micropapillary serous carcinoma of the ovary has distinct patterns of chromosomal imbalances by comparative genomic hybridization compared with atypical proliferative serous tumors and serous carcinomas. *Hum Pathol* 2002; 33: 47-59.
17. Stephens P, Hunter C, Bignell G, Edkins S, Davies H, Teague J, Stevens C, O'Meara S, Smith R, Parker A, Barthorpe A, Blow M, Brackenbury L, Butler A, Clarke O, Cole J, Dicks E, Dike A, Drozd A, Edwards K, Forbes S, Foster R, Gray K, Greenman C, Halliday K, Hills K, Kosmidou V, Lugg R,

- Menzies A, Perry J, Petty R, Raine K, Ratford L, Shepherd R, Small A, Stephens Y, Tofts C, Varian J, West S, Widaa S, Yates A, Basseur F, Cooper CS, Flanagan AM, Knowles M, Leung SY, Louis DN, Looijenga LH, Malkowicz B, Pierotti MA, Teh B, Chenevix-Trench G, Weber BL, Yuen ST, Harris G, Goldstraw P, Nicholson AG, Futreal PA, Wooster R, and Stratton MR. Lung cancer: intragenic ERBB2 kinase mutations in tumours. *Nature* 2004; 431: 525-6.
18. Shigematsu H, Takahashi T, Nomura M, Majumdar K, Suzuki M, Lee H, Wistuba, II, Fong KM, Toyooka S, Shimizu N, Fujisawa T, Minna JD, and Gazdar AF. Somatic mutations of the HER2 kinase domain in lung adenocarcinomas. *Cancer Res* 2005; 65: 1642-6.
 19. Chen YC, Davidson B, Cheng CC, Maitra A, Giuntoli RL, 2nd, Hruban RH, Wang TL, and Shih Ie M. Identification and characterization of membralin, a novel tumor-associated gene, in ovarian carcinoma. *Biochim Biophys Acta* 2005; 1730: 96-102.
 20. Singer G, Rebmann V, Y-C C, Liu H-T, Ali SZ, Reinsberg J, McMaster M, Pfeiffer K, Chan DW, Wardelmann E, Grosse-Wilde H, Kurman RJ, and Shih I-M. HLA-G is a potential tumor marker in malignant ascites. *Clin Cancer Res* 2003; 9: 4460-4.
 21. Davidson B, Elstrand MB, McMaster MT, Berner A, Kurman RJ, Risberg B, Trope CG, and Shih Ie M. HLA-G expression in effusions is a possible marker of tumor susceptibility to chemotherapy in ovarian carcinoma. *Gynecol Oncol* 2005; 96: 42-7.
 22. Chen Y-C, Pohl G, Wang T-L, Morin PJ, Risberg B, Kristensen G, Yu A, Davidson B, and Shih I-M. Apolipoprotein E is required for cell proliferation and survival in ovarian cancer. *Cancer Res* 2005; 65: 331-7.
 23. Yen MJ, Hsu CY, Mao TL, Wu TC, Roden R, Wang TL, and Shih Ie M. Diffuse mesothelin expression correlates with prolonged patient survival in ovarian serous carcinoma. *Clin Cancer Res* 2006; 12: 827-31.

APPENDICES FOR PROJECT 1 (project leader: Dr. Shih)

Selective reprints from the studies funded by this grant:

Shih IM and Kurman RJ. Ovarian tumorigenesis - a proposed model based on morphological and molecular genetic analysis (review). *Am J Pathol*, 164: 1511-1518, 2004.

Singer G, Oldt 3rd R, Cohen Y, Wang B, Sidransky D, Kurman RJ, Shih IM. Mutations in BRAF and KRAS Ras characterize the development of low-grade ovarian serous carcinoma. *J Natl Can Inst*, 95:484-486, 2003.

Chang H-W, Singer G, Cho SR, Sokoll L, Montz F, Roden R, Zhang Z, Chan DW, Kurman RJ, Shih IM. Assessment of plasma DNA levels, allelic imbalance and CA 125 as diagnostic tests for cancer. *J Natl Can Inst*, 94:1697-1703, 2002.

Nakayama K, Nakayama N, Davidson B, Sheu J, Natini Jinawath, Santillan A, Salani R, Bristow RE, Morin PJ, Kurman RJ, Wang TL, Shih IM. A BTB/POZ protein, NAC-1, is related to tumor recurrence and is essential for tumor growth and survival. *Proc Natl Acad Sci USA*, 103:18739-18744, 2006.

Yen JM, Hsu C-Y, Mao T-L, Wu, TC, Roden R, Wang T-L, Shih IM. Diffuse mesothelin expression correlates with prolonged patient survival in ovarian serous carcinoma. *Clin Cancer Res*, 12:827-831, 2006.

Shih IM, Sheu J, Yu CH, Santillan A, Yen MJ, Nakayama K, Bristow RE, Vang R, Parmigiani G, Kurman RJ, Trope CG, Davidson B and Wang T-L. Amplification of a chromatin remodeling gene, Rsf-1/HBXAP, in ovarian carcinoma. *Proc Natl Acad Sci USA*, 102:14004-14009, 2005.

Singer G, Kurman RJ, Chang H-W, Cho SKR, Shih IM. Diverse tumorigenic pathways in ovarian serous carcinoma. *Am J Pathol*, 160:1223-1228, 2002.

Park, JT, Li M, Nakayama K, Mao T-L, Davidson B, Zheng Z, Kurman RJ, Eberhart CG, Shih IM, Wang TL. Notch-3 gene amplification in ovarian cancer. *Cancer Res*, 66:6312-6318, 2006.

Buckhaults P, Zhang Z, Chen Y-C, Wang T-L, St. Croix B, Saha S, Bardelli A, Morin PJ, Polyak K, Hruban RH, Velculescu VE, Shih IM. Identifying tumor origin using a gene expression based classification map. *Cancer Res*, 63:4144-4149, 2003 (with cover illustration).

Singer G, Rebmann V, Chen Y-C, Cheng C-C, Liu H-T, Ali SZ, Reinsberg J, McMaster MT, Pfeiffer K, Chan DW, Wardelmann E, Grosse-Wilde H, Cheng CC, Kurman RJ, Shih I-M. HLA-G is a potential tumor marker in malignant effusion. *Clin Cancer Res*, 9: 4460-4466, 2003.

Shih IM and Kurman RJ. Molecular pathogenesis of ovarian borderline tumors- new insights and old challenges (review). *Clin Cancer Res*, 11:7273-7279, 2005.

Ho C-L, Kurman RJ, Dehari R, Wang T-L, Shih IM. Mutations of BRAF and KRAS precede the development of ovarian serous borderline tumors. *Cancer Res*, 64:6915-6918, 2004.

Chen Y-C, Pohl G, Wang TL, Morin PJ, Risberg B, Christesen GB, Yu A, Davidson B, Shih IM. Apolipoprotein E is required for cell proliferation and survival in ovarian cancer. *Cancer Res*, 65:331-337, 2005.

Pohl G, Ho C-L, Kurman RJ, Bristow R, Wang T-L, Shih IM. Inactivation of the MAPK pathway as a potential target-based therapy in ovarian serous tumors with KRAS or BRAF mutations. *Cancer Res*, 65:1994-2000, 2005.

Review

Ovarian Tumorigenesis

A Proposed Model Based on Morphological and Molecular Genetic Analysis

Ie-Ming Shih and Robert J. Kurman

From the Departments of Pathology, Oncology and Gynecology and Obstetrics, Johns Hopkins University School of Medicine, Baltimore, Maryland

The pathogenesis of ovarian carcinoma, the most lethal gynecological malignancy, is unknown because of the lack of a tumor progression model. Based on a review of recent clinicopathological and molecular studies, we propose a model for their development. In this model, surface epithelial tumors are divided into two broad categories designated type I and type II tumors that correspond to two main pathways of tumorigenesis. Type I tumors tend to be low-grade neoplasms that arise in a stepwise manner from borderline tumors whereas type II tumors are high-grade neoplasms for which morphologically recognizable precursor lesions have not been identified, so-called *de novo* development. As serous tumors are the most common surface epithelial tumors, low-grade serous carcinoma is the prototypic type I tumor and high-grade serous carcinoma is the prototypic type II tumor. In addition to low-grade serous carcinomas, type I tumors are composed of mucinous carcinomas, endometrioid carcinomas, malignant Brenner tumors, and clear cell carcinomas. Type I tumors are associated with distinct molecular changes that are rarely found in type II tumors, such as *BRAF* and *KRAS* mutations for serous tumors, *KRAS* mutations for mucinous tumors, and β -catenin and *PTEN* mutations and microsatellite instability for endometrioid tumors. Type II tumors include high-grade serous carcinoma, malignant mixed mesodermal tumors (carcinosarcoma), and undifferentiated carcinoma. There are very limited data on the molecular alterations associated with type II tumors except frequent p53 mutations in high-grade serous carcinomas and malignant mixed mesodermal tumors (carcinosarcomas). This model of carcinogenesis reconciles the relationship of borderline tumors to invasive

carcinoma and provides a morphological and molecular framework for studies aimed at elucidating the pathogenesis of ovarian cancer. (*Am J Pathol* 2004, 164:1511–1518)

Ovarian cancer is the most lethal gynecological malignancy and surface epithelial tumors (carcinomas) are the most common type of ovarian cancer. Despite considerable efforts aimed at elucidating the molecular mechanisms of ovarian carcinoma, its pathogenesis is still unknown, because unlike colorectal carcinoma,¹ a progression model has not been described. Ovarian carcinomas are heterogeneous and are primarily classified by cell type into serous, mucinous, endometrioid, clear cell, and Brenner (transitional) tumors corresponding to different types of epithelia in the organs of the female reproductive tract.^{2–4} The tumors in each of the categories are further subdivided into three groups, benign, malignant, and intermediate (borderline tumor) to reflect their behavior. Mucinous and endometrioid borderline tumors are often associated with invasive carcinomas but serous borderline tumors are rarely associated with serous carcinomas.² This latter observation as well as recent molecular genetic studies showing a very different frequency of p53 and *KRAS* mutations in serous carcinoma as compared to serous borderline tumors have led most investigators to conclude that serous borderline tumors and serous carcinomas are unrelated.^{5–9} The uncertainty about the nature of the borderline group of tumors, reflected by the ambiguous term “borderline,” is a major shortcoming of the current classification. Here we review recent histopathological and molecular genetic

Supported by the United States Department of Defense (research grant no. OC010017).

Accepted for publication December 22, 2003.

Address reprint requests to Robert J. Kurman or Ie-Ming Shih, Department of Pathology, Johns Hopkins Medical Institutions, Weinberg Cancer Center, Room 2242, 401 N. Broadway, Baltimore, MD 21231. E-mail: rkurman@jhmi.edu (RJK). E-mail: shihie@yahoo.com (IS).

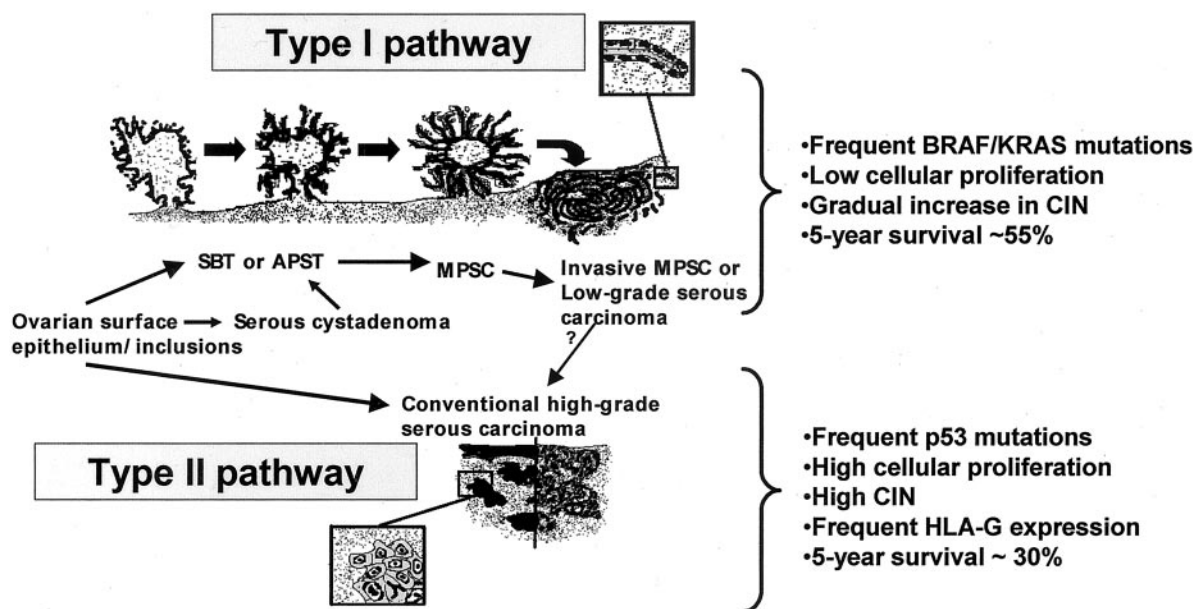


Figure 1. Schematic representation of the dualistic model depicting the development of ovarian serous carcinomas, the most common type of ovarian cancer. Low-grade serous carcinoma (MPSC) represents the prototypic type I tumor and develops in a stepwise manner from an atypical proliferative tumor through a noninvasive stage of MPSC (both of these tumors qualified as borderline) before becoming invasive. These tumors are associated with frequent *KRAS* or *BRAF* mutations. High-grade serous carcinoma represents the prototypic type II tumor and develops from the ovarian surface epithelium or inclusion cysts without morphologically recognizable intermediate stages. *KRAS* and *BRAF* mutations have been rarely found in these neoplasms. CIN, chromosomal instability.

studies to re-examine this issue and propose a model of ovarian carcinogenesis that integrates clinical, histopathological, and molecular genetic findings.

Clinical and Pathological Observations that Provide the Basis for the Proposed Model

Throughout the last 10 years, we have conducted a systematic microscopic and clinical analysis of a large number of noninvasive and invasive epithelial ovarian tumors of all histological types in an effort to delineate their pathogenesis and behavior.^{2,10-12} These studies drew attention to a subset of low-grade serous tumors designated "micropapillary serous carcinoma (MPSC)" with characteristic histopathological features, low proliferative activity, and an indolent behavior that contrasts dramatically with the conventional type of serous carcinoma, an aggressive neoplasm that is high-grade and has high proliferative activity.^{2,10-12} The term "MPSC" was originally proposed to distinguish the noninvasive form of this tumor from the more common noninvasive tumor, termed an "atypical proliferative serous tumor," both of which have been included under the rubric "borderline" or "low malignant potential."^{10,12} Histological transitions from adenofibromas and atypical proliferative serous tumors to noninvasive MPSCs are observed in nearly 75% of cases.¹³ In addition, areas of infiltrative growth (stromal invasion) immediately adjacent to the noninvasive component are found in a significant proportion of cases (Figure 1).¹³ These invasive MPSCs are synonymous with low-grade serous carcinoma. The former term describes its histopathological features and the latter its clinical behavior. The histopathological findings strongly suggest that

there is a morphological and biological spectrum beginning with a benign serous cystadenoma/adenofibroma, through a proliferative tumor (atypical proliferative serous tumor) to a noninvasive carcinoma (noninvasive MPSC) ending with an invasive low-grade serous carcinoma (invasive MPSC).

Low-grade serous carcinomas typically pursue an indolent course that may last more than 20 years.^{12,13} Approximately 50 to 60% of patients ultimately succumb because of widespread intra-abdominal carcinomatosis but the tumor maintains its low-grade appearance and low proliferative index throughout its course (Silva et al, 1997 and unpublished data).¹³ This contrasts with conventional high-grade serous carcinoma that presents as a clinically aggressive neoplasm that spreads rapidly and is associated with a poor outcome. Analysis of mucinous, endometrioid, clear cell carcinomas, and malignant Brenner tumors reveals that they are often associated with cystadenomas, borderline tumors, and intraepithelial carcinomas.² Furthermore, it has been long recognized that endometrioid carcinoma and clear cell carcinoma are associated with endometriosis in the ovary or pelvis in 15 to 50% of cases^{14,15} leading investigators to propose that endometriosis is a precursor of these tumors. Rarely, a high-grade serous carcinoma is associated with ovarian endometriosis but this is viewed as an independent, coincidental finding; a causal relationship of endometriosis and serous carcinoma has never been proposed. A recent clinical study using serial transvaginal ultrasonography has shown that ~50% of ovarian carcinomas develop from pre-existing cystic lesions whereas the remaining 50% develop in ovaries without apparent abnormality on ultrasound.¹⁶ The former group

Table 1. Precursors and Molecular Genetic Alterations of Type I Tumors of the Ovary

Type I tumors	Precursors*	Known molecular genetic alterations
Low-grade serous carcinoma (invasive MPSC)	Serous cystadenoma/adenofibroma Atypical proliferative serous tumor Noninvasive MPSC	<i>BRAF</i> and <i>KRAS</i> mutations (~67%)
Mucinous carcinoma	Mucinous cystadenoma Atypical proliferative mucinous tumor Intraepithelial carcinoma	<i>KRAS</i> mutations (>60%)
Endometrioid carcinoma	Endometriosis Endometrioid adenofibroma Atypical proliferative endometrioid tumor Intraepithelial carcinoma	LOH or mutations in <i>PTEN</i> (20%) β -catenin gene mutations (16–54%) <i>KRAS</i> mutations (4–5%) Microsatellite instability (13–50%)
Clear cell carcinoma	Endometriosis Clear cell adenofibroma Atypical proliferative clear cell tumor Intraepithelial carcinoma	<i>KRAS</i> mutations (5–16%) Microsatellite instability (~13%) TGF- β RII mutation (66%) [†]
Malignant Brenner (transitional) tumor	Brenner tumor Atypical proliferative Brenner tumor	Not yet identified

Abbreviation: MPSC, micropapillary serous carcinoma; LOH, loss of heterozygosity; TGF, transforming growth factor.

*Atypical proliferative serous tumors and noninvasive MPSC have been termed "borderline" tumors in the literature. Similarly for mucinous, endometrioid, clear cell, and Brenner tumors, atypical proliferative tumor and intraepithelial carcinoma have been combined and designated "borderline tumor" in the literature.

[†]Based on preliminary results analyzing three cases.⁵⁷

was composed mainly of mucinous, endometrioid, clear cell carcinomas, and borderline tumors whereas the latter group was composed almost exclusively of high-grade serous carcinomas. This distribution corresponds to the type I and II tumors described below.

A Proposed Model of Ovarian Carcinogenesis

Our clinicopathological and molecular genetic studies provide the basis for a proposed model of ovarian carcinogenesis in which there are two main pathways of tumorigenesis, corresponding to the development of type I and type II tumors (Tables 1 and 2). It should be emphasized that the terms, type I and type II, describe pathways of tumorigenesis and are not specific histopathological terms. Type I tumors (low-grade serous carcinoma, mucinous carcinoma, endometrioid carcinoma, malignant Brenner tumor, and clear cell carcinoma) develop in a stepwise manner from well-recognized precursors, namely borderline tumors that in turn develop from cystadenomas and adenofibromas (Figure 1 and Table 1).⁵ The latter benign tumors appear to develop from the surface epithelium or inclusion cysts in the case of serous and mucinous tumors and from endometriosis or endometriomas in the case of endometrioid and clear cell tumors. Type I tumors are slow growing as evidenced by the observation that they are large and

often confined to the ovary at diagnosis. In contrast, type II tumors are high-grade at presentation. Type II carcinomas include what are currently classified as high-grade serous carcinoma (moderately and poorly differentiated), malignant mixed mesodermal tumors (carcinosarcomas), and undifferentiated carcinoma (Figure 1 and Table 2). In addition, it is likely that some high-grade serous and undifferentiated carcinoma containing cells with clear cytoplasm have been classified as clear cell carcinoma and would be included in this group. Although malignant mixed mesodermal tumors (carcinosarcomas) were once thought to be mixed tumors comprised of carcinoma and sarcoma, recent studies have demonstrated that they are monoclonal.^{17,18} Accordingly, these tumors are now regarded as high-grade carcinomas with metaplastic sarcomatous elements. Type II carcinomas are rarely associated with morphologically recognizable precursor lesions and it has been proposed that they develop *de novo* from the surface epithelium or inclusion cysts of the ovary.⁷ They evolve rapidly, metastasize early in their course, and are highly aggressive. It is likely that the apparent *de novo* conventional high-grade serous carcinoma does develop in a stepwise manner but precursor lesions have not yet been elucidated molecularly or morphologically (Figure 1). Presumably, this is because of rapid transit from inception as a microscopic carcinoma to a clinically diagnosed neoplasm. This is supported by

Table 2. Precursors and Molecular Genetic Alterations of Type II Tumors of the Ovary

Type II tumors*	Precursors	Known molecular genetic alterations
High-grade serous carcinoma	Not yet identified	<i>p53</i> mutations (50–80%) Amplification and overexpression of <i>HER2/neu</i> gene (10%–20%) and <i>AKT2</i> gene (12%–18%) Inactivation of <i>p16</i> gene (10%–17%)
Undifferentiated carcinoma	Not yet identified	Not yet identified
Malignant mixed mesodermal tumor (carcinosarcomas)	Not yet identified	<i>p53</i> mutations (> 90%)

*Type II tumors can contain neoplastic cells with clear cytoplasm and have sometimes been classified as "clear cell carcinoma."

Table 3. Summary of Clinicopathological Features of the Prototypic Type I and Type II Tumors: Low-Grade and High-Grade Serous Carcinoma, Respectively

	Frequency	Histologic features	Precursor lesions	Clinical behavior [†]	Response to chemotherapy
Low grade	~25% of serous carcinomas*	Micropapillary architecture; low-grade nuclei; low mitotic index	Serous cystadenoma Serous atypical proliferative (borderline) tumor	Indolent; slow progression 5-year survival ~55% [‡]	Poor
High grade	~75% of serous carcinomas*	Solid nests and masses; high-grade nuclei; high mitotic index	Not known; probably from ovarian surface epithelium or inclusion cysts (<i>de novo</i>)	Aggressive; rapid progression; 5-year survival ~30%	Good, although recurrence is common

*Based on a survey at the Johns Hopkins Hospital. Most patients will eventually die from the disease after a protracted clinical course.

[†]Advanced stage tumors.

[‡]See Sehdev et al.¹³

the significantly higher Ki-67 nuclear labeling (proliferation) index in conventional high-grade serous carcinomas compared to low-grade serous carcinomas (unpublished data).¹⁹

This dualistic model is the first step in an attempt to elucidate the molecular pathogenesis of ovarian carcinoma, but should not be construed as implying that other pathways of tumorigenesis do not exist. For example, it is not certain whether there are other subsets of type II carcinomas. Molecular profiling and epidemiological studies will be important to determine whether there are distinct subsets of type II tumors. Also it is not clear whether some low-grade serous carcinomas (type I) progress to high-grade serous carcinomas (type II). We have observed serous carcinomas with high-grade nuclei and abundant mitotic activity that display a micropapillary architecture, simulating invasive MPSC (low-grade serous carcinoma). We thought that these high-grade tumors may have arisen from invasive MPSCs (low-grade serous carcinoma) but like conventional high-grade tumors without a micropapillary architecture these tumors did not harbor *KRAS* mutations, indicating that they are not derived from invasive MPSCs (low-grade serous carcinomas) (see below).²⁰ These data are preliminary and do not rule out the possibility that some low-grade serous carcinomas progress to high-grade carcinomas but the findings do support the view that ovarian serous carcinomas can be graded into low- and high-grade based on nuclear rather than architectural features. Preliminary clinicopathological studies of other type I carcinomas (mucinous, endometrioid, and clear cell carcinomas) have demonstrated that some are moderately and even poorly differentiated, suggesting that some type I carcinomas can evolve from low- to high-grade neoplasms.

Molecular Evidence Supporting the Dualistic Model

Serous carcinoma is the most common type of ovarian carcinoma and therefore low-grade and high-grade serous carcinomas serve as the prototypes of type I and type II carcinomas, respectively (Table 3). Accordingly, the molecular genetic data that are being advanced in support of the dualistic model are derived mainly from studies of serous carcinoma.

There are several distinctive molecular changes that distinguish low-grade and high-grade serous carcinomas (Table 4). Among them, the most significant molecular genetic alterations are mutations in *BRAF* and *KRAS* oncogenes. The *RAS*, *RAF*, *MEK*, *ERK*, and *MAP* cascade is important for the transmission of growth signals into the nucleus.²¹ Oncogenic mutations in *BRAF* and *KRAS* result in constitutive activation of this pathway and contribute to neoplastic transformation. Recent studies have demonstrated that *KRAS* mutations at codons 12 and 13 occur in 35% of low-grade serous carcinomas (invasive MPSCs) and 33% of borderline tumors (atypical proliferative tumor and noninvasive MPSC) but not in high-grade serous carcinomas.^{5,20} Similarly, *BRAF* mutations at codon 599 occur in 30% of low-grade serous carcinomas and 28% of borderline tumors but not in high-grade serous carcinomas.²⁰ Mutations in *BRAF* and *KRAS*, therefore, were found in 65% of low-grade invasive serous carcinomas and in 61% of atypical proliferative tumors and noninvasive MPSCs, their putative precursors, but neither of the genes was mutated in high-grade serous carcinomas. It is of interest that *BRAF* mutations were found only in tumors with wild-type *KRAS*.²⁰ The mutually

Table 4. Summary of Molecular Features of Prototypic Type I and Type II Tumors: Low-Grade and High-Grade Serous Carcinoma, Respectively

	<i>KRAS</i> mutations	<i>BRAF</i> mutations	<i>BRAF</i> or <i>KRAS</i> mutations	<i>TP53</i> mutations	HLA-G expression	Proliferation (Ki-67) index
Low grade	35%	30%	65%	0	0	~10–15%
High grade	0	0	0	50%–80%	61%	>50%

exclusive nature of *BRAF* mutations at codon 599 and *KRAS* mutations at codons 12 and 13 in ovarian carcinoma is consistent with similar findings in melanoma and colorectal carcinoma^{22,23} and lends support for the view that *BRAF* and *KRAS* mutations have an equivalent effect on tumorigenesis. Mutations of *BRAF* and *KRAS* seem to occur very early in the development of low-grade serous carcinoma as evidenced by the detection of these mutations in small atypical proliferative serous tumors but not in serous cystadenomas.²⁴ These data provide cogent evidence that the development of conventional high-grade serous carcinomas involves molecular mechanisms not related to mutations in *BRAF* and *RAS*.

In contrast to low-grade serous carcinoma in which mutations in *p53* are rare, mutations in *p53* are common in high-grade serous carcinomas. Most studies have shown that ~50 to 80% of advanced stage, presumably high-grade, serous carcinomas have mutant *p53*.²⁵⁻²⁹ It has also been reported that mutant *p53* is present in 37% of stage I and II presumably high-grade serous carcinomas.³⁰ In a study of very early microscopic stage I serous carcinomas in ovaries removed prophylactically from women who were BRCA heterozygotes, overexpression of *p53* and mutation of *p53* were found in all early invasive high-grade serous carcinomas as well as in the adjacent dysplastic surface epithelium.³¹ It is likely that inherited mutations in BRCA genes predispose the ovarian surface epithelium and inclusion cysts to neoplastic transformation through an increase in genetic instability. Although sporadic ovarian carcinomas were not analyzed in this study, the clinical and pathological features of BRCA-linked ovarian carcinomas and their sporadic counterparts are indistinguishable, suggesting that their histogenesis may be similar. Thus, although the findings are preliminary, they suggest that conventional high-grade serous carcinoma, in its very earliest stage resembles advanced stage serous carcinoma at a molecular as well as at a morphological level. Similar to high-grade serous carcinoma, malignant mixed mesodermal tumors (carcinosarcomas) also demonstrate *p53* mutations in almost all cases analyzed.³²⁻³⁴ It has been reported that the same *p53* mutations occur in the epithelial and the mesenchymal components.³² Moreover, the fact that pure carcinomatous areas are often associated with sarcomatous components suggests a common derivation of both the epithelial and the mesenchymal components in these neoplasms.³⁵ The finding that metastases from these tumors nearly always are composed exclusively of carcinoma has led investigators to suggest that malignant mixed mesodermal tumors are metaplastic carcinomas.

In addition to *p53* mutations, conventional serous carcinomas that are presumably high-grade demonstrate amplification/overexpression of HER-2/neu tyrosine kinase gene in 20 to 67%³⁶ and AKT2 serine/threonine kinase gene in 12 to 18% of samples analyzed.^{37,38} In contrast, amplification of both genes is rare in borderline tumors. Inactivation of the *p16* gene because of promoter methylation, mutation, or homozygous deletion occurs in a variety of human cancers including conventional ovarian serous carcinoma that presumably are high grade.³⁹ Because these are molecular genetic studies in which the

tumors were described simply as "serous carcinomas," we have referred to them as "presumably high-grade" because the vast majority of serous carcinomas are high grade.

Besides molecular genetic alterations, both low-grade and high-grade serous carcinomas are characterized by distinct gene expression profiles. For example, transcriptome-wide gene expression profiling has demonstrated that human leukocyte antigen-G (HLA-G) and apolipoprotein E (apoE) are overexpressed in most high-grade serous carcinomas but rarely in low-grade serous carcinomas. HLA-G immunoreactivity, ranging from focal to diffuse, was detected in 45 of 74 (61%) high-grade ovarian serous carcinomas but in none of the 18 low-grade serous carcinomas or 26 serous borderline tumors (atypical proliferative tumors and noninvasive MPSCs) that were studied.⁴⁰ A similar correlation of HLA-G expression with behavior has been observed in large cell carcinoma.⁴¹ A possible mechanism that explains the association of HLA-G expression with prognosis is that HLA-G seems to facilitate tumor cell evasion of the immune system by protecting malignant cells from lysis by natural killer cells.⁴²

Recently, apoE expression has been detected in ovarian tumors. Besides the well-known role of apoE in cholesterol transport and in the pathogenesis of atherosclerosis and Alzheimer's disease, apoE may play a novel role in the development of human cancer. In ovarian carcinomas, expression of apoE is primarily confined to type II high-grade serous carcinoma because apoE immunoreactivity has been detected in 66% of high-grade but only 12% of low-grade serous carcinomas. In contrast, apoE immunoreactivity was not detected in normal ovarian surface epithelium, serous cystadenomas, serous borderline tumors, and other type I tumors (Chen, unpublished data). Inhibition of apoE expression *in vitro* induces cell-cycle arrest and apoptosis in apoE-expressing ovarian cancer cells, suggesting that apoE expression is important for their growth and survival.

The genes that are specifically expressed in other types of ovarian carcinomas remain primarily unknown. Recently, hepatocyte nuclear factor-1 β and glutathione peroxidase 3 have been reported as molecular markers for ovarian clear cell carcinoma because both genes are highly expressed in ovarian clear cell carcinomas but rarely in other ovarian carcinomas.^{43,44}

Finally, allelic imbalance (calculated as the number of SNP markers with allelic imbalance/total SNP markers examined) has been assessed in atypical proliferative tumors, noninvasive MPSCs, and low-grade serous carcinoma (invasive MPSC).⁵ A progressive increase in the degree of allelic imbalance of chromosomes 1p, 5q, 8p, 18q, 22q, and Xp was noted when comparing atypical proliferative tumors with noninvasive and low-grade serous carcinomas (invasive MPSCs). In particular, allelic imbalance of chromosome 5q was more frequently observed in noninvasive MPSCs compared with atypical proliferative tumors and allelic imbalance of chromosome 1p was more frequently found in low-grade serous carcinoma (invasive MPSC) compared with noninvasive MPSCs. The allelic imbalance patterns in atypical proliferative

erative tumors were also found in noninvasive MPSCs containing adjacent atypical proliferative tumor components, further supporting the view that atypical proliferative tumors are the precursors of MPSCs. In contrast, all high-grade serous carcinomas including the very earliest tumors (less than 8 mm confined to one ovary) showed high levels of allelic imbalance. As allelic imbalance reflects chromosomal instability, the above findings suggest a step-wise increase in chromosomal instability in the progression to low-grade serous carcinoma in contrast to a high level of chromosomal instability in high-grade serous carcinoma even in their earliest stage of development.

The stepwise progression of borderline tumors (atypical proliferative tumor and noninvasive MPSC) to low-grade serous carcinoma (invasive MPSC) closely approximates the adenoma-carcinoma sequence in colorectal carcinoma and the progression of the other type I carcinomas, specifically mucinous and endometrioid carcinoma. In mucinous carcinoma for example, morphological transitions from cystadenoma to an atypical proliferative tumor (borderline tumor), to intraepithelial carcinoma and invasive carcinoma have been recognized for some time and an increasing frequency of *KRAS* mutations at codons 12 and 13 has been described in cystadenomas, borderline tumors, and mucinous carcinomas, respectively.^{8,45-48} In addition, using microdissection, the same *KRAS* mutation has been detected in mucinous carcinoma and in the adjacent mucinous cystadenoma and borderline tumor.⁴⁵ Likewise, in endometrioid carcinomas, mutation of β -catenin has been reported in approximately one-third of cases^{49,50} and mutation of *PTEN* in 20%, rising to 46% in those tumors with 10q23 loss of heterozygosity.⁵¹ These mutations are generally detected in well-differentiated, stage I tumors with a good prognosis, suggesting that inactivation of these genes is an early event. Moreover, similar molecular genetic alterations including loss of heterozygosity at 10q23 and mutations in *PTEN* have been reported in endometriosis, atypical endometriosis, and ovarian endometrioid carcinoma in the same specimen.⁵¹⁻⁵⁶ The molecular genetic findings together with the morphological data showing a frequent association of endometriosis with endometrioid adenofibromas, atypical proliferative (borderline) tumors, adjacent to invasive well-differentiated endometrioid carcinoma provide evidence of step-wise tumor progression in the development of endometrioid carcinoma. Clear cell carcinoma is also frequently associated with endometriosis, clear cell adenofibromas, and clear cell atypical proliferative (borderline) tumors but molecular evidence for the stepwise progression model is lacking because molecular markers specific to clear cell neoplasms have only recently been identified.^{43,44} Transforming growth factor- β receptor type II has been found to be mutated in the kinase domain in two of three clear cell carcinomas but rarely in other histological types of ovarian carcinomas.⁵⁷ Microsatellite instability is present in endometrioid and clear cell carcinoma but is only rarely detected in serous and mucinous tumors.^{58,59} These findings provide further evidence of the close relationship of endometrioid and clear cell carci-

noma and point to a common precursor lesion for these two neoplasms.

Conclusion

Based on morphological and molecular genetic analyses of a large series of ovarian tumors, we have proposed a tumor progression model for ovarian carcinoma. In this model, ovarian tumors are divided into two broad categories designated type I and type II. These designations refer to pathways of tumorigenesis and are not specific histopathological terms. Type I tumors include low-grade serous carcinoma, mucinous carcinoma, endometrioid carcinoma, malignant Brenner tumors, and clear cell carcinoma. Type II tumors are composed of what are currently classified as moderately and poorly differentiated serous carcinoma (high-grade serous carcinoma), malignant mixed mesodermal tumors (carcinosarcomas), and undifferentiated carcinoma. Some of the latter may contain cells with clear cytoplasm and have therefore been classified erroneously as clear cell carcinomas. The tumorigenic pathway for type I tumors resembles the adenoma-carcinoma sequence in colorectal cancer and is characterized by clearly recognized precursor lesions, namely, cystadenoma, atypical proliferative tumor, and noninvasive carcinoma. The latter two noninvasive tumors have traditionally been combined into one category designated "borderline." Type I tumors evolve slowly and are associated with distinct molecular changes that are rarely found in type II tumors such as mutations in *BRAF* and *KRAS* for serous tumors, *KRAS* mutations for mucinous tumors, and β -catenin and *PTEN* mutations for endometrioid tumors. In contrast, type II tumors evolve rapidly, arising directly from the surface epithelium or inclusion cysts and metastasize early in their course. There are very limited data on the molecular alterations associated with type II tumors except frequent mutations of p53 in high-grade serous carcinomas and malignant mixed mesodermal tumors (carcinosarcomas). This model reconciles the inconsistency in the current classification of ovarian tumors that regards borderline tumors as a distinct entity unrelated to invasive carcinoma and provides a morphological and molecular genetic framework for future studies aimed at elucidating the pathogenesis of ovarian cancer. Unraveling the complex molecular genetic pathways involved in ovarian carcinogenesis will require correlated morphological and molecular genetic studies. Identification and characterization of the panoply of molecular changes associated with ovarian carcinogenesis will facilitate development of diagnostic tests for early detection of ovarian cancer and for the development of novel therapies aimed at blocking key growth-signaling pathways.

Acknowledgments

We thank the members of gynecological pathology division at Johns Hopkins Medical Institutions for their review of this manuscript.

References

- Kinzler KW, Vogelstein B: The Genetic Basis of Human Cancer. Toronto, McGraw-Hill, 1998
- Seidman JD, Russell P, Kurman RJ: Surface epithelial tumors of the ovary. Blaustein's Pathology of the Female Genital Tract. Edited by RJ Kurman. New York, Springer Verlag, 2002, pp 791–904
- Scully RE: International Histological Classification of Tumors: Histological Typing of Ovarian Tumors. Geneva, World Health Organization, 1999
- Scully RE: World Health Organization International Histological Classification of Tumours. New York, Springer, 1999
- Singer G, Kurman RJ, Chang H-W, Cho SKR, Shih I-M: Diverse tumorigenic pathways in ovarian serous carcinoma. *Am J Pathol* 2002, 160:1223–1228
- Ortiz BH, Ailawadi M, Colitti C, Muto MG, Deavers M, Silva EG, Berkowitz RS, Mok SC, Gershenson DM: Second primary or recurrence? Comparative patterns of p53 and K-ras mutations suggest that serous borderline ovarian tumors and subsequent serous carcinomas are unrelated tumors. *Cancer Res* 2001, 61:7264–7267
- Bell DA, Scully RE: Early de novo ovarian carcinoma. A study of fourteen cases. *Cancer* 1994, 73:1859–1864
- Caduff RF, Svoboda-Newman SM, Ferguson AW, Johnston CM, Frank TS: Comparison of mutations of Ki-RAS and p53 immunoreactivity in borderline and malignant epithelial ovarian tumors. *Am J Surg Pathol* 1999, 23:323–328
- Dubeau L: Ovarian cancer. The Metabolic and Molecular Bases of Inherited Disease. Edited by CR Scriver, AL Beaudet, WS Sly, D Valle, B Childs, KW Kinzler, B Vogelstein. Toronto, McGraw-Hill, 2001, pp 1091–1096
- Burks RT, Sherman ME, Kurman RJ: Micropapillary serous carcinoma of the ovary. A distinctive low-grade carcinoma related to serous borderline tumors. *Am J Surg Pathol* 1996, 20:1319–1330
- Riopel MA, Ronnett BM, Kurman RJ: Evaluation of diagnostic criteria and behavior of ovarian intestinal-type mucinous tumors: atypical proliferative (borderline) tumors and intraepithelial, microinvasive, invasive, and metastatic carcinomas. *Am J Surg Pathol* 1999, 23:617–635
- Seidman JD, Kurman RJ: Subclassification of serous borderline tumors of the ovary into benign and malignant types. A clinicopathologic study of 65 advanced stage cases. *Am J Surg Pathol* 1996, 20:1331–1345
- Sehdev AES, Sehdev PS, Kurman RJ: Noninvasive and invasive micropapillary serous carcinoma of the ovary: a clinicopathologic analysis of 135 cases. *Am J Surg Pathol* 2003, 27:725–736
- Okuda T, Otsuka J, Sekizawa A, Saito H, Makino R, Kushima M, Farina A, Yuzuru K, Okai T: p53 mutations and overexpression affect prognosis of ovarian endometrioid cancer but not clear cell cancer. *Gynecol Oncol* 2003, 88:318–325
- Modesitt SC, Tortolero-Luna G, Robinson JB, Gershenson D, Wolf JK: Ovarian and extraovarian endometriosis-associated cancer. *Obstet Gynecol* 2002, 100:788–795
- Horiuchi A, Itoh K, Shimizu M, Nakai I, Yamazaki T, Kimura K, Suzuki A, Shiozawa I, Ueda N, Konishi I: Toward understanding the natural history of ovarian carcinoma development: a clinicopathological approach. *Gynecol Oncol* 2003, 88:309–317
- Masuda A, Takeda A, Fukami H, Yamada C, Matsuyama M: Characteristics of cell lines established from a mixed mesodermal tumor of the human ovary. Carcinomatous cells are changeable to sarcomatous cells. *Cancer* 1987, 60:1697–2703
- Moritani S, Moriya T, Kushima R, Sugihara H, Harada M, Hattori T: Ovarian carcinoma recurring as carcinosarcoma. *Pathol Int* 2001, 51:380–384
- Garzetti GG, Ciavattini A, Goteri G, De Nictolis M, Stramazotti D, Lucarini G, Biagini G: Ki67 antigen immunostaining (MIB 1 monoclonal antibody) in serous ovarian tumors: index of proliferative activity with prognostic significance. *Gynecol Oncol* 1995, 56:169–174
- Singer G, Oldt III R, Cohen Y, Wang BG, Sidransky D, Kurman RJ, Shih I-M: Mutations in BRAF and KRAS characterize the development of low-grade ovarian serous carcinoma. *J Natl Cancer Inst* 2003, 95:484–486
- Peyssonnaud C, Eychene A: The Raf/MEK/ERK pathway: new concepts of activation. *Biol Cell* 2001, 93:53–62
- Davies H, Bignell GR, Cox C, Stephens P, Edkins S, Clegg S, Teague J, Woffendin H, Garnett MJ, Bottomley W, Davis N, Dicks E, Ewing R, Floyd Y, Gray K, Hall S, Hawes R, Hughes J, Kosmidou V, Menzies A, Mould C, Parker A, Stevens C, Watt S, Hooper S, Wilson R, Jayatilake H, Gusterson BA, Cooper C, Shipley J, Hargrave D, Pritchard-Jones K, Maitland N, Chenevix-Trench G, Riggins GJ, Bigner DD, Palmieri G, Cossu A, Flanagan A, Nicholson A, Ho JW, Leung SY, Yuen ST, Weber BL, Seigler HF, Darrow TL, Paterson H, Marais R, Marshall CJ, Wooster R, Stratton MR, Futreal PA: Mutations of the BRAF gene in human cancer. *Nature* 2002, 417:949–954
- Rajagopalan H, Bardelli A, Lengauer C, Kinzler KW, Vogelstein B, Velculescu VE: Tumorigenesis: RAF/RAS oncogenes and mismatch-repair status. *Nature* 2002, 418:934
- Cheng EJ, Kurman RJ, Wang M, Oldt III R, Berman DM, Shih I-M: Molecular genetic analysis of ovarian serous cystadenomas. *Lab Invest* 2004, in press
- Chan W-Y, Cheung K-K, Schorge JO, Huang L-W, Welch WR, Bell DA, Berkowitz RS, Mok SC: Bcl-2 and p53 protein expression, apoptosis, and p53 mutation in human epithelial ovarian cancers. *Am J Pathol* 2000, 156:409–417
- Kohler MF, Marks JR, Wiseman RW, Jacobs IJ, Davidoff AM, Clarke-Pearson DL, Soper JT, Bast Jr RC, Berchuck A: Spectrum of mutation and frequency of allelic deletion of the p53 gene in ovarian cancer. *J Natl Cancer Inst* 1993, 85:1513–1519
- Kupryjanczyk J, Thor AD, Beauchamp R, Merritt V, Edgerton SM, Bell DA, Yandell DW: p53 gene mutations and protein accumulation in human ovarian cancer. *Proc Natl Acad Sci USA* 1993, 90:4961–4965
- Berchuck A, Carney M: Human ovarian cancer of the surface epithelium. *Biochem Pharmacol* 1997, 54:541–544
- Wen WH, Reles A, Runnebaum IB, Sullivan-Halley J, Bernstein L, Jones LA, Felix JC, Kreienberg R, el-Naggar A, Press MF: p53 mutations and expression in ovarian cancers: correlation with overall survival. *Int J Gynecol Pathol* 1999, 18:29–41
- Shelling AN, Cooke I, Ganesan TS: The genetic analysis of ovarian cancer. *Br J Cancer* 1995, 72:521–527
- Pothuri B, Leitao M, Barakat R, Akram M, Bogomolny F, Olvera N, Lin O: Genetic analysis of ovarian carcinoma histogenesis. *Gynecol Oncol* 2001, 80:Abstract (Society of Gynecologic Oncologists 32nd Annual Meeting)
- Gallardo A, Matias-Guiu X, Lagarda H, Catusas L, Bussaglia E, Gras E, Suarez D, Prat J: Malignant mullerian mixed tumor arising from ovarian serous carcinoma: a clinicopathologic and molecular study of two cases. *Int J Gynecol Pathol* 2002, 21:268–272
- Kounelis S, Jones MW, Papadaki H, Bakker A, Swalsky P, Finkelstein SD: Carcinosarcomas (malignant mixed mullerian tumors) of the female genital tract: comparative molecular analysis of epithelial and mesenchymal components. *Hum Pathol* 1998, 29:82–87
- Abeln EC, Smit VT, Wessels JW, de Leeuw WJ, Cornelisse CJ, Fleuren GJ: Molecular genetic evidence for the conversion hypothesis of the origin of malignant mixed mullerian tumours. *J Pathol* 1997, 183:424–431
- Sreenan JJ, Hart WR: Carcinosarcomas of the female genital tract. A pathologic study of 29 metastatic tumors: further evidence for the dominant role of the epithelial component and the conversion theory of histogenesis. *Am J Surg Pathol* 1995, 19:666–674
- Ross JS, Yang F, Kallakury BV, Sheehan CE, Ambros RA, Muraca PJ: HER-2/neu oncogene amplification by fluorescence in situ hybridization in epithelial tumors of the ovary. *Am J Clin Pathol* 1999, 111:311–316
- Cheng JQ, Godwin AK, Bellacosa A, Taguchi T, Franke TF, Hamilton TC, Tschlis PN, Testa JR: AKT2, a putative oncogene encoding a member of a subfamily of protein-serine/threonine kinases, is amplified in human ovarian carcinomas. *Proc Natl Acad Sci USA* 1992, 89:9267–9271
- Bellacosa A, de Feo D, Godwin AK, Bell DW, Cheng JQ, Altomare DA, Wan M, Dubeau L, Scambia G, Masciullo V: Molecular alterations of the AKT2 oncogene in ovarian and breast carcinomas. *Int J Cancer* 1995, 64:280–285
- Rocco JW, Sidransky D: p16(MTS-1/CDKN2/INK4a) in cancer progression. *Exp Cell Res* 2001, 264:42–55
- Singer G, Rebmann V, Y-C C, Liu H-T, Ali SZ, Reinsberg J, McMaster M, Pfeiffer K, Chan DW, Wardelmann E, Grosse-Wilde H, Kurman RJ, Shih I-M: HLA-G is a potential tumor marker in malignant ascites. *Clin Cancer Res* 2003, 9:4460–4464
- Urošević M, Kurrer MO, Kamarashev J, Mueller B, Weder W, Burg G,

- Stahel RA, Dummer R, Trojan A: Human leukocyte antigen G up-regulation in lung cancer associates with high-grade histology, human leukocyte antigen class I loss and interleukin-10 production. *Am J Pathol* 2001, 159:817–824
42. Urosevic M, Willers J, Mueller B, Kempf W, Burg G, Dummer R: HLA-G protein up-regulation in primary cutaneous lymphomas is associated with interleukin-10 expression in large cell T-cell lymphomas and indolent B-cell lymphomas. *Blood* 2002, 99:609–617
 43. Tsuchiya A, Sakamoto M, Yasuda J, Chuma M, Ohta T, Ohki M, Yasugi T, Taketani Y, Hirohashi S: Expression profiling in ovarian clear cell carcinoma: identification of hepatocyte nuclear factor-1beta as a molecular marker and a possible molecular target for therapy of ovarian clear cell carcinoma. *Am J Pathol* 2003, 163:2503–2512
 44. Hough CD, Sherman-Baust CA, Pizer ES, Montz FJ, Im DD, Rosenzhein NB, Cho KR, Riggins GJ, Morin PJ: Large-scale serial analysis of gene expression reveals genes differentially expressed in ovarian cancer. *Cancer Res* 2000, 60:6281–6287
 45. Mok SC, Bell DA, Knapp RC, Fishbaugh PM, Welch WR, Muto MG, Berkowitz RS, Tsao SW: Mutation of K-ras protooncogene in human ovarian epithelial tumors of borderline malignancy. *Cancer Res* 1993, 53:1489–1492
 46. Ichikawa Y, Nishida M, Suzuki H: Mutation of KRAS protooncogene is associated with histological subtypes in human mucinous ovarian tumors. *Cancer Res* 1994, 54:33–35
 47. Enomoto T, Weghorst CM, Inoue M, Tanizawa O, Rice JM: K-ras activation occurs frequently in mucinous adenocarcinomas and rarely in other common epithelial tumors of the human ovary. *Am J Pathol* 1991, 139:777–785
 48. Gemignani ML, Schlaerth AC, Bogomolny F, Barakat R, Lin O, Soslow R, Venkatraman E, Boyd J: Role of KRAS and BRAF gene mutations in mucinous ovarian carcinoma. *Gynecol Oncol* 2003, 90: 378–381
 49. Wu R, Zhai Y, Fearon ER, Cho KR: Diverse mechanisms of beta-catenin deregulation in ovarian endometrioid adenocarcinomas. *Cancer Res* 2001, 61:8247–8255
 50. Moreno-Bueno G, Gamallo C, Perez-Gallego L, deMora JC, Suarez A, Palacios J: Beta-catenin expression pattern, beta-catenin gene mutations, and microsatellite instability in endometrioid ovarian carcinomas and synchronous endometrial carcinomas. *Diagn Mol Pathol* 2001, 10:116–122
 51. Obata K, Morland SJ, Watson RH, Hitchcock A, Chenevix-Trench G, Thomas EJ, Campbell IG: Frequent PTEN/MMAC mutations in endometrioid but not serous or mucinous epithelial ovarian tumors. *Cancer Res* 1998, 58:2095–2097
 52. Sato N, Tsunoda H, Nishida M, Morishita Y, Takimoto Y, Kubo T, Noguchi M: Loss of heterozygosity on 10q23.3 and mutation of the tumor suppressor gene PTEN in benign endometrial cyst of the ovary: possible sequence progression from benign endometrial cyst to endometrioid carcinoma and clear cell carcinoma of the ovary. *Cancer Res* 2000, 60:7052–7056
 53. Saito M, Okamoto A, Kohno T, Takakura S, Shinozaki H, Isonishi S, Yasuhara T, Yoshimura T, Ohtake Y, Ochiai K, Yokota J, Tanaka T: Allelic imbalance and mutations of the PTEN gene in ovarian cancer. *Int J Cancer* 2000, 85:160–165
 54. Thomas EJ, Campbell IG: Molecular genetic defects in endometriosis. *Gynecol Obstet Invest* 2000, 50:44–50
 55. Obata K, Hoshiai H: Common genetic changes between endometriosis and ovarian cancer. *Gynecol Obstet Invest* 2000, 50:39–43
 56. Bischoff FZ, Simpson JL: Heritability and molecular genetic studies of endometriosis. *Hum Reprod Update* 2000, 6:37–44
 57. Francis-Thickpenny KM, Richardson DM, van Ee CC, Love DV, Winship IM, Baguley BC, Chenevix-Trench G, Shelling AN: Analysis of the TGF-beta functional pathway in epithelial ovarian carcinoma. *Br J Cancer* 2001, 85:687–691
 58. Fujita M, Enomoto T, Yoshino K, Nomura T, Buzard GS, Inoue M, Okudaira Y: Microsatellite instability and alterations in the hMSH2 gene in human ovarian cancer. *Int J Cancer* 1995, 64:361–366
 59. Gras E, Catusas L, Arguelles R, Moreno-Bueno G, Palacios J, Gamallo C, Matias-Guiu X, Prat J: Microsatellite instability, MLH-1 promoter hypermethylation, and frameshift mutations at coding mononucleotide repeat microsatellites in ovarian tumors. *Cancer* 2001, 92: 2829–2836
 60. Singer G, Shih Ie M, Truskinovsky A, Umudum H, Kurman RJ: Mutational analysis of K-ras segregates ovarian serous carcinomas into two types: invasive MPSC (low-grade tumor) and conventional serous carcinoma (high-grade tumor). *Int J Gynecol Pathol* 2003, 22:37–41

BRIEF COMMUNICATION

Mutations in BRAF and KRAS Characterize the Development of Low-Grade Ovarian Serous Carcinoma

Gad Singer, Robert Oldt III,
Yoram Cohen, Brant G. Wang,
David Sidransky, Robert J. Kurman,
Ie-Ming Shih

Activating mutations in KRAS and in one of its downstream mediators, BRAF, have been identified in a variety of human cancers. To determine the role of mutations in BRAF and KRAS in ovarian carcinoma, we analyzed both genes for three common mutations (at codon 599 of BRAF and codons 12 and 13 of KRAS). Mutations in either codon 599 of BRAF or codons 12 and 13 of KRAS occurred in 15 of 22 (68%) invasive micropapillary serous carcinomas (MPSCs; low-grade tumors) and in 31 of 51 (61%) serous borderline tumors (precursor lesions to invasive MPSCs). None of the tumors contained a mutation in both BRAF and KRAS. In contrast, none of the 72 conventional aggressive high-grade serous carcinomas analyzed contained the BRAF codon 599 mutation or either of the two KRAS mutations. The apparent restriction of these BRAF and KRAS mutations to low-grade serous ovarian carcinoma and its precursors suggests that low-grade and high-grade ovarian serous carcinomas develop through independent pathways. [J Natl Cancer Inst 2003; 95:484-6]

The kinase cascade involving RAS, RAF, mitogen/extracellular signal-regulated kinase (MEK), extracellular signal-regulated kinase (ERK), and mitogen-activated protein kinase (MAPK) mediates the transmission of growth signals into the nucleus (1). One of the three RAF members, BRAF, has been

recently reported to be activated by somatic mutation in many human cancers, with mutations in BRAF occurring at a particularly high rate in cutaneous melanoma and papillary carcinoma of the thyroid (2,3). All known BRAF mutations occur within the kinase domain, with a single substitution of A for the T at nucleotide position 1796 (1796T/A) accounting for at least 80% of BRAF mutations (2,4,5). This mutation converts a valine residue at amino acid position 599 to a glutamic acid (V599E); the mutant protein has elevated kinase activity and is able to transform NIH3T3 cells independent of RAS function (2). Similarly, activating mutations in codons 12 and 13 of KRAS occur frequently in carcinomas and result in constitutive activation of KRAS that contributes to tumorigenesis (1).

To investigate the role of BRAF and KRAS mutations in ovarian carcinoma, we analyzed different types of ovarian carcinomas for three common mutations in these genes—the BRAF mutation at codon 599 and the KRAS mutations at codons 12 and 13. Ovarian carcinoma, one of the major cancer types and the most lethal gynecologic malignancy, comprises a heterogeneous group of tumors with distinctly different histologic types, molecular features, and clinical behavior (6-8). The most common type of ovarian cancer is serous carcinoma which, in our previous study (9), we further divided into high-grade conventional serous carcinoma and a low-grade tumor, invasive micropapillary serous carcinoma (MPSC). All serous carcinomas are believed to develop from ovarian surface epithelium or inclusion cysts (10). In contrast to conventional serous carcinoma, for which morphologically recognizable precursor lesions have not been identified, invasive MPSC develops in a stepwise fashion from a noninvasive group of neoplasms termed serous borderline tumors. Based on our extensive morphologic and molecular studies, serous borderline tumors include a benign precursor (atypical proliferative serous tumor) and a noninvasive carcinoma designated noninvasive MPSC (9,11-14). The non-serous types of ovarian carcinoma include endometrioid carcinoma and clear-cell carcinoma, which are less common than serous carcinoma and appear to develop from endometriosis (15).

Formalin-fixed, paraffin-embedded

tissue samples of 182 ovarian tumor tissues were obtained from the surgical pathology file of the Johns Hopkins Hospital. Genomic DNA was purified from the microdissected tumor component, as previously described (9). The ovarian tumors (51 serous borderline tumors, 21 invasive MPSCs, 69 conventional serous carcinomas, 21 endometrioid carcinomas, and 20 clear-cell carcinomas), three conventional serous carcinoma cell lines (SKOV-3, OVCAR-3 and HTB-75), and one primary culture of an invasive MPSC were analyzed for the codon 599 mutation in BRAF and the codon 12 and 13 mutations in KRAS. Five normal ovarian tissues and 10 serous cystadenomas were also included in the mutation analysis. The KRAS mutation status of some of the tumor samples (22 of the serous borderline tumors, 15 of the invasive MPSCs, and 20 of the conventional serous carcinomas) has already been reported (9). Waiver of patients' consent was approved by the local Institutional Review Board. All the cases were reviewed by three gynecologic pathologists (R. J. Kurman, G. Singer, and I.-M. Shih), who concurred with the diagnoses before microdissection.

Analysis of the 1796T/A status in BRAF was performed using a polymerase chain reaction (PCR)-based restriction fragment length polymorphism (RFLP) technique (3). For this method, the BRAF PCR product of exon 15, which contains nucleotide position 1796, was digested with TspR1 (New England Biolabs, Inc., Beverly, MA) at 65°C for 3 hours. The PCR products were electrophoresed on a 10% polyacrylamide gel and were also sequenced to validate the RFLP results. As shown in Fig. 1, BRAF mutations were found

Affiliations of authors: G. Singer, R. Oldt III, B. G. Wang (Department of Pathology), Y. Cohen, D. Sidransky (Head and Neck Cancer Research Division), R. J. Kurman, I.-M. Shih (Departments of Pathology and Gynecology and Obstetrics), The Johns Hopkins University School of Medicine, Baltimore, MD.

Correspondence to: Ie-Ming Shih, M.D., Ph.D., Department of Pathology, The Johns Hopkins University School of Medicine, 418 N. Bond St., B-315, Baltimore, MD 21231 (e-mail: isih@jhmi.edu).

See "Notes" following "References."

Journal of the National Cancer Institute, Vol. 95, No. 6, © Oxford University Press 2003, all rights reserved.

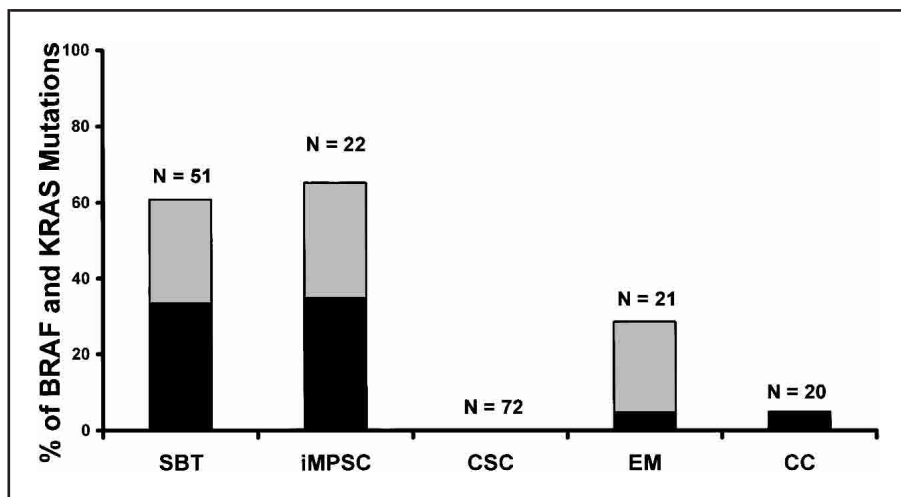


Fig. 1. Mutations of BRAF and KRAS in ovarian carcinomas. Mutational analysis of codon 599 of BRAF (gray bars) and codons 12 and 13 of KRAS (black bars) was performed in several types of ovarian neoplasm, including serous borderline tumors (SBT), invasive micropapillary serous carcinomas (iMPSC, low-grade carcinomas), conventional high-grade serous carcinomas (CSC), endometrioid carcinomas (EM), and clear-cell carcinomas (CC). The number of tumors of each type that were analyzed is indicated. None of the tumors showed both BRAF and KRAS mutations. iMPSCs and their precursor lesions, serous borderline tumors, demonstrate the highest frequency of mutations in BRAF and KRAS.

in 33% of the invasive MPSCs (including the primary culture of an invasive MPSC) and in 28% of their precursor lesions, serous borderline tumors. The BRAF mutation was not detected in the histologically normal-appearing cyst epithelium adjacent to a borderline tumor that contained the BRAF mutation (data not shown), indicating that BRAF mutations occur during progression of serous borderline tumors.

KRAS mutational status at codon 12 or 13 was analyzed either by digital PCR (9,16,17) or direct sequencing. In combination with our previous results (9), KRAS mutations were found in 35% of invasive MPSCs and 33% of serous borderline tumors. None of the tumors contained a mutation in both BRAF and KRAS; thus, considering the two genes together, a mutation in one of them was found in 68% of invasive MPSCs and in 61% of serous borderline tumors. There was no correlation between the presence of the BRAF or KRAS mutations and patient age, clinical stage, tumor size, and mismatch repair deficiency status (two-sided Spearman's rank-order correlation) (data not shown). In contrast to invasive MPSCs and their precursors, all 69 specimens of clinically aggressive conventional serous carcinomas, as well as three well-established cell lines, contained wild-type BRAF and KRAS sequences at the analyzed sites in both genes. As controls, all five normal ovarian tissues and all 10 serous cystadeno-

mas analyzed contained wild-type BRAF and KRAS.

The mutually exclusive nature of BRAF at codon 599 and KRAS mutations at codons 12 and 13 in ovarian carcinoma is consistent with a similar finding in melanoma and colorectal carcinoma and lends strong support for the view that BRAF and KRAS mutations have equivalent effects on tumorigenesis (2,5). Although the possibility that other members of the RAF family or downstream targets of RAF are mutated in conventional high-grade serous carcinomas must be investigated, it would appear that the development of high-grade conventional serous carcinomas involves a pathway distinct from the RAS signaling pathway. For example, mutations in TP53 are common in high-grade ovarian serous carcinomas (18).

We also analyzed codon 599 of BRAF and codons 12 and 13 of KRAS in less common, non-serous types of ovarian cancer, including endometrioid and clear-cell carcinomas. We did not include mucinous carcinomas involving the ovary because we had previously found that most such carcinomas are metastases from other primary sites (19,20). We detected BRAF mutations in 24% of endometrioid carcinomas but in none of the clear-cell carcinomas. No other gene has such a high mutation rate in ovarian endometrioid carcinomas, except PTEN, which is mutated in 20% of ovarian endometrioid carcinomas (21).

Only one clear-cell carcinoma and one endometrioid carcinoma had a KRAS mutation. This finding is similar to that in a previous report, which also analyzed KRAS in a small number of cases (22). Again, among the tumors we analyzed, the BRAF mutation and KRAS mutations were never both present in the same tumor.

Our results demonstrate that the mutational status of BRAF and KRAS is distinctly different among various histologic types of ovarian serous carcinoma, occurring most frequently in invasive MPSC, a clinically indolent neoplasm, and its precursors, serous borderline tumors. Thus, it appears that different histologic types of ovarian carcinomas have distinctive molecular pathways in tumor development. In addition, our analysis has extended a previous finding of BRAF mutations in four of 10 "low malignant potential" and one of 25 "malignant epithelial" ovarian neoplasms (2). Our results also have potential implications for the treatment of invasive MPSC; such lesions, unlike conventional high-grade serous carcinomas, generally do not respond well to conventional chemotherapy. Conceivably, blocking KRAS-BRAF signaling may provide more effective therapy (2).

REFERENCES

- (1) Peyssonnaud C, Eychene A. The Raf/MEK/ERK pathway: new concepts of activation. *Biol Cell* 2001;93:53-62.
- (2) Davies H, Bignell GR, Cox C, Stephens P, Edkins S, Clegg S, et al. Mutations of the BRAF gene in human cancer. *Nature* 2002; 417:949-54.
- (3) Cohen Y, Zhao XM, Mambo E, Guo Z, Wu G, Trink B, et al. BRAF mutation occurs in a majority of papillary thyroid carcinoma. *J Natl Cancer Inst.* In press 2003.
- (4) Pollock PM, Meltzer PS. A genome-based strategy uncovers frequent BRAF mutations in melanoma. *Cancer Cell* 2002;2:5-7.
- (5) Rajagopalan H, Bardelli A, Lengauer C, Kinzler KW, Vogelstein B, Velculescu VE. Tumorigenesis: RAF/RAS oncogenes and mismatch-repair status. *Nature* 2002;418: 934.
- (6) Schwartz DR, Kardia SL, Shedden KA, Kuick R, Michailidis G, Taylor JM, et al. Gene expression in ovarian cancer reflects both morphology and biological behavior, distinguishing clear cell from other poor-prognosis ovarian carcinomas. *Cancer Res* 2002;62:4722-9.
- (7) Hough CD, Sherman-Baust CA, Pizer ES, Montz FJ, Im DD, Rosenshein NB, et al. Large-scale serial analysis of gene expression reveals genes differentially expressed in ovarian cancer. *Cancer Res* 2000;60:6281-7.

- (8) Sugiyama T, Kamura T, Kigawa J, Terakawa N, Kikuchi Y, Kita T, et al. Clinical characteristics of clear cell carcinoma of the ovary: a distinct histologic type with poor prognosis and resistance to platinum-based chemotherapy. *Cancer* 2000;88:2584-9.
- (9) Singer G, Kurman RJ, Chang HW, Cho SK, Shih IM. Diverse tumorigenic pathways in ovarian serous carcinoma. *Am J Pathol* 2002;160:1223-8.
- (10) Auersperg N, Edelson MI, Mok SC, Johnson SW, Hamilton TC. The biology of ovarian cancer. *Semin Oncol* 1998;25:281-304.
- (11) Seidman JD, Kurman RJ. Ovarian serous borderline tumors: a critical review of the literature with emphasis on prognostic indicators. *Hum Pathol* 2000;31:539-57.
- (12) Seidman JD, Kurman RJ. Subclassification of serous borderline tumors of the ovary into benign and malignant types. A clinicopathologic study of 65 advanced stage cases. *Am J Surg Pathol* 1996;20:1331-45.
- (13) Burks RT, Sherman ME, Kurman RJ. Micropapillary serous carcinoma of the ovary. A distinctive low-grade carcinoma related to serous borderline tumors. *Am J Surg Pathol* 1996;20:1319-30.
- (14) Sehdev AE, Sehdev PS, Kurman RJ. Noninvasive and invasive micropapillary serous carcinoma of the ovary: a clinicopathologic analysis of 135 cases. *Am J Surg Pathol*. In press 2003.
- (15) Stern RC, Dash R, Bentley RC, Snyder MJ, Haney AF, Robboy SJ. Malignancy in endometriosis: frequency and comparison of ovarian and extraovarian types. *Int J Gynecol Pathol* 2001;20:133-9.
- (16) Vogelstein B, Kinzler KW. Digital PCR. *Proc Natl Acad Sci U S A* 1999;96:9236-41.
- (17) Shih IM, Yan H, Speyrer D, Shmookler BM, Sugarbaker PH, Ronnett BM. Molecular genetic analysis of appendiceal mucinous adenomas in identical twins, including one with pseudomyxoma peritonei. *Am J Surg Pathol* 2001;25:1095-9.
- (18) Milner BJ, Allan LA, Eccles DM, Kitchener HC, Leonard RC, Kelly KF, et al. p53 mutation is a common genetic event in ovarian carcinoma. *Cancer Res* 1993;53:2128-32.
- (19) Riopel MA, Ronnett BM, Kurman RJ. Evaluation of diagnostic criteria and behavior of ovarian intestinal-type mucinous tumors: atypical proliferative (borderline) tumors and intraepithelial, microinvasive, invasive, and metastatic carcinomas. *Am J Surg Pathol* 1999;23:617-35.
- (20) Seidman JD, Kurman RJ, Ronnett BM. Primary and metastatic mucinous adenocarcinomas in the ovaries: incidence in routine practice with a new approach to improve intraoperative diagnosis. *Am J Surg Pathol*. In press 2003.
- (21) Sato N, Tsunoda H, Nishida M, Morishita Y, Takimoto Y, Kubo T, et al. Loss of heterozygosity on 10q23.3 and mutation of the tumor suppressor gene PTEN in benign endometrial cyst of the ovary: possible sequence progression from benign endometrial cyst to endometrioid carcinoma and clear cell carcinoma of the ovary. *Cancer Res* 2000;60:7052-6.
- (22) Hough CD, Cho KR, Zonderman AB, Schwartz DR, Morin PJ. Coordinately up-regulated genes in ovarian cancer. *Cancer Res* 2001;61:3869-76.

NOTES

G. Singer, R. Oldt III, and Y. Cohen contributed equally to this work.

Supported by research grant OC010017 from the Department of Defense; Public Health Service grant CA97527 from the National Cancer Institute, National Institutes of Health, Department of Health and Human Services; and the Swiss National Science Foundation (GS).

Manuscript received September 23, 2002; revised January 7, 2003; accepted January 15, 2003.

Assessment of Plasma DNA Levels, Allelic Imbalance, and CA 125 as Diagnostic Tests for Cancer

Hsueh-Wei Chang, Shing M. Lee, Steven N. Goodman, Gad Singer, Sarah K. R. Cho, Lori J. Sokoll, Fredrick J. Montz, Richard Roden, Zhen Zhang, Daniel W. Chan, Robert J. Kurman, Ie-Ming Shih

Background: Allelic imbalance (AI), the loss or gain of chromosomal regions, is found in many cancers. AI can be detected in genomic tumor DNA released into the blood after necrosis or apoptosis. We evaluated plasma DNA concentration, allelic status in plasma DNA, and serum CA 125 level as screening tests for ovarian and other cancers. **Methods:** Plasma samples were obtained from 330 women (44 normal healthy control individuals, 122 patients with various cancers, and 164 control patients with non-neoplastic diseases). Plasma DNA concentration was determined in all samples. Allelic status was determined by digital single nucleotide polymorphism (SNP) analysis with eight SNP markers in plasma DNA from 54 patients with ovarian cancer and 31 control patients. CA 125 was determined in 63 samples. Receiver-operating characteristic (ROC) curves were plotted, and the areas under the ROC curves—a measure of the overall ability of a diagnostic test with multiple cutoffs to distinguish between diseased and nondiseased individuals—were determined. **Results:** The area under the ROC curve for plasma DNA concentration was 0.90 for patients with neoplastic disease versus healthy control individuals and 0.74 for patients with neoplastic diseases versus control patients with non-neoplastic diseases. For control subjects given a specificity of 100% (95% confidence interval [CI] = 92% to 100%), the highest sensitivity achieved was 57% (95% CI = 49% to 67%). AI in at least one SNP was found in 87% (95% CI = 60% to 98%) of patients with stage I/II ovarian cancer and 95% (95% CI = 83% to 99%) of patients with stage III/IV ovarian cancer, but AI was not found in 31 patients with non-neoplastic diseases (specificity = 100%, 95% CI = 89% to 100%). The area under the ROC curve assessing AI was 0.95. Combining the serum CA 125 level with the plasma DNA concentration increased the area under the ROC curve from 0.78 (CA 125 alone) to 0.84. **Conclusion:** Plasma DNA concentration may not be sensitive or specific enough for cancer screening or diagnosis, even when combined with CA 125. AI was detected with high specificity in plasma DNA from patients with ovarian cancer and should be studied further as a screening tool. [J Natl Cancer Inst 2002;94:1697–1703]

Tumors release a substantial amount of genomic DNA into the systemic circulatory system of many cancer patients, probably through cellular necrosis and apoptosis (1–3). This DNA can be detected by genetic and epigenetic alterations that are specific to the primary tumor, such as microsatellite alterations, translocations, mutations, and aberrant patterns of methylation (4–6). Genetic instability is a defining molecular signature of most human cancers (7,8) and is characterized molecularly by allelic imbalance (AI), representing losses or gains of defined

chromosomal regions. Analysis of AI can be used to elucidate the molecular basis of cancer and also to detect cancer. AI has been demonstrated in the serum or plasma obtained from patients with lung (9), breast (10,11), head and neck (5,12), renal (13), and ovarian (14) cancers and with melanoma (15). Some of these cancers were small early-stage neoplasms at the time of diagnosis, suggesting that detection of AI in plasma is a promising method for population-based screening (16). At least two major problems, however, are associated with the current methods for assessing AI in plasma. First, plasma DNA is a mixture of neoplastic and non-neoplastic DNA. Non-neoplastic DNA released from non-neoplastic cells can mask AI because it is difficult to quantify the allelic ratio with microsatellite markers. Second, plasma DNA is often degraded to a variable extent, artificially enriching smaller alleles when microsatellite markers are used in the analysis (17). To overcome these obstacles, we used a recently developed polymerase chain reaction (PCR)-based approach called digital single-nucleotide polymorphism (SNP) analysis, in which the paternal or maternal alleles within a plasma DNA sample are individually counted to provide a quantitative measure of such imbalance in the presence of normal DNA (18–20).

In this study, we first assessed the feasibility of using plasma DNA concentration as a screening tool for cancer. Increased levels of plasma DNA have been reported in many cancer patients but not in healthy individuals without major diseases (3); however, these studies examined relatively few patients. In this study, we tested a total of 330 plasma samples obtained from normal healthy individuals, patients with various neoplastic diseases, and patients with a variety of benign non-neoplastic diseases to reassess the specificity previously observed (3). We then used the digital SNP analysis to determine the precise allelic status of plasma DNA and to test the ability of this new technology to detect early-stage cancer. Human ovarian cancer was selected as the prototypic tumor for proof of principle, because it represents one of the most insidious and aggressive human cancers in which cost-effective screening tests have not yet been developed (21,22). Patients with ovarian cancer generally present with disseminated disease at diagnosis (23), and nearly all of these patients die of their disease. In contrast, the

Affiliation of authors: H. W. Chang, G. Singer, S. K. R. Cho, L. J. Sokoll, R. Roden, Z. Zhang (Department of Pathology), S. M. Lee, S. N. Goodman (The Oncology Center), F. J. Montz (Departments of Gynecology and Obstetrics), D. W. Chan (Department of Pathology and The Oncology Center), R. J. Kurman, I. M. Shih (Departments of Pathology, Gynecology, and Obstetrics) The Johns Hopkins University School of Medicine, Baltimore, MD.

Correspondence to: Ie-Ming Shih, M.D., Ph.D., Department of Pathology, The Johns Hopkins University School of Medicine, 418 N. Bond St., B-315, Baltimore, MD 21231 (e-mail: ishih@jhmi.edu).

See “Notes” following “References.”

© Oxford University Press

survival rate is 90% for women with tumors confined to the ovary. Thus, the development of a plasma-based molecular diagnostic test will be extraordinarily useful in identifying asymptomatic patients with early and clinically curable neoplastic diseases.

MATERIALS AND METHODS

Samples and DNA Purification

A total of 330 plasma samples obtained from females were retrieved from the Gynecological Pathology Tumor Bank and the Division of Clinical Chemistry in the Department of Pathology, The Johns Hopkins University School of Medicine. The waiver of patients' consent was obtained through the local institutional research board. Plasma samples were obtained from 54 patients with sporadic ovarian cancer, 68 patients with malignant neoplasms with other tissue origins, 164 patients with a variety of non-neoplastic diseases who were admitted to The Johns Hopkins Hospital for treatment, and 44 healthy individuals without known neoplastic diseases who visited The Johns Hopkins Hospital for a routine physical examination. Patients with non-neoplastic diseases were age-matched with the 54 patients with ovarian tumors. Of the ovarian tumors studied, 12 were stage I (the International Federation of Gynecology and Obstetrics Staging System), three were stage II, 36 were stage III, and three were stage IV. A histologic examination classified these tumors as follows: 41 serous carcinomas, six borderline tumors, three endometrioid tumors, two clear cell carcinomas, one granulosa cell tumor, and one immature teratoma. The selection of samples for this study was based on the availability of specimens in the tumor bank but not on the disease category or on other patients' clinical profiles. The plasma DNA concentration was determined for all 330 patients, and plasma DNA from the 54 patients with ovarian cancer and the 31 patients with benign diseases was analyzed by digital SNP analysis. CA 125 levels were determined for 45 patients with ovarian cancer and 18 control patients with non-neoplastic diseases.

Blood for DNA purification was collected as described (24). All cancer specimens were obtained just before surgery and therapy. Blood was collected in tubes containing EDTA and was centrifuged with the Lymphoprep reagent (Life Technologies, New York, NY) at 1000g within 2 hours after collection to separate plasma and lymphocytes, both of which were distributed into aliquots and stored at -80°C until use.

DNA was purified from plasma, lymphocytes, and paraffin-embedded tissue. Areas of interest in paraffin-embedded sections, including tumor and normal ovarian tissue or myometrium, were microdissected under a phase-contrast microscope, and DNA was isolated from each type of isolated cells. For most plasma specimens, DNA was purified from 200 μL of plasma with a QIAamp DNA Blood Kit (Qiagen, Valencia, CA). If a plasma specimen had a DNA concentration of less than 10 ng/mL, DNA was purified from 3 to 5 mL of plasma. Tissue DNA was isolated with a QIAquick PCR Purification Kit (Qiagen), and lymphocyte DNA was isolated with a QIAamp Tissue Kit (Qiagen). All the procedures follow the manufacturer's instructions.

Quantitation of Plasma DNA and Serum CA 125

The DNA concentration was measured by the PicoGreen® double-stranded DNA quantitation kit (Molecular Probes, Inc.,

Eugene, OR), according to the manufacturer's instructions. The DNA concentration is proportional to the fluorescence intensity generated by the PicoGreen® dye that binds double-stranded DNA. The fluorescence intensity was measured by a FLUOstar Galaxy fluorescence microplate reader (BMG Lab Technologies, Durham, NC). The DNA concentrations were extrapolated from the standard curves, and data are expressed as the average of six replicates for each sample. The DNA measurement was performed blinded without the knowledge of specimen identifiers.

Serum CA 125 levels were measured in 63 samples with a two-site immunoenzymometric assay on the Tosoh AIA-600 II analyzer (Tosoh Medics, South San Francisco, CA).

Digital SNP Analysis

AI was assessed in plasma DNA from 54 patients with ovarian tumors and from 31 age-matched women with non-neoplastic diseases by use of the digital SNP analysis (18–20,25). The sequences of eight SNP markers with a high frequency of allelic losses in ovarian carcinomas (26–29) were retrieved from the National Cancer Institute SNP map (<http://www.ncbi.nlm.nih.gov/entrez/query.fcgi?db=snp>). The primers and molecular beacons were synthesized by Gene Link (Thornwood, NY), and their sequences are listed in Fig. 1 (19,20,25). Molecular beacons are single-stranded oligonucleotides containing a fluorescent dye and a quencher on their 5' and 3' ends, respectively. Molecular beacons include a hairpin structure that brings the fluorophore closer to the quencher. If a nucleotide target complementary to the loop of the beacon is present in the PCR, the stem is forced apart and the quenching is relieved, thus emitting the fluorescence. Digital SNP analysis was performed as previously described (18–20,25,30). The fluorescence intensity in each well was then measured with a Galaxy FLUOstar fluorometer (BMG Lab Technologies), and the number of the specific allele in each sample was directly determined from the fluorescence measurements. The average number of informative wells containing specific alleles from an individual specimen was 200. These wells, representing maternal or paternal alleles, were used to calculate the allelic ratio (number of major alleles/number of total alleles) of that specimen. The experiment was performed in a blinded fashion.

Fraction of Tumor-Released DNA in Plasma

Digital SNP analysis was used to determine the fraction of total plasma DNA represented by tumor-released DNA as follows: let A be the number of the abundant alleles in plasma, B be the number of the minor alleles in plasma, n denote DNA derived from normal cells, and t denote DNA derived from tumor cells; then $A = A_n + A_t$ and $B = B_n + B_t$. If AI in the primary tumor is homogenous, the fraction of tumor-released DNA in plasma (f_t) is equal to $(A_t + B_t)/(A + B)$. Both alleles are in balance in DNA released from normal cells (i.e., $A_n/B_n = 1:1$ and $A_n = B_n$), because two alleles in normal cells are composed of one maternal and one paternal allele. In human tumors, AI is most often associated with loss of heterozygosity, i.e., loss of one of the parental alleles present, either the maternal or paternal allele, in the patient's normal cells (31,32). Therefore, $B_t = 0$ and $B = B_n$. Given that $A_n = B_n$ and $B_n = B$, then $f_t = (A_t + B_t)/(A + B) = (A_t)/(A + B) = (A - A_n)/(A + B) = (A - B)/(A + B)$. The numbers of A and B alleles are determined by the digital SNP analysis.

Ch	SNPs	Forward primer	Reverse primer	Molecular beacon-green	Molecular beacon-red
1p	8118	CAGGGCAAGACGCTGTGGT	AACAGAATGTGCTTCCCTCCC	CACGCTGCCAGCGCACGGCCGTG	CACGCTGCCAGTGCACGGCCGTG
5q	1578	GTCACAAGCCTTCCGTGTGAAA	GGTATAGGTTTTACTGGTGAAGTTGG	CACGCTCGCTCGTCTTCTGCCGTG	CACGATCTGCGTCTTCTTCTGCCGTG
7q	273	AGGGCTAGAGTATGAGAAGTCC	GTAATTTAGGTGAGCTATCCAGAG	CACGGTTTTTTTTCCCTATAACGTG	CACGGTTTTTTTTCTCTATAACGTG
8p	1085	CACTGAATGCTCTGCCATGA	AACCTGTCCTTGTGGGTGAT	CACGATGAGCCACAAGCAGCACGTG	CACGATGAGCCGAAGCAGCCGTG
12p	852	TGATCTGCTTCCACGA	TGGAGTCCCAGACATTGCA	CACGATCACGTCCTGGCCTCCGTG	CACGATCACGTCTGTGGCCTCCGTG
15q	1861	ACAGCCATTTATTATGTTTACTTGG	AGAATAATTGTGATAAGAATTCCCC	CACGAGCCAACACGGAGGTGACGTG	CACGAGCCAACATGGAGGTGACGTG
17p	p53	AAGACCCAGGTCCAGATGA	GGTGTAGGAGCTGCTGGTG	CACGGCTCCCCCGTGGCCCGTG	CACGGCTCCCCCGTGGCCCGTG
18q	1468	AGCGAGCATCAGAATCACCT	CGGGACAAGCAGCATCT	CACGTGGGGCTTACAAATTAGTATCGTG	CACGTGGGGCTTACGAATTAGTATCGTG

Fig. 1. Primers and probes used for digital single-nucleotide polymorphism (SNP) analysis. Ch = chromosomal arm.

Statistical Analysis

Receiver-operating characteristic (ROC) curves were used to assess the feasibility of using plasma DNA concentration and allelic status as diagnostic tools for detecting ovarian and other cancers. An ROC curve is a graphic representation of the sensitivity plotted against the false-positive rate (i.e., 1 minus specificity), and the ROC curve is used to evaluate the performance of a test at different thresholds of a diagnostic measure. The area under the ROC curve is a measure of the overall ability of a diagnostic test with multiple cutoffs to distinguish between diseased and control individuals.

For the plasma DNA concentration, two separate analyses were performed: one with patients with non-neoplastic disease as control subjects and the other with healthy patients without known major diseases as control subjects. Plasma DNA concentration was evaluated at cutoff values of 5, 10, 15, 23, 30, 40, 60, 100, 200, and 500 ng/mL. For the analysis of allelic status, the allelic proportion (abundant alleles/total alleles) was evaluated at cutoff values of 0.55, 0.60, 0.65, 0.70, 0.75, 0.80, 0.85, 0.90, and 0.95. AI is defined in this system as having at least one informative marker above the cutoff among the eight markers tested. With the use of the ROC curves, we selected the point with the highest sensitivity, given 100% specificity, and calculated the exact binomial 95% confidence interval (CI) for the corresponding sensitivity and specificity. A high specificity is desirable for screening technologies that could be applied to a population of asymptomatic individuals with a very low prevalence of disease.

Logistic regression models were used to evaluate whether the combination of plasma DNA concentration and CA 125 level increased the sensitivity and the specificity for detecting ovarian cancer and to generate ROC curves. CA 125 was used both as a continuous and dichotomous predictor; the standard clinical normal upper limit for CA 125 of 35 IU/mL was applied (21). The areas under the ROC curves with and without the inclusion of plasma DNA concentration were measured. All statistical tests were two-sided.

RESULTS

Quantitation of Plasma DNA

Plasma DNA concentrations were determined for 330 individuals: 122 patients with neoplastic disease, 164 patients with non-neoplastic diseases, and 44 healthy individuals. The specific diagnoses of the patients with neoplastic and non-neoplastic dis-

eases are presented in Table 1. Plasma DNA concentration ranged from 0 to 6707 ng/mL. The median DNA concentrations were as follows: in the 44 healthy patients, 7 ng/mL (10th–90th percentile = 0–20 ng/mL); in the patients with non-neoplastic diseases, 16 ng/mL (10th–90th percentile = 7–71 ng/mL); and in the patients with neoplastic diseases, 59 ng/mL (10th–90th percentile = 10–844 ng/mL) ($P < .001$, Kruskal–Wallis test). The area under the ROC curve assessing plasma DNA concentration was 0.90 for healthy control subjects and 0.74 for control patients with a non-neoplastic disease (Fig. 2). For healthy control subjects, given a specificity of 100% (95% CI = 92% to 100%), the highest sensitivity that could be obtained was 57% (95% CI = 49% to 67%). The sensitivity of plasma DNA concentration at any given specificity was substantially lower when applied to control patients with a non-neoplastic disease (Fig. 2). Although the number of control patients in each subgroup of benign diseases was small, no association was detected between DNA concentrations and a particular benign disease.

Table 1. Patient characteristics

Diagnosis	No. of patients
Healthy normal	44
Non-neoplastic disease	164
Anemia	8
AIDS (acquired immunodeficiency syndrome)	10
Musculoskeletal disease	10
Diabetes mellitus	7
Cardiovascular disease	13
Asthma and pulmonary disease	5
Essential hypertension	6
Infectious disease	19
Autoimmune disease	10
Status post organ transplant	23
Liver disease	9
Trauma	8
Neurologic disorder	12
Gynecologic disease	10
Drug abuse	8
Others	8
Neoplastic disease	122
Ovarian tumor	54
Endometrial/cervical carcinoma	10
Head and neck carcinoma	11
Sarcoma	4
Breast carcinoma	8
Lung carcinoma	11
Gastrointestinal carcinoma	11
Brain tumor	5
Others	6

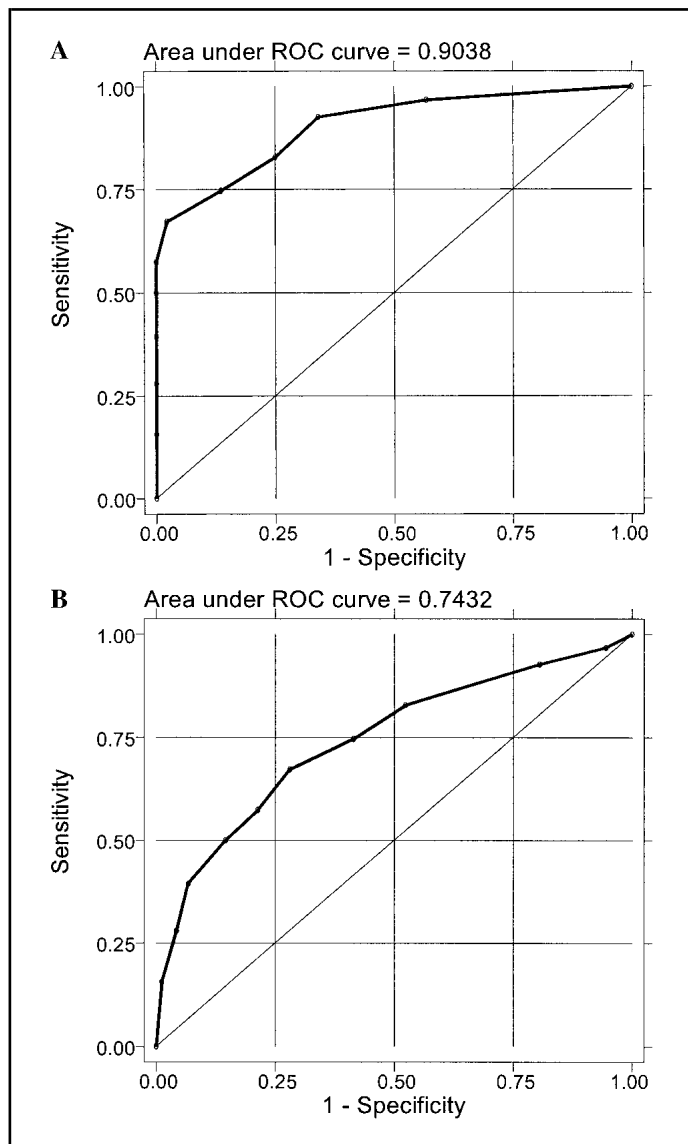


Fig. 2. **A)** Receiver-operating characteristic (ROC) curve for plasma DNA concentration with cutoff values of 5, 10, 15, 20, 30, 40, 60, 100, 200, and 500 ng/mL in 44 healthy normal individuals and 122 patients with a variety of neoplasms. **B)** ROC curve for plasma DNA concentration with cutoff values of 5, 10, 15, 20, 30, 40, 60, 100, 200, and 500 ng/mL in 164 control patients with non-neoplastic disease and 122 patients with various neoplasms.

Analysis of AI in Plasma DNA

Digital SNP analysis was performed to assess AI in plasma DNA from 54 patients with ovarian neoplasms and 31 patients with non-neoplastic diseases who had plasma DNA levels greater than 50 ng/mL. The median number of informative markers per patient was 4 (10th–90th percentile = 2–6). The highest sensitivity and specificity were obtained at a threshold level for allelic proportion of 0.6. The specificity was 100% (31 of 31, 95% CI = 89% to 100%), and the sensitivity was 93% (50 of 54, 95% CI = 82% to 98%). None of the 31 control patients with non-neoplastic diseases had AI. When the cutoff of 0.6 was used to define AI, the sensitivity of AI in patients with early-stage (I/II) ovarian cancer was 87% (13 of 15, 95% CI = 60% to 98%), and the sensitivity of AI in patients with late-stage (III/IV) ovarian cancer was 95% (37 of 39, 95% CI = 83% to

99%). The area under the ROC curve assessing AI was 0.95 (Fig. 3, A).

For comparison, the area under the ROC curve assessing plasma DNA concentration as the diagnostic tool to detect ovarian tumors was 0.75 (Fig. 3, B). Requiring a specificity of 100% (95% CI = 89% to 100%), the highest sensitivity achieved was 54% (95% CI = 40% to 67%) at a cutoff of 60 ng/mL. The sensitivity for early-stage (I/II) ovarian cancer was 47% (7 of 15, 95% CI = 21% to 73%), and the sensitivity for late-stage (III/IV) ovarian cancer was 56% (22 of 39, 95% CI = 40% to 72%).

When digital SNP analysis was used to determine the fraction of tumor-released DNA in total plasma DNA (f_t), we found that tumor-released DNA contributed substantially to the total plasma DNA in the majority of samples with an f_t average of 0.48 (95% CI = 0.43 to 0.53) and a range from 0.26 to 0.89. We

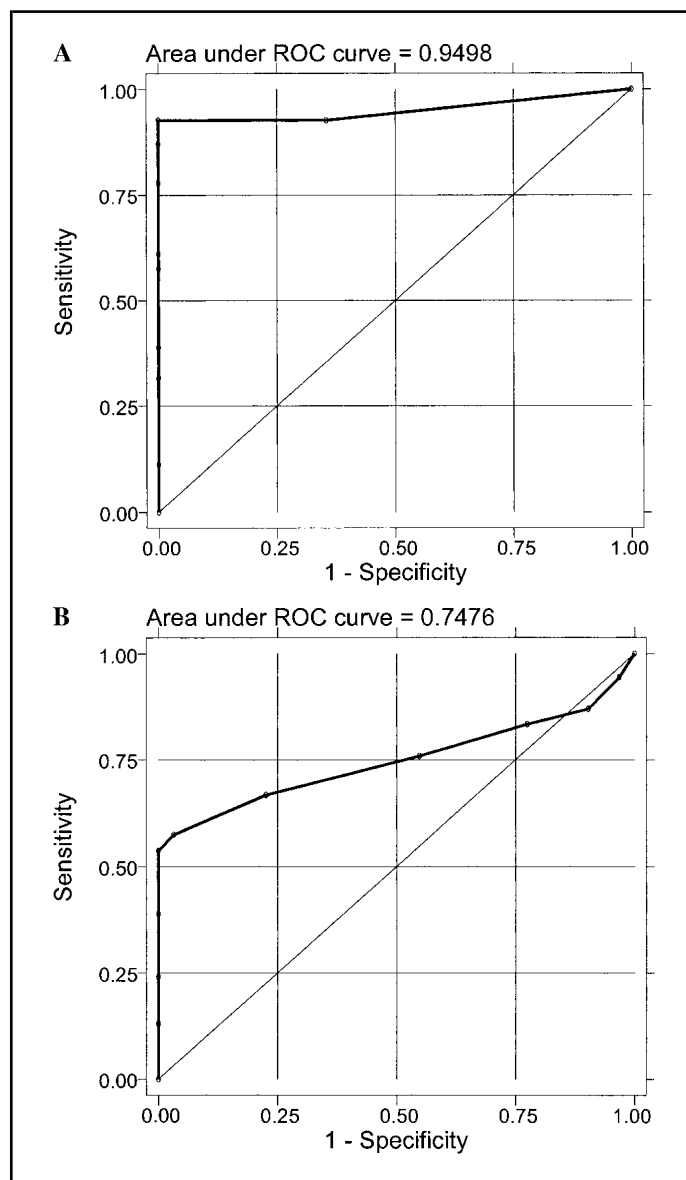


Fig. 3. **A)** Receiver-operating characteristic (ROC) curve for allelic imbalance with cutoff values in allelic ratio of 0.55, 0.60, 0.65, 0.70, 0.75, 0.80, 0.85, 0.90, and 0.95 in 54 patients with ovarian neoplasm and 31 control patients with non-neoplastic disease. **B)** ROC curve for plasma DNA concentration with cutoff values of 5, 10, 15, 20, 30, 40, 60, 100, 200, and 500 ng/mL in 54 patients with ovarian neoplasm and 31 control patients with non-neoplastic disease.

were unable to demonstrate that the f_t was associated with the amount of total plasma DNA because the r (correlation coefficient of linear regression) value was only 0.3.

The digital SNP analysis was validated by using eight representative samples, including four with AI and four with allelic balance, and repeating the digital SNP analysis three times on plasma aliquots from the same patient. The allelic ratios were consistent between the original and the repeated assays in all samples tested (data not shown). To assess the AI pattern in the corresponding primary tumors, we determined the allelic status of the tumors with the same eight SNP markers in 17 representative tumors with available tissue. Among these 17 tumors, 15 had an AI pattern identical to that of the corresponding plasma DNA sample. The remaining two tumors showed a discordant AI pattern in at least one informative SNP marker.

Combined Analysis of Plasma DNA Concentration and Serum CA 125 Level

Serum CA 125 data were determined for 63 of the 85 patients with digital SNP analyses: 45 with ovarian cancer and 18 with a non-neoplastic disease. The area under the ROC curve assessing CA 125 was 0.78 when serum CA 125 level alone was used as a continuous measure (Fig. 4, A). When a combination of plasma DNA with serum CA 125 derived from a logistic regression equation was used, the area under the ROC curve assessing the combination of CA 125 and plasma DNA concentration was 0.84 (Fig. 4, B; $P = .08$ for incremental contribution of DNA level). The areas under the curves were similar when the CA 125 cutoff value of 35 IU/ml (the standard clinical cutoff) was used. With this cutoff value, the sensitivity was 67% (95% CI = 51% to 80%) and the specificity was 89% (95% CI = 65% to 99%).

DISCUSSION

The results of this study indicate that measurement of plasma DNA concentrations has a sensitivity and specificity for cancer that may be too low for population screening. In contrast, digital SNP analysis, which allows the number of the two parental alleles in plasma to be precisely counted and the allelic status to be unequivocally determined in the background of normal DNA, appears to be a promising method for detecting at least ovarian cancer. This method should be tested more extensively on ovarian and other cancers.

Because tumors release DNA into plasma, we expected that increased amounts of plasma DNA would be detected in the majority of cancer patients and that a simple measurement of plasma DNA would offer a cost-effective approach for population-based cancer screening. In this study, even though there was a highly statistically significant difference in the average plasma DNA levels between cancer patients and both healthy control subjects and control patients with non-neoplastic disease, no cutoff value for plasma DNA concentration produced performance characteristics that would make it a good screening tool for neoplastic disease.

Why plasma DNA levels were not elevated in some patients with neoplastic disease, even when their tumors were large, is unclear. Perhaps minimal cell death resulted in a slow release of tumor DNA and/or the half-life of plasma DNA was short because of a high clearance rate. Digital SNP analysis of plasma DNA from patients with ovarian cancer and control patients with non-neoplastic diseases and with elevated plasma DNA showed that these tumors contributed a substantial fraction of DNA in

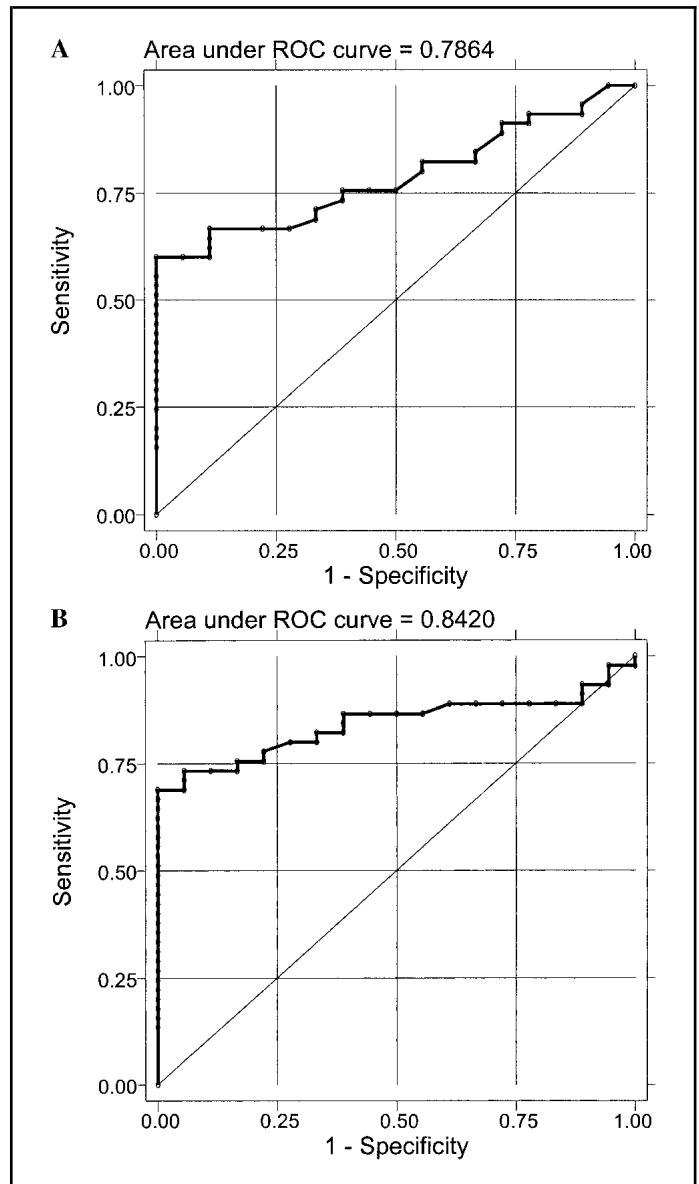


Fig. 4. A) Receiver-operating characteristic (ROC) curve for serum CA 125 levels. Data from 45 samples in patients with ovarian neoplasm and 18 samples from control patients with non-neoplastic diseases are included. B) ROC curve for plasma DNA concentrations with cutoff values of 5, 10, 15, 20, 30, 40, 60, 100, 200, and 500 ng/mL, adjusted by serum CA 125 levels. Data from 45 patients with ovarian neoplasm and 18 control patients with non-neoplastic diseases included.

the majority of patients, even in those with low absolute levels of plasma DNA. The allelic balance identified in the plasma DNA from four cancer patients could indicate that all markers tested in the corresponding primary tumors also showed allelic balance. Alternatively, AI might be masked by the overwhelming amount of normal DNA that may have originated from allelically balanced nontumor cells (3,33,34). The above findings are consistent with the conclusion from a previous report that detected AI with quantitative methylation-specific PCR (3). Although the AI pattern in plasma and in the corresponding tumor was concordant in most patients analyzed, two patients did not show the identical pattern. The discordant allelic pattern in the plasma and the primary tumor has been recently reported, and it likely reflects intratumoral clonal heterogeneity and biased tissue sampling (35).

How does our method compare with current screening approaches for ovarian cancer? Although pelvic and, more recently, vaginal sonography have been used to screen high-risk patients, both techniques lack sufficient sensitivity and specificity to screen the general population (36). CA 125 is used in the postoperative management of patients with ovarian carcinoma, but it lacks sufficient sensitivity and specificity as a screening tool. Specifically, CA 125 is negative in 30%–40% of patients with ovarian carcinomas, and its levels are elevated in a variety of benign diseases (37–39). Combining results of CA 125 and plasma DNA testing did little to enhance the predictive value of either, because they were closely correlated.

There is little evidence that measurement of AI alone would provide tissue-specific information regarding tumor sites because of the high frequency of genetic instability in a variety of cancer types. This problem may limit the usefulness of AI as a clinical diagnostic test for the early detection of a particular type of cancer. There are, however, many existing or emerging biomarkers that are relatively tissue-specific, yet their sensitivity is too low for them to be used as stand-alone diagnostic tests (21). It is possible that a combination of determining AI and testing for one or more tissue-specific serologic biomarkers could produce a diagnostic index that is cancer-type specific and has a much improved sensitivity over the original biomarkers.

This report provides preliminary evidence that AI in plasma DNA can be detected with apparently high specificity by digital SNP analysis in a substantial percentage of patients with potentially curable ovarian carcinomas. This evidence suggests that this technology might be useful in patients who present with adnexal masses. However, before digital SNP analysis becomes a practical cancer screening tool, several issues need to be addressed. In this study, the sensitivity of digital SNP analysis in diagnosing early-stage ovarian cancer was 87% (95% CI = 60% to 98%). Sensitivity might be improved by increasing the number of SNPs in the assay to determine whether sensitivity could be increased without decreasing specificity. Results of a digital SNP analysis could also be combined with results for tests of mutant genes specific for ovarian cancer. The effect on sensitivity of broadening the array of cancers tested will have to be studied.

It should be noted that the specificity and the sensitivity obtained with the optimal cutoff value from this study will probably not be as high when applied to other sets of patients. In addition, the 95% CIs in this study were fairly wide. The lower confidence bound on the 100% specificity estimate was 89%, meaning that more noncancer patients must be studied to increase the precision of that estimate before the test is widely applied. The control population in our SNP study was selected to have a high concentration of plasma DNA. Although we thought that this selection would only decrease specificity, that has not been demonstrated, and it will be important to confirm these numbers with more representative control subjects in prospective cohort studies.

Finally, it should be noted that although the current cost of digital SNP analysis is quite high (>\$200 per test), it could be fully automated by using a high-throughput format to reduce labor and reagent cost. Because digital SNP analysis is based on the discrimination of SNP on a single molecule basis, powerful new tools being developed for nanotechnology could be applicable (40,41).

REFERENCES

- (1) Leon SA, Shapiro B, Sklaroff DM, Yaros MJ. Free DNA in the serum of cancer patients and the effect of therapy. *Cancer Res* 1977;37:646–50.
- (2) Anker P, Mulcahy H, Chen XQ, Stroun M. Detection of circulating tumour DNA in the blood (plasma/serum) of cancer patients. *Cancer Metastasis Rev* 1999;18:65–73.
- (3) Jahr S, Hentze H, Englisch S, Hardt D, Fackelmayer FO, Hesch RD, et al. DNA fragments in the blood plasma of cancer patients: quantitations and evidence for their origin from apoptotic and necrotic cells. *Cancer Res* 2001;61:1659–65.
- (4) Chen XQ, Stroun M, Magnenat JL, Nicod LP, Kurt AM, Lyautey J, et al. Microsatellite alterations in plasma DNA of small cell lung cancer patients. *Nat Med* 1996;2:1033–5.
- (5) Nawroz H, Koch W, Anker P, Stroun M, Sidransky D. Microsatellite alterations in serum DNA of head and neck cancer patients. *Nat Med* 1996;2:1035–7.
- (6) Esteller M, Sanchez-Cespedes M, Rosell R, Sidransky D, Baylin SB, Herman JG. Detection of aberrant promoter hypermethylation of tumor suppressor genes in serum DNA from non-small cell lung cancer patients. *Cancer Res* 1999;59:67–70.
- (7) Lengauer C, Kinzler KW, Vogelstein B. Genetic instabilities in human cancers. *Nature* 1998;396:643–9.
- (8) Cahill DP, Kinzler KW, Vogelstein B, Lengauer C. Genetic instability and Darwinian selection in tumours. *Trends Cell Biol* 1999;9:M57–60.
- (9) Bruhn N, Beinert T, Oehm C, Jandrig B, Petersen I, Chen XQ, et al. Detection of microsatellite alterations in the DNA isolated from tumor cells and from plasma DNA of patients with lung cancer. *Ann N Y Acad Sci* 2000;906:72–82.
- (10) Shaw JA, Smith BM, Walsh T, Johnson S, Primrose L, Slade MJ, et al. Microsatellite alterations plasma DNA of primary breast cancer patients. *Clin Cancer Res* 2000;6:1119–24.
- (11) Silva JM, Dominguez G, Garcia JM, Gonzalez R, Villanueva MJ, Navarro F, et al. Presence of tumor DNA in plasma of breast cancer patients: clinicopathological correlations. *Cancer Res* 1999;59:3251–6.
- (12) Coulet F, Blons H, Cabelguenne A, Lecomte T, Lacourreye O, Brasnu D, et al. Detection of plasma tumor DNA in head and neck squamous cell carcinoma by microsatellite typing and p53 mutation analysis. *Cancer Res* 2000;60:707–11.
- (13) Goessl C, Heicappell R, Munker R, Anker P, Stroun M, Krause H, et al. Microsatellite analysis of plasma DNA from patients with clear cell renal carcinoma. *Cancer Res* 1998;58:4728–32.
- (14) Hickey KP, Boyle KP, Jepps HM, Andrew AC, Buxton EJ, Burns PA. Molecular detection of tumour DNA in serum and peritoneal fluid from ovarian cancer patients. *Br J Cancer* 1999;80:1803–8.
- (15) Fujiwara Y, Chi DD, Wang H, Keleman P, Morton DL, Turner R, et al. Plasma DNA microsatellites as tumor-specific markers and indicators of tumor progression in melanoma patients. *Cancer Res* 1999;59:1567–71.
- (16) Sozzi G, Musso K, Ratchiffe C, Goldstraw P, Pierotti MA, Pastorino U. Detection of microsatellite alterations in plasma DNA of non-small cell lung cancer patients: a prospect for early diagnosis. *Clin Cancer Res* 1999;5:2689–92.
- (17) Liu J, Zabarovska VI, Braga E, Alimov A, Klien G, Zabarovsky ER. Loss of heterozygosity in tumor cells requires re-evaluation: the data are biased by the size-dependent differential sensitivity of allele detection. *FEBS Lett* 1999;462:121–8.
- (18) Shih IM, Zhou W, Goodman SN, Lengauer C, Kinzler KW, Vogelstein B. Evidence that genetic instability occurs at an early stage of colorectal tumorigenesis. *Cancer Res* 2001;61:818–22.
- (19) Zhou W, Galizia G, Goodman SN, Romans KE, Kinzler KW, Vogelstein B, et al. Counting alleles reveals a connection between chromosome 18q loss and vascular invasion. *Nat Biotechnol* 2001;19:78–81.
- (20) Shih IM, Wang TL, Traverso G, Romans K, Hamilton SR, Ben-Sasson S, et al. Top-down morphogenesis of colorectal tumors. *Proc Natl Acad Sci U S A* 2001;98:2640–45.
- (21) Shih IM, Sokoll L, Chan DW. Tumor markers of ovarian cancer. In: Diamandis EP, Fritsche HA, Lilja H, Chan DW, Schwartz MK, editors. *Tumor markers—physiology, pathobiology and clinical applications*. 1st ed. Washington (DC): American Association for Clinical Chemistry Press; 2002. p. 239–52.

- (22) Paley PJ. Ovarian cancer screening: are we making any progress? *Curr Opin Oncol* 2001;13:399–402.
- (23) Ozols RF, Rubin SC, Thomas GB, Robboy SJ. Epithelial ovarian cancer. In: Hoskins WJ, Perez CA, Young RC, editors. *Principles and practice of gynecologic oncology*. Philadelphia (PA): Lippincott, Williams and Wilkins; 2000. p. 981–1057.
- (24) Jen J, Wu L, Sidransky D. An overview on the isolation and analysis of circulating tumor DNA in plasma and serum. *Ann N Y Acad Sci* 2000; 906:8–12.
- (25) Singer G, Kurman RJ, Chang HW, Cho SK, Shih IM. Diverse tumorigenic pathways in ovarian serous carcinoma. *Am J Pathol* 2002;160:1223–8.
- (26) Zborovskaya I, Gasparian A, Karseladze A, Elcheva I, Trofimova E, Driouch K, et al. Somatic genetic alterations (LOH) in benign, borderline and invasive ovarian tumours: intratumoral molecular heterogeneity. *Int J Cancer* 1999;82:822–6.
- (27) Cliby W, Ritland S, Hartmann L, Dodson M, Halling KC, Keeney G, et al. Human epithelial ovarian cancer allelotype. *Cancer Res* 1993;53:2393–8.
- (28) Dodson MK, Hartmann LC, Cliby WA, DeLacey KA, Keeney GL, Ritland SR, et al. Comparison of loss of heterozygosity patterns in invasive low-grade and high-grade epithelial ovarian carcinomas. *Cancer Res* 1993;53: 4456–60.
- (29) Iwabuchi H, Sakamoto M, Sakunaga H, Ma YY, Carcangiu ML, Pinkel D, et al. Genetic analysis of benign, low-grade, and high-grade ovarian tumors. *Cancer Res* 1995;55:6172–80.
- (30) Chang HW, Ali SZ, Cho SR, Kurman RJ, Shih IM. Detection of allelic imbalance in ascitic supernatant by digital SNP analysis. *Clin Cancer Res* 2002;8:2580–5.
- (31) Thiagalingam S, Laken S, Willson JK, Markowitz SD, Kinzler KW, Vogelstein B, et al. Mechanisms underlying losses of heterozygosity in human colorectal cancers. *Proc Natl Acad Sci U S A* 2001;98:2698–702.
- (32) Cavenee WK, Dryja TP, Phillips RA, Benedict WF, Godbout R, Gallie BL, et al. Expression of recessive alleles by chromosomal mechanisms in retinoblastoma. *Nature* 1983;305:779–84.
- (33) Kolble K, Ullrich OM, Pidde H, Barthel B, Diermann J, Rudolph B, et al. Microsatellite alterations in serum DNA of patients with colorectal cancer. *Lab Invest* 1999;79:1145–50.
- (34) Folkman J. Tumor angiogenesis. *Adv Cancer Res* 1985;43:175–203.
- (35) Garcia JM, Silva JM, Dominguez G, Silva J, Bonilla F. Heterogeneous tumor clones as an explanation of discordance between plasma DNA and tumor DNA alterations. *Genes Chromosomes Cancer* 2001;31:300–1.
- (36) Daly M, Ostrams GI. Epidemiology and risk assessment for ovarian cancer. *Semin Oncol* 1998;25:255–64.
- (37) Meyer T, Rustin GJ. Role of tumour markers in monitoring epithelial ovarian cancer. *Br J Cancer* 2000;82:1535–8.
- (38) Buamah P. Benign conditions associated with raised serum CA-125 concentration. *J Surg Oncol* 2000;75:264–5.
- (39) Tuxen MK, Soletormos G, Dombernowsky P. Tumor markers in the management of patients with ovarian cancer. *Cancer Treat Rev* 1995;21: 215–45.
- (40) Henrickson SE, Misakian M, Robertson B, Kasianowicz JJ. Driven DNA transport into an asymmetric nanometer-scale pore. *Phys Rev Lett* 2000; 85:3057–60.
- (41) Taton TA. Nanotechnology. Boning up on biology. *Nature* 2001;412: 491–2.

NOTES

Supported by Public Health Service grant R21CA97527 (to I.-M. Shih) from the National Cancer Institute, National Institutes of Health, Department of Health and Human Services, and the Richard TeLinde Research Fund from Johns Hopkins University School of Medicine.

We highly appreciate the excellent technical support of Dr. Q. Yan, J. Rosenzweig and Debra J. Bruzek for their blood collection and plasma preparation.

Manuscript received January 17, 2002; revised August 28, 2002; accepted September 10, 2002.

A BTB/POZ protein, NAC-1, is related to tumor recurrence and is essential for tumor growth and survival

Kentaro Nakayama*, Naomi Nakayama*, Ben Davidson[†], Jim J.-C. Sheu*, Natini Jinawath*, Antonio Santillan^{‡§}, Ritu Salani^{‡§}, Robert E. Bristow^{‡§}, Patrice J. Morin[¶], Robert J. Kurman^{**§}, Tian-Li Wang^{‡§}, and Ie-Ming Shih^{**§||}

Departments of *Pathology, [†]Oncology, and [§]Gynecology and Obstetrics, Johns Hopkins Medical Institutions, Baltimore, MD 21231; [‡]Norwegian Radium Hospital, 0310 Oslo, Norway; and [¶]Laboratory of Cellular and Molecular Biology, National Institute on Aging, National Institutes of Health, Baltimore, MD 21224

Edited by Joan S. Brugge, Harvard Medical School, Boston, MA, and approved October 8, 2006 (received for review May 18, 2006)

Recent studies have suggested an oncogenic role of the BTB/POZ-domain genes in hematopoietic malignancy. The aim of this study is to identify and characterize BTB/POZ-domain genes in the development of human epithelial cancers, i.e., carcinomas. In this study, we focused on ovarian carcinoma and analyzed gene expression levels using the serial analysis of gene expression (SAGE) data in all 130 deduced BTB/POZ genes. Our analysis reveals that NAC-1 is significantly overexpressed in ovarian serous carcinomas and several other types of carcinomas. Immunohistochemistry studies in ovarian serous carcinomas demonstrate that NAC-1 is localized in discrete nuclear bodies (tentatively named NAC-1 bodies), and the levels of NAC-1 expression correlate with tumor recurrence. Furthermore, intense NAC-1 immunoreactivity in primary tumors predicts early recurrence in ovarian cancer. Both coimmunoprecipitation and double immunofluorescence staining demonstrate that NAC-1 molecules homooligomerize through the BTB/POZ domain. Induced expression of the NAC-1 mutant containing only the BTB/POZ domain disrupts NAC-1 bodies, prevents tumor formation, and promotes tumor cell apoptosis in established tumors in a mouse xenograft model. Overexpression of full-length NAC-1 enhanced tumorigenicity of ovarian surface epithelial cells and NIH 3T3 cells in athymic *nu/nu* mice. In summary, NAC-1 is a tumor recurrence-associated gene with oncogenic potential, and the interaction between BTB/POZ domains of NAC-1 proteins is critical to form the discrete NAC-1 nuclear bodies and essential for tumor cell proliferation and survival.

oncogene | ovarian cancer | serial analysis of gene expression

The BTB (bric-a-brac tramtrack broad complex) (also known as POZ) gene family is composed of several proteins that share a conserved BTB/POZ protein-protein interaction motif at the N terminus that mediates homodimer or heterodimer formation (1–3). These proteins have been demonstrated to participate in a wide variety of cellular functions including transcription regulation, cellular proliferation, apoptosis, cell morphology, ion channel assembly, and protein degradation through ubiquitination (1). A subset of BTB/POZ proteins have been implicated in human cancer, and they include BCL-6 (4, 5), PLZF (promyelocytic leukemia zinc finger) (4, 6), leukemia/lymphoma-related factor (LRF)/Pokemon (7, 8), HIC-1 (hypermethylated in cancer-1), and Kaiso (9, 10). Among them, the BCL-6 gene is the best characterized oncogene. Frequent gene translocation or mutation has been identified in B cell lymphoma, resulting in constitutive BCL-6 expression in the tumor cells (4, 5). Peptide inhibitors that block interaction between the BCL-6 BTB/POZ domain and corepressors abrogate BCL-6 oncogenic functions in B cells, suggesting that the use of peptide inhibitors of the BTB/POZ domain may represent a therapeutic approach for B cell lymphoma (5). As the role of BTB/POZ proteins in human cancer is emerging, we have analyzed the expression patterns of tumor-associated BTB/POZ genes in ovarian cancer *in silico* using the serial analysis of gene expression

(SAGE) database. Ovarian cancer was selected in this study because this disease represents one of the most aggressive cancer types in women. Most patients with ovarian cancer are diagnosed at advanced stages when conventional therapy is less effective. As a result, most ovarian cancer patients suffer from, and eventually succumb to, recurrent disease. New therapeutic agents are urgently needed for effective treatment to improve outcome in these patients. In this study, we focused on a BTB/POZ gene, *NAC-1*, that is overexpressed in ovarian cancer, particularly in recurrent disease. We demonstrated that *NAC-1* plays a critical role in tumorigenesis and in the growth and survival of tumor cells.

Results

NAC-1 Expression Is Associated with Cancer Development. A total of 11 SAGE libraries were used to screen 130 BTB/POZ domain-containing genes for overexpression in high-grade ovarian serous carcinomas as compared with ovarian surface epithelium and benign ovarian cystadenoma. Sixteen genes were selected based on an average tag count per library >10 (Table 2, which is published as supporting information on the PNAS web site). Among these 16 genes, a gene named *NAC-1* (BTBD14B HS.531614) showed the highest ratio of average tag counts in ovarian carcinoma to controls (ovarian surface epithelium and benign ovarian cyst) and was therefore selected for validation and characterization in this study. The SAGE database was also used to analyze *NAC-1* expression in different cancer types and their corresponding normal tissues. As shown in Fig. 1, in addition to ovarian cancer, NAC-1 was up-regulated in several tumors from other organs including pancreatic, colorectal, and breast carcinomas, although the sample size of SAGE libraries in most of tumor types was too small for a statistical analysis.

To validate the SAGE results in ovarian cancer, we generated a mouse monoclonal antibody (NAC-1 Ab clone 3) that reacted to the C terminus of the NAC-1 protein and performed immunohistochemistry in 265 ovarian tumors and normal tissue samples (Table 3, which is published as supporting information on the PNAS web site). The specificity of the NAC-1 antibody was evaluated by

Author contributions: K.N., N.N., T.-L.W., and I.-M.S. designed research; K.N., N.J., and N.N. performed research; B.D., J.J.-C.S., R.E.B., P.J.M., and R.J.K. contributed new reagents/analytic tools; K.N., N.N., A.S., R.S., T.-L.W., and I.-M.S. analyzed data; and K.N., T.-L.W. and I.-M.S. wrote the paper.

The authors declare no conflict of interest.

This article is a PNAS direct submission.

Abbreviations: JHMI, Johns Hopkins Medical Institutions; MOSE, immortalized OSE cells; NRH, Norwegian National Radium Hospital; OSE, ovarian surface epithelial cells; SAGE, serial analysis of gene expression.

Data deposition: The sequence reported in this paper has been deposited in the UniGene database, www.ncbi.nlm.nih.gov/entrez/query.fcgi?db=unigene (accession no. HS.531614).

||To whom correspondence should be addressed at: Johns Hopkins Hospital, CRB II, Room 305, 1550 Orleans Street, Baltimore, MD 21231. E-mail: ishih@jhmi.edu.

© 2006 by The National Academy of Sciences of the USA

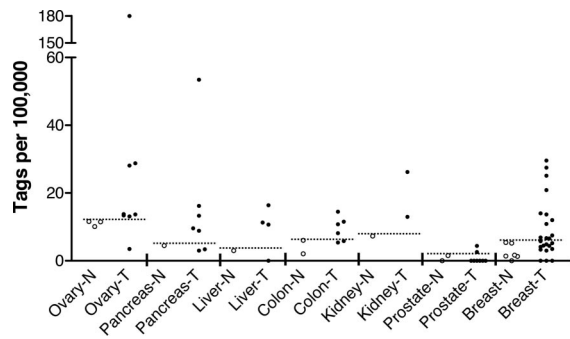


Fig. 1. Scatter plot of NAC-1 tags in several major tumor types. NAC-1 expression level is analyzed by counting NAC-1-specific tags from SAGE libraries in both cancer tissue (T, filled symbols) and the corresponding normal tissues (N, open symbols). The NAC-1 tags are normalized to tags per 100,000 (y axis). The dash line in each tumor type indicates the “ceiling” tag number in normal tissue libraries. Each symbol represents an individual specimen.

reciprocal immunoprecipitation/Western blot analyses in RK3E cells transfected with pCDNA6-V5/NAC-1 and vector control. A single band with a molecular mass of ≈ 57 kDa corresponding to NAC-1 protein was detected in NAC-1-transfected cells but not in control cells (Fig. 2A). Because the immunoreactive tumor cells always exhibited diffuse staining, we used intensity scores to quantify NAC-1 expression in tissues. In contrast to normal ovaries and benign ovarian cystadenomas, both low- and high-grade serous carcinomas demonstrated a higher NAC-1 immunoreactivity, with 27% and 40% of cases showing 2+ and 3+, respectively (χ^2 test, $P < 0.001$) (Fig. 2B–D and Table 3). The number of high-grade cases with high NAC-1 immunointensity (2+ and 3+) was significantly higher than that in low-grade carcinoma ($P < 0.01$). Immunofluorescence revealed that NAC-1 was localized to dot-like structures in those tumors showing strong NAC-1 immunointensity (2+ and 3+) (Fig. 2E and F). Ultrastructural analysis using ImmunoGold labeling, and electron microscopy further revealed that NAC-1 was localized to discrete nuclear bodies, tentatively termed “NAC-1 bodies”, with a diameter ranging from 0.3 to 1.8 μm (Fig. 2G).

Overexpression of NAC-1 Correlates with Recurrent Ovarian Cancer. It is widely accepted that recurrent tumors represent the true “killer”

Table 1. Increased NAC-1 immunoreactivity correlates with first tumor recurrence

	JHMI (solid tumors)		NRH (effusions)	
	0+/1+	2+/3+	0+/1+	2+/3+
Primary	71	39	62	49
First recurrent	21	35	22	39
Total	92	74	84	88

in cancer patients, because the primary tumors are usually removed by surgery. Identification of molecular targets that are present in recurrent tumors would be important in the development of a prognostic test and a novel therapeutic intervention for cancer patients. Thus, we addressed whether NAC-1 expression was related to tumor progression by analyzing primary and recurrent ovarian high-grade serous carcinomas using immunohistochemistry and quantitative real-time PCR. NAC-1 immunohistochemistry was performed at two institutions, Johns Hopkins Medical Institutions (JHMI, solid tumors) and Norwegian National Radium Hospital (NRH, effusions), by using independent sets of ovarian cancer specimens, and the results are presented in a 2×2 contingency table (Table 1). Among 182 JHMI high-grade carcinoma cases, we analyzed 166 samples including 110 primary and 56 first recurrent tumors. The remaining 16 specimens that were obtained from second and third recurrence were not included in the analysis. Both JHMI and NRH studies demonstrated that a higher NAC-1 staining intensity (2+ and 3+) was more frequently found in recurrent than in primary tumor tissues ($P < 0.01$ in JHMI and $P = 0.013$ in NRH, χ^2 test). To validate the immunohistochemistry results, we performed quantitative real-time PCR using samples from JHMI to assess the correlation of NAC-1 mRNA expression levels and the recurrence status. We found that an increased NAC-1 transcript level significantly correlated with recurrent disease ($P = 0.012$, Mann–Whitney test) (Fig. 3A). The association of NAC-1 expression and recurrent status was independent of clinical stage (III versus IV) at diagnosis.

Among 56 recurrent carcinomas from JHMI, there were 21 cases for which the corresponding primary tumors were available from the same patients for comparison. A statistically significant increase in NAC-1 immunointensity (2+ and 3+) was found in recurrent tumors as compared with the primary tumors from the same

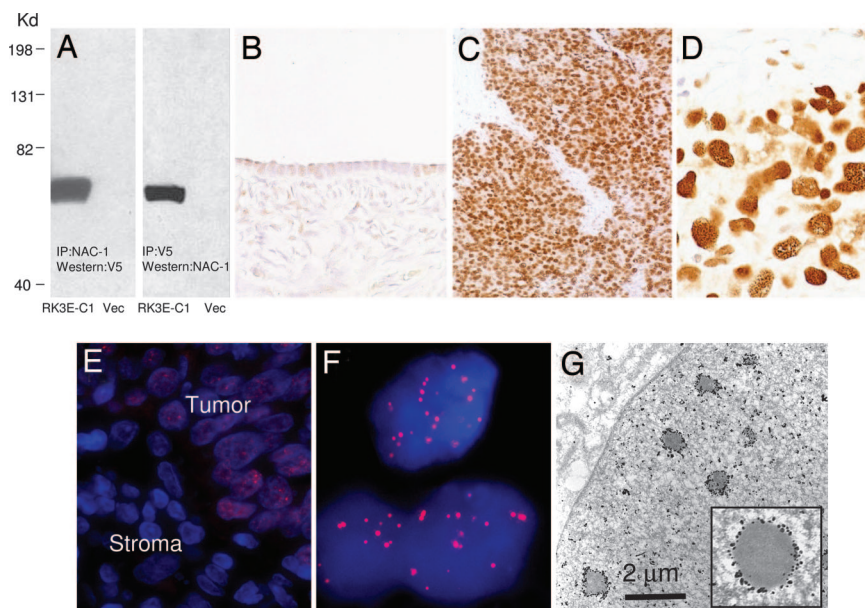


Fig. 2. Immunoreactivity of NAC-1 in ovarian cancer tissues. (A) Immunoprecipitation/Western blot analyses using NAC-1 and V5 antibodies in RK3E cells transfected with pCDNA6-NAC-1/V5 (RK3E-C1) or vector-only control (Vec). A discrete band corresponding to NAC-1 protein mass is identified in this reciprocal analysis. (B–D) The NAC-1 immunointensity is undetectable or weak in normal ovarian surface epithelium (B) but is strong in a high-grade serous carcinoma (C and D). (E and F) Immunofluorescence of NAC-1 protein localization in ovarian cancer cells in a tissue section. Tumor cells contain NAC-1 protein, which is located in discrete nuclear bodies (E). The adjacent stromal cells are negative for NAC-1 immunoreactivity. A higher magnification demonstrates the NAC-1 nuclear bodies by using a confocal fluorescence microscope (F). (G) Ultrastructure of NAC-1 bodies. ImmunoGold labeling of NAC-1-expressing RK3E cells demonstrates electron-dense bodies decorated by gold particles in the nuclear matrix.

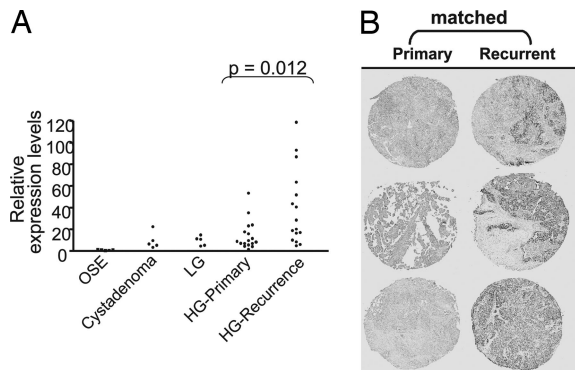


Fig. 3. NAC1 expression correlates with tumor progression in ovarian serous carcinomas. (A) Quantitative real-time PCR analysis shows higher NAC-1 expression levels in high-grade carcinomas (HG) than in ovarian surface epithelial cells (OSE), low-grade carcinomas (LG), and cystadenomas. Moreover, recurrent carcinomas have significantly higher expression levels than primary tumors ($P = 0.012$). The data are expressed as fold increase as compared with the average of OSE. (B) Immunohistochemistry demonstrates intense immunoreactivity in recurrent tumors as compared with patients' primary tumors in three representative cases.

patients ($P = 0.017$, χ^2 test) (Fig. 3B). Based on these findings, we further analyzed to see whether NAC-1 expression in primary tumors was predictive of disease-free interval (the period between primary surgery and tumor recurrence) in 57 patients with advanced-stage high-grade serous carcinomas who underwent optimal primary debulking surgery, followed by a standard chemotherapeutic regimen in the same institution (JHMI). We found that high NAC-1 immunointensity (2+ and 3+) predicted recurrence within 1 year after diagnosis with an odds ratio of 14.9 (95% CI, 3.00–74.2; $P = 0.0002$, Fisher's exact test). The median disease-free interval with NAC-1 immunointensity of ≥ 2 was 12 months, whereas when the intensity was < 2 , the interval was 18 months.

The positive correlation of NAC-1 expression and recurrent disease suggests that NAC-1 plays a role in the development of recurrent ovarian tumors. To test whether NAC-1 expression directly contributes to drug resistance, we correlated NAC-1 immunoreactivity and *in vitro* drug resistance in 60 high-grade serous carcinomas. The *in vitro* drug-resistance results were performed at Oncotech (Tustin, CA) by using the protocol described at www.oncotech.com/pdfs/edr_4_pager.pdf (11, 12). Cases were grouped according to different immunointensity scores, but there was no significant correlation ($P > 0.17$, χ^2 test) between NAC-1 expres-

sion and *in vitro* resistance to carboplatin, cisplatin, and taxol, the standard chemotherapeutic agents for ovarian cancer.

Dominant Negative Role of NAC-1 BTB/POZ Domain. Because the BTB/POZ domain has been known to be involved in protein homomerization or heteromerization, we tested whether the NAC-1 BTB/POZ domain participated in protein–protein interaction using deletion mutants of NAC-1 (Fig. 4A). Based on coimmunoprecipitation and immunofluorescence colocalization studies (Fig. 4B and C), we found that the BTB/POZ domain of NAC-1, corresponding to the 1–129 aa at the N terminus (N130 construct), was the minimal structural motif required for NAC-1 homooligomerization (Fig. 4B). The NAC-1 deletion mutants/Xpress tags were then transfected into RK3E cells that had been stably transfected with a full-length NAC-1/V5 tag expression vector. As shown in Fig. 4C, full-length NAC-1/V5 colocalized with the full-length NAC-1/Xpress in the NAC-1 bodies, indicating that NAC-1 interacted with NAC-1. As expected, both N130 and N250 deletion mutants containing the BTB/POZ domain also colocalized with full-length NAC-1, but interestingly, both mutants disrupted the formation of NAC-1 bodies by transforming them into “cotton candy”-like aggregates or large “noodle”-like structures in the nuclei (Fig. 4C). In contrast, C250 and M120 deletion mutants that did not contain the BTB/POZ domain failed to colocalize with wild-type NAC-1.

Suppression of Tumor Formation upon Induction of NAC-1 N130 Mutant.

To test whether the BTB/POZ domain is involved in tumor growth, we established an inducible (Tet-Off) system by expressing the N130 construct upon removal of doxycycline in two NAC-1-positive tumor cell lines, SKOV3, an ovarian cancer cell line, and HeLa, a cervical adenocarcinoma cell line. Cervical adenocarcinomas, like ovarian serous carcinomas, frequently overexpressed NAC-1, because a high level of NAC-1 immunoreactivity (2+ and 3+) occurred in $\approx 50\%$ (16 of 32) cervical adenocarcinomas, whereas the NAC-1 immunoreactivity in normal endocervical glands were undetectable (Fig. 7, which is published as supporting information on the PNAS web site).

For both SKOV3-N130 and HeLa-N130 cell lines, the efficiency of N130 induction was very high as evidenced by $>99\%$ of cells expressing green fluorescence based on flow cytometry (data not shown) and increased copy number of N-terminal mRNA sequence as compared with C-terminal sequence based on quantitative real-time PCR (Fig. 8A and B, which is published as supporting information on the PNAS web site) after removal of doxycycline. Like RK3E cells expressing the N130 mutant (Fig. 4C), NAC-1 nuclear bodies were transformed to cotton candy-like aggregates in

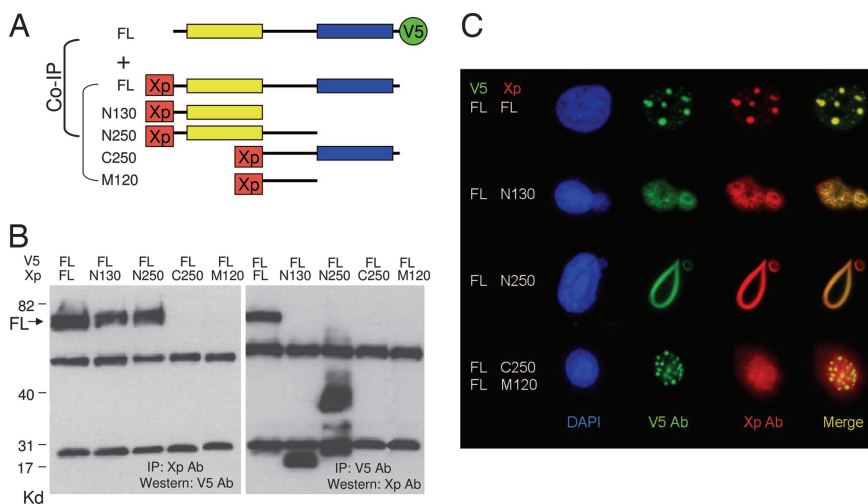


Fig. 4. Coimmunoprecipitation and colocalization of NAC-1 deletion mutants and full-length NAC-1. (A) Diagram of NAC-1 and NAC-1 deletion mutants. Full-length (FL) construct contains V5 tag at the C terminus, whereas all of the deletion mutants contain an Xpress (Xp) tag at the N terminus. The yellow box is the BTB/POZ domain; the blue box is the DUF1172 domain. (B) Coimmunoprecipitation shows that full-length NAC-1, N130, and N250 bind to NAC-1. The predicted molecular masses, not including the tag sequences, are: full-length NAC-1 (57.3 kDa), N130 (14.4 kDa), N250 (27.8 kDa), C250 (30.3 kDa), and M120 (14 kDa). (C) Cells with stable full-length NAC-1/V5 expression were transfected with different deletion mutants with the Xp tag. Double immunofluorescence shows that full-length NAC-1, N130, and N250 deletion mutants colocalize with full-length NAC-1. However, only full-length NAC-1 proteins form discrete round and oval-shaped NAC-1 nuclear bodies, whereas both N130 and N250 form irregular aggregates with the full-length NAC-1. Neither C250 nor M120 colocalizes with the full-length NAC-1 protein.

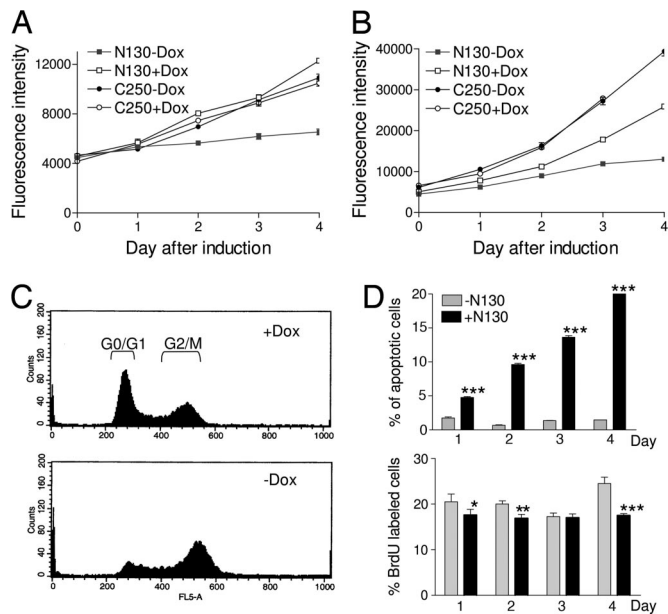


Fig. 5. Effects of N130 induction on cellular proliferation and apoptosis in 96-well plates. (A and B) Cell growth curves show that after induction of N130 (–Dox), cell growth is significantly suppressed as compared with the noninduced cells (+Dox). In contrast, induction of C250 does not have an apparent effect on cell growth in SKOV3 (A) or HeLa (B) cells. (C) Cell cycle analysis shows an increase in G₂/M fraction in N130-induced HeLa cells (Lower) as compared with noninduced cells (Upper) 24 h after induction, indicating a G₂/M block. (D) Percentages of apoptotic and proliferating cells are determined by counting annexin V- and BrdU-positive cells, respectively, in both N130-induced and -noninduced cells. Data are presented as mean \pm SD. *, $P < 0.05$; **, $P < 0.001$, ***, $P < 0.0001$, Student's *t* test.

both SKOV3 and HeLa cells after induction of *N130* (Fig. 8C). As compared with the control (induction of C250), induction of *N130* expression significantly reduced cell proliferation in both SKOV3 cells (Fig. 5A) and HeLa cells (Fig. 5B). Induction of the control C250 mutant did not have significant effects on cellular proliferation in either of the cell lines. Similarly, expression of *N130* significantly suppressed colony formation in both cell lines (Fig. 9, which is published as supporting information on the PNAS web site). The decrease in cellular growth after *N130* induction was associated with cell cycle arrest at G₂/M phase (percentage of cells in G₀/G₁-to-S-to-G₂/M = 50.3%-to-16.5%-to-33.2% in noninduced cells vs. 20.1%-to-17.4%-to-62.5% in induced cells) (Fig. 5C). *N130* induction significantly increased the number of annexin V-labeled cells and also decreased the number of BrdU-labeled cells (except on day 3), although the level in the decrease of cells with BrdU uptake is not as dramatic as the increase of annexin V-labeled cells (Fig. 5D). To further evaluate the effect of N130 on cellular proliferation and apoptosis, we used the miniN130 mutants, N65 and N30-122, in which its BTB/POZ oligomerization activity was deficient. Both N65 and N30-122 showed protein expression but were not able to coimmunoprecipitate with the full-length NAC-1 protein (Fig. 10A, which is published as supporting information on the PNAS web site). When transfecting these two constructs into the NAC-1 overexpressing SKOV3 cells, both N65 and N30-122 could not effectively suppress cellular proliferation as compared with N130 (Fig. 10B). In addition, we also knocked down NAC-1 using RNAi to determine whether there was a similar inhibitory effect to the expression of the N130 dominant-negative construct. In fact, NAC-1-expressing SKOV3 and HeLa cells had significantly reduced cell numbers after NAC-1 siRNA treatment (Fig. 11A and B, which is published as supporting information on the PNAS web site). In contrast, NAC-1 siRNA did not show a significant effect on

the cell growth of OVCAR3 cells that did not express abundant NAC-1 (Fig. 11B). Furthermore, we found that the apoptosis-inducing effect of the siRNAs used here was potent, but was less pronounced than the N130 dominant-negative NAC-1 (Fig. 11C), indicating that the latter approach could be a more effective experimental system to inactivate NAC-1 function. As a control, we expressed N130 in OVCAR3, which expressed only a minimal amount of NAC-1 protein compared with HeLa and SKOV3 cells, and found that N130 expression did not have a significant effect on the growth of OVCAR3 cells (Fig. 11D).

Based on the above findings, we investigated whether disrupting interactions between NAC-1 molecules using the N130 dominant-negative approach had a growth-inhibitory effect in HeLa (Fig. 12, which is published as supporting information on the PNAS web site) and SKOV3 (Fig. 13, which is published as supporting information on the PNAS web site) xenografts in nude mice. First, we tested whether expression of N130 could prevent tumorigenesis by inducing N130 expression 2 days after s.c. tumor injection. As shown in Figs. 12A and 13A, induction of N130 expression in HeLa and SKOV3 cells almost completely prevented the formation of s.c. tumors. In contrast, the control cells grew tumors at all injection sites. Second, we determined whether N130 could limit tumor growth in established HeLa and SKOV3 tumors. The expression of N130 was induced by removing doxycycline, when all of the mice harbor palpable tumors. Five days after discontinuation of doxycycline, induction of N130 expression was evidenced by green fluorescence in the s.c. HeLa tumors because expression of both N130 and EGFP was driven by a bicistronic promoter (Fig. 12B). As shown in Figs. 12C and 13B, tumors continued growing in control mice, whereas the tumors stopped growing or decreased in size after N130 induction. Histological examination of the tumors excised 10 days after N130 induction revealed extensive apoptosis in tumor cells, based on morphology and immunoreactivity with the M30 antibody, which recognizes the apoptosis-specific caspase-cleaved cytokeratin epitope (13, 14) (Fig. 12D).

The Oncogenic Potential of NAC-1 Expression. To test whether NAC-1 expression is tumorigenic, we randomly selected two clones from a spontaneously immortalized MOSE cell line and two NIH 3T3 clones that were stably transfected with an NAC-1 expression vector (Fig. 6). When compared with vector-transfected controls, all NAC-1-expressing clones had a higher cellular proliferation, based on growth curves and BrdU-uptake assays (Fig. 6A, D, and F). S.c. injections of NAC-1-expressing MOSE clones in athymic *nu/nu* mice produced larger tumors than the control cells transfected with the vector-only (Fig. 6B and C). MOSE clones did not grow i.p. tumors 21 days after i.p. injection. The NAC-1-expressing NIH 3T3 clones produce both s.c. and i.p. tumors in the athymic *nu/nu* mice. The i.p. tumors were always multiple, and their combined weights were measured in each mouse (Fig. 6E). In contrast, the vector-transfected NIH 3T3 cells did not grow tumors during the course of this study.

Discussion

NAC-1 was first identified and cloned as a transcript induced in the nucleus accumbens from rats treated with cocaine (15). The nucleus accumbens is a unique forebrain structure involved in reward motivation (16) and many addictive behaviors (17–19). Except for its role in cocaine-induced expression in animal brains, the cellular function of NAC-1 is unknown. In this study, we demonstrate that *NAC-1* is a previously uncharacterized cancer-associated gene, because the NAC-1 expression level is significantly increased in several types of cancers including ovarian cancer, cervical adenocarcinoma, and breast cancer. We showed that NAC-1 was required for cell proliferation and survival and was sufficient to enhance tumorigenicity in athymic *nu/nu* mice.

Cancer mortality and morbidity are related to recurrent and metastatic disease. Therefore, a positive correlation between

sequence were extracted from the Swiss-Prot/TrEMBL protein databank released on January 16, 2006 (<http://us.expasy.org/cgi-bin/get-entries?DR=PS50097&db=tr&db=sp&view=tree>). A total of 130 BTB/POZ genes were identified. The expression levels of the BTB/POZ gene family members were determined from the ovarian tumor SAGE libraries by obtaining the SAGE tag counts for each BTB/POZ gene. The libraries included the OSE cells (SV-40 immortalized IOSE29 (26) and short-term cultured HOSE4), benign cystadenoma (ML10), ovarian high-grade serous carcinoma tissues (HG63, HG48, HG92, OVT6, OVT7, and OVT8), and ovarian cancer cell lines (OVCAR3 and A2780). All libraries have been published (27), except HG63, HG48 and HG92 which were established in this study. The NAC-1-specific SAGE tags included TTCCCGGCC, TGAAGGCAGT, CCTATA-ATCG, AGTGCCAGGG, AGAATATCAG, GAGGGAGGGA, and GTTCCCCAC. By using a minimum tag count setting of >1, these NAC-1 tags were tallied and normalized per 100,000 total tags for each SAGE library. To select the candidate gene(s) for further study, we first select those with a high average tag count (>10 tags per 100,000 tags) in ovarian carcinoma libraries, followed by the highest ratio of average tag counts in ovarian carcinoma to the benign controls (IOSE29, HOSE4, and ML10).

To determine the NAC-1 expression levels among different cancer libraries, we compared NAC-1 tag counts among 81 SAGE libraries (<http://cgap.nci.nih.gov/SAGE>) (28, 29) from carcinomas and normal tissues of ovary, pancreas, liver, colon, kidney, prostate, and breast (30). NAC-1 tag counts for each library were retrieved by filtering for tag sequences that matched uniquely to NAC-1 according to the April 15, 2005 SAGEMap available on the public National Center for Biotechnology Information FTP site (<ftp://ftp.ncbi.nlm.nih.gov/pub/sage/map/Hs/NlaIII>).

Immunohistochemistry and Immunoelectron Microscopy. Paraffin-embedded tumor tissues were obtained from the Department of Pathology at the Johns Hopkins Hospital and effusion ovarian cancer samples were obtained from the Norwegian Radium National Hospital in Norway. These included 182 high-grade ovarian serous carcinoma tissues (154 stage III and 28 stage IV), 44 low-grade ovarian serous carcinoma tissues (42 stage III and 2 stage IV), 172 high-grade ovarian carcinoma effusion samples (1 stage I, 6 stage II, 97 stage III, and 68 stage IV), and 32 cervical adenocarcinomas. In addition, 21 benign ovarian cystadenomas, 18 normal ovaries, and 8 normal cervical tissues were included for comparison. Acquisition of tissue specimens and clinical information was approved by an institutional review board (Johns Hopkins Medical Institutions) or by the Regional Ethics Committee (Norwegian Radium Hospital).

For immunohistochemistry studies, we generated a mouse NAC-1 monoclonal antibody by immunizing mice with the NAC-1 recombinant protein using a standard hybridoma protocol (31). Immunohistochemistry was performed on deparaffinized sections by using the NAC-1 antibody at a dilution of 1:100 and an EnVision+System peroxidase kit (DAKO, Carpinteria, CA). Immunoreactivity was scored by two investigators as follows: 0, undetectable; 1+, weakly positive; 2+, moderately positive; and 3+, intensely positive. NAC-1 immunoreactivity was not detectable (immunointensity score = 0) or weak (1+) in normal OSE and benign serous cystadenomas. For ultrastructure study of NAC-1 bodies, we applied ImmunoGold labeling on NAC-1-expressing-RK3E cells, followed by electron microscopy.

Coimmunoprecipitation and Double Immunofluorescence Staining. A series of NAC-1-deletion mutants including N130 (encoding the amino acids 1–129 at the N terminus), N250 (amino acids 1–263 at the N terminus), M120 (amino acids 123–263 in the middle portion), and C250 (amino acids 257–528 at the C terminus) were generated by PCR. Both N130 and N250 mutants contained the BTB/POZ domain (amino acids 20–122) of NAC-1. In addition, two miniN130 expression constructs were generated, and they included N65 (encoding the first 1–65 aa of the BTB domain) and N30-122 (30–122 aa). PCR products of the NAC-1-deletion mutants were cloned into an expression vector, pCDNA4 with an Xpress tag at the N terminus. RK3E cells were first stably transfected with pCDNA6/V5/NAC-1 and then transiently transfected with the pCDNA4/NAC-1-deletion mutants. Coimmunoprecipitation was performed to assess the specific structural motifs that bound to full-length NAC-1. For immunofluorescence staining, cells were incubated with primary antibodies, followed by fluorescence-labeled secondary antibodies.

N130-Inducible Construct, Cell Proliferation, and Apoptosis Assays. The Tet-Off inducible system was used to assess the biological effects of N130. HeLa and SKOV3 cells that constitutively expressed tTA (tetracycline-controlled transactivator) were transfected with pBI-N130/EGFP or pBI-C250/V5-EGFP (control) that bicistronically expressed the products of interest and reporter EGFP upon the binding of tTA to the tetracycline-responsive element in the absence of inducer (doxycycline). Cell proliferation and apoptosis assays were performed as described (32) in 96-well plates.

We thank Mr. David Chu and Mr. M. Jim Yen for editorial assistance and Dr. C.-Y. Hsu for organization of cervical adenocarcinoma tissue microarrays. This study was supported by Department of Defense Grant OC0400600 and National Institutes of Health Grant CA103937.

- Stogios PJ, Downs GS, Jauhal JJ, Nandra SK, Prive GG (2005) *Genome Biol* 6:R82.1–R82.17.
- Bardwell VJ, Treisman R (1994) *Genes Dev* 8:1664–1677.
- Albagli O, Dhordain P, Deweindt C, Lecocq G, Leprince D (1995) *Cell Growth Differ* 6:1193–1198.
- Chen Z, Brand NJ, Chen A, Chen SJ, Tong JH, Wang ZY, Waxman S, Zelen A (1993) *EMBO J* 12:1161–1167.
- Polo JM, Dell'Oso T, Ranuncolo SM, Cerchietti L, Beck D, Da Silva GF, Prive GG, Licht JD, Melnick A (2004) *Nat Med* 10:1329–1335.
- Yeyati PL, Shaknovich R, Boterashvili S, Li J, Ball HJ, Waxman S, Nason-Burchenal K, Dmitrovsky E, Zelen A, Licht JD (1999) *Oncogene* 18:925–934.
- Maeda T, Hobbs RM, Merghoub T, Guernah I, Zelen A, Cordon-Cardo C, Teruya-Feldstein J, Pandolfi PP (2005) *Nature* 433:278–285.
- Maeda T, Hobbs RM, Pandolfi PP (2005) *Cancer Res* 65:8575–8578.
- van Roy FM, McCrea PD (2005) *Nat Rev Cancer* 5:956–964.
- Park JI, Kim SW, Lyons JP, Ji H, Nguyen TT, Cho K, Barton MC, Deroo T, Vlemingck K, Moon RT, McCrea PD (2005) *Dev Cell* 8:843–854.
- Fruehauf JP, Alberts DS (2003) *Recent Results Cancer Res* 161:126–145.
- Eltabbakh GH, Piver MS, Hempling RE, Recio FO, Lele SB, Marchetti DL, Baker TR, Blumenson LE (1998) *Gynecol Oncol* 70:392–397.
- Leers M, Kolgen W, Bjorklund V, Bergman T, Tribbick G, Persson B, Bjorklund P, Ramaekers FC, Bjorklund B, Schutte B (1999) *J Pathol* 5:567–572.
- Caulin C, Salvesen GS, Oshima RG (1997) *J Cell Biol* 138:1379–1394.
- Cha XY, Pierce RC, Kalivas PW, Mackler SA (1997) *J Neurosci* 17:6864–6871.
- Roitman MF, Wheeler RA, Carelli RM (2005) *Neuron* 45:587–597.
- Koob GF (1996) *Neuron* 16:893–896.
- Mackler SA, Korutla L, Cha XY, Koebe MJ, Fournier KM, Bowers MS, Kalivas PW (2000) *J Neurosci* 20:6210–6217.
- Kalivas PW, Duffy P, Mackler SA (1999) *Synapse* 33:153–159.
- Diaz-Montes TP, Bristow RE (2005) *Curr Oncol Rep* 7:451–458.
- Harter P, du Bois A (2005) *Curr Opin Oncol* 17:505–514.
- Gadducci A, Iacconi P, Cosio S, Fanucchi A, Cristofani R, Riccardo Genazzani A (2000) *Gynecol Oncol* 79:344–349.
- Gadducci A, Iacconi P, Fanucchi A, Cosio S, Tetti G, Genazzani AR (2000) *Anticancer Res* 20:1959–1964.
- Zang RY, Li ZT, Tang J, Cheng X, Cai SM, Zhang ZY, Teng NN (2004) *Cancer* 100:1152–1161.
- Dhordain P, Albagli O, Ansieau S, Koken MH, Deweindt C, Quief S, Lantoine D, Leutz A, Kerckaert JP, Leprince D (1995) *Oncogene* 11:2689–2697.
- Auersperg N, Pan J, Grove BD, Peterson T, Fisher J, Maines-Bandiera S, Somasiri A, Roskelley CD (1999) *Proc Natl Acad Sci USA* 96:6249–6254.
- Hough CD, Sherman-Baust CA, Pizer ES, Montz FJ, Im DD, Rosenshein NB, Cho KR, Riggins GJ, Morin PJ (2000) *Cancer Res* 60:6281–6287.
- Boon K, Osorio EC, Greenhut SF, Schaefer CF, Shoemaker J, Polyak K, Morin PJ, Buetow KH, Strausberg RL, De Souza SJ, Riggins GJ (2002) *Proc Natl Acad Sci USA* 99:11287–11292.
- Lal A, Lash AE, Altschul SF, Velculescu V, Zhang L, McLendon RE, Marra MA, Prange C, Morin PJ, Polyak K, et al. (1999) *Cancer Res* 59:5403–5407.
- Yen M-J, Hsu CY, Mao TT, Wu TC, Roden R, Wang TL, Shih IM (2006) *Clin Cancer Res* 12:827–831.
- Shih IM, Elder DE, Speicher D, Johnson JP, Herlyn M (1994) *Cancer Res* 54:2514–2520.
- Shih IM, Sheu JJ, Santillan A, Nakayama K, Yen MJ, Bristow RE, Vang R, Parmigiani G, Kurman RJ, Trope CG, et al. (2005) *Proc Natl Acad Sci USA* 102:14004–14009.

Diffuse Mesothelin Expression Correlates with Prolonged Patient Survival in Ovarian Serous Carcinoma

M. Jim Yen,¹ Chih-Yi Hsu,² Tsui-Lien Mao,¹ T-C. Wu,¹ Richard Roden,¹ Tian-Li Wang,¹ and Ie-Ming Shih¹

Abstract Purpose: Mesothelin is an emerging marker for cancer diagnosis and target-based therapy, yet relatively little is known about the clinical significance of mesothelin expression in tumors. In this study, we correlate mesothelin immunoreactivity to clinicopathologic features in ovarian serous carcinoma.

Experimental Design: Mesothelin expression levels were compared among 81 publicly available serial analysis of gene expression (SAGE) libraries of various carcinoma and normal tissue types. Immunohistochemistry using a well-characterized mesothelin monoclonal antibody (5B2) was done to evaluate mesothelin expression in 167 high-grade and 31 low-grade ovarian serous carcinomas. Immunohistochemistry staining scores were correlated with patient survival, tumor site, tumor grade, *in vitro* drug resistance, and differentiation status of tumor cells.

Results: SAGE analysis showed that mesothelin was overexpressed in 50% of ovarian and pancreatic carcinomas but rarely in other cancer types, including liver, colon, kidney, prostate, and breast. Mesothelin immunoreactivity (>5% of tumor cells) was present in 55% of ovarian serous carcinomas with no difference in expression between high-grade and low-grade serous tumors ($P = 0.82$). Based on Kaplan-Meier analysis, we found that a diffuse mesothelin staining (>50% of tumor cells) in primary high-grade ovarian carcinomas correlated significantly with prolonged survival in patients who had advanced-stage disease and had received optimal debulking surgery followed by chemotherapy ($P = 0.023$). Mesothelin expression did not correlate significantly with patient age, tumor site, *in vitro* drug resistance, or tumor differentiation status ($P > 0.10$).

Conclusion: Our results provided new evidence that mesothelin expression is associated with prolonged survival in patients with high-grade ovarian serous carcinoma.

Mesothelin is a glycoprotein that has been reported as a tumor-associated marker in several types of human cancer, including nonmucinous ovarian carcinomas and adenocarcinomas arising from the pancreaticobiliary tract, endometrium, and lung (1). Mesothelin was highly expressed in these tumors but not in a wide variety of normal tissues. The mesothelin gene was first cloned by Chang and Pastan (2), and it encodes a precursor protein that is processed to yield the 40-kDa mesothelin protein and a 31-kDa soluble fragment named

megakaryocyte-potentiating factor. Mesothelin is attached to the cell membrane by a glycosylphosphatidyl inositol linkage, and it has recently been shown to bind to CA125 (or MUC16), which is expressed in many ovarian serous carcinomas. The interaction between mesothelin and CA125 can mediate heterotypic cell adhesion as anti-mesothelin antibody blocks binding of CA125-expressing OVCAR3 cells to another cell line expressing mesothelin (3). Although the biological functions of mesothelin remain largely unknown as mesothelin knockout mice did not display detectable phenotypes (4), there is evidence that mesothelin may have potential as a new cancer diagnostic marker and a novel molecular target for gene therapy (5). For example, mesothelin alone or in combination with other gene products can provide a valuable marker for the differential diagnoses of cancer types (1). It has also been shown that a soluble form of the mesothelin (megakaryocyte-potentiating factor) family can provide useful new marker(s) for the diagnosis of ovarian carcinoma as well as monitoring its response to therapy (6). Mesothelin has been used to mediate the targeting of adenoviral vectors and an antibody-based gene therapy in mesothelin-expressing tumors (7–9).

Ovarian carcinoma is the leading cause of cancer mortality in patients who suffer from gynecologic neoplasms. Among the different types of ovarian cancer, serous carcinoma is the most

Authors' Affiliations: ¹Departments of Pathology and Oncology and Gynecology/Obstetrics, Johns Hopkins Medical Institutions, Baltimore, Maryland and ²Department of Pathology and Laboratory Medicine, Taipei Veterans General Hospital, and Pathology, National Yang-Ming University School of Medicine, Taipei, Taiwan

Received 6/27/05; revised 11/7/05; accepted 11/22/05.

The costs of publication of this article were defrayed in part by the payment of page charges. This article must therefore be hereby marked *advertisement* in accordance with 18 U.S.C. Section 1734 solely to indicate this fact.

Note: URL: <http://pathology2.jhu.edu/shihlab/index.cfm>.

Requests for reprints: Ie-Ming Shih, Department of Pathology, The Johns Hopkins Medical Institutions, 1503 East Jefferson Street, Room B-315, Baltimore, MD 21231. Phone: 410-502-7773; Fax: 410-502-7943; E-mail: ishih@jhmi.edu.

© 2006 American Association for Cancer Research.

doi:10.1158/1078-0432.CCR-05-1397

common and lethal type. Although mesothelin has been documented as a tumor-associated marker in ovarian serous carcinoma, a larger-scale analysis focusing on the correlation of mesothelin expression and clinicopathologic variables has never been done. Such a correlation study is important as it can provide a prognostic marker for predicting clinical outcome in cancer patients and shed new light on the function of mesothelin in ovarian cancer. The purpose of this study is to use immunohistochemistry to assess the clinical significance of mesothelin expression in a large series of serous carcinomas that are well annotated with clinicopathologic information.

Materials and Methods

Mesothelin expression analysis using the serial analysis of gene expression database. Mesothelin expression levels were compared among 81 publicly available serial analysis of gene expression (SAGE) libraries (<http://cgap.nci.nih.gov/SAGE>; refs. 10, 11) for carcinomas and normal tissues of ovary, pancreas, liver, colon, kidney, prostate, and breast. The selection of libraries used for analysis was based on their availability in the SAGE database. Mesothelin tag counts for each library were retrieved by filtering for tag sequences that matched uniquely to mesothelin according to the April 15, 2005 SAGEmap available on the public National Center for Biotechnology Information FTP site (ftp://ftp.ncbi.nlm.nih.gov/pub/sage/map/Hs/NlaIII/SAGEmap_tag_ug-rel.zip). Using a minimum tag count setting of >1, these mesothelin tags were tallied and normalized per 100,000 total tags for each SAGE library.

Tissue samples. Formalin-fixed, paraffin-embedded tissue samples of 198 ovarian serous tumors, including 167 serous high-grade carcinomas and 31 low-grade serous carcinomas, were retrieved from the archival file of the Department of Pathology at the Johns Hopkins Hospital. The acquisition of paraffin tissues was approved by the Johns Hopkins Institutional Review Board. The paraffin tissues were organized into tissue microarrays, which were made by removing three 1.5-mm-diameter cores of tumor from each block. The selection of areas for core was made by two pathologists (C-Y.H. and I-M.S.) based on review of the corresponding H&E slides. To evaluate whether expression of mesothelin was a prognostic marker in patients with ovarian serous carcinoma, we analyzed 105 advanced-stage, high-grade serous carcinomas, of which 92 were International Federation of Gynecology and Obstetrics stage III and 13 were International Federation of Gynecology and Obstetrics stage IV. High-grade serous carcinomas have been conventionally classified into "moderately" and "poorly" differentiated carcinomas based on whether they are predominantly papillary or solid, respectively.

Immunohistochemistry. Expression of mesothelin was assessed by immunohistochemistry using a mouse monoclonal antibody (5B2) that specifically reacts with the mesothelin (Promega, Madison, WI). This antibody has been well characterized and been used in immunohistochemistry to assess its diagnostic potential (1, 12-14). Immunohistochemistry was done on paraffin sections at a dilution of 1:500 followed by the EnVision+System using the peroxidase method (DAKO, Carpinteria, CA). The percentage of positive cells was estimated by randomly counting ~500 tumor cells from three different high-power fields ($\times 40$) within one specimen. For the negative control, an isotype (IgG1)-matched antibody, MN-4, was used in parallel (15). A positive reaction was defined as discrete localization of the brown chromagen on the cell surface. Because mesothelin immunoreactivity, if present, was always strong, we used the percentage score in this study. Cases with <5% of tumor cells positively reactive were scored as negligible. We used the following scoring system for mesothelin immunoreactivity: 0, <5%; 1+, 5% to 50%; 2+, 51% to 75%; 3+, 76% to 95%; 4+, >95%. Scoring was done by two independent investigators who concurred on the results.

A third pathologist scored the cases with discrepant scores, and the tumor was assigned based on the consensus of two.

Reverse transcriptase-PCR. To validate the immunohistochemistry results, we did reverse transcriptase-PCR to semiquantitatively measure the levels of mesothelin transcript copy number in eight representative cases with either diffuse or undetectable mesothelin immunoreactivity. mRNA was isolated from frozen tumor tissues, and cDNA was prepared as previously described (16). The sequences of forward and reverse primers were 5'-TCAGTCAGCAGAATGTGAGCA-3' and 5'-TCTAGGAC-CAGGTAGCCGTTG-3' that amplified 238 bp of mesothelin coding sequence. PCR was done as detailed in a previous report (16), and the PCR product was visualized by staining with ethidium bromide on 1.5% agarose gels.

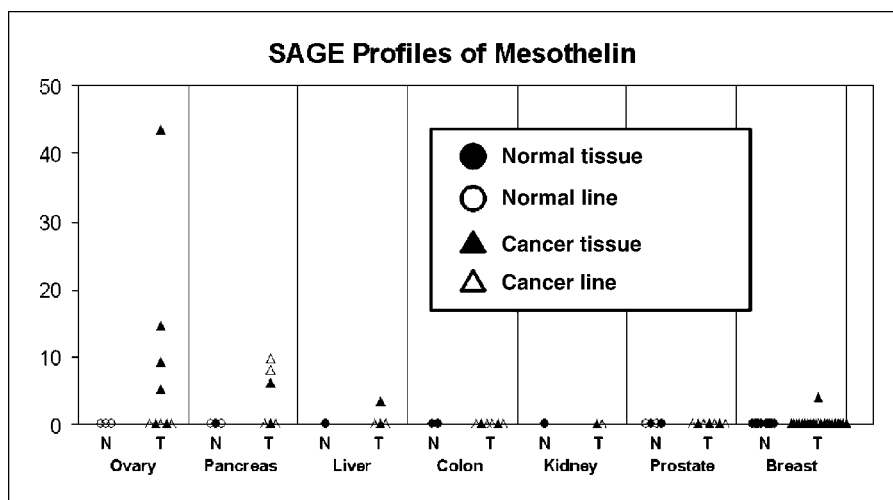
In vitro drug resistance assay. Drug sensitivity was assessed by an agar-based cell culture system with radioactive thymidine incorporation as the end point (Oncotech, Tustin, CA). There were 61 cases for which the results of this assay were available to analyze. The protocol of the assay has been detailed at <http://www.oncotech.com/innovation/PublicationDetails.asp?id=28>. Briefly, fresh tumor specimens immediately removed at the time of surgery were placed into the RPMI (Life Technologies, Gaithersburg, MD) and shipped to Oncotech for analysis. The tumor tissue was minced and enzymatically digested to disaggregate the tumor cell, which were then plated in soft agar. Tumor cells were then exposed to antineoplastic agents at a concentration of a maximum tolerated dose for 5 days *in vitro*. Tritiated thymidine was introduced during the last 2 days of culture as a measure of cell proliferation, and the drug-treated cells were compared with the untreated control. Assay results were divided into three categories: extreme, intermediate, and low drug resistance using the criteria described on the company's web site. Extreme resistance was interpreted as drug resistance, whereas intermediate and low drug resistance was interpreted as drug sensitive in this study as in previous reports (17, 18).

Statistical analysis and clinical correlation. The preexisting clinical information including clinical stage, treatment history, surgical findings during debulking, recurrence status, and survivorship was collected from clinical note, operation note, and discharge summary that were deposited in a centralized database. All the patients' identifiers were decoded before data analysis. We defined optimal debulking as the residual tumor nodules with sizes <1 cm after surgery. Survival curves were established using the Kaplan-Meier method, and their differences were analyzed using the log-rank test. Overall survival time was defined as the number of months between diagnosis and death or between diagnosis and most recent follow-up. All patients with advanced high-grade serous carcinomas were treated with combined chemotherapy, including paclitaxel and cisplatin, after optimal debulking surgery. Spearman correlation was used to determine the association between mesothelin expression and differentiation status (moderate or poor). Statistical association between mesothelin expression and patient age, tumor grade, tumor site (primary or recurrent), and *in vitro* drug resistance status was determined using Fisher's exact test.

Results

To comprehensively analyze mesothelin expression levels in common types of carcinomas, we did a sequence tag analysis based on the SAGE libraries that were available in the public database (<http://cgap.nci.nih.gov/SAGE>). SAGE provides an unbiased genome-wide analysis of all transcripts and has been used extensively in characterizing gene expression (19, 20). As shown in Fig. 1, half of the ovarian and pancreatic carcinoma libraries showed up-regulation of mesothelin (increased mesothelin-matched tag sequences) compared with their normal counterparts. Specifically, overexpression of mesothelin (normalized tag count > 5) was found in 5 of 10 ovarian carcinoma libraries and in three of six pancreatic carcinoma libraries.

Fig. 1. Mesothelin expression profiles based on SAGE analysis. Tumor (T) and normal (N) tissues or cell lines from ovary, pancreas, liver, colon, kidney, prostate, and breast were compared. Tag counts per 100,000 total tags are normalized (*y-axis*). Ovarian and pancreatic carcinomas are the two tumor types that overexpress mesothelin. Mesothelin is not expressed in any normal tissue types.



By contrast, none of the libraries representing ovarian surface epithelial cells and pancreatic ductal epithelium had mesothelin-matched tag counts of >5 . A wide variety of normal tissues also did not express mesothelin-matched tags, indicating a high specificity of mesothelin expression in carcinoma tissues.

Because ovarian carcinoma is one of the two tumor types that most frequently overexpress mesothelin based on SAGE analysis, in this study, we focused on analyzing the relationship between mesothelin expression and clinicopathologic features of ovarian serous carcinomas. Among ovarian serous carcinoma tissues, mesothelin immunoreactivity was heterogeneous with immunoreactive cells ranging from 0% to 99% (Fig. 2). Immunoreactivity of mesothelin was almost exclusively detected on the cell surface. In contrast, mesothelin immunoreactivity was absent from all six normal ovaries containing ovarian surface epithelium. Using an arbitrary cutoff of 5%, mesothelin expression ($>5\%$ of tumor cells) was found in 55% of ovarian serous carcinomas (Table 1). To validate immunohistochemistry results, we did reverse transcriptase-PCR in eight representative cases, in which the frozen samples were available and showed that PCR product of mesothelin was robust in representative tumors with diffuse mesothelin immunoreactivity (3+ and 4+) but was barely detectable in tumors with score of 0.

Next, we examined whether mesothelin expression correlated with clinicopathologic features. First, we determined if mesothelin expression was related to different types of ovarian serous carcinomas, which comprises mainly high-grade and low-grade serous carcinomas. Both types of carcinomas are characterized by distinctive clinical, morphologic, and molecular genetic features (21, 22). The frequency of mesothelin expression ($>5\%$ of tumor cells) in high-grade serous carcinomas (55%; 95% confidence interval, 47-63%) was similar to low-grade serous carcinomas (58%; 95% confidence interval, 41-75%) without statistical significance ($P = 0.82$). Second, we evaluated whether expression of mesothelin was related to a patient's overall survival in high-grade serous carcinoma. Low-grade serous carcinomas were less common, and the case number was not sufficient for statistical analysis of cumulative survival rates in this study. In high-grade serous carcinomas, we focused on

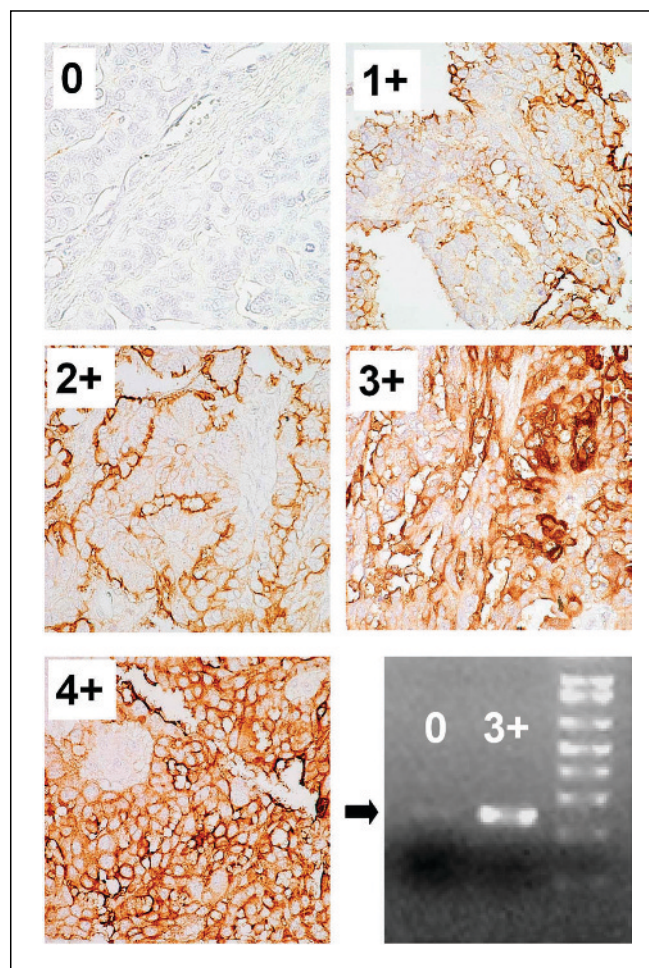


Fig. 2. Representative micrographs of mesothelin immunostaining using the antibody 5B2. Mesothelin immunoreactivity varies among high-grade ovarian serous carcinomas from score 0 to 4+. Reverse transcriptase-PCR was done on tumors with score 0 and 3+. The carcinoma with 3+ shows a robust PCR product of 238 bp that corresponds to mesothelin transcript (arrow), whereas the carcinoma without detectable mesothelin immunoreactivity only shows a barely detectable PCR product (right bottom). Molecular weight ladder (lane 3). Magnification, $\times 40$.

Table 1. Expression of mesothelin in ovarian serous tumors

Score	HGCA	LGCA	OSE
0	75	13	6
1+	52	10	0
2+	27	4	0
3+	8	1	0
4+	5	3	0
Total	167	31	6

Abbreviations: HGCA, high-grade serous carcinoma; LGCA, low-grade serous carcinoma; OSE, ovarian surface epithelium from normal ovaries.

advanced-stage diseases (92 International Federation of Gynecology and Obstetrics stage III and 13 International Federation of Gynecology and Obstetrics stage IV cases), because the vast majority of patients with high-grade serous carcinomas were diagnosed at these two stages. Among 167 high-grade cases, there were 105 patients who received optimal debulking surgery followed by paclitaxel/cisplatin-based combined chemotherapy, and their long-term follow-up information was available. Therefore, these patients were analyzed for correlation between mesothelin expression and overall survival. We separated high-grade cases into two groups: group A with diffuse immunoreactivity (immunostaining score: 2-4) and group B with negligible or focal immunoreactivity (immunostaining score: 0-1). Using this cutoff, we were able to show that patients in group A ($n = 29$) had a significantly better overall survival than patients in group B ($n = 76$; Fig. 3). The median survival was 60 months among group A patients and 34 months among group B patients. There was a statistically significant difference in overall survival between both groups ($P = 0.023$, log-rank test). The statistical significance in overall survival even improved if only stage III patients were analyzed ($P = 0.011$). Survival correlation was not done in stage IV patients, because there was a limited case number ($n = 13$) for statistical analysis. Patients in both groups had a similar age distribution (63.2 ± 12.3 versus 62.7 ± 10.9 years) and received optimal tumor debulking surgery followed by paclitaxel/cisplatin-based chemotherapy. We have also attempted to use different cutoffs to separate patients into groups (immunostaining score: 0 versus 1-4) but were unable to show any statistical significance ($P = 0.28$, log-rank test).

To further explore possible mechanisms for how mesothelin expression is related to favorable overall survival in patients with high-grade serous carcinomas, we correlated mesothelin expression with other clinical and histopathologic features. Expression of mesothelin did not correlate with the status of *in vitro* drug resistance for paclitaxel ($P = 0.106$) or cisplatin ($P = 1$), which are commonly used in treating ovarian cancer patients. We found that mesothelin was more frequently expressed in primary high-grade serous carcinomas compared with recurrent counterparts, but the difference did not reach a statistical significance ($P = 0.178$). High-grade serous carcinomas have been conventionally classified into moderately and poorly differentiated carcinomas based on whether they are predominantly papillary or solid, respectively. By classifying high-grade carcinomas into

moderately and poorly differentiated carcinomas, mesothelin expression did not correlate ($P = 0.35$) with either differentiation status category.

Discussion

Mesothelin is an emerging marker for diagnosis and target-based therapy in cancer. Ovarian cancer is one of the most common types of carcinoma that overexpresses mesothelin. In this study, we first compared the available SAGE data for mesothelin expression and then analyzed mesothelin immunoreactivity in a large number of ovarian serous carcinomas and correlated mesothelin expression to several clinicopathologic features. Our SAGE analysis confirmed previous reports (1, 2, 23-25) that mesothelin was expressed in the majority of ovarian carcinomas but not in a wide variety of normal adult tissues, suggesting that mesothelin is an ideal marker for cancer diagnosis and target-based therapy.

The most significant finding in this study is that we showed that diffuse mesothelin expression conferred a favorable clinical outcome in patients with high-grade serous carcinoma. A lack of correlation of mesothelin expression with several other clinicopathologic features, including tumor site (primary versus recurrent), tumor grade, drug resistance status, and differentiation

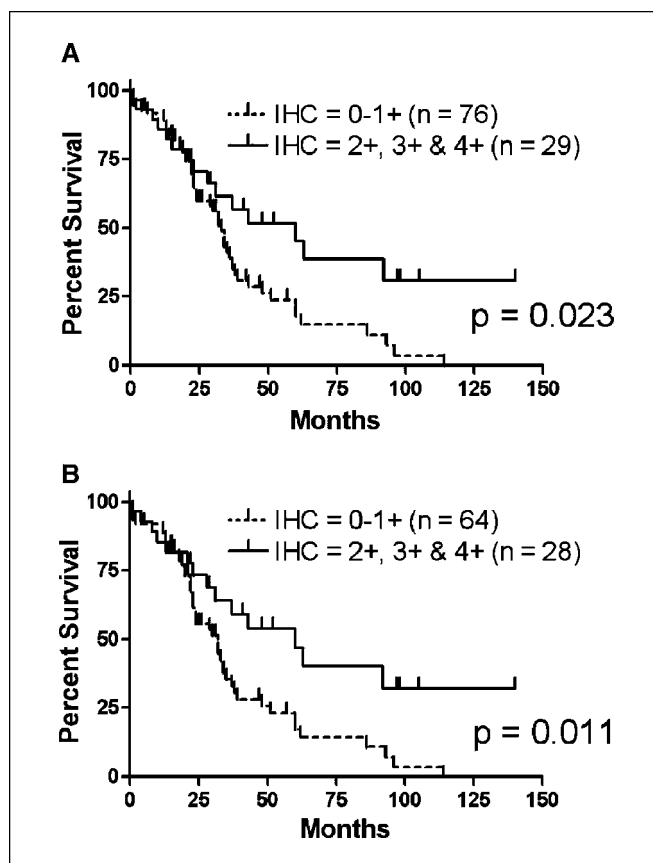


Fig. 3. Kaplan-Meier survival curves comparing tumors with negative or focal mesothelin staining (scores of 0-1 or <50% positive cells) to tumors with diffuse mesothelin staining (scores of 2+, 3+, and 4+) in (A) both stage III and stage IV high-grade primary ovarian serous carcinomas and (B) only stage III high-grade primary ovarian serous carcinoma.

status of tumor cells indicates that mesothelin seems not to be associated with these variables. The mechanisms underlying a positive correlation of mesothelin expression and a prolonged overall survival in ovarian cancer patients remain elusive but immune response to mesothelin expressing tumor cells may be one of the mechanisms. This view is supported by the following evidence. A humoral response to mesothelin has been found in patients who suffered from ovarian cancer and mesothelioma (26). Elevated levels of mesothelin-specific antibodies were detected in the sera of 41.7% of patients with ovarian cancer, and the immunogenicity of mesothelin is associated with high mesothelin expression in tumor cells. Besides the humoral response, a cell-mediated immune response may also play an important role. It has been reported that vaccination with a granulocyte macrophage colony-stimulating factor-transduced allogeneic pancreatic tumor vaccine induced human mesothelin-specific CD8⁺ T cells in pancreatic cancer patients (27). Among those patients who received the vaccine, 3 of 14 patients had prolonged survival. It is also noted that among seven pancreatic tumor genes identified by SAGE as overexpressed on pancreatic cancer, only mesothelin was recognized by T cells from the three patients but not by T cell from other patients. Therefore, the perfect correlation between the generation of vaccine-dependent T-cell responses to mesothelin and long-term survival (albeit in a limited number of patients) makes it an extremely promising candidate for mesothelin-specific immunotherapy (5).

The above finding indicates that immune response to mesothelin-expressing ovarian carcinoma cells may result in a reduction of tumor load and contribute to a prolonged patient's overall survival. It is interesting to note that a longer survival only occurred in tumors with diffuse mesothelin expression (> 50%) but not in those with focal expression. This finding implies that a tumor containing greater numbers of mesothelin-positive tumor cells was more likely to elicit a response from the immune system, whereas a tumor with focal mesothelin-positive cells would continue to progress unchecked as the majority of tumor cells fail to express the tumor antigen. Although the above view represents our most favored hypothesis, other mechanisms may also exist. For example, the cell-cell adhesion mediated by mesothelin and mucin 16 (CA125 molecules; ref. 3) may lead to cohesive tumor growth in ovarian carcinoma, which expresses mesothelin and prevents cancer cells from dissemination or metastasis in the peritoneal cavity.

In conclusion, this report represented the first large-scale analysis of mesothelin immunoreactivity in ovarian serous carcinomas and provided new evidence that diffuse mesothelin expression is associated with prolonged patient survival. Multi-institutional studies will be required to confirm whether mesothelin is an independent prognostic marker for ovarian cancer patients. It is also possible that future gene therapy directed towards enhancing mesothelin expression in cancer cells can offer improved clinical outcome to ovarian cancer patients.

References

- Ordóñez NG. Application of mesothelin immunostaining in tumor diagnosis. *Am J Surg Pathol* 2003;27:1418–28.
- Chang K, Pastan I. Molecular cloning of mesothelin, a differentiation antigen present on mesothelium, mesotheliomas, and ovarian cancers. *Proc Natl Acad Sci U S A* 1996;93:136–40.
- Rump A, Morikawa Y, Tanaka M, et al. Binding of ovarian cancer antigen CA125/MUC16 to mesothelin mediates cell adhesion. *J Biol Chem* 2004;279:9190–8.
- Bera TK, Pastan I. Mesothelin is not required for normal mouse development or reproduction. *Mol Cell Biol* 2000;20:2902–6.
- Hassan R, Bera T, Pastan I. Mesothelin: a new target for immunotherapy. *Clin Cancer Res* 2004;10:3937–42.
- Scholler N, Fu N, Yang Y, et al. Soluble member(s) of the mesothelin/megakaryocyte potentiating factor family are detectable in sera from patients with ovarian carcinoma. *Proc Natl Acad Sci U S A* 1999;96:11531–6.
- Breidenbach M, Rein DT, Everts M, et al. Mesothelin-mediated targeting of adenoviral vectors for ovarian cancer gene therapy. *Gene Ther* 2005;12:187–93.
- Hassan R, Viner JL, Wang QC, et al. Anti-tumor activity of K1–38QQR, an immunotoxin targeting mesothelin, a cell-surface antigen overexpressed in ovarian cancer and malignant mesothelioma. *J Immunother* 2000;23:473–9.
- Fan D, Yano S, Shinohara H, et al. Targeted therapy against human lung cancer in nude mice by high-affinity recombinant antimethelin single-chain Fv immunotoxin. *Mol Cancer Ther* 2002;1:595–600.
- Boon K, Osorio EC, Greenhut SF, et al. An anatomy of normal and malignant gene expression. *Proc Natl Acad Sci U S A* 2002;99:11287–92.
- Lal A, Lash AE, Altschul SF, et al. A public database for gene expression in human cancers. *Cancer Res* 1999;59:5403–7.
- Ordóñez NG. Value of mesothelin immunostaining in the diagnosis of mesothelioma. *Mod Pathol* 2003;16:192–7.
- Argani P, Iacobuzio-Donahue C, Ryu B, et al. Mesothelin is overexpressed in the vast majority of ductal adenocarcinomas of the pancreas: identification of a new pancreatic cancer marker by serial analysis of gene expression (SAGE). *Clin Cancer Res* 2001;7:3862–8.
- Frierson HF, Jr., Moskaluk CA, Powell SM, et al. Large-scale molecular and tissue microarray analysis of mesothelin expression in common human carcinomas. *Hum Pathol* 2003;34:605–9.
- Shih IM, Nesbit M, Herlyn M, Kurman RJ. A new Mel-CAM (CD146)-specific monoclonal antibody, MN-4, on paraffin-embedded tissue. *Mod Pathol* 1998;11:1098–106.
- Chen YC, Davidson B, Cheng CC, et al. Identification and characterization of membralin, a novel tumor-associated gene, in ovarian carcinoma. *Biochim Biophys Acta* 2005;1730:96–102.
- Fruehauf JP, Alberts DS. Assay-assisted treatment selection for women with breast or ovarian cancer. *Recent Results Cancer Res* 2003;161:126–45.
- Eltabbakh GH, Piver MS, Hempling RE, et al. Correlation between extreme drug resistance assay and response to primary paclitaxel and cisplatin in patients with epithelial ovarian cancer. *Gynecol Oncol* 1998;70:392–7.
- Velculescu VE, Vogelstein B, Kinzler KW. Analysing uncharted transcriptomes with SAGE. *Trends Genet* 2000;16:423–5.
- Velculescu VE, Zhang L, Vogelstein B, Kinzler KW. Serial analysis of gene expression. *Science* 1995;270:484–7.
- Shih I-M, Kurman RJ. Ovarian tumorigenesis—a proposed model based on morphological and molecular genetic analysis. *Am J Pathol* 2004;164:1511–8.
- Singer G, Oldt R III, Cohen Y, et al. Mutations in BRAF and KRAS characterize the development of low-grade ovarian serous carcinoma. *J Natl Cancer Inst* 2003;95:484–6.
- Hough CD, Sherman-Baust CA, Pizer ES, et al. Large-scale serial analysis of gene expression reveals genes differentially expressed in ovarian cancer. *Cancer Res* 2000;60:6281–7.
- Lu KH, Patterson AP, Wang L, et al. Selection of potential markers for epithelial ovarian cancer with gene expression arrays and recursive descent partition analysis. *Clin Cancer Res* 2004;10:3291–300.
- Schaner ME, Ross DT, Ciaravino G, et al. Gene expression patterns in ovarian carcinomas. *Mol Biol Cell* 2003;14:4376–86.
- Ho M, Hassan R, Zhang J, et al. Humoral immune response to mesothelin in mesothelioma and ovarian cancer patients. *Clin Cancer Res* 2005;11:3814–20.
- Thomas AM, Santarsiero LM, Lutz ER, et al. Mesothelin-specific CD8(+) T cell responses provide evidence of *in vivo* cross-priming by antigen-presenting cells in vaccinated pancreatic cancer patients. *J Exp Med* 2004;200:297–306.

Amplification of a chromatin remodeling gene, Rsf-1/HBXAP, in ovarian carcinoma

le-Ming Shih^{*†}, Jim Jinn-Chyuan Sheu^{*}, Antonio Santillan^{*}, Kentaro Nakayama^{*}, M. Jim Yen^{*}, Robert E. Bristow^{*}, Russell Vang^{*}, Giovanni Parmigiani^{*‡}, Robert J. Kurman^{*}, Claes G. Trope[§], Ben Davidson[§], and Tian-Li Wang^{*†}

^{*}Departments of Pathology, Gynecology, and Oncology, [‡]Department of Biostatistics, The Johns Hopkins University School of Medicine, Baltimore, MD 21231; and [§]Departments of Pathology and Gynecologic Oncology, Norwegian Radium Hospital, University of Oslo, Montebello, N-0310 Oslo, Norway

Edited by Bert Vogelstein, The Sidney Kimmel Comprehensive Cancer Center at Johns Hopkins, Baltimore, MD, and approved August 15, 2005 (received for review May 20, 2005)

A genomewide technology, digital karyotyping, was used to identify subchromosomal alterations in ovarian cancer. Amplification at 11q13.5 was found in three of seven ovarian carcinomas, and amplicon mapping delineated a 1.8-Mb core of amplification that contained 13 genes. FISH analysis demonstrated amplification of this region in 13.2% of high-grade ovarian carcinomas but not in any of low-grade carcinomas or benign ovarian tumors. Combined genetic and transcriptome analyses showed that Rsf-1 (HBXAPalpha) was the only gene that demonstrated consistent overexpression in all of the tumors harboring the 11q13.5 amplification. Patients with Rsf-1 amplification or overexpression had a significantly shorter overall survival than those without. Overexpression of Rsf-1 gene stimulated cell proliferation and trans-form nonneoplastic cells by conferring serum-independent and anchorage-independent growth. Furthermore, Rsf-1 gene knock-down inhibited cell growth in OVCAR3 cells, which harbor Rsf-1 amplification. Taken together, these findings indicate an important role of Rsf-1 amplification in ovarian cancer.

digital karyotyping | gene amplification | oncogene

Gene amplification is a common mechanism underlying oncogenic activation in human cancer (1). Amplifications of cyclin E, HER2/neu, AKT2, and L-Myc have been reported in ovarian cancer, and it is expected that many unknown oncogenic amplifications remain to be identified. Recent advances in molecular genetic techniques and the success of the human genome assembly have provided investigators new opportunities to explore cancer genome in great details and to identify novel cancer-associated genes. Digital karyotyping has recently been developed to provide a genomewide analysis of DNA copy number alterations at high resolution (2) and has been applied in cancer genetic studies (3–6). The principle of digital karyotyping is based on extracting and counting the 21-bp sequence tags that represent different loci in human genome. Populations of tags can be directly matched to the unique loci in genome assembly, and digital enumeration of tags provides quantitative measure of DNA copy number along chromosomes. The major advantage of digital karyotyping is that it directly counts the sequence tags, thus providing an unbiased and precise digital readout of DNA copy numbers. The current study has applied this new technology to search for DNA copy number alterations in high-grade ovarian serous carcinoma, the most common and lethal type of ovarian cancer.

Materials and Methods

Tissue Samples. Tissue samples were obtained from the Department of Pathology at The Johns Hopkins Hospital between 1990 and 2004. Effusion (peritoneal and pleural) samples were obtained from the Norwegian Radium Hospital in Norway. All ovarian carcinomas were of serous type from sporadic cases. Acquisition of tissue specimens and clinical information was approved by an institutional review board (The Johns Hopkins University) or by the Regional Ethics Committee (Norway).

Digital Karyotyping. Carcinoma cells were affinity purified by using magnetic beads conjugated with the Epi-CAM antibody (Dynal, Oslo). The purity of tumor cells was confirmed by immunostaining with an anti-cytokeratin antibody, CAM 5.2 (Becton Dickinson, San Jose, CA) and samples with greater than 95% epithelial cells were used in this study. Digital karyotyping library construction and data analysis were performed by following the protocol in refs. 2 and 3. Approximately 120,000 genomic tags were obtained for each digital karyotyping library. After removing the nucleotide repeats in the human genome, the average of filtered tags was 66,000 for each library. We set up a window size of 300 for the analysis in this study. Based on Monte Carlo simulation, the parameters used in this study can reliably detect >0.5-Mb amplicon with >5-fold amplification with >99% sensitivity and 100% positive predictive value.

FISH and Immunohistochemistry. Formalin-fixed, paraffin-embedded tissues were arranged onto tissue microarrays to facilitate FISH analysis. Three representative cores (1.5-mm diameter) from each tumor were placed on the tissue microarrays. Bacterial artificial chromosome clones containing the genomic sequences of the 11q13.5 amplicon at 77.05–77.23 Mb (RP11–1107J12) and EMSY at 75.88–76.09 Mb (CTD–2501F13) were purchased from Bacpac Resources (Children's Hospital Oakland, CA) and Invitrogen (Carlsbad, CA), respectively. The RP11–846G12 bacterial artificial chromosome clone, located at 11q11 (55.88–56.05 Mb), was used as the control probe. The method for FISH has been detailed in ref. 3. Two individuals who were not aware of the tumor grade and clinical information evaluated FISH signals. Approximately 100 tumor cells were examined for each specimen. Amplification of the Rsf-1 and EMSY genes was defined as a ratio of the gene probe signal to the control probe signal exceeding 2.

A mouse monoclonal anti-Rsf-1 antibody (gift from Danny Reinberg, University of Medicine and Dentistry of New Jersey, Piscataway, NJ) was used in the immunohistochemistry study. Immunohistochemistry was performed by standard protocol with an EnVision+System peroxidase kit (DAKO, Carpinteria, CA).

Quantitative Real-Time PCR. Real-time PCR for genomic DNA copy numbers and gene expression levels was performed by using methods described in ref. 7, and PCR primers were listed in the Tables 1 and 2, which are published as supporting information on the PNAS web site. PCR reactions were performed by using an iCycler (Bio-Rad, Hercules, CA). For quantitative PCR performed with genomic DNA, we used a cutoff ratio of 2.2 to define genomic amplification. This cutoff value was determined as the mean + 2 standard deviations based on quantitative PCR analyses of normal

This paper was submitted directly (Track II) to the PNAS office.

Abbreviations: OSE, ovarian surface epithelial; shRNA, short hairpin RNA; siRNA, short interfering RNA.

[†]To whom correspondence may be addressed. E-mail: tlw@jhmi.edu and shihie@yahoo.com.

© 2005 by The National Academy of Sciences of the USA

bly (July 2003 freeze, University of California, Santa Cruz) revealed that 13 genes were completely located within the minimal amplicon (Fig. 7, which is published as supporting information on the PNAS web site). EMSY gene, which has recently been reported as a candidate oncogene in breast and ovarian carcinomas, was located at 76 Mb (9), close to but outside the minimal region of the amplification (Fig. 1a). Two methods were used to validate the digital karyotyping results. First, dual-color FISH was performed to validate the 11q13.5 amplification in these three tumors by using a bacterial artificial chromosomes probe located at the 11q13.5 minimal amplicon (Fig. 7) and a control probe located at 11q11 (21 Mb centromeric to the minimal amplicon). As shown in Fig. 1b, we found that all three amplified tumors defined by digital karyotyping showed distinct 11q13.5 amplification. Second, quantitative real-time PCR was performed to measure the DNA copy numbers at 12 loci flanking and within the amplicon, including the EMSY gene in these three tumors (Fig. 1c). We found that increases in the DNA copy number were present at subchromosomal regions similar to the amplifications delineated by digital karyotyping. Furthermore, the fold of DNA copy number increase detected by quantitative PCR is at similar levels to that of digital karyotyping. A cutoff ratio of 2.2 was used to search for amplifications with >97.5% confidence, and the delineated common region of amplification (from Loc220032 locus to FLJ23441 locus) was consistent with that derived from digital karyotyping.

To determine the frequency of the 11q13.5 minimal amplicon, we performed dual-color FISH on 211 paraffin-embedded ovarian tissue specimens by using the FISH probe located at the minimal amplicon and the control FISH probe that is the same as described above (located on 11q11). The advantage of selecting the control FISH probe on the same chromosomal arm as the minimal amplicon is that it could facilitate distinguishing chromosome duplication from gene amplification, the latter involving smaller subchromosomal region (10). Using this method, we found 11q13.5 amplification in 16 of 121 (13.2%) high-grade serous carcinomas. In contrast, 11q13.5 gene amplification was not detected in any of 40 low-grade serous carcinomas, 14 serous borderline tumors, 19 benign cystadenomas, and 17 normal ovaries. Thus, 11q13.5 amplification was detected exclusively in high-grade serous carcinomas. Among the 16 tumors with 11q13.5 amplification, 5 cases showed a homogeneous staining region pattern, 3 cases showed a high level gain (>4.5-fold), and the remaining 8 tumors exhibited a moderate gain (between 2.5- and 4-fold). It should be noted that in addition to the 16 tumors with discrete amplification, we observed 11q polysomy in another 14 tumors based on an equal number of signals for both 11q13.5 and control probes. These tumors were not considered to have amplification specific to the 11q13.5 region in this study.

To further elucidate the physical relationship between EMSY and the minimal amplicon, we performed dual-color FISH in the same set of tumor samples by using EMSY probe and same control probe. We found that EMSY was amplified in 12 of 117 (10.3%) high-grade serous carcinomas that were available for analysis. All 12 EMSY amplified carcinomas also demonstrated amplification at 11q13.5 minimal amplicon. Conversely, 4 of the 16 carcinomas that contained 11q13.5 minimal region amplification did not harbor EMSY amplification (Fig. 8, which is published as supporting information on the PNAS web site). This result indicated that 11q13.5 minimal amplicon is more frequently amplified than its neighborhood region that contained EMSY gene in high-grade serous carcinomas.

Transcript Analysis of the 11q13.5 Minimal Amplicon. To identify the potential amplified oncogene within the 11q13.5 amplicon, we applied an approach based on the rationale that a tumor-driving gene, when amplified, almost always overexpresses to activate the tumorigenic pathway, whereas coamplified "passenger" genes that are unrelated to tumor development may or may not do so (10).

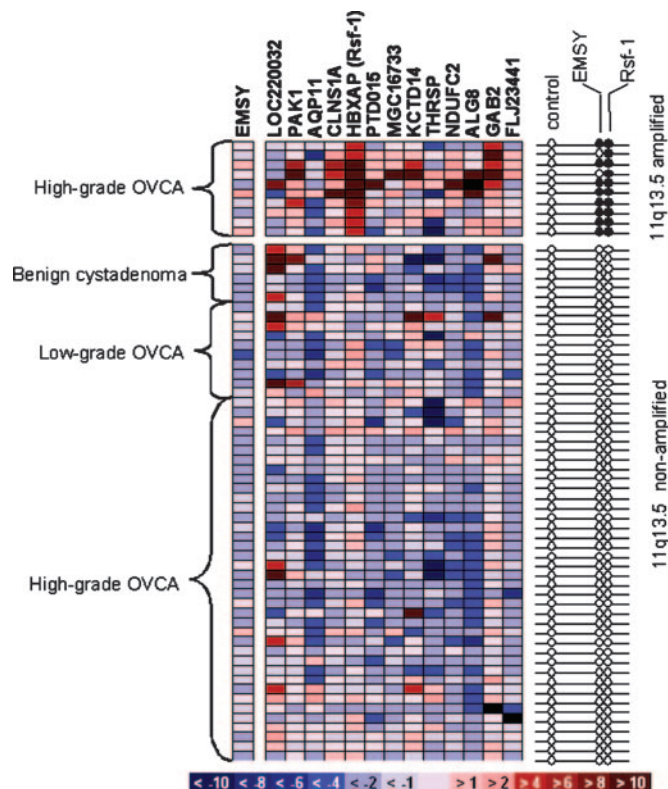


Fig. 2. Gene expression analysis of the 11q13.5 amplicon in ovarian tumors. Quantitative real-time PCR was performed for all 13 genes located within the minimal amplicon in benign cystadenomas, low-grade ovarian carcinomas and high-grade ovarian carcinomas with or without 11q13.5 amplification. The expression level of each gene (left to right: centromeric to telomeric) in individual specimen is shown as a pseudocolor gradient based on the relative expression level of a given specimen to the normal ovarian surface epithelium. (Right) The amplification status of Rsf-1, EMSY, and the 11q11 (control locus for FISH) for each specimen was determined by FISH analysis. Filled circles indicate amplification, and open circles indicate no amplification.

Therefore, we searched for genes with both DNA amplification and transcript up-regulation in the same tumor samples. Ten high-grade ovarian carcinomas that contained 11q13.5 amplification and had their frozen tissues available were analyzed by quantitative real-time PCR to assess mRNA levels in all of the genes within the minimal amplicon. The same assay was also performed in six benign cystadenomas, 10 serous borderline tumors, and 36 high-grade carcinomas that did not contain 11q13.5 amplification. Freshly brushed ovarian surface epithelium (kind gift from M. J. Birrer, National Cancer Institute, Rockville, MD), which has been considered as an appropriate normal control, was used for normalization of gene expression (11). We used the Wilcoxon test to compute and compare the difference in gene expression levels between 11q13.5 amplified versus nonamplified high-grade carcinomas. We found that among the genes within the minimal amplicon, Rsf-1 (HBXAP) had the most significant difference ($P = 8.5 \times 10^{-6}$) in expression levels between 11q13.5 amplified and nonamplified specimens. Furthermore, Rsf-1 was the only gene demonstrating consistent overexpression among the amplified tumors. Accordingly, Rsf-1 was prioritized for further characterization in this study. EMSY mRNA levels were also measured in parallel. We observed that although the EMSY gene was coamplified in eight of the tested samples, its RNA level was not consistently up-regulated as five of the tumors that harbored EMSY amplification down-regulated EMSY mRNA expression (Fig. 2).

Correlation of Rsf-1 Protein Overexpression and Gene Amplification. To demonstrate a more comprehensive correlation between Rsf-1 gene amplification and protein expression, we performed immu-

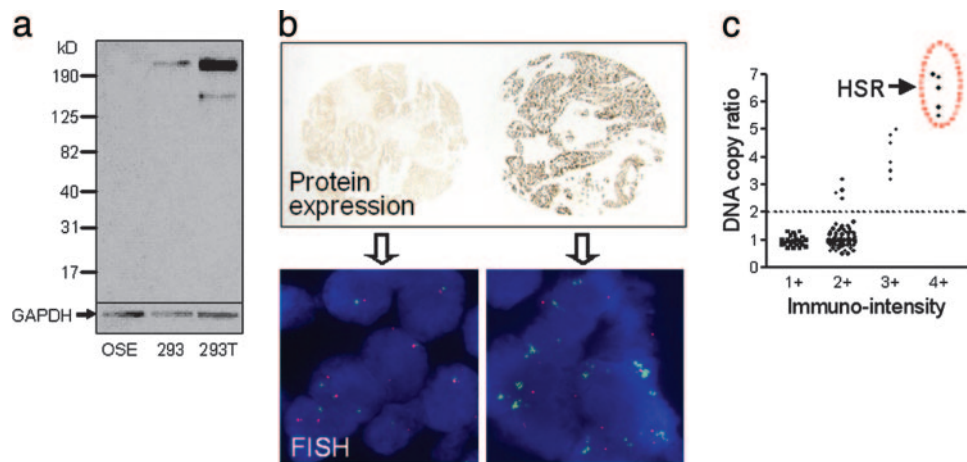


Fig. 3. Correlation of Rsf-1 DNA copy numbers and Rsf-1 protein expression in high-grade ovarian carcinomas. (a) The specificity of the anti-Rsf-1 antibody is demonstrated by Western blot analysis. 293, human embryonic kidney (HEK) 293 cells; 293T, HEK293 cells transfected with a full-length Rsf-1 gene. A predominant band of Rsf-1 protein at 215 kDa that represents the full-length Rsf-1 gene is detected in 293T cells. The faint lower band represents the degradation product of Rsf-1 protein. Endogenous Rsf-1 expression is also observed in 293 cells but not in OSE cells. (Lower) The GAPDH expression as the loading control. (b Left) A high-grade carcinoma shows weak Rsf-1 immunoreactivity (1+) and does not display Rsf-1 gene amplification. (Right) A high-grade tumor demonstrates an intense Rsf-1 immunoreactivity (4+) and displays Rsf-1 gene amplification. (c) Rsf-1 protein expression correlates with the Rsf-1 gene copy number in high-grade ovarian carcinomas. Tumors with the highest copy number of Rsf-1 DNA [manifested as homogenous staining regions (HSR)] express the highest level of Rsf-1 protein (4+). Tumors that lack Rsf-1 amplification demonstrate weak to moderate Rsf-1 immunoreactivity (1+ and 2+). Each dot represents an individual specimen. Among 16 amplified tumors, there are 15 available for immunohistochemistry.

nohistochemistry with an anti-Rsf-1 monoclonal antibody on the same panel of tissues used in FISH analysis. The specificity of the Rsf-1 monoclonal antibody has been demonstrated in ref. 12 and was independently confirmed in this study (Fig. 3a). Overall, there was a statistically significant correlation between Rsf-1 gene amplification and Rsf-1 immunoreactivity ($P < 0.001$, Spearman correlation). We found that 11q13.5 nonamplified tumors demonstrated either weak (1+, 21% of tumors) or moderate (2+, 74% of tumors) Rsf-1 immunoreactivity (Fig. 3b and c). In contrast, all of the tumors with Rsf-1 amplification demonstrated an immunointensity of 2+–4+, with the most intense immunoreactivity (4+) found in those with a homogeneous staining region pattern ($n = 5$) and a strong immunoreactivity (3+, $n = 6$) found in those with high-fold DNA gain (3- to 5-fold) (Fig. 3b and c). Four tumors with mild gain (2- to 3.5-fold) in the Rsf-1 DNA copy number demonstrated moderate immunointensity (2+), and, thus, they were similar to the majority of the high-grade tumors without Rsf-1 amplification. This finding is likely attributed to the semiquantitative nature inherent to immunohistochemistry in scoring mild to moderate immunointensity because such limitation in scoring Her2/neu immunointensity has been reported in ref. 13.

Clinical Significance of 11q13.5 Amplification and Rsf-1 Overexpression. Amplification of the Rsf-1 locus and Rsf-1 overexpression were correlated with clinical outcome in patients with high-grade ovarian serous carcinoma. Because the FISH probe used to assess 11q13.5 amplification contained the whole Rsf-1 coding region (Fig. 7), it allowed us to use the same FISH data and analyze the clinical significance of Rsf-1 amplification. A total of 107 of 121 patients were available for survival analysis. The other 14 tumors harboring chromosome 11q polysomy were excluded in the analysis because polysomy was considered as duplication of chromosomal arms or large genomic segments and could not simply be grouped to either Rsf-1 amplified or nonamplified cases.

We found that all 107 patients had advanced stage high-grade serous carcinomas (the majority at FIGO stage III). Among them, 16 patients who had Rsf-1 amplification in their tumors had a shorter overall survival compared with those without amplification ($P = 0.015$; Log-rank test) (Fig. 4a). The median overall survival was 29 months [95% confidence index (CI): 18.8–39.1 months] for the

amplified group and 36 months (95% CI: 24.3–47.7 months) for the nonamplified group. Quantitative real-time PCR was also used to measure Rsf-1 mRNA in tumor cell pellets from 53 effusion samples that were not feasible for FISH analysis. An arbitrary cutoff of the expression level (>2.4 fold compared with normal ovarian surface epithelium) was used to assign specimens to either high expression ($n = 11$) or low expression ($n = 42$) groups. The results indicated that high levels of Rsf-1 mRNA expression (>2.4 fold) were correlated with poor outcome ($P = 0.037$; Log-rank test) (Fig. 4b) with median overall survival of 19 months (95% CI: 14.5–23.6) in patients with Rsf-1 mRNA overexpression and 38 months (95% CI: 28.3–47.8) in patients without Rsf-1 mRNA overexpression. Rsf-1 amplification and overexpression appeared as independent prognostic factors based on a multivariate analysis adjusted for patient age, clinical stage, and differentiation status of tumor histology.

To further test whether the clinical significance of Rsf-1 amplification and overexpression depended on the arbitrary cutoffs, we performed a survival analysis by using continuous variables in a Cox proportional hazard model. The P values assessed by a likelihood

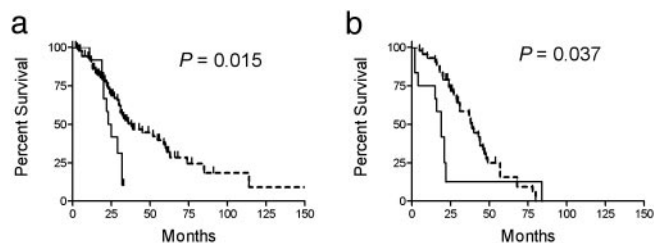


Fig. 4. Rsf-1 amplification and overexpression correlate with shorter overall survival in patients. (a) Kaplan–Meier survival analysis shows that Rsf-1 amplification (solid line, $n = 16$) is associated with a shorter overall survival compared with tumors without Rsf-1 amplification (dashed line, $n = 91$) ($P = 0.015$, Log-rank test). (b) Quantitative real-time PCR in effusion samples of ovarian high-grade serous carcinomas demonstrates that Rsf-1 overexpression (> 2.4 fold of normal ovarian surface epithelium; solid line; $n = 11$) correlates significantly with shorter overall survival than those with a low expression level (< 2.4 fold; dash line; $n = 42$) ($P = 0.037$, Log-rank test).

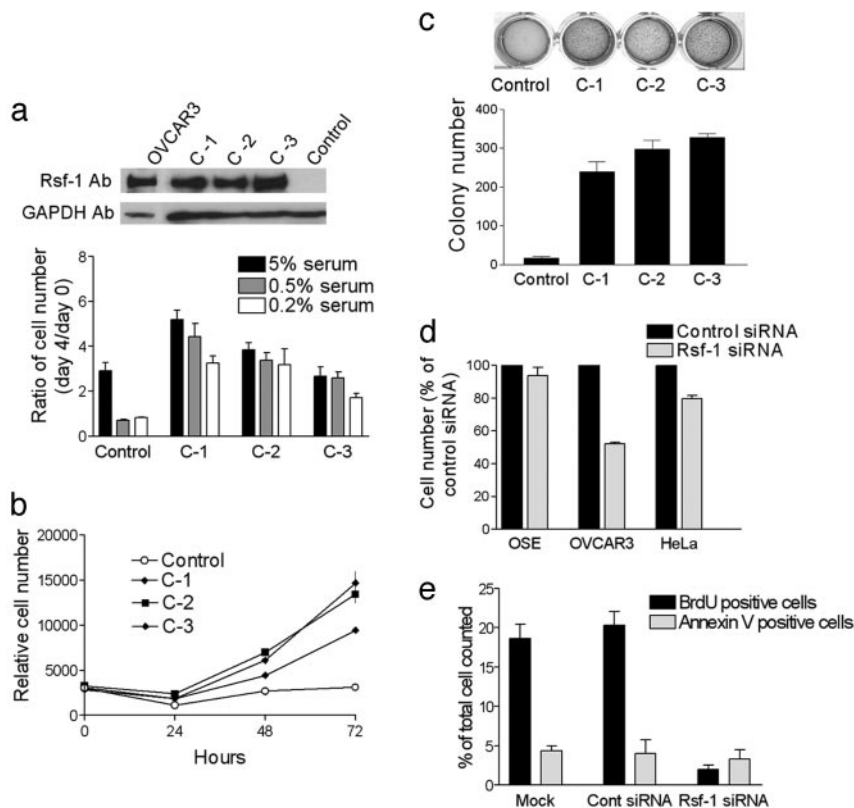


Fig. 5. Functional analyses of Rsf-1 expression. (a) Western blot analysis shows that Rsf-1-transfected RK3E clones (C-1, -2, and -3) express Rsf-1 protein with a predominant molecular mass of 215 kDa that is similar to the endogenous Rsf-1 protein expressed in OVCAR3 cells. Control RK3E cells, which are transfected with an empty vector, do not express Rsf-1 protein. As compared with the control RK3E cells, Rsf-1 clones continue proliferating at low serum concentrations (0.5% and 0.2%). (b) The Rsf-1 clones demonstrate a higher proliferative activity than the vector only control, as evidenced by a time-dependent increase in cell number at low (0.5%) serum-containing medium. (c) Anchorage-independent assay demonstrates that colonies observed in the Rsf-1 clones are more than those in the vector only control. (d) Effects of Rsf-1 gene knockdown. Knockdown of Rsf-1 significantly reduces cell number in OVCAR3 cells that harbor Rsf-1 amplification and in HeLa cells that express Rsf-1. In contrast, Rsf-1 siRNA has only a minimal effect on cell growth in OSE cells that do not express detectable Rsf-1. (e) Rsf-1 targeting siRNA reduces cell proliferation as measured by the percentage of BrdUrd-positive cells but not in control siRNA or in nontreated (mock control) OVCAR3 cells. The percentage of apoptotic cells as measured by annexin V staining is similar among Rsf-1 siRNA, control siRNA, and nontreated OVCAR3 cells.

ratio test were 0.025 for FISH assay and 0.0013 for real-time PCR. These results further indicated that Rsf-1 amplification and overexpression were significantly correlated with poor survival, independent of the cutoffs.

In this study, we further compared the statistical significance in correlating gene amplification and overexpression with overall survival of Rsf-1 gene to those of EMSY gene. For gene amplification, Rsf-1 had a more significant *P* value than that of EMSY (0.015 vs. 0.08). Similarly, for gene expression, Rsf-1 expression also had a more significant *P* value than EMSY expression by using a low stringent cutoff value of >1-fold (0.037 vs. 0.153).

Functional Analyses of Rsf-1 Expression. We therefore stably expressed the Rsf-1 gene in the nonneoplastic epithelial cells, RK3E, to assess whether Rsf-1 expression induced transformation (*Supporting Methods*, which is published as supporting information on the PNAS web site). RK3E cells have been used to evaluate the oncogenic potential of GL1, c-Myc, and mutant β -catenin and were considered as an appropriate *in vitro* model for oncogenic transformation (14–16). Using quantitative real-time PCR, we found that ovarian serous carcinomas predominantly expressed the full-length form of the Rsf-1 gene (or HBXAPa), therefore RK3E cells were transfected with a vector expressing the full-length Rsf-1, and three independent clones were randomly selected for functional analyses. Western blot analysis confirmed the Rsf-1 expression in these clones (Fig. 5a). All of the Rsf-1-expressing clones proliferated better at very low (0.2% and 0.5%) serum concentrations and showed a higher proliferative activity than control RK3E cells (transfected with vector alone) based on increased cell numbers (Fig. 5a and b) and BrdUrd incorporation (data not shown). Rsf-1-expressing clones grew anchorage independently as more colonies were observed in Rsf-1-expressing cells than in control cells (Fig. 5c). All of the above differences were of statistical significance ($P < 0.001$, *t* test).

To further determine whether Rsf-1 expression was essential for

cell survival in cell lines that overexpress Rsf-1, we used RNA interference to knock down Rsf-1 expression in three cell lines, including OVCAR3 cells (with Rsf-1 amplification and overexpression), HeLa cells (without amplification but with Rsf-1 expression), and ovarian surface epithelial (OSE; without Rsf-1 amplification or expression) cells. The effect of Rsf-1 siRNA in suppressing Rsf-1 expression was confirmed by quantitative real-time PCR (Fig. 9, which is published as supporting information on the PNAS web site). Reduction of Rsf-1 expression significantly inhibited cell growth in Rsf-1-expressing cells, including OVCAR3 and HeLa cells (Fig. 5d, $P < 0.001$, *t* test), with a more prominent inhibitory effect in Rsf-1 amplified OVCAR3 cells. In contrast, the same treatment did not affect cell growth in OSE cells, which had minimal Rsf-1 expression ($P = 0.26$, *t* test). The inhibition of cell growth after repressing Rsf-1 expression in OVCAR3 was likely a result of growth suppression as the percentage of BrdUrd-labeled cells was significantly decreased in Rsf-1 siRNA-treated cells as compared with control siRNA-treated OVCAR3 cells (Fig. 5e, $P < 0.001$). In contrast, the percentage of apoptotic cells as measured by annexin V staining was similar between the Rsf-1 siRNA and control groups. To extend the findings of Rsf-1 gene knockdown *in vitro*, we transfected OVCAR3 cells with Rsf-1 short hairpin RNA (shRNA) before injecting the cells into nude mice (*Supporting Methods*). Western blot analysis demonstrated that Rsf-1 expression was substantially reduced in Rsf-1 shRNA-transfected OVCAR3 cells as compared with the control shRNA-transfected cells (Fig. 10, which is published as supporting information on the PNAS web site). All mice injected with Rsf-1 shRNA-treated OVCAR3 cells develop much smaller intraabdominal xenograft tumors than the mice carrying control (scramble) shRNA-transfected cells (Fig. 10, $P < 0.001$, $n = 5$).

Discussion

This study provides cogent evidence that amplification of Rsf-1 within the 11q13.5 minimal amplicon is involved in ovarian

tumorigenesis based on a comprehensive study including molecular genetics, transcriptome analysis, clinical correlation, and functional characterization. Chromosome 11q13.5 amplification is one of the most frequently amplified regions in human tumors including ovarian, breast, head, and neck carcinomas. The frequency of 11q13.5 amplification in ovarian carcinoma detected in this study (13.2%) is similar to but slightly lower than that previously reported (17%) (9). This result is likely due to more stringent criteria used for FISH analysis in the current study. For example, we have used a reference probe on chromosome 11q arm instead of on chromosome 11 centromere to exclude cases that belong to polysomy or large segment duplication. It should be noted that EMSY was located near the minimal amplicon delineated in the current study. EMSY functions as a BRAC2-interacting gene and was previously thought of as a candidate oncogene for ovarian cancers (9). However, the oncogenic property of EMSY in ovarian tumor was not demonstrated in that study. Furthermore, our findings with a larger scale of ovarian tumor samples did not demonstrate a significant correlation of EMSY gene amplification and mRNA overexpression, a finding arguing against EMSY as the “driver” gene within the amplicon.

Based on our combined genetic and expression analyses, we have found that Rsf-1 is consistently overexpressed in all of the amplified tumors examined. In addition to Rsf-1, several other genes close to Rsf-1, including CLNS1A, ALG8, and GAB2, were co-up-regulated in a subset of tumors with 11q13.5 amplification. It would be interesting in the future to determine whether cooverexpression of these genes would further provide growth advantages in the development of ovarian cancer. The association of Rsf-1 amplification/overexpression with worse survival in ovarian cancer patient is similar to oncogenes, including HER2/neu in breast cancer (17, 18) and N-myc in neuroblastoma (19), in which overexpression of both oncogenes stimulates cell proliferation and confers a shorter survival. The mechanism of how Rsf-1 amplification contributes to shorter survival is not known; however, because the mortality of ovarian cancer patients is directly related to the recurrent disease after chemotherapy, it is conceivable that Rsf-1 amplification may

confer drug resistance and/or enhance cell proliferation in the chemoresistant recurrent tumors.

Our study with gene overexpression and RNA interference knockdown has established an important functional role of Rsf-1 in ovarian cancer. How can Rsf-1 contribute to tumor progression at the molecular level? Recent *in vitro* studies have indicated that Rsf-1 plays a role in chromatin remodeling (12) and transcriptional regulation (20, 21) that may contribute to tumorigenesis. Rsf-1 has been shown to function as a histone chaperone, whereas its binding partner, hSNF2H, possesses nucleosome-dependent ATPase activity. The Rsf-1/hSNF2H complex (or RSF complex) participates in chromatin remodeling by mobilizing nucleosomes in response to a variety of growth modifying signals and environmental cues. Such nucleosome remodeling is essential for transcriptional activation or repression (22), DNA replication (23), and cell cycle progression (24). Recently, a growing body of evidences has accumulated to support a novel role of chromatin remodeling in cancer (25, 26). For example, mutations and deletions of a hSNF2H homolog, Brg1, were found in different tumor types (27), and furthermore, heterozygous deletion of Brg1 in mice resulted in a cancer-prone phenotype (28, 29). It is plausible that Rsf-1 gene amplification and overexpression in tumor cells could disrupt the homeostatic kinetics in the chromatin remodeling machinery and fine tune gene regulation that facilitates tumorigenesis. Because the current study identifies and characterizes the previously undescribed Rsf-1 gene amplification in ovarian cancer, further studies are required to elucidate the etiological roles of Rsf-1 amplification and overexpression in chromatin remodeling and cancer development.

We thank Dr. M. J. Birrer for the brushed normal ovarian epithelium; Dr. D. Reinberg for the full-length Rsf-1 clone and the anti-Rsf-1 antibody; Drs. M. Shamay and Y. Shaul for the help at the initial stage of this study; Dr. Z. Wang and other members in the Molecular Genetic Laboratory for critical reading of the manuscript; and M. Skrede and Dr. Y.-W. Kim for technical assistance. This work was supported by U.S. Department of Defense Grants OC0400600 and OC010017, National Institutes of Health Grant R01 CA103937, and grants from The Alexander and Margaret Stewart Trust fund and The Richard TeLinde Endowed Fund.

- Meltzer, P. S., Kallioniemi, A. & Trent, J. M. (2002) in *The Genetic Basis of Human Cancer*, eds. Vogelstein, B. & Kinzler, K. W. (McGraw-Hill, New York), pp. 93–113.
- Wang, T.-L., Maierhofer, C., Speicher, M. R., Lengauer, C., Vogelstein, B., Kinzler, K. W. & Velculescu, V. E. (2002) *Proc. Natl. Acad. Sci. USA* **99**, 16156–16161.
- Wang, T.-L., Diaz, L. A., Jr., Romans, K., Bardelli, A., Saha, S., Galizia, G., Choti, M., Donehower, R., Parmigiani, G., Shih, I.-M., *et al.* (2004) *Proc. Natl. Acad. Sci. USA* **101**, 3089–3094.
- Di, C., Liao, S., Adamson, D. C., Parrett, T. J., Broderick, D. K., Shi, Q., Lengauer, C., Cummins, J. M., Velculescu, V. E., Fufts, D. W., *et al.* (2005) *Cancer Res.* **65**, 919–924.
- Hu, M., Yao, J., Cai, L., Bachman, K. E., van den Brule, F., Velculescu, V. & Polyak, K. (2005) *Nat. Genet.* **37**, 899–905.
- Boon, K., Eberhart, C. G. & Riggins, G. J. (2005) *Cancer Res.* **65**, 703–707.
- Buckhaults, P., Zhang, Z., Chen, Y. C., Wang, T.-L., St. Croix, B., Saha, S., Bardelli, A., Morin, P. J., Polyak, K., Hruban, R. H., *et al.* (2003) *Cancer Res.* **63**, 4144–4149.
- Shih, I.-M., Yu, J., He, T. C., Vogelstein, B. & Kinzler, K. W. (2000) *Cancer Res.* **60**, 1671–1676.
- Hughes-Davies, L., Huntsman, D., Ruas, M., Fuks, F., Bye, J., Chin, S. F., Milner, J., Brown, L. A., Hsu, F., Gilks, B., *et al.* (2003) *Cell* **115**, 523–535.
- Hogarty, M. D. & Brodeur, G. M. (2002) in *The Genetic Basis of Human Cancer*, eds. Vogelstein, B. & Kinzler, K. W. (McGraw-Hill, New York), pp. 115–128.
- Zorn, K. K., Jazaeri, A. A., Awtrey, C. S., Gardner, G. J., Mok, S. C., Boyd, J. & Birrer, M. J. (2003) *Clin. Cancer Res.* **9**, 4811–4818.
- Loyola, A., Huang, J.-Y., LeRoy, G., Hu, S., Wang, Y.-H., Donnelly, R. J., Lane, W. S., Lee, S.-C. & Reinberg, D. (2003) *Mol. Cell. Biol.* **23**, 6759–6768.
- Hicks, D. G. & Tubbs, R. R. (2005) *Hum. Pathol.* **36**, 250–261.
- Ruppert, J. M., Vogelstein, B. & Kinzler, K. W. (1991) *Mol. Cell. Biol.* **11**, 1724–1728.
- Foster, K. W., Ren, S., Louro, I. D., Lobo-Ruppert, S. M., McKie-Bell, P., Grizzle, W., Hayes, M. R., Broker, T. R., Chow, L. T. & Ruppert, J. M. (1999) *Cell Growth Differ.* **10**, 423–434.
- Kolligs, F. T., Hu, G., Dang, C. V. & Fearon, E. R. (1999) *Mol. Cell. Biol.* **19**, 5696–5706.
- Borg, A., Tandon, A. K., Sigurdsson, H., Clark, G. M., Ferno, M., Fuqua, S. A., Killander, D. & McGuire, W. L. (1990) *Cancer Res.* **50**, 4332–4337.
- Tsuda, H., Hirohashi, S., Shimosato, Y., Hirota, T., Tsugane, S., Yamamoto, H., Miyajima, N., Toyoshima, K., Yamamoto, T., Yokota, J., *et al.* (1989) *Cancer Res.* **49**, 3104–3108.
- Rubie, H., Hartmann, O., Michon, J., Frappaz, D., Coze, C., Chastagner, P., Baranzelli, M. C., Plantaz, D., Avet-Loiseau, H., Benard, J., *et al.* (1997) *J. Clin. Oncol.* **15**, 1171–1182.
- Shamay, M., Barak, O., Doitsh, G., Ben-Dor, I. & Shaul, Y. (2002) *J. Biol. Chem.* **277**, 9982–9988.
- Shamay, M., Barak, O. & Shaul, Y. (2002) *Genomics* **79**, 523–529.
- Vignali, M., Hassan, A.H., Neely, K. E. & Workman, J. L. (2000) *Mol. Cell. Biol.* **20**, 1899–1910.
- Flanagan, J. F. & Peterson, C. L. (1999) *Nucleic Acids Res.* **27**, 2022–2028.
- Cosma, M. P., Tanaka, T. & Nasmyth, K. (1999) *Cell* **97**, 299–311.
- Wolffe, A. P. (2001) *Oncogene* **20**, 2988–2990.
- Klochendler-Yeivin, A., Muchardt, C. & Yaniv, M. (2002) *Curr. Opin. Genet. Dev.* **12**, 73–79.
- Wong, A. K., Shanahan, F., Chen, Y., Lian, L., Ha, P., Hendricks, K., Ghaffari, S., Iliiev, D., Penn, B., Woodland, A. M., *et al.* (2000) *Cancer Res.* **60**, 6171–6177.
- Klochendler-Yeivin, A., Fiette, L., Barra, J., Muchardt, C., Babinet, C. & Yaniv, M. (2000) *EMBO Rep.* **1**, 500–506.
- Guidi, C. J., Sands, A. T., Zambrowicz, B. P., Turner, T. K., Demers, D. A., Webster, W., Smith, T. W., Imbalzano, A. N. & Jones, S. N. (2001) *Mol. Cell. Biol.* **21**, 3598–3603.

Short Communication

Diverse Tumorigenic Pathways in Ovarian Serous Carcinoma

Gad Singer*, Robert J. Kurman,*†
Hsueh-Wei Chang,* Sarah K.R. Cho,* and
Ie-Ming Shih*

From the Departments of Pathology* and Gynecology and
Obstetrics,† The Johns Hopkins University School of Medicine,
Baltimore, Maryland

This study was undertaken to analyze genetic alterations in 108 sporadic serous ovarian neoplasms to elucidate ovarian serous carcinogenesis. Our results demonstrate that K-ras mutations occur in approximately 50% of serous borderline tumors (SBTs), non-invasive micropapillary serous carcinomas (MPSCs), and invasive micropapillary serous carcinomas, which represent a morphological continuum of tumor progression. Moreover, progressive increase in the degree of allelic imbalance of chromosomes 1p, 5q, 8p, 18q, 22q, and Xp was observed comparing serous borderline tumors to noninvasive and invasive micropapillary serous carcinomas. In contrast, high-grade (conventional serous carcinoma) tumors contained wild-type K-ras in all 23 cases studied and a high frequency of allelic imbalance even in small (early) primary tumors similar to that found in advanced stage tumors. Based on these findings, we propose a dualistic model for ovarian serous carcinogenesis. One pathway involves a stepwise progression from SBT to noninvasive and then invasive MPSC. The other pathway is characterized by rapid progression from the ovarian surface epithelium or inclusion cysts to a conventional (high-grade) serous carcinoma. (*Am J Pathol* 2002, 160:1223–1228)

Serous carcinoma is the most common type of ovarian cancer and is the most lethal gynecologic malignancy. Delineation of the molecular pathways involved in the evolution of ovarian serous carcinoma would have profound impact on our understanding of its pathogenesis thereby providing a rational basis for the development of new diagnostic tests and therapeutic strategies. Despite considerable efforts aimed at elucidating the molecular mechanisms of ovarian serous carcinoma, its pathogen-

esis is still poorly understood¹ largely because of the lack of an established model for its development. At present, the most widely held view is that ovarian serous carcinoma consists of a relatively homogeneous group of neoplasms that arise directly from transformation of the ovarian surface epithelium or inclusion cysts through a *de novo* process², since definitive precursor lesions have not been detected. Our recent clinical and histopathological studies of a large series of serous neoplasms^{3–5} have led to the recognition of a variant of serous carcinoma, designated “micropapillary serous carcinoma” (MPSC) with distinctive histopathological and clinical features. Most MPSCs are noninvasive and are frequently associated with serous borderline tumors (SBTs) also referred to as atypical proliferative serous tumors, a benign form of serous neoplasms.⁵ Histological transitions from SBTs to noninvasive MPSCs can be observed as well as areas of infiltrative growth (stromal invasion) immediately adjacent to the MPSC component of these neoplasms (Figure 1A). The morphology of the invasive component resembles that of the noninvasive MPSC and can also be seen in frankly invasive low-grade serous carcinomas. We have designated such tumors as invasive MPSCs.³ Thus, these neoplasms appear to represent a morphological spectrum ranging from a benign proliferative tumor (SBT or atypical proliferative serous tumor) through a noninvasive carcinoma (noninvasive MPSC) to a low-grade invasive carcinoma (invasive MPSC). Our preliminary clinical data indicate that MPSCs (both noninvasive and invasive) generally pursue an indolent course. The frequency of MPSC in the general population is not known, but data from our referral material and a population-based study of noninvasive MPSCs⁶ suggest that the prevalence is around 20 to 25% of all ovarian serous tumors. In contrast to invasive MPSCs, conventional serous carcinomas present as high-grade, aggressive neoplasms that evolve rapidly (Figure 1B). The aim of this study was to

Supported by the Richard TeLinde Research Endowment from the Department of Gynecology and Obstetrics and the American Cancer Society, and The Johns Hopkins University School of Medicine. Gad Singer was supported by the Swiss National Science Foundation.

Accepted for publication January 2, 2002.

Address reprint requests to Ie-Ming Shih, M.D., Ph.D., 418 N. Bond St., B-315, Baltimore, MD 21231. E-mail: ishih@jhmi.edu.

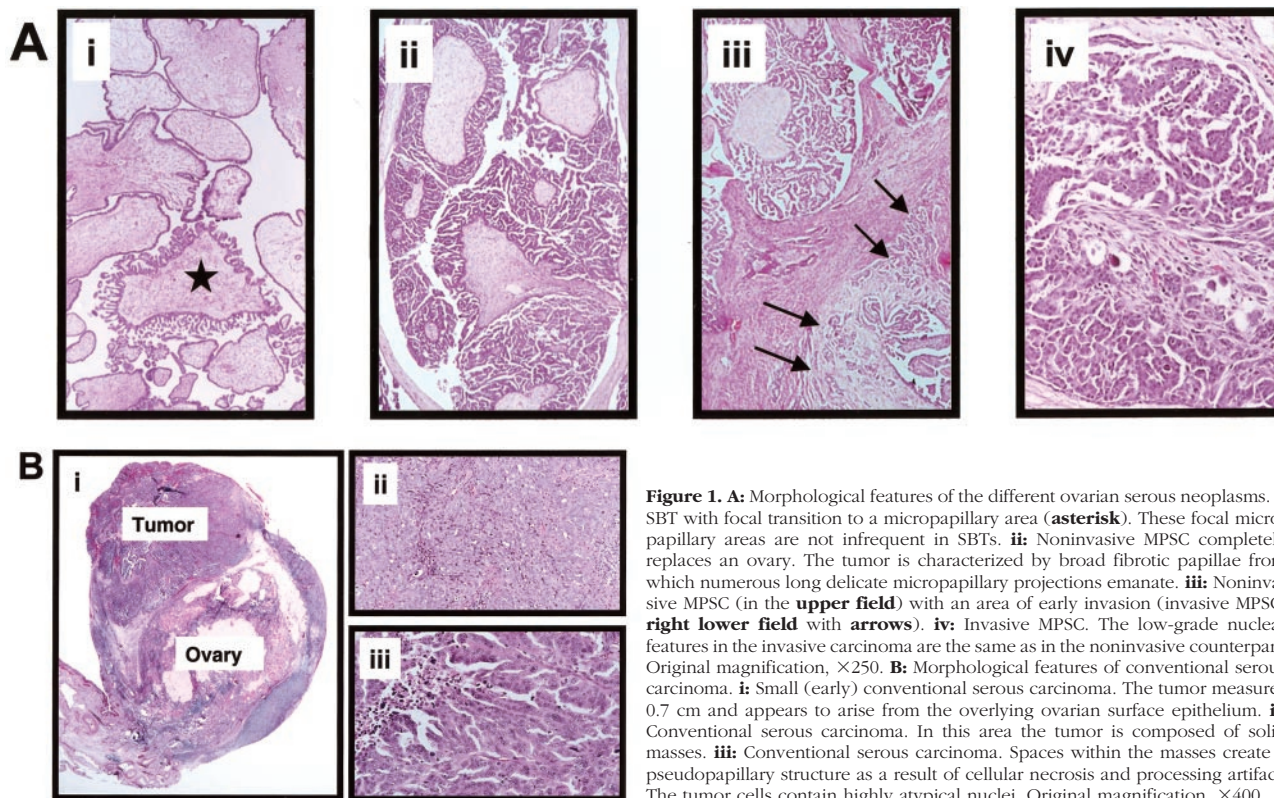


Figure 1. A: Morphological features of the different ovarian serous neoplasms. **i:** SBT with focal transition to a micropapillary area (asterisk). These focal micropapillary areas are not infrequent in SBTs. **ii:** Noninvasive MPSC completely replaces an ovary. The tumor is characterized by broad fibrotic papillae from which numerous long delicate micropapillary projections emanate. **iii:** Noninvasive MPSC (in the upper field) with an area of early invasion (invasive MPSC; right lower field with arrows). **iv:** Invasive MPSC. The low-grade nuclear features in the invasive carcinoma are the same as in the noninvasive counterpart. Original magnification, $\times 250$. **B:** Morphological features of conventional serous carcinoma. **i:** Small (early) conventional serous carcinoma. The tumor measures 0.7 cm and appears to arise from the overlying ovarian surface epithelium. **ii:** Conventional serous carcinoma. In this area the tumor is composed of solid masses. **iii:** Conventional serous carcinoma. Spaces within the masses create a pseudopapillary structure as a result of cellular necrosis and processing artifact. The tumor cells contain highly atypical nuclei. Original magnification, $\times 400$.

analyze the molecular genetic changes including K-ras mutation and allelic status of different chromosomes in these morphologically distinct ovarian serous neoplasms.

There are a variety of problems associated with traditional mutational analysis and determination of allelic status in ovarian serous tumors. These include abundant stromal contamination in tumors which can obscure tumor-associated genetic changes (Figure 1A), artifactual enrichment for one allele due to limited amounts of DNA purified from microdissected lesions, and DNA degradation of the larger microsatellite alleles which can confound the analysis of allelic status when microsatellite markers and paraffin tissue are used.⁷ To overcome these problems, we used a newly developed technique termed digital polymerase chain reaction (PCR) analysis, in which alleles (wild-type/mutant alleles or maternal/paternal alleles) are directly and precisely counted, one by one.⁸⁻¹¹ A rigorous statistical method is then used to conclude whether mutation or allelic imbalance is present in the background of normal DNA.⁸⁻¹¹

Materials and Methods

Tissues and Tumor DNA Samples

Formalin-fixed, paraffin-embedded tissue samples of 108 ovarian serous tumors were used for molecular genetic analysis. These cases were randomly retrieved from the surgical pathology files of The Johns Hopkins Hospital, Baltimore, Maryland and the consultation files of one of the authors (R.J.K.). All of the cases were re-reviewed by

three gynecological pathologists who concurred with the diagnoses before microdissection. We did not identify "well differentiated" non-MPSC among the serous carcinomas in this study. So called "moderately differentiated" serous carcinomas showed high-grade nuclear features and were included with "poorly differentiated" carcinomas as conventional serous carcinomas. The specimens included 24 SBTs (5 stage I, 8 stage II, and 11 stage III), 39 noninvasive MPSCs (16 stage I, 8 stage II, and 15 stage III), 22 invasive MPSCs (1 stage I, 1 stage II, 19 stage III, and 1 stage IV) and 23 conventional high-grade serous carcinomas (1 stage I, 2 stage II, 16 stage III, and 4 stage IV). The tumor areas and adjacent normal tissues were microdissected under an inverted microscope with the contamination from non-neoplastic cells estimated at 20 to 50% in the microdissected tumor component. DNA was purified and analyzed for mutational status of K-ras gene and allelic imbalance using digital PCR-based techniques.

Digital Single Nucleotide Polymorphism Analysis for Allelic Imbalance

We used digital single nucleotide polymorphism (SNP) analysis to assess allelic status in tumors since this new method provides a reliable and quantitative measure of the proportion of variant sequences within a mixed DNA sample as always occurs in serous tumors. To perform digital SNP analysis, SNP markers on the chromosomes 1p, 5q, 8p, 18q, 22q and Xp were retrieved from the

Table 1. Analysis of K-Ras Mutations and Allelic Imbalance in Serous Ovarian Neoplasms

Histological pattern	K-ras	Chromosome					
		1p	5q	8p	18q	22q	Xp
SBTs (<i>n</i> = 24)	12/24 (50)	1/22 (4)	4/24 (17)*	2/19 (10)	7/24 (29)	9/20 (45)	9/15 (60)
MPSCs (<i>n</i> = 39)	14/39 (36)	5/38 (13) [†]	21/38 (55)*	10/37 (27)	17/39 (44)	15/30 (50)	14/27 (52)
Invasive MPSCs (<i>n</i> = 22)	12/22 (54)	11/20 (55) [†]	11/17 (65)	8/21 (38)	8/19 (42)	10/16 (62)	10/17 (59)
CSCs (<i>n</i> = 23)	0/23 (0)	15/21 (71)	20/23 (87)	18/22 (81)	14/22 (64)	13/19 (68)	7/16 (43)

The frequency of K-ras mutations (%) and allelic imbalance (%) in SBTs, noninvasive MPSCs, invasive MPSCs, and CSCs are shown. *, †, Differences with statistical significance (*, *P* < 0.02 and †, *P* < 0.01; Student's *t* test and Mann-Whitney Rank-Sum test).

National Cancer Institute SNP map (<http://lpg.nci.nih.gov/html-snp/imagemaps.html>). These chromosomal arms were selected based on their frequent losses in serous carcinomas as previously reported.^{12–15} SNP markers within a 10 centiMorgan interval were selected from each chromosomal arm. Using these markers, we were able to find at least one heterozygous SNP for each chromosomal arm in most specimens studied.

Digital SNP analysis was performed as previously described^{9–11} with modification. In brief, DNA concentrations in the samples were first measured by the PicoGreen dsDNA quantitation kit (Molecular Probes, Eugene, OR) following the manufacturer's instructions to determine the amount of DNA to be included. DNA samples were diluted and distributed in the wells of a 384-well plate at approximately one genomic equivalent per two wells. In addition to all essential PCR reagents, the PCR cocktail contained a pair of molecular beacons (Gene Link, Thornwood, NY) along with an excess of reverse primer that allowed the generation of single-stranded DNA complementary to the molecular beacons. PCR was performed in a single step using the following protocol: 94°C (1 minute); 4 cycles of 94°C (15 seconds), 64°C (15 seconds), 70°C (15 seconds); 4 cycles of 94°C (15 seconds), 61°C (15 seconds), 70°C (15 seconds); 4 cycles of 94°C (15 seconds), 58°C (15 seconds), 70°C (15 seconds); 60 cycles of 94°C (15 seconds), 55°C (15 seconds), 70°C (15 seconds); 94°C (1 minute) and 60°C (5 minutes). The fluorescence intensity in each well was then measured in a Galaxy FLUOstar fluorometer (BMG Lab Technologies, Durham, NC) and the number of specific alleles in each sample was directly determined from the fluorescence measurements.

Digital PCR Analysis for K-ras Mutations

K-ras mutations at codon 12 and 13 were analyzed using digital PCR and molecular beacons as described in previous reports.^{8,16}

Statistical Analysis

To determine whether there was statistical significance for allelic imbalance, we used the Sequential Probability Ratio test.^{9,10} An allelic imbalance index was determined for each tumor as the number of chromosomal arms with allelic imbalance divided by the total number of chromosomal arms with informative markers. Differences between the allelic imbalance index in different groups and

the percentage of allelic imbalance in individual chromosomal arms in different groups were tested using the Student's *t*-test and the Mann-Whitney rank-sum test as appropriate. The correlation between tumor size in different groups and allelic imbalance index was assessed using Spearman's rank-order correlation.

Results

K-ras mutations in codon 12 or 13 were found in 50% of SBTs, 36% of noninvasive, and 54% of invasive MPSCs (Table 1). In contrast, K-ras mutations were not found in any of the 23 conventional (high-grade) serous carcinomas examined.

Comparing SBTs to noninvasive and invasive MPSCs (Table 1 and Figure 2), revealed an increased allelic imbalance index in the progression from SBT to noninvasive MPSC (*P* < 0.01) and to invasive MPSC (*P* < 0.02). In particular, allelic imbalance of chromosome 5q was more frequently observed in noninvasive MPSCs compared to SBTs (*P* < 0.02) and allelic imbalance of chromosome 1p was more frequently found in invasive MPSCs compared to noninvasive MPSCs (*P* < 0.01). Identical allelic imbalance patterns and K-ras mutations were found in the areas of SBT and noninvasive MPSC, or in the areas of

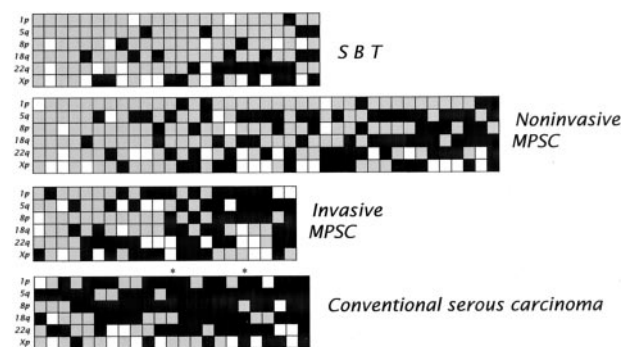


Figure 2. Summary of the results of allelic status in ovarian serous tumors. Each panel represents a group of serous tumors: SBT, noninvasive MPSC, invasive MPSC, and conventional serous carcinoma. Chromosomal arms in which the SNP markers are located are indicated on the left of each panel. In the vertical columns, each column represents one case. Black squares represent chromosomal arms in which allelic imbalance is identified based on the digital SNP analysis, while gray squares represent chromosomal arms in which both alleles were in balance. Blank squares indicate chromosomal arms that cannot be evaluated because the allelic ratio in the SPRT analysis does not achieve a statistical significant difference or because all SNP markers tested are uninformative in the normal tissue. The very small conventional serous carcinomas (maximal dimension 0.6 and 0.7 cm) are marked with asterisks.

Table 2. K-ras Mutational Status and Allelic Imbalance in Bilateral Noninvasive and Invasive MPSCs

	Case no.															
	1R	1L	2R	2L	3R	3L	4R	4L	5R	5L	6R	6L	7R	7L	8R	8L
K-ras status (codon with mutation)	wt	GCT (12)	GAT (12)	IGC (13)	wt	GAT (12)	IGT (12)	wt	wt	wt	AGC (13)	GAT (12)	wt	wt	wt	wt
Allelic imbalance	5q 18q Xp	5q 18q 22q	1p 5q 18q 22q Xp	8p 18q	5q 8p	5q 18q	5q 18q	5q 18q	22q Xp	Xp	5q 22q	5q 18q	22q	18q Xp	1p 5q	5q 18q 8p 18q Xp
	Case no.															
	9R	9L	10R	10L	11R	11L	12R	12L	13R	13L	14R	14L	15R	15L	16R	16L
K-ras status	wt	wt	IGT (12)	wt	AGC (13)	wt	GAC (13)	wt	GAC (13)	GAC (13)	wt	GAC (13)	wt	wt	wt	wt
Allelic imbalance	No	8p 22q	1p 8p 22q	18q 22q Xp	5q 18q 22q	5q 8p 22q	5q 18q 22q Xp	5q 8p 18q 22q	1p Xp	1p Xp	1p	1p 8p 22q	22q Xp	5q 22q Xp	5q 18q 22q Xp	5q 22q Xp

Corresponding case numbers indicate the same patients. Noninvasive MPSCs are the cases 1 to 11, invasive MPSCs are the cases 12 to 16. R, right; L, left; no, no allelic imbalance.

noninvasive and invasive MPSC in the 34 tumors containing two components representing stages in progression (SBTs and noninvasive MPSCs or noninvasive and invasive MPSCs). There was no correlation between the allelic imbalance index and the size of the tumors in the different groups. Conventional serous carcinomas showed a high level of allelic imbalance in almost all of the investigated tumors irrespective of their size (Figure 2).

Sixteen patients with noninvasive MPSCs (cases 1 to 11) and invasive MPSCs (cases 12 to 16) presented with tumors in both ovaries. These bilateral tumors were of similar size and had a similar gross and microscopic appearance. Comparison of the tumors involving both ovaries in these patients revealed that 15 (94%) of 16 had a discordant pattern of K-ras mutation or allelic imbalance (Table 2).

Discussion

By stratifying ovarian serous carcinomas into two histopathologically distinct groups, a low-grade carcinoma designated invasive micropapillary serous carcinoma with its putative precursors (SBT and noninvasive MPSC), and a high-grade carcinoma (conventional serous carcinoma), we were able to demonstrate that these neoplasms displayed very different and characteristic molecular genetic alterations.

First, K-ras mutations were found in nearly half of the invasive MPSCs and their putative precursors, but not in conventional serous carcinoma, suggesting that aberration in the K-ras signaling pathway may play an important role in the development of invasive MPSC. Previous studies of K-ras mutations in SBTs and ovarian serous carcinomas have differed in their findings and interpretation. Some have detected K-ras mutations in SBTs but not in carcinoma and concluded that they are unrelated¹⁷ whereas others have detected them in nearly 40% of SBTs and 30% of serous carcinomas and concluded that

SBTs may be precursors of serous carcinoma.¹⁸ Since MPSC (noninvasive and invasive) was not recognized as a distinct entity in these studies, their results cannot be directly compared to ours. Second, we found that the allelic imbalance index gradually increased from SBTs to noninvasive and then to invasive MPSCs. In contrast, all conventional serous carcinomas including the very earliest (tumors less than 0.8 cm confined to one ovary) showed high levels of allelic imbalance. Since the alterations on chromosomes 5q and 1p were not exclusively observed in noninvasive and invasive MPSCs, respectively, and can rarely be demonstrated in SBTs, it is likely that critical genetic alterations may precede the morphological changes. This view is further supported by the identical allelic imbalance patterns and K-ras mutations in the tumors containing different morphological stages of progression (SBTs and noninvasive MPSC or noninvasive and invasive MPSC). Third, our findings that nearly 95% of bilateral ovarian MPSCs have discordant patterns of K-ras mutation or allelic imbalance suggest that they develop independently, although divergent progression from the same early neoplastic lesion cannot be entirely excluded. This contrasts with conventional serous carcinomas in which bilateral tumors have been reported to be monoclonal in most cases.¹⁶

Clear-cut morphologically recognizable precursor lesions of conventional serous carcinomas are rarely observed. In our study, conventional serous carcinomas (including two tumors measuring 0.6 and 0.7 cm), showed massive, clonal allelic imbalance among the different chromosomal arms (Figure 2). This finding together with the morphological observations that early conventional serous carcinomas are high-grade¹⁹ underlies the notion that they arise "de novo." It must be acknowledged, however, that the absence of morphologically established intermediate steps may be due to a higher rate of cellular proliferation resulting in rapid evolution to conventional serous carcinoma, obscuring discrete mor-

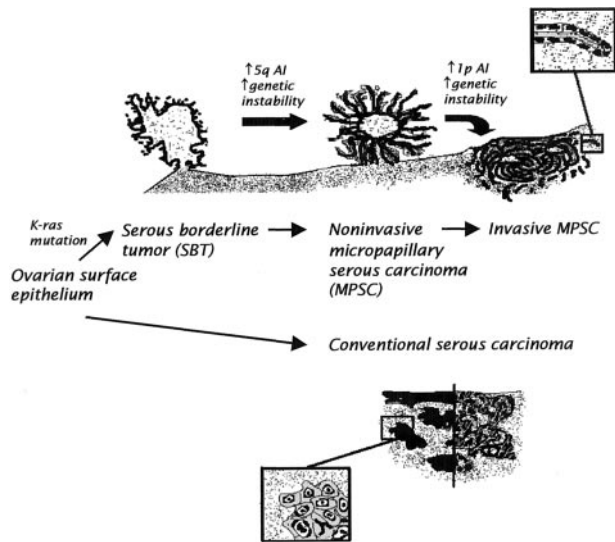


Figure 3. Schematic representation of the dualistic model depicting the development of ovarian serous carcinomas, the most common type of ovarian cancer. In one pathway invasive MPSC develops in a stepwise fashion from a SBT through a noninvasive stage of MPSC before becoming invasive. These tumors are associated with frequent K-ras mutations. Increased allelic imbalance of chromosome 5q is associated with the progression from SBT to MPSC and increased allelic imbalance of chromosome 1p with the progression from noninvasive to invasive MPSC. In the second pathway, conventional serous carcinoma, a high-grade neoplasm, exhibits a solid and/or pseudopapillary morphology and develops from the ovarian surface epithelium without morphologically recognizable intermediate stages. K-ras mutations have not been found in all these neoplasms tested.

phological intermediate stages. This is supported by a substantially higher Ki-67 nuclear labeling (proliferative) index in early conventional serous carcinoma as compared with SBT, noninvasive and invasive MPSC,²⁰ (and our unpublished data). Thus, the rapid progression of conventional serous carcinoma suggests that a profound loss of cell cycle regulation occurs very early in its development. This interpretation is supported by the finding of p53 mutations in small conventional serous carcinomas confined to the ovary and in adjacent "dysplastic" epithelium.²¹ In contrast, p53 mutations have as yet not been detected in MPSC.⁴ However, it should be noted that a comprehensive analysis of the pathogenesis of conventional serous carcinoma will require a large collaborative study since early tumors are rarely encountered.

In summary, the molecular findings in this study in conjunction with morphological data support the stratification of ovarian serous carcinomas into two distinct groups with two different pathways of tumorigenesis (Figure 3). In one pathway, a low-grade carcinoma (invasive MPSC) develops in a stepwise fashion from a SBT (atypical proliferative serous tumor) and then a noninvasive MPSC. This tumor and its precursors exhibit frequent K-ras mutations. As the precursors evolve into invasive MPSC they gradually acquire more genetic abnormalities. In the second pathway, a high-grade carcinoma (conventional serous carcinoma) develops by transformation from the ovarian surface epithelium or inclusion cysts without morphologically recognizable intermediate stages. These tumors, even early in their development, demonstrate wild-type K-ras and frequent allelic imbal-

ance. This proposed dualistic model is the first step in an attempt to elucidate the pathogenesis of serous ovarian carcinoma, but should not be construed as implying that other pathways of tumorigenesis do not exist. Future studies focusing on gene expression profiles and the early molecular genetic alterations of these two types of serous carcinomas will be necessary to further elucidate the molecular pathogenesis of ovarian serous carcinoma.

Acknowledgments

We thank Drs. Bert Vogelstein and Tian-Li Wang at The Johns Hopkins Oncology Center for the critical comments.

References

- Dubeau L: Ovarian cancer. The Metabolic and Molecular Bases of Inherited Disease. Edited by CR Scriver, AL Beaudet, WS Sly, D Valle, B Childs, KW Kinzler, B Vogelstein. New York, McGraw-Hill, 2001, pp 1091-1096
- Auersperg N, Edelson MI, Mok SC, Johnson SW, Hamilton TC: The biology of ovarian cancer. *Semin Oncol* 1998, 25:281-304
- Seidman JD, Kurman RJ: Subclassification of serous borderline tumors of the ovary into benign and malignant types: a clinicopathologic study of 65 advanced stage cases. *Am J Surg Pathol* 1996, 20:1331-1345
- Katabuchi H, Tashiro H, Cho KR, Kurman RJ, Hedrick Ellenson L: Micropapillary serous carcinoma of the ovary: an immunohistochemical and mutational analysis of p53. *Int J Gynecol Pathol* 1998, 17: 54-60
- Burks RT, Sherman ME, Kurman RJ: Micropapillary serous carcinoma of the ovary: a distinctive low-grade carcinoma related to serous borderline tumors. *Am J Surg Pathol* 1996, 20:1319-1330
- Slomovitz BM, Caputo TA, Economos K, Gretz H: Non-invasive ovarian proliferations with micropapillary architecture are part of the spectrum of serous borderline tumor. *Mod Pathol* 2001, 14:146A
- Liu J, Zabarovska VI, Braga E, Alimov A, Kliem G, Zabarovsky ER: Loss of heterozygosity in tumor cells requires re-evaluation: the data are biased by the size-dependent differential sensitivity of allele detection. *FEBS Lett* 1999, 462:121-128
- Vogelstein B, Kinzler KW: Digital PCR. *Proc Natl Acad Sci USA* 1999, 96:9236-9241
- Shih IM, Zhou W, Goodman SN, Lengauer C, Kinzler KW, Vogelstein B: Evidence that genetic instability occurs at an early stage of colorectal tumorigenesis. *Cancer Res* 2001, 61:818-822
- Zhou W, Galizia G, Goodman SN, Romans KE, Kinzler KW, Vogelstein B, Choti MA, Montgomery EA: Counting alleles reveals a connection between chromosome 18q loss and vascular invasion. *Nature Biotechnol* 2001, 19:78-81
- Shih IM, Wang TL, Traverso G, Romans K, Hamilton SR, Ben-Sasson S, Kinzler KW, Vogelstein B: Top-down morphogenesis of colorectal tumors. *Proc Natl Acad Sci USA* 2001, 98:2640-2645
- Zborovskaya I, Gasparian A, Karseladze A, Elcheva I, Trofimova E, Driouch K, Trassard M, Tatosyan A, Lidereau R: Somatic genetic alterations (LOH) in benign, borderline and invasive ovarian tumours: intratumoral molecular heterogeneity. *Int J Cancer* 1999, 82:822-826
- Cliby W, Ritland S, Hartmann L, Dodson M, Halling KC, Keeney G, Podratz KC, Jenkins RB: Human epithelial ovarian cancer allelotype. *Cancer Res* 1993, 53:2393-2398
- Dodson MK, Hartmann LC, Cliby WA, DeLacey KA, Keeney GL, Ritland SR, Su JQ, Podratz KC, Jenkins RB: Comparison of loss of heterozygosity patterns in invasive low-grade and high-grade epithelial ovarian carcinomas. *Cancer Res* 1993, 53:4456-4460

15. Iwabuchi H, Sakamoto M, Sakunaga H, Ma YY, Carcangiu ML, Pinkel D, Yang-Feng TL, Gray JW: Genetic analysis of benign, low-grade, and high-grade ovarian tumors. *Cancer Res* 1995, 55:6172–6180
16. Shih IM, Yan H, Speyrer D, Shmookler BM, Sugarbaker PH, Ronnett BM: Molecular genetic analysis of appendiceal mucinous adenomas in identical twins, including one with pseudomyxoma peritonei. *Am J Surg Pathol* 2001, 25:1095–1099
17. Caduff RF, Svoboda-Newman SM, Ferguson AW, Johnston CM, Frank TS: Comparison of mutations of Ki-RAS and p53 immunoreactivity in borderline and malignant epithelial ovarian tumors. *Am J Surg Pathol* 1999, 23:323–328
18. Mok SC, Bell DA, Knapp RC, Fishbaugh PM, Welch WR, Muto MG, Berkowitz RS, Tsao SW: Mutation of K-ras protooncogene in human ovarian epithelial tumors of borderline malignancy. *Cancer Res* 1993, 53:1489–1492
19. Bell DA, Scully RE: Early de novo ovarian carcinoma: a study of fourteen cases. *Cancer* 1994, 73:1859–1864
20. Garzetti GG, Ciavattini A, Goteri G, De Nictolis M, Stramazotti D, Lucarini G, Biagini G: Ki67 antigen immunostaining (MIB 1 monoclonal antibody) in serous ovarian tumors: index of proliferative activity with prognostic significance. *Gynecol Oncol* 1995, 56:169–174
21. Pothuri B, Leitao M, Barakat R, Akram M, Bogomolny F, Olvera N, Lin O: Genetic analysis of ovarian carcinoma histogenesis. *Gynecol Oncol* 2001, 80:277

Notch3 Gene Amplification in Ovarian Cancer

Joon T. Park,^{1,2} Mei Li,¹ Kentaro Nakayama,² Tsui-Lien Mao,² Ben Davidson,³ Zhen Zhang,² Robert J. Kurman,^{1,2} Charles G. Eberhart,² Ie-Ming Shih,^{1,2} and Tian-Li Wang¹

Departments of ¹Gynecology and Obstetrics and Oncology, and ²Pathology, The Johns Hopkins Medical Institutions, Baltimore, Maryland; and ³Department of Pathology, Norwegian Radium Hospital, University of Oslo, Oslo, Norway

Abstract

Gene amplification is one of the common mechanisms that activate oncogenes. In this study, we used single nucleotide polymorphism array to analyze genome-wide DNA copy number alterations in 31 high-grade ovarian serous carcinomas, the most lethal gynecologic neoplastic disease in women. We identified an amplicon at 19p13.12 in 6 of 31 (19.5%) ovarian high-grade serous carcinomas. This amplification was validated by digital karyotyping, quantitative real-time PCR, and dual-color fluorescence *in situ* hybridization (FISH) analysis. Comprehensive mRNA expression analysis of all 34 genes within the minimal amplicon identified *Notch3* as the gene that showed most significant overexpression in amplified tumors compared with nonamplified tumors. Furthermore, *Notch3* DNA copy number is positively correlated with *Notch3* protein expression based on parallel immunohistochemistry and FISH studies in 111 high-grade tumors. Inactivation of *Notch3* by both γ -secretase inhibitor and *Notch3*-specific small interfering RNA suppressed cell proliferation and induced apoptosis in the cell lines that overexpressed *Notch3* but not in those with minimal amount of *Notch3* expression. These results indicate that *Notch3* is required for proliferation and survival of *Notch3*-amplified tumors and inactivation of *Notch3* can be a potential therapeutic approach for ovarian carcinomas. (Cancer Res 2006; 66(12): 6312-8)

Introduction

Gene amplification is one of the key mechanisms in activating oncogenes in human cancer (1). Ovarian cancer is the most malignant gynecologic neoplasm. Each year, ~16,000 women will succumb to this disease. In ovarian carcinomas, amplifications of *cyclin E1* (2), *Her2/neu* (3), *AKT2* (4), *L-Myc* (5), and *Rsf-1* (6) have been reported. Because these amplifications occur only in a subset of tumors, it is expected that additional oncogenic amplifications will be identified. Recent developments of molecular genetic techniques that allow a genome-wide exploration of DNA copy number in cancer have provided investigators unprecedented opportunities to analyze cancer genome in great details. For example, single nucleotide polymorphism (SNP) array has been recently shown as an effective tool in discovering amplified chromosomal regions (7, 8). In the current study, we did SNP array analysis on 31 high-grade ovarian serous carcinomas purified

from fresh clinical samples and identified a chromosomal region at 19p13.12 that is frequently amplified. One of the genes within this amplicon, *Notch3*, showed the most significant correlation between gene copy numbers and transcript expression in ovarian cancer, suggesting that *Notch3* is a candidate oncogene in the chr19p13.12 amplicon.

Materials and Methods

Tumor specimens. For SNP arrays, tissue samples, including 31 high-grade and 7 low-grade ovarian serous carcinomas, were obtained from the department of pathology at the Johns Hopkins Hospital and the Norwegian Radium Hospital in Norway. Tumor cells were affinity purified by anti-EPCAM-conjugated beads. In addition, genomic DNA from 13 normal ovarian tissues was prepared for controls. For quantitative reverse transcription-PCR (RT-PCR), 89 frozen tumor tissues were used to extract RNA, and nine normal ovarian tissues were also included as controls. Acquisition of tissue specimens and clinical information was approved by an institutional review board (Johns Hopkins University) or by the Regional Ethics Committee (Norway).

SNP array. SNPs were genotyped using 10K arrays (Affymetrix, Santa Clara, CA) in the Microarray Core Facility at the Dana-Farber Cancer Institute (Boston, MA). A detailed protocol is available at the Core center web page.⁴ Briefly, genomic DNA was cleaved with the restriction enzyme, *XbaI*, ligated with linkers, followed by PCR amplification. The PCR products were purified and then digested with DNaseI to a size ranging from 250 to 2,000 bp. Fragmented PCR products were then labeled with biotin and hybridized to the array. Arrays were then washed on the Affymetrix fluidics stations. The bound DNA was then fluorescently labeled using streptavidin-phycoerythrin conjugates and scanned using the Gene Chip Scanner 3000.

dChip software version 1.3 was used to analyze the SNP array data as described previously (7, 8). Data was normalized to a baseline array with median signal intensity at the probe intensity level using the invariant set normalization method. A model-based (PM/MM) method was used to obtain the signal values for each SNP in each array. Signal values for each SNP were compared with the average intensities from 13 normal samples. To infer the DNA copy number from the raw signal data, we used the Hidden-Markov model (7) based on the assumption of diploidy for normal samples. Mapping information of SNP locations and cytogenetic band were based on curation of Affymetrix and University of California Santa Cruz hg15. A cutoff of >2.8 copies in more than three consecutive SNPs was defined as amplification.

Digital karyotyping. Purified carcinoma cells as described in the SNP array method were used to generate digital karyotyping library as previously described (9). Approximate 120,000 genomic tags were obtained for each digital karyotyping library. After removing the nucleotide repeats in human genome, the average of filtered tags was 66,000 for each library. We set up a window size of 300 (300 virtual tags) for the analysis in this study. Based on Monte Carlo simulation, the variables used in this study can reliably detect >0.6 Mb amplicon with >5-fold amplification with >99% sensitivity and 100% positive predictive value.

Note: Supplementary data for this article are available at Cancer Research Online (<http://cancerres.aacrjournals.org/>).

Requests for reprints: Tian-Li Wang, Departments of Gynecology/Obstetrics and Oncology, Johns Hopkins University School of Medicine, CRBII, 1550 East Jefferson Street, Room 306, Baltimore, MD 21231. Phone: 410-502-7774; Fax: 410-502-7943; E-mail: tlw@jhmi.edu.

©2006 American Association for Cancer Research.
doi:10.1158/0008-5472.CAN-05-3610

⁴ <http://chip.dfci.harvard.edu/lab/services.php>.

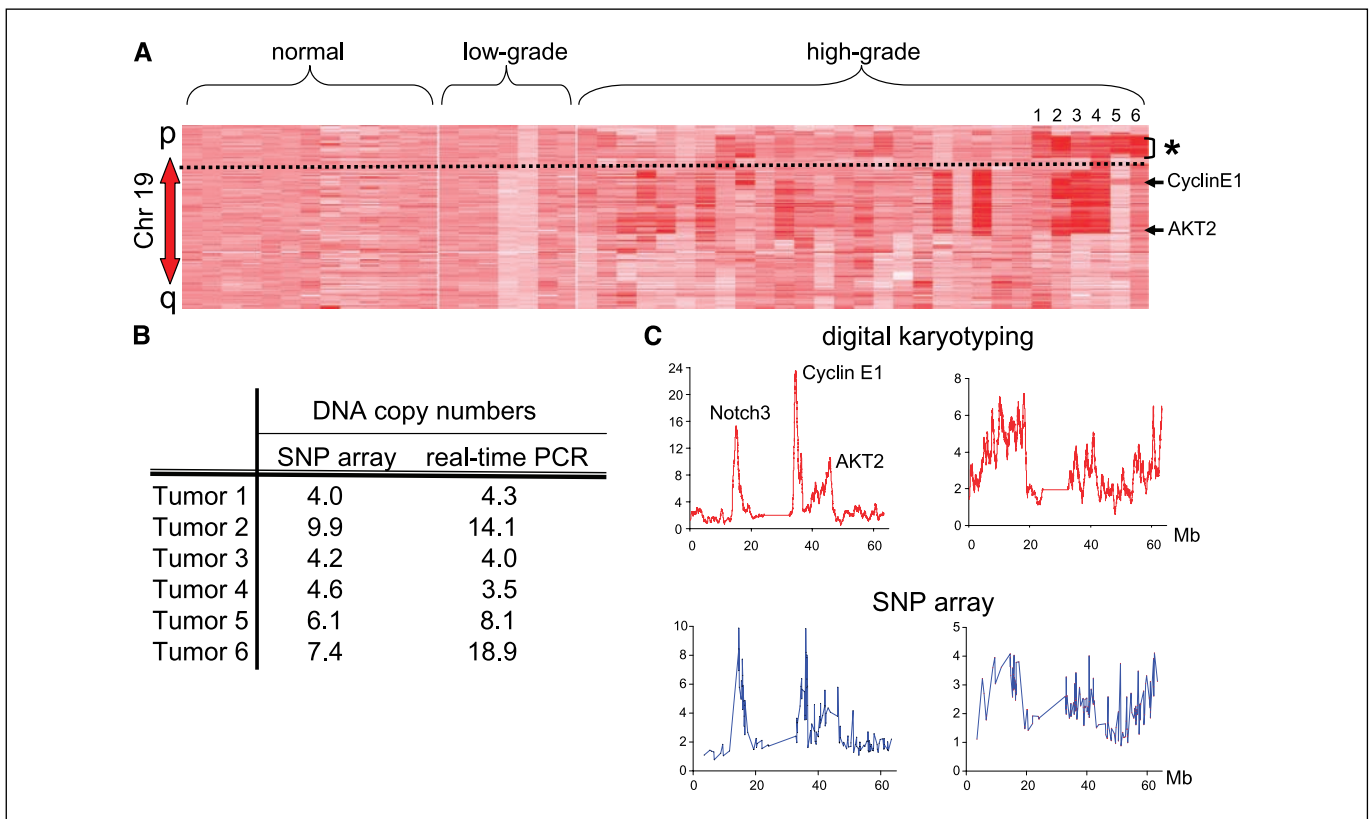


Figure 1. Identification of chr19p13.12 amplification in high-grade ovarian serous carcinomas. *A*, SNP array analysis shows several distinct amplicons on chromosome 19 (top to bottom, p to q arm) including the *cyclin E1* and *AKT2* loci and a novel amplicon at chr19p13.12 (bracket). An increase in DNA copy number is indicated by a gradient in color with 0 copy in white and five or more copies in red. Each column represents an individual tumor sample. *B*, quantitative real-time PCR on genomic DNA validates the amplification on the six tumors with chr19p13.12 amplification identified by the SNP array analysis. *C*, comparison of DNA copy number using SNP array and digital karyotyping on chromosome 19. The data of SNP array is compared with that of digital karyotyping analysis on two representative specimens. *Left*, tumor 2, which contains a high copy number amplification at chr19p13.12. *Right*, tumor 1, which contains a low copy number gain at chr19p13.12. Both SNP array and digital karyotyping analyses show a similar pattern of DNA copy number alterations.

Fluorescence in situ hybridization and quantitative real-time PCR.

BAC clones (RP11-937H1 and RP11-319O10) containing the genomic sequences of the 19p13.12 amplicon at 15.00 to 15.25 Mb were purchased from Bacpac Resources (Children’s Hospital, Oakland, CA). BAC clone (RP11-752A21), located at 19q13.42 (59.26-59.46 Mb), was used to generate the reference probe. The method for fluorescence *in situ* hybridization (FISH) has been detailed in a previous report (6).

Relative gene expression and genomic amplification levels were measured by quantitative real-time PCR using methods previously described (9, 10). PCR primers were designed using the Primer 3 program and the nucleotide sequences of the primers for determining transcript expression were listed in Supplementary Table S1. The primer sequences to determine the 19p13.12 genomic amplification were 5’-GCCTGTGGCTGAAAATTAAGG-3’ and 5’-TCAATGTCCACCTCGCAATAG-3’.

Immunohistochemistry. A rabbit polyclonal anti-Notch3 antibody was purchased from Santa Cruz Biotechnology (Santa Cruz, CA) and was used in the immunohistochemistry. An EnVision+System peroxidase kit (DAKO, Carpinteria, CA) was used for staining following the protocol provided by the manufacturer. Tissue microarrays (triplicate 1.5 mm cores from each specimen) including 111 high-grade serous carcinomas and 10 normal ovaries were used to facilitate immunohistochemistry. Immunointensity was scored as negative (0), negligible (1+), moderate (2+), and intense (3+), and two investigators independently scored all the samples. For discordant cases, a third investigator scored and the final intensity score was determined by the majority scores.

Cell proliferation and apoptosis assays. Cells were grown in 96-well plates at a density of 4,000 per well. Type 1 γ -secretase inhibitor was purchased from Calbiochem (San Diego, CA) and was dissolved in DMSO

as 4 mmol/L stock solution. Cells were treated with γ -secretase inhibitor with DMSO final concentration <0.1%. Notch3-specific small interfering RNA (siRNA) (rGrUrCrArArUrGrUrUrCrArCrUrUrCrGrCrArGrUrU and rGrCrGrUrGrGrArUrUrCrGrGrArCrArGrUrCrUrGrArGrArGrGrG) and control siRNA that targets the *Luciferase* gene (rGrArUrArArUrCrUrUrCrUrArGrCrGrArCrUrUrCrUrUrCrGrC) were synthesized by Integrated DNA Technologies (Coralville, IA). Cells were treated with siRNA at a final concentration of 200 nmol/L.

Cell number was measured by the fluorescence intensity of SYBR green I nucleic acid gel stain (Molecular Probes, Eugene, OR) using a fluorescence microplate reader (Fluostar from BMG, Durham, NC). Data was determined from five replicates and was expressed as the percentage of the inhibitor or Notch3 siRNA-treated cells versus DMSO or control siRNA-treated cells. BrdUrd uptake and staining were done using a cell proliferation kit (Amersham, Buckinghamshire, England, United Kingdom) and apoptotic cells were detected using an Annexin V staining kit (BioVision, Mountain View, CA). The percentage of BrdUrd-positive and Annexin V-positive cells was determined by counting ~400 cells from each well in 96-well plates. The data was expressed as mean \pm 1 SD from triplicates.

Results and Discussion

Amplification of chromosome 19 in ovarian serous carcinomas. SNP arrays were used to search for genome-wide DNA copy number alterations in 31 high-grade and 7 low-grade ovarian serous carcinomas. In addition, 13 normal ovarian tissues were analyzed as controls. We found several distinct amplifications on

chromosome 19 specific to high-grade serous carcinomas. Among them, amplification of the *cyclin E1* locus was present in 10 of 31 (32.2%) samples and amplification of *AKT2* locus in 9 of 31 (29%) samples. Both *cyclin E1* and *AKT2* have been previously reported as potential oncogenes that are frequently amplified in ovarian cancer. More importantly, a novel amplification on chr19p13.12 was identified in 6 of 31 (19.5%) high-grade carcinomas. The peak copy number changes in these six amplified tumors ranged from four to nine copies based on SNP array analysis (Fig. 1A and B). In contrast to high-grade serous carcinomas, no evidence of amplification at 19p13.12, or *cyclin E1* or *AKT2* loci could be detected in low-grade ovarian tumors or normal ovarian tissues.

Three independent methods were used to validate the 19p13.12 amplification. First, digital karyotyping was done on a tumor with low level of gain (four copies) and a tumor with high level of amplification (nine copies) based on SNP array analysis. Digital karyotyping is a recently developed genome-wide technology that allows a precise measurement of DNA copy number at high resolution (9). The method has been used to identify new amplicons in human cancer (6, 11–13) and using digital karyotyping, we found similar location and amplitude of these amplicons detected by SNP arrays (Fig. 1C). Second, quantitative real-time PCR was used to measure the copy number of the predicted amplification in all of the six tumors (Fig. 1B). The amplification levels based on the SNP arrays were generally in agreement with quantitative PCR but with an underestimation of copy number in

those samples with high amplitude of amplifications. This could be due to the saturation of probe hybridization signal associated with array platform. Third, dual-color FISH analysis was done on all six amplified tumors using a BAC clone located at the 19p13.12 amplicon and a BAC clone located at the 19q as the reference. All of the six cases showed increased target signals compared with the reference signals. Among them, four cases showed a pattern of chromosomal gain and two cases showed a pattern of homogeneously staining region. Taken together, the above results confirmed amplification of 19p13.12 in high-grade ovarian serous carcinomas.

Notch3 as the candidate cancer-related gene in the 19p13.12 amplicon. To select the most promising tumor-associated gene within the minimal amplicon, we aligned the amplicons from these six tumors and delineated a common region of amplification (minimal amplicon), which spanned from 14.60 to 16.47 Mb on chromosome 19p and contained 34 genes (Fig. 2). To identify the candidate-amplified tumor-associated gene within the amplicon, we correlated the gene copy number and gene expression levels for all 34 genes based on the rationale that a tumor-driving gene, when amplified, should overexpress to activate its tumorigenic pathway, whereas coamplified “passenger” genes that are not related to tumor development may or may not do so (14). This approach can be useful to narrow down the candidate gene lists, although some amplification events may not necessarily have overexpression of the gene of interest. The mRNA levels were measured using quantitative RT-PCR on five high-grade carcinomas with 19p13.12

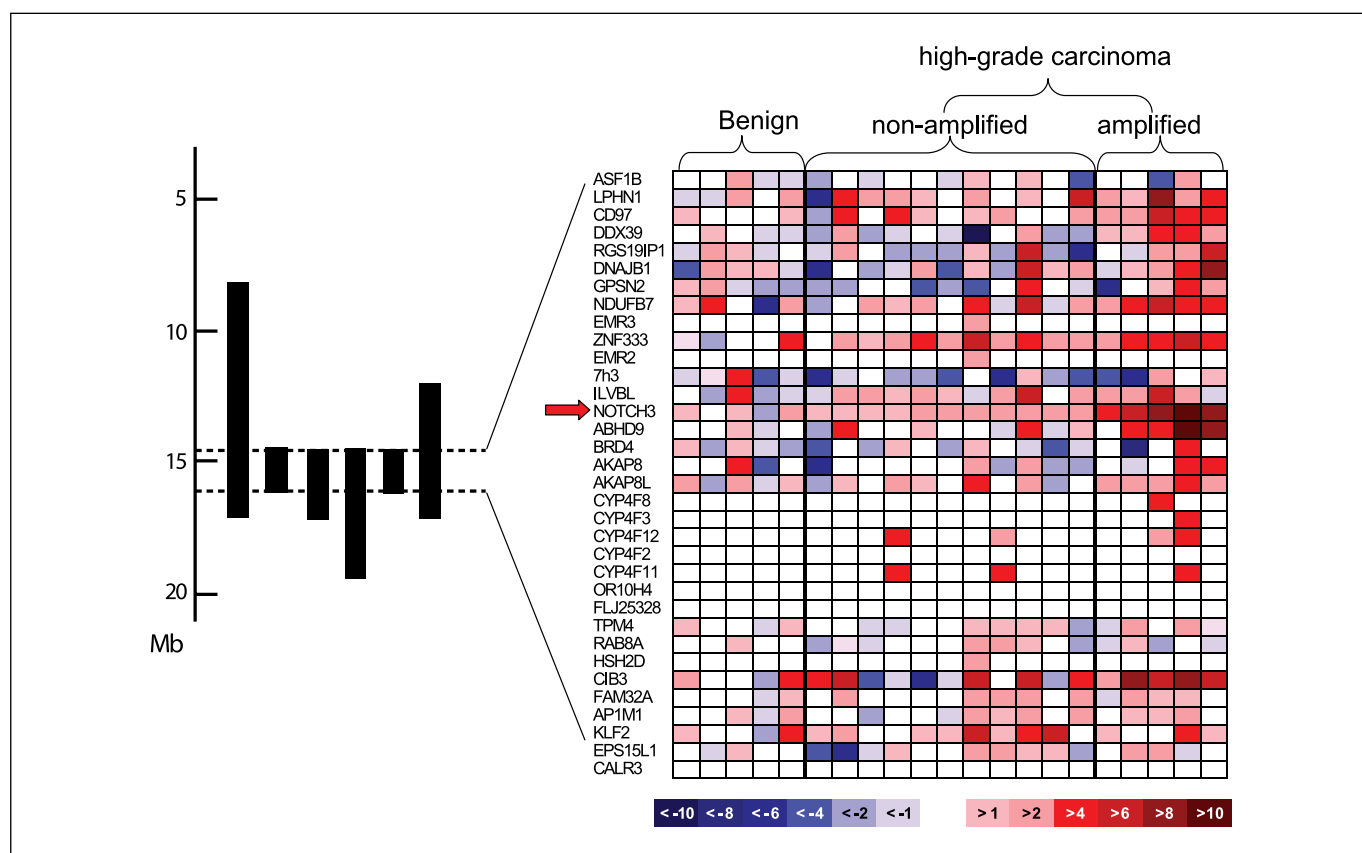


Figure 2. Gene expression analysis of the 19p13.12 amplicon in ovarian tumors. *Left*, alignment of the amplicons from the 19p13.12-amplified tumors reveals a common region of amplification spanning from 14.60 to 16.47 Mb at chromosome 19p. *Right*, quantitative real-time PCR was done for all 34 genes located within the minimal amplicon in high-grade serous carcinomas with or without 19p13.12 amplification and benign OSE cells were used as controls. The expression level of each gene (*top to bottom*, centromeric to telomeric) in individual specimen is shown as a pseudocolor gradient based on the relative expression level of a given specimen to the average value derived from five benign OSE samples.

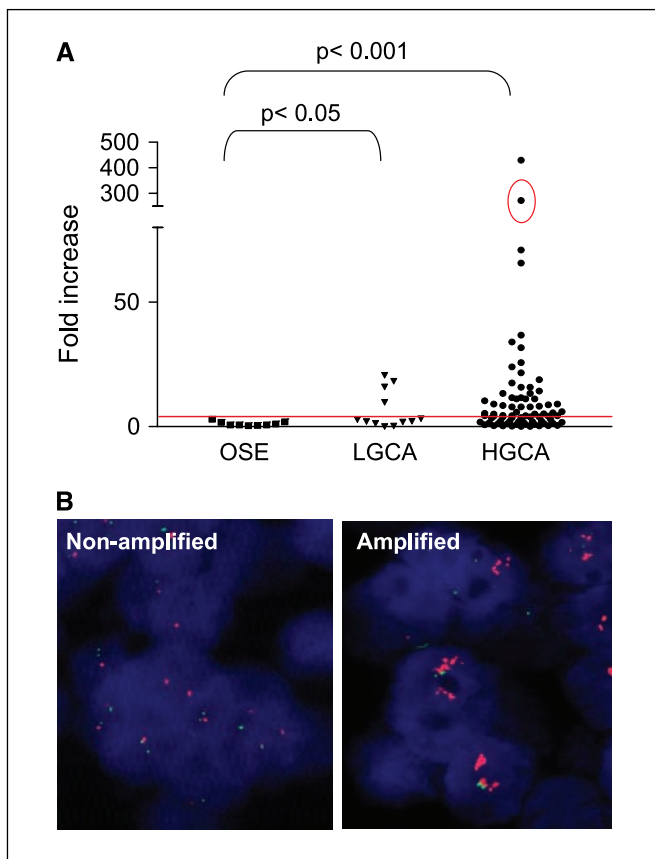


Figure 3. Overexpression and amplification of Notch3 in high-grade ovarian carcinomas. *A*, mRNA expression level of Notch3 for each specimen is measured by quantitative RT-PCR and is expressed as fold increase relative to the average value derived from nine OSE samples. Each symbol represents one specimen. The sample with circle harbored 19p13.12 amplification, which is shown in (*B*). *B*, FISH analysis shows a homogeneously stained region in an amplified tumor (*right*) with a high level of mRNA expression. A nonamplified tumor (*left*) is also shown as a control.

amplification, 11 high-grade tumors without such amplification, and five benign ovarian tissues including four OSE samples and a benign ovarian cyst. The expression levels for each gene were normalized to the average value of benign tissues (Fig. 2). Mann-Whitney *U* test was used to compute and compare the difference in gene expression levels between the 19p13.12 amplified versus nonamplified high-grade carcinomas. Among the 34 genes within the minimal amplicon, *Notch3* showed the most consistent and significant up-regulation in 19p13.12-amplified tumors compared with nonamplified tumors ($P = 0.0018$). Other genes in the amplicon, such as *DDX39* and *ADHD9*, also showed a significant overexpression in the amplified versus nonamplified tumors ($P = 0.01$ and $P = 0.02$, respectively). It is plausible that these genes also contribute to the tumorigenesis in ovarian cancer. In this study, we selected *Notch3* for further characterization because it showed the most significant *P* value. We further correlated *Notch3* DNA and mRNA copy number in a set of 31 samples in which both tissues and RNA samples were available for FISH and quantitative RT-PCR analyses. Our data showed a moderate positive correlation of these two variables with a correlation coefficient of 0.481 (Spearman rank-order test, $P < 0.05$).

The above results, together with previous reports showing that *Notch3* participates in both development and oncogenesis, suggest

that *Notch3* is a candidate “driving” gene in the 19p13.12 amplicon. Therefore, *Notch3* was prioritized for further characterization in this study. We then did quantitative RT-PCR on a large panel of ovarian serous tumors to determine *Notch3* mRNA levels. As shown in Fig. 3*A*, *Notch3* was overexpressed in 66% (51 of 77) of high-grade tumors, but only in 33% (4 of 12) of low-grade tumor compared with normal ovarian surface epithelium (OSE). In addition, the top five tumors with the highest *Notch3* mRNA expression harbored 19p13.12 amplification (Fig. 3*B*), further supporting *Notch3* as a candidate amplified gene that is important in tumor development. Mann-Whitney *U* test showed that there was a statistically significant difference in the levels of *Notch3* expression between OSE and high-grade serous carcinomas ($P < 0.001$) and between OSE and low-grade serous carcinomas ($P < 0.05$). However, there was no significant difference between low-grade and high-grade carcinomas ($P = 0.3187$).

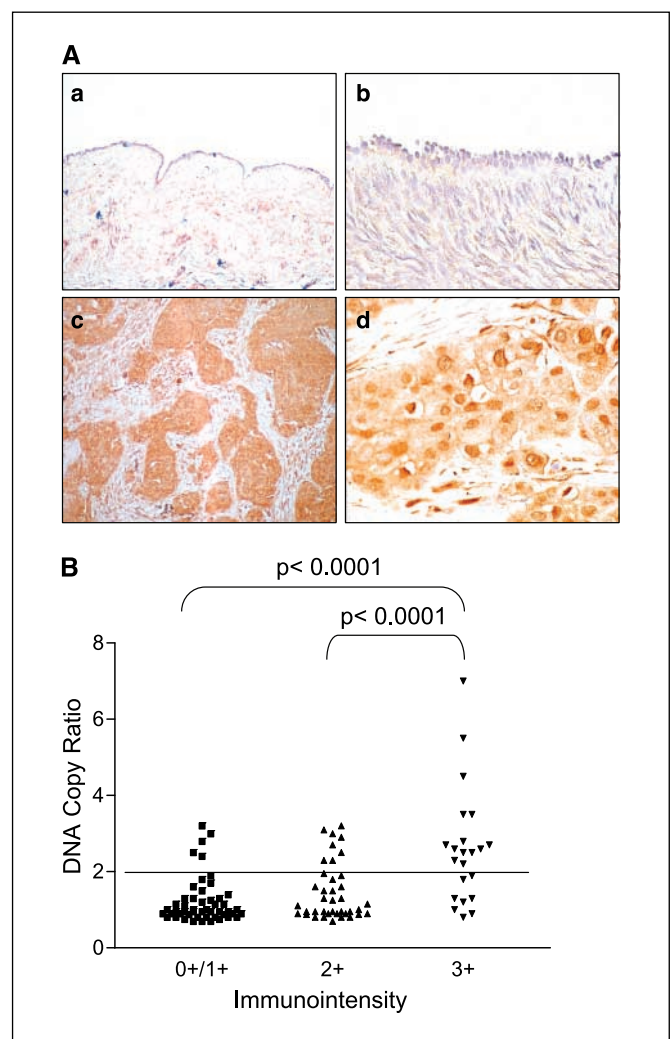


Figure 4. Immunoreactivity of Notch3 in ovarian tumors. *A*, immunoreactivity of Notch3 is not detectable in normal OSE (*a* and *b*) but is overexpressed in 55% of high-grade serous carcinoma. Immunolocalization of Notch3 is detected in both nucleus and cytoplasm in the tumor cells (*c* and *d*). *B*, correlation of Notch3 immunointensity and DNA copy number ratio in high-grade serous carcinomas. The intensity of Notch3 immunoreactivity positively correlates with the Notch3 DNA copy ratio based on FISH analysis. Furthermore, there is a statistically significant difference between tumors with intense staining intensity (3+) and those without (Mann-Whitney *U* test).

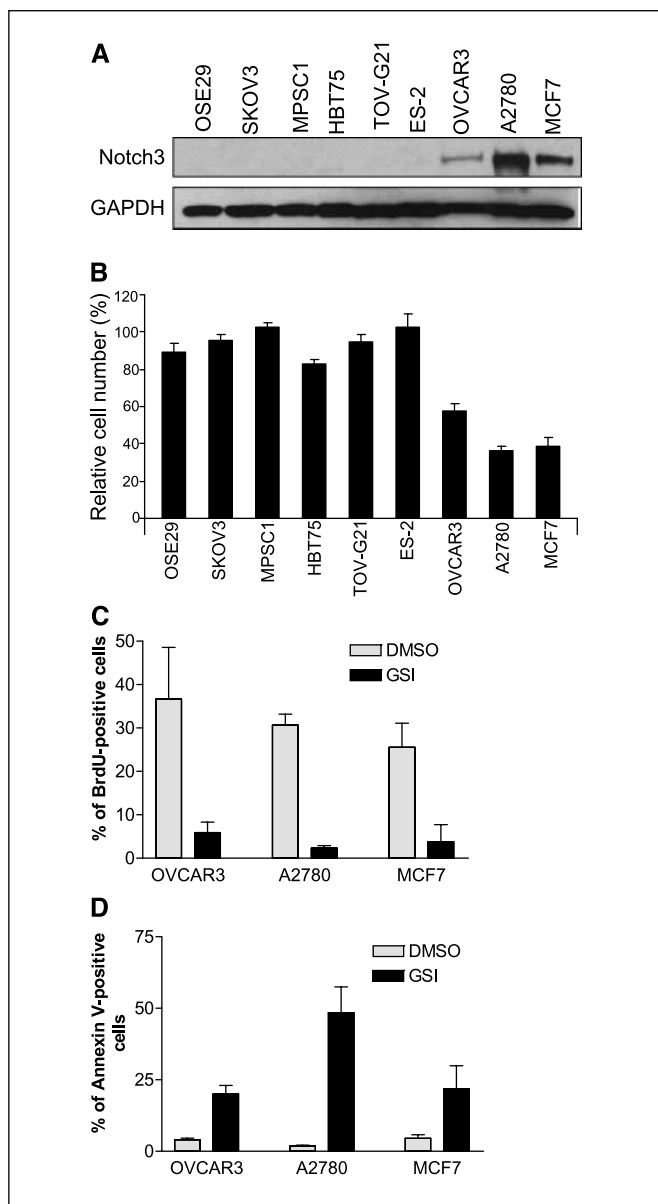


Figure 5. Effects of γ -secretase inhibitor on cell proliferation and apoptosis in cell lines. *A*, Western blot analysis shows a higher expression level of Notch3 protein in OVCAR3, A2780, and MCF-7 cells compared with the other cell lines in which the Notch3 protein is not detectable. *B*, γ -secretase inhibitor significantly reduces the cell number in cell lines with Notch3 overexpression, including OVCAR3, A2780, and MCF-7 compared with those without Notch3 overexpression. γ -Secretase inhibitor decreases DNA synthesis (*C*) and increases apoptosis (*D*) in OVCAR, A2780, and MCF-7 cells based on measurement of BrdUrd uptake and Annexin V labeling assays, respectively.

Immunohistochemistry and FISH were done in parallel on 111 tumor samples to correlate protein expression and *Notch3* DNA copy number. Notch3 immunoreactivity was detected in both nucleus and cytoplasm of tumor cells in 61 of 111 (55%) carcinomas but not in normal ovarian epithelial cells (Fig. 4A). Notch3 immunointensity was scored as negative (0), negligible (1+), moderate (2+), and intense (3+) and was correlated with *Notch3* DNA copy number ratio based on FISH analysis (Fig. 4B). Specifically, the intensity of Notch3 staining positively correlated with the *Notch3* DNA copy ratio (Spearman rank-order correlation coefficient = 0.4). Furthermore, there is statistically significant

difference between tumors with intense staining intensity (3+) and those without (intensity score = 0, 1+, and 2+; Mann-Whitney *U* test, $P < 0.0001$). We observed that 8 of 22 carcinomas are with Notch3 overexpression (3+) but without *Notch3* gene amplification (gene copy ratio ≤ 2). This finding implies that in addition to gene amplification, mechanisms such as epigenetic activation of the *Notch3* promoter in response to environmental cues may contribute to Notch overexpressing in those tumors. Although a positive correlation of *Notch3* gene copy ratio and protein expression was observed, there are some tumors (5 of 50 tumors)

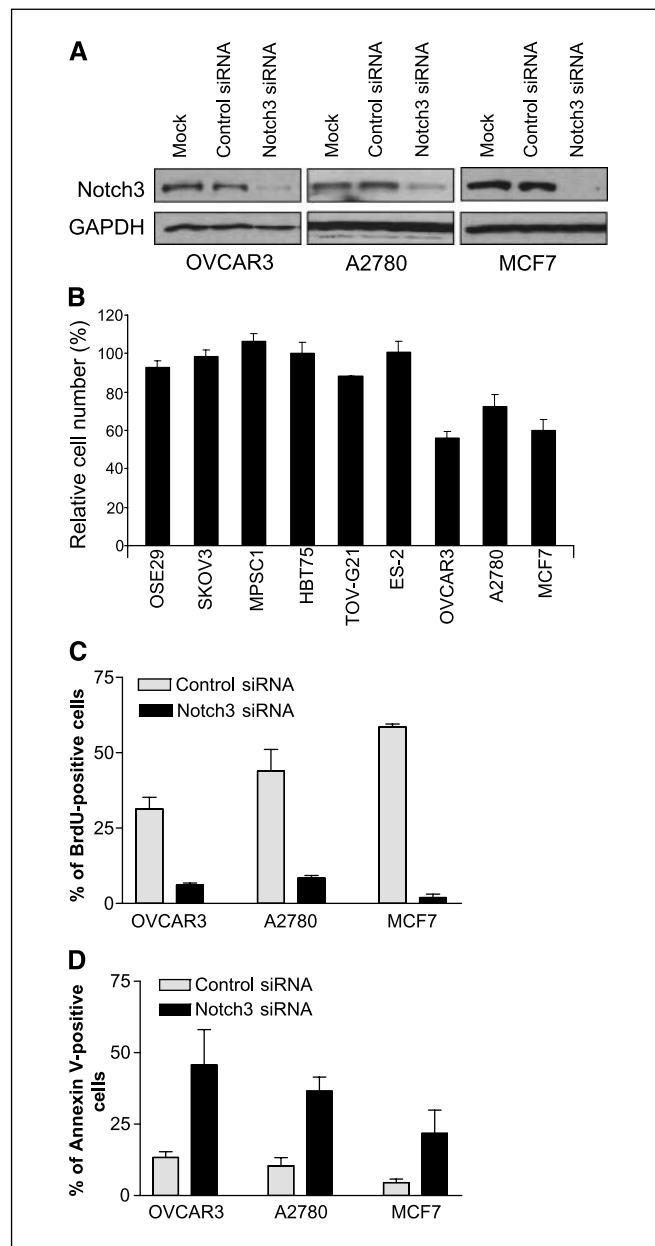


Figure 6. Effects of Notch3 knockdown on cell proliferation and apoptosis in cell lines. *A*, Western blot analysis shows a significant reduction of Notch3 protein in Notch3 siRNA-treated cells compared with the mock or control siRNA-treated cells. *B*, Notch3 siRNA significantly reduces the cell number in cell lines with Notch3 overexpression, including OVCAR3, A2780, and MCF-7 compared with those without. Treatment with Notch3 siRNA decreases DNA synthesis as measured by BrdUrd uptake (*C*) and increases apoptosis as measured by Annexin V labeling (*D*) in OVCAR3, A2780, and MCF-7 cells.

with *Notch3* DNA copy ratio >2 but with only weak Notch3 protein expression (0/1+). This result suggests that these carcinomas may use other oncogene(s) that resides on the same chromosomal arm as the *Notch3* locus to promote tumor progression in ovarian serous carcinomas.

Notch receptors participate in signal transduction by translocating their cytoplasmic domain to the nucleus where it activates an array of downstream effectors that can play important roles in cell proliferation and survival (15). The association of genetic changes in *Notch3* and human cancer has been recently established in lung carcinoma. Translocation of t(15;19) was identified in non-small-cell lung cancer cell lines and the breakpoint has been mapped to 50 bp upstream of the *Notch3* locus. The translocation of chromosome 19p was found to correlate with overexpression of Notch3 full-length mRNA (16). Our data here provide new evidence that besides translocation, gene amplification is another mechanism to activate Notch3 in human cancer.

The genetic findings are supported by mouse models. For example, expression of the intracellular domain (a constitutively active form) of Notch3 in mouse thymus induced T-cell leukemia/lymphoma (17). Furthermore, constitutive expression of activated Notch3 in the central nervous system initiates the formation of brain tumors in the choroid plexus in mice (18), suggesting that deregulation of Notch3 plays a role in neoplastic transformation.

Functional analysis of Notch3 expression. To determine if Notch3 is essential for cell growth and survival in cell lines that overexpress Notch3, we used γ -secretase inhibitor 1, which prevents the activation of Notch3 by inhibiting the proteolysis and translocation of Notch3 cytoplasmic domain to the nucleus. This compound has been shown to be a potent and specific inhibitor of Notch pathway (19, 20). γ -Secretase inhibitor was applied to the culture medium in nine cell lines, including three cancer cell lines with Notch3 overexpression (OVCAR3, A2780, and MCF7), an immortalized OSE cell line (OSE 29), and five cancer cell lines (SKOV3, MPSC1, HTB75, TOV-G21, and ES-2) without Notch3 overexpression (Fig. 5A). We first determined the concentration of γ -secretase inhibitor to be used and found that the IC₅₀ was lowest in OVCAR3 (1 μ mol/L). Therefore, we treated different cell lines with inhibitor at 1 μ mol/L in culture and found that there was a substantial reduction in cell number of OVCAR3, A2780, and MCF7 cells that overexpressed Notch3 compared with other cell lines that did not have Notch3 overexpression (Fig. 5B, $P < 0.001$, Student's t test). To assess the mechanisms underlying the growth inhibition by the γ -secretase inhibitor in OVCAR3, A2780, and MCF-7 cells, we measured the percentage of BrdUrd-labeled cells for cellular proliferation and Annexin V-labeled cells for apoptosis (Fig. 5C and D). We found that γ -secretase inhibitor significantly reduced cellular proliferation and induced apoptosis in all three cell lines with Notch3 overexpression compared with the DMSO controls ($P < 0.001$, Student's t test). siRNA was used to knock down the expression of Notch3 in the same nine cell lines used for

the γ -secretase inhibitor assay. The knockdown effect of siRNA was shown by Western blot (Fig. 6A). siRNA treatment significantly reduced the Notch3 protein expression compared with the mock or control siRNA-treated groups. Similar to the effects of γ -secretase inhibitor, Notch3 siRNA reduced cell number most significantly in OVCAR3, A2780, and MCF7 cells, which overexpressed Notch3 compared with the other cell lines (Fig. 6B, $P < 0.001$, Student's t test). The BrdUrd-positive cells decreased and the Annexin V-labeled cells increased in Notch3 siRNA-treated cells compared with control siRNA-treated cells (Fig. 6C and D, $P < 0.001$, Student's t test).

Our *in vitro* data to inactivate Notch3 by γ -secretase inhibitor and siRNA may have clinical implications for ovarian cancer patients and suggest that Notch3 can be a candidate therapeutic target. γ -Secretase inhibitors have been studied in the past several years as a potential therapeutic intervention in Alzheimer's disease. Very recently, γ -secretase inhibitors have been shown to inhibit the epithelial cell proliferation and induce goblet cell differentiation in intestinal adenomas *Apc*^{-/-} (min) mice (20). Furthermore, γ -secretase was shown to be able to inhibit the growth of Kaposi's sarcoma cells in mouse tumor model (19). Therefore, with the promising effects at both *in vitro* and *in vivo* systems, γ -secretase inhibitors can be used as new target-based therapy for those tumors with Notch3 activation.

The current study suggests that *Notch3* is a strong candidate oncogene among the genes within the ch19p13.12 amplicon in ovarian carcinomas. This is because *Notch3* gene shows a high correlation of gene amplification and overexpression and is functionally essential for tumor growth and survival. Although the above represents our preferred interpretation, other alternative interpretations should be pointed out. For example, *Notch3* may not be the only gene with high correlation of DNA copy number and gene expression level after analyzing a large series of amplified and nonamplified tumors. It is possible that other coamplified gene(s) within the *Notch3* amplicon also plays a role in tumorigenesis and they may cooperate with Notch3 in propelling tumor progression.

In conclusion, we have identified *Notch3* as a candidate amplified oncogene that overexpressed in 66% of ovarian serous carcinomas. Our findings suggest that *Notch3* amplification may play an important role in the development of ovarian carcinomas; moreover, these findings provide a rationale for future development of Notch3-based therapy for ovarian cancer.

Acknowledgments

Received 10/6/2005; revised 3/10/2006; accepted 4/11/2006.

Grant support: Department of Defense grant OC0400600 and NIH grant CA103937.

The costs of publication of this article were defrayed in part by the payment of page charges. This article must therefore be hereby marked *advertisement* in accordance with 18 U.S.C. Section 1734 solely to indicate this fact.

We thank Dr. Edward Fox and Dr. Changzhong Chen at the microarray core facility of the Dana-Farber Cancer Institute for valuable suggestions.

References

- Meltzer PS, Kallioniemi A, Trent JM. Chromosome alterations in human solid tumors. In: Vogelstein B, Kinzler KW, editors. The genetic basis of human cancer. New York: McGraw-Hill; 2002. p. 93-113.
- Farley J, Smith LM, Darcy KM, et al. Cyclin E expression is a significant predictor of survival in advanced, suboptimally debulked ovarian epithelial cancers: a Gynecologic Oncology Group study. *Cancer Res* 2003;63:1235-41.
- Slamon DJ, Godolphin W, Jones LA, et al. Studies of the HER-2/neu proto-oncogene in human breast and ovarian cancer. *Science* 1989;244:707-12.
- Cheng JQ, Godwin AK, Bellacosa A, et al. AKT2, a putative oncogene encoding a member of a subfamily of protein-serine/threonine kinases, is amplified in human ovarian carcinomas. *Proc Natl Acad Sci U S A* 1992;89: 9267-71.
- Wu R, Lin L, Beer DG, et al. Amplification and overexpression of the L-MYC proto-oncogene in ovarian carcinomas. *Am J Pathol* 2003;162: 1603-10.
- Shih I-M, Sheu JJ, Santillan A, et al. Amplification of a

- chromatin remodeling gene, Rsf-1/HBXAP, in ovarian carcinoma. *Proc Natl Acad Sci U S A* 2005;102:14004–9.
7. Zhao X, Li C, Paez JG, et al. An integrated view of copy number and allelic alterations in the cancer genome using single nucleotide polymorphism arrays. *Cancer Res* 2004;64:3060–71.
 8. Zhao X, Weir BA, LaFramboise T, et al. Homozygous deletions and chromosome amplifications in human lung carcinomas revealed by single nucleotide polymorphism array analysis. *Cancer Res* 2005;65:5561–70.
 9. Wang TL, Maierhofer C, Speicher MR, et al. Digital karyotyping. *Proc Natl Acad Sci U S A* 2002;99:16156–61.
 10. Buckhaults P, Zhang Z, Chen YC, et al. Identifying tumor origin using a gene expression-based classification map. *Cancer Res* 2003;63:4144–9.
 11. Wang TL, Diaz LA, Jr., Romans K, et al. Digital karyotyping identifies thymidylate synthase amplification as a mechanism of resistance to 5-fluorouracil in metastatic colorectal cancer patients. *Proc Natl Acad Sci U S A* 2004;101:3089–94.
 12. Boon K, Eberhart CG, Riggins GJ. Genomic amplification of orthodenticle homologue 2 in medulloblastomas. *Cancer Res* 2005;65:703–7.
 13. Di C, Liao S, Adamson DC, et al. Identification of OTX2 as a medulloblastoma oncogene whose product can be targeted by *all-trans* retinoic acid. *Cancer Res* 2005;65:919–24.
 14. Hogarty MD, Brodeur GM. Gene amplification in human cancers: biological and clinical significance. In: Vogelstein B, Kinzler KW, editors. *The genetic basis of human cancer*. New York: McGraw-Hill; 2002. p. 115–28.
 15. Allenspach EJ, Maillard I, Aster JC, Pear WS. Notch signaling in cancer. *Cancer Biol Ther* 2002;1:466–76.
 16. Dang TP, Gazdar AF, Virmani AK, et al. Chromosome 19 translocation, overexpression of Notch3, and human lung cancer. *J Natl Cancer Inst* 2000;92:1355–7.
 17. Bellavia D, Campese AF, Alesse E, et al. Constitutive activation of NF- κ B and T-cell leukemia/lymphoma in Notch3 transgenic mice. *EMBO J* 2000;19:3337–48.
 18. Dang L, Fan X, Chaudhry A, Wang M, Gaiano N, Eberhart CG. Notch3 signaling initiates choroid plexus tumor formation. *Oncogene* 2005;25:487–91.
 19. Curry CL, Reed LL, Golde TE, Miele L, Nickoloff BJ, Foreman KE. γ -Secretase inhibitor blocks Notch activation and induces apoptosis in Kaposi's sarcoma tumor cells. *Oncogene* 2005;24:6333–44.
 20. van Es JH, van Gijn ME, Riccio O, et al. Notch/ γ -secretase inhibition turns proliferative cells in intestinal crypts and adenomas into goblet cells. *Nature* 2005;435:959–63.

Identifying Tumor Origin Using a Gene Expression-based Classification Map¹

Phillip Buckhaults, Zhen Zhang, Yu-Chi Chen, Tian-Li Wang, Brad St. Croix, Saurabh Saha, Alberto Bardelli, Patrice J. Morin, Kornelia Polyak, Ralph H. Hruban, Victor E. Velculescu, and Ie-Ming Shih²

The Sidney Kimmel Comprehensive Cancer Center at Johns Hopkins [P. B., T-L. W., S. S., A. B., V. E. V.] and The Department of Pathology [Z. Z., Y-C. C., R. H. H., I-M. S.], Johns Hopkins Medical Institutions, Baltimore, Maryland 21231; The National Cancer Institute, Frederick, Maryland [B. St. C.]; National Institute on Aging, Baltimore, Maryland [P. J. M.]; and Dana-Farber Cancer Institute, Boston, Massachusetts [K. P.]

ABSTRACT

Identifying the primary site in cases of metastatic carcinoma of unknown origin has profound clinical importance in managing cancer patients. Although transcriptional profiling promises molecular solutions to this clinical challenge, simpler and more reliable methods for this purpose are needed. A training set of 11 serial analysis of gene expression (SAGE) libraries was analyzed using a combination of supervised and unsupervised computational methods to select a small group of candidate genes with maximal power to discriminate carcinomas of different tissue origins. Quantitative real-time PCR was used to measure their expression levels in an independent validation set of 62 samples of ovarian, breast, colon, and pancreatic adenocarcinomas and normal ovarian surface epithelial controls. The diagnostic power of this set of genes was evaluated using unsupervised cluster analysis methods. From the training set of 21,321 unique SAGE transcript tags derived from 11 libraries, five genes were identified with expression patterns that distinguished four types of adenocarcinomas. Quantitative real-time PCR expression data obtained from the validation set clustered tumor samples in an unsupervised manner, generating a self-organized map with distinctive tumor site-specific domains. Eighty-one percent (50 of 62) of the carcinomas were correctly allocated in their corresponding diagnostic regions. Metastases clustered tightly with their corresponding primary tumors. A classification map diagnostic of tumor types was generated based on expression patterns of five genes selected from the SAGE database. This expression map analysis may provide a reliable and practical approach to determine tumor type in cases of metastatic carcinoma of clinically unknown origin.

INTRODUCTION

In the United States, ~51,000 patients (or 4% of all new cancer cases) present annually with metastases arising from occult primary carcinomas of unknown origin (1). Adenocarcinomas represent the most common metastatic tumors of unknown primary site. Although these patients often present at a late stage, outcome can be positively affected by accurate diagnoses followed by appropriate therapeutic regimens specific to different types of adenocarcinoma (2). The lack of unique microscopic appearance of the different types of adenocarcinomas challenges morphological diagnosis of adenocarcinomas of unknown origin. The application of tumor-specific serum markers in identifying cancer type is theoretically feasible, but such markers are generally not available at present (3, 4). Transcription profiling of thousands of genes using DNA microarrays has successfully classified tumors according to the site of origin (5, 6), but the need for relatively large amounts of RNA and lack of a unified standard for both data collection and analysis make it difficult to deploy the current platform

in a clinical setting. SAGE,³ on the other hand, measures absolute expression levels through a tag counting approach, allowing data to be obtained and compared from different samples analyzed in isolation. However, the throughput of this approach is low, making it inappropriate for routine clinical applications. Quantitative real-time PCR is a reliable method for assessing gene expression levels from relatively small amounts of tissue (7). Although this approach has recently been successfully applied to the molecular classification of breast tumors into prognostic subgroups based on the analysis of 2,400 genes (8), the measurement of such a large number of randomly selected genes by PCR is clinically impractical.

To overcome the above limitations, we developed a rational strategy that uses a combination of supervised and unsupervised computational methods to analyze SAGE-derived gene expression data and identify a minimum number of genes with maximum ability to separate adenocarcinomas according to their tissue origins. We then used quantitative real-time PCR to query the expression levels of these genes and used novel unsupervised computational analyses to prospectively evaluate their ability to correctly categorize adenocarcinomas of the ovary, breast, colon, and pancreas.

MATERIALS AND METHODS

Tissue Samples. A total of 62 surgically removed samples were retrieved from the tumor bank, Department of Pathology, Johns Hopkins Hospital. The acquisition of human tissue material was approved by the local Institutional Review Board. The panel of carcinomas included 20 ovarian serous carcinomas (11 primaries and 9 metastases), 11 breast carcinomas (10 primaries and 1 metastasis), 6 pancreatic carcinomas (all primaries), and 20 colorectal carcinomas (9 primaries and 11 metastases). Total RNA was purified, and cDNA was synthesized using standard protocols. Briefly, frozen tissues were minced and placed in the TRIzol reagent (Invitrogen, Carlsbad, CA). Total RNA was isolated, and contaminating genomic DNA was removed using the DNA-free kit (Ambion, Austin, TX). cDNA was prepared using oligo dT primers and diluted for PCR. H&E-stained sections were prepared from a portion of the frozen tumors and reviewed by a surgical pathologist (I-M. S.) to confirm the diagnosis and assess the percentage of viable tumor cells in the tissue sections. Tissue samples with >60% stromal contamination or <50% viable tumor cells were not included in analysis. Five primary cultures of ovarian surface epithelium were obtained from normal ovaries that were surgically removed, along with uteri, because of benign uterine disorders.

Analysis Software. UMSA is a modified Support Vector Machine learning algorithm that allows the incorporation of estimated data distribution into the derivation of an optimal soft-margin classifier (9). ProPeak (3Z Informatics, Charleston, SC) is a Java-based software package that implements the UMSA algorithm. Unsupervised clustering with SOM was performed using SOM toolbox 2.0 for Matlab (10).⁴ Additional Matlab code was developed by the authors to display the estimated two-dimensional probability distribution patterns of each of the tumor sites and define the diagnostic regions within a derived SOM. PCR primers for the selected genes were designed using Primer3.⁵

Received 12/26/02; accepted 5/7/03.

The costs of publication of this article were defrayed in part by the payment of page charges. This article must therefore be hereby marked *advertisement* in accordance with 18 U.S.C. Section 1734 solely to indicate this fact.

¹ Supported by Public Health Service Grants CA97527 (to I-M. S.) and P50-CA62924 (to R. H. H.) from the National Cancer Institute, NIH, Department of Health and Human Services, and the United States Department of Defense Research Grant OC010017 (to I-M. S.).

² To whom requests for reprints should be addressed, at The Department of Pathology, The Johns Hopkins University School of Medicine, 418 North Bond Street, B-315, Baltimore, MD 21231. E-mail: ishih@jhmi.edu.

³ The abbreviations used are: SAGE, serial analysis of gene expression; UMSA, unified maximum separability analysis; SOM, self-organizing map; Ct, threshold cycle number; APP, amyloid precursor protein.

⁴ Internet address: <http://www.cis.hut.fi>.

⁵ Internet address: http://www-genome.wi.mit.edu/genome_software/other/primer3.html.

Tag Selection from the SAGE Database. SAGE libraries were sequenced, and the resulting gene expression data were collated and warehoused as part of the Cancer Genome Anatomy Project public database for gene expression (11). The hematopoietic cell library was reported previously (12). Tags and their expression levels were retrieved from the Internet (12–17).⁶ Molecular information regarding the libraries analyzed, as well as the primary expression data, are available under the following ProbeSet ID numbers: Colon Cancer 1 (CoCa1) GSM756; Colon Cancer 2 (CoCa2) GSM755; Ovarian Cancer 1 (OvCa1) GSM735; Ovarian Cancer 2 (OvCa2) GSM736; Ovarian Cancer 3 (OvCa3) GSM737; Pancreatic Cancer 1 (PaCa1) GSM743; Pancreatic Cancer 2 (PaCa2) GSM744; Breast Cancer 1 (BrCa1) GSM670; Breast Cancer 1 Metastasis (BrCa1Met) GSM671; Breast Cancer 2 (BrCa2) GSM672; and Breast Cancer 2 Metastasis (BrCa2Met) GSM673. In the supervised selection process, the tags were first filtered to retain only those that were abundant (greater than eight tags/100,000 total tags) in tumors and absent in hematopoietic cells. Tag counts were subsequently analyzed by the UMSA algorithm in ProPeak to select several top-ranked tags for each of the four tumor sites according to their contribution in separating the specific carcinoma from the rest of the data. The resultant most informative tags were then subjected to unsupervised two-way hierarchical cluster analysis (centered correlation similarity metric with complete linkage clustering, no transformation or normalization; Ref. 18)⁷ to evaluate the site specificity of the tumor-associated groups of tags. The tags were matched to the Unigene database, and well-characterized genes were selected for PCR primer design and further analysis.

Gene Expression. Quantitative real-time PCR was performed to determine gene expression levels in a panel of 20 ovarian carcinomas (11 primaries and 9 metastases), 11 breast carcinomas (10 primaries and 1 metastasis), 6 pancreatic carcinomas (all primaries), 20 colorectal carcinomas (9 primaries and 11 metastases), and five normal ovarian surface epithelial cultures using the protocol described previously (19). Primers were designed for representative well-characterized candidate genes to test the performance in quantitative real-time PCR, and those containing robust and specific PCR products without detectable primer dimers were selected for analysis. Approximately 16–100 ng of cDNA were included in the real-time PCR, which was performed using an iCycler, and Cts were obtained using the iCycler Optical system interface software (Bio-Rad Lab, Hercules, CA). Averages in the Ct of duplicate measurements were obtained. The results were expressed as the difference between the Ct of the diagnostic gene and Ct of a control gene (APP), for which expression is relatively constant among the SAGE libraries analyzed. In cases where no gene expression was observed, a cutoff Ct value of 45 cycles was used.

RESULTS

Identification of Diagnostic Genes. Analysis of SAGE libraries constructed from surgical samples of ovarian, breast, pancreatic, and colon adenocarcinomas identified a total of 21,321 unique SAGE tags that were observed two or more times (Fig. 1). To identify genes that were potential candidates for differential diagnosis of these tumor types, we selected tags that were highly expressed (eight or more occurrences/100,000 total tags) in one or more of the tumor samples. This resulted in the identification of 6,396 unique and highly expressed cancer-associated tags. To remove transcripts derived from hematopoietic infiltrates present in variable amounts in these tumors, we eliminated tags that were also present in a SAGE library constructed from tumor-derived, purified hematopoietic cells (12). As a result, a total of 3,747 unique, cancer-specific tags was obtained and subjected to further analysis.

UMSA (9) was used to identify a subset of genes that would provide the most discriminating differential gene expression information. The UMSA approach evaluates and ranks the contribution of each transcript tag toward the optimal separation of SAGE libraries derived from different tissues. Although we only analyzed four tumor sites, this UMSA approach can become valuable in analyzing SAGE

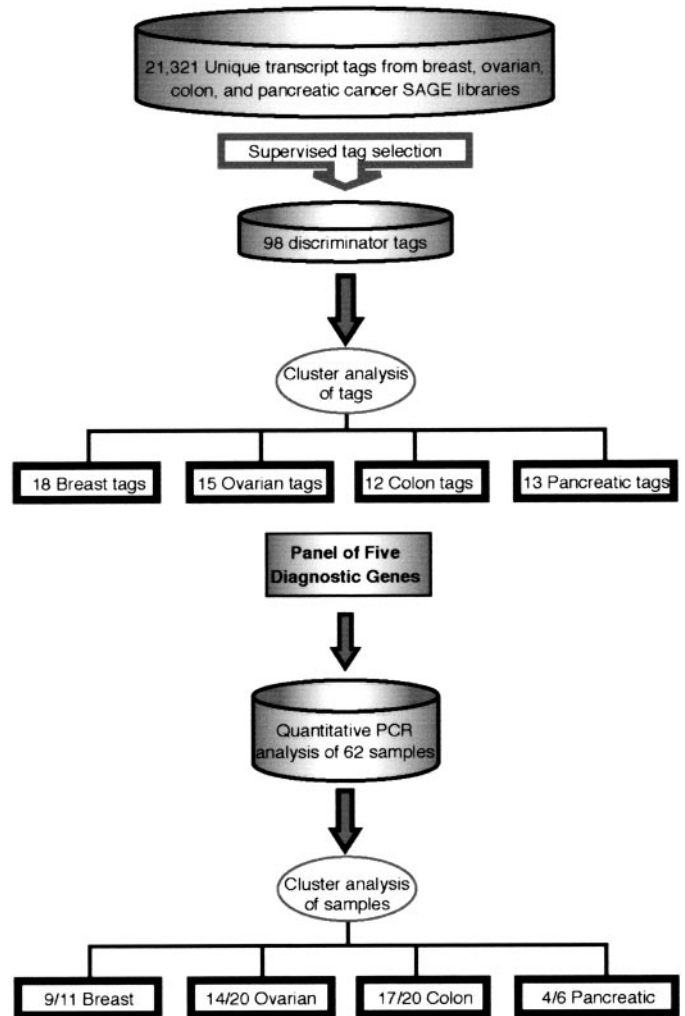


Fig. 1. Outline of data analysis. Tags were subjected to a combination of supervised and unsupervised selection algorithms. Expression levels of genes corresponding to informative transcript tags were measured by quantitative real-time PCR, and the expression data were used to identify tissue type in a test set of 62 clinical samples.

libraries obtained from many tissue sites in the future extended study. This analysis resulted in a total of 98 unique transcript tags including 15 tags for ovarian, 12 tags for colon, 13 tags for pancreatic, and 18 tags for breast carcinomas that were calculated to be most informative for tumor site-specific classification. This was corroborated by a two-way hierarchical cluster analysis of both tumors and tags based on the expression levels of this reduced number of tags. This relatively small subset of transcript tags (<0.5% of all tags) was sufficient to correctly cluster the SAGE libraries into groups of similar tissue origins (Fig. 2, horizontal tree). Additionally, tags clustered into nodes of similar expression patterns and had clearly visible associations with the above carcinomas arising from different tissue types (Fig. 2, vertical tree). The tags were matched to the Unigene database,⁸ and three well-characterized genes from each node were randomly selected to evaluate their performance in quantitative real-time PCR. Five of these genes showed robust and specific PCR products without detectable primer dimer formation and were further analyzed for their diagnostic potential (Table 1). The selection of these five genes from the candidate pool was arbitrary and driven by technical limitations (*i.e.*, capacity and success of real-time PCR). Most tags present in the pancreatic cluster did not match known genes and were not pursued

⁶ Internet address: <http://www.ncbi.nlm.nih.gov/SAGE/>.

⁷ Internet address: <http://rana.lbl.gov/EisenSoftware.htm>.

⁸ Internet address: <http://www.ncbi.nlm.nih.gov/UniGene/>.

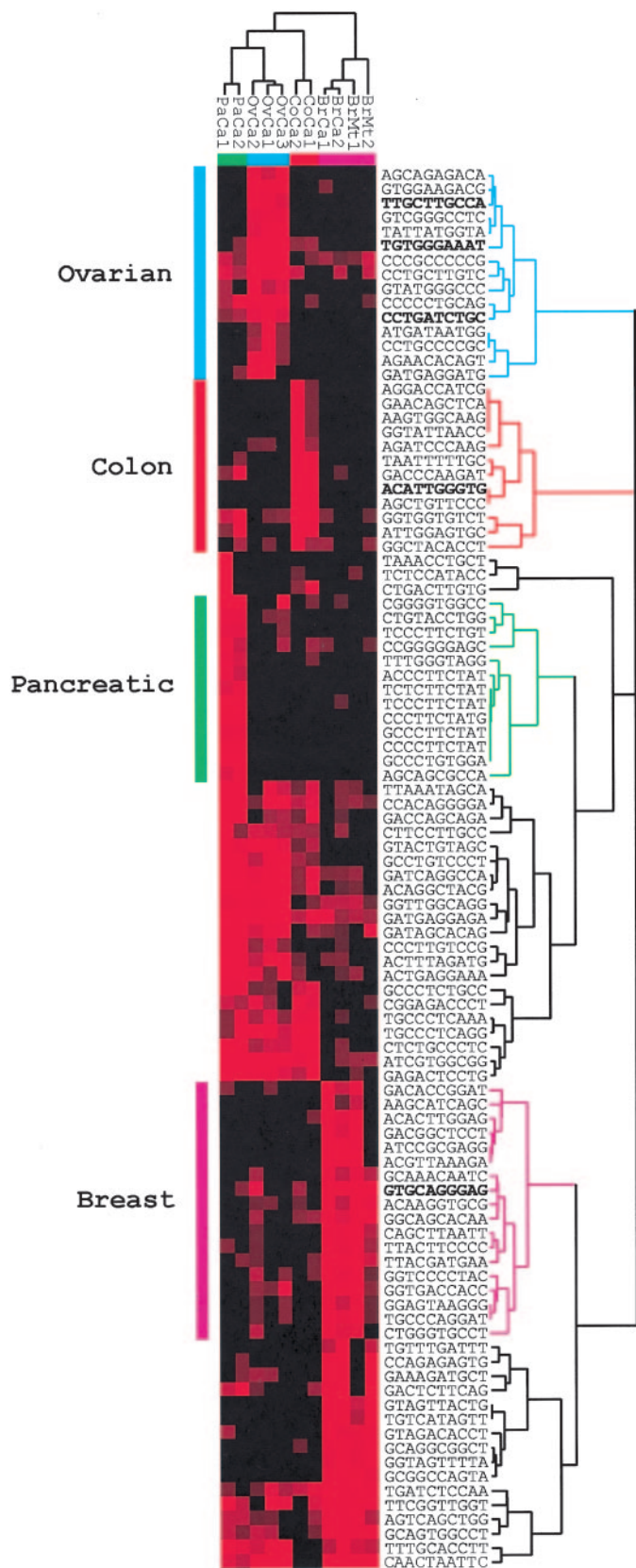


Fig. 2. Cluster analysis and identification of diagnostic tags. The most informative 98 tags (vertical tree) were subjected to two-way hierarchical cluster analysis with different SAGE libraries (horizontal tree) as the training set. Seventy-one cancer type-specific tags are identified and include 15 tags for ovarian, 12 tags for colon, 16 tags for pancreatic, and 28 tags for breast carcinomas. A total of five genes with their tag sequences bolded were selected for real-time PCR. *PaCa*, primary pancreatic carcinoma; *OvCa*, primary ovarian carcinoma; *BrCa*, primary breast carcinoma; *BrMt*, breast carcinoma metastases.

further. Among all of the genes analyzed in the SAGE libraries, APP (Unigene ID 177486) demonstrated a relatively constant expression level and was selected as the control for subsequent expression analyses.

Validation of Diagnostic Genes. To prospectively evaluate their diagnostic power, the expression levels of the five genes selected from the above training set were evaluated by quantitative real-time PCR in a separate set of 62 samples of breast, colon, ovarian, and pancreatic primary carcinomas and metastases and normal ovarian surface epithelium. Ct differences between each diagnostic gene and the control gene (APP) were calculated, and the expression data obtained from this validation set were subjected to unsupervised hierarchical cluster analysis. This analysis was able to correctly classify 44 of 62 samples according to their sites of origin (Fig. 3). A pancreatic cluster was not evident by this analysis. With a sensitivity of 71% (44 of 62), real-time PCR results clearly validated the diagnostic genes' ability to classify different types of adenocarcinomas

In an attempt to improve the resolving power of the expression data, and display results in terms of diagnostic probability, an unsupervised two-dimensional SOM analysis of the quantitative real-time PCR data was performed (10). As shown in Fig. 4, each of the five genes demonstrated a gradient in expression levels with the highest expression present in certain types of cancers. For practical application of this analysis, we generated a two-dimensional gene expression-based classification map according to different cancer types (Fig. 5). Most adenocarcinomas clustered within their well-defined map districts bounded by iso-probability curves. This type of analysis allowed for a rapid visual assessment of the probabilities of each cancer diagnosis. Based on our computational analysis, most of the probability maps demonstrated a single diagnostic domain with the exception of the breast carcinoma probability map, which exhibited two diagnostic domains. By integrating the spatial distribution patterns of these five individual estimated tissue type cancer probability maps, a combined classification map was established (Fig. 5, right bottom corner) with borders between the domains determined by maximizing the overall sensitivity for all diagnostic domains. This allowed categorization of the adenocarcinomas and normal samples into their specific domains with a sensitivity of 80.6% (50 of 62). Metastases clustered tightly with their corresponding primary tumors. In the ovarian cancer probability map, all ovarian cancer specimens were of serous types, the most common type of ovarian cancer, with the exception of two specimens, which were located outside the border of the ovarian cancer diagnostic domain. Histologically, both cases were retrospectively found to be unusual nonserous subtypes of ovarian cancer (20).

DISCUSSION

The results described above demonstrate that expression analysis of a small set of genes can reliably discriminate adenocarcinomas of different tissue origins. These findings suggest that gene expression-based probability maps composed of spatial domains computed by the expression patterns of a few informative genes can provide a molecular platform to predict adenocarcinoma of clinically unknown origin. It is noteworthy that the expression patterns of several genes selected by this computational process have been observed previously by other methods to be relatively tissue specific for certain types of carcinomas, e.g., MUC16 has been recently identified as the gene encoding the CA125 antigen (21, 22), which has long been known as an ovarian cancer-associated marker and routinely used to monitor the response of therapy and detect tumor recurrence in ovarian cancer patients (20). Additionally, ceruloplasmin and SLPI have been reported among the most highly up-regulated markers in ovarian carcinoma (13). Similar to a previous report (23), our finding supports the utility of the SAGE

Table 1 Panel of diagnostic genes

Category	SAGE tag	Unigene no.	Gene	Transcript tag counts from cancer SAGE libraries ^a										
				CoCa1	CoCa2	OvCa1	OvCa2	OvCa3	BrCa1	BrCa1MET	BrCa2	BrCa2MET	PaCa1	PaCa2 ^b
Colon	ACATTGGGTG	351719	FABP1	56	221	0	0	0	0	0	0	0	0	0
Ovarian	TTGCTTGCCA	296634	CP	0	0	23	41	12	0	0	0	0	0	
Ovarian	CCTGATCTGC	98502	MUC16	0	0	28	14	12	0	0	0	3	5	
Ovarian	TGTGGGAAAT	251754	SLPI	3	5	34	62	143	0	0	0	0	3	
Breast	GTGCAGGAG	79414	PDEF	5	0	0	12	0	61	63	58	44	0	3
Control	GTGAAACCCC	177486	APP	681	834	508	381	387	269	213	546	415	681	562

^a Normalized to 100,000 total tags.

^b CoCa, colon cancer; OvCa, ovarian cancer; BrCa, breast cancer; PaCa, pancreatic cancer; BrCaMET, breast cancer metastasis.

database and robustness of our computational methods in identifying candidate genes for validation. Among those tumor samples that failed to cluster into their diagnostic domains, two ovarian carcinomas were retrospectively found to be nonserous subtypes. This result suggests that our method could be used to define histological subtypes within a tumor type.

As compared with the global transcriptional profiling that analyzes thousands of genes, our reductionist approach, deploying a two-dimensional, expression-based classification map based on a few highly informative genes, has several advantages in determining the origin of a metastatic carcinoma of clinically unknown primary: (a) only a relatively small amount of tissue material is required. This feature is particularly attractive because minimally invasive tech-

niques such as small biopsies using fine needle, endoscope, and laparoscope approaches are frequently used; (b) by reducing thousands of genes to a limited set of informative genes, the background noise introduced by the vast majority of irrelevant genes can be minimized, and the information gained from each sample is maximized. A similar approach has been shown effective in a specialized cDNA array with only hundreds of genes (24). Accordingly, sensitivity can be improved using this approach; (c) quantitative real-time PCR has become a reliable assay without the need for sophisticated instrumentation (7). In contrast to DNA array hybridization and SAGE, the assays can be performed in a shorter period of time (~5 h) at low cost; and (d) although bioinformatics tools have recently been applied to microarray data and shown utility in predicting both cancer

Fig. 3. Hierarchical cluster analysis of gene expression in a validation set of 62 carcinoma specimens. Quantitative real-time PCR data were evaluated using unsupervised hierarchical cluster analysis. Forty of 50 colon, ovarian, and breast carcinomas cluster to their site of origin. Four of five normal ovarian surface epithelial controls also clustered. No pancreatic cluster was observed. *P*, pancreatic carcinoma; *O*, ovarian carcinoma; *C*, colon carcinoma; *B*, breast carcinoma; *N*, normal ovarian surface epithelial controls.

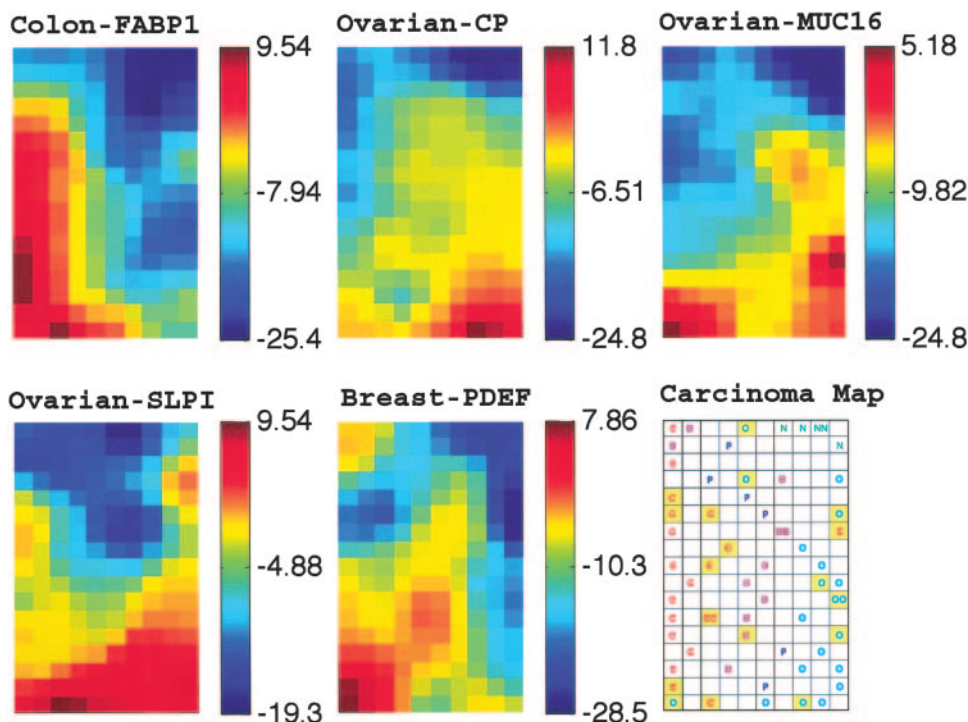
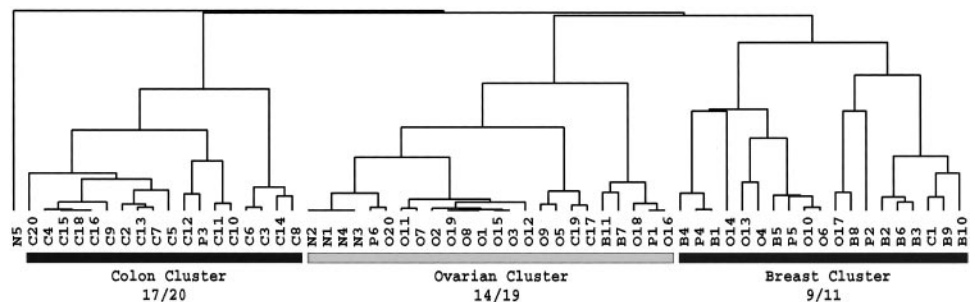
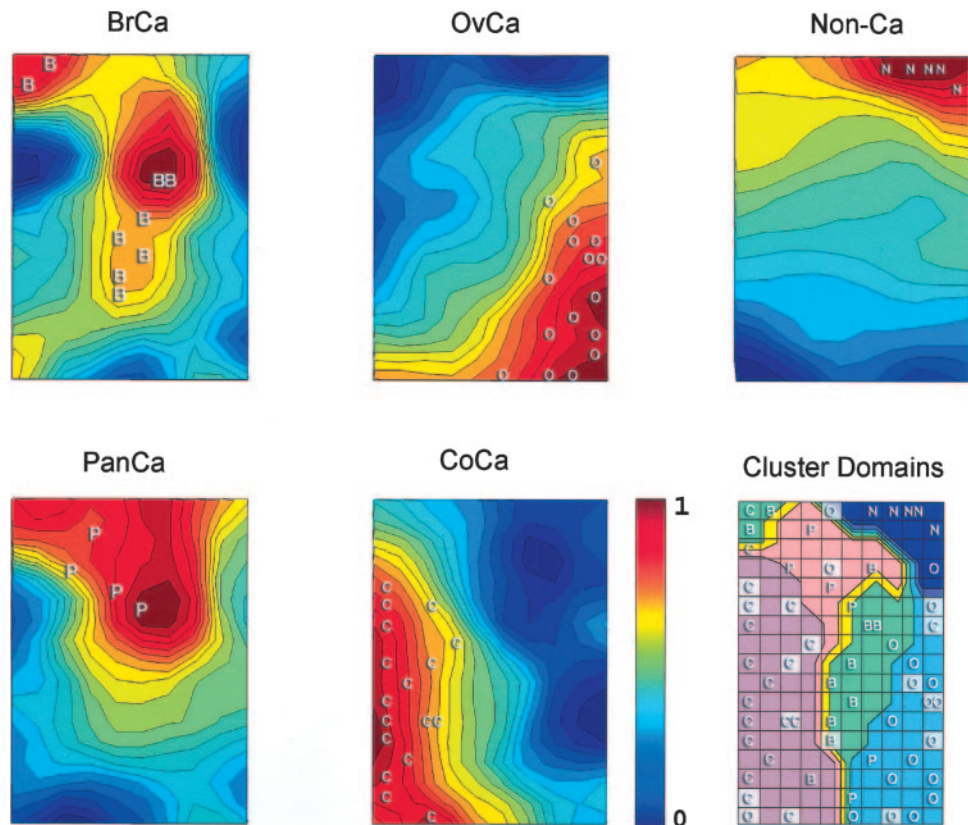


Fig. 4. Distribution of samples and gene expression levels using SOM analysis. Expression data from quantitative real-time PCR analyses are represented as pseudo-color gradients corresponding to the Ct differences between experimental and control genes (bars to the right of each panel). The placements of corresponding clinical samples by SOM are indicated in the right bottom panel. *O*, ovarian carcinoma; *B*, breast carcinoma; *P*, pancreatic carcinoma; *C*, colon carcinoma; *N*, normal ovarian surface epithelial controls. Metastases are noted by the yellow boxes.

Fig. 5. Expression-based classification map for primary site determination. A probability surface shown as a pseudo-color map was estimated for each cancer type, and individual clinical samples were projected onto the map according to their positions by SOM. The highest probability (*J*) is shown in *red* and lowest (*O*) in *blue*. Iso-probability curves for all carcinoma types are outlined. The landscape of the integrated classification map from the five individual tissue-type probability maps is shown in the *right bottom panel*. The borders were generated along the contiguous saddle points, which represent equal probability between neighboring domains, and maximize the diagnostic sensitivity for all five tissue types. *P*, pancreatic carcinoma; *O*, ovarian carcinoma; *C*, colon carcinoma; *B*, breast carcinoma; *N*, normal ovarian surface epithelial controls. Metastases are noted in the lighter shaded boxes.



diagnosis (25) and outcome (26), our computational modeling of expression data through a surface probability map provides a quantitative appreciation of the probability of tissue origin in the tested sample. The results of this cancer classification map in combination with clinical profiles, including patients' demography, the prevalence-specific cancer types, and other clinical parameters, could be clinically useful in determining the cancer origin from unknown primary.

In conclusion, this report provides evidence that a gene expression-based probability map could prove to be a powerful tool aiding the diagnosis of metastatic carcinomas of unknown origin. However, before this approach becomes a practical cancer diagnostic tool, several issues need to be addressed. In this study, the sensitivity in differentiating various types of samples was 80.6%. Sensitivity might be improved in the following ways. Additional gene markers from the candidate list of SAGE tags (Fig. 2) can be tested to determine whether either can be increased over that obtained from the current selected genes. Our approach can also be used in conjunction with emerging protein or peptide markers that are relatively tissue specific, yet are of suboptimal sensitivity or specificity. Although this report only included four major cancer types to demonstrate the feasibility of this method, it would be important to extend our approach to a larger set of samples from a wide variety of common cancer types and generate a more comprehensive cancer diagnostic map. Finally, a more precise landscape of the probabilities and classification map will evolve as more samples are analyzed.

ACKNOWLEDGMENTS

We thank Drs. K. Kinzler and B. Vogelstein and the members of The Molecular Genetics laboratory, Johns Hopkins Oncology Center, for their critical comments.

REFERENCES

1. ACS Cancer Facts & Figures 2001: American Cancer Society, 2001.
2. Hillen, H. F. Unknown primary tumours. *Postgrad. Med. J.*, 76: 690–693, 2000.
3. Milovic, M., Popov, I., and Jelic, S. Tumor markers in metastatic disease from cancer of unknown primary origin. *Med. Sci. Monit.*, 8: MT25–MT30, 2002.
4. Diamandis, E. P., Fritsche, H. A., Lilja, H., Chan, D. W., and Schwartz, D. R. (eds.). *Tumor Markers: Physiology, Pathobiology, Technology and Clinical Applications*. Washington, DC: AACR Press, 2002.
5. Ramaswamy, S., Tamayo, P., Rifkin, R., Mukherjee, S., Yeang, C. H., Angelo, M., Ladd, C., Reich, M., Latulippe, E., Mesirov, J. P., Poggio, T., Gerald, W., Loda, M., Lander, E. S., and Golub, T. R. Multiclass cancer diagnosis using tumor gene expression signatures. *Proc. Natl. Acad. Sci. USA*, 98: 15149–15154, 2001.
6. Yeang, C. H., Ramaswamy, S., Tamayo, P., Mukherjee, S., Rifkin, R. M., Angelo, M., Reich, M., Lander, E., Mesirov, J., and Golub, T. Molecular classification of multiple tumor types. *Bioinformatics*, 17: S316–S322, 2001.
7. Freeman, W. M., Walker, S. J., and Vrana, K. E. Quantitative RT-PCR: pitfalls and potential. *Biotechniques*, 26: 112–122, 115–124, 1999.
8. Iwao, K., Matoba, R., Ueno, N., Ando, A., Miyoshi, Y., Matsubara, K., Noguchi, S., and Kato, K. Molecular classification of primary breast tumors possessing distinct prognostic properties. *Hum. Mol. Genet.*, 11: 199–206, 2002.
9. Zhang, Z., Page, G., and Zhang, H. (eds.). *Applying Classification Separability Analysis to Microarray Data*. New York: Kluwer Academic Publishers, 2001.
10. Kohonen, T. (ed.). *Self-organizing Maps*, Ed. 1. New York: Springer-Verlag, 1995.
11. Lal, A., Lash, A. E., Altschul, S. F., Velculescu, V., Zhang, L., McLendon, R. E., Marra, M. A., Prange, C., Morin, P. J., Polyak, K., Papadopoulos, N., Vogelstein, B., Kinzler, K. W., Strausberg, R. L., and Riggins, G. J. A public database for gene expression in human cancers. *Cancer Res.*, 59: 5403–5407, 1999.
12. St. Croix, B., Rago, C., Velculescu, V., Traverso, G., Romans, K. E., Montgomery, E., Lal, A., Riggins, G. J., Lengauer, C., Vogelstein, B., and Kinzler, K. W. Genes expressed in human tumor endothelium. *Science*, 289: 1197–1202, 2000.
13. Hough, C. D., Sherman-Baust, C. A., Pizer, E. S., Montz, F. J., Im, D. D., Renshew, N. B., Cho, K. R., Riggins, G. J., and Morin, P. J. Large-scale serial analysis of gene expression reveals genes differentially expressed in ovarian cancer. *Cancer Res.*, 60: 6281–6287, 2000.
14. Hough, C. D., Cho, K. R., Zonderman, A. B., Schwartz, D. R., and Morin, P. J. Coordinately up-regulated genes in ovarian cancer. *Cancer Res.*, 61: 3869–3876, 2001.
15. Porter, D. A., Krop, I. E., Nasser, S., Sgroi, D., Kaelin, C. M., Marks, J. R., Riggins, G., and Polyak, K. A SAGE (serial analysis of gene expression) view of breast tumor progression. *Cancer Res.*, 61: 5697–5702, 2001.
16. Zhang, L., Zhou, W., Velculescu, V. E., Kern, S. E., Hruban, R. H., Hamilton, S. R., Vogelstein, B., and Kinzler, K. W. Gene expression profiles in normal and cancer cells. *Science*, 276: 1268–1272, 1997.

17. Lash, A. E., Tolstoshev, C. M., Wagner, L., Schuler, G. D., Strausberg, R. L., Riggins, G. J., and Altschul, S. F. SAGEmap: a public gene expression resource. *Genome Res.*, 10: 1051–1060, 2000.
18. Eisen, M. B., Spellman, P. T., Brown, P. O., and Botstein, D. Cluster analysis and display of genome-wide expression patterns. *Proc. Natl. Acad. Sci. USA*, 95: 14863–14868, 1998.
19. Morrison, T. B., Weis, J. J., and Wittwer, C. T. Quantification of low-copy transcripts by continuous SYBR Green I monitoring during amplification. *Biotechniques*, 24: 954–958, 960–962, 1998.
20. Shih, I-M., Sokoll, L. J., and Chan, D. W. Tumor markers in ovarian cancer. *In*: E. P. Diamandis, H. A. Fritsche, H. Lilja, D. W. Chan, and M. K. Schwartz (ed.), *Tumor Markers Physiology, Pathobiology, Technology and Clinical Applications*, pp. 239–252. Philadelphia: AACR Press, 2002.
21. Yin, B. W., and Lloyd, K. O. Molecular cloning of the CA125 ovarian cancer antigen: identification as a new mucin, MUC16. *J. Biol. Chem.*, 276: 27371–27375, 2001.
22. Yin, B. W., Dnistrian, A., and Lloyd, K. O. Ovarian cancer antigen CA125 is encoded by the MUC16 mucin gene. *Int. J. Cancer*, 98: 737–740, 2002.
23. Dennis, J. L., Vass, J. K., Wit, E. C., Keith, W. N., and Oien, K. A. Identification from public data of molecular markers of adenocarcinoma characteristic of the site of origin. *Cancer Res.*, 62: 5999–6005, 2002.
24. Sawiris, G. P., Sherman-Baust, C. A., Becker, K. G., Cheadle, C., Teichberg, D., and Morin, P. J. Development of a highly specialized cDNA array for the study and diagnosis of epithelial ovarian cancer. *Cancer Res.*, 62: 2923–2928, 2002.
25. Golub, T. R., Slonim, D. K., Tamayo, P., Huard, C., Gaasenbeek, M., Mesirov, J. P., Coller, H., Loh, M. L., Downing, J. R., Caligiuri, M. A., Bloomfield, C. D., and Lander, E. S. Molecular classification of cancer: class discovery and class prediction by gene expression monitoring. *Science*, 286: 531–537, 1999.
26. Pomeroy, S. L., Tamayo, P., Gaasenbeek, M., Sturla, L. M., Angelo, M., McLaughlin, M. E., Kim, J. Y., Goumnerova, L. C., Black, P. M., Lau, C., Allen, J. C., Zagzag, D., Olson, J. M., Curran, T., Wetmore, C., Biegel, J. A., Poggio, T., Mukherjee, S., Rifkin, R., Califano, A., Stolovitzky, G., Louis, D. N., Mesirov, J. P., Lander, E. S., and Golub, T. R. Prediction of central nervous system embryonal tumour outcome based on gene expression. *Nature*, 415: 436–442, 2002.

HLA-G Is a Potential Tumor Marker in Malignant Ascites

Gad Singer, Vera Rebmann, Yu-Chi Chen, Hsu-Tai Liu, Syed Z. Ali, Jochen Reinsberg, Michael T. McMaster, Kerstin Pfeiffer, Daniel W. Chan, Eva Wardelmann, Hans Grosse-Wilde, Chih-Chien Cheng, Robert J. Kurman, and Ie-Ming Shih¹

Department of Pathology [G. S., Y-C. C., S. Z. A., D. W. C., C-C. C., R. J. K., I-M. S.], and Department of Epidemiology [H-T. L., Johns Hopkins University Medical Institutions, Baltimore Maryland 21231; Department of Immunology, University Hospital of Essen, Essen, Germany [V. R., H. G-W.]; Departments of Gynecology and Obstetrics [J. R., K. P.], and Department of Pathology [E. W.], University of Bonn, Bonn, Germany; and Department of Stomatology, University of California, San Francisco, California [M. T. M.]

ABSTRACT

Purpose: Molecular approaches as supplements to cytological examination of malignant ascites may play an important role in the clinical management of cancer patients. HLA-G is a potential tumor-associated marker and that one of its isoforms, HLA-G5, produces a secretory protein. This study is to assess the clinical utility of secreted HLA-G levels in differential diagnosis of malignant ascites.

Experimental Design: We used ELISA to assess whether secretory HLA-G (sHLA-G) could serve as a marker of malignant ascites in ovarian and breast carcinomas, which represent the most common malignant tumors causing ascites in women.

Results: On the basis of immunohistochemistry, 45 (61%) of 74 ovarian serous carcinomas and 22 (25%) invasive ductal carcinomas of the breast demonstrated HLA-G immunoreactivity ranging from 2 to 100% of the tumor cells. HLA-G staining was not detected in a wide variety of normal tissues, including ovarian surface epithelium and normal breast tissue. Reverse transcription-PCR demonstrated the presence of HLA-G5 isoform in all of the tumor samples expressing HLA-G. ELISA was performed to measure the sHLA-G in 42 malignant and 18 benign ascites

supernatants. sHLA-G levels were significantly higher in malignant ascites than in benign controls ($P < 0.001$). We found that the area under the receiver-operating characteristic curve for sHLA-G was 0.95 for malignant versus benign ascites specimens. At 100% specificity, the highest sensitivity to detect malignant ascites was 78% (95% confidence interval, 68–88%) at a cutoff of 13 ng/ml.

Conclusions: Our findings suggest that measurement of sHLA-G is a useful molecular adjunct to cytology in the differential diagnosis of malignant versus benign ascites.

INTRODUCTION

Ascites is commonly associated with a variety of infectious diseases, inflammatory disorders, and cardiac, liver, and renal diseases as well as benign and malignant neoplasms (1–3). Cytological examination of ascites is performed in an effort to diagnose malignant tumors, but the sensitivity of cytology has been estimated to be 60% at best (4). The low sensitivity may be because of small numbers of tumor cells in the ascites or the presence of a large amount of leukocytes, mesothelial cells, and blood that can obscure the malignant cells. For example, inflammation that is often associated with a malignant ascites can result in reactive changes in mesothelial cells that make their morphological distinction from carcinoma cells extremely difficult (4). Thus, a molecular test that is able to distinguish malignant from benign ascites could have great diagnostic utility.

HLA-G is a nonclassical MHC class I antigen that interacts with natural killer cells (5). HLA-G expression has not been detected in normal tissues except in trophoblast in placentas from early gestation (6–8). In contrast, HLA-G expression has been detected in several human cancers including melanoma, renal cell carcinoma, breast carcinoma, and large cell carcinoma of the lung (9–14). HLA-G expression in cancer cells has been shown to be important for the escape of immunosurveillance by host T-lymphocytes and natural killer cells (6, 9–11, 15, 16). Recently, an HLA-G-specific ELISA was developed to measure sHLA-G, a product of an HLA-G5 isoform (17–19). Because HLA-G is not detected in normal adult tissues but is expressed by some carcinomas, we hypothesized that the detection of sHLA-G² using the newly developed ELISA might be useful in the detection of cancer in ascites. In this study, we tested this hypothesis by assessing the expression pattern of HLA-G in women with ovarian serous carcinomas and invasive ductal carcinomas of the breast because these are the most common malignant tumors in women that produce ascites. We measured sHLA-G in peritoneal fluid supernatant to evaluate its potential as a marker for malignant ascites.

Received 2/24/03; revised 5/20/03; accepted 5/21/03.

The costs of publication of this article were defrayed in part by the payment of page charges. This article must therefore be hereby marked *advertisement* in accordance with 18 U.S.C. Section 1734 solely to indicate this fact.

This work was supported in part by the United States Department of Defense OC 010017 Grant, the Richard TeLinde Research Fund from The Johns Hopkins University (JHU) School of Medicine, the JHU-American Cancer Society, and the Swiss National Science Foundation (to G. S.).

¹To whom requests for reprints should be addressed, at The Johns Hopkins Medical Institutions, 418 North Bond Street, Room B-315, Baltimore, MD 21231. Phone: (410) 502-774; Fax: (410) 502-7943; E-mail: ishah@jhmi.edu.

²The abbreviations used are: sHLA-G, secretory or soluble HLA-G; CI, confidence interval; RT-PCR, reverse transcription-PCR; ROC, receiver operating characteristic (curve).

MATERIALS AND METHODS

Tissue Samples and Ascites Specimens. The acquisition of paraffin tissues and ascites specimens was approved by the local Institutional Review Boards. A total of 180 formalin-fixed, paraffin-embedded tissue samples including 74 ovarian serous carcinomas, 88 breast invasive ductal carcinomas, 8 normal ovaries, and 10 benign breast tissues were retrieved from the surgical pathology files. Peritoneal fluid specimens (3–5 ml) were obtained from the Cytopathology Division of the University of Bonn, Bonn, Germany, and from the Johns Hopkins Medical Institutions; they included 41 cytology-confirmed malignant ascites samples (24 ovarian serous carcinomas and 17 breast carcinomas) and 19 cytology-negative benign specimens in which the patients did not have concurrent malignant diseases. There was a cytology-false-negative specimen that was initially diagnosed by cytopathologists as benign, but the patients had stage III ovarian cancer, and the ascites sample contained ovarian serous carcinoma cells in culture (20). Thus, this sample was later classified into the ovarian cancer group in this study. The ascites samples were centrifuged at $2000 \times g$ for 5 min within 6 h after collection. The supernatant and cell pellets were aliquoted and frozen until use. All of the specimens were obtained from female adult patients.

Immunohistochemistry and Western Blot Analysis. Expression of HLA-G was studied in surgical specimens using immunohistochemistry and Western blot analysis. Paraffin sections were used for immunohistochemistry with an HLA-G-specific monoclonal antibody, 4H84 (1:600), which reacted to the denatured HLA-G heavy chain (6), followed by the avidin-biotin peroxidase method (8, 15). The frequency of positive cells was estimated by randomly counting more than 500 tumor cells from three different high-power fields ($\times 40$). Western blot analysis was performed using the 4H84 antibody (1:1000) on five ovarian serous carcinomas that showed positive HLA-G immunostaining, two specimens of epithelium isolated from ovarian serous cystadenomas, one primary culture from normal ovarian surface, one sample of normal ovarian tissue, and one sample of isolated peripheral leukocytes. Similar amounts of total protein from each lysate were loaded and separated on 12% Tris-Glycine-SDS polyacrylamide gels (Novex, San Diego, CA) and electroblotted to Millipore Immobilon-P polyvinylidene difluoride membranes. Western blots were developed by chemiluminescence (Pierce, Rockford, IL).

RT-PCR. RT-PCR was performed to validate the HLA-G expression and to determine the isoforms expressed in a panel of 11 ovarian and 5 breast carcinomas using the protocol described previously (21). The assay was not performed in samples that stained negative for the HLA-G antibody. The primer sequences for all of the HLA-G isoforms were: 5'-ggaagaggagacacgaaca-3' and 5'-gcagctccagtactacgc-3'. The primer sequences for HLA-G5-specific primers were: 5'-accgacctgtaaggtctt-3' and 5'-caatgtgctgaacaaggagag-3'. Total RNA was purified and cDNA was synthesized using standard protocols. Briefly, frozen tissues were minced and placed in the TRIzol reagent (Invitrogen, Carlsbad, CA). Total RNA was isolated, and contaminating genomic DNA was removed using the DNA-free kit (Ambion, Austin, TX). cDNA was prepared using oligo(dT) primers and was diluted for PCR.

H&E-stained sections were prepared from a portion of the frozen tumors and were reviewed by a surgical pathologist (I-M. S.) to confirm the diagnosis. The PCR products were separated by 2% agarose gels.

ELISA. sHLA-G was measured using ELISA, which has been described previously by us (18, 19). Briefly, soluble HLA-A, B, C, E molecules (sHLA-I) were selectively depleted from samples using immunomagnetic beads (Dynabeads M280; Dynal, Hamburg, Germany) coupled with the monoclonal antibody TP25.99. The remaining sHLA-G molecules were measured in an ELISA format using monoclonal antibody W6/32 [0.2 $\mu\text{g/ml}$ in PBS (pH 7.2)] as the capture reagent. After the blocking of free binding sites with BSA in PBS (2%), diluted samples (1:2) were added and incubated for 1 h at room temperature. Unbound antigens were removed by intensive washing with PBS-Tween (0.05%). Bound sHLA-G heavy chains were detected by the sequential addition of pox-labeled antihuman $\beta 2$ -microglobulin antiserum (Dakopatts, Hamburg, Germany), and substrate [0.075% H_2O_2 , 0.1% ortho-phenylenediamine in 0.035 M citrate buffer (pH 5.0)]. The absorbance was measured at 490 nm (BIO-TEK Instruments, Winooski, VT). The intra- and interassay variations were 3.5 and 13.1%, respectively. The sensitivity of the assay in detecting sHLA-G was 3 ng/ml. ELISA was performed in a blinded fashion.

Statistical Analysis. The feasibility of using sHLA-G levels as a diagnostic tool for detecting malignant *versus* benign ascites was assessed using the ROC curve analysis. A ROC curve is a graphic presentation of the sensitivity against the false-positive rate (1-specificity), and the areas under the ROC curves were measured to evaluate test performance at different thresholds of a diagnostic measure. The χ^2 test (one-sided) of the medians was used to analyze the difference in sHLA-G levels in malignant *versus* benign ascites samples. The CIs were estimated for the sensitivity of the HLA-G ELISA.

RESULTS

Expression of HLA-G in Ovarian and Breast Cancer Tissues. Immunohistochemical analysis of ovarian and breast carcinomas revealed HLA-G immunoreactivity in 45 (61%) of 74 high-grade ovarian serous carcinomas and in 22 (25%) of 88 invasive ductal carcinomas of the breast (Fig. 1). The positive tumor cells showed a discrete membranous staining pattern, and the proportion of positive cells varied from 2 to 100% in any given specimen. HLA-G staining was not detected in low-grade ovarian serous carcinomas and normal tissues including ovarian surface epithelium, mammary ducts, and lobules. We also assessed HLA-G immunoreactivity in benign ovarian and breast lesions. HLA-G expression was not detected in 8 ovarian serous cystadenomas, 12 ovarian borderline tumors (atypical proliferative serous tumors and noninvasive micropapillary serous carcinomas), nor 10 intraductal hyperplasias of the breast. Only rare HLA-G-positive tumor cells were identified in 2 of 10 intraductal carcinomas of the breast. The specificity of HLA-G immunostaining was confirmed by Western blot analysis and RT-PCR as shown in Fig. 2. A 39 kDa band corresponding to the HLA-G protein was identified in five ovarian serous carcinomas but not in two ovarian cystadenomas, ovarian surface epithelium, and stroma. RT-PCR was performed in ovarian

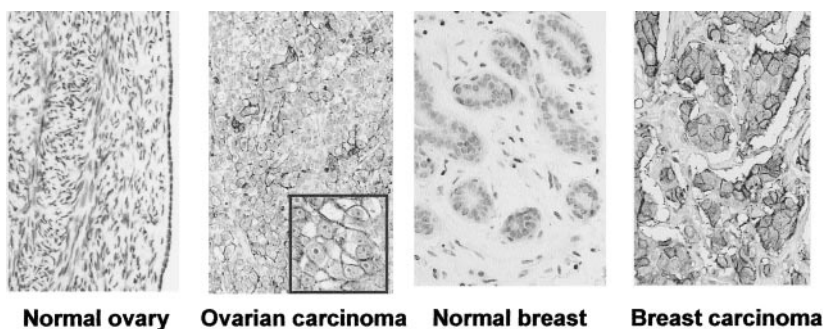


Fig. 1 HLA-G expression based on immunohistochemistry in ovarian serous carcinomas and breast ductal carcinomas. HLA-G immunoreactivity is predominantly localized in the cell membrane of tumor cells (inset) in ovarian serous carcinoma and breast ductal carcinoma. There is no detectable HLA-G immunoreactivity in ovarian surface epithelium of normal ovary and normal breast tissue. The stromal cells and inflammatory cells are negative.

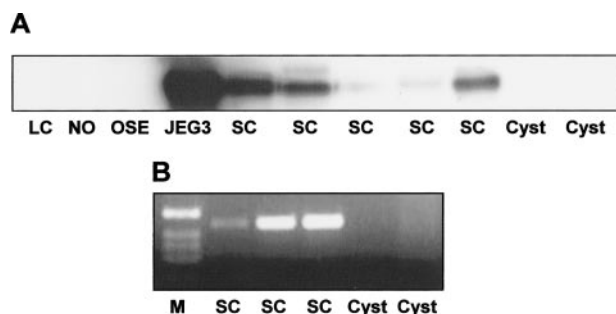


Fig. 2 Western blot analysis. A, a 39 kDa band corresponding to HLA-G protein is demonstrated in all five of the ovarian serous carcinomas (SC) and the positive control, JEG3 choriocarcinoma cell line, but not in peripheral leukocytes (LC), normal ovarian stromal tissue (NO), ovarian surface epithelium (OSE), and cyst epithelium (Cyst) from two ovarian serous cystadenomas. B, RT-PCR. HLA-G5 PCR products were present in three ovarian cancer tissues that express HLA-G using immunohistochemistry but not in two ovarian serous cysts that fail to show HLA-G immunostaining. M, 1-Kb DNA marker.

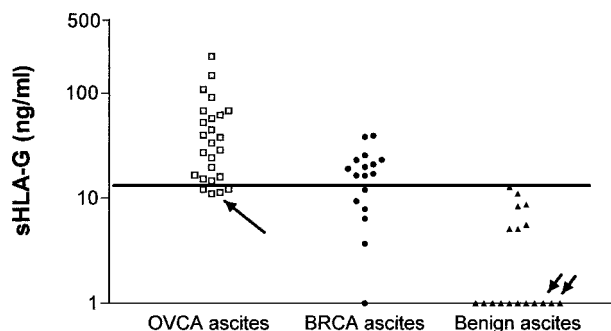


Fig. 3 Scatter plot showing sHLA-G concentrations in a total of 60 ascites samples as determined by ELISA. All of the 25 ovarian cancer (OVCA) patients (□) and 16 of 17 breast cancer (BRCA) patients (●) have detectable HLA-G levels. Long arrow, the patient with malignant ascites but with a negative cytology. In contrast, 7 of 18 benign ascitic fluid samples in the age-matched control group (▲) has a detectable but low HLA-G level. Short arrows, the two patients with ovarian cystadenomas. As compared with benign group, the levels of sHLA-G are significantly higher in ovarian ($P < 0.001$) and breast cancer groups ($P < 0.001$). solid line, an arbitrary cutoff (13 ng/ml) to give 100% specificity in diagnosing malignant ascites.

serous carcinomas and invasive ductal carcinomas of the breast using primers that amplified all HLA-G isoforms. The PCR products were isolated by electrophoresis to reveal a predominance of the HLA-G1 and G5 isoforms. HLA-G5 RNA transcript, a secretory isoform, was specifically amplified using the HLA-G5-specific primers in all five of the representative ovarian serous carcinomas and in the two invasive ductal carcinomas of breast that expressed HLA-G (Fig. 2). This finding prompted us to assess whether sHLA-G could be detected in peritoneal fluid samples in ovarian and breast cancer patients.

Measurement of sHLA-G in Ascites Specimens.

sHLA-G levels were measured in the supernatant of ascites from 60 samples using ELISA. All but one malignant ascites supernatant contained detectable sHLA-G, including one specimen that had been missed on cytology (20). In contrast, 7 of 18 benign specimens contained detectable but low levels of sHLA-G. As shown in Fig. 3, the levels of sHLA-G were significantly higher in malignant as compared with benign ascites ($P < 0.001$). Among 11 benign ascites specimens with undetectable sHLA-G, 2 were obtained from patients with ovarian serous cystadenomas that could be confused with ovarian cancer on clinical examination. The remaining seven benign samples with detectable sHLA-G were from patients with non-neoplastic diseases including liver, cardiac, and renal diseases.

ROC curves were used to evaluate the performance of sHLA-G in detecting ovarian and breast cancer in ascites using multiple cutoff values. The area under the ROC curve was 0.95 in assessing sHLA-G levels as the diagnostic tool to detect ovarian and breast cancer. More specifically, the areas under the ROC curve were 0.99 and 0.90 for ovarian cancer versus benign samples and breast cancer versus benign samples, respectively (Fig. 4). Given 100% specificity, the highest sensitivity achieved to detect cancer was 78% (95% CI, 68–88%) at a cutoff of 13 ng/ml. The sensitivity to diagnose ovarian cancer and breast cancer was 84% (95% CI, 70–98%) and 65% (95% CI, 42–87%), respectively, at this arbitrary cutoff. With a specificity of 94.4%, the sensitivity was 100% (95% CI, 100%) and 71% (95% CI, 49–93%) for ovarian cancer and breast cancer, respectively.

Correlation of HLA-G expression in tissue or ascites cell pellets and the sHLA-G level in ascites supernatants was performed in 31 patients as the corresponding surgical specimens or cell pellets were available for analysis. In 21 malignant ascites samples with detectable sHLA-G, HLA-G expression was demonstrated in 12 tissue specimens and ascites cell pellets by immunohistochemistry or Western blot analysis (data not

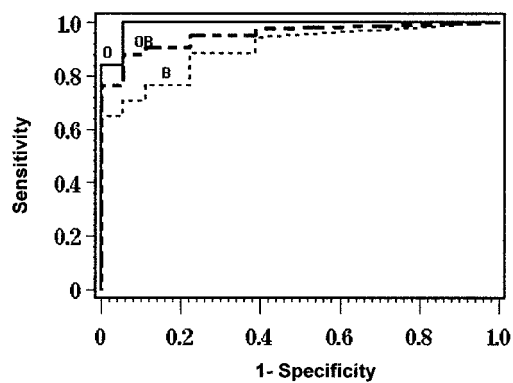


Fig. 4 ROC curve analysis based on 60 samples to assess the performance of sHLA-G levels in diagnosing malignant ascites. The area under the ROC curve assessing sHLA-G levels as the diagnostic tool to detect ovarian and breast cancer is 0.95. Specifically, the areas under the ROC curve are 0.99 and 0.90 for ovarian cancer *versus* benign samples and breast cancer *versus* benign samples, respectively. O: ovarian cancer; B, breast cancer; OB, ovarian and breast cancer.

shown). In 10 benign ascites samples (5 with detectable sHLA-G), there was no HLA-G expression detectable in ascites cell pellets using Western blot analysis.

DISCUSSION

The results of this study provide evidence that HLA-G is expressed in ovarian and breast carcinomas and that measurement of sHLA-G using ELISA is a highly sensitive technique to diagnose malignant ascites. Ninety-eight % of specimens with malignant cells, identified by cytology, had detectable sHLA-G levels. In addition, sHLA-G was detected in one specimen that was ultimately shown to be a false-negative case by cytological examination. The areas under the ROC curve were 0.99 and 0.90 for ovarian cancer *versus* benign samples and breast cancer *versus* benign samples, respectively. The better performance of sHLA-G in detecting ovarian cancer as compared with breast cancer is consistent with our immunohistochemical findings that ovarian cancers express HLA-G more frequently than breast cancers.

How does HLA-G compare with other soluble tumor-associated markers in diagnosing malignant ascites? Several protein markers have been studied including CA125 (22), tissue polypeptide-specific antigen, soluble interleukin-2 receptor α (23), soluble aminopeptidase N/CD13 (24), α -fetoprotein (25), carcinoembryonic antigen, CA 19-9, CA 15-3 (25), and several cytokines (26), but none are specific enough for cancer diagnosis because a variety of normal tissues, benign tumors, and nonneoplastic diseases also express these markers (24, 27-28). Using a cutoff value to achieve >90% specificity in detecting malignant ascites, the sensitivity of these markers was generally very low and, therefore, unacceptable for clinical application. In contrast, HLA-G has very limited tissue distribution because only a subpopulation of trophoblast (intermediate trophoblast) is known to express this molecule (7, 8) suggesting that sHLA-G would be more specific for cancer diagnosis. The findings in this study confirm this impression because the HLA-G ELISA

achieved a sensitivity of 78% and a specificity of 100% for diagnosing malignant ascites at a cutoff of 13 ng/ml.

The finding that almost all of the malignant ascites samples contained detectable sHLA-G contrasted with the lower rate of HLA-G expression in the tumors based on immunohistochemistry, because 61% of ovarian and only 25% of breast cancer tissue specimens were positive. In addition, some malignant ascites supernatants contained elevated sHLA-G levels, whereas HLA-G immunoreactivity was not detected in the corresponding tissue specimens and cell pellets from ascites by immunohistochemistry. This discordant finding can be explained by the fact that HLA-G is only focally expressed in most tumors and, therefore, may be undetected in representative tissue specimens selected for immunostaining or immunoblotting. It is likely that carcinoma cells in ascitic fluid secrete sHLA-G, resulting in high sHLA-G levels in ascites. If only a few tumor cells are present in the peritoneal fluid they may not be detected by cytology. Although these are our favorite explanations, other possibilities, albeit unlikely, should be also pointed out. For example, sHLA-G is expressed by other tissues in response to malignant diseases. The low level of sHLA-G in benign ascites may be attributable to nonspecific binding (background noise) of the antibody used in the ELISA. Alternatively, there may be unknown tissue resources that express sHLA-G and contribute to the low level of sHLA-G in ascites samples.

In summary, HLA-G is a tumor-associated molecule that is expressed by ovarian serous carcinoma and ductal carcinomas of the breast, the most common malignant tumors that produce ascites in women. Malignant ascites specimens contained much higher levels of sHLA-G than the benign ascites specimens. The detection of sHLA-G in ascitic fluid may provide a novel molecular approach to supplement cytological examination in the evaluation of ascites. It should be noted that the sensitivity of sHLA-G ELISA to diagnose malignant ascites may not be as high as shown in this study because the threshold to distinguish benign and malignant ascites could be higher than 13 ng/ml after a larger number of benign samples are analyzed. In order for this new marker to have clinical utility, several issues must be addressed. Although the sensitivity of sHLA-G ELISA in diagnosing malignant ascites in this study was 78% with 100% specificity, higher sensitivity would be desirable. Sensitivity could be improved by combining the measurement of sHLA-G with other tumor-associated markers (20, 29). It will be necessary to compare the performance of the sHLA-G ELISA and routine cytological examination by testing a large number of cytology-negative but biopsy-positive samples. It will also be important to address how age, menopausal status, histological grade and other clinical parameters affect HLA-G levels in ascites. Lastly, the potential use of sHLA-G in other body fluids such as plasma should be further investigated.

ACKNOWLEDGMENTS

We thank John Lauro at the Johns Hopkins Medical Institutions for his excellent technical support. This study is in memory of Dr. Frederick J. Montz of the Kelly Gynecologic Oncology Service at Johns Hopkins Hospital.

REFERENCES

- Senger, D. R., Galli, S. J., Dvorak, A. M., Perruzzi, C. A., Harvey, V. S., and Dvorak, H. F. Tumor cells secrete a vascular permeability factor that promotes accumulation of ascites fluid. *Science (Wash. DC)*, *219*: 983–985, 1983.
- Nagy, J. A., Herzberg, K. T., Dvorak, J. M., and Dvorak, H. F. Pathogenesis of malignant ascites formation: initiating events that lead to fluid accumulation. *Cancer Res.*, *53*: 2631–2643, 1993.
- Garrison, R. N., Galloway, R. H., and Heuser, L. S. Mechanisms of malignant ascites production. *J. Surg. Res.*, *42*: 126–132, 1987.
- Motherby, H., Nadjari, B., Friegel, P., Kohaus, J., Ramp, U., and Bocking, A. Diagnostic accuracy of ascites cytology. *Diagn. Cytopathol.*, *20*: 350–357, 1999.
- van der Ven, K., Pfeiffer, K., and Skrablin, S. HLA-G polymorphisms and molecule function—questions and more questions—a review. *Placenta*, *21* (Suppl. A): S86–S92, 2000.
- McMaster, M., Zhou, Y., Shorter, S., Kapasi, K., Geraghty, D., Lim, K. H., and Fisher, S. HLA-G isoforms produced by placental cytotrophoblasts and found in amniotic fluid are due to unusual glycosylation. *J. Immunol.*, *160*: 5922–5928, 1998.
- McMaster, M. T., Librach, C. L., Zhou, Y., Lim, K. H., Janatpour, M. J., DeMars, R., Kovats, S., Damsky, C. S., and Fisher, S. J. Human placental HLA-G expression is restricted to differentiated cytotrophoblasts. *J. Immunol.*, *154*: 3771–3778, 1995.
- Singer, G., Kurman, R. J., McMaster, M., and Shih, I-M. HLA-G immunoreactivity is specific for intermediate trophoblast in gestational trophoblastic disease and can serve as a useful marker in differential diagnosis. *Am. J. Surg. Pathol.*, *26*: 914–920, 2002.
- Paul, P., Rouas-Freiss, N., Khalil-Daher, I., Moreau, P., Riteau, B., Le Gal, F. A., Avril, M. F., Dausset, J., and Guillet, J. G. HLA-G expression in melanoma: a way for tumor cells to escape from immunosurveillance. *Proc. Natl. Acad. Sci. USA*, *95*: 4510–4515, 1998.
- Ibrahim, E. C., Guerra, N., Lacombe, M. J., Angevin, E., Chouaib, S., Carosella, E. D., Caignard, A., and Paul, P. Tumor-specific up-regulation of the nonclassical class I HLA-G antigen expression in renal carcinoma. *Cancer Res.*, *61*: 6838–6845, 2001.
- Urosevic, M., Kurrer, M. O., Kamarashev, J., Mueller, B., Weder, W., Burg, G., Stahel, R. A., Dummer, R., and Trojan, A. Human leukocyte antigen G up-regulation in lung cancer associates with high-grade histology, human leukocyte antigen class I loss and interleukin-10 production. *Am. J. Pathol.*, *159*: 817–824, 2001.
- Polakova, K., and Russ, G. Expression of the non-classical HLA-G antigen in tumor cell lines is extremely restricted. *Neoplasma*, *47*: 342–348, 2000.
- Davies, B., Hiby, S., Gardner, L., Loke, Y. W., and King, A. HLA-G expression by tumors. *Am. J. Reprod. Immunol.*, *45*: 103–107, 2001.
- Real, L. M., Cabrera, T., Collado, A., Jimenez, P., Garcia, A., Ruiz-Cabello, F., and Garrido, F. Expression of HLA G in human tumors is not a frequent event. *Int. J. Cancer*, *81*: 512–518, 1999.
- Lefebvre, S., Antoine, M., Uzan, S., McMaster, M., Dausset, J., Carosella, E. D., and Paul, P. Specific activation of the non-classical class I histocompatibility HLA-G antigen and expression of the ILT2 inhibitory receptor in human breast cancer. *J. Pathol.*, *196*: 266–274, 2002.
- Urosevic, M., Willers, J., Mueller, B., Kempf, W., Burg, G., and Dummer, R. HLA-G protein up-regulation in primary cutaneous lymphomas is associated with interleukin-10 expression in large cell T-cell lymphomas and indolent B-cell lymphomas. *Blood*, *99*: 609–617, 2002.
- Paul, P., Cabestre, F. A., Ibrahim, E. C., Lefebvre, S., Khalil-Daher, I., Vazeux, G., Quiles, R. M., Bermond, F., Dausset, J., and Carosella, E. D. Identification of HLA-G7 as a new splice variant of the HLA-G mRNA and expression of soluble HLA-G5, -G6, and -G7 transcripts in human transfected cells. *Hum. Immunol.*, *61*: 1138–1149, 2000.
- Rebmann, V., Pfeiffer, K., Passler, M., Ferrone, S., Maier, S., Weiss, E., and Grosse-Wilde, H. Detection of soluble HLA-G molecules in plasma and amniotic fluid. *Tissue Antigens*, *53*: 14–22, 1999.
- Ugurel, S., Rebmann, V., Ferrone, S., Tilgen, W., Grosse-Wilde, H., and Reinhold, U. Soluble human leukocyte antigen-G serum level is elevated in melanoma patients and is further increased by interferon- α immunotherapy. *Cancer (Phila.)*, *92*: 369–376, 2001.
- Chang, H-W, Ali, S. Z., Cho, S. K. R., Kurman, R. J., and Shih, I-M. Detection of allelic imbalance in ascitic supernatant by Digital SNP analysis. *Clin. Cancer Res.*, *8*: 2580–2585, 2002.
- Morrison, T. B., Weis, J. J., and Wittwer, C. T. Quantification of low-copy transcripts by continuous SYBR Green I monitoring during amplification. *Biotechniques*, *24*: 954–958, 960, 962, 1998.
- Sevinc, A., Sari, R., and Buyukberber, S. Cancer antigen 125: tumor or serosal marker in case of ascites? *Arch. Intern. Med.*, *161*: 2507–2508, 2001.
- Sedlacek, P., Frydecka, I., Gabrys, M., Van Dalen, A., Einarsson, R., and Harlozinska, A. Comparative analysis of CA125, tissue polypeptide specific antigen, and soluble interleukin-2 receptor α levels in sera, cyst, and ascitic fluids from patients with ovarian carcinoma. *Cancer (Phila.)*, *95*: 1886–1893, 2002.
- van Hensbergen, Y., Broxterman, H. J., Hanemaaijer, R., Jorna, A. S., van Lent, N. A., Verheul, H. M. W., Pinedo, H. M., and Hoekman, K. Soluble aminopeptidase N/CD13 in malignant and nonmalignant ascites and intratumoral fluid. *Clin. Cancer Res.*, *8*: 3747–3754, 2002.
- Sari, R., Yildirim, B., Sevinc, A., Bahceci, F., and Hilmioğlu, F. The importance of serum and ascites fluid alpha-fetoprotein, carcinoembryonic antigen, CA 19-9, and CA 15-3 levels in differential diagnosis of ascites etiology. *Hepatogastroenterology*, *48*: 1616–1621, 2001.
- Punnonen, R., Teisala, K., Kuoppala, T., Bennett, B., and Punnonen, J. Cytokine production profiles in the peritoneal fluids of patients with malignant or benign gynecologic tumors. *Cancer (Phila.)*, *83*: 788–796, 1998.
- Shahab, N. Tumor markers in malignant ascites. *Arch. Intern. Med.*, *162*: 949–950, 2002.
- Topalak, O., Saygili, U., Soyuturk, M., Karaca, N., Batur, Y., Uslu, T., and Erten, O. Serum, pleural ascites, and ascites CA-125 levels in ovarian cancer and nonovarian benign and malignant diseases: a comparative study. *Gynecol. Oncol.*, *85*: 108–113, 2002.
- Shih, I-M., Sokoll, L. J., and Chan, D. W. Tumor markers in ovarian cancer. In: E. P. Diamandis, H. A. Fritsche, H. Lilja, D. W. Chan, and M. K. Schwartz (eds.), *Tumor Markers physiology, Pathobiology, Technology and Clinical Applications*, pp. 239–252. Philadelphia: AACR Press, 2002.

Molecular Pathogenesis of Ovarian Borderline Tumors: New Insights and Old Challenges

le-Ming Shih and Robert J. Kurman

Abstract Ovarian borderline (low malignant potential) tumors are a puzzling group of neoplasms that do not fall neatly into benign or malignant categories. Their behavior is enigmatic, their pathogenesis unclear, and their clinical management controversial, especially for serous borderline tumors (SBT), the most common type of ovarian borderline tumor. Clarifying the nature of borderline tumors and their relationship to invasive carcinoma has puzzled investigators since the category was created over 30 years ago. Much of the confusion and controversy concerning these tumors is due to a lack of understanding of their pathogenesis and an absence of a model for the development of ovarian carcinoma. This review summarizes recent molecular studies of ovarian borderline tumors with special emphasis on the role of SBT in tumor progression and its relationship to ovarian serous carcinoma.

Ovarian cancer is composed of a heterogeneous group of tumors that are derived from the surface epithelium of the ovary or from surface inclusions. They are classified into serous, mucinous, endometrioid, clear cell, and Brenner (transitional) types corresponding to the different types of epithelia in the organs of the female reproductive tract (1–3). Each histologic subcategory is further divided into three groups: benign, intermediate (borderline tumor), and malignant, reflecting their clinical behavior (1). In developed countries, serous tumors account for about 60% of all ovarian epithelial tumors; therefore, serous borderline tumors (SBT) are the major focus of this review.

The modern history of SBTs begins in the 1950s and 1960s when investigators from the United States and Europe recognized that there was a subset of serous carcinomas that had a significantly better prognosis even when they presented as advanced stage tumors and were inadequately treated (4). The International Federation of Gynecology and Obstetrics in 1971 and subsequently the WHO in 1973 therefore created a separate category for these tumors, designating them “borderline” or “low malignant potential” (5). In addition, because women with advanced-stage borderline tumors had a very good prognosis, extraovarian lesions were classified as “implants” rather than metastases. The biggest challenge in the management of women with these tumors is to identify

the subset that will behave in a malignant fashion and to develop effective treatment for them. This challenge can only be addressed if the pathogenesis of these tumors is elucidated.

Molecular Studies of Ovarian Borderline Tumors

Ovarian serous carcinoma has been traditionally graded as well differentiated, moderately differentiated, and poorly differentiated, implying that serous carcinoma begins as a well-differentiated neoplasm that progresses over time to a poorly differentiated tumor. The recent molecular studies summarized below, however, have challenged this view and offered an alternative “dualistic” model of serous carcinogenesis.

Molecular genetic findings. Molecular genetic studies aimed at delineating the pathogenesis of SBTs have highlighted the importance of the KRAS signaling pathway. Activating mutations in KRAS and one of its downstream mediators, BRAF, have been identified in a variety of human cancers, and mutations of either KRAS or BRAF result in constitutive activation of the RAS/RAF/mitogen-activated protein kinase (MAPK) kinase (MEK)/MAPK signaling pathway (6). KRAS mutations were first reported in SBT by Mok et al. (7). Recent studies have verified the original finding and further showed that mutations in KRAS and BRAF characterize SBTs and low-grade serous carcinomas (8–11). Mutations in either codons 12 and 13 of KRAS or codon 599 of BRAF occur in two thirds of SBT and low-grade serous carcinomas (8, 9). In contrast, none of the 112 high-grade serous carcinomas (usual type of serous carcinoma) that we have analyzed contained KRAS or BRAF mutations. These findings provide compelling evidence indicating that KRAS and BRAF mutations are predominantly confined to low-grade serous ovarian carcinomas and their putative precursor, SBTs. The frequent mutations in KRAS and BRAF in SBTs in the progression of low-grade ovarian serous carcinoma tumor are analogous to melanoma and colorectal carcinoma in which mutations in RAS (KRAS in colorectal

Authors' Affiliation: Departments of Pathology, Oncology, and Gynecology/Obstetrics, Johns Hopkins Medical Institutions, Baltimore, Maryland
Received 4/7/05; revised 6/29/05; accepted 7/21/05.

Grant support: U.S. Department of Defense grants OC010017 and OC040060 and National Cancer Institute/NIH grant RO1 CA103937.

The costs of publication of this article were defrayed in part by the payment of page charges. This article must therefore be hereby marked *advertisement* in accordance with 18 U.S.C. Section 1734 solely to indicate this fact.

Requests for reprints: le-Ming Shih, Johns Hopkins Medical Institutions, 1503 East Jefferson Street, Room B-315, Baltimore, MD 21231. Phone: 410-502-7774; Fax: 410-502-7943; E-mail: ishih@jhmi.edu.

© 2005 American Association for Cancer Research.
doi:10.1158/1078-0432.CCR-05-0755

tumor and NRAS in melanoma) and *BRAF* genes also occur in their preinvasive stages, nevus and adenomatous polyp, respectively (12–15). Thus, it is likely that mutations in *RAS* and *RAF* genes are involved in early tumorigenesis, but the mutations are not sufficient for a malignant transformation. Interestingly, none of these three types of tumor that were analyzed showed mutations in both *RAS* and *BRAF* and lends further support to the view that *RAS* and *BRAF* mutations have an equivalent effect on tumorigenesis. In view of the absence of *KRAS* and *BRAF* mutations in high-grade serous carcinoma, it would seem that the development of high-grade serous carcinoma involves a pathway not related to the mutations in the *RAS/RAF/MEK/MAPK* signaling pathway. This conclusion is supported by the finding of p53 mutations in >50% of high-grade ovarian serous carcinomas and the rare finding of mutant p53 in SBTs and low-grade serous carcinomas (16, 17).

Two recent studies have employed mutational analysis to characterize the early molecular genetic events in the development of SBTs. In one study, 30 consecutive serous cystadenomas, the putative precursor of SBTs, were analyzed for *KRAS* and *BRAF* mutations and none were found (18). A subsequent study that analyzed eight serous cystadenomas containing small SBTs compared the mutational status of *KRAS* and *BRAF* in the SBT and the adjacent epithelium from the cystadenoma (19). It was found that four SBTs contained activating *KRAS* mutations at codon 12 and three SBTs contained mutant *BRAF* at codon 599. One case contained wild-type *KRAS* and *BRAF*. Moreover, the mutation detected in the SBT component of the tumor was identical to the mutation in the cystadenoma epithelium adjacent to the SBTs in 86% of informative cases. Unlike SBTs, cystadenoma epithelium lacks cytologic atypia. These findings have several important implications in thus far as the pathogenesis of SBT is concerned. First, they suggest that mutations of *KRAS* and *BRAF* are early events associated with tumor initiation as occurs in melanoma (14) and colorectal carcinoma (20). Moreover, it would seem that they precede the development of a SBT indicating that some cystadenomas are precursors of SBTs. Second, the frequency of mutations in *KRAS* and *BRAF* in cystadenomas associated with SBTs was significantly higher than those without SBTs. This finding together with the fact that SBTs are relatively uncommon compared with cystadenomas (1, 21–24) suggests that only a small proportion of serous cystadenomas are neoplastic with the potential to progress to SBTs.

The biological effects and clinical implication of *KRAS* and *BRAF* mutations in serous borderline tumor. The biological effects of mutations in *KRAS* and *BRAF* in the development of low-grade carcinoma are likely mediated by the constitutive activation of MAPK, the downstream target of the *KRAS/BRAF/MEK/MAPK* (extracellular signal-regulated kinase) signaling pathway (25). This is supported by the observation that activating mutations in these genes are oncogenic in experimental cell culture systems (12, 26, 27) probably through a constitutive activation of MAPK which in turn regulate many downstream targets that are important for tumor development (28, 29). It should be noted that activated MAPK or extracellular signal-regulated kinase can also be observed in conventional high-grade serous carcinomas probably through an epigenetic mechanism other than activating mutations of *KRAS* and *BRAF* (25, 30), because mutations in both genes are rarely found in high-grade serous carcinomas.

What is the biological significance of activation in the MAPK signaling pathway in SBT and low-grade serous carcinoma? Pohl et al. applied long serial analysis of gene expression to identify genes that are regulated by activated MAPK in low-grade serous carcinoma cells that harbor a *BRAF* mutation (31). The transcriptome of these cells was compared with that of CI-1040-treated cells, a compound that selectively inhibits MEK, the upstream regulator of MAPK (28). The most striking changes after MEK inhibition were down-regulation of cyclin D1, COBRA1, and transglutaminase-2 and up-regulation of tumor necrosis factor-related apoptosis-inducing ligand, thrombospondin-1, optineurin, and palladin. Among all the differentially expressed genes, *cyclin D1* showed the greatest alteration of gene expression. Cyclin D1 plays an important role in the cell cycle transition from G₁ to S phase through its association with cyclin-dependent kinases 4 and 6 (32, 33). In ovarian tumors, overexpression of cyclin D1 is associated with low-grade tumors (34–36), a finding consistent with our view that cyclin D1 is a downstream target of active MAPK, which is constitutively expressed in most low-grade ovarian tumors because of frequent activating mutations in *KRAS* and *BRAF*. Future experiments are necessary to determine whether mutations of *KRAS* and *BRAF* are sufficient to initiate the development of SBTs or whether additional genetic “hits” are required in tumorigenesis.

Because CI-1040 can inhibit the *KRAS/BRAF/MEK/MAPK* pathway, it is likely that this compound and other emerging MEK inhibitors may be an effective therapeutic agent for patients with SBTs and low-grade serous carcinomas. Pohl et al. have recently shown that CI-1040-treated ovarian serous tumors harboring either *KRAS* or *BRAF* mutations showed marked growth suppression (G₁ cell cycle arrest) compared with tumors containing wild-type *KRAS* and *BRAF* *in vitro* (31). Normal cells including ovarian surface epithelial cultures and ovarian stromal cells did not show significant growth inhibition by CI-1040 treatment. In addition, CI-1040-induced apoptosis occurred more frequently in tumor cells with either *KRAS* or *BRAF* mutations than in those with wild-type sequences. These findings indicate that an activated MAPK pathway is critical in tumor growth and survival of ovarian tumors with *KRAS* or *BRAF* mutations and suggest that the CI-1040-induced phenotypes depend on the mutational status of *KRAS* and *BRAF* in ovarian tumors. Because SBTs and low-grade serous carcinomas have a high frequency of mutations in *KRAS* and *BRAF*, it will be important to determine if treatment with CI-1040 can prolong disease-free interval and overall survival in patients with advanced-stage SBTs.

Genetic instability in serous borderline tumors. Microsatellite instability and changes in DNA copy number (or chromosomal instability) reflect the genetic instability in tumor cells (37). Microsatellite instability has been studied in SBTs using 69 microsatellite markers (38). Similar to high-grade serous carcinoma in which frequency of microsatellite instability is rare (39), SBTs did not show evidence for microsatellite instability in 19 SBTs studied. In contrast, SBTs showed DNA copy number changes as evidenced by chromosomal and allelic imbalance based on comparative genomic hybridization and digital PCR analysis, respectively. Two independent studies using comparative genomic hybridization have shown that the level of chromosomal imbalance in SBTs and low-grade serous carcinomas is similar to each other and is

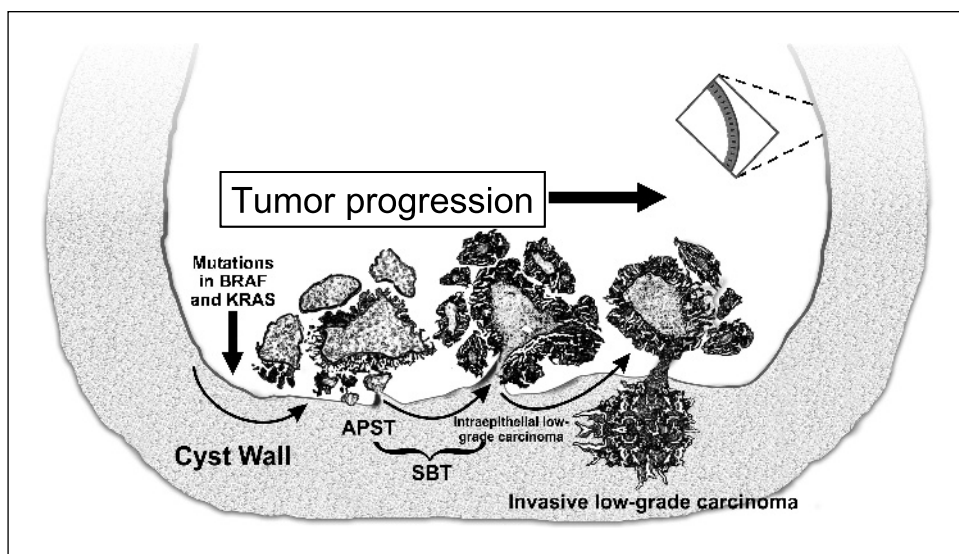
significantly lower than that of high-grade serous carcinomas, reflecting a lesser degree of chromosomal instability in SBT and low-grade serous carcinoma compared with high-grade serous carcinoma (40, 41). In another study, digital PCR analysis showed an increased allelic imbalance index paralleling the progression from SBT to invasive low-grade serous carcinoma (9). Specifically, allelic imbalance of chromosome 1p, which harbors tumor suppressor genes, including *MYCL1* and *NOERY/ARH1*, is frequently found in SBTs (9, 42). Allelic imbalance at certain chromosomal regions in the areas of SBT can be found in the adjacent invasive low-grade serous carcinomas (9, 42), further supporting the tumor progression model of SBT (Fig. 1).

Gene expression profiling in serous borderline tumors. Recently, high-density oligonucleotide microarrays have been done to profile gene expression in SBTs and serous carcinomas of the ovary (41, 43). Meinhold-Heerlein et al. showed that SBTs are distinct from high-grade serous carcinomas based on both unsupervised and supervised analysis of gene expression. Interestingly, well-differentiated serous carcinomas in their study, which are equivalent to low-grade serous carcinomas showed a similar profile to STBs compared with moderately and poorly differentiated carcinomas that correspond to high-grade serous carcinomas. Among the differentially expressed genes, a cell cycle regulator, *p21/WAF1*, is consistently expressed in the majority of SBTs and low-grade carcinomas but not in high-grade carcinomas. Similarly, Gilks et al. reported a complete separation between SBTs and conventional high-grade serous carcinomas based on unsupervised clustering analysis of gene expression. In their study, the genes that were most differentially expressed in SBTs included *mucin 10* (subtype B), *kallikrein 6*, *B7 protein*, *claudin 10*, and *keratin 17* (43). Moreover, the authors found that many genes previously identified as up-regulated in ovarian carcinoma relative to normal ovarian surface epithelium are expressed at even higher levels in SBT. These genes include *mucin 1*, *mesothelin*, *HE4*, *PAX 8*, and *apolipoprotein J/clusterin*. These gene expression profiles further show that SBT and low-grade serous carcinoma have a similar expression signature, which is distinct from conventional high-grade serous carcinoma.

Relationship of Serous Borderline Tumor to Ovarian Serous Carcinoma in Tumor Progression

In the past, the role of SBTs in the progression of ovarian serous carcinoma was not clear (11, 44–47). Until recently, molecular genetic studies together with clinicopathologic observations suggested that SBTs were unrelated to serous carcinoma (11, 46, 48, 49). Recent molecular genetic and morphologic studies, however, suggest there are two main pathways of tumorigenesis that correspond to the development of low-grade and high-grade serous carcinoma (50–55). This has led to the proposal of a new model of serous carcinogenesis, which reconciles the lack of association of SBTs with serous carcinoma on the one hand and the occasional malignant behavior of SBTs on the other (54). In one pathway, invasive low-grade serous carcinoma develops from a noninvasive (i.e., *in situ* tumor) traditionally termed SBT (56), mimicking the adenoma-carcinoma sequence in colorectal carcinoma in which carcinoma evolves through a continuum of histologically recognizable precursor lesions (ref. 57; Fig. 1). Detailed histopathologic analysis shows that SBTs consist of two noninvasive tumors at different stages of tumor progression, a benign tumor that has been termed “atypical proliferative serous tumor” and an intraepithelial (in *situ*) carcinoma termed “low-grade serous carcinoma” (noninvasive micropapillary serous carcinoma), which is the immediate precursor of invasive low-grade serous carcinoma (9, 54). Atypical proliferative serous tumor and intraepithelial low-grade serous carcinoma can be thought of as analogous to dysplasia and carcinoma *in situ* of the cervix. That is to say, the atypical proliferative serous tumor is a benign proliferative lesion that can progress to intraepithelial low-grade serous carcinoma, which is the immediate precursor of invasive low-grade serous cancer. Recurrence of SBT as high-grade serous carcinoma has been reported (58). Ortiz et al. have compared mutational profiles of *p53* and *KRAS* genes in SBTs and the subsequent serous carcinomas from the same patients and found that SBTs were molecular genetically different from the serous carcinomas (46). Although these serous carcinomas were considered as grade 1 in that study,

Fig. 1. Schematic representation of the relationship of SBT to low-grade serous carcinoma. Histopathologic and molecular genetic studies suggest that atypical proliferative serous tumor (APST) may arise from cystadenoma or ovarian surface epithelium. Some of the atypical proliferative serous tumors can progress to intraepithelial then invasive low-grade serous carcinoma. Conventionally, both atypical proliferative serous tumor and intraepithelial low-grade serous carcinoma are referred to SBT. Mutations of *KRAS* and *BRAF* occur at a very early stage of progression (i.e., the cystadenoma stage), which precedes the development of SBT.



it is not clear what they classified as grade 1 corresponds to what we classify as low-grade serous carcinomas or high-grade serous carcinoma.

Peritoneal Implants Associated with Serous Borderline Tumor

SBTs are frequently associated with peritoneal implants that are extraovarian lesions. This terminology, "implants," was used because it was not clear to early investigators what these lesions were. They may be benign implants from the SBT, analogous to implants of endometriosis, or they may be benign reactive lesions that develop independently on peritoneal surfaces (i.e., mesothelial hyperplasia; ref. 59). Alternatively, they are indeed metastases from the ovarian tumor or an independent primary peritoneal carcinoma. In the late 1970s and 1980s, investigators, thinking that the implants may be prognostic indicators, subdivided them into "noninvasive" and "invasive" types based on their microscopic appearance (60). Although initially there was considerable debate regarding the prognostic significance of this distinction, a recent review of the literature showed that the presence of invasive as opposed to noninvasive implants was the most important prognostic indicator (61). It is generally accepted that mortality in patients with SBTs is limited to those with extraovarian disease, but there is considerable controversy about how they should be treated, particularly because the distinction between noninvasive and invasive implants can be difficult.

Only a few molecular analyses have been done on peritoneal implants and have been limited to noninvasive implants. The results are conflicting. Investigators assessing allelic imbalance and the mutational status of *KRAS* have shown identical findings in SBTs and the synchronous implants of the same patient, supporting the implantation theory (42, 62, 63). On the other hand, clonality assays using X chromosome inactivation have shown different inactivation patterns in the SBTs and peritoneal lesions, providing evidence that some implants arise independently (64, 65). Elucidating the molecular features of the invasive as well as different types of noninvasive implants will clarify their nature and will have a major effect on the management of patients with advanced stage tumors.

Molecular Alterations in Nonserous Borderline Tumors

Unlike SBTs, mucinous, endometrioid, and clear cell borderline tumors are often associated with their corresponding carcinomas. Accordingly, these nonserous borderline tumors have been thought to possibly represent an intermediate stage in the stepwise progression to carcinoma (Table 1). In mucinous carcinoma for example, morphologic transitions from cystadenoma to a borderline tumor and to intraepithelial carcinoma and invasive carcinoma have been recognized for some time. In addition, an increasing frequency of *KRAS* mutations at codons 12 and 13 has been described in cystadenomas, borderline tumors, and mucinous carcinomas, respectively (7, 11, 66–68) and using microdissection, the same *KRAS* mutation has been detected in mucinous carcinoma and in the adjacent mucinous cystadenoma and borderline tumor (7). Other than *KRAS* mutations, molecular genetic changes, including microsatellite instability, have rarely been reported in mucinous borderline tumors (38). Similarly, morphologic data showing a frequent association of endometriosis with endometrioid adenofibromas and endometrioid borderline tumors and their topographical distribution, adjacent to invasive well-differentiated endometrioid carcinoma, suggest a of stepwise progression in the development of endometrioid carcinoma. These tumors are characterized by frequent mutation in β -catenin (69, 70), and to a lesser extent, mutation in *PTEN* (71). Moreover, similar molecular genetic alterations, including loss of heterozygosity at 10q23 and mutations in *PTEN*, have been reported in different stages of tumor progression in the same specimen (71–75). The molecular genetic and histopathologic findings suggest a precursor role of endometrioid borderline tumors in the development of ovarian endometrioid carcinoma. A recent report using an engineered mouse model shows that *KRAS* and *PTEN* mutations play an important role in the development of endometriosis and endometrioid carcinoma of the ovary (76). In that study, expression of oncogenic *KRAS* or conditional *PTEN* deletion within the ovarian surface epithelium gave rise to preneoplastic ovarian lesions with an endometrioid glandular morphology. Furthermore, the combination of the two mutations in the ovary led to the induction of invasive and

Table 1. Ovarian borderline tumors and associated molecular genetic changes in tumor progression

Type of ovarian borderline tumor	Major molecular genetic alterations	Precursor lesions and invasive carcinomas
Serous	<i>BRAF</i> and <i>KRAS</i> mutations (~67%)	Precursor: serous cystadenoma or adenofibroma; Progression to: invasive low-grade serous carcinoma
Mucinous	<i>KRAS</i> mutations (>60%)	Precursor: mucinous cystadenoma; Progression to: intraepithelial carcinoma then to invasive mucinous carcinoma
Endometrioid	LOH or mutations in <i>PTEN</i> (20%), β -catenin gene mutations (~50%), microsatellite instability (13-50%)	Precursor: endometriosis, endometrioid adenofibroma; Progression to: intraepithelial carcinoma then to invasive endometrioid carcinoma
Clear cell	<i>KRAS</i> mutations (5-16%), microsatellite instability (~13%)	Precursor: endometriosis, clear cell adenofibroma; Progression to: intraepithelial carcinoma then to invasive clear cell carcinoma
Brenner (transitional type)	Not yet identified	Precursor: Brenner tumor; Progression to: malignant Brenner (transitional cell) carcinoma

widely metastatic endometrioid ovarian carcinomas. The ovarian cancer model provides cogent molecular evidence of the role of KRAS and PTEN in the development of endometrioid carcinoma. Like endometrioid tumors, clear cell borderline tumors are also frequently associated with endometriosis, clear cell adenofibromas, and clear cell carcinoma, but molecular evidence for the stepwise progression is lacking, because molecular markers specific to clear cell neoplasms have only recently been identified (77, 78). These findings also provide further evidence of the close relationship of endometrioid and clear cell carcinoma and point to a common precursor lesion for these two neoplasms.

Future Directions

Despite recent advances, there are several challenges unique to borderline tumors that must be overcome to better understand the behavior and pathogenesis of SBTs and develop new management strategies. Several examples are discussed below.

Etiologic role of KRAS and BRAF mutations in initiating serous borderline tumor. Although the RAS signaling pathway has been extensively studied in SBTs, it is not known whether mutations of KRAS and BRAF alone are sufficient to induce SBTs *in vivo*. Murine models must be established to express the mutant forms of KRAS and BRAF to determine if expression of mutant KRAS and BRAF induces SBT-like lesions in mice. Furthermore, analysis of SBT genomes is critical for the identification of potential molecular genetic alterations that play a key role in tumorigenesis. New technologies, including digital karyotyping, array comparative genomic hybridization, and high-throughput mutational analysis, are now available to address these issues (79). The molecular genetic studies of SBTs will not only provide the essential data for future identification of new oncogenes and tumor suppressors in these tumors but will also provide molecular markers to refine the diagnostic and prognostic criteria of primary tumors and implants.

One of the challenges in studying SBTs is how to isolate and enrich tumor cells, because in SBTs, unlike most solid tumors, the tumor cells are arranged as a single layer and overlie abundant stroma. Therefore, the tumor represents only a small fraction of the pooled sample. Laser capture microdissection is a powerful technique for isolating tumor cells from SBTs; however, it is labor intensive and difficult to obtain sufficient DNA and RNA for assays. Several techniques may be useful to overcome these difficulties. For example, tumor cells can be isolated from fresh SBTs and short-term cultured (31). Genomic DNA can be then purified, and cell biology assays done on the cultured cells. In addition, genomic DNA and RNA can be directly purified from the fresh tissues using *in situ* lysis by applying a mild extraction buffer directly onto the surface of fresh SBTs (80).

Molecular definition of peritoneal implants. It is important to determine whether molecular genetic features may be superior to morphologic features as prognostic markers. For example, pathologists acknowledge that the distinction of noninvasive and invasive implants at times can be very difficult. Molecular genetic studies including mutational analysis and allelic imbalance will determine whether different kinds of implants have distinct molecular genetic profiles and whether these profiles can predict outcome. Correlation of the molecular genetic findings with the morphology and behavior of implants may disclose previously unrecognized morphologic features

that may assist the surgical pathologist in making the correct diagnosis.

Target-based therapy for serous borderline tumor at advanced stages. Novel therapeutic targets can be identified to improve the management of SBT patients with advanced-stage tumors (i.e., with metastatic low-grade carcinoma). Although SBTs occur in women of all ages, most present in women of reproductive age. In perimenopausal and menopausal women, hysterectomy and bilateral salpingo-oophorectomy are generally the treatments of choice, but in reproductive age women, issues of fertility and sterilization must be weighed against treatment for what is regarded as cancer, albeit a low-grade one. Because SBTs and low-grade serous carcinoma are indolent tumors, they do not respond to conventional cytotoxic chemotherapy; therefore, there is considerable debate regarding the best therapy for women with advanced-stage disease. Although many women are followed with no treatment, there are no reliable tumor markers that can be used to monitor the disease process. Recent molecular genetic studies may provide clues for the development of novel target-based therapy. For example, in most SBTs and low-grade serous carcinomas, there is constitutive activation of the MAPK signaling pathway due to frequent mutations in the *KRAS* and *BRAF* genes, the upstream regulators of MAPK. Accordingly, it will be important to test whether CI-1040 and other MEK inhibitors can prolong disease-free interval and overall survival in patients with advanced-stage of SBTs.

Conclusions

Recent molecular studies, including analyses of mutational status, DNA copy number changes, and gene expression profiles, have shed new light on the pathogenesis of SBTs and provide a model for studying the development of ovarian serous carcinoma. In this model, serous carcinoma is subdivided into low-grade and high-grade types that have distinct pathways of tumorigenesis (54). Low-grade serous carcinomas develop in a slow stepwise fashion from SBTs and intra-epithelial carcinoma, whereas the majority of high-grade serous carcinomas develop rapidly, presumably from inclusion cysts or ovarian surface epithelium. In the dualistic model, the SBT is a distinct entity that represents the putative precursor of invasive low-grade serous carcinoma and is unrelated to high-grade (usual type) serous carcinoma. This model is the first step in an attempt to elucidate the molecular pathogenesis of ovarian carcinoma but should not be construed as implying that other pathways of tumorigenesis do not exist. For example, we have observed high-grade serous carcinomas associated with a SBT or a low-grade carcinoma on rare occasions. In these cases, both low-grade and high-grade components shared the same mutations, suggesting that high-grade serous carcinomas may occasionally develop from a preexisting SBT or low-grade serous carcinoma.¹

Acknowledgments

We thank M. Jim Yen for his help in the preparation of illustrations and for editorial assistance.

¹ R. Dehari, unpublished data.

References

1. Seidman JD, Russell P, Kurman RJ. Surface epithelial tumors of the ovary. In: Kurman RJ, editor. Blaustein's pathology of the female genital tract. 5th ed. New York: Springer-Verlag; 2002. pp. 791–904.
2. Scully RE. World Health Organization international histological classification of tumours. 2nd ed. New York (NY): Springer; 1999.
3. Scully RE. International histological classification of tumors: histological typing of ovarian tumors. Geneva: WHO; 1999.
4. Kottmeier H. Carcinoma of the cervix, endometrium and ovary. Chicago: Year Book; 1962. p. 285–98.
5. Serov SF, Scully RE, Sobin LH. International histological classification and staging of tumors, histologic typing of ovarian tumors. Geneva: WHO; 1973.
6. Vogelstein B, Kinzler KW. Cancer genes and the pathways they control. *Nat Med* 2004;10:789–99.
7. Mok SC, Bell DA, Knapp RC, et al. Mutation of K-ras protooncogene in human ovarian epithelial tumors of borderline malignancy. *Cancer Res* 1993; 53:1489–92.
8. Singer G, Oldt R III, Cohen Y, et al. Mutations in BRAF and KRAS characterize the development of low-grade ovarian serous carcinoma. *J Natl Cancer Inst* 2003;95: 484–6.
9. Singer G, Kurman RJ, Chang H-W, Cho SKR, Shih I-M. Diverse tumorigenic pathways in ovarian serous carcinoma. *Am J Pathol* 2002;160:1223–8.
10. Sieben NL, Macropoulos P, Roemen GM, et al. In ovarian neoplasms, BRAF, but not KRAS, mutations are restricted to low-grade serous tumours. *J Pathol* 2004;202:336–40.
11. Caduff RF, Svoboda-Newman SM, Ferguson AW, Johnston CM, Frank TS. Comparison of mutations of Ki-RAS and p53 immunoreactivity in borderline and malignant epithelial ovarian tumors. *Am J Surg Pathol* 1999;23:323–8.
12. Davies H, Bignell GR, Cox C, et al. Mutations of the BRAF gene in human cancer. *Nature* 2002;417: 949–54.
13. Rajagopalan H, Bardelli A, Lengauer C, et al. Tumorigenesis: RAF/RAS oncogenes and mismatch-repair status. *Nature* 2002;418:934.
14. Pollock PM, Harper UL, Hansen KS, et al. High frequency of BRAF mutations in nevi. *Nat Genet* 2003; 33:19–20.
15. Kumar R, Angelini S, Snellman E, Hemminki K. BRAF mutations are common somatic events in melanocytic nevi. *J Invest Dermatol* 2004;122:342–8.
16. Milner BJ, Allan LA, Eccles DM, et al. p53 mutation is a common genetic event in ovarian carcinoma. *Cancer Res* 1993;53:2128–32.
17. Singer G, Stohr R, Cope L, et al. Patterns of p53 mutations separate ovarian serous borderline tumors and low- and high-grade carcinomas and provide support for a new model of ovarian carcinogenesis: a mutational analysis with immunohistochemical correlation. *Am J Surg Pathol* 2005;29:218–24.
18. Cheng EJ, Kurman RJ, Wang M, et al. Molecular genetic analysis of ovarian serous cystadenomas. *Lab Invest* 2004;84:778–84.
19. Ho C-L, Kurman RJ, Dehari R, Wang T-L, Shih I-M. Mutations of BRAF and KRAS precede the development of ovarian serous borderline tumors. *Cancer Res* 2004;64:6915–8.
20. Chan TL, Zhao W, Leung SY, Yuen ST. BRAF and KRAS mutations in colorectal hyperplastic polyps and serrated adenomas. *Cancer Res* 2003;63:4878–81.
21. Mink PJ, Sherman ME, Devesa SS. Incidence patterns of invasive and borderline ovarian tumors among white women and black women in the United States. Results from the SEER Program, 1978–1998. *Cancer* 2002;95:2380–9.
22. Conway C, Zalud I, Dilella M, et al. Simple cyst in the postmenopausal patient: detection and management. *J Ultrasound Med* 1998;17:369–72; quiz 73–4.
23. Oyelese Y, Kueck AS, Barter JF, Zalud I. Asymptomatic postmenopausal simple ovarian cyst. *Obstet Gynecol Surv* 2002;57:803–9.
24. Christensen JT, Boldsen JL, Westergaard JG. Functional ovarian cysts in premenopausal and gynecologically healthy women. *Contraception* 2002;66:153–7.
25. Hsu C-Y, Bristow R, Cha M, et al. Characterization of active mitogen-activated protein kinase in ovarian serous carcinomas. *Clin Cancer Res* 2004; 10:6432–6.
26. Peyssonnaud C, Eychene A. The Raf/MEK/ERK pathway: new concepts of activation. *Biol Cell* 2001; 93:53–62.
27. Malumbres M, Barbacid M. RAS oncogenes: the first 30 years. *Nat Rev Cancer* 2003;3:459–65.
28. Allen LF, Sebolt-Leopold J, Meyer MB. Ci-1040 (PD184352), a targeted signal transduction inhibitor of MEK (MAPKK). *Semin Oncol* 2003;30:105–16.
29. Satyamoorthy K, Li G, Gerrero MR, et al. Constitutive mitogen-activated protein kinase activation in melanoma is mediated by both BRAF mutations and autocrine growth factor stimulation. *Cancer Res* 2003;63:756–9.
30. Davidson B, Givant-Horwitz V, Lazarovici P, et al. Matrix metalloproteinases (MMP), EMMPRIN (extracellular matrix metalloproteinase inducer) and mitogen-activated protein kinases (MAPK): co-expression in metastatic serous ovarian carcinoma. *Clin Exp Metastasis* 2003;20:621–31.
31. Pohl G, Ho CL, Kurman RJ, et al. Inactivation of the mitogen-activated protein kinase pathway as a potential target-based therapy in ovarian serous tumors with KRAS or BRAF mutations. *Cancer Res* 2005;65: 1994–2000.
32. Sherr CJ, Roberts JM. CDK inhibitors: positive and negative regulators of G₁-phase progression. *Genes Dev* 1999;13:1501–12.
33. Sherr CJ. Cell cycle control and cancer. *Harvey Lect* 2000;96:73–92.
34. Worsley SD, Ponder BA, Davies BR. Overexpression of cyclin D1 in epithelial ovarian cancers. *Gynecol Oncol* 1997;64:189–95.
35. Gilks CB. Subclassification of ovarian surface epithelial tumors based on correlation of histologic and molecular pathologic data. *Int J Gynecol Pathol* 2004; 23:200–5.
36. Sui L, Tokuda M, Ohno M, Hatase O, Hando T. The concurrent expression of p27 (kip1) and cyclin D1 in epithelial ovarian tumors. *Gynecol Oncol* 1999;73: 202–9.
37. Lengauer C, Kinzler KW, Vogelstein B. Genetic instabilities in human cancers. *Nature* 1998;396:643–9.
38. Shih YC, Kerr J, Hurst TG, et al. No evidence for microsatellite instability from allelotyping analysis of benign and low malignant potential ovarian neoplasms. *Gynecol Oncol* 1998;69:210–3.
39. Allen HJ, DiCioccio RA, Hohmann P, Piver MS, Tworek H. Microsatellite instability in ovarian and other pelvic carcinomas. *Cancer Genet Cytogenet* 2000; 117:163–6.
40. Staebler A, Heselmeyer-Haddad K, Bell K, et al. Micropapillary serous carcinoma of the ovary has distinct patterns of chromosomal imbalances by comparative genomic hybridization compared with atypical proliferative serous tumors and serous carcinomas. *Hum Pathol* 2002;33:47–59.
41. Meinhold-Heerlein I, Bauerschlag D, Hilpert F, et al. Molecular and prognostic distinction between serous ovarian carcinomas of varying grade and malignant potential. *Oncogene* 2005;24:1053–65.
42. Krishnamurti U, Sasatomi E, Swalsky PA, Jones MW, Finkelstein SD. Microdissection-based mutational genotyping of serous borderline tumors of the ovary. *Int J Gynecol Pathol* 2005;24:56–61.
43. Gilks CB, Vanderhyden BC, Zhu S, van de Rijn M, Longacre TA. Distinction between serous tumors of low malignant potential and serous carcinomas based on global mRNA expression profiling. *Gynecol Oncol* 2005;96:684–94.
44. Schuijjer M, Berns EM. TP53 and ovarian cancer. *Hum Mutat* 2003;21:285–91.
45. Feeley KM, Wells M. Precursor lesions of ovarian epithelial malignancy. *Histopathology* 2001;38: 87–95.
46. Ortiz BH, Ailawadi M, Colitti C, et al. Second primary or recurrence? Comparative patterns of p53 and K-ras mutations suggest that serous borderline ovarian tumors and subsequent serous carcinomas are unrelated tumors. *Cancer Res* 2001;61:7264–7.
47. Teneriello MG, Ebina M, Linnoila RI, et al. p53 and Ki-ras gene mutations in epithelial ovarian neoplasms. *Cancer Res* 1993;53:3103–8.
48. Dubeau L. Ovarian cancer. In: Scriver CR, Beaudet AL, Sly WS, et al. editors. *The metabolic and molecular bases of inherited disease*. 8th ed. Vol. 1. McGraw-Hill; 2001. pp. 1091–6.
49. Bell DA, Scully RE. Early *de novo* ovarian carcinoma. A study of fourteen cases. *Cancer* 1994;73: 1859–64.
50. Zheng JP, Robinson WR, Ehlen T, Yu MC, Dubeau L. Distinction of low grade from high grade human ovarian carcinomas on the basis of losses of heterozygosity on chromosomes 3, 6, and 11 and HER-2/*neu* gene amplification. *Cancer Res* 1991;51:4045–51.
51. Zheng J, Wan M, Zweig S, et al. Histologically benign or low-grade malignant tumors adjacent to high-grade ovarian carcinomas contain molecular characteristics of high-grade carcinomas. *Cancer Res* 1993;53:4138–42.
52. Zheng J, Benedict WF, Xu HJ, et al. Genetic disparity between morphologically benign cysts contiguous to ovarian carcinomas and solitary cystadenomas [see comments]. *J Natl Cancer Inst* 1995;87:1146–53.
53. Wolf NG, Abdul-Karim FW, Schork NJ, Schwartz S. Origins of heterogeneous ovarian carcinomas. A molecular cytogenetic analysis of histologically benign, low malignant potential, and fully malignant components. *Am J Pathol* 1996;149:511–20.
54. Shih I-M, Kurman RJ. Ovarian tumorigenesis: a proposed model based on morphological and molecular genetic analysis. *Am J Pathol* 2004;164:1511–8.
55. Bell DA. Origins and molecular pathology of ovarian cancer. *Mod Pathol* 2005;218 Suppl:S19–32.
56. Burks RT, Sherman ME, Kurman RJ. Micropapillary serous carcinoma of the ovary. A distinctive low-grade carcinoma related to serous borderline tumors. *Am J Surg Pathol* 1996;20:1319–30.
57. Kinzler KW, Vogelstein B. Colorectal Tumors. In: Vogelstein B, Kinzler KW, editors. *The genetic basis of human cancer*. New York: McGraw-Hill; 1998. pp. 565–87.
58. Parker RL, Clement PB, Chervcover DJ, Sornarajah T, Gilks CB. Early recurrence of ovarian serous borderline tumor as high-grade carcinoma: a report of two cases. *Int J Gynecol Pathol* 2004;23:265–72.
59. Sehdev AES, Sehdev PS, Kurman RJ. Noninvasive and invasive micropapillary serous carcinoma of the ovary: a clinicopathologic analysis of 135 cases. *Am J Surg Pathol* 2003;27:725–36.
60. Hart WR. Borderline epithelial tumors of the ovary. *Mod Pathol* 2005;18 Suppl 2:S33–50.
61. Seidman JD, Kurman RJ. Ovarian serous borderline tumors: a critical review of the literature with emphasis on prognostic indicators. *Hum Pathol* 2000;31: 539–57.
62. Diebold J, Seemuller F, Lohrs U. K-RAS mutations in ovarian and extraovarian lesions of serous tumors of borderline malignancy. *Lab Invest* 2003;83:251–8.
63. Zanotti KM, Hart WR, Kennedy AW, Belinson JL, Casey G. Allelic imbalance on chromosome 17p13 in borderline (low malignant potential) epithelial ovarian tumors. *Int J Gynecol Pathol* 1999;18:247–53.
64. Gu J, Roth LM, Younger C, et al. Molecular evidence for the independent origin of extra-ovarian papillary serous tumors of low malignant potential. *J Natl Cancer Inst* 2001;93:1147–52.
65. Lu KH, Bell DA, Welch WR, Berkowitz RS, Mok SC. Evidence for the multifocal origin of bilateral and advanced human serous borderline ovarian tumors. *Cancer Res* 1998;58:2328–30.
66. Ichikawa Y, Nishida M, Suzuki H. Mutation of KRAS

- protooncogene is associated with histological subtypes in human mucinous ovarian tumors. *Cancer Res* 1994;54:33–5.
67. Enomoto T, Weghorst CM, Inoue M, Tanizawa O, Rice JM. K-ras activation occurs frequently in mucinous adenocarcinomas and rarely in other common epithelial tumors of the human ovary. *Am J Pathol* 1991;139:777–85.
68. Gemignani ML, Schlaerth AC, Bogomolny F, et al. Role of KRAS and BRAF gene mutations in mucinous ovarian carcinoma. *Gynecol Oncol* 2003;90:378–81.
69. Wu R, Zhai Y, Fearon ER, Cho KR. Diverse mechanisms of β -catenin deregulation in ovarian endometrioid adenocarcinomas. *Cancer Res* 2001;61:8247–55.
70. Moreno-Bueno G, Gamallo C, Perez-Gallego L, et al. β -Catenin expression pattern, β -catenin gene mutations, and microsatellite instability in endometrioid ovarian carcinomas and synchronous endometrial carcinomas. *Diagn Mol Pathol* 2001;10:116–22.
71. Obata K, Morland SJ, Watson RH, et al. Frequent PTEN/MMAC mutations in endometrioid but not serous or mucinous epithelial ovarian tumors. *Cancer Res* 1998;58:2095–7.
72. Sato N, Tsunoda H, Nishida M, et al. Loss of heterozygosity on 10q23.3 and mutation of the tumor suppressor gene PTEN in benign endometrial cyst of the ovary: possible sequence progression from benign endometrial cyst to endometrioid carcinoma and clear cell carcinoma of the ovary. *Cancer Res* 2000;60:7052–6.
73. Thomas EJ, Campbell IG. Molecular genetic defects in endometriosis. *Gynecol Obstet Invest* 2000;50:44–50.
74. Obata K, Hoshiai H. Common genetic changes between endometriosis and ovarian cancer. *Gynecol Obstet Invest* 2000;50:39–43.
75. Bischoff FZ, Simpson JL. Heritability and molecular genetic studies of endometriosis. *Hum Reprod Update* 2000;6:37–44.
76. Dinulescu DM, Ince TA, Quade BJ, et al. Role of K-ras and Pten in the development of mouse models of endometriosis and endometrioid ovarian cancer. *Nat Med* 2005;11:63–70.
77. Tsuchiya A, Sakamoto M, Yasuda J, et al. Expression profiling in ovarian clear cell carcinoma: identification of hepatocyte nuclear factor-1 β as a molecular marker and a possible molecular target for therapy of ovarian clear cell carcinoma. *Am J Pathol* 2003;163:2503–12.
78. Hough CD, Sherman-Baust CA, Pizer ES, et al. Large-scale serial analysis of gene expression reveals genes differentially expressed in ovarian cancer. *Cancer Res* 2000;60:6281–7.
79. Shih Ie M, Wang TL. Apply innovative technologies to explore cancer genome. *Curr Opin Oncol* 2005;17:33–8.
80. Berman DM, Shih Ie M, Burke LA, et al. Profiling the activity of G proteins in patient-derived tissues by rapid affinity-capture of signal transduction proteins (GRASP). *Proteomics* 2004;4:812–8.

Mutations of BRAF and KRAS Precede the Development of Ovarian Serous Borderline Tumors

Chung-Liang Ho,¹ Robert J. Kurman,^{1,2} Reiko Dehari,¹ Tian-Li Wang,² and Ie-Ming Shih^{1,2}

Departments of ¹Pathology, ²Oncology and Gynecology and Obstetrics, Johns Hopkins Medical Institutions, Baltimore, Maryland

ABSTRACT

Molecular genetic changes that are associated with the initiating stage of tumor development are important in tumorigenesis. Ovarian serous borderline tumors (SBTs), putative precursors of low-grade serous carcinomas, are among the few human neoplasms with a high frequency of activating mutations in *BRAF* and *KRAS* genes. However, it remains unclear as to how these mutations contribute to tumor progression. To address this issue, we compared the mutational status of *BRAF* and *KRAS* in both SBTs and the adjacent epithelium from cystadenomas, the presumed precursor of SBTs. We found that three of eight SBTs contained mutant *BRAF*, and four SBTs contained mutant *KRAS*. All specimens with mutant *BRAF* harbored wild-type *KRAS* and vice versa. Thus, seven (88%) of eight SBTs contained either *BRAF* or *KRAS* mutations. The same mutations detected in SBTs were also identified in the cystadenoma epithelium adjacent to the SBTs in six (86%) of seven informative cases. As compared to SBTs, the cystadenoma epithelium, like ovarian surface epithelium, lacks cytological atypia. Our findings provide cogent evidence that mutations of *BRAF* and *KRAS* occur in the epithelium of cystadenomas adjacent to SBTs and strongly suggest that they are very early events in tumorigenesis, preceding the development of SBT.

INTRODUCTION

It has been shown that tumors result from an accumulation of genetic alterations that result in uncontrolled cellular proliferation. Identification of the alterations that occur early in tumor development is critical to understanding carcinogenesis and can provide insight into potential markers for early detection (1–3). Ovarian cancer is one of the most lethal neoplasms in women, and serous carcinoma is the most common type (4), but the molecular events that underlie the development of ovarian serous carcinoma are largely unknown. Recent studies have shown that ovarian serous carcinoma develops along two distinct pathways, and we have proposed a model of ovarian carcinogenesis that reflects this concept (5–7). In one pathway, invasive low-grade serous carcinoma develops from a noninvasive (or *in situ*) tumor that has traditionally been termed “serous borderline tumor” (SBT; ref. 8). The progression of SBT to invasive low-grade carcinoma mimics the adenomacarcinoma sequence in colorectal carcinoma (1). Detailed analysis of SBTs shows that SBTs consist of two tumors at different stages of tumor progression, a benign tumor termed “atypical proliferative serous tumor,” and an intraepithelial low-grade (noninvasive micropapillary serous) carcinoma, the immediate precursor of invasive low-grade serous carcinoma (5, 7). SBTs are frequently associated with serous cystadenomas that develop from ovarian surface epithelium through a hyperplastic process (9). Like ovarian surface epithelium, the epithelial cells of a cystadenoma do not show cytological atypia, and their proliferation index is extremely low (9). In the second pathway, high-grade serous carcinoma develops

from ovarian surface epithelium or from surface inclusion cysts (10), but precursor lesions have not been well characterized. Accordingly, this process has been described as “*de novo*” (5).

Molecular genetic analysis has shown that SBTs and invasive low-grade serous carcinomas are characterized by mutations of *BRAF* and *KRAS* in 61 to 68% of cases (6, 7, 11, 12), but p53 mutations are rare (12–14). In contrast, high-grade serous carcinomas frequently contain p53 mutations (>50%) but rarely *BRAF* and *KRAS* mutations (6, 7, 13–17). These studies analyzed advanced stage tumors in which putative precursor lesions may have been obliterated by the tumor. In this study, we confined our analysis to small SBTs and associated cystadenomas to delineate the early molecular genetic events in their pathogenesis. Specifically, we compared the mutational status of *BRAF* and *KRAS* in SBTs and the adjacent nontransformed epithelium of serous cystadenomas.

MATERIALS AND METHODS

A total of eight small SBTs (corresponding to what has been classified as atypical proliferative tumor) and the associated cystadenomas were collected. The acquisition of tumor samples was approved by the Johns Hopkins institutional review board. The SBTs ranged from 8 to 20 mm (average 16 mm) in greatest dimension and associated cystadenomas ranged from 5 to 8 cm (average 6.8 cm). The SBTs occupied 5 to 15% of the total surface area of the cystadenomas. Only a small number of cases were studied because although cystadenomas and SBTs are not uncommon, cystadenomas containing synchronous small SBTs are relatively rare. Microscopically, the SBTs contained a hierarchical branching papillae lined by epithelial cells with mild to moderate cellular atypia (Fig. 1). The epithelium of the SBTs merged abruptly with the cystadenoma epithelium that was composed of a single layer of flat to columnar cells without atypia (Fig. 1). The Palm laser capture microdissection microscope (Zeiss) was used to separately collect the epithelium from the SBTs and adjacent cystadenoma. The PicoPure DNA extraction kit (Arcturus, Mountain View, CA) was used to prepare genomic DNA. PCR was then done, and an ABI 3100 sequencer (ABI, Foster City, CA) was used to do nucleotide sequencing. Exon 1 of *KRAS* and exon 15 of *BRAF* were both sequenced as each exon harbors almost all of the mutations in both genes (6, 7, 11, 18). The primers for PCR and sequencing were as follows: for *BRAF*, 5'-tgcttctgataggaaaatga-3' (forward); 5'-ccacaaaatggatccagacaac-3' (reverse); and 5'-gaaatgagatctactgttttcttcta-3' (sequencing); for *KRAS*, 5'-taaggcctgctgaaatgactg-3' (forward); 5'-tgcttctgaccagtaaatgc-3' (reverse); and 5'-ctgcaccagtaatatgcattaaaac-3' (sequencing). The Lasergene program (DNASTAR, Madison, WI) was used to analyze the sequences.

RESULTS

The results of the mutational status correlated with the SBT or cystadenoma component of the tumors are shown in Table 1. We found that four SBTs (cases 1, 4, 5, and 8) contained activating *KRAS* mutations at codon 12 (three mutations of GGT to GAT and one mutation of GGT to GTT) and three SBTs (cases 3, 5, and 6) had *BRAF* mutations at codon 599 (all of T1796A mutation). As in our previous report (6), the presence of *KRAS* and *BRAF* mutations was mutually exclusive. Thus, seven (88%) of eight SBTs had either a *BRAF* or a *KRAS* mutation. Case 2 contained wild-type *KRAS* and *BRAF*. Analysis of the mutational status in the epithelium from the cystadenomas adjacent to the SBTs revealed that both the cystade-

Received 6/15/04; accepted 7/26/04.

Grant support: Supported by a research grant OC010017 from the United States Department of Defense.

The costs of publication of this article were defrayed in part by the payment of page charges. This article must therefore be hereby marked *advertisement* in accordance with 18 U.S.C. Section 1734 solely to indicate this fact.

Requests for reprints: Ie-Ming Shih, The Johns Hopkins Medical Institutions, 1503 E. Jefferson Street, Room B-315, Baltimore, MD 21231. Phone: 410-502-7774; Fax: 410-502-7943; E-mail: ishih@jhmi.edu.

©2004 American Association for Cancer Research.

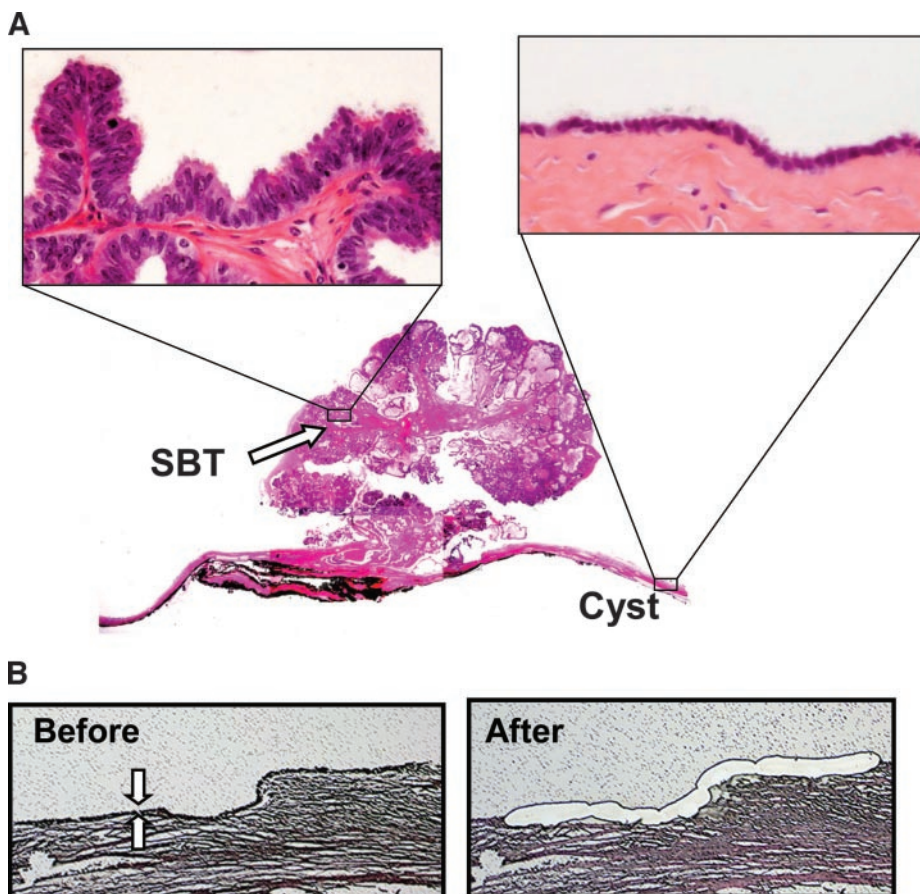


Fig. 1. A, small serous borderline tumor and associated serous cystadenoma (case E). The tumor measures 0.8 cm in greatest dimension and is composed of hierarchical branching papillae lined by cells with mild to moderate atypia (*left inset*). The adjacent cystadenoma epithelium is composed of a single layer of epithelium without cytological atypia (*right inset*). B, laser capture microdissection with minimal contamination from the underlying stromal cells were used to isolate epithelial cells lining the cystadenoma (between *arrows*).

noma and SBT components contained identical mutations in six of seven informative cases. Representative sequence analyses are shown in Fig. 2. The frequent mutations of *KRAS* and *BRAF* in small SBTs are consistent with previous reports showing mutations in either *BRAF* or *KRAS* in 66 to 68% of large SBTs (6, 11). The higher frequency of mutations (88%) in the current report is probably because of the use of purer tumor cell samples obtained by laser capture microdissection or may have resulted from the small sample size in the present analysis.

DISCUSSION

The findings in this study provide important insights into the molecular pathogenesis of low-grade ovarian serous tumors (Fig. 3). Because we only analyzed a single time point in the sequence of cystadenoma to SBTs, we can only infer that the findings truly describe the events in early tumor progression. However, the coexistence of a cystadenoma with a SBT strongly suggests that the latter arises from the former (Fig. 3). Accordingly, the presence of identical mutations in the cystadenoma epithelium that displayed no evidence of cytological atypia strongly suggests that mutations of *BRAF* and *KRAS* occur before the development of a SBT and indicates that cystadenomas are the precursors of SBTs. Our results support the view that mutations of *BRAF* and *KRAS* (or *NRAS*) are early events associated with tumor initiation as occurs in melanoma (19) and colorectal carcinoma (20).

We have recently studied 30 consecutive pure cystadenomas without SBTs and have shown an absence of *BRAF* and *KRAS* mutations in all of them (9). The frequency of mutations in *BRAF* and *KRAS* in cystadenomas associated with SBTs was significantly higher than

those without SBTs ($P < 0.001$, Fisher's exact test; Table 2). This finding together with the fact that SBTs are relatively uncommon as compared to cystadenomas (21–25) suggests that only a small proportion of serous cystadenomas are neoplastic with the potential to progress to SBTs. Finally, our findings suggest a “gatekeeper” role of *BRAF* and *KRAS* genes in the development of low-grade serous carcinomas (26). This is supported by the observation that activating mutations in these genes are oncogenic in experimental cell culture systems (19, 27, 28) probably through a constitutive activation of mitogen-activated protein kinase (29, 30). Future experiments will determine whether mutations of *BRAF* and *KRAS* are sufficient to initiate the development of SBTs or additional genetic “hits” are required in tumorigenesis. Because mutations of *BRAF* and *KRAS* in serous cystadenomas are associated with the development of SBTs, detection of *BRAF* and *KRAS* mutations could facilitate the differen-

Table 1 *Mutational status of KRAS and BRAF genes in eight small serous borderline tumors and associated cystadenomas*

Gene	Case 1	Case 2	Case 3	Case 4	Case 5	Case 6	Case 7	Case 8
<i>KRAS</i>								
SBT	G35A* G12D†	WT	WT	G35T G12V	G35A G12D	WT	WT	G35A G12D
Cyst	G35A G12D	WT	WT	WT	G35A G12D	WT	WT	G35A G12D
<i>BRAF</i>								
SBT	WT	WT	T1796A V599E	WT	WT	T1796A V599E	T1796A V599E	WT
Cyst	WT	WT	T1796A V599E	WT	WT	T1796A V599E	T1796A V599E	WT

Abbreviation: WT, wild-type.

* Alteration in nucleotide sequence.

† Alteration in amino acid sequence.

Fig. 2. Chromatograms of nucleotide sequences of *BRAF* and *KRAS* in two representative cases. *Left panel* (case 1) shows a point mutation in the *KRAS* gene in both SBT and the adjacent cystadenoma (Cyst) of the same specimen. *Right panel* (case 6) shows a point mutation in the *BRAF* gene in both the serous borderline tumor and the corresponding cystadenoma.

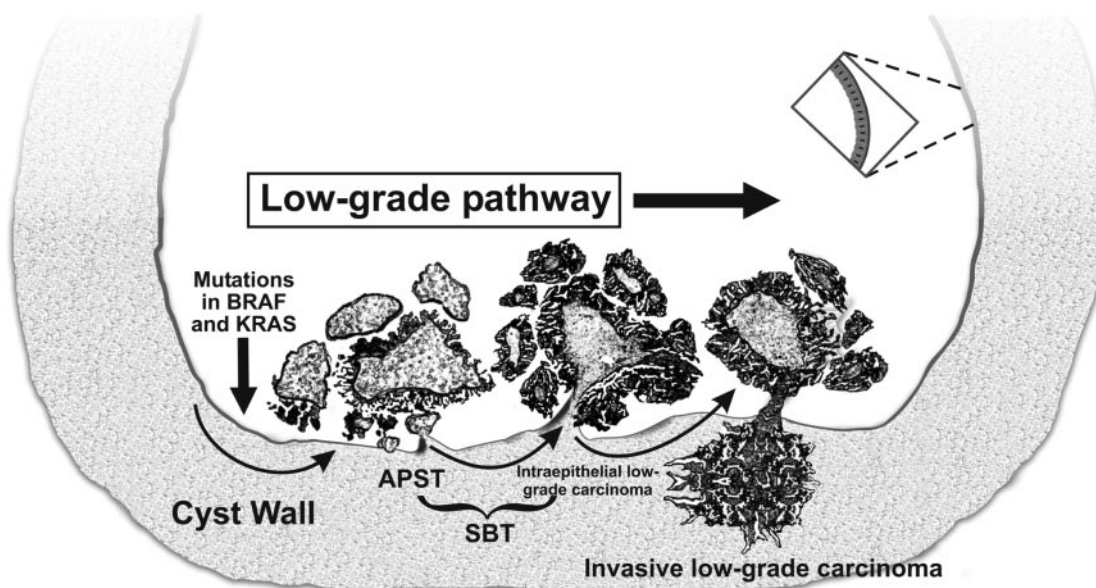
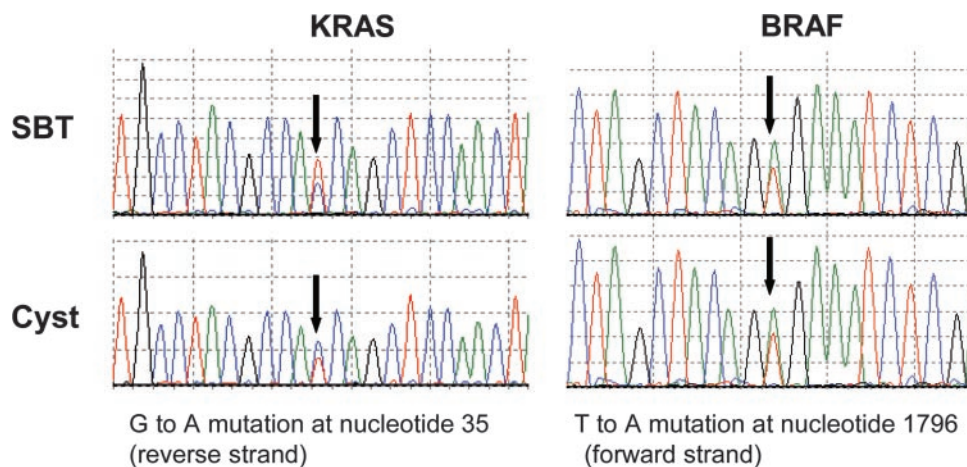


Fig. 3. Schematic representation of tumor progression in low-grade serous carcinoma. Mutations of *BRAF* and *KRAS* occur in a small proportion of cystadenomas that may contribute to the development of a SBT. Some serous borderline tumors progress further to intraepithelial and then to invasive low-grade serous carcinoma. APST, atypical proliferative serous tumor.

tiation of cystadenomas with a high risk of progression from the vast majority of cystadenomas that lack *BRAF* or *KRAS* mutations and have a very low risk of progression. Development of molecular assays (31, 32) that can detect such mutations (in cyst fluid, for example) could play an important role in the management of patients with ovarian cystadenomas, particularly young women who would prefer fertility-sparing treatment.

ACKNOWLEDGMENTS

We gratefully acknowledge the technical support of the Oncology Imaging Core at the Johns Hopkins Medical Institutions for the photomicrographs and the laser capture microdissection.

REFERENCES

1. Kinzler KW, Vogelstein B. The genetic basis of human cancer. Toronto: McGraw-Hill, 1998.
2. Kinzler KW, Vogelstein B. Landscaping the cancer terrain. *Science* (Wash D C) 1998;280:1036-7.
3. Kern SE. Advances from genetic clues in pancreatic cancer. *Curr Opin Oncol* 1998;10:74-80.
4. Seidman JD, Horkayne-Szakaly I, Haiba M, et al. The histologic type and stage distribution of ovarian carcinomas of surface epithelial origin. *Int J Gynecol Pathol* 2004;23:41-4.
5. Shih I-M, Kurman RJ. Ovarian tumorigenesis- a proposed model based on morphological and molecular genetic analysis. *Am J Pathol* 2004;164:1511-8.
6. Singer G, Oldt R 3rd, Cohen Y, et al. Mutations in *BRAF* and *KRAS* characterize the development of low-grade ovarian serous carcinoma. *J Natl Cancer Inst* (Bethesda) 2003;95:484-6.
7. Singer G, Kurman RJ, Chang H-W, et al. Diverse tumorigenic pathways in ovarian serous carcinoma. *Am J Pathol* 2002;160:1223-8.

Table 2 Frequency of mutations in *BRAF* and *KRAS* in cystadenomas with associated serous borderline tumor and pure cystadenomas

	cystadenoma	
	SBT	
	Cystadenoma associated with SBT	Pure cystadenoma
Mutations in <i>BRAF</i> or <i>KRAS</i>	6	0
Wild-type in <i>BRAF</i> and <i>KRAS</i>	2	30
Total cases	8	30

8. Burks RT, Sherman ME, Kurman RJ. Micropapillary serous carcinoma of the ovary. A distinctive low-grade carcinoma related to serous borderline tumors. *Am J Surg Pathol* 1996;20:1319–30.
9. Cheng EJ, Kurman RJ, Wang M, et al. Molecular genetic analysis of ovarian serous cystadenomas. *Lab Invest* 2004;84:778–84.
10. Yang DH, Smith ER, Cohen C, et al. Molecular events associated with dysplastic morphologic transformation and initiation of ovarian tumorigenicity. *Cancer (Phila)* 2002;94:2380–92.
11. Sieben NLG, Macropoulos P, Roemen G, et al. In ovarian neoplasms, BRAF, but not KRAS, mutations are restricted to low-grade serous tumors. *J Pathol* 2004;202:336–40.
12. Cuatrecasas M, Erill N, Musulen E, et al. K-ras mutations in nonmucinous ovarian epithelial tumors: a molecular analysis and clinicopathologic study of 144 patients. *Cancer (Phila)* 1998;82:1088–95.
13. Zheng J, Benedict WF, Xu HJ, et al. Genetic disparity between morphologically benign cysts contiguous to ovarian carcinomas and solitary cystadenomas [see comments]. *J Natl Cancer Inst (Bethesda)* 1995;87:1146–53.
14. Teneriello MG, Ebina M, Linnoila RI, et al. p53 and Ki-ras gene mutations in epithelial ovarian neoplasms. *Cancer Res* 1993;53:3103–8.
15. Leitao MM, Soslow RA, Baergen RN, et al. Mutation and expression of the TP53 gene in early stage epithelial ovarian carcinoma. *Gynecol Oncol* 2004;93:301–6.
16. Kappes S, Milde-Langosch K, Kressin P, et al. p53 mutations in ovarian tumors, detected by temperature-gradient gel electrophoresis, direct sequencing and immunohistochemistry. *Int J Cancer* 1995;64:52–9.
17. Singer G, Stohr R, Dehari R, et al. Patterns of p53 mutations separate ovarian serous borderline tumors, low- and high-grade carcinomas and provide support for a new model of ovarian carcinogenesis. *Am J Surg Pathol*. In press 2004.
18. Davies H, Bignell GR, Cox C, et al. Mutations of the BRAF gene in human cancer. *Nature (Lond)* 2002;417:949–54.
19. Pollock PM, Harper UL, Hansen KS, et al. High frequency of BRAF mutations in nevi. *Nat Genet* 2003;33:19–20.
20. Chan TL, Zhao W, Leung SY, et al. BRAF and KRAS mutations in colorectal hyperplastic polyps and serrated adenomas. *Cancer Res* 2003;63:4878–81.
21. Mink PJ, Sherman ME, Devesa SS. Incidence patterns of invasive and borderline ovarian tumors among white women and black women in the United States. Results from the SEER Program, 1978–1998. *Cancer (Phila)* 2002;95:2380–9.
22. Conway C, Zalud I, Dilena M, et al. Simple cyst in the postmenopausal patient: detection and management. *J Ultrasound Med* 1998;17:369–72; quiz 373–4.
23. Oyelese Y, Kueck AS, Barter JF, et al. Asymptomatic postmenopausal simple ovarian cyst. *Obstet Gynecol Surv* 2002;57:803–9.
24. Christensen JT, Boldsen JL, Westergaard JG. Functional ovarian cysts in premenopausal and gynecologically healthy women. *Contraception* 2002;66:153–7.
25. Seidman JD, Russell P, Kurman RJ. Surface epithelial tumors of the ovary. In: Kurman RJ, editor. *Blaustein's pathology of the female genital tract*, edition 5. New York: Springer Verlag, 2002. p. 791–904.
26. Kinzler KW, Vogelstein B. Cancer-susceptibility genes. Gatekeepers and caretakers [news; comment]. *Nature (Lond)* 1997;386:761, 763.
27. Peyssonnaud C, Eychene A. The Raf/MEK/ERK pathway: new concepts of activation. *Biol Cell* 2001;93:53–62.
28. Malumbres M, Barbacid M. RAS oncogenes: the first 30 years. *Nat Rev Cancer* 2003;3:459–65.
29. Allen LF, Sebolt-Leopold J, Meyer MB. CI-1040 (PD184352), a targeted signal transduction inhibitor of MEK (MAPKK). *Semin Oncol* 2003;30(5 Suppl 16):105–16.
30. Satyamoorthy K, Li G, Gerrero MR, et al. Constitutive mitogen-activated protein kinase activation in melanoma is mediated by both BRAF mutations and autocrine growth factor stimulation. *Cancer Res* 2003;63:756–9.
31. Vogelstein B, Kinzler KW. Digital PCR. *Proc Natl Acad Sci USA* 1999;96:9236–41.
32. Dressman D, Yan H, Traverso G, et al. Transforming single DNA molecules into fluorescent magnetic particles for detection and enumeration of genetic variations. *Proc Natl Acad Sci USA* 2003;100:8817–22.

Apolipoprotein E Is Required for Cell Proliferation and Survival in Ovarian Cancer

Yu-Chi Chen,¹ Gudrun Pohl,¹ Tian-Li Wang,² Patrice J. Morin,³ Björn Risberg,⁴ Gunnar B. Kristensen,⁵ Albert Yu,¹ Ben Davidson,⁴ and Ie-Ming Shih^{1,2}

Departments of ¹Pathology, ²Gynecology and Oncology, Johns Hopkins University Medical Institutions and ³National Institute of Aging, Baltimore, Maryland and Departments of ⁴Pathology and ⁵Gynecologic Oncology, The Norwegian Radium Hospital, University of Oslo, Montebello, Oslo, Norway

Abstract

Apolipoprotein E (ApoE) has been recently identified as a potential tumor-associated marker in ovarian cancer by serial analysis of gene expression. ApoE has long been known to play a key role in lipid transport, and its specific isoforms may participate in atherosclerogenesis. However, its role in human cancer is not known. In this study, apoE expression was frequently detected in ovarian serous carcinomas, the most common and lethal type of ovarian cancer. It was not detected in serous borderline tumors and normal ovarian surface epithelium. Inhibition of apoE expression using an apoE-specific siRNA led to G₂ cell cycle arrest and apoptosis in an apoE-expressing ovarian cancer cell line, OVCAR3, but not in apoE-negative cell lines. Furthermore, the phenotype of apoE siRNA-treated OVCAR3 cells was reversed by expressing engineered mutant apoE with introduced silent mutations in the siRNA target sequence. Expression of apoE in nuclei was significantly associated with a better survival in patients who presented peritoneal effusion at the time of diagnosis (5-year follow-up, $P = 0.004$). This study suggests a new role of apoE in cancer as apoE expression is important for the proliferation and survival in apoE-expressing ovarian cancer cells. (Cancer Res 2005; 65(1): 331-7)

Introduction

Identification of tumor-associated markers is critical not only in understanding tumorigenesis but also in providing new markers for diagnosis and prognosis (1, 2). Discovery of new markers seems more urgent for clinically aggressive cancers like ovarian carcinoma in which the current diagnostic and therapeutic approaches are limited (3). Recent advances in transcriptome-wide technologies have led to the discovery of a host of emergent tumor-associated markers (4–6). Comparing gene expression profiles in ovarian cancer to benign ovarian surface epithelial cells using serial analysis of gene expression (SAGE), Hough et al. (7) have identified a number of genes that are differentially expressed in ovarian cancer. We selected one of these genes, apolipoprotein E (*ApoE*), for further characterization because it is potentially involved in a number of signal transduction pathways that may be critical in regulating cancer cell proliferation and survival.

ApoE has long been known as an essential constituent of plasma lipoproteins responsible for cholesterol transport and metabolism.

Plasma apoE is produced mainly in the liver but also in the brain, adrenal glands, kidney, and macrophages. It associates with cholesterol-rich proteins such as low-density lipoprotein (LDL) and enables these protein-lipid complexes to bind to the members of the LDL receptor family present in a variety of tissues (8). The binding of apoE and certain LDL receptor family members not only leads to endocytosis and subsequent importation of lipid-protein complex into the cells but also initiates signal transduction (9, 10). For example, one of the LDL receptor family members, gp330, has been known to mediate intracellular signaling through Src-homology recognition motifs for the PI3 kinase, protein kinase C, casein kinase II, and cyclic AMP-dependent protein kinase (11). The signaling pathways that are initiated by these receptor-ligand interactions on the cell membrane affect the proliferation of various normal cell types, including vascular smooth muscle (12–16), inhibit platelet aggregation (17), regulate inflammatory gene expression (18), and affect the metabolism and survival in neurons through the Akt pathway (19). In addition to the exogenous source of apoE, some cells produce endogenous apoE by transcriptional activation of the *apoE* gene. In contrast to exogenous apoE that binds to cell-surface LDL receptors and mediates endocytosis, endogenous apoE is mainly associated with Golgi compartments in the cytosol (20). The cellular functions of endogenous apoE are less well understood, but it may be secreted and act as an autocrine or paracrine growth factor, thereby modifying the microenvironment. For example, it has been shown that endogenous apoE stimulates serum-independent cell proliferation. In addition, endogenous apoE derived from macrophages plays an important role in the etiology of atherosclerosis (12).

Besides its well-recognized role in lipid metabolism and atherosclerogenesis, apoE has been shown to involve in several pathophysiologic processes not directly related to lipid transport. Specific isoforms of apoE participate in the development of Alzheimer's disease, immunoregulation, and neurite outgrowth (20–23), suggesting that apoE may play a more general role than simply lipid transport. In order to explore the new roles of apoE in human cancer, we evaluated apoE expression in tumor tissues and established a cell culture model to study its cellular function by knocking down apoE expression in apoE overexpressing ovarian cancer cells. Besides, the prognostic relevance of apoE expression was determined to show its potential application as a marker to predict clinical outcome in ovarian cancer patients.

Materials and Methods

Tissue Samples. The acquisition of paraffin tissues and frozen specimens was approved by the Institutional Review Boards at Johns Hopkins University and the informed consent was obtained from the Norwegian Radium Hospital. A total of 194 ovarian carcinomas from the ovary, 119

Note: Yu-Chi Chen and Gudrun Pohl contributed equally.

Requests for reprints: Ie-Ming Shih, Johns Hopkins Medical Institutions, 1503 East Jefferson Street, Room B-315, Baltimore, MD 21231. Phone: 410-502-7774; Fax: 410-502-7943; E-mail: ishih@jhmi.edu.

©2005 American Association for Cancer Research.

metastatic serous carcinomas, 148 specimens of effusion containing serous carcinomas, 10 ovarian serous borderline tumors, 10 ovarian serous cysts, and 10 normal ovarian surface epithelium were retrieved from the department of Pathology at the Johns Hopkins Hospital and the Norwegian Radium Hospital. More than 95% of ovarian carcinoma was of serous type and of high grade except 20 low-grade serous carcinomas. Formalin-fixed paraffin-embedded tissue blocks from the above cases were obtained from archival material. We also included eight frozen tissue samples of high-grade ovarian serous carcinoma and seven primary cultures of ovarian surface epithelium for Western blot analysis. The diagnoses of the paraffin and fresh tissue specimens were confirmed by microscopic examination on the tissue sections before analysis. All the eight fresh ovarian cancer tissues had corresponding paraffin tissue for immunohistochemistry. The diagnosis of effusion samples was established by evaluation of smears and cell block sections from formalin-fixed paraffin-embedded pellets by experienced cytopathologists (B.R. and B.D.) and were then further characterized using immunocytochemistry with broad antibody panels against carcinoma, mesothelial, and leukocyte epitopes, as previously described (24, 25). The procedures for fixation and block preparation for effusion specimens were identical to those employed for tissue samples.

Immunohistochemistry and Western Blot Analysis. Expression of apoE was studied by immunohistochemistry and Western blot analysis. The antibody used for immunohistochemistry was an apoE-specific monoclonal antibody (Transduction Lab, Lexington, KY) at a dilution of 1:600 followed by the EnVision + System using the peroxidase method (DAKO, Carpinteria, CA). The frequency of positive cells was estimated by randomly counting ~500 tumor cells from three different high-power fields ($\times 40$). For the negative control, an isotype (IgG1)-matched antibody, MN-4, was used in parallel (26). A positive reaction was defined as discrete localization of the brown chromogen in the cytoplasm or nucleus. A specimen was scored in a blinded fashion by observers according to the following criteria: negative, 1% to 5%, 6% to 50%, 51% to 100% of immunoreactive neoplastic cells with cytoplasmic/nuclear staining. Any discrepancy between the two observers was resolved through rescoring by another investigator.

Western blot analysis was done using the same antibody (1:1,000) on seven specimens of ovarian surface epithelial cell cultures, eight high-grade serous carcinoma tissues and four ovarian cancer cell lines, including OVCAR3, SKOV-3, OV-90, and CAOV3. Similar amounts of total protein from each lysate were loaded and separated on 12% Tris-Glycine-SDS polyacrylamide gels (Novex, San Diego, CA) and electroblotted to Millipore Immobilon-P polyvinylidene difluoride membranes. Western blots were developed by chemiluminescence (Pierce, Rockford, IL).

Cell Culture, Reagents, and Mitosis Counting. Four ovarian cell lines including OVCAR3, SKOV-3, OV-90, and CAOV3 and the kidney 293 cell line were purchased from the American Type Culture Collection (Rockville, MD). All the cell lines were maintained in the RPMI 1640 (Life Technologies, Gaithersburg, MD) supplemented with 10% fetal bovine serum (HyClone, Logan, UT), 100 units/mL of penicillin, and 100 μ g/mL of streptomycin. Nocodazole (Sigma, St. Louis, MO) was used to trap mitoses in cell cultures at 70 ng/mL in the culture medium. Mitotic indices were determined at 3, 6, and 12 hours after adding nocodazole. The mitotic index was expressed as the percentage of mitotic figures by counting at least 500 4',6'-diamidino-2-phenylindole (DAPI)-stained cells under a fluorescence microscope. To detect the secretory form of apoE, we cultured 5×10^5 OVCAR3 cells in 1 mL of serum-free RPMI 1640 using a 6-well plate. After filtering the condition medium to remove floating cells and cell debris, an aliquot (50 μ L) was obtained at 24, 48, 72, and 96 hours for Western blot analysis.

Gene Knockdown Using siRNA. Short interfering RNA that specifically targeted the apoE RNA was used to reduce apoE expression (27). We selected OVCAR3 cells as the representative cell line for siRNA treatment because other ovarian cancer cell lines (SKOV3, OV90, and CAOV3) we have examined did not show detectable level of apoE expression and they were used as controls. The siRNA was generated by Silencer siRNA Construction Kit (Ambion, Austin, TX) or by chemical synthesis (Dharmacon, Lafayette, CO). Cultured cells were grown on 24-well plates and were transfected with siRNA using an oligofectamine reagent (Invitrogen, Carlsbad, CA). The target sequences for apoE siRNA were

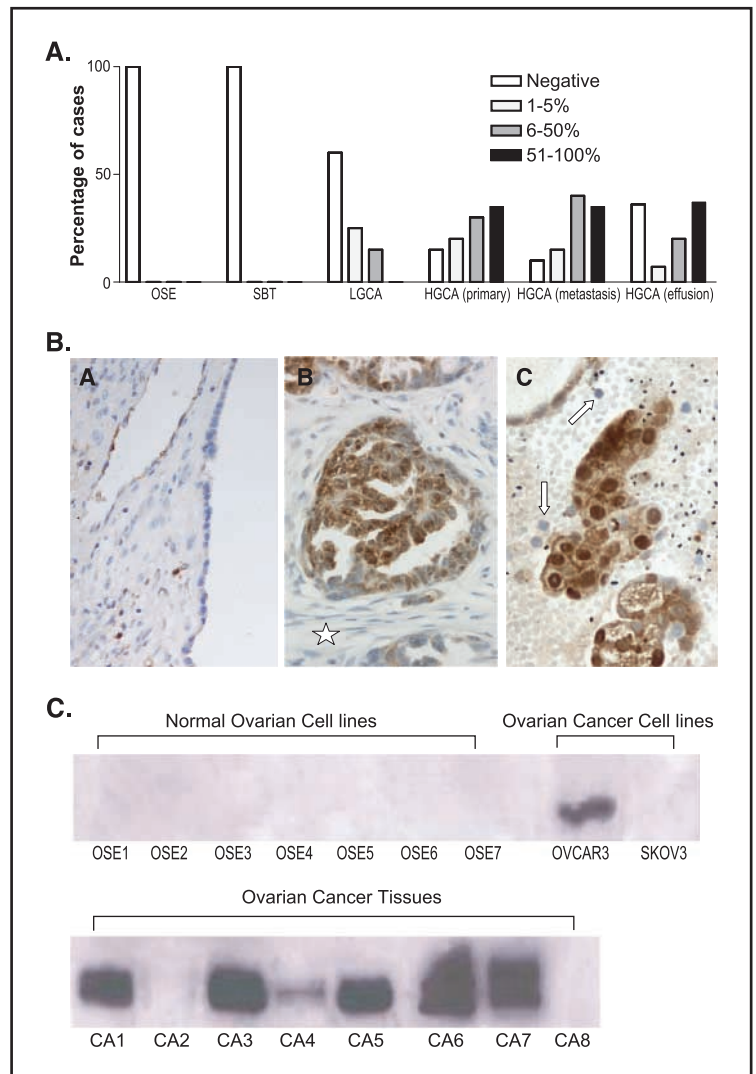
5'-aaggtggagcaagcgggtggag-3' (siRNA-1) and 5'-ggagttgaaggcctacaaa-3' (siRNA-2). The sequences for the control siRNA were 5'-aactggcactgggtcgtttt-3' (siRNA-3) and 5'-aaggagttgaaggcctacaaa-3' (siRNA-4). The sequences of target and control siRNA were derived from the apoE coding region, but the control siRNA did not have an effect on apoE expression. Blast analysis (<http://www.ncbi.nlm.nih.gov/BLAST/>) did not reveal overlapping regions between both target sequences and other human genes. Both adherent and floating cells were harvested for Western blot, cell cycle analysis, and apoptosis detection at different time points.

Cell Cycle Analysis and Apoptosis Detection. Both attached and floating cells were harvested for study. For DAPI staining, 3×10^5 cells were resuspended in 50 μ L of PBS and 350 μ L of staining solution containing 0.6% NP40, 3% paraformaldehyde, and 10 μ g/mL DAPI. DAPI-stained cells were subject to cell cycle analysis using a BD-LSR flow cytometer (Becton Dickinson, Mountain View, CA). The sub-G₁ population in the cell cycle analysis was defined as the fraction of apoptotic cells. To confirm the apoptotic cells, DAPI- or annexin V-stained cells were also examined under a fluorescence microscope. The staining of annexin V has been described in our previous report (28). Briefly, 10^5 cells were suspended in 100 mL of annexin-binding buffer and were then incubated with 5 μ L of Alexa568-bound annexin V (Molecular Probes, Eugene, OR) at room temperature for 15 minutes. Apoptotic cells were defined as those cells that were fluorescent after annexin V staining. The percentage of annexin V-positive cells was measured by the flow cytometer.

Rescue Assay by Expression of Engineered ApoE with Silent Mutations. In order to show the specificity of apoE siRNA in targeting apoE, we did a rescue assay by expressing engineered mutant apoE that was not sensitive for apoE siRNA-1 silencing in OVCAR3 cells. To achieve this, we introduced silent mutations into apoE cDNA, encoding the targeted gene that were thought to destroy complementarity with the siRNA, whereas maintaining the wild-type amino acid sequence. The cDNA of ApoE was prepared from OVCAR3 cells, PCR amplified, and cloned to a mammalian expression vector, pCDNA6 (Invitrogen) using the following primers: 5'-accatgaagttctgtgggctg-3' (forward primer) and 5'-gtgattgtcgtgggacaca-3' (reverse primer). Site-directed mutagenesis was used to generate mutant apoE with silent mutations using the template of wild-type pCDNA6/apoE. The silent mutations were designed to be located in the apoE siRNA-1 targeting sequence. Two primers were designed to generate two mutated nucleotide residues. To generate the mutation close to the 3' end, we use the reverse primer, 5'-ccaggccaaAgtggagcaGcgggtggagacagagccg-3' (mutated nucleotides were capitalized). Using the forward primer designed from the wild-type, this created a 74-bp fragment. To generate another mutation close to the 5' end, we designed the forward primer 5'-Gcgggtggagacagagccg-3', which in combination with the reverse primer used above resulted in an 888-bp fragment. Another PCR was done with both of the fragments to create a fusion PCR product containing the mutations using the PCR condition as follows: denaturation for 2 minutes at 94°C followed by three cycles of denaturation at 94°C for 10 seconds, annealing at 67°C for 30 seconds and extension at 68°C followed by three cycles of denaturation at 94°C for 10 seconds, annealing at 47°C for 30 seconds and extension at 68°C followed by three cycles of denaturation at 94°C for 10 seconds, annealing at 61°C for 30 seconds and extension at 68°C followed by 27 cycles of denaturation at 94°C for 10 seconds, annealing at 56°C for 30 seconds and extension at 68°C. The PCR product was cloned to pCDNA6 to generate pCDNA/mApoE and it was sequenced to validate the mutations.

For an efficient transfection, OVCAR3 and 293 cells were transfected with the pCDNA/mApoE or vector (pCDNA) by electroporation using a Nucleofector II (Amaxa, Köln, Germany). The cells were cultured in 24-well plates for 18 hours. The cells were transfected with apoE siRNAs or control siRNAs. Western blot analysis was done in 293 cells to assess whether mutant apoE expression was not sensitive for apoE siRNA silencing. OVCAR3 cells were analyzed for cell cycle progression and apoptosis. We determined if pCDNA/mApoE-transfected cells could rescue the apoE siRNA-1-induced phenotypes.

Figure 1. ApoE expression in ovarian serous tumors and normal ovarian surface epithelium. *A*, percentage of cases showing apoE immunoreactivity in normal ovarian surface epithelium (*OSE*), serous borderline tumor (*SBT*), low-grade serous carcinoma (*LGCA*), and high-grade serous carcinomas (*HGCA*) from different stages including the primary tumors, omental metastases, and effusions. The immunostaining pattern is scored as a four-tiered system based on the percentage of immunoreactive tumor cells. *B*, representative photomicrographs of apoE staining in normal ovarian surface epithelium (*A*), a metastasis of serous carcinoma in the omentum (*B*), and an effusion specimen containing serous carcinoma cells (*C*). As compared with normal ovarian surface epithelium, which lacks of apoE immunoreactivity, the serous carcinoma shows diffuse staining in the cytoplasm and nucleus. The stromal cells (*star* in *B*) and lymphocytes (*arrows* in *C*) are negative for apoE. *C*, Western blot analysis of apoE expression in ovarian surface epithelial cell cultures, ovarian carcinoma tissues, and cell lines. All seven ovarian surface epithelial (*OSE*) cultures are negative for apoE expression. OVCAR3 but not SKOV3 cells show a 34-kDa band (*top*). Most of ovarian serous carcinoma tissues (*CA*) are positive for apoE expression (*bottom*).



ApoE Expression Analysis Using the SAGE Database. To further extend our findings of apoE expression in ovarian serous carcinomas, we compared the gene expression levels in the SAGE libraries of carcinomas that are deposited in the public database (<http://www.ncbi.nlm.nih.gov/SAGE/index.cgi?cmd=tagsearch>). A total of 34 libraries were retrieved and they included carcinoma libraries and normal counterparts from pancreas, prostate, breast, stomach, and colon in addition to ovary. The selection of libraries for analysis was based on their availability in the SAGE database (till January 2004). The tag number from each library was retrieved by requesting the apoE tag sequence (CGACCCACG) from the SAGE database. They were expressed and normalized as the number of tags of apoE per one million of total tags in a given SAGE library.

Statistical Analysis. Statistical analysis was done by applying the SPSS-PC package (version 10.1, SPSS, Chicago, IL, 2001). $P < 0.05$ was considered statistically significant. Clinical and pathologic data were available for the majority of patients. Studies of the association between apoE expression in effusions and solid tumors and clinicopathologic parameters were undertaken using the two-sided χ^2 test. Univariate survival analyses were done using the Kaplan-Meier method and log-rank test. Expression categories in the clinical sample survival analysis were clustered as described in figure legend so as to allow for a sufficient number of cases to be included in each category. Student's t test was used to evaluate the difference in cell number in culture.

Results

ApoE Expression in Ovarian Cancer Tissues. To assess the biological roles of apoE in tumor progression, we first did immunohistochemistry on surgically removed ovarian tumors and their benign counterparts. ApoE immunoreactivity was present in 85% of primary high-grade serous carcinomas, 90% of solid metastatic high-grade serous carcinomas, and 64% of effusion specimens containing high-grade serous carcinomas. In contrast, apoE stain was not detectable in benign counterparts, including 10 normal ovarian surface epithelium, 10 serous cystadenomas, and 10 serous borderline tumors (Fig. 1). Cytoplasmic staining was shown in 81% of specimens and nuclear immunoreactivity was observed in 19% of cases. Low-grade serous carcinoma, a less common type of serous tumors, was positive for apoE in only 40% of cases and the staining pattern was always focal. The staining intensity was always strong in positive cells and therefore percentage scoring was used in this study. The specificity of apoE immunoreactivity in tissues was validated by Western blot analysis. As shown in Fig. 1, a predominant ~34-kDa band corresponding to apoE protein was present in immunostaining-positive samples (CA1 and CA3-7) but not in immunostaining-negative specimens

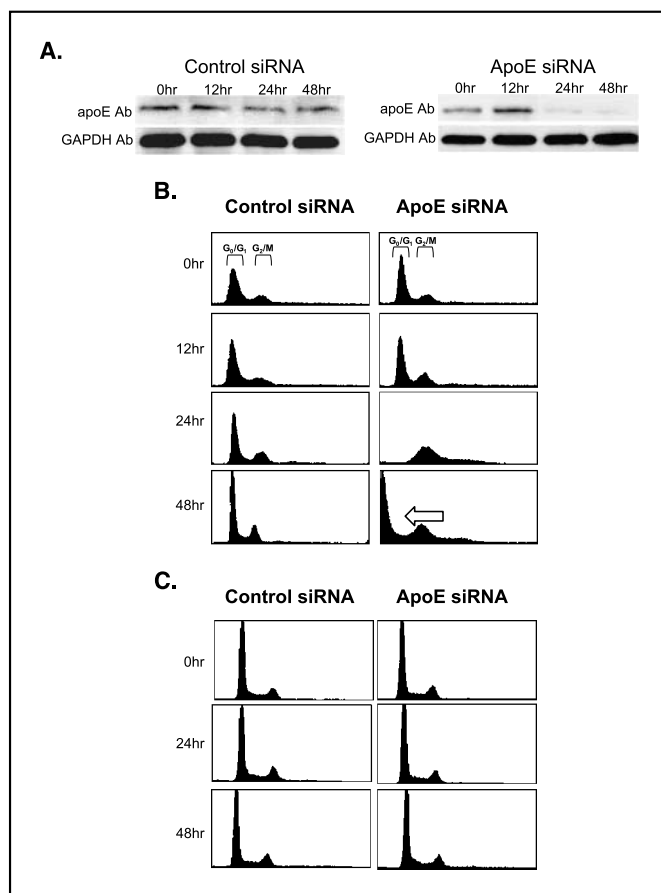


Figure 2. ApoE siRNA treatment in OVCAR3 cells. *A*, Western blot analysis of a significant decrease in apoE protein amount in apoE siRNA-treated cells as compared with the control siRNA-treated cells 24 hours after the siRNA treatment. Similar amount of total proteins were loaded as evidenced by a similar GAPDH intensity. *B*, cell cycle analysis shows a G₂-M block in OVCAR3 cells 24 hours after apoE siRNA treatment. A marked sub G₀-G₁ fraction is noted in treated cells (*arrow*), indicating an increased number of apoptotic cells. In contrast, there is no detectable alteration in the progression of cell cycle in the control siRNA treated cells. *C*, effect of apoE siRNA on SKOV3 cells. ApoE siRNA does not affect the cell cycle progression in SKOV3 cells.

(CA2 and CA8). ApoE protein was also present in the cytoplasm of the OVCAR3 ovarian cancer cell line but not in the SKOV3, CAOV3, and OV90 ovarian cancer cell lines. In addition, apoE immunoreactivity was not detected in any of the normal ovarian surface epithelial cultures (Fig. 1). To determine whether OVCAR3 cells secreted apoE, we did Western blot on the conditioned serum-free medium of OVCAR3 cells. There was no detectable apoE protein found in the conditioned medium up to 96 hours after incubation (data not shown).

The Phenotypes after apoE Knockdown. In order to characterize the functional role of apoE in ovarian carcinogenesis, we did an apoE knockdown assay using apoE specific siRNAs to reduce its expression in the OVCAR3 cell line that expresses apoE and in a control cell line, SKOV3 that does not express apoE based on Western blotting (Fig. 1). We designed a total of four sets of siRNA that targeted different regions of the apoE open reading frame. Based on Western blot analysis, two siRNAs (siRNA-1 and siRNA-2) showed a knockdown effect and the other two (siRNA-3 and control siRNA-4) did not. Therefore,

siRNA-3 and siRNA-4 were used as control siRNAs. Both apoE siRNAs (siRNA-1 and siRNA-2) were used in the biological assays. As compared with apoE siRNA-2, apoE siRNA-1 was more effective in silencing apoE expression. As shown in Fig. 2*A*, apoE expression was significantly reduced 24 hours after treatment of apoE siRNAs in OVCAR3 cells but not in the same cells treated with the control siRNAs or a mock transfection. Cell cycle analysis showed a G₂-M phase arrest in OVCAR3 cells 24 hours after siRNA-1 administration (Fig. 2*B*). The cell cycle arrest was reflected by a significant decrease in the numbers of viable cells at 48 hours after apoE siRNA treatment. The number of viable OVCAR3 cells was $139 \pm 33 \times 10^4$ /mL (average \pm SD) which was lower than $298 \pm 12 \times 10^4$ /mL in the mock treated cells and $247 \pm 21 \times 10^4$ /mL in the control siRNA treated cells ($P < 0.01$, *t* test). Nocodazole trapping was then used to distinguish G₂-phase versus M-phase arrest by counting the mitotic index in OVCAR3 cells 24 hours after apoE siRNA targeting. There was no substantial increase in the mitotic index among nocodazole treated cells at 3, 6, and 12 hours after adding nocodazole ($P > 0.1$). The cell cycle arrest was associated with an increase in apoptotic OVCAR3 cells. As compared with the control siRNAs, an increased number of apoptotic cells were observed in OVCAR3 cells treated with apoE siRNAs ($P < 0.01$) as detected by annexin V and DAPI staining (Fig. 3). The annexin V-positive cells occurred as early as 24 hours after treatment when rare cells showed morphologic features of apoptosis

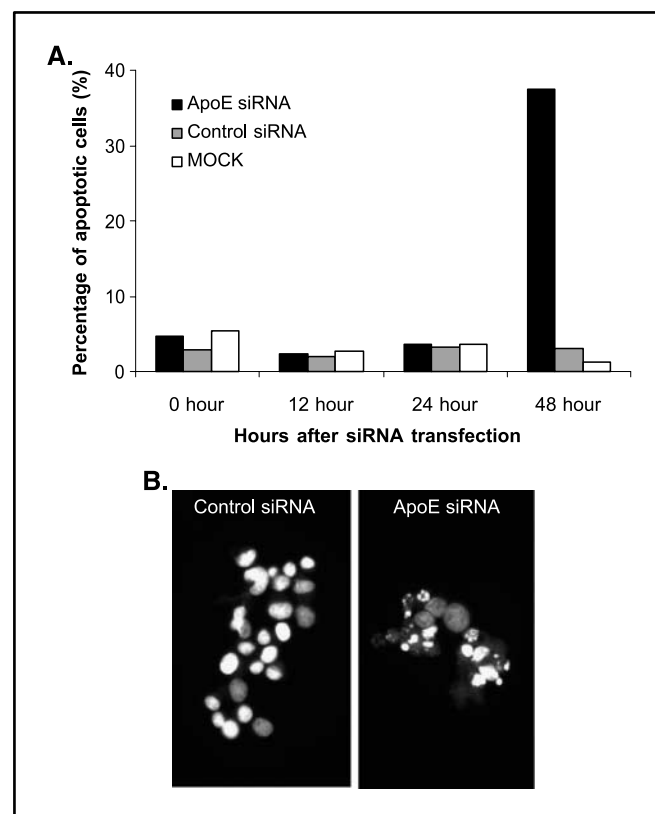


Figure 3. Detection of apoptosis in OVCAR3 cells. *A*, based on cell cycle analysis, a significant increase in apoptotic cells is noted in apoE siRNA-treated OVCAR3 cells at 48 hours. In contrast, both mock transfection and control siRNA transfection do not induce apoptosis. *B*, representative view of DAPI-stained OVCAR3 cells 48 hours after control siRNA (*left*) and apoE siRNA (*right*) treatment. Apoptotic cells were defined as those cells containing condensed and/or fragmented nuclei.

by DAPI staining. In contrast, the phenotypic changes seen in the apoE siRNA-treated OVCAR3 cells were absent in apoE siRNA-treated ovarian cancer cells such as SKOV3, OV-90, and CAOV3, which did not express detectable apoE. A representative cell cycle analysis of SKOV3 cells after apoE siRNA treatment was shown in Fig. 2C.

To validate the specificity of the siRNA approach, we tested if the phenotypes observed in apoE siRNA-treated OVCAR3 cells could be rescued by expression of an engineered mutant version of apoE containing silent mutations in the target sequence that were refractory to siRNA silencing. As compared with native wild-type apoE (Fig. 2A), expression of full-length mutant apoE with silent mutations was not suppressed by apoE siRNA based on Western blot analysis (Fig. 4). Cell cycle analysis showed a similar cell cycle distribution with minimal apoptotic cell (sub-G₁ fraction) in apoE mutant-transfected OVCAR3 cells 48 hours after treatment of apoE and control siRNA, indicating that cell cycle arrest was not detected in the cells expressing the mutant form of apoE with silent mutations in the siRNA targeted sequence (Fig. 4).

ApoE Tag Distribution in Other Human Cancers. In order to extend the apoE expression profile to other common types of carcinomas, we did a tag counting analysis based on the SAGE libraries that were available in the public database (<http://www.ncbi.nlm.nih.gov/SAGE/index.cgi?cmd=tagsearch>). In addition to ovarian cancer in which the apoE expression is up-regulated, almost all the libraries, including pancreas, prostate, breast, stomach, and colon carcinomas, showed an increase in the number of apoE tags compared with their normal counterparts, indicating that apoE was overexpressed in these cancer types (Fig. 5).

Clinical Significance of apoE Expression. In this study, we further assessed whether apoE expression had prognostic relevance in ovarian cancer patients by correlating apoE expression patterns and clinical outcome in patients who presented peritoneal effusion and did not receive prior chemotherapy (Fig. 6). After a comprehensive analysis by correlating apoE expression patterns and different clinical parameters, we found that the only statistically significant correlation was apoE immunoreactivity in nucleus of tumor cells in effusion samples and the overall survival. Using Kaplan-Meier survival analysis, patients with carcinoma cells showing

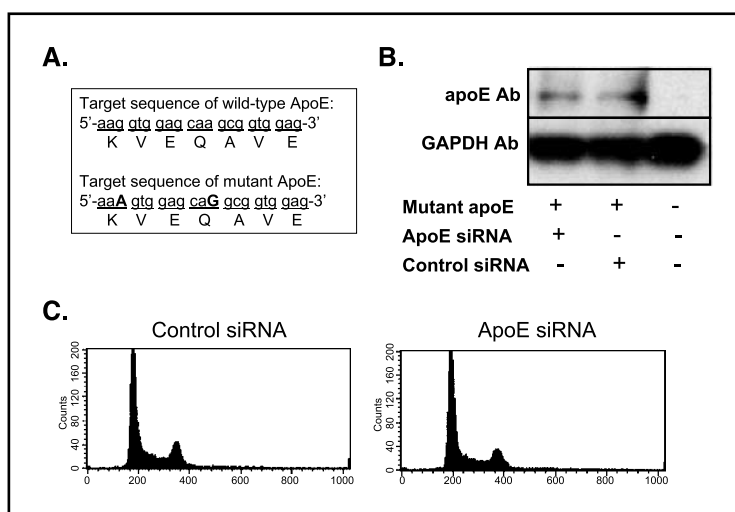
any level of nuclear expression in effusion samples had significantly better survival than those with effusions showing negative expression (43 versus 28 months for median overall survival, log-rank test, $P = 0.004$). However, there was no significant difference in overall survival between apoE-positive and apoE-negative cases in solid tumors (primary and metastasis). Kaplan-Meier survival analysis of apoE expression (nuclear or cytoplasmic) in carcinoma cells of 63 primary tumors shows similar median survival (29 months) for apoE-positive ($n = 19$) and apoE-negative ($n = 44$) tumors (log-rank test, $P = 0.79$).

Discussion

The results in this report showed that most ovarian serous carcinomas express apoE, thus confirming the previous SAGE result (7). Overexpression of apoE may not be confined to ovarian serous carcinomas because analysis of the SAGE database (<http://www.nlm.nih.gov/SAGE/>) showed that apoE expression was also up-regulated in other tumor types, including breast carcinomas, pancreatic carcinomas, stomach carcinomas, colon carcinomas, and prostate carcinomas (Fig. 5). The above findings suggest that apoE represents a tumor-associated marker in a wide variety of human cancers. The significantly higher frequency of apoE expression in high-grade compared with low-grade ovarian serous carcinomas is of great interest, and the finding suggests that both low-grade and high-grade tumors are distinct in gene expression, further supporting a dualistic pathway for the development of ovarian serous carcinoma (29). In that model, low-grade and high-grade ovarian serous carcinomas develop independently and are characterized by different molecular genetic changes and gene expression profiles (30–32).

Although siRNA is an effective and convenient approach to assess functional roles of genes by silencing their expression, it is essential to ensure that the phenotype changes after siRNA treatment are the results of specific gene knockdown rather than the “off-target” effects associated with the siRNA approach (33). In this study, we carefully designed our experiments and controls to avoid the specificity problems. We used two apoE siRNAs and several control siRNAs in experiments to show similar phenotypes in growth inhibition and apoptosis induction by the

Figure 4. Expression of mutant apoE protects OVCAR3 cells from apoE siRNA-induced cell cycle arrest and apoptosis. *A*, site-directed mutagenesis was done to generate silent mutations in siRNA-targeted sequence of apoE. *B*, Western blot analysis shows that expression of the mutant apoE in 293 cells is similar between apoE siRNA- and control siRNA-treated cells. The parental 293 cells do not express detectable apoE protein. *C*, cell cycle analysis demonstrates that cell cycle appears not arrested 48 hours after apoE siRNA-1 treatment in OVCAR3 cells that express the mutant apoE.



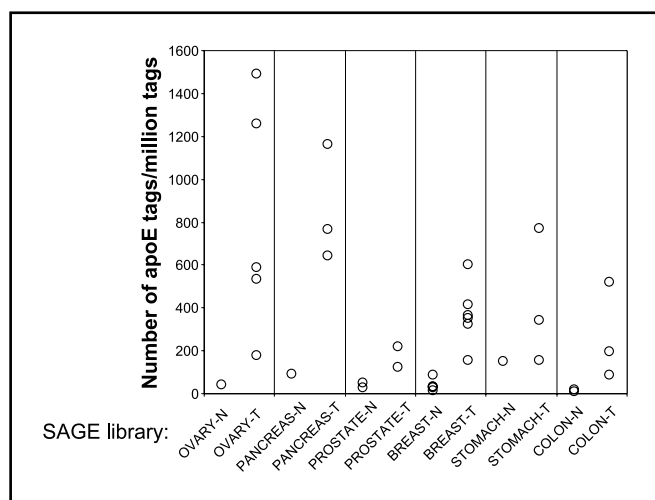


Figure 5. Analysis of apoE expression pattern in different carcinomas based on an analysis of SAGE database. All the SAGE libraries from carcinomas and normal counterparts from ovary, pancreas, colon, breast, stomach, and prostate in the SAGE database are selected. The expression level is shown as the number of apoE tag per one million of total tag counts (*y*-axis). Circle, SAGE library; T, tumor; N, normal counterpart.

targeting siRNAs. The phenotype changes can only be shown in ovarian cancer cells with apoE expression but not in those without detectable apoE expression. More importantly, we have shown that expression of a mutant version of apoE that cannot be recognized by the siRNA reverted the phenotypes. Overexpression of the engineered mutant apoE with silent mutations tolerated the siRNA silencing and rescued the cells after treatment of the target siRNA. The above results indicated the specificity of apoE siRNA that was used in this study.

Reduction of apoE expression resulted in a cell cycle arrest and apoptosis in apoE-expressing OVCAR3 cells, indicating that apoE is essential for proliferation and survival of OVCAR3 cells. One of the possible mechanisms is that endogenous apoE molecules enhance the lipid transport (endocytosis) into the tumor cells through the LDL receptor family members, which are expressed in OVCAR3 cells (data not shown). Besides, apoE mediates signal transduction upon binding to the LDL receptor members. This autocrine loop leads to activation and/or expression of downstream proliferative and anti-apoptotic signals. This view is supported by a number of studies showing that apoE, upon binding to LDL receptor family members, initiates cell signaling and exerts a variety of biological effects (8, 12, 22). During tumor progression of ovarian serous carcinomas, some carcinomas acquire and become dependent on the strategy by overexpressing endogenous apoE to maintain cell growth and prevent apoptosis through the autocrine mechanism of ligand-receptor binding. Therefore, inhibition of apoE expression abolishes the apoE related pathway(s), causing cell cycle arrest and apoptosis.

Other than lipid transport and signal transduction, apoE may modify the tumor microenvironment to maintain tumor proliferation and survival. Support for this comes from a study showing that apoE induces expression of subendothelial heparan sulfate proteoglycan (34), which may be important for apoE in preventing apoptosis in kidney mesangial cells (35). Based on the studies using apoE knockout mice (36–38), it has been reported

that macrophage-derived apoE interacts with the extracellular matrix and that such interactions result in the retention of lipoproteins in the vessel wall and affect the bioavailability of cytokines and growth factors sequestered in the extracellular matrix (39). Further studies are required to determine if a similar paracrine mechanism operates in ovarian carcinomas.

Prognostic markers that can predict clinical outcome, including treatment response and overall survival, have substantial clinical impacts in the management of ovarian cancer patients (40). To further explore the clinical relevance of apoE expression in ovarian serous carcinomas, we correlated its expression and the overall survival in patients with peritoneal effusion who did not receive prior chemotherapy. Interestingly, we found a positive correlation of a favorable prognosis and apoE expression in nuclei of tumor cells. Our finding contrasts with a recent report showing positive correlation of cytoplasmic apoE immunointensity and clinical aggressiveness in prostate cancer (41). This difference in the prognostic significance between ovarian and prostate carcinomas is intriguing and probably reflects different roles of the apoE in different tumor types. Besides, the nuclear apoE may have different cellular functions from cytoplasmic apoE. Further studies should assess whether nuclear apoE sensitizes ovarian cancer cells to chemotherapeutic agents, including paclitaxel and carboplatin *in vivo*. The positive correlation of apoE expression and better survival can only be shown in effusion samples but not in solid tumors. This finding is consistent with the view that the mortality of ovarian cancer is attributed to the effusion rather than to the solid tumor (42). Therefore, assessment of apoE expression in tumor cells from the effusion samples is more relevant in analysis of overall survival.

In summary, this study shows a new role of apoE in human cancer. Cancer cells may depend on apoE for cell survival in apoE-expressing tumors. ApoE knockdown in OVCAR3 cells represents an experimental model for the future studies aimed at elucidating the basic mechanisms by which apoE expression contributes to cell proliferation and survival in cancer. Finally, apoE expression has clinical relevance by serving as a prognostic marker in ovarian cancer patients.

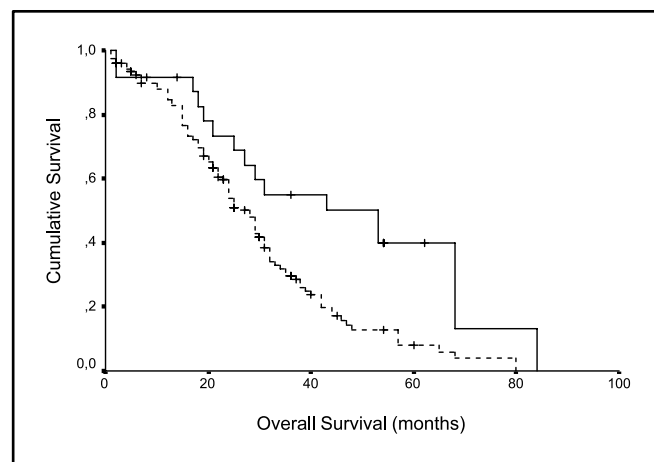


Figure 6. Kaplan-Meier survival analysis shows that previously untreated patients with carcinoma cells in effusion showing nuclear immunoreactivity of apoE ($n = 24$, solid line) had significantly better survival than those with effusions showing negative expression ($n = 121$, dashed line; 43 versus 28 for median overall survival; $P = 0.004$).

Acknowledgments

Received 5/26/2004; revised 10/21/2004; accepted 11/2/2004.

Grant support: U.S. Department of Defense grant OC010017 and National Cancer Institute/NIH grant CA103937.

The costs of publication of this article were defrayed in part by the payment of page

charges. This article must therefore be hereby marked advertisement in accordance with 18 U.S.C. Section 1734 solely to indicate this fact.

We thank the excellent technical support from Leslie Meszler (Johns Hopkins Imaging Core Facility); Inger-Liv Nordli, Mai Nguyen, Erika Thorbjørnsen and Ann Larsen at the Department of Pathology at the Norwegian Radium Hospital, Norway; and Dr. C-Y Hsu for statistical analysis.

References

- Diamandis EP. Tumor markers: past, present and future. In: Diamandis EP, editor. *Tumor markers*. 1st ed. Washington (DC): American Association for Clinical Chemistry; 2002. p. 3-8.
- Diamandis EP, Yousef GM. Human tissue kallikreins: a family of new cancer biomarkers. *Clin Chem* 2002;48:1198-205.
- Shih I-M, Sokoll LJ, Chan DW. Tumor markers in ovarian cancer. In: Diamandis EP, Fritsche HA, Lilja H, Chan DW, Schwartz MK, editors. *Tumor markers physiology, pathobiology, technology and clinical applications*. Philadelphia: AACR Press; 2002. p. 239-52.
- Velculescu VE, Zhang L, Vogelstein B, et al. Serial analysis of gene expression. *Science* 1995;270:484-7.
- Velculescu VE, Madden SL, Zhang L, et al. Analysis of human transcriptsomes. *Nat Genet* 1999;23:387-8.
- Lash AE, Tolstoshev CM, Wagner L, et al. SAGEmap: a public gene expression resource. *Genome Res* 2000;10:1051-60.
- Hough CD, Sherman-Baust CA, Pizer ES, et al. Large-scale serial analysis of gene expression reveals genes differentially expressed in ovarian cancer. *Cancer Res* 2000;60:6281-7.
- Gliemann J. Receptors of the low density lipoprotein (LDL) receptor family in man. Multiple functions of the large family members via interaction with complex ligands. *Biol Chem* 1998;379:951-64.
- Li Y, Cam J, Bu G. Low-density lipoprotein receptor family: endocytosis and signal transduction. *Mol Neurobiol* 2001;23:53-67.
- Herz J, Bock HH. Lipoprotein receptors in the nervous system. *Annu Rev Biochem* 2002;71:405-34.
- Hjalm G, Murray E, Crumley G, et al. Cloning and sequencing of human gp330, a Ca(2+)-binding receptor with potential intracellular signaling properties. *Eur J Biochem* 1996;239:132-7.
- Ho YY, Deckelbaum RJ, Chen Y, et al. Apolipoprotein E inhibits serum-stimulated cell proliferation and enhances serum-independent cell proliferation. *J Biol Chem* 2001;276:43455-62.
- Vogel T, Guo NH, Guy R, et al. Apolipoprotein E: a potent inhibitor of endothelial and tumor cell proliferation. *J Cell Biochem* 1994;54:299-308.
- Browning PJ, Roberts DD, Zabrenetzky V, et al. Apolipoprotein E (ApoE), a novel heparin-binding protein inhibits the development of Kaposi's sarcoma-like lesions in BALB/c *nu/nu* mice. *J Exp Med* 1994;180:1949-54.
- Ishigami M, Swertfeger DK, Hui MS, et al. Apolipoprotein E inhibition of vascular smooth muscle cell proliferation but not the inhibition of migration is mediated through activation of inducible nitric oxide synthase. *Arterioscler Thromb Vasc Biol* 2000;20:1020-6.
- Ishigami M, Swertfeger DK, Granholm NA, et al. Apolipoprotein E inhibits platelet-derived growth factor-induced vascular smooth muscle cell migration and proliferation by suppressing signal transduction and preventing cell entry to G₁ phase. *J Biol Chem* 1998;273:20156-61.
- Riddell DR, Graham A, Owen JS. Apolipoprotein E inhibits platelet aggregation through the L-arginine: nitric oxide pathway. Implications for vascular disease. *J Biol Chem* 1997;272:89-95.
- Lynch JR, Morgan D, Mance J, et al. Apolipoprotein E modulates glial activation and the endogenous central nervous system inflammatory response. *J Neuroimmunol* 2001;114:107-13.
- Laffont I, Takahashi M, Shibukawa Y, et al. Apolipoprotein E activates Akt pathway in neuro-2a in an isoform-specific manner. *Biochem Biophys Res Commun* 2002;292:83-7.
- Mahley RW. Apolipoprotein E: cholesterol transport protein with expanding role in cell biology. *Science* 1988;240:622-30.
- Nathan BP, Jiang Y, Wong GK, et al. Apolipoprotein E4 inhibits, and apolipoprotein E3 promotes neurite outgrowth in cultured adult mouse cortical neurons through the low-density lipoprotein receptor-related protein. *Brain Res* 2002;928:96-105.
- Mahley RW, Rall SC Jr. Apolipoprotein E: far more than a lipid transport protein. *Annu Rev Genomics Hum Genet* 2000;1:507-37.
- Raber J, Wong D, Yu GQ, et al. Apolipoprotein E and cognitive performance. *Nature* 2000;404:352-4.
- Davidson B, Risberg B, Kristensen G, et al. Detection of cancer cells in effusions from patients diagnosed with gynaecological malignancies. Evaluation of five epithelial markers. *Virchows Arch* 1999;435:43-9.
- Davidson B, Nielsen S, Christensen J, et al. The role of desmin and N-cadherin in effusion cytology: a comparative study using established markers of mesothelial and epithelial cells. *Am J Surg Pathol* 2001;25:1405-12.
- Shih IM, Nesbit M, Herlyn M, et al. A new Mel-CAM (CD146)-specific monoclonal antibody, MN-4, on paraffin-embedded tissue. *Mod Pathol* 1998;11:1098-106.
- Dykxhoorn DM, Novina CD, Sharp PA. Killing the messenger: short RNAs that silence gene expression. *Nat Rev Mol Cell Biol* 2003;4:457-67.
- Shih IM, Yu J, He TC, et al. The β -catenin binding domain of adenomatous polyposis coli is sufficient for tumor suppression. *Cancer Res* 2000;60:1671-6.
- Shih I-M, Kurman RJ. Ovarian tumorigenesis: a proposed model based on morphological and molecular genetic analysis. *Am J Pathol* 2004;164:1511-8.
- Singer G, Oldt R III, Cohen Y, et al. Mutations in BRAF and KRAS characterize the development of low-grade ovarian serous carcinoma. *J Natl Cancer Inst* 2003;95:484-6.
- Singer G, Rebmann V, Chen Y-C, et al. HLA-G is a potential tumor marker in malignant ascites. *Clin Cancer Res* 2003;9:4460-4.
- Singer G, Kurman RJ, Chang H-W, et al. Diverse tumorigenic pathways in ovarian serous carcinoma. *Am J Pathol* 2002;160:1223-8.
- Hannon GJ, Rossi JJ. Unlocking the potential of the human genome with RNA interference. *Nature* 2004;431:371-8.
- Pillarsetti S. Lipoprotein modulation of subendothelial heparan sulfate proteoglycans (perlecan) and atherogenicity. *Trends Cardiovasc Med* 2000;10:60-5.
- Chen G, Paka L, Kako Y, et al. A protective role for kidney apolipoprotein E. Regulation of mesangial cell proliferation and matrix expansion. *J Biol Chem* 2001;276:49142-7.
- Linton MF, Atkinson JB, Fazio S. Prevention of atherosclerosis in apolipoprotein E-deficient mice by bone marrow transplantation. *Science* 1995;267:1034-7.
- Boisvert WA, Spangenberg J, Curtiss LK. Treatment of severe hypercholesterolemia in apolipoprotein E-deficient mice by bone marrow transplantation. *J Clin Invest* 1995;96:1118-24.
- Boisvert WA, Curtiss LK. Elimination of macrophage-specific apolipoprotein E reduces diet-induced atherosclerosis in C57BL/6J male mice. *J Lipid Res* 1999;40:806-13.
- Mazzone T. Apolipoprotein E secretion by macrophages: its potential physiological functions. *Curr Opin Lipidol* 1996;7:303-7.
- Scott M, Hall PA. Prognostic and predictive factors. *Methods Mol Med* 2004;97:1-11.
- Venanzoni MC, Giunta S, Muraro GB, et al. Apolipoprotein E expression in localized prostate cancers. *Int J Oncol* 2003;22:779-86.
- Davidson B, Risberg B, Reich R, et al. Effusion cytology in ovarian cancer: new molecular methods as aids to diagnosis and prognosis. *Clin Lab Med* 2003;23:729-54, viii.

Inactivation of the Mitogen-Activated Protein Kinase Pathway as a Potential Target-Based Therapy in Ovarian Serous Tumors with KRAS or BRAF Mutations

Gudrun Pohl,¹ Chung-Liang Ho,¹ Robert J. Kurman,^{1,2} Robert Bristow,² Tian-Li Wang,² and Ie-Ming Shih^{1,2}

Departments of ¹Pathology and ²Oncology and Gynecology and Obstetrics, Johns Hopkins Medical Institutions, Baltimore, Maryland

Abstract

Activation of mitogen-activated protein kinase (MAPK) occurs in response to various growth stimulating signals and as a result of activating mutations of the upstream regulators, KRAS and BRAF, which can be found in many types of human cancer. To investigate the roles of MAPK activation in tumors harboring KRAS or BRAF mutations, we inactivated MAPK in ovarian tumor cells using CI-1040, a compound that selectively inhibits MEK, an upstream regulator of MAPK and thus prevents MAPK activation. Profound growth inhibition and apoptosis were observed in CI-1040-treated tumor cells with mutations in either KRAS or BRAF in comparison with the ovarian cancer cells containing wild-type sequences. Long serial analysis of gene expression identified several differentially expressed genes in CI-1040-treated MPSC1 cells harboring an activating mutation in BRAF (V599L). The most striking changes were down-regulation of cyclin D1, COBRA1, and transglutaminase-2 and up-regulation of tumor necrosis factor-related apoptosis-induced ligand, thrombospondin-1, optineurin, and palladin. These patterns of gene expression were validated in other CI-1040-treated tumor cells based on quantitative PCR. Constitutive expression of cyclin D1 partially reversed the growth inhibitory effect of CI-1040 in MPSC1 cells. Our findings indicate that an activated MAPK pathway is critical in tumor growth and survival of ovarian tumors with KRAS or BRAF mutations and suggest that the CI-1040 induced phenotypes depend on the mutational status of KRAS and BRAF in ovarian tumors. (Cancer Res 2005; 65(5): 1994-2000)

Introduction

Ovarian cancer is one of the most lethal malignant diseases in women and of these, serous carcinoma is the most common type (1). Our previous studies have shown that a subset of serous tumors that include low-grade serous carcinoma and its precursor, serous borderline tumor (2–4) harbor mutations in either KRAS or BRAF (2, 3). Based on mutational analysis, we found that mutations in either BRAF or KRAS occur in 65% to 88% of these low-grade tumors. Furthermore, we found that mutations in BRAF at codon 599 and KRAS at codons 12 and 13 were mutually exclusive (2, 5), a finding consistent with the data in melanoma and colorectal

carcinoma (6, 7). This lends further support to the view that BRAF and KRAS mutations have an equivalent effect on tumorigenesis. Mutations in either KRAS or BRAF occur very early in the development of low-grade serous tumors as the same mutations of KRAS or BRAF can be detected in both serous borderline tumor and adjacent cystadenoma epithelium, a presumed precursor of serous borderline tumor (5). In contrast, mutations in KRAS and BRAF are rare in high-grade serous carcinomas, which are characterized by frequent (>50%) p53 mutations (8).

Mutations of either BRAF or KRAS lead to constitutive activation (phosphorylation) of the downstream target, mitogen-activated protein kinase (MAPK), also known as extracellular signal-regulated protein kinase (ERK; refs. 9, 10). In a previous study, we showed a correlation between mutations in BRAF or KRAS and overexpression of activated MAPK in ovarian tumor tissues further supporting the above view (11). Activation of MAPK activates downstream cellular targets (12, 13) including a variety of cellular and nuclear proteins. Although the function and downstream effectors of the RAS/RAF/MEK/MAPK (ERK) pathway have been recently studied (14), the biological role of this pathway in the development of ovarian serous tumors has not been explored.

Based on our recent studies demonstrating that mutations in KRAS or BRAF occur very early in the tumor development (5) and that these mutations are associated with activation of MAPK in ovarian serous tumors (11), we hypothesize that constitutive activation of MAPK plays a key role in the development of serous tumors containing mutant KRAS or BRAF. To test this hypothesis, we compared the phenotypes and gene expression profiles in cultured ovarian serous tumor cells after treatment with a highly potent and selective inhibitor of MEK1/2, CI-1040 (formerly known as PD184352; refs. 15–18) that prevents the activation (phosphorylation) of MAPK. One of the differentially expressed genes, *cyclin D1*, was the most dramatically and consistently down-regulated by CI-1040 and accordingly, it was selected for further study for its biological role in mediating MAPK activation and cell proliferation.

Materials and Methods

Cell Culture and Cell Lines

OVCA3, SKOV3, and CAOV3 ovarian cancer cell lines were obtained from American Tissue Culture Center (Rockville, MD). MPSC1 cell line was established from a low-grade serous carcinoma. A set of primary cultures was established from ovarian serous tumors, including OVPC-1, OVPC-2, OVPC-3, OVPC-4, OVPC-5, OVPC-6, OVPC-7, OVPC-8, and OVPC-9. In addition, primary cultures of normal ovarian surface epithelium and ovarian stroma were also obtained from ovarian tissues without neoplastic diseases. The acquisition of anonymous tissue specimens was approved by the local institutional review board. The diagnoses were confirmed by a surgical pathologist (I.S.) before harvesting tumor samples

Note: G. Pohl and C-L. Ho contribute equally.

C-L. Ho is currently at the Department of Pathology, National Cheng-Kung University, Tainan, Taiwan.

Requests for reprints: Ie-Ming Shih, Johns Hopkins Medical Institutions, 1503 East Jefferson Street, Room B-315, Baltimore, MD 21231. Phone: 410-502-7774; Fax: 410-502-7943; E-mail: ishih@jhmi.edu.

©2005 American Association for Cancer Research.

for experiments. Primary tumor cultures were established from freshly isolated tumor samples by immunosorting or trypsinization. For immunosorting, fresh tumor tissues were minced and incubated with collagenase A (2 mg/mL) at 37°C for 40 minutes. After filtration through sieve membranes (with 100- μ m pores), tumor cells were immunosorted using an anti-Ep-CAM antibody bound to the Dynal beads (Dynal, Oslo, Norway) following the vendor's instructions. For direct trypsinization, large fragments of fresh serous borderline tumor tissues (~1 cm) were incubated with trypsin-EDTA (Life Technologies, Grand Island, NY) at 37°C for 10 minutes with agitation. The detached epithelial cells were harvested by centrifugation. This procedure significantly minimized stromal cell contamination by detaching tumor epithelial cells directly from the tumor surface whereas keeping the underlying stroma intact. Freshly isolated tumor cells were allowed to grow in culture and were used for experiments within two passages. Culturing ovarian surface epithelium was done by gently scraping the surface of normal ovaries after incubation with trypsin-EDTA at 37°C for 15 minutes. The purity of epithelial cells was determined by the cytokeratin-8 immunoreactivity. Samples with >98% cytokeratin-8-positive cells were used. The culture of ovarian stromal cells was established by mincing a piece of normal ovary after removing the surface epithelium. All cultures were maintained in RPMI 1640 supplemented with 10% fetal bovine serum and 1% antibiotics. Selection of pCMV/cyclin D1 stable clones was done by minimal dilution in a selection medium containing 18 μ g/mL of Blasticidin (Sigma, St Louis, MO).

Mutational Analysis of BRAF and KRAS

Genomic DNA was purified from all the cell lines and primary cultures using a Qiaquick PCR purification kit (Qiagen, Valencia, CA). PCR was then done followed by nucleotide sequencing at the Agencourt Bioscience (Beverly, MA). Exon 1 of *KRAS* and exon 15 of *BRAF* were both sequenced as each exon harbors almost all mutations of both genes (2–4, 6). The primers for PCR and sequencing were manufactured by GeneLink (Hawthorne, NY) and their sequences were described in a previous report (5). The sequences were analyzed using the Lasergene program, DNASTAR (Madison, WI).

LongSAGE Library Construction. Total RNA was isolated from MPSC1 cells after 9-hour incubation with 5 μ mol/L CI-1040 (a gift from M. Kolodney, Department of Medicine, UCLA School of Medicine, Los Angeles, CA; ref. 19) and DMSO control. The concentration of CI-1040 was used because this was the minimal concentration that abolished the expression of active MAPK in MPSC-1 cells based on Western blot analysis in MPSC-1 cells. LongSAGE was done with 2 μ g mRNA using the standard SAGE protocol that has been detailed at http://www.sagenet.org/sage_protocol.htm with the modifications previously described (20). Linkers containing the *MmeI* recognition site were ligated to 3' cDNA ends after *NlaIII* digestion [linker 1A (5'-TTTGGATTGCTGGTGCAGTACAAC TAGGCTTAATATCCGACATG-3') and linker 1B (5'-TCGGATATTAAGCCTAGTTGTACTGCACCAGCAAATCCC7-amino-modified-3')] followed by annealing together and ligation to half the cDNA population, and linker 2A (5'-TTTCTGCTCGAATCAAGTTCAACGATGTACGTCGACATG-3') and linker 2B (5'-TCGGACGTACATCGTTAGAAGCTTGAATTCGAGCAGC7-amino-modified-3') were annealed together and ligated to the remaining half of the cDNA. Linker tag molecules were released from the cDNA using the *MmeI* type IIS restriction endonuclease (21). Digestion was done at 37°C for 2.5 hours using 40 units *MmeI* in 300 μ L of 10 mmol/L HEPES (pH 8.0), 2.5 mmol/L potassium acetate, 5 mmol/L magnesium acetate, 2 mmol/L DTT, and 40 μ mol/L *S*-adenosylmethionine. The linker 1 tag and linker 2 tag molecules were not polished and were directly ligated together in a 6 μ L reaction containing 4 units T4 DNA ligase (Invitrogen, Carlsbad, CA) in the supplied buffer for 2.5 hours at 16°C. The ligation mixture was used to transform bacteria and ~3,840 clones were sequenced to obtain ~50,000 to 60,000 tags from each LongSAGE library (Agencourt, MA). The SAGE software was modified to allow extraction of 21-bp tags from sequences of concatemer clones.

Quantitative PCR Analysis of Candidate Genes. Single-stranded cDNA was synthesized from CI-1040 and DMSO-treated MPSC1, OVPC-1, OVPC-3, SKOV3, and OVCAR3 cells at 24 hours using the Superscript II reverse

transcriptase (Invitrogen) following the manufacturer's protocol, and mock template preparations were prepared in parallel without the addition of reverse transcriptase. After analysis of LongSAGE data, we selected the top 20 candidates of CI-1040 induced up-regulated and down-regulated genes for real-time PCR analysis. As we expected that most tags would correspond to the last exon of the candidate LongSAGE genes, primers were designed using the Primer 3 interface (http://www-genome.wi.mit.edu/cgi-bin/primer/primer3_www.cgi) to span a 100- to 200-bp region that included the tag, and were synthesized by GeneLink (Hawthorne, NY). Quantitative PCR was done using an iCycler (Bio-Rad, Hercules, CA) using Pico Green dye (Molecular Probes, Eugene, OR), and threshold numbers were collected using the iCycler software version 1.0. Averages in the threshold cycle number (Ct) of duplicate measurements were obtained. The results were expressed as the difference between the Ct of the gene of interest and the Ct of a control gene (*APP*) for which expression is relatively constant among the SAGE libraries analyzed (22).

Western Blot Analysis

Cell lysates were prepared by dissolving cell pellets in the Laemmli sample buffer (Bio-Rad) supplemented with 5% of β -mercaptoethanol (Sigma). Western blot analysis was done on ovarian cancer cell lines/cultures, including MPSC1, OVCAR3, SKOV3, and OVPC-5. Similar amounts of total protein from each lysate were loaded and separated on 10% Tris-Glycine-SDS polyacrylamide gels (Novex, San Diego, CA) and electroblotted to the Millipore Immobilon-P polyvinylidene difluoride membranes. The membranes were probed with the anti-active MAPK antibody (pTEpY, 1:5,000; Promega, Madison, WI) or an anti-cyclin D1 antibody (CD1.1, 1:200; abcam, Cambridge, MA) followed by a peroxidase conjugated anti-mouse or anti-rabbit immunoglobulin (1:20,000). The same membrane was probed with an antibody that reacts with glyceraldehyde-3-phosphate dehydrogenase for loading controls. Western blots were developed by chemiluminescence (Pierce, Rockford, IL).

Cell Growth and Cell Cycle Assays

For cell growth assay, cells were plated at the same density (10^5 cells per well) in 24-well plates and cell growth assay was done by counting the number of viable cells 72 hours after treating the cells with CI-1040 at 5 μ mol/L and DMSO (control). The data was expressed as percentage of the DMSO control. The mean and SD were obtained from three experiments. To assess if cyclin D1 can revert the growth inhibitory effect of CI-1040, we constructed a mammalian expression vector, pCMV/cyclin D1 with a V5 tag at the COOH terminus. The cDNA of cyclin D1 was prepared from the MPSC1 cells, PCR and cloned to a mammalian expression vector, pcDNA6/V5-His A (Invitrogen). The clone was sequenced to ensure a wild-type coding sequence of cyclin D1. pCMV/cyclin D1 was stably transfected into MPSC1 cells using the Nucleofector II electroporator (Amaxa, Köln, Germany) under a selection marker of Blasticidin (18 μ g/mL). MPSC1 cells with both pCMV/cyclin D1- and pcDNA6/V5-His A-transfected cells were treated with either CI-1040 or DMSO (control). Cell number was counted at 0, 24, 48, and 72 hours. For cell cycle analysis, both attached and floating cells were harvested for study. Approximately 3×10^5 cells were resuspended in 50 μ L of PBS, which was then mixed with 350 μ L of staining solution containing 0.6% NP40, 3% paraformaldehyde, and 10 μ g/mL 4',6-Diamidino-2-phenylindole. 4',6-diamidino-2-phenylindole-stained cells were subject to cell cycle analysis using a BD-LSR flow cytometer (Becton Dickinson, Mountain View, CA). The sub-G₁ population in the cell cycle analysis was defined as a fraction of apoptotic cells. To confirm the presence of apoptotic cells, 4',6-diamidino-2-phenylindole-stained cells were also examined under a Nikon fluorescence microscope or stained with Annexin V dye.

Results

Effects of MAPK Inactivation on Ovarian Serous Tumors. A panel of ovarian serous tumor cell lines and primary cultures were first analyzed for their mutation status in the *KRAS* and *BRAF* genes. Their mutational status was correlated with growth

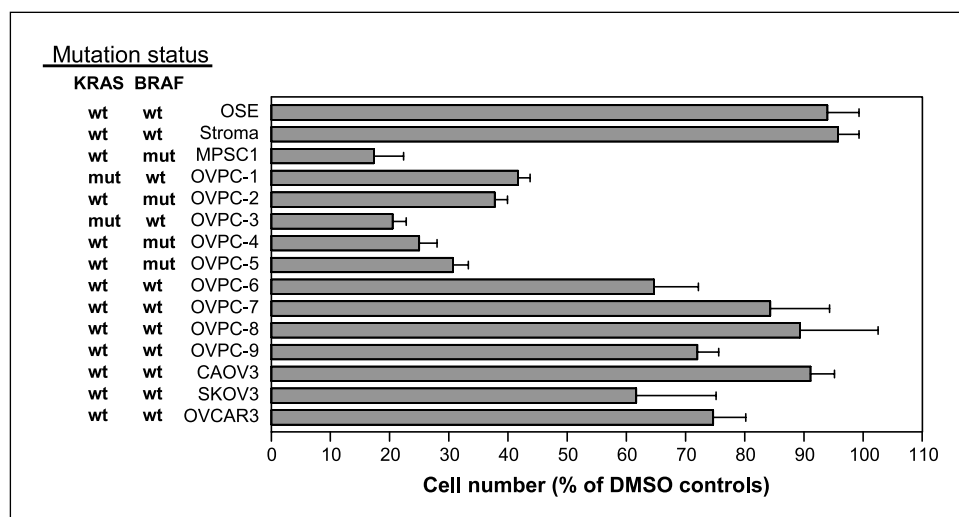


Figure 1. Effects of CI-1040 on cell proliferation. Cell number was counted after 72 hours of CI-1040 or DMSO (control) treatment. The mutational status of KRAS and BRAF for each sample is shown next to the tumor cell cultures and cell lines. Ovarian tumors with mutations in either KRAS or BRAF are more sensitive to growth inhibition by CI-1040 than those with wild-type sequences.

inhibition and apoptosis induction by CI-1040 which inhibits MEK and thus prevents activation of its downstream target, MAPK (ERK). Western blot analysis showed a dose-dependent effect on the expression of active MAPK in MPSC1 cells and active MAPK was not detectable 6 hours after treating the cells with CI-1040 at 5 $\mu\text{mol/L}$, which was the concentration used in this study. As shown in Fig. 1, six of the tumors harboring either KRAS or BRAF mutations showed a marked reduction (<50% of DMSO control) in the cell number in CI-1040-treated group as compared with the other seven tumors containing wild-type KRAS and BRAF ($P < 0.001$). Normal cells including ovarian surface epithelial cultures and ovarian stromal cells did not show a significant effect on growth inhibition by CI-1040. Cell cycle analysis showed a time-dependent cell cycle arrest at G_1 phase in MPSC1 cells that contained an activating mutation in BRAF (V599L), but such arrest was not apparent in SKOV3 and OVCAR3 cells which did not have mutations in KRAS or BRAF (Fig. 2). Besides, CI-1040 induced apoptosis was more remarkable in the cell cultures and cell lines with either KRAS or BRAF mutations than those with wild-type sequences (Fig. 3).

LongSAGE. To determine the molecules that are potentially regulated by MAPK activation in ovarian serous tumors, we compared the gene expression profiles between the MPSC1 cells (with mutant BRAF) treated with CI-1040 and DMSO control using LongSAGE which is a technique modified from conventional SAGE. LongSAGE uses a different mapping enzyme to analyze longer tags that allows for direct and comprehensive comparison in gene expression profiles (20, 23). To identify the early alteration in gene expression, we did LongSAGE in MPSC1 cells 9 hours after CI-1040 treatment when the cell cycle arrest began to become evident and the active MAPK was undetectable. A total of 55,546 and 50,716 tags (transcripts) were obtained from CI-1040 and DMSO LongSAGE libraries, respectively. Tags ($n = 168$) were selected based on the CHIDIST value of ≥ 0.8896 and among them, 93 tags were further chosen based on the ratio of tag number of each library (i.e., DMSO/ CI-1040 or CI-1040/DMSO) >3 . Thus, almost all the genes showed a similar tag count (<3-fold) in both libraries except those 93 genes that represented 0.46% of ~20,250 unique tags. We selected the top 20 genes for validation based on the largest fold difference in tag number between CI-1040 and DMSO

LongSAGE libraries. The validation was done in two steps using an independent assay, the quantitative real-time PCR. First, 14 candidate genes were selected as the pattern of gene expression was identical between LongSAGE and real-time PCR in MPSC1 cells. The gene names, unigene number, possible functions, and expression levels of LongSAGE and real-time PCR are listed in Table 1. In the second step, the genes identified in step 1 were further tested in CI-1040- and DMSO-treated OVPC-1, OVPC-3, and OVPC-5 primary cultures in which sufficient RNA was available for multiple real-time PCR analyses. Of the 14 genes, we found that 10 genes showed consistent alteration in gene expression in at least

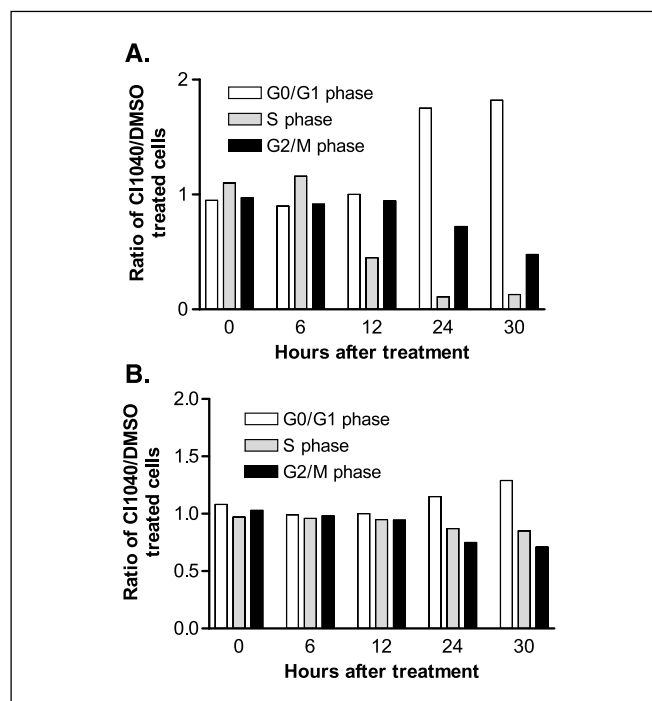


Figure 2. Cell cycle analysis of MPSC1 cells (A) and OVCAR3 cells (B). CI-1040-treated MPSC1 cells harboring a BRAF mutation show a gradual loss of S and G_2 -M peaks and an accumulation of cells in the G_1 phase. In contrast, OVCAR3 cells with wild-type KRAS and BRAF show only a mild G_1 arrest.

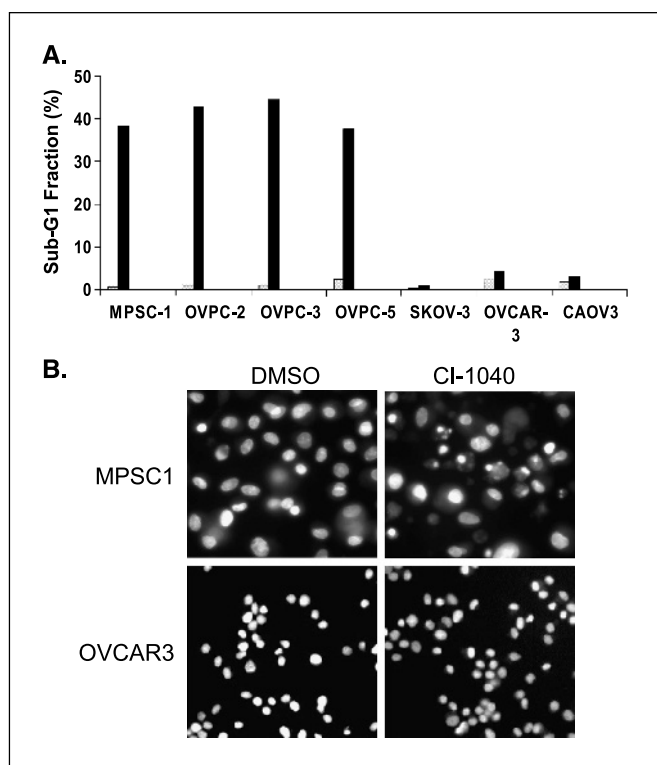


Figure 3. Detection of apoptotic cells. *A*, apoptotic cells are quantified by the sub-G₁ fraction in four cell cultures with mutations in KRAS or BRAF (MPSC1, OVPC-2, OVPC-3, and OVPC-5) and in three cell lines with wild-type sequence (SKOV3, OVCAR3, and CAOVS3). The experiment was done 72 hours after CI-1040 or DMSO treatment. *B*, many of the CI-1040-treated cells but not OVCAR3 cells show morphologic features typical of apoptosis.

three of four low-grade tumors including MPSC1, OVPC-1, OVPC-3, and OVPC-5 (Table 2). The up-regulated genes included tumor necrosis factor-related apoptosis-induced ligand (*TRAIL*), *thrombospondin-1*, *optineurin*, *palladin*, and *pannexin* and the down-regulated genes contained *cyclin D1*, *COBRA1* (cofactor of BRCA1), *transglutaminase-2*, *HSPC152* (not yet annotated) and protein phosphatase (*PP1R14B*). In fact, down-regulation of cyclin D1 and COBRA1 and up-regulation of pannexin were observed in all four cultures.

Constitutive Expression of Cyclin D1. Among the differentially expressed genes, *cyclin D1* showed the most dramatic changes in the expression level (23-fold less by LongSAGE and 11-fold less by real-time PCR) in MPSC1 cells and in all other three tumors by real-time PCR after CI-1040 treatment. It was therefore selected for further study to assess its biological role in MAPK-mediated effects. Western blot analysis showed that cyclin D1 protein was undetectable in MPSC1, OVCAR3, SKOV3, and OVPC-2 cells 24 hours after treating the cells with CI-1040 (Fig. 4). Because it has been reported that cyclin D1 promoter is related to the activation of MAPK (24, 25), we established an expression vector (pCMV/cyclin D1) that constitutively expressed cyclin D1. MPSC1 cells were transfected with pCMV/cyclin D1 or the empty vector alone (as the control) and stable clones were selected for cell growth assay. Expression of engineered cyclin D1 was detected by Western blot analysis using an anti-V5 antibody which recognized the V5-cyclin D1 fusion protein (data not shown). As shown in Fig. 5, Western blot analysis showed that the endogenous cyclin D1 was reduced to an

undetectable level after CI-1040 treatment in both pCMV/cyclin D1-transfected and control MPSC1 cells. In contrast, the engineered cyclin D1 expression was not affected by CI-1040. Cell proliferation was determined by counting the cell number at various time points. Constitutive expression of cyclin D1 did not show significant changes in cell number as compared with the controls (Fig. 5). Interestingly, expression of cyclin D1 driven by a cytomegalovirus promoter partially reversed the growth inhibitory effect of CI-1040 as the cell counts significantly increased as compared with the CI-1040-treated cells transfected with the control vector although it did not achieve to a similar level of cells treated with DMSO.

Discussion

Although the biological roles of the RAS/RAF/MEK/MAPK (ERK) pathway in human cancer have been studied for several years, it is not known whether its role in tumor progression differs in tumors with and without activating KRAS or BRAF mutations. In this study, we did a genotype-phenotype correlation of ovarian tumor cells using a MEK inhibitor, CI-1040, and provided evidence that the biological effects of the MAPK signaling pathway depend on the mutation status of its upstream regulator (i.e., *KRAS* and *BRAF* genes). Ovarian tumors with mutations in either KRAS or BRAF were more sensitive to growth inhibition and apoptosis induction by the MAPK inhibitor, CI-1040. This observation suggests that ovarian tumors with mutations in either KRAS or BRAF depend much more on the activation of the RAS/RAF/MEK/MAPK pathway for cell proliferation and survival than those without such mutations. Thus, inactivation of MAPK results in a marked growth inhibition in ovarian tumors with mutations in KRAS or BRAF and only a modest effect in tumors with wild-type KRAS and BRAF. Our result is consistent with a recent report showing that CI-1040 significantly inhibited proliferation in melanoma cell lines harboring mutant BRAF, but not in the cell line with wild-type *KRAS* and *BRAF* genes (19). The above observations lend strong support to the view of "kinase addiction" by which the activating mutations in the kinase pathway confer susceptibility of the tumors to the inhibitor (16, 26). As ovarian serous tumors with KRAS or BRAF mutations are almost exclusively low grade (2, 3), which are generally not sensitive to conventional chemotherapeutic agents (27, 28), our findings may have practical implication. Thus, CI-1040 can become a potential drug for the treatment of ovarian tumors with KRAS or BRAF mutations. This is further supported by the effectiveness of CI-1040 in treating experimental tumors in mice with colon carcinomas of either mouse or human origin (16). In that study, efficacy was achieved with a wide range of doses and was correlated with a reduction in the levels of activated, phosphorylated MAPK in tumors excised from treated animals without overt toxicity. In this study, we focused on CI-1040 because it inhibited the common downstream target in the RAS signaling pathway and the compound may provide a convenient therapeutic strategy for patients with either KRAS or BRAF mutations. Besides, CI-1040 has a relatively high selectivity in inhibiting MEK; therefore, it provides a reliable tool to study the biological effects of KRAS/BRAF/MEK/MAPK pathway in low-grade serous tumors. Future studies will be done to address whether the inhibitors of KRAS and BRAF have similar effects on low-grade ovarian serous tumors.

Table 1. Differentially expressed genes after inactivation of MAPK in MPSC1 cells

Gene name	UniGene number	Possible functions	Tag count CI-1040-treated cells	Tag count DMSO-treated cells	Fold of difference by real-time PCR
<i>Cyclin D1</i>	371468	Cell cycle progression of G ₁ phase; proto-oncogene.	1	23	10.9-fold down
<i>COBRA1</i>	410095	Binds to chromatin-unfolding domains of BRCA1 and induces chromatin decondensation	0	6	3.7-fold down
<i>HSPC152</i>	333579	Unknown function, hypothetical protein	2	12	3.1-fold down
<i>NFκB</i>	458276	Transcription factor, involved in the inflammatory and immune response	0	6	3.6-fold down
<i>PPP1R14B</i>	120197	PPP; Ser/Thr phosphatases implicated in a multitude of cellular functions	16	37	2.9-fold down
<i>PPP2R5D</i>	118244		0	7	3.5-fold down
<i>Transglutaminase-2</i>	512708	Catalyze cross-linking of proteins. Maybe involved in apoptosis.	3	27	4.4-fold down
<i>TRAIL</i>	387871	Mediator of apoptosis, immune regulation and inflammation.	17	3	2.5-fold up
<i>Thrombospondin-1</i>	164226	Inhibits angiogenesis and tumorigenesis, extracellular matrix protein	11	0	2-fold up
<i>Calnexin</i>	155560	Type-I integral membrane protein (lectin) that serves as molecular chaperone for glycoproteins in the endoplasmic.	6	0	2.3-fold up
<i>Nucleobindin</i>	172609	Might play a role in G protein- and Ca ²⁺ -regulated signal transduction	6	0	3-fold up
<i>Optineurin</i>	390162	Cellular target for adenovirus E3. Affecting cell death through the tumor necrosis factor receptor.	8	0	2.5-fold up
<i>Palladin</i>	194431	Actin-associated protein that control cell shape, adhesion, and contraction.	23	8	3.4-fold up
<i>Pannexin</i>	32163	Induced formation of intercellular channels.	7	0	2.7-fold up

NOTE: Expression level in CI-1040- versus DMSO-treated MPSC1 cells. Abbreviation: PPP, protein phosphatase.

In this study, we applied LongSAGE as a discovery tool to identify genes in which their expression was altered shortly (9 hours) after CI-1040 treatment. Among all the differentially expressed genes, *cyclin D1* showed the greatest fold in the

alteration of gene expression. Cyclin D1 plays an important role in the cell cycle transition from G₁-to-S phase by association with cyclin-dependent kinases (cdk) 4 and 6 which phosphorylate the retinoblastoma protein, blocking its growth inhibitory activity and

Table 2. Validation of differentially expressed genes by quantitative PCR

Gene name	MPSC1	OVPC-1	OVPC-3	OVPC-5	
<i>Cyclin D1</i>					20 fold down
<i>COBRA1</i>					-15
<i>HSPC152</i>					-5
<i>NF-KB</i>					-4
<i>PPP1R14B</i>					-3
<i>PPP2R5D</i>					-2
<i>Transglutaminase-2</i>					0 No change
<i>TRAIL</i>					2
<i>Thrombospondin-1</i>					3
<i>Calnexin</i>					4
<i>Nucleobindin</i>					5
<i>Optineurin</i>					10
<i>Palladin</i>					15
<i>Pannexin</i>					20 20 fold up

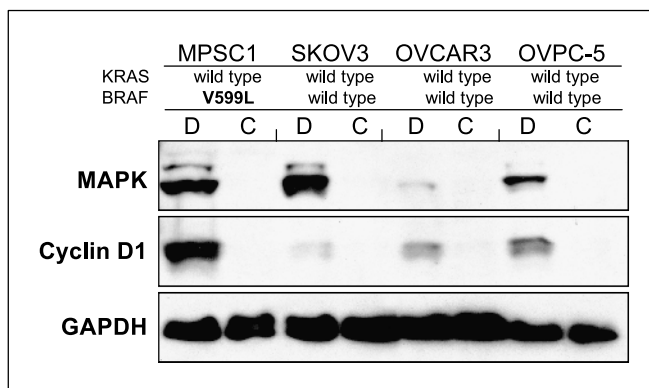
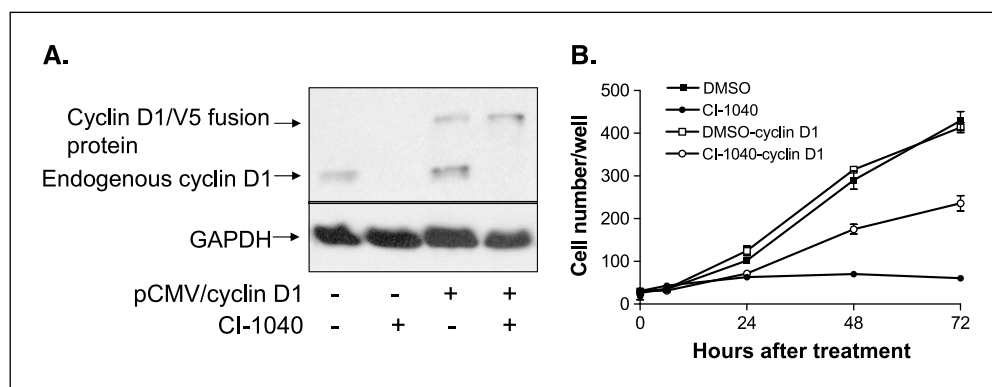


Figure 4. Western blot analysis. Expression of active MAPK and cyclin D1 is undetectable in all CI-1040-treated samples. A similar amount of protein was loaded in CI-1040- and DMSO-treated samples as evidenced by a similar intensity of glyceraldehyde-3-phosphate dehydrogenase (*GAPDH*). D, DMSO treatment; C, CI-1040 treatment.

Figure 5. Effect of engineered cyclin D1 expression in MPSC1 cells.

A. Western blot analysis shows expression of cyclin D1/V5 fusion protein that is independent of CI-1040 as the gene expression is driven by pCMV/cyclin D1. In contrast, the endogenous cyclin D1 is undetectable after CI-1040 treatment. **B.** pCMV/cyclin D1-transfected MPSC1 cells are less sensitive to CI-1040 treatment as shown by the growth curve.



promoting the release of bound E2F transcription factor. These events facilitate the activation of cyclin E-cdk 2 and cyclin A-cdk 2, molecules required for the entry into and completion of S phase (29, 30). Thus, the G₁ cell cycle arrest as observed in CI-1040-treated MPSC1 cells is consistent with the function of cyclin D1. Several studies have reported that overexpression of cyclin D1 occurs in several types of human cancer including ovarian serous tumors based on immunohistochemistry (31). In ovarian tumors, overexpression of cyclin D1 is associated with low-grade tumors (31), a finding consistent with our view that cyclin D1 is a downstream target of active MAPK which is constitutively expressed in most low-grade ovarian tumors because of their frequent activating mutations in KRAS and BRAF. In the present study, Western blot analysis showed a significant decrease of cyclin D1 in all the ovarian tumor cell lines and primary cultures examined independent of their mutational status in KRAS and BRAF. This observation is in accordance with a previous report showing that inhibition of the ERK1 and ERK2 MAPK signaling by expression of dominant-negative forms of MAPK or by MAP kinase phosphatase strongly inhibited cyclin D1 promoter (24). In addition, expression of cyclin D1 and overexpression of constitutively active MKK1 mutant dramatically increased cyclin D1 promoter activity and cyclin D1 protein expression (24). To address whether cyclin D1 is required for active MAPK-mediated cell proliferation, we established a stable MPSC1 line that constitutively expresses cyclin D1 and showed that the transfected cells were less sensitive to the growth inhibitory effect of CI-1040, providing cogent evidence to support the role of cyclin D1 as a downstream target in the MAPK pathway. Although cyclin D1 expression rescues growth suppression by CI-1040, it may not recapitulate all the functions in cell proliferation of active MAPK. This is because alterations in other genes may occur later and are therefore not detected by LongSAGE before it was done. It is interesting to note that the ovarian cancer cells with wild-type KRAS and BRAF were less dependent on cyclin D1 for cell proliferation because the expression level of cyclin D1 was down-regulated to an undetectable level by CI-1040, whereas the growth in those tumor cells was only mildly inhibited.

TRAIL represents a well-known gene that is up-regulated after CI-1040 treatment. *TRAIL* is a member of the death ligand family and consists of an extracellular *TRAIL* binding domain and a cytoplasmic "death domain." Binding of *TRAIL* to its receptor facilitates the induction of apoptosis (32–34). Our finding of up-regulation of *TRAIL* after MAPK inhibition in ovarian tumor cells with mutations in KRAS/BRAF but not in those with wild-type

sequences suggests that CI-1040 induced apoptosis is related to the expression of *TRAIL*. This finding complements a recent report showing that activation of MAPK suppressed the expression of *TRAIL* in nontransformed mammalian epithelial cells based on gene expression profiling using oligonucleotide expression arrays (14).

The functional roles of other CI-1040-responsive genes are less clear in the development of ovarian cancer. COBRA1 is a novel cofactor of the BRCA1 protein and has been cloned from a human ovarian cDNA library (35). It binds to the chromosome site by the first BRCT repeat of BRCA1 protein and is itself sufficient to induce chromatin unfolding. Thrombospondin is an extracellular matrix protein that plays a role in tumor progression by modifying tumor microenvironment. It has been shown that thrombospondin expression is repressed by RAS and MYC (36). Thrombospondin also inhibits tumorigenesis by suppressing the activity of matrix metalloproteinase-9 (37) and inhibits angiogenesis by binding to the CD36 receptor protein, which is present on endothelial cell surfaces (38). Thrombospondin is able to inhibit cancer cell growth and prevents metastasis in several tumor models, including breast, skin, and lung carcinomas and melanoma and malignant gliomas; its repression also promotes tumor growth (39–41). Transglutaminase-2 is an enzyme that catalyzes the post-translational modification of proteins by the formation of cross-links (42). Future studies will focus on demonstrating the functions of these genes in response to activation of the RAS/RAF/MEK/MAPK pathway in ovarian tumors.

In summary, we have shown a genotype (mutation status of KRAS/BRAF)-dependent phenotypic change (i.e., cell proliferation and apoptosis), in ovarian serous tumors in response to MAPK inactivation. The findings in this study provide new insight into the biological roles of the RAS/RAF/MEK/MAPK signaling pathway in ovarian serous tumors and have important therapeutic implication in ovarian cancer patients with KRAS or BRAF mutations. Ovarian tumors with KRAS or BRAF mutations are clinically low-grade and they are refractory to conventional cytotoxic chemotherapy (27, 28). Detection of KRAS and BRAF mutations in ovarian cancers may identify patients who will benefit from CI-1040 treatment.

Acknowledgments

Received 10/7/2004; revised 12/9/2004; accepted 12/29/2004.

Grant support: NIH grant RO1 CA 103937, U.S. Department of Defense grants OC010017 and OC040060, and Austrian Forum against Cancer (G. Pohl).

The costs of publication of this article were defrayed in part by the payment of page charges. This article must therefore be hereby marked advertisement in accordance with 18 U.S.C. Section 1734 solely to indicate this fact.

We thank the comments from the members in the Molecular Genetics Laboratory of Ovarian Cancer.

References

1. Seidman JD, Horkayne-Szakaly I, Haiba M, et al. The histologic type and stage distribution of ovarian carcinomas of surface epithelial origin. *Int J Gynecol Pathol* 2004;23:41-4.
2. Singer G, Oldt R 3rd, Cohen Y, et al. Mutations in BRAF and KRAS characterize the development of low-grade ovarian serous carcinoma. *J Natl Cancer Inst* 2003;95:484-6.
3. Singer G, Kurman RJ, Chang H-W, et al. Diverse tumorigenic pathways in ovarian serous carcinoma. *Am J Pathol* 2002;160:1223-8.
4. Sieben NLG, Macropoulos P, Roemen G, et al. In ovarian neoplasms, BRAF, but not KRAS, mutations are restricted to low-grade serous tumors. *J Pathol* 2004; 202:336-40.
5. Ho C-L, Kurman RJ, Dehari R, et al. Mutations of BRAF and KRAS precede the development of ovarian serous borderline tumors. *Cancer Res* 2004;64:6915-8.
6. Davies H, Bignell GR, Cox C, et al. Mutations of the BRAF gene in human cancer. *Nature* 2002;417:949-54.
7. Rajagopalan H, Bardelli A, Lengauer C, et al. Tumorigenesis: RAF/RAS oncogenes and mismatch-repair status. *Nature* 2002;418:934.
8. Singer G, Stohr R, Dehari R, et al. Patterns of p53 mutations separate ovarian serous borderline tumors, low and high-grade carcinomas and provide support for a new model of ovarian carcinogenesis. *Am J Surg Pathol*. In press 2005.
9. Wan PT, Garnett MJ, Roe SM, et al. Mechanism of activation of the RAF-ERK signaling pathway by oncogenic mutations of B-RAF. *Cell* 2004;116:855-67.
10. Olson JM, Hallahan AR. p38 MAP kinase: a convergence point in cancer therapy. *Trends Mol Med* 2004;10:125-9.
11. Hsu C-Y, Bristow R, Cha M, et al. Characterization of active mitogen-activated protein kinase in ovarian serous carcinomas. *Clin Cancer Res* 2004;10:6432-6.
12. Peyssonnaud C, Eychene A. The Raf/MEK/ERK pathway: new concepts of activation. *Biol Cell* 2001; 93:53-62.
13. Allen LF, Sebolt-Leopold J, Meyer MB. CI-1040 (PD184352), a targeted signal transduction inhibitor of MEK (MAPKK). *Semin Oncol* 2003;30:105-16.
14. Grill C, Gheys F, Dayananth P, et al. Analysis of the ERK1,2 transcriptome in mammary epithelial cells. *Biochem J* 2004;381:635-44.
15. Schaeffer HJ, Weber MJ. Mitogen-activated protein kinases: specific messages from ubiquitous messengers. *Mol Cell Biol* 1999;19:2435-44.
16. Sebolt-Leopold JS, Dudley DT, Herrera R, et al. Blockade of the MAP kinase pathway suppresses growth of colon tumors *in vivo*. *Nat Med* 1999;5:810-6.
17. Sebolt-Leopold JS, Van Becelaere K, Hook K, et al. Biomarker assays for phosphorylated MAP kinase. Their utility for measurement of MEK inhibition. *Methods Mol Med* 2003;85:31-8.
18. Sebolt-Leopold JS. MEK Inhibitors: a therapeutic approach to targeting the Ras-MAP kinase pathway in tumors. *Curr Pharm Des* 2004;10:1907-14.
19. Collisson EA, De A, Suzuki H, et al. Treatment of metastatic melanoma with an orally available inhibitor of the Ras-Raf-MAPK cascade. *Cancer Res* 2003;63: 5669-73.
20. Saha S, Sparks AB, Rago C, et al. Using the transcriptome to annotate the genome. *Nat Biotechnol* 2002;20:508-12.
21. Boyd AC, Charles IG, Keyte JW, et al. Isolation and computer-aided characterization of *Mme1*, a type II restriction endonuclease from *Methylophilus methylotrophus*. *Nucleic Acids Res* 1986;14:5255-74.
22. Buckhaults P, Zhang Z, Chen YC, et al. Identifying tumor origin using a gene expression-based classification map. *Cancer Res* 2003;63:4144-9.
23. Velculescu VE, Zhang L, Vogelstein B, et al. Serial analysis of gene expression. *Science* 1995;270:484-7.
24. Lavoie JN, L'Allemain G, Brunet A, et al. Cyclin D1 expression is regulated positively by the p42/p44MAPK and negatively by the p38/HOGMAPK pathway. *J Biol Chem* 1996;271:20608-16.
25. Balmanno K, Cook SJ. Sustained MAP kinase activation is required for the expression of cyclin D1, p21Cip1 and a subset of AP-1 proteins in CCL39 cells. *Oncogene* 1999;18:3085-97.
26. Arteaga CL, Baselga J. Tyrosine kinase inhibitors: why does the current process of clinical development not apply to them? *Cancer Cell* 2004;5:525-31.
27. Bristow RE, Gossett DR, Shook DR, et al. Micropapillary serous ovarian carcinoma: surgical management and clinical outcome. *Gynecol Oncol* 2002;86: 163-70.
28. Bristow RE, Gossett DR, Shook DR, et al. Recurrent micropapillary serous ovarian carcinoma. *Cancer* 2002; 95:791-800.
29. Sherr CJ, Roberts JM. CDK inhibitors: positive and negative regulators of G₁-phase progression. *Genes Dev* 1999;13:1501-12.
30. Sherr CJ. Cell cycle control and cancer. *Harvey Lect* 2000;96:73-92.
31. Worsley SD, Ponder BA, Davies BR. Overexpression of cyclin D1 in epithelial ovarian cancers. *Gynecol Oncol* 1997;64:189-95.
32. Wiley SR, Schooley K, Smolak PJ, et al. Identification and characterization of a new member of the TNF family that induces apoptosis. *Immunity* 1995;3:673-82.
33. Schneider P, Thome M, Burns K, et al. TRAIL receptors 1 (DR4) and 2 (DR5) signal FADD-dependent apoptosis and activate NF- κ B. *Immunity* 1997;7: 831-6.
34. Pan G, O'Rourke K, Chinnaiyan AM, et al. The receptor for the cytotoxic ligand TRAIL. *Science* 1997;276:111-3.
35. Ye Q, Hu YF, Zhong H, et al. BRCA1-induced large-scale chromatin unfolding and allele-specific effects of cancer-predisposing mutations. *J Cell Biol* 2001;155: 911-21.
36. Watnick RS, Cheng YN, Rangarajan A, et al. Ras modulates Myc activity to repress thrombospondin-1 expression and increase tumor angiogenesis. *Cancer Cell* 2003;3:219-31.
37. Rodriguez-Manzanique JC, Lane TF, Ortega MA, et al. Thrombospondin-1 suppresses spontaneous tumor growth and inhibits activation of matrix metalloproteinase-9 and mobilization of vascular endothelial growth factor. *Proc Natl Acad Sci U S A* 2001;98:12485-90.
38. Dawson DW, Pearce SF, Zhong R, et al. CD36 mediates the *In vitro* inhibitory effects of thrombospondin-1 on endothelial cells. *J Cell Biol* 1997;138: 707-17.
39. Bleuel K, Popp S, Fusenig NE, et al. Tumor suppression in human skin carcinoma cells by chromosome 15 transfer or thrombospondin-1 overexpression through halted tumor vascularization. *Proc Natl Acad Sci U S A* 1999;96:2065-70.
40. Streit M, Velasco P, Brown LF, et al. Overexpression of thrombospondin-1 decreases angiogenesis and inhibits the growth of human cutaneous squamous cell carcinomas. *Am J Pathol* 1999;155: 441-52.
41. Volpert OV, Pili R, Sikder HA, et al. Id1 regulates angiogenesis through transcriptional repression of thrombospondin-1. *Cancer Cell* 2002;2:473-83.
42. Griffin M, Casadio R, Bergamini CM. Transglutaminases: nature's biological glues. *Biochem J* 2002;368: 377-96.

Award Number: OC010017

TITLE:

PATHOGENESIS OF OVARIAN SEROUS CARCINOMA AS THE BASIS FOR IMMUNOLOGIC DIRECTED
DIAGNOSIS AND TREATMENT: PROJECT 2 IDENTIFICATION OF AUTOLOGOUS ANTIGENS IN EARLY
STAGE SEROUS CARCINOMA

PRINCIPAL INVESTIGATOR:

RICHARD RODEN, Ph.D.

CONTRACTING ORGANIZATION:

The Johns Hopkins School of Medicine
720 Rutland Avenue,
Baltimore, MD 21205

REPORT DATE: Dec 6, 2006

TYPE OF REPORT:

Final Progress report

PREPARED FOR: U.S. Army Medical Research and Materiel Command
Fort Detrick, Maryland 21702-5012

DISTRIBUTION STATEMENT: Approved for Public Release;
Distribution Unlimited

The views, opinions and/or findings contained in this report are those of the
author(s) and should not be construed as an official Department of the Army
position, policy or decision unless so designated by other documentation.

REPORT DOCUMENTATION PAGE			Form Approved OMB No. 074-0188	
Public reporting burden for this collection of information is estimated to average 1 hour per response, including the time for reviewing instructions, searching existing data sources, gathering and maintaining the data needed, and completing and reviewing this collection of information. Send comments regarding this burden estimate or any other aspect of this collection of information, including suggestions for reducing this burden to Washington Headquarters Services, Directorate for Information Operations and Reports, 1215 Jefferson Davis Highway, Suite 1204, Arlington, VA 22202-4302, and to the Office of Management and Budget, Paperwork Reduction Project (0704-0188), Washington, DC 20503				
1. AGENCY USE ONLY (Leave blank)	2. REPORT DATE Dec 6, 2006	3. REPORT TYPE AND DATES COVERED FINAL (7/1/02-6/30/05 and no cost extension)		
4. TITLE AND SUBTITLE PATHOGENESIS OF OVARIAN SEROUS CARCINOMA AS THE BASIS FOR IMMUNOLOGIC DIRECTED DIAGNOSIS AND TREATMENT: PROJECT 2 Identification of Autologous Antigens in Early Stage Serous Carcinoma			5. FUNDING NUMBERS OC010017	
6. AUTHOR(S) RICHARD RODEN, Ph.D.				
7. PERFORMING ORGANIZATION NAME(S) AND ADDRESS(ES) Department of Pathology, The Johns Hopkins School of Medicine E-Mail:roden@jhmi.edu			8. PERFORMING ORGANIZATION REPORT NUMBER	
9. SPONSORING / MONITORING AGENCY NAME(S) AND ADDRESS(ES) U.S. Army Medical Research and Materiel Command Fort Detrick, Maryland 21702-5012			10. SPONSORING / MONITORING AGENCY REPORT NUMBER	
11. SUPPLEMENTARY NOTES				
12a. DISTRIBUTION / AVAILABILITY STATEMENT Approved for Public Release; Distribution Unlimited			12b. DISTRIBUTION CODE	
13. ABSTRACT (<i>Maximum 200 Words</i>) Our goal is to develop an early detection screening test for serous carcinoma. Specific aim 1: Obtain cDNAs of autologous tumor antigens recognized by sera of patients with early stage serous carcinoma, but not controls. Progress: We employed patient sera to immunoprecipitate proteins from autologous cancer cells and identified these antigens by mass spectrometry. Two antigens were identified including SMAP-1 which has homology to genes that facilitate cell division. We derived An autoantibody model that generated an AUC of 0.86 (95% CI: 0.78-0.90) for discrimination between sera of EOC patients and healthy patients using antibody specific to p53, NY-CO-8 and HOXB7. Specific aim 2: Identify autologous tumor antigens expressed in serous carcinoma but absent from, or a low level in normal tissue. Progress: We have determined GC-UNC-45 expression in normal tissue and ovarian tumors by grade and stage. We also show elevated levels of proteasomes and ubiquitinated cellular proteins.				
14. SUBJECT TERMS			15. NUMBER OF PAGES 11	
			16. PRICE CODE	
17. SECURITY CLASSIFICATION OF REPORT	18. SECURITY CLASSIFICATION OF THIS PAGE	19. SECURITY CLASSIFICATION OF ABSTRACT Unclassified	20. LIMITATION OF ABSTRACT	

NSN 7540-01-280-5500

Standard Form 298 (Rev. 2-89)
Prescribed by ANSI Std. Z39-18
298-102

Table of Contents

Cover.....	1
SF 298.....	2
Table of Contents.....	3
Introduction.....	4
Body.....	4
Key Research Accomplishments.....	12
Reportable Outcomes.....	12
Conclusions.....	12
References.....	13
Appendices.....	Five
Erkanli et al, 2006	
Bazzaro et al, 2006	
Bazzaro et al, submitted	
Yang et al, 2006	
Coukos et al, 2005	

Introduction

The immune system constantly surveys the body for 'non-self' antigens, and generates a response in the appropriate context. A key finding of cancer biology is that cancer patients often generate antibody to neoantigens specifically expressed in their tumor (1). Autologous antibodies have been documented in patients afflicted with a variety of different cancers, (2-4) including ovarian cancer (5). Autologous antibodies generated by cancer patients have been used to screen expression libraries for tumor antigens. This technique, originally described by Sahin *et al* and termed SEREX (serologic analysis of recombinant cDNA expression libraries of human tumors with autologous serum), has been used to obtain tumor antigen cDNA clones. SEREX has been applied to tumors of many organs (6) and antibody specific for antigens identified by SEREX in other cancer types have been demonstrated in ovarian cancer patients (7, 8). Tumor-specific autoantigens that are common among ovarian cancer patients but not recognized by sera of healthy volunteers have been identified by us e.g. HOXA7 and HOXB7, and others e.g. cathepsin D and GRP78 (9). Although expressed, Cathepsin D and GRP78 derived from normal tissue were not recognized by sera from ovarian cancer patients implying that they contain tumor-specific epitopes (9). Detection of these autologous antibody responses to ovarian cancer antigens appears to have prognostic significance (10). SEREX antigens derived from early stage serous carcinoma may represent useful biomarkers for the dissection of molecular pathways of serous carcinoma (Dr Shih, Project 1). SEREX antigens are also potential targets for cancer immunotherapy (11) (Dr Wu, Project 3).

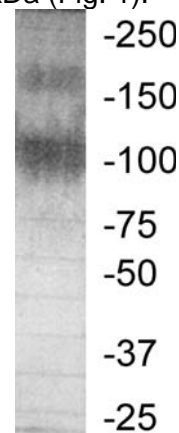
Body

Objective 1: Obtain cDNAs of autologous tumor antigens recognized by sera of patients with early stage serous carcinoma, but not controls.

Task 1.1. Screen sera of patients (n=12) with early stage serous carcinoma by Western blot analysis to identify those patients with high titer autologous tumor-reactive antibody (months 0-2).

We have performed Western blot analysis to select sera suitable for immunoscreening of a cDNA expression library. We have screened with sera from patients with micropapillary serous carcinoma, which has been proposed as a precursor/intermediate of serous carcinoma. We also tested immunoprecipitation, rather than Western blot, as a method to identify autologous tumor antigens. We derived a cell line from a micropapillary serous carcinoma of patient JH514. Affinity purified serum immunoglobulin from the same patient was covalently coupled to Sepharose beads, and these beads used to immunoprecipitate antigens from detergent lysate of the autologous JH514 cell line. The serum antibody from this patient recognized two autologous tumor associated antigens of approximately 100kDa and 200kDa (Fig. 1).

Figure 1. Immunoaffinity purification of autologous tumor antigens for micropapillary serous carcinoma of the ovary. Serum from a patient with MPSC, JH514, was passed over a protein-G spin column. After washing, the antibody was covalently linked with a cross-linker. The column was then washed with low pH elution buffer followed by PBS. A detergent lysate was prepared from a MPSC cell line derived from the same patient. This lysate was passed through the column. After washing, the column was eluted in low pH. The eluate was separated by SDS-PAGE on an 8% gel. The proteins were stained with Coomassie Blue. Antigens of ~100kDa and ~200kDa were excised for mass spectrometry.



Task 1.2. Generate serous carcinoma cDNA expression libraries and immuno-screen with autologous patient (n=3) serum antibody to identify SEREX antigens (months 2-14).

The generation of a cDNA expression library derived from the serous carcinoma cell line OVCAR-3 is ongoing. During the first year of funding we have also developed a complementary technology for the identification of autologous tumor antigens that is based upon immunoprecipitation and antigen identification using mass spectrometry. This approach has a key advantage over SEREX screening in that the antigen is expressed in its native conformation and with the appropriate post-translational modifications. Therefore we

excised the bands from the gel shown in Figure 1, subjected the antigens to trypsin digest and determine the charge/mass ratio for the peptides present by mass spectrometry (Fig 2 and not shown).

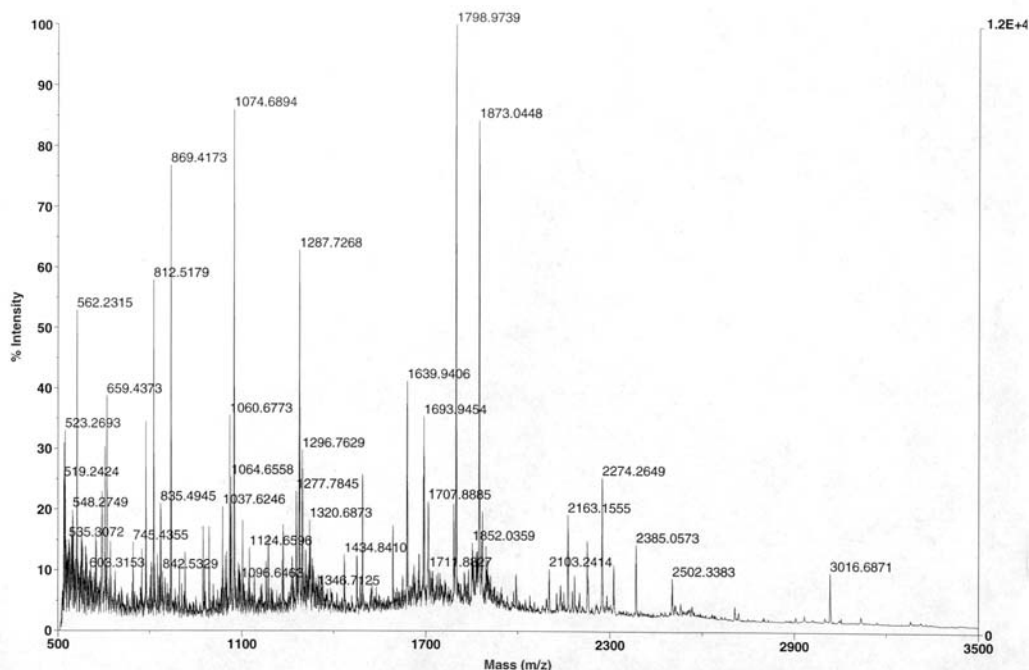


Figure 2. Mass spectrometry of tryptic peptides derived from the ~100kDa ovarian cancer-associated antigen.

Task 1.3. Sequence SEREX antigen cDNAs identified in screen and analyze sequences using BLAST searches (months 14-15).

The prospector website was used to search for proteins with matching peptides. The ~100kDa and ~200kDa antigens were identified by their peptide signatures as SMAP-1 (101kDa) (shown for SMAP-1 in Table 1) and KIAA1529 (195kDa). Nothing is known about the KIAA1529 antigen and no significant homologies or domains were identified. SMAP-1 has three TPR domains, and a recent report suggests that this protein is a chaperone that interacts with HSP90 and facilitates myosin motor assembly.

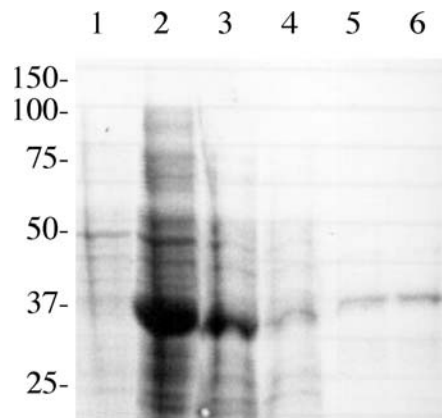
Table 1. Expected and observed M/z for peptides of SMAP-1 and the 100kDa antigen. Matched peptides cover 12% of the SMAP-1 protein, with 53 unmatched masses. 13/66 peptides match SMAP-1(AB014729), estimated MW of 101676.3Da, and SMAP-1b(AB014736).

M/z submitted	MH+ matched	ΔDa	Missed cleavages	Database Sequence
523.2691	523.2186	0.050	0	(K)CSEK(D)
562.2315	562.3201	-0.089	1	(K)GTEKK(Q)
1074.6897	1074.5618	0.13	1	(R)CVSLEPKNK(V)
1179.6649	1179.5618	0.085	0	(K)SWFEGQGLAGK(L)
1186.7039	1186.5414	0.16	0/1Met-ox	(K)LGSAGGTDFSMK(Q)
1287.7267	1287.7749	-0.048	1	(R)TVATLSILGTRR(V)
1320.6865	1320.7527	-0.066	0	(R)ASFITANGVSLK(D)
1661.9771	1661.8606	0.12	0	(R)LLDMGETDLMLAALR(T)
1677.9307	1677.8556	0.075	0/1Met-ox	(R)LLDMGETDLMLAALR(T)
1693.9454	1693.8505	0.095	0/2Met-ox	(R)LLDMGETDLMLAALR(T)
1797.9774	1797.9063	0.071	0	(R)WAVEGLAYLTFDADVK(E)
2225.2600	2225.1119	0.15	0	(R)EIASTLMESEMMEILSVLAK(G)
2273.2726	2273.0966	0.18	0/3Met-ox	(R)EIASTLMESEMMEILSVLAK(G)

Task 1.4 Express SEREX antigens and purify from bacteria (months 15-21).

We obtained the full length cDNAs for human (MGC-999) and mouse SMAP-1 (MGC-7875). We expressed full length human SMAP-1 with a 6His tag in bacteria and purified the protein. Similarly, we expressed a central conserved region of murine SMAP-1 with a 6His tag and purified this protein from bacteria (Fig 3).

Figure 3. Purification of recombinant SMAP-1 conserved peptide from E.coli. A central portion of murine SMAP-1 was subcloned into pProExHT. Transformed E.coli DH5 α were induced for 6h in 1mM IPTG. Affinity purification on a Ni-NTA Sepharose column was performed according to Qiagen's protocol. Fractions were separated in a 12% SDS-PAGE gel and stained with Coomassie Blue. Lane 1: Uninduced E.coli, Lane 2: Induced E.coli, Lane 3: Lysate of induced E.coli, Lane 4: Column flow through, Lanes 5 and 6: Elution fraction.



Task 1.5 Determine the prevalence of serum antibody specific to each SEREX antigen by direct ELISA in a case/control study (months 21-27). (100 ovarian carcinoma patient sera, 102 sera from patients with benign ovarian tumors and 200 control sera will be tested.)

To explore the utility of autologous serum antibody specific to particular TAAs as an additional tool for discrimination of sera from cancer patients and healthy women, we generated recombinant protein from 13 markers previously identified as candidate TAAs (see Table 6) and selected 5 presumptive control reagents (uncoated beads and beads coated with anti-human IgG, human IgG, vector alone extracts and calmodulin, see Table 6). Sera from both healthy women and ovarian cancer patients derived from two different academic centers were tested in parallel for reactivity to all 18 panel elements. Initially we tested sera of 23 healthy patients as controls and sera from 86 stage III/IV ovarian cancer patients. This set of sera was analyzed for reactivity to microspheres of discrete sizes coated with individual recombinant TAA or control protein. The presence of antibody bound to the beads was detected with PE-labeled anti-human IgG and the fluorescence quantified using a Luminex plate reader. Since 5 presumptive control elements were included in the panel, absolute MFI values without background subtraction were employed.

Our analytical strategy consisted of fitting a logistic regression model for cases and controls. A Bayesian Model/Variable Selection approach using a Markov Chain Monte Carlo (Gelfand and Smith, 1990) computations was implemented in the WinBugs (Spiegelhalter et al., 2003) programming environment. A full description of the model selection and details of our Bayesian Computations using Gibbs Sampling are provided in Appendix 3. The MCMC variable (here the 13 markers and 5 controls) selection approach is a stochastic search algorithm that effectively visits all $2^{18} = 216,144$ different models obtained from including/excluding any of the markers or controls in a logistic regression for the probability of ovarian cancer. For numerical stability, we transformed the measured MFI levels of the markers and controls to logarithmic scale. Our approach adjusts for the associations amongst the 13 markers, and effects of the 5 controls. Given the limited number of cases and controls, we focused on an additive model assuming no interactions among the markers, controls, and between markers and controls. A priori, each specific marker or control is assumed to be equally likely to be included/excluded (i.e., with probability of 0.5) in the model. This corresponds to an equally likely prior probability of $1/2^{18}$ for each possible configuration in the model space. The inclusion probability for a specific marker or control is then updated by their posterior probability using all the available information about the other markers and controls, conditional on the observed ovarian cancer status. Although, in principle, one can compute the posterior probability of each of the 2^{18} models using the Bayesian analysis, a simpler alternative is to use the Bayes factor (BF) (Carlin and Louis, 1996), defined as the posterior and prior odds ratio, to select relevant markers or controls for future analyses. For a specific marker or control, larger values of BF provide evidence in favor of inclusion, while smaller values support exclusion from the model. Usually, a value between 1 and 3 is considered weak, between 3 and 10 as substantial, between 10 and 100 as strong, and greater than 100 as very strong (Kass and Raftery, 1995).

By using $BF \geq 3$ as a selection criterion, we picked the best model and computed multiple sensitivity, specificity, ROC curve and AUC by varying a probability cutoff between 0.01 to 1.00 (Table 2, Figure 4). The AUC was calculated as 0.86 (95% confidence interval 0.78-0.90) for this best fitting model (Table 2). We also compared the best model for discrimination of cases and controls with detection of absolute level of CA125 or p53-specific antibody or both. The AUC was calculated as 0.83 (95% confidence interval 0.81-0.83) for the standard CA125 assay alone. Detection of p53 antibody alone was not useful for discrimination of cases and controls in this serum set (AUC of 0.52 with 95% confidence interval 0.20-0.58) and combination of absolute CA125 level and serum reactivity to p53 provided an AUC of 0.81 (95% confidence interval 0.79-0.83).

Table 2. Modeling of serum responses to the 18 element panel in cases and controls. Identification of the best fitting model for discrimination between sera of 23 healthy patients as controls, versus sera from 866 stage III/IV ovarian cancer patients as cases using the 18 element panel either without CA125 (A) or with CA125 (B). The table shows the posterior estimates (mean and standard deviations) of $\Pr(d_j = 1|Data)$, the regression coefficients $\{\theta_j = d_j b_j\}$, and the Bayes Factors for 13 markers and 5 controls using the data set of ULSM cases, and MDACC cases and controls. The regression coefficients θ_j are assumed to be statistically independent, and each have a two-component mixture prior distribution with a point mass at zero (when $d_j = 0$) with probability of 0.5, and a normal distribution $N(0, \sigma_j^2)$ (when $d_j = 1$) with probability 0.5.

A				B			
Marker	$\Pr(d_j = 1 Data)$	θ_j	BF_j	$\Pr(d_j = 1 Data)$	θ_j	BF_j	
FLJ21522	0.49 (0.50)			0.37 (0.48)			
NY-CO-8	0.98 (0.15)	-1.49 (0.62)	49	0.90 (0.31)	-1.18 (0.67)	9	
NY-CO-16	0.45 (0.49)			0.44 (0.50)			
ABC7	0.65 (0.48)			0.53 (0.50)			
α HslgG	0.42 (0.49)			0.35 (0.48)			
Calmodulin	0.42 (0.49)			0.42 (0.49)			
HOXB7	0.92 (0.27)	1.42 (0.76)	11.5	0.87 (0.33)	1.17 (0.73)	6.7	
Hsp70	0.57 (0.49)			0.33 (0.47)			
Hsp90	0.49 (0.50)			0.41 (0.49)			
HslgG	0.43 (0.49)			0.36 (0.48)			
No Antigen	0.60 (0.49)			0.52 (0.50)			
NY-ESO-1	0.48 (0.50)			0.41 (0.50)			
p53	0.96 (0.20)	1.21 (0.58)	24	0.76 (0.43)	0.73 (0.62)	3.2	
Ubiquilin-1	0.61 (0.49)			0.52 (0.50)			
ZFP161	0.28 (0.45)			0.49 (0.50)			
Vector	0.40 (0.49)			0.41 (0.50)			
HOXA7	0.42 (0.49)			0.43 (0.49)			
Hsp27	0.42 (0.49)			0.37 (0.48)			
CA125				0.99 (0.07)	0.90 (0.37)	99	
	Post. Mean (Std D.)	95% CI interval for AUC		Post. Mean (Std D.)	95% CI interval for AUC		
AUC	0.86 (0.03)	0.78	0.90	0.89 (0.03)	0.84	0.92	

We tested whether addition of absolute serum level of CA125 as an element of the panel conferred additional predictive value upon re-analysis of the serum set (Table 6B). The posterior distributions of the regression parameters are displayed in Figure 3C and the ROC curve is given in Figure 3D. Although there is improvement in terms of the accuracy of the fitted model (AUC with CA125 goes slightly up from 0.86 (95% confidence interval 0.78-0.90) to 0.89 (95% confidence interval 0.84-0.92), the same markers NY-CO-8, HOXB7, and p53 are again selected as most informative along with CA125. Our study examines the

applicability of multiplex detection of autologous antibody to TAAs as a diagnostic tool for cancer. The detection of autologous antibody to this 3 member panel of TAAs, in addition to CA125, shows merit as an approach for ovarian cancer detection. However, much larger studies are required to assess its sensitivity at the high specificity required for screening healthy women. In particular it warrants further examination in high-risk populations such as female first-degree relatives of ovarian cancer patients or women carrying mutations that predispose toward cancer. The application of longitudinal screening may also significantly increase the positive predictive value of the test (McIntosh and Urban, 2003; McIntosh et al., 2002). Sera collected over four time points from individual patients with ovarian (n=5) or breast (n=5) cancer were analyzed for the stability of TAA reactivity. The reactivity were generally stable over several years despite therapy indicating that this approach is not useful to monitor therapy (not shown).

Our modeling of TAA-specific antibody poorly discriminates those patients with ovarian cancer from patients with cancer of other organ sites (not shown). This reflects the use of p53 as a diagnostic marker and its importance in cancers in addition to ovarian cancer (Soussi, 2000). However, other investigators have made progress to this end (Koziol et al., 2003; Zhang et al., 2003). Three of the seven TAAs tested proved useful in detecting particular cancer types (Koziol et al., 2003; Zhang et al., 2003). Over 2000 TAAs have been entered into the SEREX database (<http://www.licr.org/SEREX.html>). Several other approaches have also been used to identify candidate TAAs including mass spectrometric analysis of immunoprecipitates (Chinni et al., 1997) and screening of phage display libraries (Fossa et al., 2004; Mintz et al., 2003). Inclusion of other TAAs using similar, highly multiplexed approaches (Scanlan et al., 2002), in large case/control studies may provide better discrimination between cancer types.

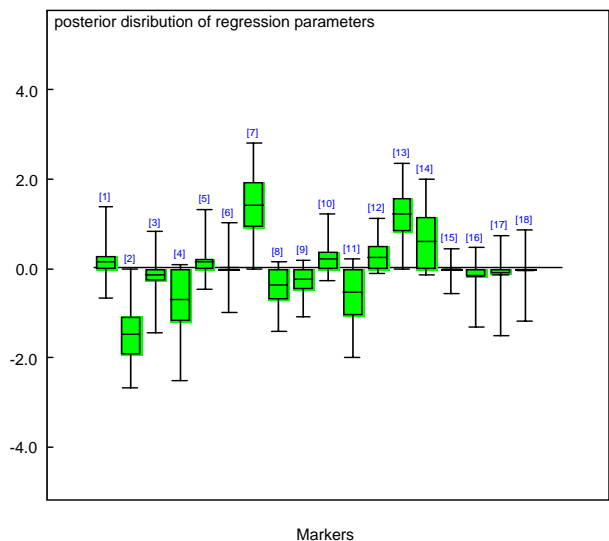
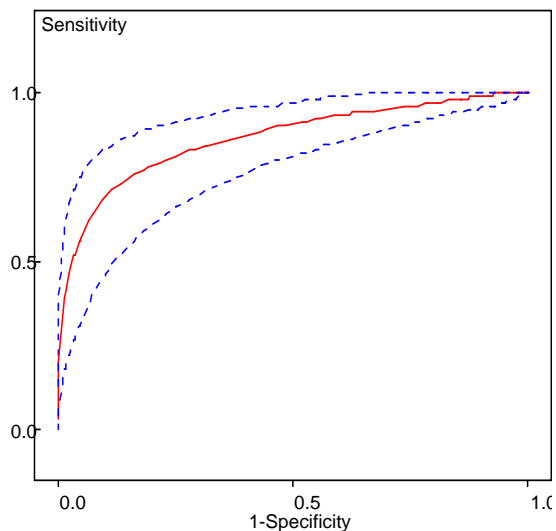
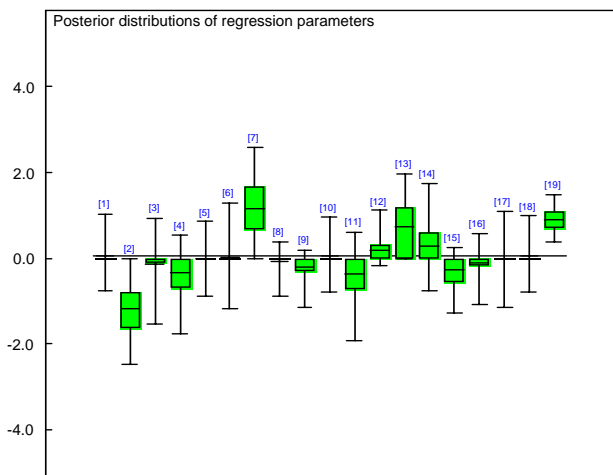
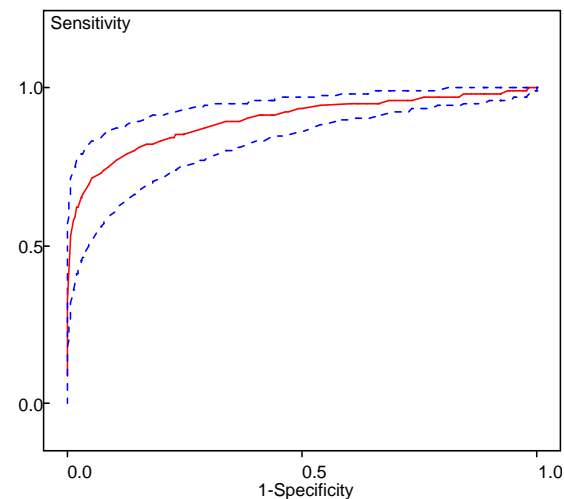
Pattern recognition analysis of proteomic profiles has been used to discriminate sera of ovarian cancer patients from those of healthy women, but the biological underpinning of these patterns is as yet unclear (Petricoin et al., 2002). By contrast the significance of the TAAs p53 and HOXB7 in cancer biology has been studied extensively for ovarian and other cancers (Care et al., 1998; Care et al., 1996; Care et al., 1999; Naora et al., 2001b; Shih Ie and Kurman, 2004). A partial cDNA sequence NY-CO-8 was initially identified as a colon cancer antigen. The full length gene was recently cloned and its product, CCCAP, shown to associate with centrosomes (Kenedy et al., 2003). Subsequent analysis of the serologic reactivity to NY-CO-8 suggests that it is a naturally occurring autoantigen (Scanlan et al., 2002). The presence of NY-CO-8-reactive antibody in healthy controls may account for its negative association with ovarian cancer in our study. The possibility of a protective effect warrants further investigation as described recently for MUC1 (Cramer et al., 2005).

Figure 4 (Next Page). A. Posterior distributions of $\{\theta_j\}$ in the variable selection algorithm for data of Table 6A.

B. Posterior estimate of ROC curve for markers NY-CO-8, HOXB7 and p53 with 95% Credible Interval for cut off values ranging from 0.01 and 1.00 for data of Table 6A. C. Posterior distributions of $\{\theta_j\}$ for all 18

candidate markers plus CA125 levels (marked as [19] above) in the variable selection algorithm for data of Table 6B. D. Posterior estimate of ROC curve for training set using NY-CO-8, HOXB7, p53, and CA125 with

95% Credible Interval for cut off values ranging from 0.01 and 1.00 for data of Table 6B.

Figure 4 A**B****C****D**

Objective 2: Select autologous tumor antigens expressed in early stage serous carcinoma but absent from, or a low level in normal tissue.

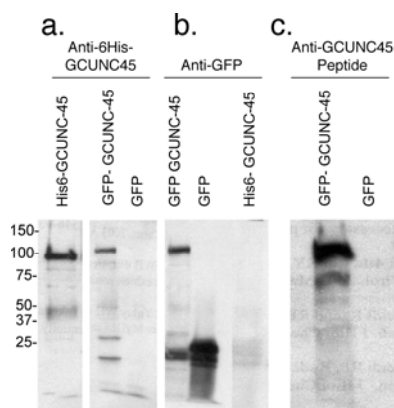
- Task 2.1. Generate rat antiserum to SEREX antigens (months 27-29)
- Task 2.2. Affinity purify and validate specificity of antibodies (months 29-32).
- Task 2.3. Examine the expression pattern of each SEREX antigen by immunohistochemical staining in normal ovary and a spectrum of ovarian tumors (months 32-36)

In order to evaluate GC-UNC-45 expression in ovarian tumors and normal tissue we generated rabbit antisera against KLH coupled to a peptide comprising the final 18 residues of human GC-UNC-45. Peptide binding antibody was affinity purified on a peptide column. The specificity of the affinity purified peptide antibody was analysed by Western blot using 6His-Tagged human GC-UNC-45 purified from E.coli (not shown) and 293T cells transfected with pEGFP-C1-GC-UNC-45 or pEGFP-C1 (Figure 5c). The antibody specifically recognized recombinant GC-UNC-45 with either the 6His or GFP tags (Figure 5c). We optimized conditions for detection of GC-UNC-45 in paraffin-embedded human tissue using the affinity purified peptide antibody. Immunohistochemical staining suggested a cytoplasmic localization for GC-UNC-45 (Figure 6),

consistent with our *in vitro* studies using GFP-GC-UNC-45 (not shown). A similar immunohistochemical staining pattern was observed using the rabbit antiserum to full length GC-UNC-45 (not shown).

In order to assess whether GC-UNC-45 is differentially expressed in ovarian serous carcinoma, we performed immunohistochemical staining of tissue microarrays using GC-UNC-45-specific antibody for low grade (14 cases) and high grade (32 cases) serous carcinoma. Staining was scored blind as absent=0, weak=1, intermediate=2, and intense=3. Using this scoring system we observed that high grade serous carcinomas stained more intensely than low grade serous carcinoma ($p=0.027$, Figure 6e). Conversely, staining of normal ovarian surface epithelium (12 cases) and benign serous cystadenoma ($n=4$) were not significantly different from each other ($p=0.29$, Figure 6e) or from low grade serous carcinoma ($p=0.48$ and $p=0.21$ respectively). In contrast, staining of normal ovarian surface epithelium (12 cases) and benign serous cystadenoma ($n=4$) was significantly weaker than for high grade serous carcinoma (32 cases, $p=0.0028$ and $p=0.0065$ respectively, Figure 6e). The GC-UNC-45 antibody staining of low stage (stages 1-2) serous carcinoma (18 cases) was also significantly weaker than for high stage (stages 3-4) serous carcinoma (32 cases, $P=0.0021$, Figure 6f).

Figure 5. Specificity of GC-UNC-45 antisera. Rabbits were inoculated with either full length 6His-tagged human GC-UNC-45 or KLH-coupled peptide HTSAASPAVSLLSGLPLQ of human GC-UNC-45. Western blot analysis using antiserum to full length human GC-UNC-45 (a), rabbit antiserum to GFP (b) or rabbit serum against GC-UNC-45 peptide (c). Reactivity has been tested against 6His-tagged human GC-UNC-45 purified from *E. coli* and 293T cells transfected with pEGFP-C1-GC-UNC-45 or pEGFP-C1 vector alone.



Our recent analyses by microarray suggested that the proteasome components are co-ordinately upregulated in ovarian cancer. The ubiquitin-proteasome system (UPS) mediates targeted protein degradation. Notably, the UPS determines levels of key checkpoint proteins controlling apoptosis and proliferation by controlling protein half-life. We find that ovarian carcinoma manifests an overstressed UPS by comparison to normal tissues by accumulation of ubiquitinated proteins despite elevated proteasome levels. Elevated levels of total ubiquitinated proteins and 19S and 20S proteasome subunits are evident in both low grade and high grade ovarian carcinoma tissue relative to benign ovarian tumors and in ovarian carcinoma cell lines relative to immortalized surface epithelium (Figure 7). We find that ovarian carcinoma cell lines exhibit greater sensitivity to apoptosis in response to proteasome inhibitors than immortalized ovarian surface epithelial cells. This sensitivity correlates with increased cellular proliferation rate and UPS stress rather than absolute proteasome levels. Proteasomal inhibition *in vitro* induces cell cycle arrest and the accumulation of p21 and p27, and triggers apoptosis via activation of caspase-3. Furthermore, treatment with the licensed proteasomal inhibitor PS-341 slows the growth of ES-2 ovarian carcinoma xenograft in immunodeficient mice. In sum, elevated proliferation and metabolic rate resulting from malignant transformation of the epithelium stresses the UPS and renders ovarian carcinoma more sensitive to apoptosis in response to proteasome inhibition. Furthermore, we hypothesize that the accumulation of malformed and ubiquitinated protein in cancers cells as a result of UPS may contribute to the development of autoantibodies in ovarian cancer patients. These data are published in Bazzaro et al, 2006 (appendix).

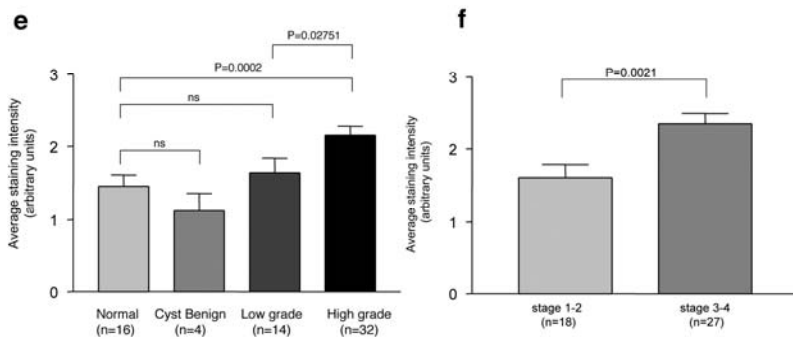
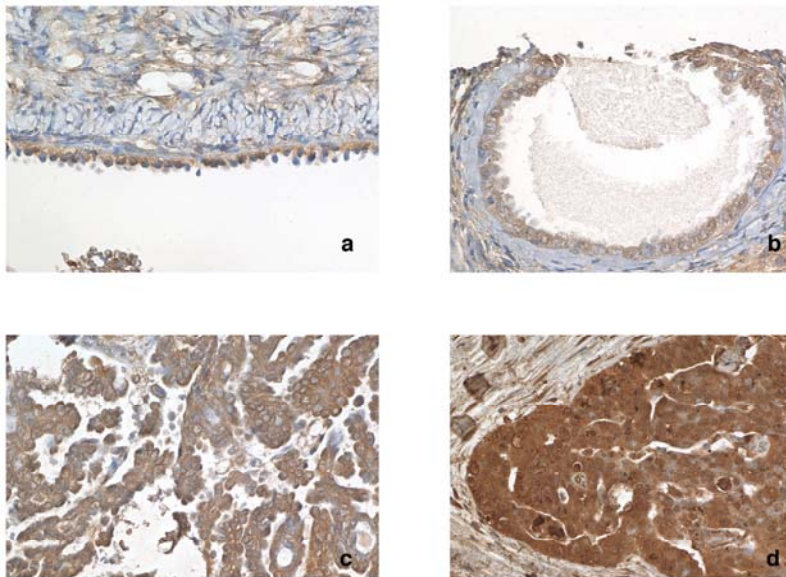


Figure 6. GC-UNC-45 expression in normal tissue and ovarian tumors by grade and stage. Representative histological sections showing immunohistochemical staining for GC-UNC-45 and hematoxylin counterstaining of **a.** Normal ovarian surface epithelium (160X), **b.** benign serous cystadenoma (160X), **c.** Low grade ovarian carcinoma (160X), and **d.** High grade ovarian carcinoma (100X) specimens on an ovarian tissue microarray. **e.** Immunohistochemical staining intensity for GC-UNC-45 in normal ovarian surface epithelium (12 cases), benign serous cystadenoma (4 cases), low grade (14 cases) and high grade (32 cases) serous carcinoma specimens was scored. GC-UNC-45 staining is not statistically different in normal or cystic epithelium or low grade ovarian carcinoma. However GC-UNC-45 staining is significantly elevated in high grade ovarian cancer ($p=0.0002$) versus low grade versus high grade ovarian cancer ($p=0.0275$). **f.** Immunohistochemical staining intensity for GC-UNC-45 in early (18 cases) and advanced stage (32 cases) serous carcinoma specimens was scored. GC-UNC-45 staining was significantly higher in advanced stage (3-4) versus early stage (1-2) ovarian carcinoma.

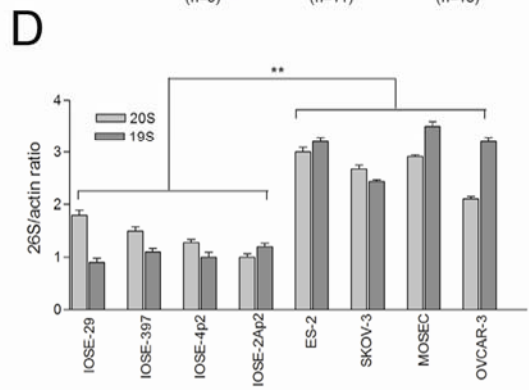
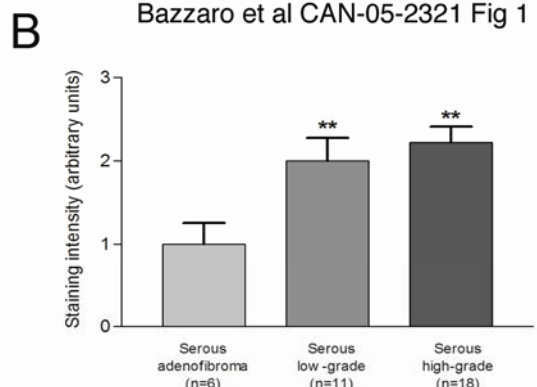
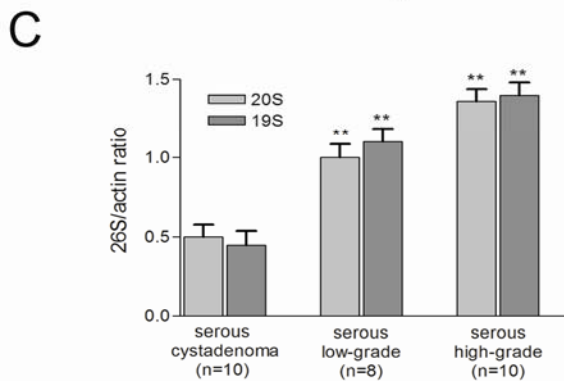
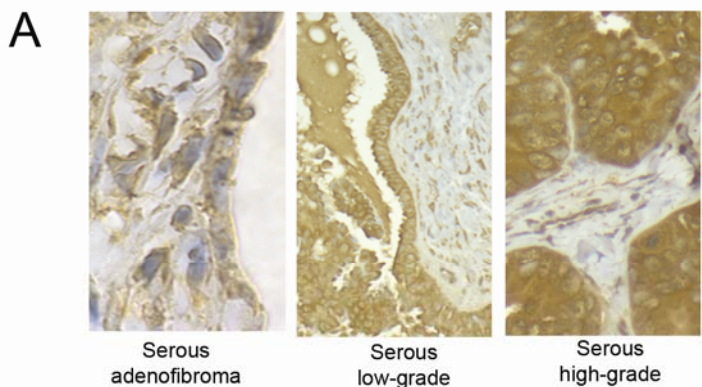


Fig.7 In vivo and in vitro proteasome over-expression in ovarian carcinoma. a. Immunohistochemical staining of α -4 subunits of 20S proteasome in ovarian tumors. Shown are representative examples of intense

20S staining in serous high-grade (40X) and low-grade (40X) ovarian carcinomas and weaker staining in serous adenofibroma (100X). **b.** Staining intensity for each case was graded as 0= no staining, 1= weak staining, 2= moderate staining, 3= intense staining. Statistical significance in staining intensities among indicated groups was assessed by the Mann-Whitney U test (**=p<0.02). **c.** Tissue lysates were immunoblotted with an antibody recognizing subunits of the 19S or the 20S proteasome. The ratio between 26S proteasome (α -3 and Rpt4 sub-unit) and β -actin in tissue lysates from serous cystadenoma (10 cases), low-grade serous ovarian carcinoma (8 cases) or high-grade serous ovarian carcinoma (10 cases) is presented (**=p<0.02). **d.** Ratio between 26S proteasome (β -4 and Rpt4 sub-unit) and β -actin in cell lysates of IOSEs (IOSE-29, IOSE-397, IOSE-4p2, IOSE-2Ap2) and ovarian cancer cell lines (ES-2, SKOV-3, MOSEC, OVCAR-3).

Key Research Accomplishments

- Developed a new, complementary approach for the identification of tumor-associated antigens
- Identification of 2 new tumor associated antigens for serous carcinoma using the new methodology
- Expression analysis for SMAP-1 transcripts in normal tissue and ovarian tumors
- Finding of over-expression and mislocalization of the SEREX antigen HOXB7 in serous carcinoma
- An autoantibody model. The best model generated an AUC of 0.86 (95% CI: 0.78-0.90) for discrimination between sera of EOC patients and healthy patients using antibody specific to p53, NY-CO-8 and HOXB7.
- Demonstration of proteasome overexpression in ovarian cancer
- Proteasomes shown to be promising drug target in ovarian cancer

Reportable Outcomes

- Cell line derived from a micropapillary serous carcinoma
- Antisera to HOXB7 and SMAP-1/GC-UNC-45
- Five manuscripts

Conclusions

We have made significant progress in the period of grant funding (and our no-cost extension), and have performed all of the tasks in our Statement of Work. We have developed a methodology for the identification of ovarian cancer-associated antigens that is complementary to SEREX. While we are generating the cDNA expression library for SEREX screening, we have used this alternate immunoprecipitation and mass spectrometry-based approach to identify two new ovarian cancer associated antigens. Almost nothing is known about the function of either antigen. For one of these new antigens, SMAP-1, we have performed a survey of transcript expression and have developed a specific antibody reagent. Furthermore, we have built upon our previous work in which HOXB7 was identified by SEREX as an ovarian cancer antigen. We have demonstrated over expression of the HOXB7 protein in ovarian cancer, as compared to normal surface epithelium. This immunohistochemical data supports our previous analysis of HOXB7 transcript expression. We also observed a mislocalization of HOXB7 in ovarian cancer. The significance of this exciting finding is under investigation. We tested multiplex detection of antibodies to candidate ovarian TAAs and statistical modeling for discrimination of sera of EOC patients and controls. Binding of serum antibody of women with EOC or healthy controls to candidate TAA-coated microspheres was assayed in parallel. A Bayesian model/variable selection approach using Markov Chain Monte Carlo computations was applied to these data, and serum CA125 values to determine the best predictive model. The selected model was subjected to area under the receiver-operator curve (AUC) analysis. The best model generated an AUC of 0.86 (95% CI: 0.78-0.90) for discrimination between sera of EOC patients and healthy patients using antibody specific to p53, NY-CO-8 and HOXB7. Inclusion of CA125 in the model provided an AUC of 0.89 (95% CI: 0.84-0.92), as compared to an AUC of 0.83 (95% CI: 0.81-0.85) using CA125 alone. However, using TAA responses alone, the model discriminated between independent sera of women with non-malignant gynecologic conditions and those with early advanced or early stage EOC with AUCs of 0.71 (95% CI: 0.67, 0.76) and 0.70 (95% CI: 0.48-0.75) respectively. We conclude that serum antibody to p53 and HOXB7 is positively associated with EOC, whereas NY-CO-8-specific antibody shows negative association. Bayesian modeling of these TAA-specific serum antibody responses exhibits similar

discrimination of patients with early and advanced EOC from women with non-malignant gynecologic conditions, and may be complementary to CA125.

References

1. L. J. Old, Y. T. Chen, *J Exp Med* 187, 1163-7 (1998).
2. U. Sahin *et al.*, *Proc Natl Acad Sci U S A* 92, 11810-3 (1995).
3. N. Brass *et al.*, *Hum Mol Genet* 6, 33-9 (1997).
4. M. J. Scanlan *et al.*, *Int J Cancer* 76, 652-8 (1998).
5. J. R. Dawson, P. M. Lutz, H. Shau, *Am J Reprod Immunol* 3, 12-7 (1983).
6. U. Sahin, O. Tureci, M. Pfreundschuh, *Curr Opin Immunol* 9, 709-16 (1997).
7. O. Tureci *et al.*, *Cancer Res* 56, 4766-72 (1996).
8. E. Stockert *et al.*, *J Exp Med* 187, 1349-54 (1998).
9. S. R. Chinni *et al.*, *Clin Cancer Res* 3, 1557-64 (1997).
10. S. R. Chinni, C. Gercel-Taylor, G. E. Conner, D. D. Taylor, *Cancer Immunol Immunother* 46, 48-54 (1998).
11. E. Jager *et al.*, *J Exp Med* 191, 625-30 (2000).

PROJECT 2 APPENDICES

1. Erkanli et al, 2006
2. Bazzaro et al, submitted
3. Bazzaro et al, 2006
4. Yang et al, 2006
5. Coukos et al, 2005

Application of Bayesian Modeling of Autologous Antibody Responses against Ovarian Tumor-Associated Antigens to Cancer Detection

Al Erkanli,¹ Douglas D. Taylor,³ Deyrick Dean,⁴ Faria Eksir,⁴ Daniel Egger,² James Geyer,⁴ Brad H. Nelson,⁵ Brad Stone,⁶ Herbert A. Fritsche,⁷ and Richard B.S. Roden⁸

¹Department of Biostatistics and Bioinformatics, Duke University Medical Center; ²Eno River Capital, Durham, North Carolina; ³Departments of Obstetrics and Gynecology and Radiation Oncology, University of Louisville School of Medicine, Louisville, Kentucky; ⁴Amplistar, Inc., Winston-Salem, North Carolina; ⁵Deeley Research Centre, British Columbia Cancer Agency, Victoria, British Columbia, Canada; ⁶Benaroya Research Institute, Seattle, Washington; ⁷University of Texas M.D. Anderson Cancer Center, Houston, Texas; and ⁸Department of Pathology, Johns Hopkins School of Medicine, Baltimore, Maryland

Abstract

Biomarkers for early detection of epithelial ovarian cancer (EOC) are urgently needed. Patients can generate antibodies to tumor-associated antigens (TAAs). We tested multiplex detection of antibodies to candidate ovarian TAAs and statistical modeling for discrimination of sera of EOC patients and controls. Binding of serum antibody of women with EOC or healthy controls to candidate TAA-coated microspheres was assayed in parallel. A Bayesian model/variable selection approach using Markov Chain Monte Carlo computations was applied to these data, and serum CA125 values, to determine the best predictive model. The selected model was subjected to area under the receiver-operator curve (AUC) analysis. The best model generated an AUC of 0.86 [95% confidence interval (95% CI), 0.78-0.90] for discrimination between sera of EOC patients and healthy patients using antibody specific to p53, NY-CO-8, and HOXB7. Inclusion of CA125 in the model provided an AUC of 0.89 (95% CI, 0.84-0.92) compared with an AUC of 0.83 (95% CI, 0.81-0.85) using CA125 alone. However, using TAA responses alone, the model discriminated between independent sera of women with nonmalignant gynecologic conditions and those with advanced-stage or early-stage EOC with AUCs of 0.71 (95% CI, 0.67-0.76) and 0.70 (95% CI, 0.48-0.75), respectively. Serum antibody to p53 and HOXB7 is positively associated with EOC, whereas NY-CO-8-specific antibody shows negative association. Bayesian modeling of these TAA-specific serum antibody responses exhibits similar discrimination of patients with early-stage and advanced-stage EOC from women with nonmalignant gynecologic conditions and may be complementary to CA125. (Cancer Res 2006; 66(3): 1792-8)

Note: Under a licensing agreement between Amplistar, Inc., and Johns Hopkins University, R.B.S. Roden is entitled to a share of royalty received by the University on sales of products related to the research described in this article. The terms of this arrangement are being managed by the Johns Hopkins University in accordance with its conflict of interest policies.

Supplementary data for this article are available at Cancer Research Online (<http://cancerres.aacrjournals.org/>).

Requests for reprints: Richard B.S. Roden, Department of Pathology, Johns Hopkins School of Medicine, Ross Research Building, Room 512, 720 Rutland Avenue, Baltimore, MD 21205. Phone: 410-502-5161; Fax: 443-287-4295; E-mail: roden@jhmi.edu.

©2006 American Association for Cancer Research.
doi:10.1158/0008-5472.CAN-05-0669

Introduction

Conventional treatment has limited efficacy against advanced-stage epithelial ovarian cancer (EOC), whereas >80% patients with early-stage disease survive 5 years after diagnosis. However, because there is no diagnostic tool for reliable screening and detection of premalignant or localized ovarian cancer, 70% of patients with ovarian cancer have advanced disease on initial diagnosis (1).

Measurement of serum CA125 levels was approved as a prognostic indicator to monitor disease recurrence (2). Normal healthy donors (~1%) have serum CA125 levels greater than 35 units/mL. Elevated levels of CA125 are detected in >90% of sera of disseminated ovarian cancer cases (stages II-IV) but in only 50% of patients with stage I disease (2). Thus, the CA125 assay is inappropriate as a "stand-alone" population screen for early-stage ovarian cancer, although its positive predictive value can be improved by combination with other screening tools (e.g., serial measurements, transvaginal sonography, or combinations with other markers and statistical modeling).

The immune system constantly surveys the body for "nonself" antigens and generates a response in the appropriate context. Significantly, cancer patients often mount a humoral response to autologous tumor-associated antigens (TAAs; ref. 3). Autologous antibodies have been documented in patients afflicted with a variety of different cancers, including those of the breast, head and neck, colon, lung, kidney, and melanoma (4-6). Ovarian tumor-reactive antibodies have been detected in patient serum and ascites (7) and their antigens are identified by mass spectrometry of immunoprecipitates (8) or by SEREX (refs. 9-11; e.g., ubiquilin-1, ZFP161, FLJ21522, ABC7, HOXA7, and HOXB7). Antibodies to many TAAs are present in several cancer types (e.g., p53 and NY-ESO-1; ref. 12).

Several studies indicate that autologous antibodies specific for TAAs are prevalent in cancer patients but are absent from or infrequent in healthy volunteers. This suggests that autologous antibodies specific to relevant TAAs may have potential as serum biomarkers (13). Therefore, we sought from the literature TAAs associated with ovarian cancer and colon cancer, because the latter often resembles mucinous carcinomas of the ovary. Perhaps the autoantigen best studied in ovarian cancer patients is p53 (14). In stage I/II ovarian disease, 22% of patients had p53 antibody, 31% in stage III, and 50% in stage IV (15). Although there was no association of p53 antibody with clinical stage, tumor histologic type, or overall patient survival (16, 17), detection of autologous

antibody to some ovarian cancer antigens seems to have prognostic significance (18). Notably, detection of serum antibody to p53 has been shown to predict subsequent development of cancer (19).

The relevance to carcinogenesis of most TAAs is unclear, with the exception of known cell cycle regulators, such as p53, ras, c-myc, c-myb, and HER-2/*neu* (20). The ovarian TAA HOXB7 is overexpressed in ovarian and several other cancers and is associated with enhancement of fibroblast growth factor production and angiogenesis (9, 21). The mechanisms that trigger antibody responses to these autologous TAAs are not known. Although p53 is frequently mutated in cancer, many of these TAAs are not. Many TAAs are overexpressed in the cancer relative to normal tissue or not normally expressed in the tissue, such as the cancer/testis family (22). One study noted that many ovarian TAAs are encoded on chromosome arm 17q (e.g., HER-2/*neu* and HOXB7; ref. 11). Autoantibody to heat shock proteins (Hsp), notably Hsp27 and Hsp90 (23–25), has also been associated with ovarian cancer, and this may reflect the ability of certain Hsps, such as Hsp70, to bind and activate dendritic cells (26).

Although many other TAAs have been identified,⁹ the percentage of ovarian cancer patients with reactivity to individual TAAs is generally low. We hypothesized that detection of antibodies to a panel of known TAAs could discriminate sera from ovarian cancer patients and healthy women and potentially improve on the performance of the CA125 assay. However, a statistically rigorous approach to marker selection is required to develop such a clinically applicable diagnostic test by avoiding problems arising from high correlations among potential markers. Herein, we describe the application of multiplex detection of autologous antibodies to a panel of previously described ovarian TAAs and the Bayesian model/variable selection approach using Markov Chain Monte Carlo (MCMC) computations to determine the relevant TAA biomarkers and the most predictive model. MCMC variable selection is a model-based approach with a specified statistical model that puts no distributional restriction on the predictors (markers). Our model-based approach provides probabilistic assessments of uncertainty through Bayesian learning. A unique feature of the Bayesian approach is the easy incorporation of previously described markers in a natural way into existing models, which cannot be achieved by ad hoc procedures, such as recursive partitioning (27–29). Our application of multiplex detection of autologous antibodies to ovarian TAA and Bayesian model selection for detection of EOC complements the CA125 test and implicates p53, HOXB7, and NY-CO-8 in the biology of EOC.

Materials and Methods

Samples. Sera were collected as part of informed consent protocols approved by the local institutional review boards, and the study was approved by the Johns Hopkins University Institutional Review Board. Blood samples were allowed to clot at room temperature and then centrifuged at $400 \times g$ to remove clot and cells. Clarified sera were stored at -70°C . A learning set of 59 sera and a validation set of 37 sera were obtained at the University of Louisville School of Medicine (ULSM; Louisville, KY) from women with stage III/IV ovarian cancer and 32 sera from women attending a gynecology clinic for conditions other than

ovarian cancer as controls. Sera were also obtained at the University of Texas M. D. Anderson Cancer Center (MDACC; Houston, TX). This set was obtained from women with breast cancer ($n = 18$), colon cancer ($n = 6$), lung cancer ($n = 10$), and stage III/IV ovarian cancer ($n = 27$) and from healthy women ($n = 23$). Finally, a set of sera of women with early-stage ovarian cancer ($n = 14$) was provided by the Gynecologic Oncology Group (GOG; Bethesda, MD).

Preparation of recombinant TAA. TAAs were cloned from PCR products into the prokaryotic expression vector pBADgIII (Invitrogen, Carlsbad, CA). ABC7 (AF133659), HOXA7 (AF032095; ref. 10), HOXB7 (NM_004502; ref. 9), NY-ESO-1 (U87459; ref. 30), ubiquilin-1 (NM_013438), ZFP161 (Y12726), FLJ21522 (AK025175; ref. 11), calmodulin (Invitrogen), and p53 (X02469; ref. 14) were amplified from published constructs, whereas NY-CO-8 (AF039690) and NY-CO-16 (AF039694; ref. 6) were amplified directly from commercial cDNA libraries. Constructs were validated using Automated Laser Fluorescent Sequencing. Bacterial cultures were grown in Terrific broth supplemented with 1% (v/v) glycerol and 100 $\mu\text{g}/\text{mL}$ ampicillin at 37°C to mid-log phase (A_{650} , 0.6–0.7) and induced with 0.02% (w/v) L-(+)-arabinose for 2 to 3 hours. Induction was done at 30°C with 0.002% (w/v) L-(+)-arabinose for HOXA7 and HOXB7. Cell pellets from 1 L cultures were solubilized by sonication in 20 mL of 8 mol/L urea, 3.7 mL of 10% (w/v) sodium *N*-lauroyl-sarcosinate and brought to 50 mL with 20 mmol/L Tris-HCl (pH 8.0)/0.2 mol/L NaCl/10% (v/v) glycerol and 0.1% (w/v) sodium *N*-lauroyl-sarcosinate. After centrifugation at $12,000 \times g$ for 30 minutes at 4°C , the supernatant was loaded onto a Ni-NTA Superflow (Qiagen, Valencia, CA) column. The column was washed with a step gradient of 10, 20, 50, 100, and 0.5 mol/L imidazole in 20 mmol/L Tris-HCl (pH 8.0)/0.2 mol/L NaCl/10% (v/v) glycerol and 0.1% (v/v) Triton X-100. The purity and size of the purified proteins was determined by staining SDS-PAGE gels for total protein (Sypro Ruby) and performing Western blotting on duplicate gels for His₆-labeled antigen using horseradish peroxidase-labeled anti-His₆ and chemiluminescent substrate.

Coupling to microspheres and Luminex analysis. Monoclonal antibody to His₆ was coupled to 11 distinct sets of LabMAP carboxylated microspheres (following the manufacturer's protocol),¹⁰ which were then individually bound overnight at 4°C with 30 μg each purified His₆-tagged recombinant TAA. Similarly, a further six distinct sets of LabMAP carboxylated microspheres were directly coupled to 25 μg purified Hsp27, Hsp70, and Hsp90 (Stressgen, Victoria, British Columbia, Canada; refs. 25, 31, 32) or, as controls, 25 μg glutathione *S*-transferase (GST) or pBAD vector alone, 5 $\mu\text{g}/\text{mL}$ anti-human IgG (Sigma Chemical Co., St. Louis, MO), or 50 $\mu\text{g}/\text{mL}$ human IgG. Equivalent counts of each set of protein-coupled microspheres were mixed to a concentration of 5,000 per set per 50 $\mu\text{L}/\text{well}$ in PBS containing 10% normal mouse serum (The Jackson Laboratory, West Grove, PA). The beads were shaken with 50 μL patient serum diluted 1:25 in a 96-well filter-bottomed microtiter plate for 1 hour in the dark at ambient temperature. The beads were washed thrice with 100 μL buffer by filtration and then shaken in 100 $\mu\text{L}/\text{well}$ R-phycoerythrin (PE)-conjugated donkey anti-human IgG diluted 1:200 in PBS/bovine serum albumin [BSA; 10 g/L BSA, 1.4 g/L $\text{NaH}_2\text{PO}_4 \cdot \text{H}_2\text{O}$, 8.77 g/L NaCl, 0.5 g/L NaN_3 (pH 7.4)] for 45 minutes in the dark. After three washes, the beads were resuspended in 100 $\mu\text{L}/\text{well}$ PBS/BSA and their mean fluorescence intensity (MFI) was assayed on a Luminex 100 plate reader. The MFI of 100 of each set of microspheres was determined for each well. A small panel of 10 patient sera was run on all assay plates to allow an assessment of interassay variability and bead variability or stability. Several presumptive positive and negative control antigens were included within the bead set, including human IgG (HsIgG to monitor the addition of PE-conjugated secondary antibody), anti-human IgG (αHsIgG to show addition of the human sera to each well), calmodulin (a presumptive irrelevant autoantigen associated with viral hepatitis), or vector alone (controlling for bacterial contaminants in the antigen preparations) and uncoated beads (for assessment of nonspecific binding).

⁹ <http://www.licr.org/SEREX.html>.

¹⁰ <http://www.luminexcorp.com>.

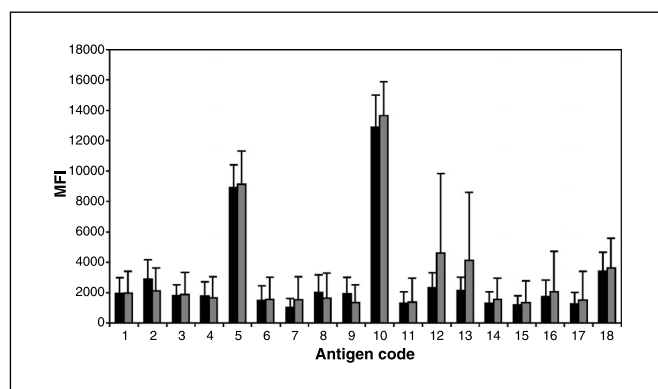


Figure 1. MFI of the beads coated with individual markers (mean \pm SD) in normal volunteers (*black columns*) and ovarian cancer patients (*gray columns*). Antigen codes: 1, FLJ21522; 2, NY-CO-8; 3, NY-CO-16; 4, ABC7; 5, α HsIgG; 6, calmodulin; 7, HOXB7; 8, HSP70; 9, HSP90; 10, HsIgG; 11, no antigen; 12, NY-ESO-1; 13, p53; 14, ubiquilin-1; 15, GST; 16, ZFP161; 17, HOXA7; 18, HSP27.

Statistical analyses. A Bayesian logistic regression model/variable selection approach using MCMC (33) computations was implemented in the WinBUGS (34) programming environment. A full description of the model selection and details of our Bayesian computations using Gibbs sampling are provided in the Supplementary Materials.

The motivation behind the variable selection approach was the fact that all the markers and controls were highly correlated (data not shown), which is known as multicollinearity and likely reflects background effects of using serum at high concentration. Thus, simultaneous use of all the markers and controls in a statistical model will obscure the statistical significance of the core variables that are functions of the others. Consequently, the information contained in all the variables is already represented in the core variables, and a dimension/variable selection technique can be used to identify them. In preliminary analyses (data not shown), we ran a logistic regression model that contained all the 13 TAAs and 5 controls and found out that none of the markers and controls were significant, which resulted in poor discrimination of EOC.

The MCMC variable selection approach is a stochastic search algorithm that effectively visits all $2^{18} = 216,144$ different models obtained from including/excluding any of the 18 TAAs or controls in a logistic regression for the probability of ovarian cancer. The outcome of this procedure is the model with the highest number of visits (the most probable model) supported by the data. For numerical stability, we transformed the measured MFI levels of the markers and controls to logarithmic scale. Our approach adjusts for the associations among the 13 markers and the effects of the 5 controls. Given the limited number of cases and controls, we focused on an additive model assuming no interactions among the markers, controls, and between markers and controls. *A priori*, each specific marker or control is assumed to be equally likely to be included/excluded (i.e., with probability of 0.5) in the model. This corresponds to an equally likely prior probability of $1/2^{18}$ for each possible configuration in the model space. The inclusion probability for a specific marker or control is then updated by their posterior probability using all the available information about the other markers and controls, conditional on the observed ovarian cancer status. Although, in principle, one can compute the posterior probability of each of the 2^{18} models using the Bayesian analysis, a simpler alternative is to use the Bayes factor (BF; ref. 35), defined as the posterior and prior odds ratio, to select relevant markers or controls for future analyses. For a specific marker or control, larger values of BF provide evidence in favor of inclusion, whereas smaller values support exclusion from the model. Usually, a value between 1 and 3 is considered weak, between 3 and 10 as substantial, between 10 and 100 as strong, and >100 as very strong (36).

Results

To explore the utility of autologous serum antibody specific to particular TAAs as an additional tool for discrimination of sera from cancer patients and healthy women, we generated recombinant protein from 13 markers identified previously as candidate TAAs and selected 5 presumptive control reagents. Sera from both healthy women and EOC patients were tested in parallel for reactivity to all 18 panel elements. Initially, we tested sera of 23 healthy women from MDACC as controls and sera from 59 stage III/IV ovarian cancer patients obtained at ULSM and 27 from MDACC as cases, respectively. This set of sera was analyzed for reactivity to microspheres of discrete sizes coated with individual recombinant TAA or control protein. The presence of antibody bound to the beads was detected with PE-labeled anti-human IgG and the fluorescence was quantified using a Luminex plate reader. Because 5 presumptive control elements were included in the panel, absolute MFI values without background subtraction were employed (Fig. 1).

Our analytic strategy consisted of fitting the logistic regression model in Eq. 1 (see Supplementary Materials) for ULSM and MDACC cases and controls. By using $BF \geq 3$ as a selection

Table 1. Modeling of serum responses to the 18-element panel in cases and controls

Marker	$\Pr(d_j = 1 Data)$	θ_j	BF_j
FLJ21522	0.49 (0.50)		
NY-CO-8	0.98 (0.15)	-1.49 (0.62)	49
NY-CO-16	0.45 (0.49)		
ABC7	0.65 (0.48)		
α HsIgG	0.42 (0.49)		
Calmodulin	0.42 (0.49)		
HOXB7	0.92 (0.27)	1.42 (0.76)	11.5
Hsp70	0.57 (0.49)		
Hsp90	0.49 (0.50)		
HsIgG	0.43 (0.49)		
No antigen	0.60 (0.49)		
NY-ESO-1	0.48 (0.50)		
p53	0.96 (0.20)	1.21 (0.58)	24
Ubiquilin-1	0.61 (0.49)		
ZFP161	0.28 (0.45)		
Vector	0.40 (0.49)		
HOXA7	0.42 (0.49)		
Hsp27	0.42 (0.49)		
	Post. mean (SD)	95% CI for AUC	
AUC	0.86 (0.03)	0.78	0.90

NOTE: Identification of the best-fitting model for discrimination between sera of 23 healthy patients from MDACC as controls and sera from 59 stage III/IV ovarian cancer patients obtained at ULSM and 27 from MDACC as cases using the 18-element panel. Data are posterior estimates (mean and SD) of $\Pr(d_j = 1|Data)$ for all the variables, the regression coefficients $\{\theta_j = d_j b_j\}$, and BFs for the best markers and controls (selected by the Bayesian approach) using the data set of ULSM and MDACC cases and controls. The regression coefficients θ_j are assumed to be statistically independent, and each have a two-component mixture prior distribution with a point mass at 0 (when $d_j = 0$) with probability of 0.5 and a normal distribution $N(0, \sigma_j^2)$ (when $d_j = 1$) with probability 0.

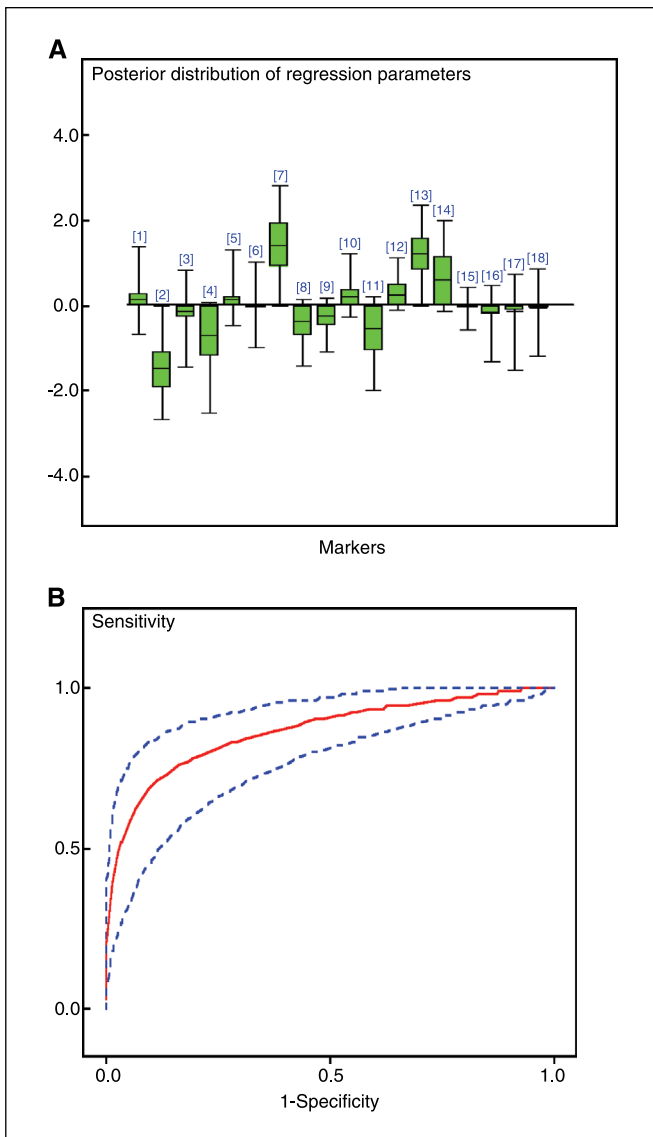


Figure 2. Posterior distributions and estimate of ROC for markers NY-CO-8, HOXB7, and p53. A, posterior distributions of $\{\theta_j\}$ in the variable selection algorithm for data of Table 1. Numbers inside brackets, elements in Table 1 (i.e., [1] corresponds to FLJ21522, etc.). B, posterior estimate of ROC for markers NY-CO-8, HOXB7, and p53 with 95% credible interval for cutoff values ranging from 0.01 to 1.00 for data of Table 1.

criterion, we picked the best model and computed multiple sensitivity, specificity, ROC, and area under the receiver-operator curve (AUC) by varying a probability cutoff between 0.01 and 1.00 (Table 1; Fig. 2). The AUC was calculated as 0.86 [95% credible interval (Bayesian analogue of confidence interval), 0.78-0.90] for this best-fitting model (Table 1). The best model used three TAA markers: p53 and HOXB7, which showed a positive association, and NY-CO-8, which showed a negative association (Table 1).

We also compared the best model for discrimination of cases and controls with detection of absolute serum level of CA125 or p53-specific antibody or both. The AUC was calculated as 0.83 [95% confidence interval (95% CI), 0.81-0.85] for the standard CA125 assay alone. Detection of p53 antibody alone was not useful for discrimination of cases and controls in this serum set

(AUC, 0.52; 95% CI, 0.20-0.58) and combination of absolute CA125 level and serum reactivity to p53 provided an AUC of 0.81 (95% CI, 0.79-0.83). We tested whether addition of absolute serum level of CA125 as an element of the panel conferred additional predictive value on reanalysis of the serum set (Table 2). The posterior distributions of the regression variables are displayed in Fig. 3A and the ROC is given in Fig. 3B (along with 95% credible bands). Although there is improvement in terms of the accuracy of the fitted model [AUC with CA125 goes slightly up from 0.86 (95% CI, 0.78-0.90) to 0.89 (95% CI, 0.84-0.92)], the same markers NY-CO-8, HOXB7, and p53 are again selected as most informative along with CA125.

We conducted a cross-validation analysis to determine the self-consistency of the best model. Here, a leave-one-out approach was used where each data point D_i was removed from the data set and predicted (using the best-fitting model in Table 1 and posterior predictive distribution $[D^*_i|D_{\{-i\}}]$) by the remaining cases $D_{\{-i\}}, i = 1, 2, \dots, n$ with $\{-i\}$ denoting the data, except for the i th observation and D^*_i is a predicted value of D_i . The resulting cross-validated ROC in Fig. 4A was very close in shape to ROC given in Fig. 2B. The posterior mean of the cross-validated AUC was 0.85, with a slightly wider 95% credible interval of 0.76 to 0.92 reflecting additional uncertainty arising from predictions. Therefore, for this data set, our model is self-consistent.

Several conditions unrelated to ovarian cancer result in an elevated serum CA125 level. Furthermore, the sensitivity of the CA125 for detection of early-stage disease is limited. To validate

Table 2. Modeling of the serum responses to the 18-element panel and CA125 level in cases and controls

Marker	$Pr(d_j = 1 Data)$	θ_j	BF_j
FLJ21522	0.37 (0.48)		
NY-CO-8	0.90 (0.31)	-1.18 (0.67)	9
NY-CO-16	0.44 (0.50)		
ABC7	0.53 (0.50)		
α HsIgG	0.35 (0.48)		
Calmodulin	0.42 (0.49)		
HOXB7	0.87 (0.33)	1.17 (0.73)	6.7
Hsp70	0.33 (0.47)		
Hsp90	0.41 (0.49)		
HsIgG	0.36 (0.48)		
No Antigen	0.52 (0.50)		
NY-ESO-1	0.41 (0.50)		
p53	0.76 (0.43)	0.73 (0.62)	3.2
Ubiquilin-1	0.52 (0.50)		
ZFP161	0.49 (0.50)		
Vector	0.41 (0.50)		
HOXA7	0.43 (0.49)		
Hsp27	0.37 (0.48)		
CA125	0.99 (0.07)	0.90 (0.37)	99
	Post. mean (SD)	95% CI for AUC	
AUC	0.89 (0.03)	0.84	0.92

NOTE: Identification of the best-fitting model for discrimination between sera of 23 healthy patients from MDACC as controls and sera from 59 stage III/IV ovarian cancer patients obtained at ULSM and 27 from MDACC as cases using the 18-element panel and absolute CA125 level. Statistical analysis was done as described for Table 1.

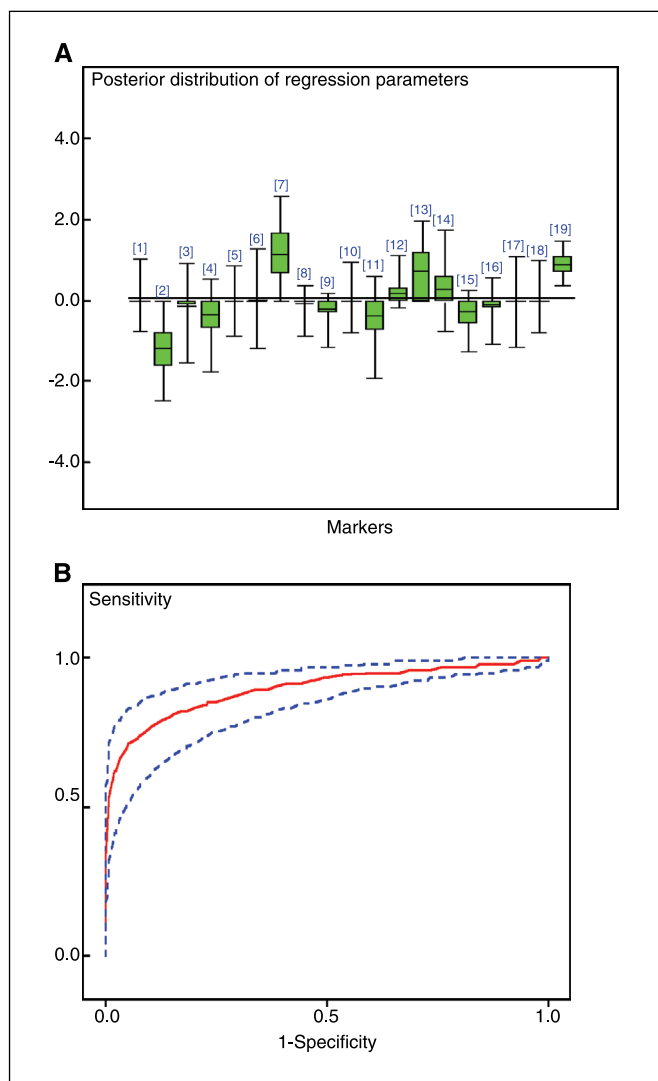


Figure 3. Posterior distributions and estimate of ROC for markers NY-CO-8, HOXB7, p53, and CA125. *A*, posterior distributions of $\{\theta_j\}$ for all 18 candidate markers plus CA125 levels (*19*) in the variable selection algorithm for data of Table 2. *B*, posterior estimate of ROC for training set using NY-CO-8, HOXB7, p53, and CA125 with 95% credible interval for cutoff values ranging from 0.01 to 1.00 for data of Table 2.

our 18-element panel and modeling in a serum set in which the CA125 assay would perform poorly, we studied sera of 32 women attending a gynecology clinic at ULSM (including 3 with CA125 levels >35 units/mL) but who had no evidence of ovarian cancer as controls. As cases, we tested sera from either 37 women with advanced-stage (III/IV) ovarian cancer or 14 women with early-stage (I/II) ovarian cancer (Fig. 4*B* and *C*). These test sets of independent sera were analyzed in parallel for reactivity to the panel of TAAs and controls, and the data were analyzed using the previously determined best-fitting model excluding CA125 (described in Table 1). The ROC analyses are provided in Fig. 4*B* and *C*. The model provided an AUC of 0.71 (95% CI, 0.67-0.76) for discrimination between women with advanced-stage ovarian cancer and those attending the gynecology clinic at ULSM and an AUC of 0.70 (95% CI, 0.48-0.75) for discrimination between early-stage ovarian cancer and women attending the gynecology clinic at ULSM.

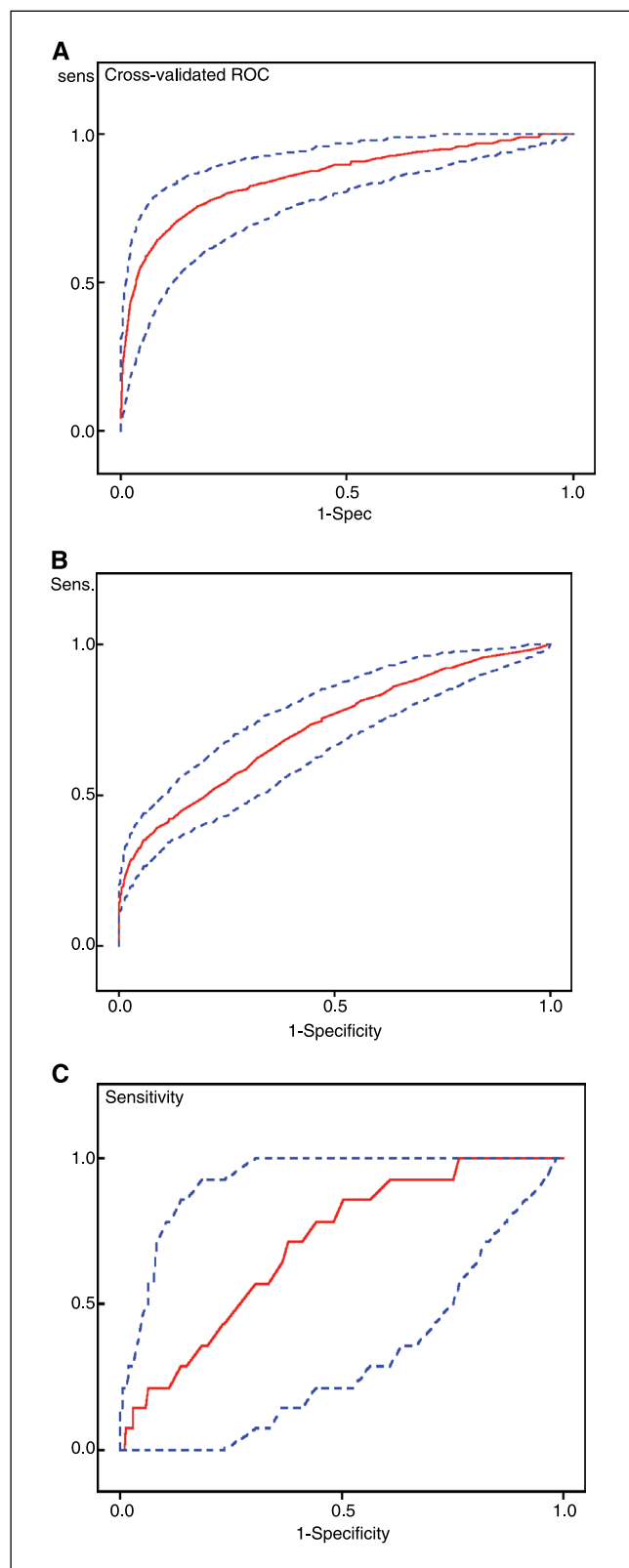


Figure 4. Validation steps. *A*, cross-validated estimate of ROC for the best-fitting model summarized in Table 1. *B* and *C*, cross-validation of the best-fitting model for p53-, NY-CO-8-, and HOXB7-specific antibody reactivity (see Table 1) using an independent set of sera from 37 advanced-stage ovarian cancer patients (*B*) or 14 early-stage ovarian cancer patients (*C*) as cases and 32 women attending a gynecology clinic for conditions other than ovarian cancer as controls in (*B* and *C*).

Discussion

Our study examines the applicability of multiplex detection of autologous antibody to TAAs as a diagnostic tool for cancer. The detection of autologous antibody to this three-member panel of TAAs, in addition to CA125, shows merit as an approach for ovarian cancer detection. However, much larger studies are required to assess its sensitivity at the high specificity required for screening healthy women. In particular, it warrants further examination in high-risk populations, such as female first-degree relatives of ovarian cancer patients or women carrying mutations that predispose toward cancer. The application of longitudinal screening may also significantly increase the positive predictive value of the test (37, 38). Sera collected over up to four time points from individual patients with ovarian ($n = 5$) or breast ($n = 5$) cancer were analyzed for the stability of TAA reactivity. The reactivity to individual TAAs was generally stable over several years despite therapy, indicating that this approach is not useful to monitor therapy (data not shown).

Our modeling of TAA-specific antibody discriminates poorly the patients with ovarian cancer from those with cancer of other organ sites, notably women with breast cancer ($n = 18$), colon cancer ($n = 6$), and lung cancer ($n = 10$; data not shown). This reflects the use of p53 as a diagnostic marker and its importance in cancers in addition to ovarian cancer (14). However, other investigators have improved specificity for a particular cancer type by the inclusion of additional markers (29, 39). Over 2,000 TAAs have been entered into the SEREX database.⁹ Several other approaches have also been used to identify candidate TAAs, including mass spectrometric analysis of immunoprecipitates (8) and screening of phage display libraries (40, 41). Inclusion of other TAAs using similar, highly multiplexed approaches (42) in large case-control studies may provide better discrimination between ovarian and other cancer types.

A more conventional approach to data analysis using logistic regression where all the 13 markers and 5 controls were forced to stay in the model (with prior probability of inclusion being 100% for each) failed to provide a useful model (data not shown), as an AUC of only ~ 0.60 was obtained. Here, we describe the application of Bayesian model/variable selection approach using MCMC computations, implemented in the freely available WinBUGS program, to determine the best predictive model. The MCMC variable selection is a model-based approach with a specified statistical model on the cases and controls (in our case, binomial distribution with logistic link) but puts no distributional restriction on the predictors (markers). It represents an alternative to the existing ad hoc statistical approaches, such as recursive partitioning (27–29), and provides formal assessment of uncertainty (in probabilistic terms) through Bayesian learning and updating. A unique feature of our methods is the easy incorporation in a natural way into existing models of prior information obtained from earlier clinical studies or scientist's experience that cannot be used in other procedures.

We conducted a cross-validation analysis initially using a leave-one-out approach to determine the self-consistency of our best model for discrimination between healthy volunteers and women with advanced-stage ovarian cancer. The model has proven to be internally consistent; therefore, we sought further validation using an independent serum set. Unlike advanced-stage disease, ovarian cancer diagnosed while still confined to the ovaries is highly curable using current interventions. Thus, we examined the ability of our model to discriminate sera from patients with advanced-

stage and early-stage disease. The model was tested in another set of sera that included 14 from patients with stage I/II ovarian cancer or 37 sera from advanced-stage ovarian cancer patients. Furthermore, as a more rigorous test, we used sera from women with nonmalignant gynecologic conditions as controls. The model achieved an AUC of 0.70 (95% CI, 0.48–0.75) for discrimination between sera of early-stage ovarian cancer patients and controls. The wider credible intervals partially reflect the relatively small number of early-stage cases ($n = 14$). This outcome represents a significantly poorer performance than for advanced-stage cases versus healthy volunteers for which an AUC of 0.86 (95% CI, 0.78–0.90) was derived. However, we obtained an AUC of 0.71 (95% CI, 0.67–0.76) for discrimination between advanced-stage ovarian cancer and women with nonmalignant gynecologic conditions suggesting that these markers, like CA125, are affected by nonmalignant gynecologic conditions.

Many other biomarkers, including CA125, are significantly less predictive for early-stage ovarian cancer patients. It is therefore interesting that the autoantibody-based test may be similarly effective for discrimination of sera of both early-stage and late-stage ovarian cancer patients from healthy women. Although no information is available on the relationship of NY-CO-8 and ovarian carcinogenesis, both p53 mutation (14, 16, 43) and HOXB7 overexpression have been described in early-stage ovarian cancer (11, 21).

Differences in specimen processing can confound biomarker studies. The similar AUCs obtained using ovarian cancer cases from different institutions (ULSM and GOG) suggests that this autoantibody-based test is likely resistant to the confounding effects of collection at different sites.

Pattern recognition analysis of proteomic profiles has been used to discriminate sera of ovarian cancer patients from those of healthy women. However, the biological underpinning of these patterns is yet unclear (44). By contrast to proteomic profiles, the significance of the TAAs p53 and HOXB7 in cancer biology has been studied extensively for ovarian and other cancers (9, 43, 45–47). A partial cDNA sequence NY-CO-8 was initially identified as a colon cancer antigen. However, subsequent analysis of the serologic reactivity to NY-CO-8 suggests that it is a naturally occurring autoantigen (42). The presence of NY-CO-8-reactive autoantibody in healthy controls that are suppressed in cancer patients may account for its negative association with ovarian cancer in our study. However, we observed no generalized suppression of antibody levels in ovarian cancer patients (Fig. 1); thus, the possibility of a protective effect warrants further investigation. Indeed, a similar phenomenon was recently described for MUC1-specific antibody (48). The full-length NY-CO-8 gene was recently cloned, and its product, CCCAP, was shown to associate with centrosomes (49). Intriguingly, disruption of the centrosomes is an early event in the genesis of ovarian cancer. Furthermore, the breast and ovarian cancer hereditary susceptibility genes BRCA1 and BRCA2 contribute to a centrosome function that is believed to help maintain the integrity of the chromosome segregation process (50, 51).

Acknowledgments

Received 2/25/2005; revised 10/19/2005; accepted 11/16/2005.

Grant support: Department of Defense grant OC010017 (R.B.S. Roden) and USPHS grant CA98166 (D.D. Taylor).

The costs of publication of this article were defrayed in part by the payment of page charges. This article must therefore be hereby marked *advertisement* in accordance with 18 U.S.C. Section 1734 solely to indicate this fact.

References

1. Rosenthal A, Jacobs I. Ovarian cancer screening. *Semin Oncol* 1998;25:315-25.
2. Jacobs I, Bast RC, Jr. The CA 125 tumour-associated antigen: a review of the literature. *Hum Reprod* 1989; 4:1-12.
3. Old LJ, Chen YT. New paths in human cancer serology. *J Exp Med* 1998;187:1163-7.
4. Sahin U, Tureci O, Schmitt H, et al. Human neoplasms elicit multiple specific immune responses in the autologous host. *Proc Natl Acad Sci U S A* 1995;92: 11810-3.
5. Brass N, Heckel D, Sahin U, Pfreundschuh M, Sybrecht GW, Meese E. Translation initiation factor eIF-4 γ is encoded by an amplified gene and induces an immune response in squamous cell lung carcinoma. *Hum Mol Genet* 1997;6:33-9.
6. Scanlan MJ, Chen YT, Williamson B, et al. Characterization of human colon cancer antigens recognized by autologous antibodies. *Int J Cancer* 1998;76:652-8.
7. Dawson JR, Lutz PM, Shau H. The humoral response to gynecologic malignancies and its role in the regulation of tumor growth: a review. *Am J Reprod Immunol* 1983;3:12-7.
8. Chinni SR, Falchetto R, Gercel-Taylor C, Shabanowitz J, Hunt DE, Taylor DD. Humoral immune responses to cathepsin D and glucose-regulated protein 78 in ovarian cancer patients. *Clin Cancer Res* 1997;3:1557-64.
9. Naora H, Yang YQ, Montz FJ, Seidman JD, Kurman RJ, Roden RB. A serologically identified tumor antigen encoded by a homeobox gene promotes growth of ovarian epithelial cells. *Proc Natl Acad Sci U S A* 2001; 98:4060-5.
10. Naora H, Montz FJ, Chai CY, Roden RB. Aberrant expression of homeobox gene HOXA7 is associated with müllerian-like differentiation of epithelial ovarian tumors and the generation of a specific autologous antibody response. *Proc Natl Acad Sci U S A* 2001;98: 15209-14.
11. Stone B, Schummer M, Paley PJ, et al. Serologic analysis of ovarian tumor antigens reveals a bias toward antigens encoded on 17q. *Int J Cancer* 2003; 104:73-84.
12. Odunsi K, Jungbluth AA, Stockert E, et al. NY-ESO-1 and LAGE-1 cancer-testis antigens are potential targets for immunotherapy in epithelial ovarian cancer. *Cancer Res* 2003;63:6076-83.
13. Stockert E, Jager E, Chen YT, et al. A survey of the humoral immune response of cancer patients to a panel of human tumor antigens. *J Exp Med* 1998; 187:1349-54.
14. Soussi T. p53 Antibodies in the sera of patients with various types of cancer: a review. *Cancer Res* 2000;60: 1777-88.
15. Gadducci A, Ferdeghini M, Buttitta F, et al. Preoperative serum antibodies against the p53 protein in patients with ovarian and endometrial cancer. *Anticancer Res* 1996;16:3519-23.
16. Angelopoulou K, Rosen B, Stratis M, Yu H, Solomou M, Diamandis EP. Circulating antibodies against p53 protein in patients with ovarian carcinoma. Correlation with clinicopathologic features and survival. *Cancer* 1996;78:2146-52.
17. Gadducci A, Ferdeghini M, Buttitta F, et al. Assessment of the prognostic relevance of serum anti-p53 antibodies in epithelial ovarian cancer. *Gynecol Oncol* 1999;72:76-81.
18. Chinni SR, Gercel-Taylor C, Conner GE, Taylor DD. Cathepsin D antigenic epitopes identified by the humoral responses of ovarian cancer patients. *Cancer Immunol Immunother* 1998;46:48-54.
19. Li Y, Karjalainen A, Koskinen H, et al. p53 autoantibodies predict subsequent development of cancer. *Int J Cancer* 2005;114:157-60.
20. Canevari S, Pupa SM, Menard S. 1975-1995 Revised anti-cancer serological response: biological significance and clinical implications. *Ann Oncol* 1996;7:227-32.
21. Care A, Felicetti F, Meccia E, et al. HOXB7: a key factor for tumor-associated angiogenic switch. *Cancer Res* 2001;61:6532-9.
22. Old LJ. Cancer vaccines 2003: opening address. *Cancer Immunol* 2003;3 Suppl 2:1.
23. Korneeva I, Bongiovanni AM, Girotra M, Caputo TA, Witkin SS. IgA antibodies to the 27-kDa heat-shock protein in the genital tracts of women with gynecologic cancers. *Int J Cancer* 2000;87:824-8.
24. Korneeva I, Bongiovanni AM, Girotra M, Caputo TA, Witkin SS. Serum antibodies to the 27-kd heat shock protein in women with gynecologic cancers. *Am J Obstet Gynecol* 2000;183:18-21.
25. Luo LY, Herrera I, Soosaipillai A, Diamandis EP. Identification of heat shock protein 90 and other proteins as tumour antigens by serological screening of an ovarian carcinoma expression library. *Br J Cancer* 2002;87:339-43.
26. Tsan MF, Gao B. Endogenous ligands of Toll-like receptors. *J Leukoc Biol* 2004;76:514-9.
27. Breiman L, Freidman JH, Olshen RA, Stone CJ. Classification and regression trees. Monterey (CA): Wadsworth; 1984.
28. Zhang H, Singer B. Recursive partitioning in the health sciences. New York: Springer; 1999.
29. Koziol JA, Zhang JY, Casiano CA, et al. Recursive partitioning as an approach to selection of immune markers for tumor diagnosis. *Clin Cancer Res* 2003;9: 5120-6.
30. Chen YT, Scanlan MJ, Sahin U, et al. A testicular antigen aberrantly expressed in human cancers detected by autologous antibody screening. *Proc Natl Acad Sci U S A* 1997;94:1914-8.
31. Castelli M, Cianfriglia F, Manieri A, et al. Anti-p53 and anti-heat shock proteins antibodies in patients with malignant or pre-malignant lesions of the oral cavity. *Anticancer Res* 2001;21:753-8.
32. Kaur J, Srivastava A, Ralhan R. Serum p53 antibodies in patients with oral lesions: correlation with p53/HSP70 complexes. *Int J Cancer* 1997;74:609-13.
33. Gelfand AE, Smith AFM. Sampling based approaches to calculation marginal densities. *J Am Stat Assoc* 1990; 85:398-40.
34. Spiegelhalter D, Thomas A, Best N, Lunn D. WinBUGS user manual version 1.4. Cambridge (United Kingdom): MRC Biostatistics Unit; 2003.
35. Carlin BP, Louis TA. Bayes and empirical Bayes methods for data analysis. London: Chapman and Hall; 1996.
36. Kass RE, Raftery AE. Bayes factors. *J Am Stat Assoc* 1995;90:773-95.
37. McIntosh MW, Urban N, Karlan B. Generating longitudinal screening algorithms using novel biomarkers for disease. *Cancer Epidemiol Biomarkers Prev* 2002;11:159-66.
38. McIntosh MW, Urban N. A parametric empirical Bayes method for cancer screening using longitudinal observations of a biomarker. *Biostatistics* 2003;4:27-40.
39. Zhang JY, Casiano CA, Peng XX, Koziol JA, Chan EK, Tan EM. Enhancement of antibody detection in cancer using panel of recombinant tumor-associated antigens. *Cancer Epidemiol Biomarkers Prev* 2003;12:136-43.
40. Mintz PJ, Kim J, Do KA, et al. Fingerprinting the circulating repertoire of antibodies from cancer patients. *Nat Biotechnol* 2003;21:57-63.
41. Fossa A, Alsøe L, Cramer R, Funderud S, Gaudernack G, Smeland EB. Serological cloning of cancer/testis antigens expressed in prostate cancer using cDNA phage surface display. *Cancer Immunol Immunother* 2004;53:431-8.
42. Scanlan MJ, Welt S, Gordon CM, et al. Cancer-related serological recognition of human colon cancer: identification of potential diagnostic and immunotherapeutic targets. *Cancer Res* 2002;62:4041-7.
43. Shih Ie M, Kurman RJ. Ovarian tumorigenesis: a proposed model based on morphological and molecular genetic analysis. *Am J Pathol* 2004;164:1511-8.
44. Petricoin EF, Ardekani AM, Hitt BA, et al. Use of proteomic patterns in serum to identify ovarian cancer. *Lancet* 2002;359:572-7.
45. Care A, Silvani A, Meccia E, et al. HOXB7 constitutively activates basic fibroblast growth factor in melanomas. *Mol Cell Biol* 1996;16:4842-51.
46. Care A, Silvani A, Meccia E, Mattia G, Peschle C, Colombo MP. Transduction of the SkBr3 breast carcinoma cell line with the HOXB7 gene induces bFGF expression, increases cell proliferation and reduces growth factor dependence. *Oncogene* 1998;16:3285-9.
47. Care A, Valtieri M, Mattia G, et al. Enforced expression of HOXB7 promotes hematopoietic stem cell proliferation and myeloid-restricted progenitor differentiation. *Oncogene* 1999;18:1993-2001.
48. Cramer DW, Titus-Ernstoff L, McKolanis JR, et al. Conditions associated with antibodies against the tumor-associated antigen MUC1 and their relationship to risk for ovarian cancer. *Cancer Epidemiol Biomarkers Prev* 2005;14:1125-31.
49. Kenedy AA, Cohen KJ, Loveys DA, Kato GJ, Dang CV. Identification and characterization of the novel centrosome-associated protein CCCAP. *Gene* 2003;303:35-46.
50. Hsu LC, Kapali M, DeLoia JA, Gallion HH. Centrosome abnormalities in ovarian cancer. *Int J Cancer* 2005; 113:746-51.
51. Ban S, Shinohara T, Hirai Y, Moritaku Y, Cologne JB, MacPhee DG. Chromosomal instability in BRCA1- or BRCA2-defective human cancer cells detected by spontaneous micronucleus assay. *Mutat Res* 2001;474: 15-23.

UCS protein GC UNC-45 is Over-Expressed in Ovarian Cancer and Promotes Cell Proliferation**Martina Bazzaro¹, Antonio Santillan^{1,2}, Taylor Tang¹, Robert E Bristow^{2,3}, le-Ming Shih^{1,2,3}, and Richard BS Roden^{1,2,3*}****Departments of Pathology¹, Obstetrics and Gynecology², and Oncology³, The Johns Hopkins School of Medicine, Baltimore, MD 21205.**

* Corresponding author. Please send reprint requests to Richard Roden, Cancer Research Building 2, Room 308, 1550 Orleans St, Baltimore, MD 21231 USA

Tel: 410 502 5161

Fax: 443 287 4295

email: roden@jhmi.edu

Grant support was provided by the US Department of Defense Grant OC010017 (R.B.S.R., R.B. and I.-M. S.) and the HERA foundation (M.B. and A.S.). We thank Mike Lee for proof reading our manuscript and Sean Patrick for her encouragement and fund raising activities.

Running title: GC UNC-45 expression in ovarian carcinoma (36 of 40 word maximum)

Abbreviations:

GC: General cell isoform

UNC-45: uncoordinated mutant-45

UCS: UNC-45/CRO1/She4p, a family of related chaperones of myosins

GFP: green fluorescent protein

MALDI-TOF: matrix-assisted laser desorption ionization time-of-flight analysis

IOSE: Immortalized ovarian surface epithelial cell

MGC-999: full length cDNA for human GC UNC-45, Genbank ID BC006214

XTT: 2,3-bis[2-methoxy-4-nitro-5-sulphophenyl]-2-H-tetrazolium-5-carboxanilide

GAPDH: glyceraldehyde-3-phosphate dehydrogenase

HSP: Heat shock protein

Abstract

Aberrant protein expression contributes to carcinogenesis and can trigger a specific humoral immune response in cancer patients. To identify aberrantly expressed proteins that are potentially relevant to the development of ovarian cancer, we derived a tumor cell line from a patient with serous carcinoma and immunoprecipitated tumor-associated antigens from tumor cell lysate using autologous serum antibody. The General Cell isoform of UNC-45 (GC UNC-45) was identified in the immunoprecipitate by matrix-assisted laser desorption ionization time-of-flight analysis. *GC UNC-45* transcripts were higher in high grade disease than immortalized ovarian surface epithelium in 53% of cases. GC UNC-45 protein levels were also elevated in ovarian cancer cells lines as compared to immortalized ovarian surface epithelial cell lines. Although GC UNC-45 is present in normal surface epithelium and benign cystadenoma, elevated GC UNC-45 expression was associated with serous carcinoma ($P < 0.02$). Furthermore, elevated GC UNC-45 expression positively correlated with higher grade and advanced stage of serous carcinoma ($P < 0.02$). GC UNC-45 is a member of the UCS (UNC-45/CRO1/She4p) family of proteins necessary to chaperone myosin assembly and critical for cytokinesis in fungi and nematodes. GC UNC-45 co-localized with myosin II in ovarian cancer cells during interphase, and concentrated with myosin II at the cleavage furrow during cytokinesis. Ectopic over-expression of GC UNC-45 enhanced the rate of ovarian cancer cell proliferation in vitro. Knockdown of GC UNC-45 with siRNA reduced the rate of proliferation without affecting myosin levels, consistent with a role in facilitating correct myosin assembly and division of ovarian cancer cells.

Introduction

Ovarian cancer is the most lethal gynecological malignancy. Ovarian cancer comprises a heterogeneous group of tumors but serous carcinoma accounts for more than 60% of all cases. Efforts to develop new targeted treatments and diagnostic tests for serous carcinoma have been limited by our limited understanding of ovarian carcinogenesis. There is currently no established morphologic precursor lesion for conventional serous carcinoma and it has thus been described as arising 'de novo' (1). As a consequence of the lack of an effective screening test for early detection, serous carcinoma is rarely diagnosed in stage I when conventional treatment is frequently curative. Serous carcinoma is believed to arise in the ovarian surface epithelium, although it may also develop from the mesothelium or the fallopian tube epithelium (2). Controversy with respect to the origins of this disease (3) and the paucity of animal models for serous carcinoma have complicated the study of the early events of ovarian carcinogenesis.

The immune system constantly surveys for "non-self" antigens which often results in generation of autologous antibodies against tumor associated antigens aberrantly expressed or mutated in cancer (4). As an alternative to the typical genetic and proteomic approaches that are applied to identify differentially expressed proteins in cancer, the isolation of tumor associated antigens by immunoprecipitation using autologous serum antibody from patients may be of utility for identification of proteins that are aberrantly expressed in ovarian cancer (5, 6). For example, mutation of p53 is a critical early event in ovarian carcinogenesis, and p53-specific autologous serum antibody is frequently detected even in patients (7). However, the role of , most

antigens identified using autologous antibodies in cancer biology is unclear, and additional studies are critical to validate disease relevance (4).

Herein we utilized autologous antibody to identify the mammalian general cell (GC) isoform of UNC-45 (8), an aberrantly expressed protein in metastatic serous carcinoma and explored its disease relevance. Elevated GC UNC-45 expression is associated with high grade and high stage serous carcinoma. Further, we show that GC UNC-45 expression level modulates the proliferation rate of ovarian cancer cells, and that GC UNC-45 concentrates with myosin II, a molecular motor essential for cell division, at the cleavage furrow during cytokinesis.

Materials and Methods

Human specimens. Studies using human tissue were performed with the approval of the Johns Hopkins Institutional review board. Fresh tumor tissue and peripheral blood were obtained at the Johns Hopkins Hospital with patient consent. Archival tissues were obtained from the Department of Pathology of the Johns Hopkins Hospital and assembled in tissue microarrays by a core facility.

Identification of GC UNC-45 antigen. 0.5ml of 0.2 μ m-filtered sera from patient JH514 was bound to a Sieze-X[®] protein G spin column (Pierce, Rockland NJ) and IgG cross-linked with disuccinimidyl suberate according to the manufacturers' instructions. Cultured JH514 ovarian cancer cells were lysed in M-PER[®] (Pierce) and clarified by centrifugation and passage through a protein G spin column. JH514 cell lysate (7.6mg/ml) was reacted with the autologous antibody column for 1h at 4°C. After

extensive washing, captured antigen was eluted at pH2.5. Eluates were precipitated with 10% trichloroacetic acid and analyzed by sodium dodecyl sulphate polyacrylamide gel electrophoresis and silver staining. The ~100 kDa and ~200kDa protein bands were each excised and digested with L-1-Chloro-3-[4-tosylamido]-4-phenyl-2-butanone-treated sequencing grade trypsin (Worthington Biochemical Corp., Lakewood, NJ) as previously described (9). Masses of the resulting peptides were measured by matrix-assisted laser desorption ionization time-of-flight (MALDI-TOF) on a Voyager DE STR (Applied Biosystems, Foster City, Ca). Positive ion mass spectra were analyzed using Data Explorer (version 3.5). Mass accuracy was better than 100 ppm. GC UNC-45 was identified by searching the monoisotopic masses acquired from the 100kDa protein against the National Center for Biotechnology Information non-redundant database using the MS-Fit search engine on the protein Prospector web site (prospector.ucsf.edu).

Cell culture. IOSE-29, IOSE-397, IOSE-386 cell lines were kindly provided by Nelly Auesperg (University of British Columbia, Vancouver, British Columbia, Canada) and cultured in Medium 199 and MCDB105 (1:1) with 10% fetal bovine serum and 50 μ g/mL gentamycin (Invitrogen). OVCAR-3, SKOV-3, ES-2 and 293T cell lines were obtained from American Type Culture Collection, (Manassas, VA) and cultured according their specification. JH514 cell line was derived from a tumor excised from an 83 year old woman with stage IV low grade serous carcinoma of the ovary and cultured in Dulbecco's modified Eagles's medium (DMEM) supplemented with 10% fetal calf serum, penicillin (100IU/ml, and streptomycin (100 μ g/ml) at 5% CO₂.

Expression and purification of recombinant GC UNC-45 protein. Full length human GC UNC-45 coding sequence (Genbank ID BC006214) was subcloned from MGC-999 (American Type Culture Collection, Manassas, VA) into pProExHTc vector (Invitrogen, Carlsbad, CA). After transformation the bacteria were grown to an OD₆₀₀ of 0.6 and induced with 1 mM isopropylthio- β -D-galactoside (1 mM) for 6h. 6His-tagged protein was purified on nickel-nitriloacetic acid resin columns under denaturing conditions according to the manufacturer (Qiagen, Valencia, CA). 100ng/ml well 6His-tagged human GC UNC-45 was used for ELISA, with 1:100 diluted human sera and peroxidase-linked anti-human IgG secondary antibody (KPL, Gaithersburg, MD).

Generation of rabbit antisera. Rabbits were immunized with 250 μ g of antigen in Freund's Complete Adjuvant and boosted with 125 μ g of antigen in Freund's Incomplete Adjuvant on days 14, 28 and 35. Rabbits were inoculated with the following antigens: full length 6His-tagged human GC UNC-45 and Keyhole limpet cyanogen-coupled peptide HTSAASPAVSLLSGLPLQ human GC UNC-45. Immunizations and peptide affinity purification were performed by Proteintech Laboratories (Chicago, IL) using their standard protocol.

Antibodies and Western blot analysis. Antibodies were utilized for Western blot analysis at the concentration recommended by the manufacturer: rabbit polyclonal anti-myosin V and mouse anti-myosin VI (Sigma, St. Louis, MO), rabbit anti-myosin II (Covance, Berkeley, CA), anti- β -actin (Sigma, St. Louis, MO); and peroxidase-linked anti-rabbit or anti-mouse Immunoglobulin G (Amersham, Piscataway, NJ). Rabbit antisera to GC UNC-45 were used at 1:1000 dilution.

Immunohistochemistry of tissue microarrays. Immunohistochemical analysis of paraffin-embedded tissues was done as previously described (10). Briefly, 5µm tissue microarray sections were deparaffinized and rehydrated. Antigen retrieval was performed and slides were incubated for 5 min with 3% hydrogen peroxide; washed and incubated in antibody dilution 1:250 for 60 min at room temperature. The avidin-biotin-peroxidase complex method from DAKO (Glostrup, Denmark) was used to visualize antibody binding, and slides were subsequently counterstained with hematoxylin.

Generation of GC UNC-45 transient transfectants. Full-length *GC UNC-45* cDNA (Genbank ID BC006214) was into pcDNA3.1 (Invitrogen, Carlsbad, CA) and pEGFP-C1 (Clontech, Mountain View, CA). Subconfluent cultures of 293T or SKOV-3 cells were transfected with plasmids DNA by using Lipofectamine 2000 reagent (Life Technologies, Carlsbad, CA).

Transfection of ovarian carcinoma cells with short interfering RNA (siRNA) oligomers.

Sequences of siRNA oligomers (synthesized by Qiagen, Valencia, CA) were as follows: GC UNC-45 siRNA-1, 5'-GCUGGAAGAUUACGACAAAdTdT-3'; GC UNC-45 siRNA-2, 5'-ACCUCAAGCUGGAAGAUUAdTdT-3'. ES-2 cells were transfected with oligomers by using Lipofectamine 2000 reagent (Life Technologies, Carlsbad, CA). Efficacy of GC UNC-45 knock-down was tested by using oligomers at a range of concentration (20, 50, 100nM) over a period of 24, 48 and 96 hours by Western blot analysis. As control, ES-2 cells were transfected with nonsilencing fluorescein-labeled siRNA (Qiagen, Valencia, CA) under the same conditions used for GC UNC-45 siRNAs.

Proliferation assay.

Fluorescent SKOV-3 cells were imaged and manually counted after 12, 24 and 48 hours from the transfection in a 20X power field under a Nikon Eclipse TE200 inverted fluorescence microscope. 6 fields per each condition were counted. Alternatively, cell were seeded at the concentration of 1,000 cells per well in 100 μ l medium in 96-well plate and after the indicated periods, cells were incubated with 2,3-bis[2-methoxy-4-nitro-5-sulphophenyl]-2-H-tetrazolium-5-carboxanilide inner salt (XTT) (Roche Diagnostic GmbH, Mannheim, Germany) according to the manufacturer's protocol. Formazan dye was quantified using a spectrophotometric plate reader to measure the absorbance at 405nm (ELISA reader 190; Molecular Devices, Sunnyvale, CA). All experiments were done in triplicate.

Cellular localization of GC UNC-45. SKOV-3 cells were seeded 12 hours after transfection at 2,000 cells/500 μ l per well in Lab-Tek II chambered coverglass (Nalge Nunc International, Rochester, NY) and nuclei were visualized by Hoechst staining. Mounted samples were viewed under a Nikon Eclipse TE 200 inverted microscope and images captured with Spot 3.5.8 acquisition software.

Results**Identification and characterization of GC UNC-45.**

Aberrant expression of tumor cell proteins is often accompanied by generation of specific autologous antibodies by cancer patients. In order to identify proteins that are aberrantly expressed during ovarian carcinogenesis, we utilized matrix-assisted laser

desorption ionization time-of-flight analysis (MALDI-TOF) to identify ovarian tumor cell proteins precipitated by autologous patient IgG. A cell line was derived from a patient with stage IV low grade serous carcinoma, and detergent lysate prepared for immunoprecipitation. Autologous serum antibody immunoprecipitated two proteins with estimated molecular mass of ~100kDa and ~200kDa (Fig.1A insert panel). Each band was excised from the gel and identified by trypsin digestion and MALDI-TOF of the tryptic fragments. The ~200kDa antigen was identified as KIAA1529 (195kDa). The ~100kDa was identified as GC UNC-45 (GC UNC-45) (11) which has a predicted mass of 101kDa (Figure 1A and Supplementary data Table 1). While nothing is known about KIAA1529, GC UNC-45 is a conserved member of the UCS (UNC-45/CRO1/She4p) family of the chaperone proteins. Studies of the function of UCS proteins have been primarily restricted to model organisms such as nematodes and fungi (8). They suggest that UCS proteins exert chaperone activity on both conventional and non-conventional myosins and thereby play a key role in cytokinesis and cell proliferation (12-17).

GC UNC-45 aberrant expression associates with ovarian cancer cells *in vivo*.

GC UNC-45 transcripts were detected in all 17 serous carcinoma specimens tested. The SV40 large T-immortalized surface epithelial cell line IOSE-29 has been used to model a pre-malignant state of ovarian carcinogenesis (18-20). Initial analysis of GC UNC-45 mRNA levels in 17 ovarian cancer samples using Q-PCR showed that, after normalization to the transcript of housekeeping gene GAPDH, GC UNC-45 transcripts levels were at least 2-fold higher than the levels in the SV40 large T-immortalized surface epithelial cell line IOSE-29 in 8 of 15 (53%) high grade serous carcinomas

(Fig.1B). GC UNC-45 transcripts were elevated 2-fold in both the tumor tissue and cell line of the patient with GC UNC-45-specific antibody.

Given this evidence of GC UNC-45 transcript levels tended to be higher in ovarian cancer with respect to the SV40 large T-immortalized surface epithelial cell line IOSE-29, we generated polyclonal rabbit antisera (Fig. 2A) to aid the examination of GC UNC-45 protein expression in benign cysts and normal ovarian surface epithelium. First we performed immunoblot analysis to validate the specificity of the antibody and compare GC UNC-45 expression levels in specimens of serous carcinomas versus benign serous cystadenoma. As shown in Fig. 2B specimens of serous carcinoma are associated with significantly ($P<0.02$) higher levels of GC UNC-45 compared to the benign serous cystadenoma. A semiquantitative analysis of the ratio between GC UNC-45 and β -actin is given in Fig. 2C. To address the possibility that aberrant expression of GC UNC-45 may be associated with a more aggressive behavior of ovarian cancer, we performed immunohistochemical staining of tissue microarrays. A total of 64 clinical specimens representing, normal ovarian surface epithelia ($n=14$), benign cysts of the ovary ($n=7$), low-grade ovarian carcinomas ($n=14$) and high-grade ovarian carcinomas ($n=32$) were subjected to immunohistochemical staining for GC UNC-45 expression (Fig. 3A). The staining intensity was scored by three independent evaluators, blinded to the severity of the tumors, as no staining=0, weak staining=1, moderate staining=2, and intense staining=3. Using this scoring system high grade serous carcinomas was associated with more intense staining for GC UNC-45 than the low-grade serous carcinomas ($p<0.02$). Staining of normal ovarian surface epithelium and benign serous

cystadenoma were not significantly different from each other ($p=n.s$) (Fig. 3B, upper panel). GC UNC-45 antibody staining was significantly less intense in low stage (1-2) versus high stage (stages 3-4) serous carcinoma ($p<0.02$) (Fig. 3B, lower panel). However, despite the aberrant expression of GC UNC-45 in a significant fraction of ovarian cancer cases, GC-UNC-45-specific antibodies were detected by ELISA using full length 6His-tagged recombinant protein in only 2/82 sera of patients with ovarian carcinoma, and 0/50 patients with non-malignant gynecologic disorders (data not shown), suggesting that it is not highly immunogenic.

GC UNC-45 is aberrantly expressed in ovarian cancer cell lines and regulates cell proliferation

To establish a suitable *in vitro* model for investigating the biological significance of GC UNC-45 overexpression in ovarian cancer, a panel of immortalized, but not tumorigenic, ovarian surface epithelial cells (IOSE-29, IOSE-386 and IOSE-397) and a panel of ovarian cancer cell lines (SKOV-3, OVCAR-3, ES-2 and JH-514) were subjected to immunoblot analysis for GC UNC-45. The ovarian cancer cell lines exhibited higher levels of GC UNC-45 as compared to IOSEs suggesting that aberrant expression of GC UNC-45 associated with malignant phenotype is maintained in established ovarian cancer cell lines. A semiquantitative analysis of the ratio between GC UNC-45 and β -actin is given in Fig. 4B. Similar results were obtained by using both antisera, but immunoblot analysis using the affinity-purified peptide antibody is shown.

Immunohistochemical analysis of GC UNC-45 expression in clinical specimens revealed that the endogenous protein is predominantly localized in the cytosolic compartment. Similarly, GFP-tagged GC UNC-45 localized predominantly in the cytoplasmic cellular compartment when ectopically expressed in multiple different ovarian cancer cell lines using the pEGFP-C1 GC UNC-45 construct (data not shown).

Genetic studies in model systems suggest a role for GC UNC-45 in cell proliferation (8). To address the significance of the elevated levels of GC UNC-45 present in ovarian cancer, we investigated whether modulation of GC UNC-45 expression levels via ectopic over-expression or siRNA knock-down reciprocally regulated cell proliferation of the cells. The ovarian cancer cell line SKOV-3 was chosen for experiments of ectopic over-expression because western blot analysis revealed an intermediate expression level of GC UNC-45. The SKOV-3 cell line was transiently transfected with vectors expressing GFP alone (pEGFP-C1) or GFP-GC UNC-45 fusion protein (pEGFP-C1 GC UNC-45) and the number of fluorescent cells were counted at 12, 24 and 36h after transfection. The results show significant more rapid proliferation by cells transfected with pEGFP-C1-GC UNC-45 as compared to pEGFP-C1 vector alone ($P < 0.02$ at both 24h and 48h post transfection) (Fig. 5A). To exclude the possibility that GFP fusion affects the function of GC UNC-45 or potential toxic effects of GFP expression, we compared the proliferation rate of SKOV-3 cells transiently transfected with pEGFP-C1 plus pcDNA3 (vector control) versus pEGFP-C1 plus pcDNA3-GC UNC-45. The proliferation rates were followed by counting the number of fluorescent cells at 12, 24

and 36 hours post-transfection. Again, ectopic expression of GC UNC-45 was associated with an increased cell proliferation in SKOV-3 cells ($P < 0.02$, Fig.5B).

To determine if higher basal levels of GC UNC-45 contribute to higher proliferation rate of ovarian cancer cells, we performed GC UNC-45 knock-down experiments using siRNA in ES-2 ovarian cancer cell line. The GC UNC-45 expression was unaffected upon transient transfection of non-silencing control siRNA (negative control siRNA), while both GC UNC-45 siRNA-1 and GC UNC-45 siRNA-2 considerably reduced the protein expression levels within 24 hours of siRNA treatment (Fig. 5C). After assessing the protein knock-down conditions, the proliferation rate was determined by using the XTT assay. A significant reduction in proliferation rate of ES-2 cell line was observed for both the siRNAs 1-and 2 as compared to the proliferation rate of the cell transfected with the neg.control-siRNAs (Fig. 5D). This is consistent with anti-sense experiments conducted on proliferating myoblasts shows that their proliferation rate is severely compromise by the reduction of GC UNC-45 expression level (11).

Colocalization of GC UNC-45 with myosin and the effect of GC UNC-45 levels on myosin expression.

Genetic and biochemical studies reveal that UCS domain proteins have chaperone activity during assembly and maturation of conventional and non-conventional myosins (16). Specifically, GC UNC-45 paralogues in yeast and nematodes act on myosin types II and V and thereby play a fundamental role during cytokinesis (12, 13, 15, 17). To

address the hypothesis that GC UNC-45 plays a similar role in ovarian cancer cells, we performed co-localization studies by immunofluorescence microscopy. While there was partial overlap between GC UNC-45 and myosin V immunostaining (Fig. 6A) the GC UNC-45 and myosin II extensively co-localized within the cytoplasm of interphase ovarian cancer cells (Fig. 6B). Using confocal immunofluorescence microscopy, we were able to show that endogenous GC UNC-45 colocalizes with myosin II in interphase cells (Supplemental Figures 1 and 2). Myosin II is also known to accumulate at the cleavage furrow (Fig. 6C) and thereby drive cytokinesis (21, 22). Immunohistochemical staining also revealed the co-localization of GC UNC-45 with myosin II at the cleavage furrow in mitotic cells (Fig. 6C), consistent with the role of GC UNC-45 as chaperone that facilitates the correct assembly of myosin II.

Genetic studies suggest that cytokinesis is very sensitive to appropriate levels and folding of myosin (23). Thus the inhibition in cell proliferation of ovarian cancer cell lines following knockdown might occur via unfolding and/or destabilization of myosins in the presence of insufficient GC UNC-45 chaperone. Thus, we examined whether knockdown of GC UNC-45 expression would destabilize and thereby reduce the levels of conventional (myosin II) and non-conventional (V and VI) myosins. For this purpose GC UNC-45 expression levels were knocked-down by siRNA in ES-2 ovarian cancer and the expression levels of myosins II, V and VI were assessed by immunoblot analysis. As shown in Fig.6D, reduction of GC UNC-45 expression levels did not have obvious effects on the levels of myosin II, V or VI in siRNA treated ES-2 cell lines at 48 hours post-transfection. At 96 hours post-siRNA treatment the levels of myosin V was

notably decreased. Because the effect of the GC UNC-45 down-regulation on proliferation of ovarian cancer cells was already evident between 24-48 hours post-transfection with GC UNC-45 siRNA, it is not likely that the decrease in myosin levels is responsible for the slowed cell proliferation following GC UNC-45 down-regulation.

Discussion

In this study we identified GC UNC-45, a member of the UCS family (UNC-45/CRO1/She4p), as an autologous antigen in ovarian cancer. Although GC UNC-45 reactive antibody was rare in ovarian cancer patients, nevertheless, GC UNC-45 is aberrantly over-expressed in ovarian cancer cells *in vivo* and *in vitro* with a pattern of protein over-expression that correlates with the more aggressive high grade, high stage ovarian cancer versus low grade and low stage disease.

To address the significance of GC UNC-45 over-expression in ovarian cancer and its biological function we examined the consequences of manipulating its level, and examined the localization of GC UNC-45 with respect to known interacting proteins. Prior studies conducted on proliferating versus quiescent myoblasts as well as on mouse embryos throughout the differentiation process, indicated a direct correlation between GC UNC-45 expression levels and proliferation (11). Here we show that ectopic over-expression or knockdown of GC UNC-45 increased and reduced the proliferation rate of ovarian cancer cells respectively, suggesting that GC UNC-45 over-expression may both contribute to and be necessary for rapid ovarian cancer expansion.

GC UNC-45 paralogues in fungi and nematodes act as chaperone molecules for the assembly and folding of conventional and non-conventional myosins, including myosins II and V (8, 23). Furthermore the function of GC UNC-45 paralogues and myosins II and V are critical during cytokinesis in these model organisms (12-17). Immunofluorescence studies in ovarian cancer cells suggest that GC UNC-45 co-localizes with myosins, and myosin II in particular. This colocalization occurs during interphase but is most obvious during cytokinesis whereupon GC UNC-45 and myosin II accumulate and co-localize within the cleavage furrow. Gene dosage studies in model organisms suggest that cytokinesis is extremely sensitive to the levels of myosin (24-26). Further, studies have shown that UCS protein binds directly to and prevents thermal aggregation of the myosin head domain and are necessary for its activity (16, 27). Consistent with the genetic studies, our study shows that knockdown of GC UNC-45 slows the rate of ovarian cancer cell proliferation within 48h, although levels of myosins II, V and VI do not change during this period. This suggests that continued chaperone-function of GC UNC-45 for correct folding of myosins is required for maintenance of cell proliferation in cancer cells. Conversely, ectopic over-expression of GC UNC-45 in SKOV-3 cells increases the rate of cell proliferation, suggesting that GC UNC-45 levels may be limiting for the proliferation of SKOV-3 cells.

High grade ovarian cancer typically invades and metastasizes rapidly. Metastasis is associated with changes in cancer cell morphology and motility, processes regulated by the cytoskeleton and myosin motors. Myosin II is an important determinant of force generation in cellular motility and the myosin II-specific inhibitor blebbistatin inhibits

pancreatic adenocarcinoma cellular invasiveness (28). Myosin II accumulates at the lamellipodia leading edges in cancer cells and interacts with the S100A4 metastasis factor (29). A higher level of GC UNC-45 expression was observed in advanced versus early stage disease suggesting a hypothesis that elevated GC UNC-45 expression may also contribute to ovarian cancer metastasis by facilitating myosin II assembly.

UCS proteins act in concert with HSP90 to chaperone the assembly of myosin (30).

Interestingly the HSP90 inhibitors geldanamycin and its analogues are active against ovarian cancer (31-33), and inhibit cytokinesis in model organisms (30). However, it is important to note that HSP90 acts as a chaperone for the folding of many proteins besides the myosins and these agents may effect other cellular functions (34, 35).

Thus, future study is required to determine if defects in GC-UNC-45 function is a consequence of Hsp90 inhibition in cancer cells. Regardless, given the ubiquitous role of GC-UNC-45 and myosin function in cell proliferation, elevated GC-UNC-45 expression may be important in ovarian cancer biology. Finally, GC-UNC-45 may represent a target for developing drugs to slow cancer progression.

(3,594 words)

Figure Legends

Figure 1. Immunoprecipitation and identification of GC UNC-45. A. Autologous serum from patient JH514 bound to protein-G immunoprecipitated two antigens of ~100kDa and ~200kDa from cell lysates of JH-514 ovarian cancer cell line (*insert panel*). Both antigens were subjected to tryptic digestion and mass spectrometry analysis. Shown is the mass spectrum derived from tryptic digestion of ~100kDa band corresponding to GC UNC-45. B. Levels of GC UNC-45 transcripts were determined relative to GAPDH in JH514 primary tumor tissue (JH514tt), JH514 cell line (JH514cl) and 15 additional primary serous carcinoma specimens (sc). The GC UNC-45 transcript levels in serous carcinoma are presented relative to the level present in the immortalized ovarian surface epithelial cell line IOSE-29. For a few samples, the levels of GC UNC-45 transcripts were dramatically higher and the fold increases are shown in parenthesis.

Figure 2. GC UNC-45 expression is higher malignant versus benign ovarian tumors. A, rabbit antisera to 6His-tagged GC UNC-45 full length antigen (*left panel*), GC UNC-45 peptide (*middle panel*) or GFP (*right panel*) were tested by immunoblot analysis for reactivity to 6His-tagged GC UNC-45 purified protein and cell lysates of 293T cells transduced with control vector (pEGFP-C1) or pEGFP-C1-GC UNC45 expressing GFP-tagged GC UNC-45 protein. B, lysate of samples of serous cystadenoma (lanes 1-4) and serous carcinoma (lanes 5-10) were immunoblotted using GC UNC-45 peptide-specific rabbit antibody. Equal loading was verified by using an

antibody directed against β -actin. C, Ratio between GC UNC-45 and β -actin in tissue lysates from serous cystadenoma (4 cases) and serous carcinoma (6 cases). ** $P < 0.02$.

Figure 3. Immunohistochemical staining of GC UNC-45 in clinical specimens. A, shown are representative examples of intense GC UNC-45 staining in high grade serous carcinoma (X40), moderate staining intensity in low-grade serous carcinoma (X40) and weak staining intensity in benign cyst and normal ovarian surface epithelium (X40). B, staining intensity for each case was graded as 0 (no staining), 1 (weak staining), 2 (moderate staining), and 3 (intense staining). **, $P < 0.02$ statistical significance in staining intensities among indicated groups (Mann-Whitney U test).

Figure 4. GC UNC-45 over-expression *in vitro* and its cellular localization.

A, lysates of Immortalized Ovarian Surface Epithelial cell lines (IOSE-29, IOSE-386, IOSE-397) and ovarian cancer cell lines (SKOV-3, OVCAR-3, ES-2 and JH-514) were immunoblotted with anti-GC UNC-45 peptide rabbit antibody. Equal loading was verified by using an antibody directed against β -actin. B, Ratio between GC UNC-45 and β -actin in tissue lysates from IOSEs and ovarian cancer cell lines, ** $P < 0.02$. C, representative immunofluorescence image of SKOV-3 cells ectopically expressing either pEGFP-C1 vector alone or pEGFP-C1-tagged GC UNC-45 and stained with DAPI.

Figure 5. Effect of GC UNC-45 expression levels on ovarian cancer cell proliferation.

A, proliferation rate of SKOV-3 cells ectopically expressing either GFP (pEGFP-C1 vector alone) or GFP -tagged GC UNC-45 (pEGFP-C1-GC UNC-45) was determined by counting the number of fluorescent cells 12, 24 and 36 hours post transfection. ***, $P < 0.001$. B, proliferation rate of SKOV-3 co-transfected with either pEGFP-C1 and pcDNA3 or pEGFP-C1 and pcDNA3-GC UNC-45 was determined by counting the number of fluorescent cells 12, 24 and 36 hours post transfection. ***, $P < 0.001$. C, the efficiency of GC UNC-45 knockdown in ES-2 cells transduced with one of two different GC UNC-45 siRNA oligomers (GC UNC-45-siRNA-1, -2) or with nonsilencing siRNA (neg. control-siRNA) at the indicated concentration was tested by immunoblot analysis at 48 hours post-transfection. Equal loading was verified by using an antibody directed against β -actin. D, proliferation rate of ES-2 cell line transfected with either nonsilencing siRNA, GC UNC-45-siRNA-1 or GC UNC-45-siRNA-2, was measured by XTT assay starting from 12 hours post transfection. Results are expressed in terms of daily proliferation rate. ** $P < 0.02$, *** $P < 0.001$.

Figure 6. Effect of GC UNC-45 knock-down on myosin levels.

A-C. GC-UNC-45 transfected SKOV-3 cells were stained with the DNA stain DAPI (A1, B1, C1), anti-myosin V (A3), anti-myosin II (B2, C2) and anti-GC UNC-45 peptide antibody (A2, B2, C2). Staining for DNA is blue, myosin is red and GC UNC-45 is green. Merged immunofluorescence images are presented (A4, B4, C4). D. The cellular localization of GC UNC-45 only partially overlaps myosin V (A). In particular, while significant myosin V staining is present over the nuclei, very little GC UNC-45 is present over the nuclei. In contrast, there is a significant and robust colocalization of GC UNC-

45 with myosin II in interphase (B) and mitotic cells (C). Lysate of negative control siRNA or GC UNC-45-siRNA-1 treated ES-2 cells for the time indicated was immunoblotted with antibodies against Myosin II, Myosin V or Myosin VI. Equal protein loading was verified by using an antibody directed against β -actin.

SUPPLEMENTARY DATA

Supplemental Table 1. Expected and observed M/z for peptides of GC UNC-45 and the ~100kDa antigen. Matched peptides cover 12% of the GC UNC-45 protein.

M/z submitted	MH+ matched	Δ Da	Missed cleavages	Database Sequence
523.2691	523.2186	0.050	0	(K)CSEK(D)
562.2315	562.3201	-0.089	1	(K)GTEKK(Q)
1074.6897	1074.5618	0.13	1	(R)CVSLEPKNK(V)
1179.6649	1179.5618	0.085	0	(K)SWFEGQGLAGK(L)
1186.7039	1186.5414	0.16	0/1Met-ox	(K)LGSAGGTDFSMK(Q)
1287.7267	1287.7749	-0.048	1	(R)TVATLSILGTRR(V)
1320.6865	1320.7527	-0.066	0	(R)ASFITANGVSLK(D)
1661.9771	1661.8606	0.12	0	(R)LLDMGETDLMLAALR(T)
1677.9307	1677.8556	0.075	0/1Met-ox	(R)LLDMGETDLMLAALR(T)
1693.9454	1693.8505	0.095	0/2Met-ox	(R)LLDMGETDLMLAALR(T)
1797.9774	1797.9063	0.071	0	(R)WAVEGLAYLTFDADV(K)
2225.2600	2225.1119	0.15	0	(R)EIASTLMESEMMEILSVLAK(G)
2273.2726	2273.0966	0.18	0/3Met-ox	(R)EIASTLMESEMMEILSVLAK(G)

Supplemental Figures 1 and 2. Confocal immunofluorescence micrograph showing localization of GC UNC-45 (green), Myosin II (red) and DNA staining with DAPI (blue).

REFERENCES

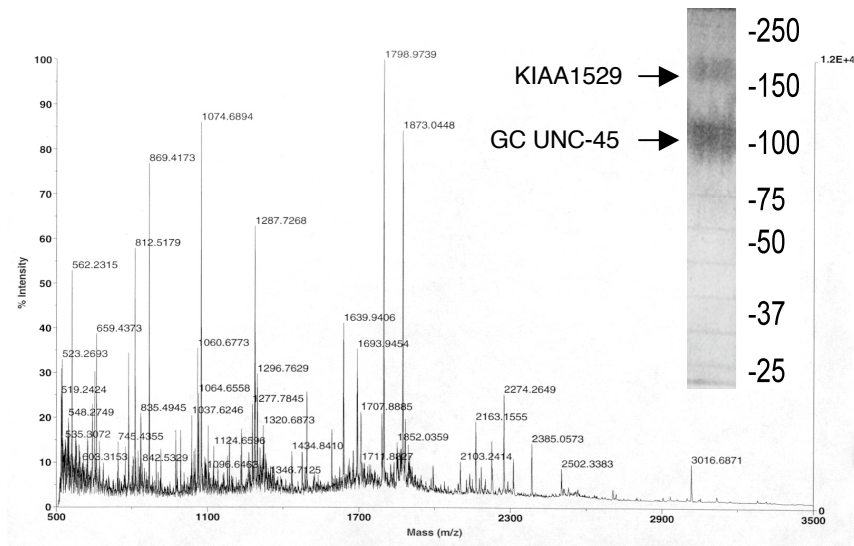
1. Shih le, M. and Kurman, R. J. Ovarian tumorigenesis: a proposed model based on morphological and molecular genetic analysis. *Am J Pathol* 2004; **164**: 1511-1518.
2. Lee, Y., Medeiros, F., Kindelberger, D., Callahan, M. J., Muto, M. G., and Crum, C. P. Advances in the recognition of tubal intraepithelial carcinoma: applications to cancer screening and the pathogenesis of ovarian cancer. *Adv Anat Pathol* 2006; **13**: 1-7.
3. Dubeau, L. The cell of origin of ovarian epithelial tumors and the ovarian surface epithelium dogma: does the emperor have no clothes? *Gynecol Oncol* 1999; **72**: 437-442.
4. Old, L. J. and Chen, Y. T. New paths in human cancer serology. *J Exp Med* 1998; **187**: 1163-1167.
5. Chinni, S. R., Falchetto, R., Gercel-Taylor, C., Shabanowitz, J., Hunt, D. F., and Taylor, D. D. Humoral immune responses to cathepsin D and glucose-regulated protein 78 in ovarian cancer patients. *Clin Cancer Res* 1997; **3**: 1557-1564.
6. Soussi, T. p53 Antibodies in the sera of patients with various types of cancer: a review. *Cancer Res* 2000; **60**: 1777-1788.
7. Gadducci, A., Ferdeghini, M., Buttitta, F., Fanucchi, A., Annicchiarico, C., Prontera, C., et al. Preoperative serum antibodies against the p53 protein in patients with ovarian and endometrial cancer. *Anticancer Res* 1996; **16**: 3519-3523.
8. Hutagalung, A. H., Landsverk, M. L., Price, M. G., and Epstein, H. F. The UCS family of myosin chaperones. *J Cell Sci* 2002; **115**: 3983-3990.
9. Yang, R., Yutzy, W. H. t., Viscidi, R. P., and Roden, R. B. Interaction of L2 with beta-actin directs intracellular transport of papillomavirus and infection. *J Biol Chem* 2003; **278**: 12546-12553.
10. Bazzaro, M., Lee, M. K., Zoso, A., Stirling, W. L., Santillan, A., Shih le, M., et al. Ubiquitin-proteasome system stress sensitizes ovarian cancer to proteasome inhibitor-induced apoptosis. *Cancer Res* 2006; **66**: 3754-3763.
11. Price, M. G., Landsverk, M. L., Barral, J. M., and Epstein, H. F. Two mammalian UNC-45 isoforms are related to distinct cytoskeletal and muscle-specific functions. *J Cell Sci* 2002; **115**: 4013-4023.
12. Wong, K. C., D'Souza V, M., Naqvi, N. I., Motegi, F., Mabuchi, I., and Balasubramanian, M. K. Importance of a myosin II-containing progenitor for actomyosin ring assembly in fission yeast. *Curr Biol* 2002; **12**: 724-729.
13. Wong, K. C., Naqvi, N. I., Iino, Y., Yamamoto, M., and Balasubramanian, M. K. Fission yeast Rng3p: an UCS-domain protein that mediates myosin II assembly during cytokinesis. *J Cell Sci* 2000; **113 (Pt 13)**: 2421-2432.
14. Toi, H., Fujimura-Kamada, K., Irie, K., Takai, Y., Todo, S., and Tanaka, K. She4p/Dim1p interacts with the motor domain of unconventional myosins in the budding yeast, *Saccharomyces cerevisiae*. *Mol Biol Cell* 2003; **14**: 2237-2249.

15. Wesche, S., Arnold, M., and Jansen, R. P. The UCS domain protein She4p binds to myosin motor domains and is essential for class I and class V myosin function. *Curr Biol* 2003; **13**: 715-724.
16. Barral, J. M., Hutagalung, A. H., Brinker, A., Hartl, F. U., and Epstein, H. F. Role of the myosin assembly protein UNC-45 as a molecular chaperone for myosin. *Science* 2002; **295**: 669-671.
17. Kachur, T., Ao, W., Berger, J., and Pilgrim, D. Maternal UNC-45 is involved in cytokinesis and colocalizes with non-muscle myosin in the early *Caenorhabditis elegans* embryo. *J Cell Sci* 2004; **117**: 5313-5321.
18. Auersperg, N., Maines-Bandiera, S. L., Dyck, H. G., and Kruk, P. A. Characterization of cultured human ovarian surface epithelial cells: phenotypic plasticity and premalignant changes. *Lab Invest* 1994; **71**: 510-518.
19. Auersperg, N., Pan, J., Grove, B. D., Peterson, T., Fisher, J., Maines-Bandiera, S., et al. E-cadherin induces mesenchymal-to-epithelial transition in human ovarian surface epithelium. *Proc Natl Acad Sci U S A* 1999; **96**: 6249-6254.
20. Auersperg, N., Edelson, M. I., Mok, S. C., Johnson, S. W., and Hamilton, T. C. The biology of ovarian cancer. *Semin Oncol* 1998; **25**: 281-304.
21. Matsumura, F. Regulation of myosin II during cytokinesis in higher eukaryotes. *Trends Cell Biol* 2005; **15**: 371-377.
22. Balasubramanian, M. K., Bi, E., and Glotzer, M. Comparative analysis of cytokinesis in budding yeast, fission yeast and animal cells. *Curr Biol* 2004; **14**: R806-818.
23. Landsverk, M. L. and Epstein, H. F. Genetic analysis of myosin II assembly and organization in model organisms. *Cell Mol Life Sci* 2005; **62**: 2270-2282.
24. May, K. M., Win, T. Z., and Hyams, J. S. Yeast myosin II: a new subclass of unconventional conventional myosins? *Cell Motil Cytoskeleton* 1998; **39**: 195-200.
25. Bezanilla, M., Forsburg, S. L., and Pollard, T. D. Identification of a second myosin-II in *Schizosaccharomyces pombe*: Myp2p is conditionally required for cytokinesis. *Mol Biol Cell* 1997; **8**: 2693-2705.
26. Mulvihill, D. P. and Hyams, J. S. Role of the two type II myosins, Myo2 and Myp2, in cytokinetic actomyosin ring formation and function in fission yeast. *Cell Motil Cytoskeleton* 2003; **54**: 208-216.
27. Lord, M. and Pollard, T. D. UCS protein Rng3p activates actin filament gliding by fission yeast myosin-II. *J Cell Biol* 2004; **167**: 315-325.
28. Duxbury, M. S., Ashley, S. W., and Whang, E. E. Inhibition of pancreatic adenocarcinoma cellular invasiveness by blebbistatin: a novel myosin II inhibitor. *Biochem Biophys Res Commun* 2004; **313**: 992-997.
29. Li, Z. H. and Bresnick, A. R. The S100A4 metastasis factor regulates cellular motility via a direct interaction with myosin-IIA. *Cancer Res* 2006; **66**: 5173-5180.
30. Mishra, M., D'Souza V, M., Chang, K. C., Huang, Y., and Balasubramanian, M. K. Hsp90 protein in fission yeast Swo1p and UCS protein Rng3p facilitate myosin II assembly and function. *Eukaryot Cell* 2005; **4**: 567-576.

31. Neckers, L. and Ivy, S. P. Heat shock protein 90. *Curr Opin Oncol* 2003; **15**: 419-424.
32. Nishiyama, N., Nori, A., Malugin, A., Kasuya, Y., Kopeckova, P., and Kopecek, J. Free and N-(2-hydroxypropyl)methacrylamide copolymer-bound geldanamycin derivative induce different stress responses in A2780 human ovarian carcinoma cells. *Cancer Res* 2003; **63**: 7876-7882.
33. Banerji, U., Walton, M., Raynaud, F., Grimshaw, R., Kelland, L., Valenti, M., et al. Pharmacokinetic-pharmacodynamic relationships for the heat shock protein 90 molecular chaperone inhibitor 17-allylamino, 17-demethoxygeldanamycin in human ovarian cancer xenograft models. *Clin Cancer Res* 2005; **11**: 7023-7032.
34. Schnur, R. C., Corman, M. L., Gallaschun, R. J., Cooper, B. A., Dee, M. F., Doty, J. L., et al. Inhibition of the oncogene product p185erbB-2 in vitro and in vivo by geldanamycin and dihydrogeldanamycin derivatives. *J Med Chem* 1995; **38**: 3806-3812.
35. Xu, W., Marcu, M., Yuan, X., Mimnaugh, E., Patterson, C., and Neckers, L. Chaperone-dependent E3 ubiquitin ligase CHIP mediates a degradative pathway for c-ErbB2/Neu. *Proc Natl Acad Sci U S A* 2002; **99**: 12847-12852.
36. Korneeva, I., Bongiovanni, A. M., Girotra, M., Caputo, T. A., and Witkin, S. S. IgA antibodies to the 27-kDa heat-shock protein in the genital tracts of women with gynecologic cancers. *Int J Cancer* 2000; **87**: 824-828.

Figure 1

A



B

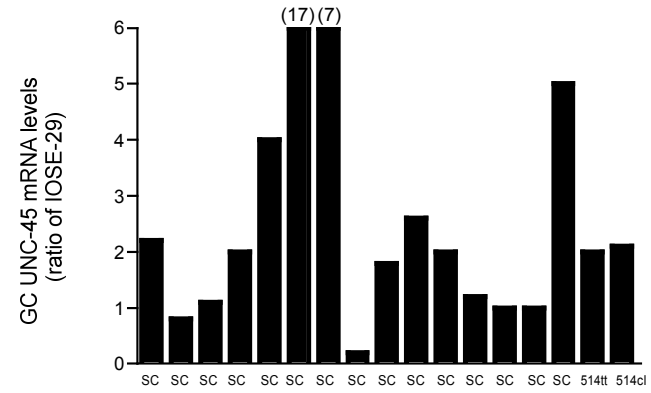


Figure 2

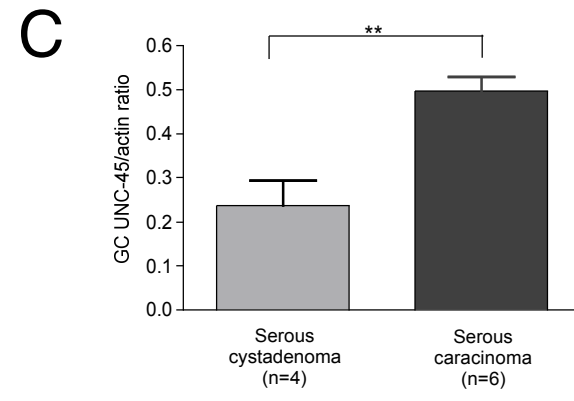
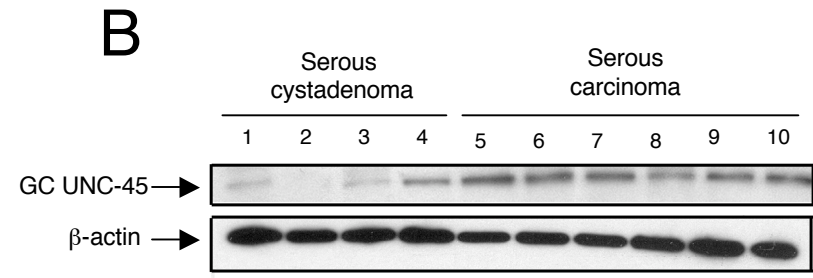
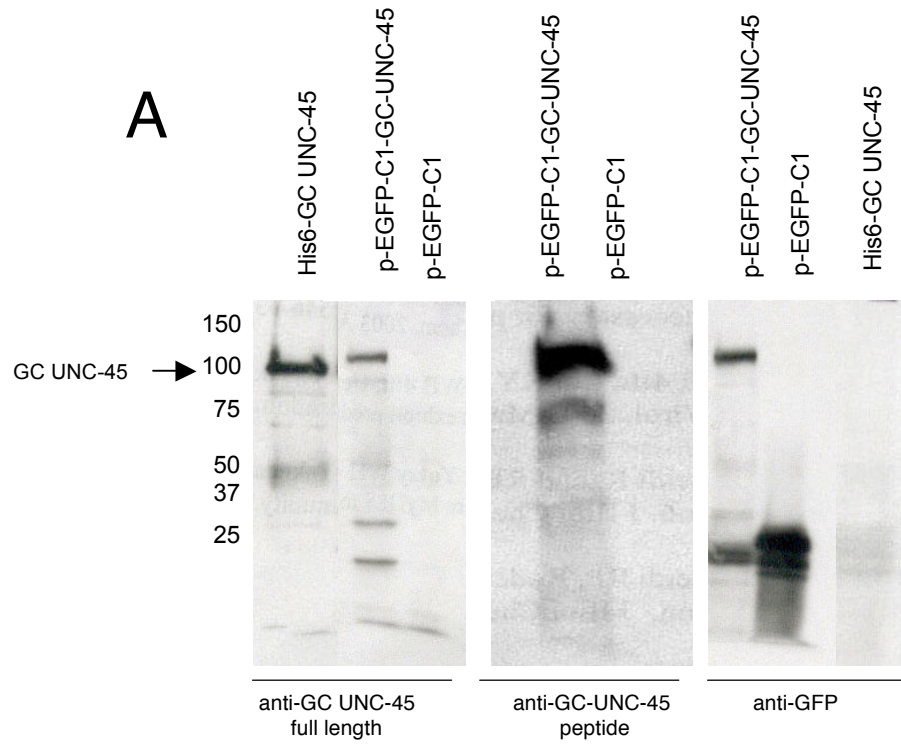
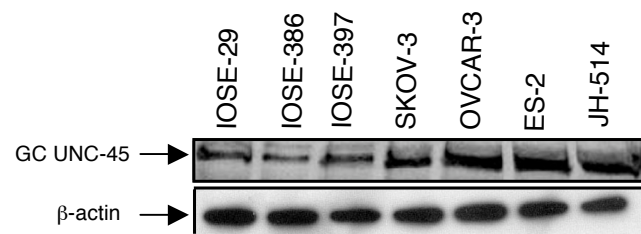
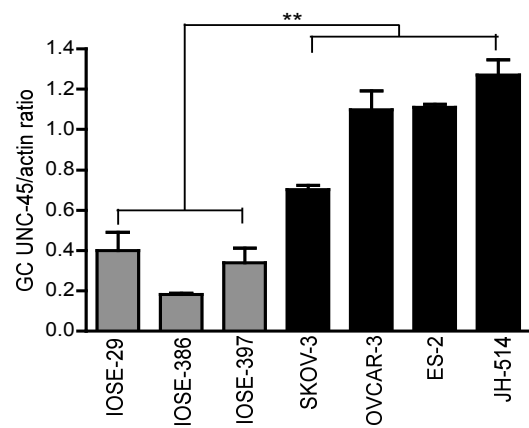


Figure 4

A



B



C

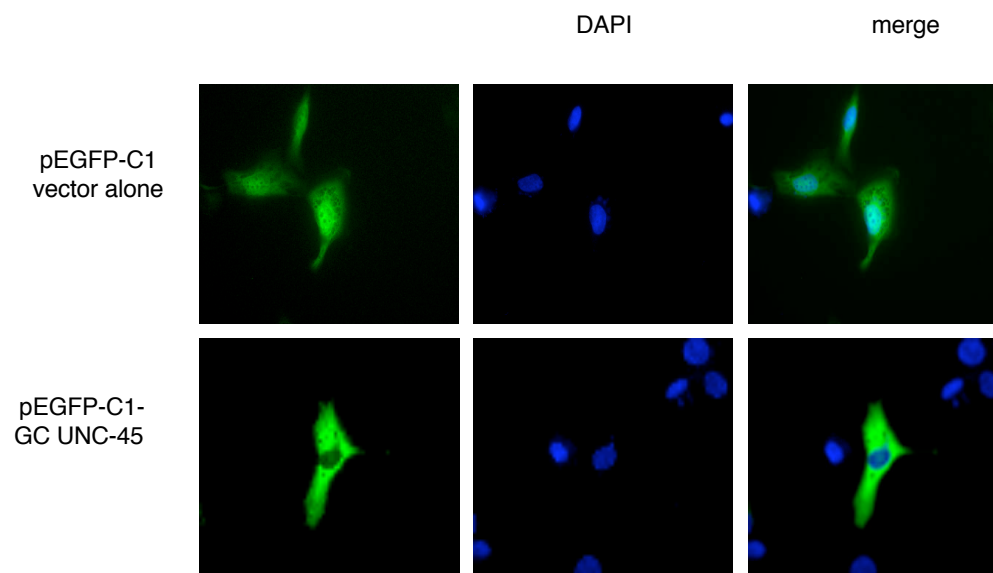
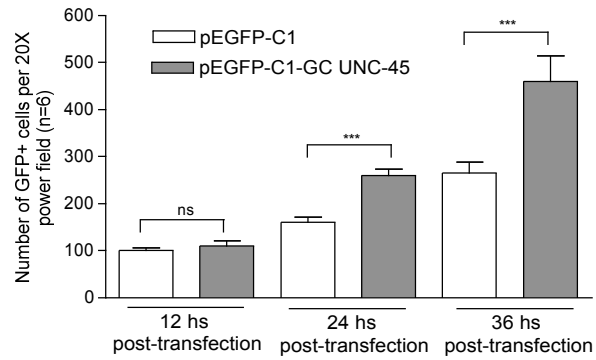
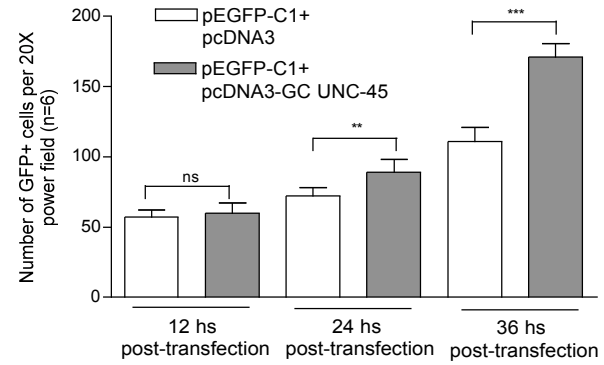


Figure 5

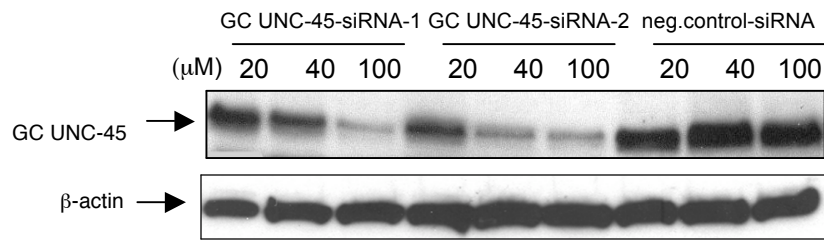
A



B



C



D

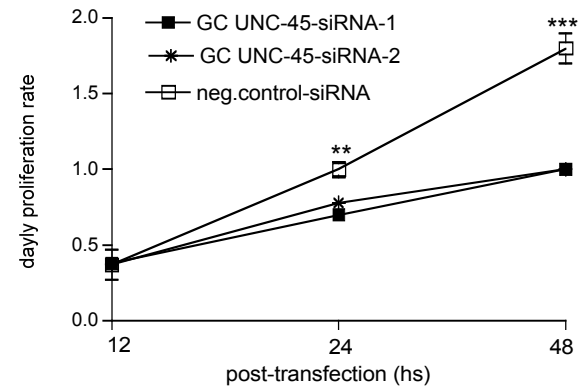
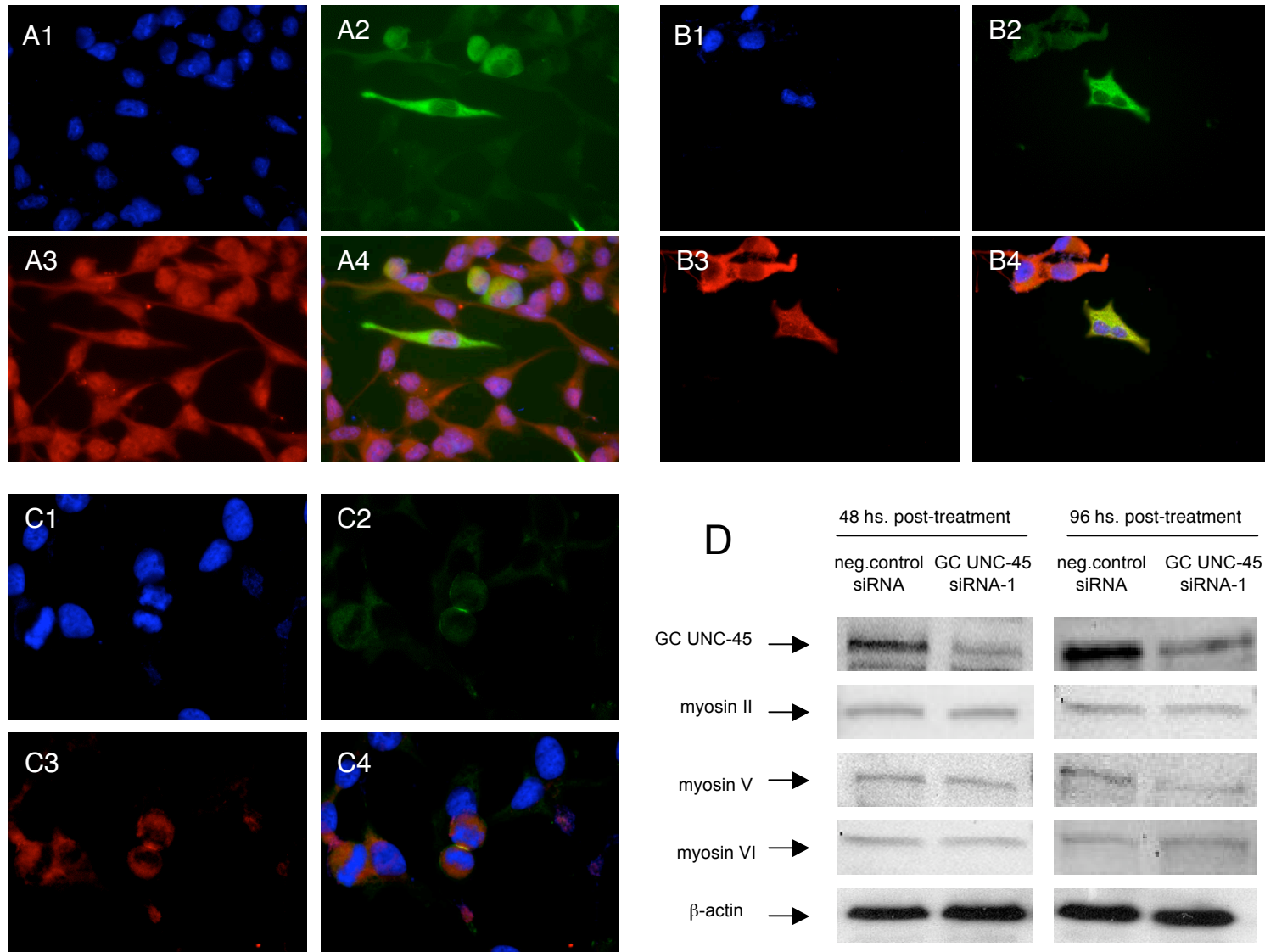


Figure 6



Ubiquitin-Proteasome System Stress Sensitizes Ovarian Cancer to Proteasome Inhibitor-Induced Apoptosis

Martina Bazzaro,¹ Michael K. Lee,¹ Alessia Zoso,¹ Wanda L.H. Stirling,¹ Antonio Santillan,² Ie-Ming Shih,^{1,2,3} and Richard B.S. Roden^{1,2,3}

Departments of ¹Pathology, ²Obstetrics and Gynecology, and ³Oncology, The Johns Hopkins School of Medicine, Baltimore, Maryland

Abstract

The ubiquitin-proteasome system (UPS) mediates targeted protein degradation. Notably, the UPS determines levels of key checkpoint proteins controlling apoptosis and proliferation by controlling protein half-life. Herein, we show that ovarian carcinoma manifests an overstressed UPS by comparison with normal tissues by accumulation of ubiquitinated proteins despite elevated proteasome levels. Elevated levels of total ubiquitinated proteins and 19S and 20S proteasome subunits are evident in both low-grade and high-grade ovarian carcinoma tissues relative to benign ovarian tumors and in ovarian carcinoma cell lines relative to immortalized surface epithelium. We find that ovarian carcinoma cell lines exhibit greater sensitivity to apoptosis in response to proteasome inhibitors than immortalized ovarian surface epithelial cells. This sensitivity correlates with increased cellular proliferation rate and UPS stress rather than absolute proteasome levels. Proteasomal inhibition *in vitro* induces cell cycle arrest and the accumulation of p21 and p27 and triggers apoptosis via activation of caspase-3. Furthermore, treatment with the licensed proteasome inhibitor PS-341 slows the growth of ES-2 ovarian carcinoma xenograft in immunodeficient mice. In sum, elevated proliferation and metabolic rate resulting from malignant transformation of the epithelium stresses the UPS and renders ovarian carcinoma more sensitive to apoptosis in response to proteasomal inhibition. (Cancer Res 2006; 66(7): 3754-63)

Introduction

The ubiquitin-proteasome system (UPS) is responsible for >80% of the intracellular protein degradation in eukaryotes and has two components: the ubiquitin-conjugating system and the 26S proteasome (1). The UPS catabolic machinery is located in the 26S proteasome, which consists of a 20S catalytic core that degrades ubiquitinated protein, and two 19S regulatory subunits that regulate the entrance of the targeted substrates into the core. Tight regulation of UPS-mediated proteolysis is maintained to control half-lives of proteins involved in cell cycle regulation, transcriptional control, antigen processing, angiogenesis, and removal of incorrectly folded or damaged proteins (2).

Despite evidence that dysregulation of the catalytic processes mediated by the UPS system is associated with tumorigenesis,

tumor progression, and drug resistance, the relationship between proteasome expression and cancer progression is still poorly understood. Indeed, whereas proteasome down-regulation has been described in solid tumors, abnormally high proteasome levels have been observed in hematopoietic tumor cells. In addition to the proteasome, ubiquitin-specific proteases may be overexpressed in several cancer and transformed cell lines (3).

Consistent with a greater requirement for proteasomal function in cancer cells and other rapidly proliferating cells, proteasomal inhibition causes increased cell death in lymphoma cell lines when compared with normal lymphoblasts (4). Further, rapidly proliferating cells, such as embryonic endothelial cells, are extremely sensitive to apoptosis induced by proteasomal inhibition (5). These observations suggest that rapidly proliferating cells, particularly cancer cells, have a greater requirement for proteasomal activity than their normal counterpart. The evidence linking the proliferative status of a particular cell with sensitivity to proteasomal inhibition indicates that the proteasome represents a promising target for cancer therapy. Currently, a proteasome inhibitor PS-341 (bortezomib, Velcade) is undergoing clinical testing for treatment of several tumors and has been Food and Drug Administration approved for treatment of multiple myeloma (6–14).

Better treatments for ovarian cancer are urgently needed. Despite the ubiquitous nature of proteasome function and the potential of proteasome chemotherapy in a variety of tumors, it is currently unknown whether abnormalities in UPS system and elevated sensitivity to proteasomal inhibition are associated with epithelial ovarian cancer. Our findings herein show that ovarian cancer cells are under significant UPS stress and suggest that proteasome inhibitors may have utility in the treatment of ovarian cancer.

Materials and Methods

Animals. Six-week-old female immunodeficient BNX (*beige nude xid*) mice were obtained from National Cancer Institute-Frederick (Frederick, MD) and maintained in a pathogen-free animal facility at least 1 week before use. All animal studies were done in accordance with institutional guidelines.

Cell culture. IOSE-29 and IOSE-397 cell lines were kindly provided by Nelly Auesperg (University of British Columbia, Vancouver, British Columbia, Canada) and cultured in Medium 199 and MCDB105 (1:1) with 10% fetal bovine serum and 50 µg/mL gentamicin. IOSE-2Ap2 and IOSE-4p2 were kindly provided by Hidetaka Katabuchi (Kumamoto University School of Medicine, Kumamoto, Japan). OVCAR-3, ES-2, and SKOV-3 cell lines were obtained from American Type Culture Collection (Manassas, VA) and cultured according to their specifications. MOSEC cells were kindly provided by Dr. Katherine F. Roby (University of Kansas, Kansas City, KS; ref. 15). Unless otherwise specified, cell lines were maintained in DMEM supplemented with 10% FCS, 100 IU/mL penicillin, and 100 µg/mL streptomycin at 5% CO₂.

Drugs. The proteasome inhibitors MG132 and epoxomicin were purchased from Affiniti Research Products Ltd. (Exeter, United Kingdom)

Note: Supplementary data for this article are available at Cancer Research Online (<http://cancerres.aacrjournals.org/>).

Requests for reprints: Richard B.S. Roden, The Johns Hopkins School of Medicine Cancer Research Building 2, Room 3.08, 1550 Orleans Street, Baltimore, MD 21231. Phone: 410-502-5161; Fax: 443-287-4295; E-mail: roden@jhmi.edu.

©2006 American Association for Cancer Research.
doi:10.1158/0008-5472.CAN-05-2321

and dissolved in DMSO. The proteasome inhibitor PS-341 (Millenium Pharmaceuticals, Inc., Cambridge, MA) mixed with mannitol was dissolved in 0.9% NaCl at the appropriate concentration before each drug injection.

Xenograft murine model. Mice were inoculated s.c. into the right flank with 1×10^7 ES-2 cells in 100 μ L DMEM. When tumor was measurable, mice were randomly assigned into two groups receiving PS-341 or 0.9% saline. Treatment with PS-341 was given i.v. twice weekly via tail vein at 1 mg/kg PS-341. The control group received the vehicle alone at the same schedule. Caliper measurements of the longest perpendicular tumor diameters were done every 2 days to estimate the tumor volume (mean \pm SE; mm³), using the following formula: $4\pi / 3 \times (\text{width} / 2)^2 \times (\text{length} / 2)$, representing the three-dimensional volume of an ellipse. Animals were sacrificed when their tumors reached 2 cm.

Cell viability assay. Cell viability was determined by 2,3-bis[2-methoxy-4-nitro-5-sulphophenyl]-2H-tetrazolium-5-carboxanilide inner salt (XTT) assay (Roche Diagnostics GmbH, Mannheim, Germany). Cells seeded at the concentration of 1,000 per well in 100 μ L medium in 96-well plate were treated with proteasome inhibitors at specified concentrations. After the indicated periods, cells were incubated according to the manufacturer's protocol with the XTT labeling mixture for 4 hours. Formazan dye was quantified using a spectrophotometric plate reader to measure the absorbance at 405 nm (ELISA reader 190; Molecular Devices, Sunnyvale, CA). All experiments were done in triplicate.

Rate of proliferation. Cell lines were seeded at a density of 5,000 cells per well (12-well plate) under the specified culturing conditions. At the indicated time points, cells were trypsinized and counted in a hemocytometer in the presence of trypan blue to exclude dead cells. Proliferation rate was determined from the steepest slope.

Antibodies and Western blot analysis. We used the following reagents for concentration with standard Western blot analysis techniques at the concentration recommended by the manufacturer: anti-19S subunit Rpt4, HC9 anti-proteasomal subunit α 3, rabbit polyclonal antibody to human 20S proteasome subunit β 5, and rabbit polyclonal antibody to human 20S proteasome subunit β 4 (Affiniti Research Products); anti-ubiquitin (clone 5-25; Signet, Dedham, MA); anti-p21^{WAF1} and anti-p27^{KIP1} (BD Biosciences, San Diego, CA); anti- β -actin (Sigma, St. Louis, MO); and peroxidase-linked anti-rabbit or anti-mouse IgG (Amersham, Piscataway, NJ).

Flow cytometry. Cell cycle status was analyzed with a FACSCalibur flow cytometer (Becton Dickinson, San Diego, CA) by measuring fluorescence from cells stained with propidium iodide (PI; Sigma). For Annexin V experiments, cells were treated for indicated amount of time, harvested, and immediately stained for Annexin V/FITC (BD Pharmingen, San Diego, CA) and PI according to the protocol provided by the manufacturer.

Caspase-3 activity assay. Caspase-3-like activity assay was done with the colorimetric substrate Ac-Asp-Glu-Val-Asp-p-nitroaniline (Ac-DEVD-pNA) in accordance with the protocol supplied by the manufacturer (Chemicon International, Temecula, CA). To determine the specificity of the caspase-3 activity, the caspase-3-specific inhibitor Ac-DEVD-CMK was added to the assay mixture. To determine caspase-like activity, the pan-caspase inhibitor Z-VAD-CMK was incubated together with proteasome inhibitors and the cell viability was then tested. All the experiments were conducted in triplicates.

Terminal deoxynucleotidyl transferase-mediated dUTP nick end labeling assay. Paraffin-embedded tissue sections were processed for terminal deoxynucleotidyl transferase-mediated dUTP nick end labeling (TUNEL) using an established method to assay for cell death-associated DNA double-strand breaks (16).

Immunohistochemical analysis. Immunohistochemical analyses of human tissues were done with the approval of The Johns Hopkins University Institutional Review Board. Sections of a microarray (3-4 μ m) of paraffin-embedded tissues were used for immunohistochemistry. The tissue microarray was deparaffinized in fresh xylenes and rehydrated through sequential graded ethanol steps. Antigen retrieval was done by citrate buffer incubation [18 mmol/L citric acid, 8 mmol/L sodium citrate (pH 6)] using a household vegetable steamer (Black & Decker, Shelton, CT) for 60 minutes. The microarray was incubated for 5 minutes with 3% H₂O₂, washed in 20 mmol/L Tris, 140 mmol/L NaCl, and 0.1% Tween

20 (pH 7.6), and incubated with the mouse monoclonal antibody to 20S proteasome subunit α 4 HC6 (Affiniti Research Products) diluted 1:250 for 60 minutes at room temperature. The avidin-biotin-peroxidase complex method from DAKO (Glostrup, Denmark) was used to visualize antibody binding, and the tissues were counterstained with hematoxylin. For immunohistochemical analyses of mouse tissues, tumors from mice were excised, fixed in 10% neutral buffered formalin, and embedded in paraffin according to standard histologic procedures. For microvessel density (MVD) assay, 10- μ m frozen sections were briefly fixed in acetone and immunohistochemically stained for mouse CD34 expression. MVD was determined by light microscopy. Neovascularized areas were identified by scanning tumor sections at low-power magnification (\times 40) and then counted at high-power magnification (\times 200). Five separate \times 200 field were analyzed per each condition.

Results

Proteasomal overexpression is associated with ovarian cancer cells *in vivo* and *in vitro*. It has been reported that proteasomes are expressed at abnormally high levels in various hematopoietic tumor cells, including leukemic cells (17, 18). We sought to determine whether the link between proteasomal overexpression and malignant transformation is restricted to hematologic tumors or it can be expanded to other tumor malignancies, particularly ovarian carcinoma. Therefore, we examined whether increase in proteasomal levels could be documented in ovarian tumors compared with normal surface epithelium. The expression pattern of the 20S proteasome was assessed in specimens of benign adenofibroma, low-grade ovarian carcinomas, and high-grade ovarian carcinomas by immunocytochemical analysis. The results showed that cells of both low-grade and high-grade serous carcinomas are associated with more robust 20S proteasome (anti- α 4) staining than the ovarian surface epithelial cells in serous adenofibroma (Fig. 1A). A semiquantitative analysis of the staining intensity is given in Fig. 1B. Although the 20S staining was slightly slower in low-grade compared with high-grade serous carcinoma, this difference did not reach statistical significance. Several other 20S proteasomal subunits were found to be similarly up-regulated in malignant versus benign tumors (data not shown), suggesting that this phenomenon is not restricted to the α 3 subunit. Consistent with the immunocytochemical study, semiquantitative immunoblot analyses showed that both low-grade and high-grade serous carcinomas are associated with the significantly ($P < 0.02$) higher relative levels of 20S and 19S proteasomal subunits when compared with benign cystadenoma (Supplementary Fig. S1A). A semiquantitative analysis of the ratio between 26S proteasome and actin *in vivo* is given in Fig. 1C. Again, the proteasomal subunit levels were lower in low-grade versus high-grade serous carcinoma, but the difference was not statistically significant.

To establish a suitable *in vitro* model for investigating the biological significance of proteasomal levels in ovarian cancer, we tested if the trend of proteasomal overexpression occurred in ovarian cancer cell lines compared with immortalized, but not tumorigenic, surface epithelial cells (IOSE). A panel of IOSEs (IOSE-29, IOSE-397, IOSE-4p2, and IOSE-2Ap2) and ovarian cancer cell lines (OVCA3, SKOV-3, and ES-2) and a new murine model of epithelial ovarian cancer (MOSEC) was tested for the expression of 19S and 20S proteasome subunits. In line with the *in vivo* profile of proteasome expression, all the ovarian cancer cell lines tested show considerably higher levels of 20S and 19S proteasome subunits when compared with IOSE (Supplementary Fig. S1B). A semiquantitative analysis of the ratio between

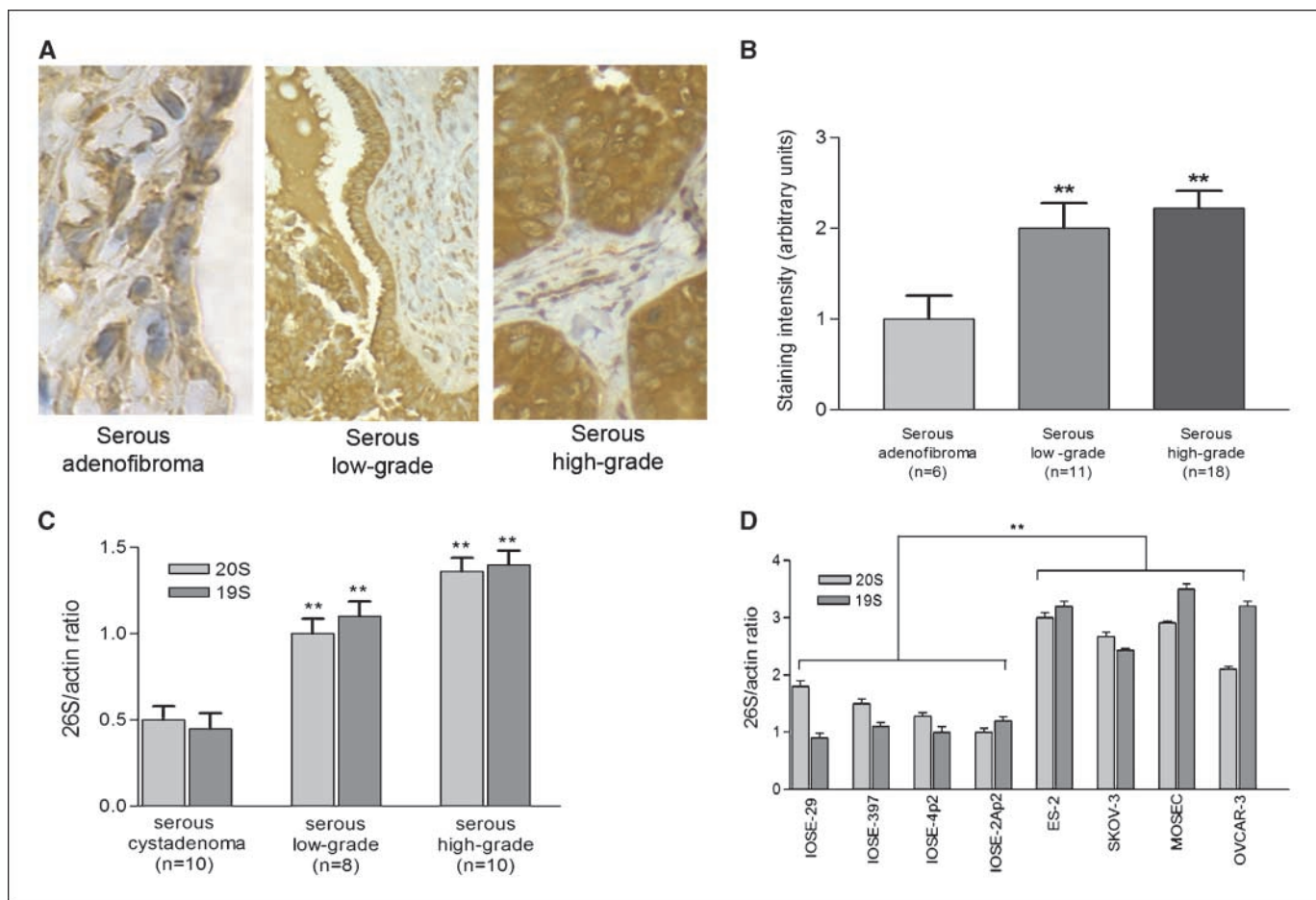


Figure 1. *In vivo* and *in vitro* proteasomal overexpression in ovarian carcinoma. *A*, immunohistochemical staining of $\alpha 4$ subunit of 20S proteasome in ovarian tumors. Representative examples of intense 20S staining in serous high-grade ($\times 40$) and low-grade ($\times 40$) ovarian carcinomas and weaker staining in serous adenofibroma ($\times 100$). *B*, staining intensity for each case was graded as 0 (no staining), 1 (weak staining), 2 (moderate staining), and 3 (intense staining). **, $P < 0.02$, statistical significance in staining intensities among indicated groups (Mann-Whitney U test). *C*, tissue lysates were immunoblotted with an antibody recognizing subunits of the 19S or 20S proteasome. Ratio between 26S proteasome ($\alpha 3$ and Rpt4 subunits) and β -actin in tissue lysates from serous cystadenoma (10 cases) and low-grade serous ovarian carcinoma (8 cases) or high-grade serous ovarian carcinoma (10 cases). **, $P < 0.02$. *D*, ratio between 26S proteasome ($\beta 4$ and Rpt4 subunits) and β -actin in cell lysates of IOSEs (IOSE-29, IOSE-397, IOSE-4p2, and IOSE-2Ap2) and ovarian cancer cell lines (ES-2, SKOV-3, MOSEC, and OVCAR-3).

26S proteasome and actin in IOSEs and ovarian cancer cell lines is given in Fig. 1D.

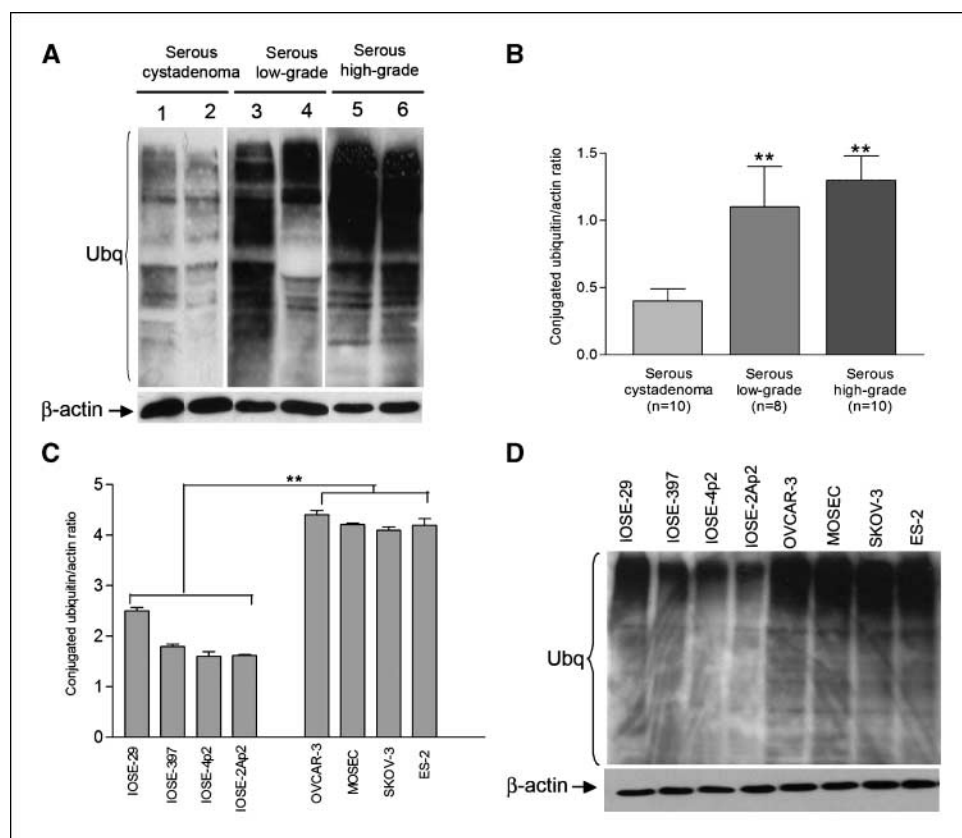
***In vivo* and *in vitro* evidence of UPS stress in ovarian cancer.**

The UPS system is responsible for the degradation of polyubiquitinated proteins within the cells (1). Because ovarian cancer cells express abnormally high levels of 26S proteasome *in vivo* and *in vitro*, we next asked whether alteration in the levels of polyubiquitinated proteins is associated with proteasomal overexpression. Immunoblot analysis of polyubiquitinated protein expression in serous cystadenoma (10 cases) and low-grade (8 cases) and high-grade (10 cases) serous carcinomas revealed that ovarian cancer cells of both low-grade and high-grade serous carcinomas are associated with more robust anti-ubiquitin staining than epithelial cells of serous cystadenoma (Fig. 2A). A semiquantitative analysis of the polyubiquitinated protein levels show that the actin-normalized levels of polyubiquitinated proteins are ~2- to 3-fold higher in malignant tumors compared with cystadenoma (Fig. 2B). Consistent with these *in vivo* findings, immunoblot analysis of IOSEs (IOSE-29, IOSE-397, IOSE-4p2, and IOSE-2Ap2) and ovarian cancer cell lines (OVCAR-3, MOSEC, SKOV-3, and ES-2) revealed that polyubiquitinated proteins are

present at significantly higher levels ($P < 0.02$) in cancer cell lines versus their immortalized but nontumorigenic ovarian surface epithelial cell lines (Fig. 2C). A representative example of immunoblot analysis of polyubiquitinated in IOSEs and ovarian cancer cell lines is given in Fig. 2D. Thus, despite the increase in proteasomal levels, ovarian cancer cells accumulate more polyubiquitinated proteins. Taken together, these results suggest that ovarian cancer cells are under greater UPS stress than their normal counterpart.

Proteasomal inhibition induces G₂-M cell cycle arrest and caspase-mediated apoptosis in ovarian cancer cell lines. The higher demand for proteasomal activity in ovarian cancer cell lines versus their nontransformed counterpart may render the cells more sensitive to proteasomal inhibition. To test this hypothesis, we compared the effect of the proteasome inhibitors MG132 and epoxomicin on the panels of IOSEs (IOSE-29, IOSE-397, IOSE-4p2, and IOSE-2ap2) and ovarian cancer cell lines (OVCAR-3, SKOV-3, ES-2, and JH-514, which is derived from a low-grade serous carcinoma and the mouse ovarian cancer model MOSEC). Both MG132 and epoxomicin (Fig. 3A, *left* and *right*, respectively) diminished cell viability of ovarian cancer cell lines by 24 hours of

Figure 2. UPS stress in ovarian cancer. **A**, level of ubiquitinated proteins was evaluated in lysate from clinical specimens of serous cystadenoma (10 cases; lanes 1 and 2), low-grade serous ovarian carcinoma (8 cases; lanes 3 and 4), or high-grade serous ovarian carcinoma (10 cases; lanes 5 and 6). **B**, ratio between ubiquitinated proteins in clinical specimens and β -actin. **, $P < 0.02$. **C**, ratio between ubiquitinated proteins and actin was evaluated in lysate of IOSEs (IOSE-29, IOSE-397, IOSE-4p2, and IOSE-2Ap2) and ovarian cancer cell lines (SKOV-3, ES-2, MOSEC, and OVCAR-3). **, $P < 0.02$. **D**, representative immunoblot using lysate from IOSEs (IOSE-29, IOSE-397, IOSE-4p2, and IOSE-2Ap2) and ovarian cancer cell lines (OVCAR-3, MOSEC, SKOV-3, and ES-2) with an antibody recognizing conjugated ubiquitin.



treatment in a dose-dependent manner. In contrast, the IOSEs were resistant to high concentrations of both MG132 and epoxomicin (Fig. 3A, left and right, respectively).

The UPS modulates levels of key cell cycle regulatory proteins whose dysregulation is expected to affect the cell cycle and viability (19, 20). To test whether the reduced cell viability of ovarian cancer cell lines is associated with cell cycle dysregulation, ES-2 cells were incubated for various times with the proteasome inhibitor MG-132 and the cell cycle status was analyzed by flow cytometry after staining with PI. After 24-hour incubation with MG132, the percentage of cells in G₀-G₁ phase was reduced by nearly half compared with control, with the treated cells accumulating in S and G₂-M (Fig. 3B, left and right, respectively). To investigate the fate of the cells accumulated in G₂-M following proteasomal inhibition, we analyzed them by flow cytometric after staining with Annexin V. Annexin V protein specifically binds phosphatidylserine; this phospholipid is normally localized on the inner leaflet of the plasma membrane but flips to the outer leaflet during early apoptotic signaling (21). As shown in Supplementary Fig. S1C, treatment with 20 μ Mol/L MG132 for 8 hours results in an increase in Annexin V staining cells (4.8% in control versus 35.5% in MG132-treated). Similarly, the fraction of cells taking up PI, a feature of both advanced apoptosis and necrosis, is elevated from 6.5% in control to 22.4% in treated cells. These findings support our hypothesis that proteasomal inhibition triggers apoptosis in ovarian cancer cells.

Progression through the phases of cell cycle is regulated by periodic activation of several cyclin-dependent kinases (CDK) whose levels are controlled through ubiquitination and proteasomal degradation (20, 22, 23). In particular, levels of CDK inhibitors (CDKI) p21^{WAF1} and p27^{KIP1} have been shown previously to be

dysregulated following proteasomal inhibition (24–28). Western blot analysis of the levels of p21^{WAF1} and p27^{KIP1} in ovarian cancer cell lines (ES-2) following MG-132 treatment revealed an accumulation of both p21^{WAF1} and p27^{KIP1} starting at 16 hours after inhibition. These data suggest a role for p21^{WAF1} and p27^{KIP1} in blocking the G₂-M transition of the cells after proteasomal inhibition. The induction of p21^{WAF1} and apoptosis on proteasomal inhibition suggested a possible role for p53 in apoptosis. To address this possibility, we explored the relative levels of the 19S and 20S proteasome subunits in serous carcinoma specimens with wild-type and mutant p53. A similar elevation in proteasomal subunit levels was observed between these serous carcinoma specimens with respect to serous cystadenoma (Supplementary Fig. S2A and B). Similarly, there was no significant difference in the levels of polyubiquitinated proteins in p53 wild-type versus mutant serous carcinoma specimens, although both were elevated with respect to serous cystadenoma specimens (Supplementary Fig. S2C and D). Finally, three ovarian cancer cell lines bearing wild-type p53 exhibited similar proliferation rates and sensitivity to proteasomal inhibition-induced apoptosis as three lines bearing null or mutated p53 (Supplementary Fig. S2E and F). Taken together, these findings suggest that cell death induced by proteasomal inhibition occurs independently of p53 mutation status.

Furthermore, cleavage products of both CDKs p21 and p27 (19- and 22-kDa bands, respectively) were also detected in ES-2 cell lysate collected 24 hours after addition of the proteasome inhibitor MG132, suggesting caspase-3 activation as the apoptotic mechanism associated with the decrease in cell viability (Fig. 3C; ref. 20).

To confirm that activation of caspase-3 was induced by proteasome inhibitors, subconfluent ES-2 cells were treated for up

to 24 hours with 20 $\mu\text{mol/L}$ MG132 or 1 $\mu\text{mol/L}$ epoxomicin and the caspase-3 activity was evaluated by measuring the cleavage of the caspase-3-specific substrate Ac-DEVD-pNA. Proteolytic activity for the caspase-3-specific substrate was detected in ES-2 cell lysate starting at 16 hours after addition of proteasome inhibitors, increasing ~ 10 -fold by 24 hours of treatment (Fig. 3D, left). To determine whether caspase-3 activation was entirely responsible for proteasome inhibitor-induced cell death, caspase-3-specific (Ac-DEVD-CMK) and pan-caspase (Z-VAD-CMK) inhibitors were tested. Whereas pan-caspase inhibition results in almost complete protection, caspase-3 inhibition provides only partial protection from cell death in the presence of MG132 or epoxomicin. This result indicated that although proteasomal inhibition caused cell death via activation of caspases there may be more than one effector caspase involved (Fig. 3D, right).

Proteasomal sensitivity is dependent on proliferation rate and UPS stress. A correlation between proliferation rate and proteasome inhibitor-mediated apoptosis has been shown previously in rapidly proliferating leukemic and endothelial cells versus their quiescent counterparts (4, 5, 9, 26, 29). Thus, we hypothesized that the differential effect in terms of cell viability following proteasomal inhibition may be associated with the greater proliferation rates of ovarian cancer cell lines versus the IOSE counterpart. To test this hypothesis, we examined whether the previously characterized IOSEs and ovarian cancer cell lines proliferate at different rates. Consistent with their greater sensitivity to proteasome inhibitor-induced cell death, the proliferation rate of ovarian cancer cell lines was significantly ($P < 0.02$) higher than in IOSEs (Fig. 4A). To exclude that the difference in sensitivity was a cell type-dependent effect and to

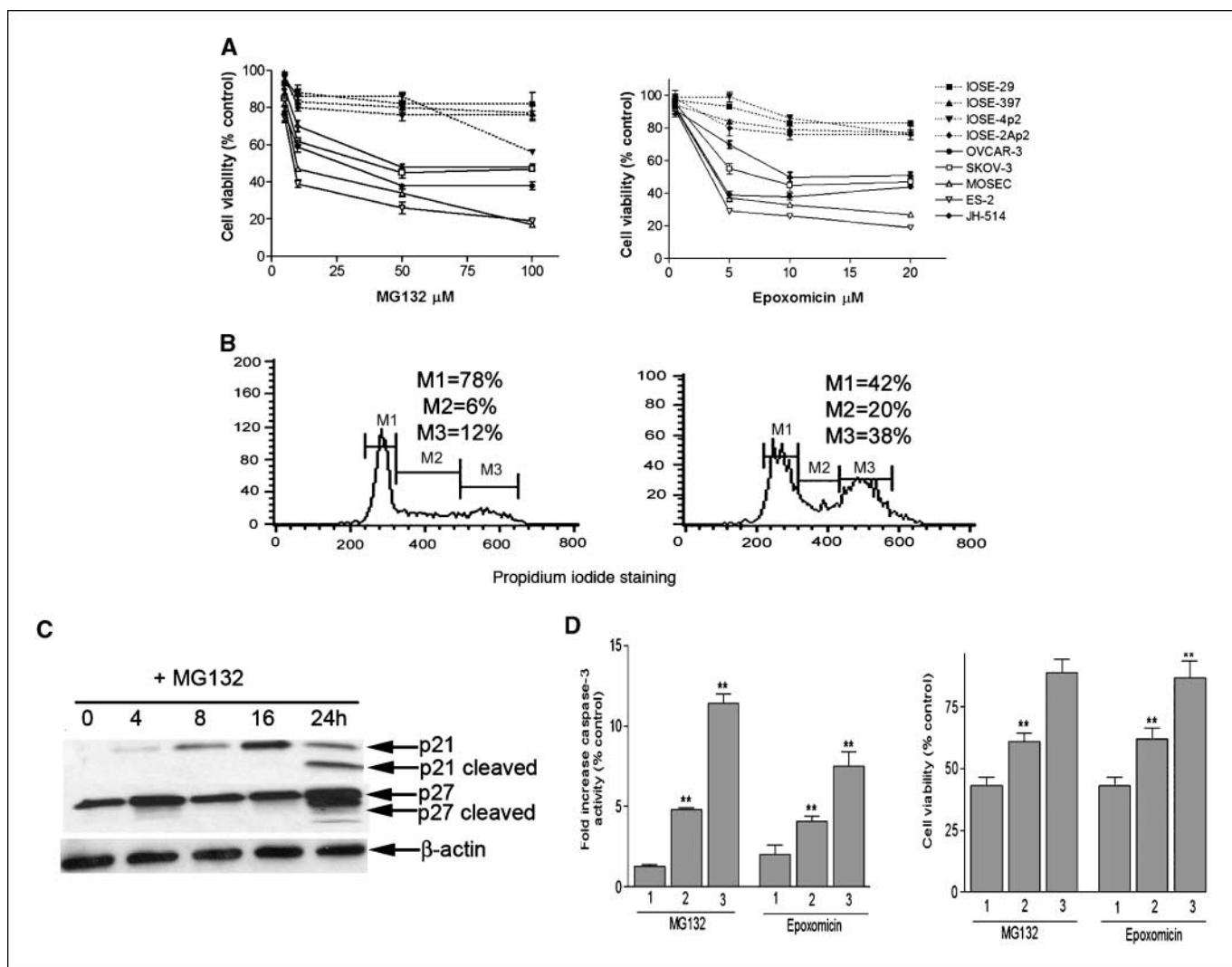


Figure 3. Proteasomal inhibition induces G₂-M cell cycle arrest and caspase-mediated apoptosis in ovarian cancer cell lines. **A**, dose-dependent inhibition of the cell viability of ovarian cancer cell lines and IOSEs using proteasome inhibitors. Cell viability was measured by XTT assay after culturing the cells for 24 hours in presence of MG132 (left) or epoxomicin (right) at the concentrations indicated. Percentage of viable cells relative to mock-treated controls. **B**, cell cycle distribution of ES-2 cells, either mock treated (left) or treated with 20 $\mu\text{mol/L}$ MG132 (right) for 24 hours, was evaluated by PI staining and flow cytometric analysis. Percentage G₁ phase (M1), S phase (M2), and G₂-M phase (M3). **C**, lysate of ES-2 cells that had been treated with 20 $\mu\text{mol/L}$ MG132 for the time indicated was immunoblotted with antibodies recognizing p21 and p27 and their corresponding cleavage products. Equal protein loading was verified by using an antibody directed against β -actin. **D**, ES-2 cells were treated for 8, 16, or 24 hours (1-3, respectively) in the presence of MG132 (20 $\mu\text{mol/L}$) or epoxomicin (5 $\mu\text{mol/L}$) and the caspase-3 activity was then evaluated by measuring the cleavage of the caspase-3-specific substrate Ac-DEVD-pNA (left). Fold increase caspase-3 activity relative to control. **, $P < 0.02$. Right, ES-2 cells were treated for 24 hours with 20 $\mu\text{mol/L}$ MG132 or 5 $\mu\text{mol/L}$ epoxomicin alone (column 1) in the presence of caspase-3-specific inhibitor Ac-DEVD-CMK (column 2) or pan-caspase inhibitor Z-VAD-CMK (column 3) and the cell viability was then tested by XTT assay. Percentage of viable cells relative to mock treated controls. **, $P < 0.02$.

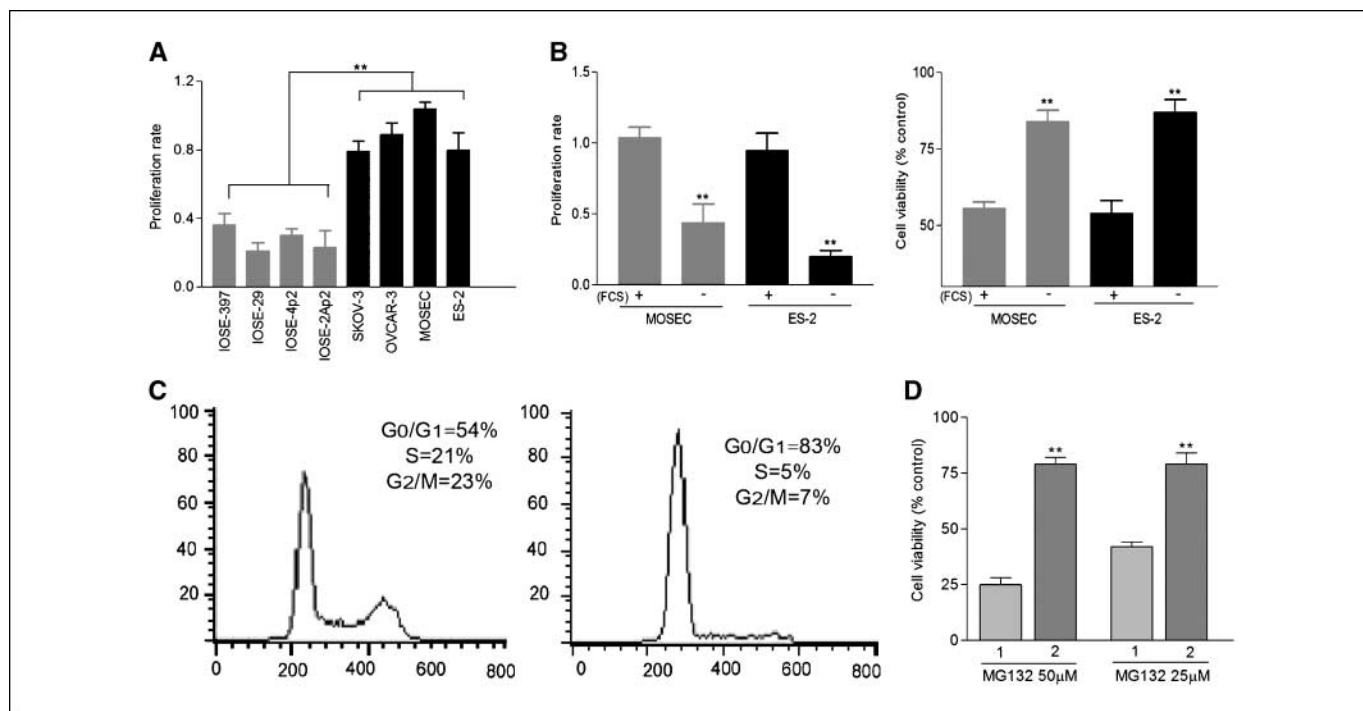


Figure 4. Sensitivity to proteasome inhibitors is dependent on proliferation rate and UPS stress. *A*, proliferation rate of IOSEs and ovarian cancer cell lines measured by XTT assay under normal culture conditions (i.e., 10% FCS). Results are expressed in terms of daily proliferation rate. **, $P < 0.02$. *B*, proliferation rate (left; expressed in terms of daily proliferation rate) and viability (right; expressed as percentage of viable cells relative to mock-treated controls) of ovarian cancer cell lines (ES-2 and MOSEC) measured by XTT assay after culturing them in presence of 10% (+) or 0.1% (-) FCS. **, $P < 0.02$. *C*, subconfluent (left) and confluent (right) ES-2 cell lines were analyzed by PI staining and flow cytometric analysis to determine their cell cycle distribution. Insets, corresponding percentage of cells in G₀-G₁, S, and G₂-M phases of the cell cycle. *D*, cell viability of subconfluent (1) and confluent (2) ES-2 cell line was evaluated presence of either 25 or 50 μmol/L MG132. Percentage of viable cells relative to mock treated controls. **, $P < 0.02$.

more directly link the proliferation rate with the proteasomal sensitivity, we lowered the proliferation rate of MOSEC and ES-2 ovarian cancer cell lines by two independent methods and tested sensitivity to proteasomal inhibition in relation to proliferation rate.

In the first set of experiments, the proliferation rate of MOSEC and ES-2 cell lines was compared under normal culture conditions (10% FCS) and after an extended period of serum starvation (0.1% FCS). Ovarian cancer cell lines cultured in presence of 10% FCS grow exponentially, whereas under serum starvation the level of cell proliferation is significantly reduced ($P < 0.02$; Fig. 4*B*, left). Normally cultured or starved MOSEC and ES-2 cells were subsequently subjected to proteasomal inhibition and the viability was determined compared with control untreated cells (Fig. 4*B*, right). Whereas the proteasomal inhibition leads to significantly attenuated cell viability in the proliferating ES-2 and MOSEC cells in 10% FCS, serum starvation protects ES-2 and MOSEC cells from the cytotoxic effects of proteasome inhibitor (Fig. 4*B*, right). This effect is dose dependent and is seen with epoxomicin treatment (data not shown).

For the second set of experiments, the proliferation rate of ES-2 cells was slowed by contact inhibition, and the sensitivity to proteasomal inhibition was tested. After 3 days in culture, ES-2 cells plated at high density were 100% confluent, whereas those plated at low density were subconfluent ($\leq 50\%$; data not shown). Fluorescence-activated cell sorting analysis confirmed that the percentage of ES-2 cells within the G₀-G₁ phase of the cell cycle was 83% in confluent cultures compared with 54% of subconfluent ES-2 cells (Fig. 4*C*, left and right, respectively). Under these conditions,

reduction of the cell viability for subconfluent ES-2 cell is significantly ($P < 0.02$) higher than for confluent ES-2 cells in the presence of either 25 or 50 μmol/L MG132, whereas vehicle alone had no effect (Fig. 4*D*).

Because a decreased proliferation rate of the ovarian cancer cells led to a significant decrease in the toxicity associated with proteasomal inhibition, we examined whether a decrease in proliferation rate of cells is similarly accompanied by a reduction in UPS stress. First, we examined the levels of 20S proteasome in ovarian cancer cells after either 4 or 15 days of serum starvation in comparison with cells in standard culture conditions (10% FCS). The results show that proteasome levels are maintained at high levels for up to 4 days of serum starvation, consistent with the known long half-life of the proteasome, but significantly decrease with prolonged serum starvation up to 15 days (Fig. 5*A*). The ES-2 ovarian cancer cells already show attenuated sensitivity to proteasomal inhibition by the third day of starvation, although proteasome levels are still high, suggesting that proteasome levels are not the primary determinant of sensitivity to proteasome inhibitor in ovarian cancer cell lines.

We then evaluated the overall levels of ubiquitinated proteins as a function of cell proliferation. The immunoblot analysis shows that the levels of ubiquitinated proteins decrease rapidly with serum starvation and better correlate with timing of decreased sensitivity to proteasomal inhibition (Fig. 5*B*). This implies that the degree of UPS stress more directly relates to rate of proliferation and sensitivity to proteasomal inhibition than the absolute level of proteasome. A semiquantitative analysis of the ratio between 20S proteasome and β-actin in normally cultured and serum-starved

ovarian cancer cell lines is given in Fig. 5C, whereas the semiquantification between polyubiquitinated proteins and β -actin is given in Fig. 5D.

In vivo activity of proteasome inhibitor PS-341 against an ovarian cancer xenograft. The proteasome inhibitor PS-341/Velcade has shown efficacy for the treatment of multiple myeloma as well as other hematologic and solid tumors (30, 31). Our observation that ovarian cancer cells, like multiple myeloma, exhibit significant UPS stress *in vivo* and enhanced sensitivity to proteasome inhibitor-induced apoptosis *in vitro* suggests the potential for therapeutic responses to treatment of ovarian cancer with proteasome inhibitors *in vivo*. Therefore, the ability of proteasome inhibitor PS-341 to inhibit ES-2 tumor growth was examined with a mouse xenograft model of ovarian cancer. BNX mice were inoculated s.c. in the right flank with 1×10^7 ES-2 cells and 93% animals developed a measurable tumor after within 7 days of inoculation. Mice were then randomly assigned to PS-341 treatment group (1 mg/kg; $n = 15$) or 0.9% normal saline-treated control groups ($n = 15$) and treated by i.v. injection twice weekly. The average tumor volume was 212 mm^3 at the initiation of treatment with no significant difference in tumor volume between treatment and control groups at day 0. As shown in Fig. 6A, a significant reduction in tumor volume was observed in mice treated with PS-341 versus the control group by day 5 of treatment

($P < 0.05$). The difference became more significant by day 9 ($P < 0.0001$), whereupon some control animals were sacrificed due to their large tumor burden. A survival curve for mice in each group is shown in Fig. 6B. A log-rank test revealed a significant prolongation in overall survival in animals treated with PS-341 versus controls ($P < 0.0001$). Notably, by day 18 of treatment, all of the control mice were sacrificed due to their tumor burden, whereas only 15% of mice in the PS-341 treatment arm had to be euthanized. Our *in vitro* study clearly indicated that the viability of ovarian cancer cells is highly compromised following proteasomal inhibition due to the rapid onset of apoptosis. Further, to investigate the *in vivo* effect of PS-341, tumor sections harvested from control mice and mice treated with proteasome inhibitor were subjected to TUNEL assay and scored outside of necrotic regions. As shown in Fig. 6C, whereas the percentage of apoptotic cells in the control group is 7.2% (SE ± 1.3) and the percentage of apoptotic figures in PS-341 animals is 53.8% (SE ± 4.1). Previous studies have shown an antiangiogenic effect of proteasome inhibitors as a result of apoptotic effect on endothelial cells. To assess the relative contribution of the antiangiogenic effect of the reduction of tumor growth after PS-341 treatment, tumor sections harvested from control mice and mice treated with proteasome inhibitor were evaluated for MVD by immunohistochemical analysis for CD34 expression. As shown in Fig. 6D, we found a

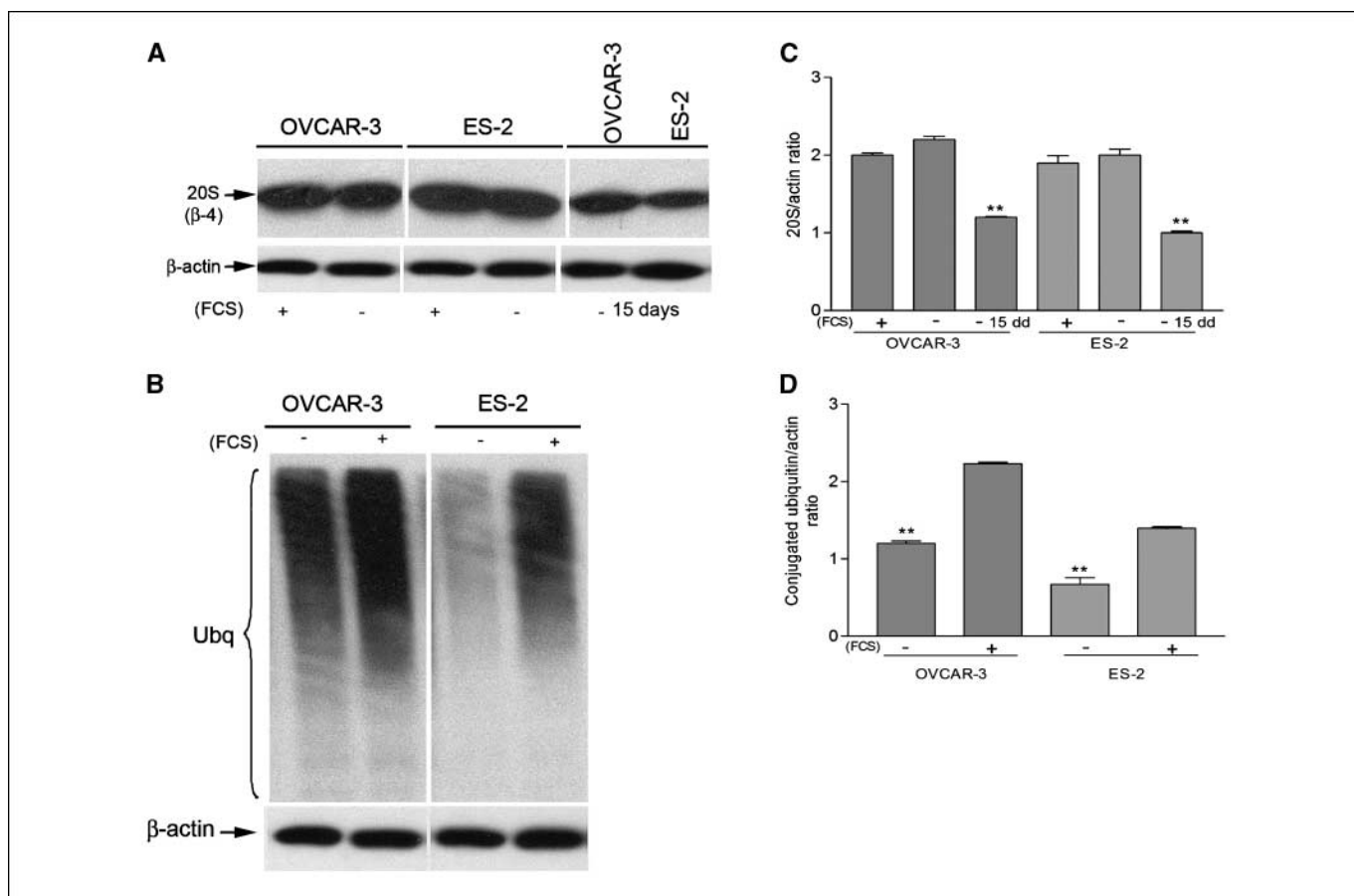


Figure 5. Levels of UPS stress regulate the sensitivity to proteasome inhibitors. *A*, lysate of OVCAR-3 and ES-2 cultured in presence of 10% FCS (+), 0.1% FCS over a period of 4 days (-), or 0.1% FCS over a period of 15 days (-15 days) was immunoblotted with an antibody recognizing the β 4 subunit of the 20S proteasome. *B*, lysate of OVCAR-3 and ES-2 cultured in presence of 10% FCS (+) or 0.1% FCS over a period of 4 days (-) was immunoblotted with an antibody recognizing conjugated ubiquitin. Equal protein loading in all four panels was verified by using an antibody directed against β -actin. Quantitation of the ratio between 20S proteasome subunit (*C*) or conjugated ubiquitin (*D*) versus actin protein levels is presented. ** $P < 0.02$.

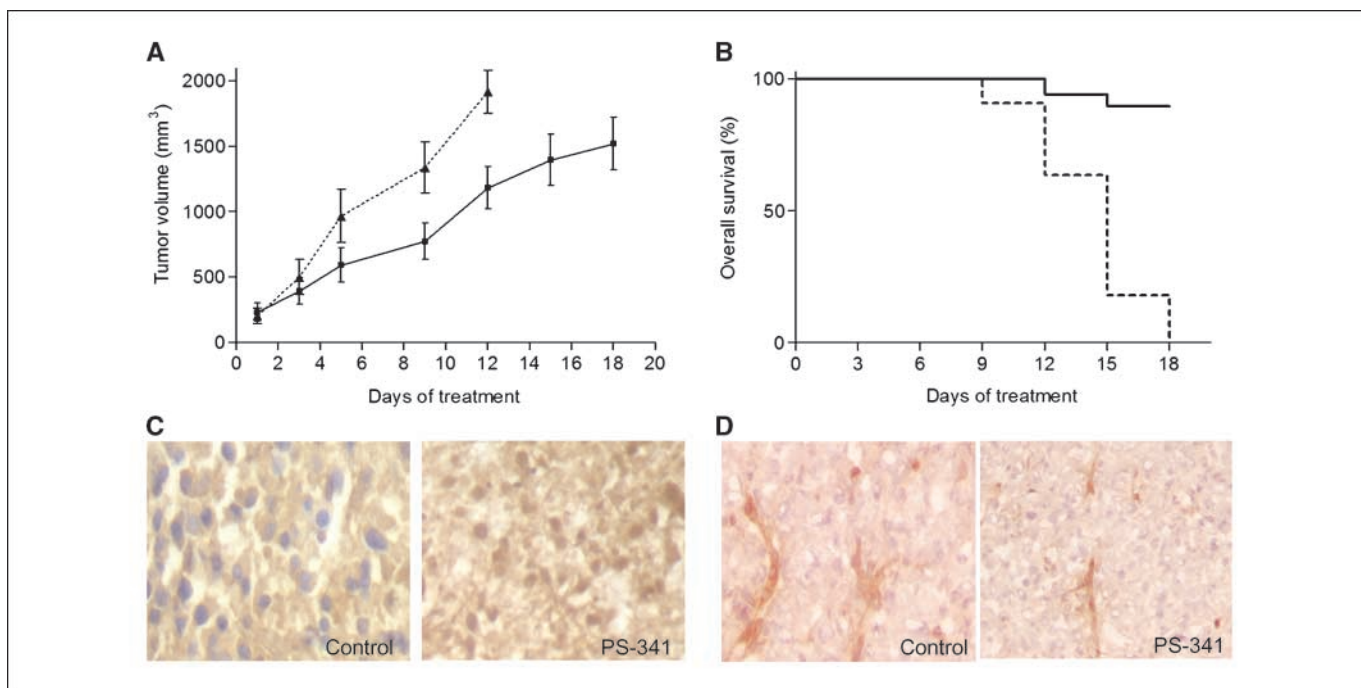


Figure 6. Proteasome inhibitor PS-341 inhibits growth of ES-2 xenograft. **A**, BNX mice were inoculated with 1×10^7 ES-2 in the right flank. On detection of measurable tumor (day 1), mice were treated twice weekly with i.v. injection of 1 mg/kg proteasome inhibitor PS-341 ($n = 15$; solid line) or 0.9% saline ($n = 15$; dotted line). Caliper measurement of the longest perpendicular tumor diameters was done to estimate the tumor volume (mean \pm SE; mm^3), using the following formula: $4\pi / 3 \times (\text{width} / 2)^2 \times (\text{length} / 2)$, corresponding to the three-dimensional volume of an ellipse. Statistically significant differences in terms of tumor growth were observed starting from the day 2 after the first treatment ($P \leq 0.05$) and increased over the time ($P \leq 0.001$). **B**, effect of PS-341 on survival of mice bearing ES-2 xenograft. Survival was evaluated from the first day after the treatment until all the control group mice had to be sacrificed (tumor diameter, 2 cm). A significant difference in overall survival between PS-341-treated and control animals ($P < 0.001$) by log-rank test. **C**, TUNEL assay done on histologic specimens from a control mouse (left) and mouse treated with 1 mg/kg PS-341 (right). **D**, representative tumor sections from a control mouse (left) and from a PS-341 mouse (right) evaluated for MVD staining for CD34.

statistically significant decrease in terms of MVD in sections obtained from PS-341-treated versus control mice: 16.8 ± 5.3 blood vessels per high-power field ($\times 200$) in control versus 36.1 ± 7.7 in PS-341-treated mice ($P = 0.05$).

Discussion

In this study, we show that up-regulation of proteasome subunit levels occurs in ovarian cancer *in vivo* and *in vitro*. However, despite the up-regulation of total proteasome levels, ovarian carcinogenesis is associated with increased accumulation of polyubiquitinated proteins. This suggests that the up-regulation of the proteasome levels is insufficient to meet the increased demand generated by the greater metabolic rate of ovarian cancer cells, and this situation is reflected in greater UPS stress. Consistent with this evidence of increased proteasomal stress in ovarian carcinoma *in vivo* and *in vitro*, ovarian cancer cell lines show increased sensitivity to proteasome inhibitor-induced apoptosis *in vitro*. Furthermore, treatment with a proteasome inhibitor slows the growth of a human ovarian cancer xenograft model in mice.

Alteration in proteasomal expression and activity has been linked previously to a variety of biological and pathologic conditions (32–37). In this study, we show that the up-regulation of proteasome protein levels not only is a phenomenon confined to malignancies of hematopoietic origin but also occurs in ovarian cancer. This suggests that, as in leukemic cells, ovarian cancer cells may have a greater requirement for proteasomal activity than their untransformed counterpart. We cannot rule out that the additional

proteasomes are not fully functional perhaps because a component is not coordinately up-regulated and is therefore rate limiting. However, our analysis shows that all the proteasome subunits tested (consisting of α , β , and 19S subunits) are coordinately up-regulated.

A correlation between proliferation rate and proteasome inhibitor-mediated apoptosis has been found previously in rapidly proliferating leukemic and endothelial cells versus their quiescent counterpart (4, 5). Our study also extends these previous finding by showing that level of UPS stress and sensitivity to proteasomal inhibition both correlate with cell proliferation rate. Specifically, we show that a decrease in proliferation rate of ovarian cancer cell lines leads to a significant decrease of polyubiquitinated proteins levels and decreased toxicity of proteasomal inhibition without changes in the proteasome levels. Thus, cellular levels of UPS stress more directly relate to rate of proliferation and sensitivity to proteasomal inhibition than the absolute levels of proteasome subunits. The decrease in proliferation rate is accompanied by reduction in sensitivity to proteasomal inhibition, whereas the steady levels of 20S proteasome subunits are maintained at high levels for up to 4 days of serum starvation. However, with continued serum starvation, the proteasome levels decrease. This is consistent with the known long half-life of the proteasome (38). Thus, our findings show that the degree of UPS stress regulates the levels of proteasome expression in cells.

Proteasome inhibitors can induce apoptosis by targeting various classes of protein involved in the regulation of the cell cycle (19). Prior investigations have shown that proteasomal inhibition of several types of solid tumors blocks the cells at the G_2 -M phase

of the cell cycle (24–26, 39). In this study, we show treatment of ovarian cancer cell lines with proteasome inhibitors caused accumulation of p21^{WAF1} and p27^{KIP1}, whose levels are regulated by the UPS, and accumulation of the cells in G₂-M phase. The concomitant accumulation of the cells in G₂-M of the cell cycle together with accumulation of CDKs, such as p21^{WAF1} and p27^{KIP1}, is actually consistent. Although p21^{WAF1} is typically associated with arrest in G₁-S transition, a role for p21^{WAF1} at the G₂-M-phase transition has also been proposed (25). This suggests that accumulation of p21^{WAF1} and p27^{KIP1} following proteasomal inhibition may cause a temporary stall of the cells in G₁ followed by a block in G₂-M. Further, studies have shown that pro-caspase-3 overexpression sensitizes ovarian cancer cells to proteasome inhibitor-induced apoptosis (40, 41). This may occur via Bik/NBK stabilization (42). Here, we show that although caspase-3 activation is certainly involved in proteasome inhibitor-mediated cell death, caspase-3 is not entirely responsible for the apoptotic process on proteasomal inhibition. This is consistent with a study of mediators of endoplasmic reticulum stress-induced cell death on proteasomal inhibition showing activation of caspase-12 and caspase-8 in addition to caspase-3 (43).

PS-341 represents a novel class of myeloma therapy, several studies have shown the efficacy of the proteasome inhibitor PS-341 in a variety of tumor cell lines, and its synergistic antitumor activity has been shown in combination with other chemotherapy (8, 44–47). Our *in vitro* data suggest a differential sensitivity of highly proliferating ovarian cancer cells to proteasomal inhibition. Such selectivity suggests proteasome inhibitors as a candidate new

chemotherapeutic agent for ovarian cancer treatment. The current study provides *in vivo* evidence suggesting that trials of PS-341 in patients with ovarian cancer are warranted perhaps in combination with other chemotherapeutic agents. Indeed, a phase I trial of bortezomib in recurrent ovarian or primary peritoneal cancer is currently in progress (14). Treatment of mice bearing palpable ovarian cancer xenograft with PS-341 profoundly retarded tumor growth. Consistent with the *in vitro* effects of the proteasome inhibitors, we observed a profound increase in the level of apoptosis in ES-2 xenograft of treated mice. Further, a ~50% reduction in the MVD was observed within the ES-2 tumor of treated mice. This is also in line with the previously described antiangiogenic effects of proteasome inhibitors (46, 48–50), although the mechanism driving these effects is poorly understood. These findings are particularly encouraging given our evidence of significant UPS stress in ovarian carcinoma specimens and numerous studies showing the importance of angiogenesis in development of ovarian cancer.

Acknowledgments

Received 7/1/2005; revised 12/29/2005; accepted 1/20/2006.

Grant support: HERA Foundation (M. Bazzaro and A. Santillan) and Department of Defense Ovarian Cancer Congressionally Directed Medical Research Program OC010017 (R.B.S. Roden).

The costs of publication of this article were defrayed in part by the payment of page charges. This article must therefore be hereby marked *advertisement* in accordance with 18 U.S.C. Section 1734 solely to indicate this fact.

We thank Drs. Nelly Auesperg, Hidetaka Katabuchi, and Katherine F. Roby for the gift of cell lines and Millenium Pharmaceuticals for the gift of PS-341.

References

- Ciechanover A. The ubiquitin-proteasome proteolytic pathway. *Cell* 1994;79:13–21.
- Baumeister W, Walz J, Zuhl F, Seemuller E. The proteasome: paradigm of a self-compartmentalizing protease. *Cell* 1998;92:367–80.
- Ovaa H, Kessler BM, Rolen U, Galardy PJ, Ploegh HL, Masucci MG. Activity-based ubiquitin-specific protease (USP) profiling of virus-infected and malignant human cells. *Proc Natl Acad Sci U S A* 2004; 101:2253–8.
- Soligo D, Servida F, Delia D, et al. The apoptogenic response of human myeloid leukaemia cell lines and of normal and malignant haematopoietic progenitor cells to the proteasome inhibitor PS1. *Br J Haematol* 2001;113: 126–35.
- Drexler HC, Risau W, Konerding MA. Inhibition of proteasome function induces programmed cell death in proliferating endothelial cells. *FASEB J* 2000;14: 65–77.
- Richardson PG, Barlogie B, Berenson J, et al. A phase 2 study of bortezomib in relapsed, refractory myeloma. *N Engl J Med* 2003;348:2609–17.
- Adams J, Kauffman M. Development of the proteasome inhibitor Velcade (bortezomib). *Cancer Invest* 2004; 22:304–11.
- Richardson PG, Hideshima T, Anderson KC. Bortezomib (PS-341): a novel, first-in-class proteasome inhibitor for the treatment of multiple myeloma and other cancers. *Cancer Control* 2003;10:361–9.
- Orlowski RZ, Eswara JR, Lafond-Walker A, Grever MR, Orlowski M, Dang CV. Tumor growth inhibition induced in a murine model of human Burkitt's lymphoma by a proteasome inhibitor. *Cancer Res* 1998;58:4342–8.
- Mitsiades N, Mitsiades CS, Richardson PG, et al. The proteasome inhibitor PS-341 potentiates sensitivity of multiple myeloma cells to conventional chemotherapeutic agents: therapeutic applications. *Blood* 2003;101: 2377–80.
- Rajkumar SV, Richardson PG, Hideshima T, Anderson KC. Proteasome inhibition as a novel therapeutic target in human cancer. *J Clin Oncol* 2005;23:630–9.
- Richardson PG, Mitsiades C, Hideshima T, Anderson KC. Proteasome inhibition in the treatment of cancer. *Cell Cycle* 2005;4:290–6.
- Aghajanian C, Soignet S, Dizon DS, et al. A phase I trial of the novel proteasome inhibitor PS341 in advanced solid tumor malignancies. *Clin Cancer Res* 2002;8:2505–11.
- Aghajanian C. Clinical update: novel targets in gynecologic malignancies. *Semin Oncol* 2004;31:22–6; discussion 33.
- Roby KF, Taylor CC, Sweetwood JP, et al. Development of a syngeneic mouse model for events related to ovarian cancer. *Carcinogenesis* 2000;21:585–91.
- Gavrieli Y, Sherman Y, Ben-Sasson SA. Identification of programmed cell death *in situ* via specific labeling of nuclear DNA fragmentation. *J Cell Biol* 1992;119: 493–501.
- Kumatori A, Tanaka K, Inamura N, et al. Abnormally high expression of proteasomes in human leukemic cells. *Proc Natl Acad Sci U S A* 1990;87:7071–5.
- Shimbara N, Orino E, Sone S, et al. Regulation of gene expression of proteasomes (multi-protease complexes) during growth and differentiation of human hematopoietic cells. *J Biol Chem* 1992;267:18100–9.
- Glotzer M, Murray AW, Kirschner MW. Cyclin is degraded by the ubiquitin pathway. *Nature* 1991;349: 132–8.
- Levkau B, Koyama H, Raines EW, et al. Cleavage of p21^{Cip1/Waf1} and p27^{Kip1} mediates apoptosis in endothelial cells through activation of Cdk2: role of a caspase cascade. *Mol Cell* 1998;1:553–63.
- van Engeland M, Nieland LJ, Ramaekers FC, Schutte B, Reutelingsperger CP. Annexin V-affinity assay: a review on an apoptosis detection system based on phosphatidylserine exposure. *Cytometry* 1998;31:1–9.
- Coulombe P, Rodier G, Bonneil E, Thibault P, Meloche S. N-terminal ubiquitination of extracellular signal-regulated kinase 3 and p21 directs their degradation by the proteasome. *Mol Cell Biol* 2004;24:6140–50.
- Pagano M, Tam SW, Theodoras AM, et al. Role of the ubiquitin-proteasome pathway in regulating abundance of the cyclin-dependent kinase inhibitor p27. *Science* 1995;269:682–5.
- Adams J, Palombella VJ, Sausville EA, et al. Proteasome inhibitors: a novel class of potent and effective antitumor agents. *Cancer Res* 1999;59:2615–22.
- Dulic V, Stein GH, Far DF, Reed SI. Nuclear accumulation of p21^{Cip1} at the onset of mitosis: a role at the G₂-M-phase transition. *Mol Cell Biol* 1998;18:546–57.
- Yin D, Zhou H, Kumagai T, et al. Proteasome inhibitor PS-341 causes cell growth arrest and apoptosis in human glioblastoma multiforme (GBM). *Oncogene* 2005;24:344–54.
- Hideshima T, Richardson P, Chauhan D, et al. The proteasome inhibitor PS-341 inhibits growth, induces apoptosis, and overcomes drug resistance in human multiple myeloma cells. *Cancer Res* 2001;61:3071–6.
- Sun J, Nam S, Lee CS, et al. CEP161, a dipeptidyl proteasome inhibitor, induces p21^{WAF1} and p27^{KIP1} expression and apoptosis and inhibits the growth of the human lung adenocarcinoma A-549 in nude mice. *Cancer Res* 2001;61:1280–4.
- Nasr R, El-Sabban ME, Karam JA, et al. Efficacy and mechanism of action of the proteasome inhibitor PS-341 in T-cell lymphomas and HTLV-I associated adult T-cell leukemia/lymphoma. *Oncogene* 2005;24:419–30.
- Gardner RC, Assinder SJ, Christie G, et al. Characterization of peptidyl boronic acid inhibitors of mammalian 20S and 26S proteasomes and their inhibition of proteasomes in cultured cells. *Biochem J* 2000;346 Pt 2:447–54.
- Rivett AJ, Gardner RC. Proteasome inhibitors: from *in vitro* uses to clinical trials. *J Pept Sci* 2000;6:478–88.
- Petrucelli L, O'Farrell C, Lockhart PJ, et al. Parkin protects against the toxicity associated with mutant α -synuclein: proteasome dysfunction selectively affects catecholaminergic neurons. *Neuron* 2002;36:1007–19.

33. Bence NF, Sampat RM, Kopito RR. Impairment of the ubiquitin-proteasome system by protein aggregation. *Science* 2001;292:1552-5.
34. Johnsen A, France J, Sy MS, Harding CV. Down-regulation of the transporter for antigen presentation, proteasome subunits, and class I major histocompatibility complex in tumor cell lines. *Cancer Res* 1998;58:3660-7.
35. Gobbi G, Mirandola P, Micheloni C, et al. Expression of HLA class I antigen and proteasome subunits LMP-2 and LMP-10 in primary vs. metastatic breast carcinoma lesions. *Int J Oncol* 2004;25:1625-9.
36. Meissner M, Reichert TE, Kunkel M, et al. Defects in the human leukocyte antigen class I antigen processing machinery in head and neck squamous cell carcinoma: association with clinical outcome. *Clin Cancer Res* 2005; 11:2552-60.
37. Shimbara N, Sato C, Takashima M, Tanaka T, Tanaka K, Ichihara A. Down-regulation of ubiquitin gene expression during differentiation of human leukemia cells. *FEBS Lett* 1993;322:235-9.
38. Ciechanover A. The ubiquitin-proteasome pathway: on protein death and cell life. *EMBO J* 1998;17:7151-60.
39. Ling YH, Liebes L, Jiang JD, et al. Mechanisms of proteasome inhibitor PS-341-induced G(2)-M-phase arrest and apoptosis in human non-small cell lung cancer cell lines. *Clin Cancer Res* 2003;9:1145-54.
40. Tenev T, Marani M, McNeish I, Lemoine NR. Pro-caspase-3 overexpression sensitises ovarian cancer cells to proteasome inhibitors. *Cell Death Differ* 2001;8:256-64.
41. Kudo Y, Takata T, Ogawa I, et al. p27^{Kip1} accumulation by inhibition of proteasome function induces apoptosis in oral squamous cell carcinoma cells. *Clin Cancer Res* 2000;6:916-23.
42. Zhu H, Zhang L, Dong F, et al. Bik/NBK accumulation correlates with apoptosis-induction by bortezomib (PS-341, Velcade) and other proteasome inhibitors. *Oncogene* 2005;24:4993-9.
43. Landowski TH, Megli CJ, Nullmeyer KD, Lynch RM, Dorr RT. Mitochondrial-mediated dysregulation of Ca²⁺ is a critical determinant of Velcade (PS-341/bortezomib) cytotoxicity in myeloma cell lines. *Cancer Res* 2005;65: 3828-36.
44. Richardson P. Clinical update: proteasome inhibitors in hematologic malignancies. *Cancer Treat Rev* 2003;29 Suppl 1:33-9.
45. Jagannath S, Barlogie B, Berenson J, et al. A phase 2 study of two doses of bortezomib in relapsed or refractory myeloma. *Br J Haematol* 2004;127:165-72.
46. Sunwoo JB, Chen Z, Dong G, et al. Novel proteasome inhibitor PS-341 inhibits activation of nuclear factor- κ B, cell survival, tumor growth, and angiogenesis in squamous cell carcinoma. *Clin Cancer Res* 2001;7: 1419-28.
47. Frankel A, Man S, Elliott P, Adams J, Kerbel RS. Lack of multicellular drug resistance observed in human ovarian and prostate carcinoma treated with the proteasome inhibitor PS-341. *Clin Cancer Res* 2000;6: 3719-28.
48. LeBlanc R, Catley LP, Hideshima T, et al. Proteasome inhibitor PS-341 inhibits human myeloma cell growth *in vivo* and prolongs survival in a murine model. *Cancer Res* 2002;62:4996-5000.
49. Nawrocki ST, Sweeney-Gotsch B, Takamori R, McConkey DJ. The proteasome inhibitor bortezomib enhances the activity of docetaxel in orthotopic human pancreatic tumor xenografts. *Mol Cancer Ther* 2004;3: 59-70.
50. Williams S, Pettaway C, Song R, Papatandreu C, Logothetis C, McConkey DJ. Differential effects of the proteasome inhibitor bortezomib on apoptosis and angiogenesis in human prostate tumor xenografts. *Mol Cancer Ther* 2003;2:835-43.

CD80 in Immune Suppression by Mouse Ovarian Carcinoma–Associated Gr-1⁺CD11b⁺ Myeloid Cells

Rongcun Yang,^{1,2,4,6} Zhong Cai,³ Yuan Zhang,¹ William H. Yutzy IV,⁴ Katherine F. Roby,⁷ and Richard B.S. Roden^{4,5,6}

¹Department of Immunology, College of Medicine; ²Key Laboratory of Bioactive Materials, Ministry of Education, Nankai University; ³Clinical Laboratory, Tianjin Chest Hospital, Tianjin, China; Departments of ⁴Pathology, ⁵Oncology, and ⁶Gynecology and Obstetrics, The Johns Hopkins School of Medicine, Baltimore, Maryland; and ⁷Department of Anatomy and Cell Biology, University of Kansas Medical Center, Kansas City, Kansas

Abstract

An elevated number of Gr-1⁺CD11b⁺ myeloid cells has been described in mice bearing transplantable tumors, and has been associated with immune suppression. We examined the role of such myeloid suppressor cells in mice bearing the spontaneously transformed syngeneic mouse ovarian surface epithelial cell line, 1D8. We observed high levels of CD80 expression by Gr-1⁺CD11b⁺ cells from spleen, ascites, and tumor tissue of mice bearing 1D8 ovarian carcinoma, whereas CD40 and CD86 were absent. CD80 expression was not detected on Gr-1⁺CD11b⁺ cells from naïve mice. However, the expression of CD80 by Gr-1⁺CD11b⁺ cells from naïve mice was promoted by coculture with 1D8 cells. Because irradiated 1D8 cells, but not 1D8-conditioned medium, up-regulate CD80 expression by Gr-1⁺CD11b⁺ cells, this phenomenon likely requires direct interaction. Gr-1⁺CD11b⁺ cells derived from 1D8 tumor-bearing mice provided significant suppression of antigen-specific immune responses, but Gr-1⁺CD11b⁺ cells from naïve mice did not. Both short interfering RNA-mediated knockdown and genetic knockout of CD80 expression by Gr-1⁺CD11b⁺ cells of 1D8 tumor-bearing mice alleviated the suppression of antigen-specific immune responses. Suppression via CD80 on Gr-1⁺ CD11b⁺ myeloid cells was mediated by CD4⁺CD25⁺ T regulatory cells and required CD152. CD80 knockout or antibody blockade of either CD80 or CD152 retarded the growth of 1D8 tumor in mice, suggesting that expression of CD80 on Gr-1⁺CD11b⁺ myeloid cells triggered by 1D8 ovarian carcinoma suppresses antigen-specific immunity via CD152 signaling and CD4⁺CD25⁺ T regulatory cells. Thus, CD80-dependent responses to myeloid suppressor cells may contribute to tumor tolerance and the progression of ovarian carcinoma. (Cancer Res 2006; 66(13): 6807-15)

Introduction

The interaction of T cells with immunosuppressive versus activated regulatory antigen-presenting cells triggers antigen-specific T cell tolerance as opposed to priming (1–3). Recently, specific subsets of dendritic cells (DC) such as regulatory DC (4), tolerogenic DC (1), and Gr-1⁺CD11b⁺ myeloid cells (5, 6) have been found to play a critical role in inducing immunosuppression.

Tumor progression is associated with the accumulation of myeloid suppressor cells (MSC) that include immature macrophages, granulocytes, DCs, and myeloid cells (7–10). These MSCs share common features such as myeloid origin, macrophage-like morphology, the phenotype of surface receptors, and the ability to suppress T cells after culture *in vitro* (7–10). The Gr-1⁺CD11b⁺ surface markers are most often associated with a population of immature myeloid cells in the spleen of tumor-bearing mice (5, 11, 12). Such immature myeloid cells are present in the bone marrow and spleen of healthy mice, and differentiate into mature myeloid cells under normal conditions (12). The accumulation of Gr-1⁺CD11b⁺ cells in large numbers of tumor-bearing mice probably results from various tumor-derived factors. Release of interleukin-10 (13), transforming growth factor- β (14), interleukin-6 (15), vascular endothelial growth factor (16), prostanoids (17), prostaglandin E₂ (18), and stromal-derived factor α (19) by tumors have been implicated in preventing the differentiation and maturation of immunoregulatory cells and hampering the induction of antitumor immunity. These cells are also associated with immune suppression during viral infection, transplantation, UV irradiation, and cyclophosphamide treatment (20).

Receptors and their ligands on T cells and antigen-presenting cells are critical in delivering inhibitory or stimulatory signals that enable immune cells to remain dormant or to respond effectively to various stimuli (21). The CD28-B7 and TNFR/TNF super-families contain many of these molecules. B7 family members, including B7-1, B7-2, ICOS ligand, PD-L1, PD-L2, B7-H3, and B7-H4, are expressed on professional antigen-presenting cells as well as on cells within nonlymphoid organs, providing regulation of T cell activation and tolerance in peripheral tissues. The interaction of CD28 with CD80 (B7-1) or CD86 (B7-2) not only promotes initial T cell activation but also regulates self-tolerance by supporting CD4⁺CD25⁺ T regulatory (T_{reg}) cell homeostasis. B7 both enhances the development of Ag-specific CD4⁺CD25⁺ T_{reg} in the thymus in response to self-Ag recognition and also maintains these cells in peripheral lymphoid organs (22). A low-level expression of CD80/CD86 is required for CD4⁺CD25⁺ T_{reg} survival. CD152 (CTLA-4), which binds with higher affinity to CD80/CD86 than CD28, is predominantly expressed on CD4⁺CD25⁺ T_{reg} cells (23, 24).

Several mechanisms have been described for the induction of tolerance. These include release of soluble mediators like NO, lack of costimulation, Fas/FasL interaction and the induction of several types of regulatory T cells including Tr1, Th3, NKT cells, and CD4⁺CD25⁺ T_{reg} cells (25, 26). Tumor-associated myeloid cells may inhibit T cell responses by inducing the apoptosis of activated T cells via up-regulation of NO production and arginase activity (12, 27). Prostaglandin E₂ and tumor necrosis factor- α function in

Requests for reprints: Richard Roden, Department of Pathology, Room 308, CRB2, 1550 Orleans SE, Baltimore, MD 21231. Phone: 410-502-5161; Fax: 443-287-4295; E-mail: roden@jhmi.edu or Rongcun Yang. E-mail: ryang@nankai.edu.cn.

©2006 American Association for Cancer Research.
doi:10.1158/0008-5472.CAN-05-3755

macrophage-mediated T cell suppression (28, 29). Although a number of studies show that strict cell-cell contact between MSCs and T cells is required for T cell suppression in mice and humans (30–34), the mechanism by which direct cell-cell contact with such tumor-associated Gr-1⁺CD11b⁺ cells suppress CD8⁺ T cells in an antigen-specific manner is not clear. Herein, we show that the murine model of ovarian carcinoma, mouse ovarian surface epithelial cell (MOSEC) line 1D8 triggers the accumulation of Gr-1⁺CD11b⁺ myeloid cells and CD4⁺CD25⁺ T_{reg} cells can be found in spleen, ascites, and tumor tissue in mice. Gr-1⁺CD11b⁺ cells from tumor-free mice do not detectably express CD80, CD40, or CD86. However, Gr-1⁺CD11b⁺ cells in mice bearing MOSEC tumor express high levels of CD80, although neither CD40 nor CD86 are detected. We show that direct contact of Gr-1⁺CD11b⁺ cells with MOSEC ovarian carcinoma cells causes the expression of CD80. CD80 expressed by these Gr-1⁺CD11b⁺ MSCs plays a critical role in immunosuppression induced by MOSEC tumors. The action of CD4⁺CD25⁺ T_{reg} cells and signaling via CD152 are also critical to immunosuppression by MOSEC tumors.

Materials and Methods

Mice. Six- to 8-week-old male C57BL/6 (NCI) and CD80^{-/-} (B6, 129S4-CD80^{TM1SHR}) mice were maintained in a pathogen-free animal facility at least 1 week before use. Experiments were done in accordance with institutional guidelines. For *in vivo* blockade studies, mice were injected i.p. with 250 µg of anti-CTLA-4 monoclonal antibody (UC10-4F10-11; BD PharMingen, San Diego, CA) or anti-CD80 (mB7-1 affinity-purified goat IgG, AF740; R&D, Minneapolis, MN) on days -6, -4, -2, and +1.

MOSEC ovarian carcinoma model. A syngeneic mouse model for epithelial ovarian cancer based on a spontaneously transformed MOSEC cell line (1D8) has been previously described (35). MOSEC did not express the costimulatory molecules CD40, CD80, CD86, CD22.2, CD72, CTLA-4, or other markers CD5, B220, CD11b, and CD11c (data not shown). However, the MOSEC 1D8 cells expressed CD44 and very low levels of costimulatory molecules B7-H1, PD-1, and MHC class II (data not shown). Multiple tumors formed within 60 days after the i.p. injection of 1 × 10⁷ MOSEC (data not shown) in syngeneic C57BL/6 mice. Tissue samples were collected 2 month after the i.p. MOSEC injection. To monitor tumor growth rate, 1 × 10⁷ MOSEC cells were injected s.c. in the right leg.

Flow cytometric analysis and isolation of Gr-1+CD11b+ myeloid cells from ascites of mice with ovarian carcinoma. FITC-conjugated anti-CD11c (N418), anti-mouse CD86 (GL1), anti-mouse CD80 (16-10A1), anti-mouse CD40 (3/23), and phycoerythrin (PE)-labeled anti-CD4 (L3T4), anti-mouse CD8α (53-6.6), anti-mouse CD45 R/B220 (RA36B2), anti-mouse CD11b (M1/70), as well as purified anti-mouse I-A^b (25-9-17), and FITC-labeled anti-mouse Ly-6G (RB6-8C5), allophycocyanin anti-mouse Ly-6G (RB6-8C5), PE or FITC-labeled anti-CD25 (7D4), and PE-labeled CTLA-4 (UC10-4F10-11) were purchased from PharMingen. Single or multiple staining was done using different monoclonal antibodies. For each analysis, isotype-matched control monoclonal antibody was used as a negative control. Cells were then washed twice, resuspended in PBS containing 1% paraformaldehyde and 1% FCS and kept at 4°C prior to flow cytometric analysis (FACScan, Becton Dickinson, San Diego, CA).

Ascites or splenic cells from mice with ovarian carcinoma were directly stained with FITC- or allophycocyanin-labeled anti-Gr-1 antibodies and PE-labeled anti-CD11b. After washing, cells were gated for myeloid cell characteristics, i.e., high forward and side scatter and bright staining for CD11b. These selected cells were then sorted using FACScan based on the staining for CD11b and for Gr-1 or the absence of staining for both. The purity of Gr-1⁺CD11b⁺ cells was >95%. CD4⁺CD25⁺ T_{reg} cells were also sorted using FACScan by staining with FITC-labeled anti-CD4 and PE-labeled CD25 antibodies.

Preparation of bone marrow cells. Bone marrow cells (BMC) were prepared as we have previously described (36). Briefly, BMCs were collected by removing the femur bones of mice, cutting off each end, and flushing out the bone marrow with RPMI 1640 using a syringe. The pooled cells were harvested by centrifugation at 1,600 rpm for 10 minutes and resuspended in 2 mL of ACK buffer for 5 minutes at room temperature to lyse RBC. These cells were washed in medium and cultured in RPMI 1640 with 10% FCS and 1% penicillin and streptomycin. To determine the effect of ovarian carcinoma cells on the BMCs, 5 × 10⁴ ovarian carcinoma cells with or without irradiation (10⁴ Rad) or 50% (final concentration) supernatant from tumor cultures were added into BMCs, respectively. The Gr-1⁺CD11b⁺ cells were isolated and surface markers were analyzed by flow cytometry.

Short interfering RNA design, synthesis, and transfection. Short interfering RNA (siRNA) sequences used for targeted silencing of human CD80 were designed according to protocols in the Ambion Inc., (Austin, TX) web site, <http://www.ambion.com>, and had the following sequences: sense 5'-UGGAAGAGAAUACCUGGCTT and antisense 5'-GCCAGGUAUUUCU-CUUCATT. Nonsilencing control siRNA is an irrelevant siRNA with random nucleotides (5'-ACUATCUAAGUUAUACTACCCCTT). Sequences were synthesized and annealed by the Johns Hopkins University Genetics Core Facility (Baltimore, MD). Searches of the mouse genome database (BLAST) were carried out to ensure that the sequence would not target other gene transcripts. Cells were transduced with the siRNAs using GeneSilencer (Gene Therapy Systems, San Diego, CA), which was used according to the manufacturer's protocol.

Inhibition of antigen-specific responses by ovarian carcinoma-associated Gr-1+CD11b+ cells. Gr-1⁺CD11b⁺ cells obtained from mice with or without MOSEC tumor, as indicated, splenocytes from mice immunized with human papillomavirus type 16 virus-like particles (VLP), and VLPs were, respectively, used as suppressor, responders, and stimulator. To investigate suppressive role of ovarian carcinoma-associated Gr-1⁺CD11b⁺ cells in the antigen-specific response, 2 × 10⁶ splenocytes were cocultured with VLP (final concentration, 25 µg/mL) in triplicate in 24-well flat-bottomed plates (Falcon, BD Biosciences, Franklin Lakes, NJ) in 200 µL of RPMI 1640 according to our prior methods (36). CD4⁺ cell and CD8⁺ beads were prepared according to the described protocol (MACS). Gr-1⁺CD11b⁺ MSCs (5 × 10⁴ per well unless otherwise stated) were added into culture of splenocytes during VLP stimulation. To determine the suppressive effect of MSCs on VLP-induced splenocyte proliferation, splenocytes from mice immunized with VLPs were labeled with 2.5 µmol/L of CFSE for 10 minutes at room temperature (with gentle agitation every 2-3 minutes), and then washed thrice with PBS. The CFSE-labeled splenocytes were stimulated with VLP and cocultured with Gr-1⁺CD11b⁺ MSCs. The cells and supernatants were harvested separately at 4 days. The cells were analyzed by flow cytometry and IFN-γ in the supernatant was assayed by capture ELISA. To determine the effect of CD4⁺CD25⁺ T_{reg} cells on the VLP-specific responses, CD25⁺ T_{reg} cells were depleted using magnetic beads or the sorted CD25⁺ T_{reg} cells by FACScan were added into culture. CD4⁺CD25⁺ T_{reg}s (1 × 10⁴) were used in all experiments unless otherwise stated. After 3 days, the supernatant was collected and IFN-γ was analyzed.

Blocking experiments were used to determine the role of costimulatory molecules on the ovarian carcinoma-associated Gr-1⁺CD11b⁺ cells in which various neutralizing antibodies were added into the culture to 10 µg/mL, including anti-CD80 (goat IgG) and anti-mouse CTLA-4 (UC10-4F10-11, hamster IgG₁). The supernatants were collected after 3 days and release of IFN-γ was analyzed. All monoclonal antibodies had an endotoxin level of <1 endotoxin units/mL.

RT-PCR analysis. Total cellular RNA was prepared using TRIzol reagent (Invitrogen, Carlsbad, CA) followed by RNA clean-up with RNeasy Mini kit (Qiagen, Valencia, CA). RT-PCR was done by SuperScript one-step RT-PCR with Platinum Taq according to the protocol provided (Invitrogen). For cDNA synthesis and predenaturation, we used 1 cycle (50°C for 15 minutes, 94°C for 2 minutes); and for PCR amplification, we used 40 cycles (denature, 94°C for 15 seconds, anneal, 55°C for 30 seconds, extend 72°C for 1 min/kb); and for final extension, we used 1 cycle (72°C for 10 minutes). The primers included: mouse Foxp3, sense 5'-ATGCCCAACCTAGGCCACG

and antisense 5'-TCAAGGGCAGGGATTGGAGCC; mouse CD80, sense 5'-ATGGCTTGCAATTGTCAAGTTG and antisense 5'-CTAAAGGAAGACGGTCTG; GAPDH, sense 5'-ATGGTGAAGGTGGTGTGAACGGATTGGC and antisense 5'-CATCGAAGGTGGAAGAGTGGGAGTTGCTGT.

ELISA. Commercial sandwich ELISA kits were used for the quantitation of IFN γ (Pierce Endogen, Rockford, IL). The absorbance of each of the samples were measured at 450 nm using a SpectraMax 190 ELISA plate reader. Cytokine levels were quantified from two to three titrations using standard curves, and expressed in pg/mL.

Results

Murine model of ovarian carcinoma induces Gr-1⁺CD11b⁺ MSCs. Previous studies of mice bearing transplantable tumors (37) have shown the accumulation of a Gr-1⁺CD11b⁺ MSC population. We find that mice bearing the transplantable model of ovarian carcinoma MOSEC 1D8 exhibit a distinct Gr-1⁺CD11b⁺ population of myeloid cells present in the spleen, ascites, and also tumor tissue that was absent from tumor-free mice (Fig. 1A). Consistent with their surface marker phenotype, the Gr-1⁺CD11b⁺ population of

cells exhibited myeloid features by Giemsa staining (data not shown). This phenomenon also occurs in mice bearing Lewis lung carcinoma (LLC) but not the cervical carcinoma model TC-1 (data not shown).

To determine whether the Gr-1⁺CD11b⁺ population of cells suppressed antigen-specific T cell responses as previously described, we used a potent heterologous antigen from our previous studies; human papillomavirus type 16 L1 VLPs. This xenogenic antigen induces potent L1-specific antibody and T cell responses in mice. When VLPs are added to the splenocytes of vaccinated mice, antigen-presenting cells such as DCs and B cells in splenocytes could capture, process, and present VLP and then induce strong VLP-specific T cell responses. We observed that the Gr-1⁺CD11b⁺ myeloid cells derived from mice bearing ovarian carcinoma suppressed VLP-specific T cell responses *in vitro*, including both proliferation and release of IFN γ (Fig. 1B-D). Importantly, antigen-specific T responses were suppressed by Gr-1⁺CD11b⁺ cells from mice bearing MOSEC 1D8 tumor but not those of tumor-free mice (Fig. 1B-D). This suggests that Gr-1⁺CD11b⁺ cells from mice bearing

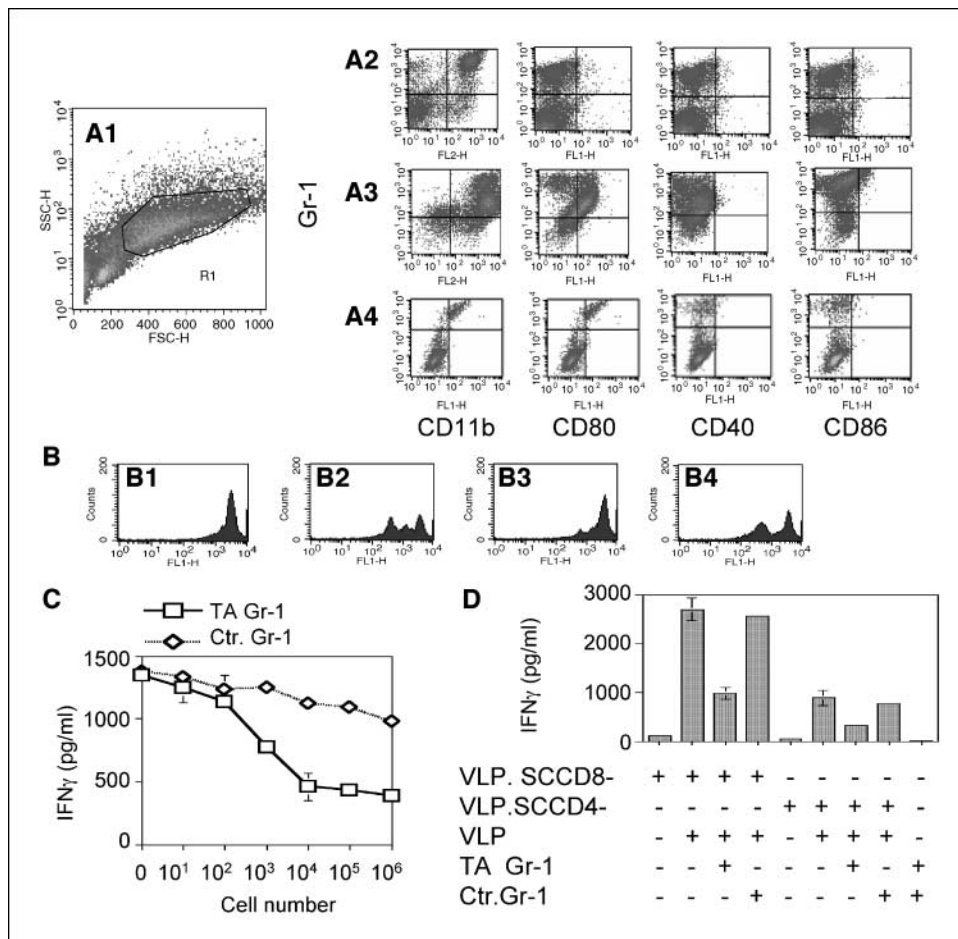


Figure 1. Characteristics of MOSEC 1D8 ovarian carcinoma-associated Gr-1⁺CD11b⁺ MSCs. **A**, flow cytometric analysis of splenocytes from a tumor-free mouse. Gating on forward and side scatter (1), and staining for Gr-1 versus CD11b, CD80, CD86, and CD40 (2); 3, similar to (2), but using splenocytes of mice bearing MOSEC 1D8 tumors; 4, flow cytometric analysis of MOSEC 1D8 ascites cells. The cells were gated on side and forward scatter, and larger cells were analyzed. The cells were stained by FITC-labeled antimouse CD11b, CD80, CD40, and CD86, PE-labeled antimouse Gr-1 antibodies, and larger cells were analyzed. **B**, mouse ovarian carcinoma-associated Gr-1⁺CD11b⁺ cells inhibited VLP-specific proliferation of CFSE-labeled splenocytes: 1, splenocytes from mice immunized by VLPs without stimulation; 2, splenocytes from mice immunized by VLPs stimulated with VLPs; 3, similar to (2), but MOSEC 1D8 tumor-associated Gr-1⁺CD11b⁺ cells (5×10^4) were added into the culture; 4, similar to (2) but Gr-1⁺CD11b⁺ cells isolated from tumor-free mice were added into the culture. Splenocytes from mice immunized with human papillomavirus type 16 L1 VLPs (36) were labeled with 2.5 μ mol/L of CFSE for 10 minutes and then stimulated by VLP. **C**, mouse ovarian carcinoma-associated Gr-1⁺CD11b⁺ cells inhibited VLP-specific production of IFN γ . The indicated numbers of Gr-1⁺CD11b⁺ cells were sorted by flow cytometry from mice bearing MOSEC 1D8 tumor (TA-Gr-1) or tumor-free mice (Ctrl.Gr-1 cells) and were cocultured with 2×10^6 VLP-specific splenocytes (VLP.SC). **D**, splenocytes from VLP-vaccinated mice, depleted for either CD8⁺ (VLP.SCCD8⁻) or CD4⁺ cells (VLP.SCCD4⁻), and either stimulated with VLP or not, were cultured with Gr-1⁺CD11b⁺ cells from either control or 1D8 tumor-bearing mice.

MOSEC 1D8 tumor are functionally different from those of naïve mice. Furthermore, Gr-1⁺CD11b⁺ cells from mice bearing LLC suppress ovalbumin-specific T cell release of IFN γ , suggesting that this phenomenon is neither unique to VLP-specific T cell responses nor Gr-1⁺CD11b⁺ cells from mice bearing MOSEC 1D8 tumor (data not shown).

Some prior studies indicate that MSCs inhibit MHC class I-restricted CD8⁺ T cells and have no effect on CD4⁺ T cells (16, 38), whereas others find that Gr-1⁺CD11b⁺ MSCs also inhibit CD4⁺ T cell function (39). We addressed this issue in the MOSEC 1D8 model. When ovarian carcinoma-associated Gr-1⁺CD11b⁺ cells were added into CD8-depleted or CD4-depleted VLP-specific splenocytes, VLP-dependent production of IFN γ was significantly reduced in both splenocyte preparations (Fig. 1D). Again, suppression was not observed using Gr-1⁺CD11b⁺ cells from naïve mice. This suggests that mouse ovarian carcinoma-associated Gr-1⁺CD11b⁺ cells inhibit antigen-specific release of IFN γ by both CD4⁺ and CD8⁺ cells.

Bronte et al. (5) described that Gr-1⁺CD11b⁺ myeloid cells expressed MHC class II, B220, F4/80, CD86, CD16/32, and DEC205. In contrast, Gabrilovich et al. (16, 40) reported the expression of MHC class I and the absence of MHC class II and costimulatory molecules, suggesting that there may be significant differences in the phenotypes and functions of Gr-1⁺CD11b⁺ myeloid cells induced by different tumors. Therefore, we examined the surface markers for Gr-1⁺CD11b⁺ MSCs from mice with 1D8 ovarian carcinoma and found no detectable expression of MHC class II, CD14, B220 (data not shown), or the CD40 and CD86 costimulatory molecules (Fig. 1A).

Direct contact of mouse ovarian carcinoma with Gr-1⁺CD11b⁺ myeloid cells promotes CD80 expression. A number of tumor-derived signals (17, 40) have been implicated in preventing the differentiation and maturation of immunoregulatory cells and hampering the induction of antitumor immunity. Our findings suggest that Gr-1⁺CD11b⁺ cells from mice bearing MOSEC 1D8 tumor are functionally different from those of disease-free mice. Thus, it is possible that 1D8 ovarian carcinoma-derived factors could render Gr-1⁺CD11b⁺ cells of naïve mice immunosuppressive. CD80 expression has been described as a surface marker of MSCs expanded in mice with disseminated candidiasis, and its depletion increased IFN γ -mediated antifungal resistance (20, 41). This finding suggested a possible suppressive role for CD80 in the activity of MSCs. Therefore, we examined the levels of CD80 on Gr-1⁺CD11b⁺ cells from splenocytes of naïve and MOSEC 1D8 tumor-bearing mice (Fig. 1A). CD80 expression was present in the Gr-1⁺CD11b⁺ cells of tumor-bearing (Fig. 1A3), but not naïve mice (Fig. 1A2). Likewise, Gr-1⁺CD11b⁺ cells in 1D8 ascites also expressed CD80 (Fig. 1A4).

To address whether CD80 expression on Gr-1⁺CD11b⁺ cells was a direct effect of the 1D8 tumor cells, we isolated Gr-1⁺CD11b⁺ cells from the bone marrow of tumor-free mice and cocultured them for 3 days with 1D8 cells at a ratio of 1:10 (1D8 cells/Gr-1⁺CD11b⁺ cells), irradiated 1D8 cells at a ratio of 1:10 (1D8 cells/Gr-1⁺CD11b⁺ cells), or in 25% supernatant conditioned using 1D8 *in vitro* cultures. Total RNA from Gr-1⁺CD11b⁺ cells with each different exposure was analyzed by RT-PCR for CD80 transcript expression. The semiquantitative RT-PCR analysis suggested that CD80 transcripts were significantly up-regulated when Gr-1⁺CD11b⁺ cells from the bone marrow of tumor-free mice were cocultured with 1D8 tumor cells (Fig. 2A). A similar effect was observed upon coculture with irradiated 1D8 cells. However, 25% (v/v) conditioned

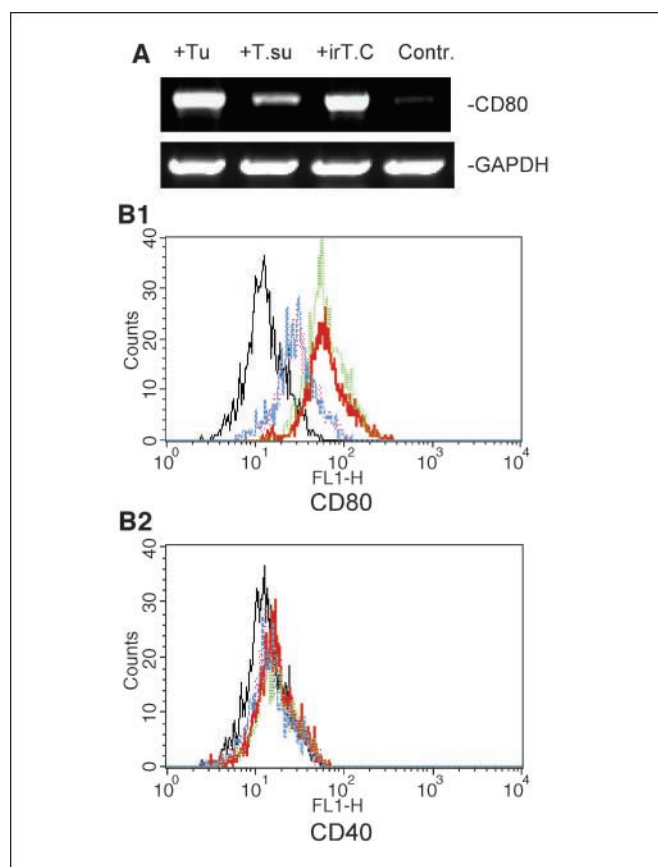


Figure 2. Direct contact between MOSEC 1D8 cells induces expression of CD80 on Gr-1⁺CD11b⁺ cells. *A*, semiquantitative RT-PCR showing the effect of cocultured live (*T.C*) or irradiated MOSEC 1D8 cells (*irT.C*) or MOSEC 1D8 cell-conditioned medium (*T.Su*) versus control medium (*Contr.*) on CD80 transcript levels in Gr-1⁺CD11b⁺ cells. *B*, flow cytometric analysis of surface CD80 (1) and CD40 (2) expression on Gr-1⁺CD11b⁺ cells cultured in the presence of tumor cells (red solid line), irradiated cells (green stippled line), 1D8 cell-conditioned medium (red stippled line), medium alone (blue line), or isotypic control (solid black line).

supernatant from 1D8 cultures had a lesser effect on CD80 transcript expression.

We examined the up-regulation by 1D8 cells of CD80 on Gr-1⁺CD11b⁺ cells from the bone marrow of tumor-free mice at the protein level using flow cytometry (Fig. 2B). In parallel with the RT-PCR findings for CD80 transcripts, surface expression of CD80 (Fig. 2B1), but not CD40 (Fig. 2B2), on Gr-1⁺CD11b⁺ cells from the bone marrow of tumor-free mice was up-regulated in those cultured with both live and irradiated 1D8 cells, but not cells cultured in 25% 1D8-conditioned medium. Thus, MOSEC 1D8 tumor cells not only cause the accumulation of Gr-1⁺CD11b⁺ MSCs but also induce the expression of CD80. This phenomenon depends on direct contact between MOSEC 1D8 ovarian carcinoma cells and Gr-1⁺CD11b⁺ MSCs, but not tumor cell proliferation (Fig. 2).

Antibody blockade of CD80 decreases the suppressive potential of mouse ovarian carcinoma-associated Gr-1⁺CD11b⁺ MSCs. CD80 is a prototypic member of the B7-CD28 family of costimulatory molecules. However, reports differ in the outcome of CD80-dependent signaling in regulating T cell activity (42). Thus, we hypothesized that CD80 expression by the ovarian carcinoma-associated Gr-1⁺CD11b⁺ MSCs might contribute to the suppression of antigen-specific immunity and the induction of

tumor immunotolerance (20, 41). To address the role of CD80 in the suppressive effects of Gr-1⁺CD11b⁺ MSCs on antigen-specific T cell responses, we again used splenocytes from mice vaccinated with the potent heterologous antigen, HPV16 L1 VLPs. The presence of CD80-specific neutralizing antibody, but control antibody, inhibited the suppressive effect of ovarian carcinoma-associated Gr-1⁺CD11b⁺ MSCs upon VLP-specific and T cell-dependent IFN γ release (Fig. 3A). Furthermore, CD80-specific neutralizing antibody did not alter VLP-specific and T cell-dependent IFN γ release in the absence of Gr-1⁺CD11b⁺ MSCs suggesting that the effect is mediated by binding of CD80 antibody to CD80⁺Gr-1⁺CD11b⁺ MSCs. Because antibody blockade suggests that CD80 signaling contributes to the suppression of antigen-specific immune responses by ovarian carcinoma-associated CD80⁺Gr-1⁺CD11b⁺ MSCs, we reasoned that blockade of the CD80 ligand CD152 might produce a similar effect. As shown in Fig. 3A, antibody blockade of CD152 also significantly decreased the suppression of VLP-specific and T cell-dependent IFN γ release by ovarian carcinoma-associated CD80⁺Gr-1⁺CD11b⁺ MSCs. CD152 antibody

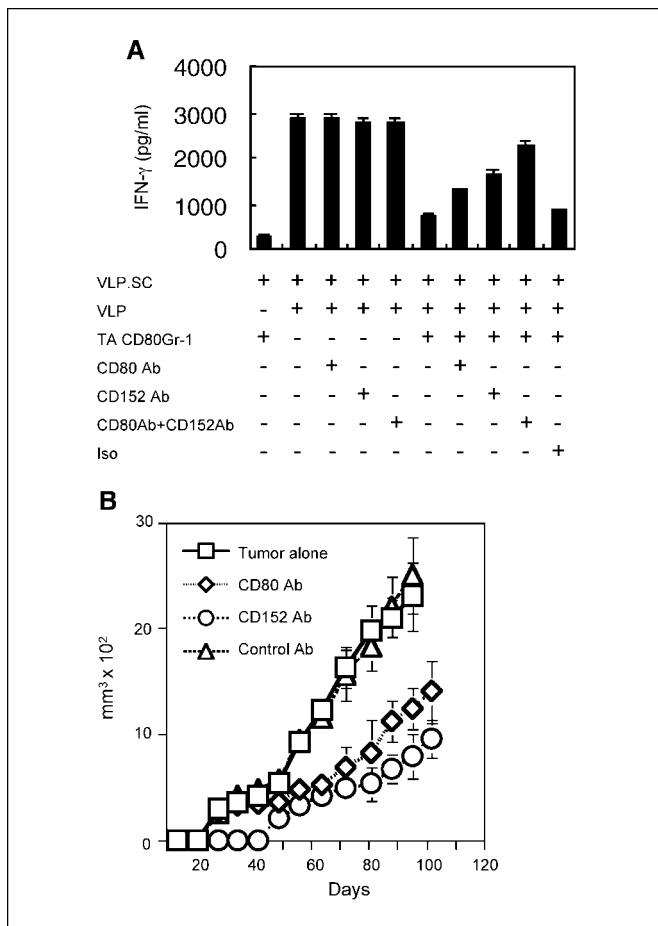


Figure 3. Blockade of CD80 or CD152 reduced antigen-specific T cell suppression by mouse ovarian carcinoma-associated Gr-1⁺CD11b⁺ cells and slowed tumor growth. **A**, effect of neutralizing antibody (10 μ g/mL) to CD80 or CD152 on the generation of IFN γ by VLP-specific splenocytes (VLP.SC) in the presence of mouse ovarian carcinoma-associated CD11b⁺Gr-1⁺ cells (TA CD80Gr-1) and CD4⁺CD25⁺ cells. Supernatants of cultures were collected after 24 hours and IFN γ was assayed by capture ELISA. Iso, control antibody. **B**, *in vivo* injection of neutralizing antibody to CD80 or CD152 significantly slowed and retarded tumor growth. Mice (six/group) were injected using MOSEC 1D8 cells (s.c. with 5×10^6) and i.p. with 250 μ g of control antibody or antibody specific for CD152 or CD80 on days -6, -4, -2, and +1.

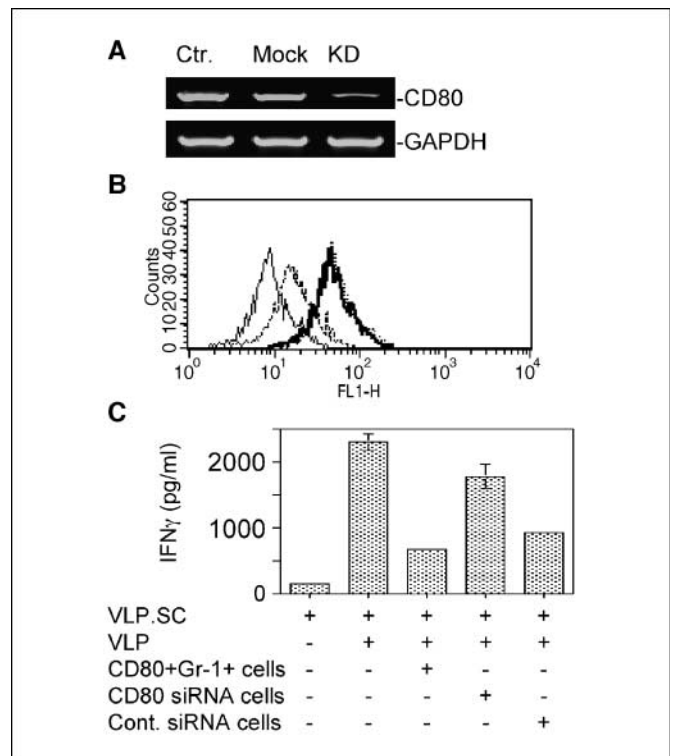


Figure 4. Knockdown of CD80 by siRNA decreased the suppressive potential of ovarian carcinoma-associated CD80⁺Gr-1⁺CD11b⁺ MSCs. **A**, CD80 siRNA reduced the level of CD80 but not GAPDH transcript expression in transfected ovarian carcinoma-associated Gr-1⁺CD11b⁺ cells, as assessed by RT-PCR. **B**, CD80 siRNA, but not nonspecific siRNA, reduced the level of surface CD80 expression in transfected ovarian carcinoma-associated Gr-1⁺CD11b⁺ cells, as assessed by flow cytometric analysis: isotype control (thin black line), expression of CD80 on ovarian carcinoma-associated Gr-1⁺CD11b⁺ MSCs (thick black line), expression of CD80 on ovarian carcinoma-associated Gr-1⁺CD11b⁺ cells by control siRNA (dotted line), and expression of CD80 on ovarian carcinoma-associated Gr-1⁺CD11b⁺ cells transfected with CD80-specific siRNA (dashed line). **C**, CD80 siRNA inhibited the suppression by ovarian carcinoma-associated Gr-1⁺CD11b⁺ cells of VLP-induced generation of IFN γ in VLP-specific splenocyte cultures (VLP.SC). CD80⁺Gr-1⁺ cells, cells sorted from the ascites of mice with MOSEC 1D8 ovarian carcinoma; CD80siRNA cells, CD80⁺Gr-1⁺ cells transfected with CD80 siRNA; Cont. siRNA cells, CD80⁺Gr-1⁺ cells transfected with control siRNA.

produces a significantly stronger inhibition than CD80 antibody ($P < 0.05$) and their effects seem to be additive. CD152 functions as a negative signaling molecule not only expressed by T_{reg} cells, but also in many different kinds of lymphocytes. In contrast, CD80 is mainly expressed in monocyte-derived cells such as antigen-presenting cells. This may account for stronger inhibition of T cell suppression by antibody blockade of CD152 as compared with CD80 blockade.

To further address the role of CD80-dependent signaling on tumor tolerance, we examined the effect of both CD80- and CD152-specific neutralizing antibodies on the growth of the MOSEC 1D8 ovarian carcinoma model in C57BL/6 mice. The administration of either CD80- or CD152-specific neutralizing antibody (250 μ g i.p.) on days -6, -4, -2, and +1 around the s.c. inoculation with 10^7 1D8 cells delayed the growth of tumor with respect to mice that did not receive antibody, whereas control antibody failed to retard tumor growth (Fig. 3B). When CD80 or CD152 neutralizing antibodies are injected into mice 1 week after inoculation with LLC cells (data not shown), the delay in tumor growth was similar to that seen with the protocol for CD80 antibody injection on days

-6, -4, -2, and +1 observed in mice challenged with 1D8 tumor (Fig. 3B). Furthermore, the infusion of CD80⁺Gr-1⁺CD11b⁺ MSCs from mice with large carcinoma burden into naïve mice produces more rapid tumor outgrowth upon subsequent LLC tumor challenge (data not shown). This suggests that expansion of the CD80⁺Gr-1⁺CD11b⁺ MSC population suppresses immunity against both tumor types. Furthermore, stronger inhibition of T cell suppression by antibody blockade of CD152 as compared with CD80 blockade (Fig. 3A) is consistent with the greater reduction of 1D8 and LLC tumor growth by treatment of mice with CD152 antibody versus CD80 antibody (Fig. 3B; data not shown).

CD80 knockdown by siRNA decreased the suppressive potential of ovarian carcinoma-associated Gr-1⁺CD11b⁺ MSCs. Antibody blocking studies suggest that signaling via CD80 contributes to the induction of immunosuppression by MOSEC 1D8 ovarian carcinoma. Because antibody treatment can induce nonspecific effects, we sought to further confirm the role of CD80 in the suppression of antigen-specific T cell responses by Gr-1⁺CD11b⁺ MSCs using CD80-targeted and nonspecific control siRNA. Upon transfection, the CD80-targeted siRNA reduced the CD80 transcript (Fig. 4A) and surface protein (Fig. 4B) levels with respect to untreated ovarian carcinoma-associated Gr-1⁺CD11b⁺ MSCs, whereas the control siRNA did not. Flow cytometric analysis showed that neither CD80-targeted nor nonspecific control siRNA altered the level of CD40 or CD86 in these cells (data not shown). Ovarian carcinoma-associated Gr-1⁺CD11b⁺ MSCs transfected with CD80-targeted siRNA or control siRNA were added into the culture of VLP-specific splenocytes with VLPs. Ovarian carcinoma-associated Gr-1⁺CD11b⁺ MSCs transfected with CD80-targeted siRNA exhibited significantly reduced suppressive potential for VLP-specific and T cell-dependent induction of IFN γ release as compared with control siRNA-treated cells.

Growth of MOSEC 1D8 tumor is retarded in CD80-deficient mice. Both antibody blockade and siRNA knockdown studies support the involvement of CD80 on the Gr-1⁺CD11b⁺ cells in inducing immune suppression against MOSEC 1D8 tumor. Therefore, we explored this phenomenon further in CD80-deficient mice. When MOSEC 1D8 cells were injected s.c. into CD80^{-/-} and CD80^{+/+} mice, tumor appeared later and growth was clearly slower in CD80^{-/-} as compared with CD80^{+/+} mice, further supporting a role for CD80-dependent signaling in the induction of immune suppression (Fig. 5A).

CD80 deficiency decreases the suppressive potential of ovarian carcinoma-associated Gr-1⁺CD11b⁺ cells. Because MOSEC 1D8 tumor appeared later and growth was clearly slower in CD80-deficient as compared with wild-type mice, we isolated the Gr-1⁺CD11b⁺ cells derived from these CD80^{-/-} mice and wild-type mice bearing tumors, and examined their ability to suppress antigen-specific T cell responses. Gr-1⁺CD11b⁺ cells derived from wild-type mice bearing MOSEC 1D8 tumor exhibited significant suppression on the VLP-specific immune responses, whereas those isolated from CD80^{-/-} mice with the equivalent tumor load showed a reduced effect (Fig. 5B).

Recent findings suggest that TLR signaling, notably TLR9 activation by CpG, in the appropriate context, could overcome immune tolerance. Using RT-PCR, we determined that Gr-1⁺CD11b⁺ MSCs express transcripts for TLR2, TLR4, and TLR9 (data not shown). To explore this possibility, Gr-1⁺CD11b⁺ MSCs isolated from CD80^{-/-} or CD80^{+/+} mice bearing ovarian carcinomas were stimulated by the CpG ODN2006 (or lipopolysaccharide) to determine the effect of TLR9 activation on antigen-specific T cell suppression. Although control and lipopolysaccharide-treated (data not shown) Gr-1⁺CD11b⁺ MSCs suppressed VLP-specific and T cell-dependent release of IFN γ , CpG-treated Gr-1⁺CD11b⁺ cells

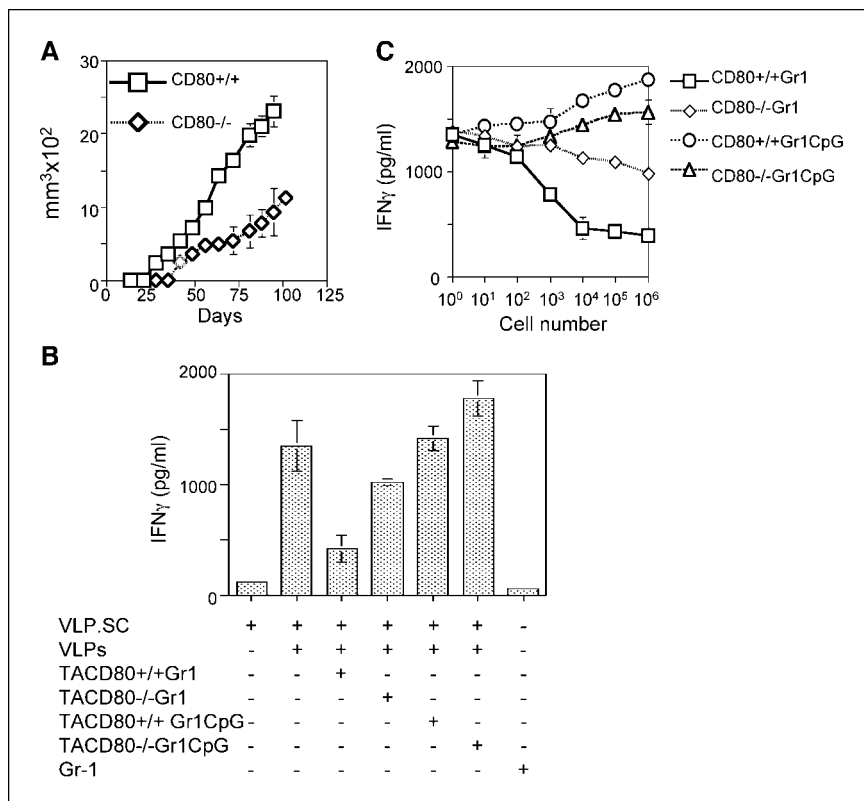


Figure 5. Effect of CD80 deficiency on ovarian carcinoma-associated Gr-1⁺CD11b⁺ cell suppression of T cell responses and tumor tolerance. **A**, the growth of MOSEC 1D8 tumor is delayed and slower in CD80 knockout mice as compared with wild-type mice (six/group). **B** and **C**, Gr-1⁺CD11b⁺ cells from CD80^{-/-} mice with ovarian carcinoma exhibited a decreased suppression of VLP-induced production of IFN γ in VLP-specific splenocyte cultures. CD80^{-/-} Gr-1⁺CD11b⁺ cells and CD80^{+/+} Gr-1⁺CD11b⁺ cells were sorted from splenocytes of CD80^{-/-} mice and wild-type mice with ovarian carcinoma, respectively. Isolated Gr-1⁺CD11b⁺ cells were cocultured with or without CpG (5 nmol/L, ODN2006; InvivoGen, San Diego, CA). These cells were washed and then added into the culture to assess the influence of CpG treatment of Gr-1⁺CD11b⁺ cells on their suppression of VLP-specific T cell production of IFN γ . Supernatants of T cell cultures were collected after 24 hours and IFN γ assayed by capture ELISA.

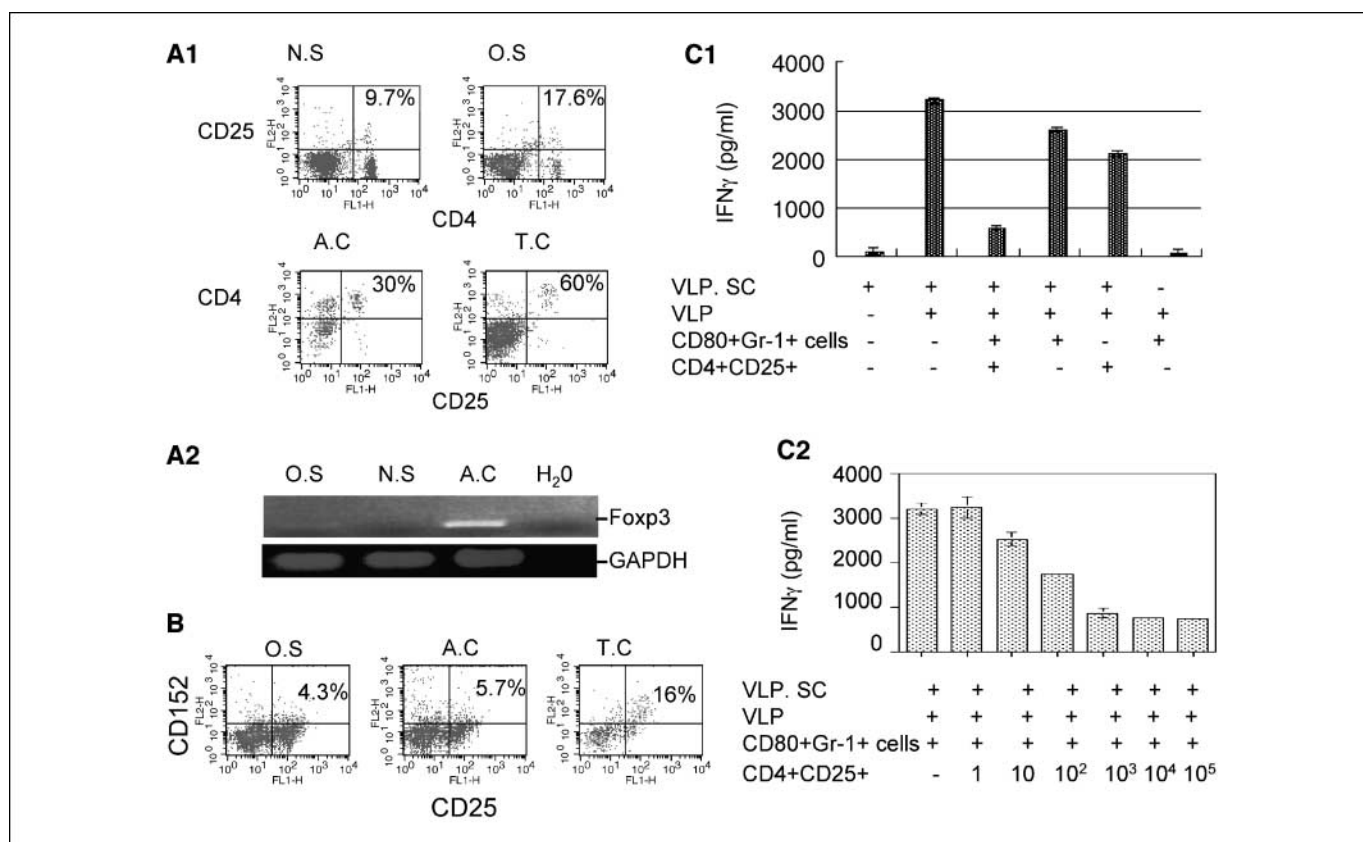


Figure 6. Inhibition of antigen-specific responses by CD80⁺Gr-1⁺CD11b⁺ cells via CD4⁺CD25⁺ T_{reg} cells. **A**, flow cytometric analysis (1) of CD4⁺CD25⁺ T_{reg} cells isolated from splenocytes of tumor-free mice (N.S), splenocytes from mice with ovarian carcinoma (O.S), ascites cells from mice with ovarian carcinoma (A.C), and ovarian tumor-infiltrating lymphocytes (T.C). The figures reflect the percentage of CD4⁺ T cells that express CD25. 2, the above cells were analyzed for Foxp3 and GAPDH transcript expression by RT-PCR. **B**, expression of CD152 on CD25⁺ T cells isolated from mice bearing MOSEC 1D8 ovarian carcinoma. **C**, CD4⁺CD25⁺ T_{reg} cells are required for the suppression of VLP-induced production of IFN γ in VLP-specific splenocyte cultures by MSCs. VLP-specific splenocytes were depleted of CD25⁺ cells using microbeads (VLP.SC) and stimulated with VLP. CD80⁺Gr-1⁺ cells and CD4⁺CD25⁺ cells were isolated from the ascites of mice with MOSEC 1D8 ovarian carcinoma by flow cytometry and then added into culture at the numbers indicated.

from tumor-bearing CD80^{+/+} mice failed to effectively suppress this response. Notably, CpG-treated Gr-1⁺CD11b⁺ cells from CD80^{-/-} mice bearing ovarian carcinoma significantly enhanced VLP-specific and T cell-dependent release of IFN γ (Fig. 5B). These phenomena were dependent on the number of MSCs added to the VLP-specific splenocyte cultures (Fig. 5C).

Role of CD4⁺CD25⁺ T_{reg} cells in the suppression of antigen-specific responses by Gr-1⁺CD11b⁺ MSCs. CD4⁺CD25⁺ T_{reg} cells suppress antitumor immunity and are expanded in patients with ovarian cancer and correlate with poor clinical outcome (43). We also observed an increase in the splenic population of CD4⁺CD25⁺ T cells in mice bearing MOSEC 1D8 tumor (Fig. 6A1). Furthermore, a greatly increased proportion of CD4⁺CD25⁺ T_{reg} cells were observed in MOSEC 1D8 ascites (30% of total CD4⁺ T cells) and tumor tissue (60% of total CD4⁺ T cells; Fig. 6A1). The expression of transcripts of the T_{reg} marker Foxp3 were detected in CD4⁺CD25⁺ cells isolated from MOSEC 1D8 ascites (Fig. 6A2). Weak Foxp3 transcript expression was also detected in CD4⁺CD25⁺ splenocytes from mice bearing MOSEC 1D8 tumors, but not those from tumor-free mice (Fig. 6A2). We also observed a higher proportion (18.2%) of CD4⁺ splenocytes of mice bearing ovarian tumor stains for Foxp3 using antibody FJK-16s (eBioscience, San Diego, CA) as compared with CD4⁺ splenocytes of control tumor-free mice (only 5.7%). These numbers are consistent with the 17.6% and 9.7% of CD4⁺ splenocytes staining with CD25 in splenocytes

from mice bearing ovarian tumor versus those of control tumor-free mice, respectively (Fig. 6A1), suggesting that the majority of CD4⁺CD25⁺ cells detected are indeed Foxp3⁺ T_{reg} rather than activated conventional T cells. A significant fraction of CD25⁺ T cells from tumor tissue were CD152-positive (Fig. 6B), which may account for the ability of CD152 antibody blockade to blunt the suppression of antigen-specific T cell responses (Fig. 3A) and retard tumor growth (Fig. 3B).

We sought to address the role of CD4⁺CD25⁺ T_{reg} cells in ovarian carcinoma-associated Gr-1⁺CD11b⁺ cell-mediated suppression of antigen-specific T responses. Thus, CD25⁺ cells were depleted from the splenocytes of VLP-vaccinated mice. Treatment of these CD25-depleted splenocyte cultures with VLP induced a robust IFN γ response (Fig. 6C1). Notably, the addition of both CD4⁺CD25⁺ T cells and Gr-1⁺CD11b⁺ MSCs from tumor-bearing mice were required for the suppression of VLP-induced release of IFN γ by CD25-depleted splenocyte cultures of VLP-vaccinated mice. To address whether T_{reg} cells require Gr-1⁺CD11b⁺ MSCs to inhibit the function of T cells in our model, we compared the immunosuppressive effect of CD4⁺CD25⁺ T cells either with or without Gr-1⁺CD11b⁺ cells. Although 10⁵ CD4⁺CD25⁺ T cells without Gr-1⁺CD11b⁺ cells could slightly reduce the T cell response (Fig. 6C1), the immunosuppression was much more potent in the presence of Gr-1⁺CD11b⁺ cells. Because this suppression was not seen in the absence of CD4⁺CD25⁺ T cells (Fig. 6C1), this experiment suggests

a critical role for T_{reg} in the suppression of antigen-specific immunity by $Gr-1^+CD11b^+$ MSCs of tumor-bearing mice. Finally, suppression of VLP-induced release of $IFN\gamma$ by CD25-depleted splenocyte cultures of VLP-vaccinated mice could be titrated with the addition of increasing numbers of $CD4^+CD25^+$ T cells (Fig. 6C2).

Discussion

In this study, we describe the accumulation of $Gr-1^+CD11b^+$ MSCs and $CD4^+CD25^+FoxP3^+$ T_{reg} cells in the spleen, ascites, and tumor tissue of mice bearing the MOSEC 1D8 model of ovarian carcinoma. Mice bearing LLC, but not the cervical carcinoma model, TC-1 (data not shown), also accumulate $Gr-1^+CD11b^+$ MSCs, implying that this phenomenon is neither restricted to the 1D8 model, nor common to all tumor models. The absence of $Gr-1^+CD11b^+$ MSC accumulation from the spleens of mice bearing TC-1 suggests that other mechanisms are responsible for tolerance of this tumor. It is clear that tumors use multiple mechanisms to induce immune tolerance involving T_{reg} cells, tolerant DCs, and the tumor cell itself.

We show that the mouse ovarian carcinoma-associated $Gr-1^+CD11b^+$ MSCs expressed a high level of CD80, whereas other costimulatory molecules, i.e., CD40 and CD86, are not detected. We find that direct interaction of MOSEC 1D8 ovarian carcinoma cells causes $Gr-1^+CD11b^+$ cells to up-regulate surface expression of CD80. We show that CD80 expressed by ovarian carcinoma-associated $Gr-1^+CD11b^+$ cells plays a critical role in immunosuppression induced and maintained by $Gr-1^+CD11b^+$ cells.

How does direct contact between tumor and splenic $Gr-1^+CD11b^+$ cells occur for CD80 up-regulation? One possibility is via circulating tumor cells that seed metastases. This is consistent with the requirement of extensive disease burden for this effect and the previous description of metastasis of both MOSEC 1D8 and LLC, but interestingly, not TC-1 tumor. It is also possible that blood cells, especially bone marrow stem cells, pass through tumor tissue before entering the spleen (44). Another possibility is that membrane fragments shed from 1D8 tumor cells trigger CD80 up-regulation on splenic MSCs because viable tumor cells are not required for this phenomenon *in vitro* (Fig. 2). Indeed, ovarian cancer sheds high concentrations of membrane fragments into the peripheral blood of patients (45). These shed tumor membrane fragments have been shown to suppress CD3- ζ expression and induce T cell apoptosis *in vitro* (45). Clearly there are multiple opportunities for contact between blood and tumor cells, but defining the mechanism of $Gr-1^+CD11b^+$ spleen cell expansion and CD80 up-regulation requires further study.

Recently, several studies have addressed the roles of CD80 and CD86 in regulating immune responses. CD80 and CD86 are sometimes considered interchangeable costimulators. However, it has been proposed that CD80 is the initial ligand responsible for maintaining aspects of immune tolerance through interaction with

CD152 (46). These inhibitory functions might then be overridden by the up-regulation of CD86 on DCs as a result of inflammatory stimuli, leading to immune activation. In addition, CD80 and CD86 may have distinct preferences for CD28 and CD152. Our studies strongly support a role for CD80 as the initial ligand responsible for maintaining aspects of immune tolerance through interaction with CD152. CD80 expressed on the $Gr-1^+CD11b^+$ cells induces antigen-specific immunosuppression by modulating the activity of T_{reg} cells. Indeed we find that a significant fraction of $CD4^+CD25^+$ T_{reg} cells isolated from mice bearing the MOSEC 1D8 ovarian carcinoma express CD152. Others have also found a high level of CD152 on $CD4^+CD25^+$ T cells in different systems (47). Furthermore, interference with this role of CD152 suffices to elicit autoimmune disease in otherwise normal animals, presumably through affecting $CD4^+CD25^+$ T cell-mediated control of self-reactive T cells (24). $CD4^+CD25^+$ T_{reg} cells produce interleukin-10, transforming growth factor- β , interleukin-6, and $IFN-\gamma$ to induce the T cell immunotolerance (48). This unique function of CD152 could be used to modulate T cell-mediated immunoregulation, and induce immunologic tolerance, or control autoimmunity.

Binding of CD80 and CD152 may affect the function of $Gr-1^+CD11b^+$ cells. Indeed, binding of CD152-Ig to DCs induces the expression of indoleamine-2,3-dioxygenase (IDO), an enzyme that degrades the essential amino acid tryptophan (49). Tryptophan metabolites suppress T cell response *in vitro* and *in vivo* (50) as well as T cell clonal expansion (49). Recent studies suggest that triggering of IDO requires the ligation of CD80/CD86 molecules displayed on DCs by CD152/CD28 expressed on T cells (49). Subpopulations of $CD4^+CD25^+$ T_{reg} may constitutively express CD152. Indeed, both mouse $CD4^+CD25^+$ T_{reg} cells and a CD152-transfected cell line induced IDO activity in mouse DCs *in vitro* in a CD152-dependent manner. The adaptive immune system could promote tolerance through signals from T_{reg} cells that express CD152 and induce IDO-competent DCs to express IDO, thereby suppressing T cell responses and promoting tolerance. The IDO-catalyzed tryptophan metabolites are toxic for T cells, especially activated T cells. IDO-expressing DC might also promote the development of T_{reg} cells in a feed-forward mechanism (49). Further study is necessary to determine the role of IDO and tryptophan metabolites in immunosuppression produced by ovarian carcinoma-associated $CD80^+Gr-1^+CD11b^+$ MSCs.

Acknowledgments

Received 10/18/2005; revised 3/13/2006; accepted 4/14/2006.

Grant support: Department of Defense funding, OC010017. Congressionally Directed Medical Research Program, PHS grant RO1 CA122581 and the Richard TeLinde Endowment (R.B.S. Roden), and by the University of Nankai and NSFC grant 30540022 (R. Yang).

The costs of publication of this article were defrayed in part by the payment of page charges. This article must therefore be hereby marked *advertisement* in accordance with 18 U.S.C. Section 1734 solely to indicate this fact.

We thank the HERA foundation and Sean Patrick for their encouragement and support of our research program.

References

- Steinman RM, Hawiger D, Nussenzweig MC. Tolerogenic dendritic cells. *Annu Rev Immunol* 2003;21:685-711.
- Probst HC, Lagnel J, Kollias G, van den Broek M. Inducible transgenic mice reveal resting dendritic cells as potent inducers of CD8 $^+$ T cell tolerance. *Immunity* 2003;18:713-20.
- Moser M. Dendritic cells in immunity and tolerance—do they display opposite functions? *Immunity* 2003;19:5-8.
- Juedes AE, Von Herrath MG. Using regulatory APCs to induce/maintain tolerance. *Ann N Y Acad Sci* 2003;1005:128-37.
- Bronte V, Serafini P, Apolloni E, Zanovello P. Tumor-induced immune dysfunctions caused by myeloid suppressor cells. *J Immunother* 2001;24:431-46.
- Li Q, Pan PY, Gu P, Xu D, Chen SH. Role of immature myeloid $Gr-1^+$ cells in the development of antitumor immunity. *Cancer Res* 2004;64:1130-9.
- Young MR, Wright MA, Matthews JP, Malik I, Prechel M. Suppression of T cell proliferation by tumor-induced granulocyte-macrophage progenitor cells producing transforming growth factor- β and nitric oxide. *J Immunol* 1996;156:1916-22.
- Otsuji M, Kimura Y, Aoe T, Okamoto Y, Saito T.

- Oxidative stress by tumor-derived macrophages suppresses the expression of CD3 ζ chain of T-cell receptor complex and antigen-specific T-cell responses. *Proc Natl Acad Sci U S A* 1996;93:13119–24.
9. Kono K, Salazar-Onfray F, Petersson M, et al. Hydrogen peroxide secreted by tumor-derived macrophages down-modulates signal-transducing ζ molecules and inhibits tumor-specific T cell- and natural killer cell-mediated cytotoxicity. *Eur J Immunol* 1996;26:1308–13.
 10. Fu YX, Watson GA, Kasahara M, Lopez DM. The role of tumor-derived cytokines on the immune system of mice bearing a mammary adenocarcinoma. I. Induction of regulatory macrophages in normal mice by the *in vivo* administration of rGM-CSF. *J Immunol* 1991;146:783–9.
 11. Melani C, Chiodoni C, Forni G, Colombo MP. Myeloid cell expansion elicited by the progression of spontaneous mammary carcinomas in c-erbB-2 transgenic BALB/c mice suppresses immune reactivity. *Blood* 2003;102:2138–45.
 12. Kusmartsev S, Gabrilovich DI. Inhibition of myeloid cell differentiation in cancer: the role of reactive oxygen species. *J Leukoc Biol* 2003;74:186–96.
 13. Goddard S, Youster J, Morgan E, Adams DH. Interleukin-10 secretion differentiates dendritic cells from human liver and skin. *Am J Pathol* 2004;164:511–9.
 14. Halliday GM, Le S. Transforming growth factor- β produced by regressor tumors inhibits, whereas IL-10 produced by regressor tumors enhances, Langerhans cell migration from skin. *Int Immunol* 2001;13:1147–54.
 15. Chomarar P, Banchereau J, Davoust J, Palucka AK. IL-6 switches the differentiation of monocytes from dendritic cells to macrophages. *Nat Immunol* 2000;1:510–4.
 16. Gabrilovich DI, Chen HL, Girgis KR, et al. Production of vascular endothelial growth factor by human tumors inhibits the functional maturation of dendritic cells. *Nat Med* 1996;2:1096–103.
 17. Hammad H, de Heer HJ, Soullie T, et al. Prostaglandin D2 inhibits airway dendritic cell migration and function in steady state conditions by selective activation of the D prostanoid receptor 1. *J Immunol* 2003;171:3936–40.
 18. Jing H, Vassiliou E, Ganea D. Prostaglandin E₂ inhibits production of the inflammatory chemokines CCL3 and CCL4 in dendritic cells. *J Leukoc Biol* 2003;74:868–79.
 19. Schnurr M, Toy T, Shin A, et al. Role of adenosine receptors in regulating chemotaxis and cytokine production of plasmacytoid dendritic cells. *Blood* 2004;103:1391–7.
 20. Serafini P, De Santo C, Marigo I, et al. Derangement of immune responses by myeloid suppressor cells. *Cancer Immunol Immunother* 2004;53:64–72.
 21. Subudhi SK, Alegre ML, Fu YX. The balance of immune responses: costimulation versus coinhibition. *J Mol Med* 2005;83:193–202.
 22. Lohr J, Knoechel B, Kahn EC, Abbas AK. Role of B7 in T cell tolerance. *J Immunol* 2004;173:5028–35.
 23. Tang Q, Henriksen KJ, Boden EK, et al. Cutting edge: CD28 controls peripheral homeostasis of CD4+CD25+ regulatory T cells. *J Immunol* 2003;171:3348–52.
 24. Read S, Malmstrom V, Powrie F. Cytotoxic T lymphocyte-associated antigen 4 plays an essential role in the function of CD25(+)/CD4(+) regulatory cells that control intestinal inflammation. *J Exp Med* 2000;192:295–302.
 25. Allez M, Mayer L. Regulatory T cells: peace keepers in the gut. *Inflamm Bowel Dis* 2004;10:666–76.
 26. Mills KH, McGuirk P. Antigen-specific regulatory T cells—their induction and role in infection. *Semin Immunol* 2004;16:107–17.
 27. Mazzoni A, Bronte V, Visintin A, et al. Myeloid suppressor lines inhibit T cell responses by an NO-dependent mechanism. *J Immunol* 2002;168:689–95.
 28. Saio M, Radoja S, Marino M, Frey AB. Tumor-infiltrating macrophages induce apoptosis in activated CD8(+) T cells by a mechanism requiring cell contact and mediated by both the cell-associated form of TNF and nitric oxide. *J Immunol* 2001;167:5583–93.
 29. Alleva DG, Burger CJ, Elgert KD. Tumor-induced regulation of suppressor macrophage nitric oxide and TNF- α production. Role of tumor-derived IL-10, TGF- β , and prostaglandin E₂. *J Immunol* 1994;153:1674–86.
 30. Apolloni E, Bronte V, Mazzoni A, et al. Immortalized myeloid suppressor cells trigger apoptosis in antigen-activated T lymphocytes. *J Immunol* 2000;165:6723–30.
 31. Bronte V, Wang M, Overwijk WW, et al. Apoptotic death of CD8+ T lymphocytes after immunization: induction of a suppressive population of Mac-1+/Gr-1+ cells. *J Immunol* 1998;161:5313–20.
 32. Bronte V, Chappell DB, Apolloni E, et al. Unopposed production of granulocyte-macrophage colony-stimulating factor by tumors inhibits CD8+ T cell responses by dysregulating antigen-presenting cell maturation. *J Immunol* 1999;162:5728–37.
 33. Serafini P, Borrello I, Bronte V. Myeloid suppressor cells in cancer: recruitment, phenotype, properties, and mechanisms of immune suppression. *Semin Cancer Biol* 2006;16:53–65.
 34. Almand B, Clark JI, Nikitina E, et al. Increased production of immature myeloid cells in cancer patients: a mechanism of immunosuppression in cancer. *J Immunol* 2001;166:678–89.
 35. Roby KF, Taylor CC, Sweetwood JP, et al. Development of a syngeneic mouse model for events related to ovarian cancer. *Carcinogenesis* 2000;21:585–91.
 36. Yang R, Murillo FM, Cui H, et al. Papillomavirus-like particles stimulate murine bone marrow-derived dendritic cells to produce α interferon and Th1 immune responses via MyD88. *J Virol* 2004;78:11152–60.
 37. Bronte V, Apolloni E, Cabrelle A, et al. Identification of a CD11b(+)/Gr-1(+)/CD31(+) myeloid progenitor capable of activating or suppressing CD8(+) T cells. *Blood* 2000;96:3838–46.
 38. Dikov MM, Oyama T, Cheng P, et al. Vascular endothelial growth factor effects on nuclear factor- κ B activation in hematopoietic progenitor cells. *Cancer Res* 2001;61:2015–21.
 39. Cauley LS, Miller EE, Yen M, Swain SL. Superantigen-induced CD4 T cell tolerance mediated by myeloid cells and IFN- γ . *J Immunol* 2000;165:6056–66.
 40. Gabrilovich DI, Velders MP, Sotomayor EM, Kast WM. Mechanism of immune dysfunction in cancer mediated by immature Gr-1+ myeloid cells. *J Immunol* 2001;166:5398–406.
 41. Mencacci A, Montagnoli C, Bacci A, et al. CD80+Gr-1+ myeloid cells inhibit development of antifungal Th1 immunity in mice with candidiasis. *J Immunol* 2002;169:3180–90.
 42. Zheng Y, Manzotti CN, Liu M, et al. CD86 and CD80 differentially modulate the suppressive function of human regulatory T cells. *J Immunol* 2004;172:2778–84.
 43. Curiel TJ, Coukos G, Zou L, et al. Specific recruitment of regulatory T cells in ovarian carcinoma fosters immune privilege and predicts reduced survival. *Nat Med* 2004;10:942–9.
 44. Yamaguchi H, Wyckoff J, Condeelis J. Cell migration in tumors. *Curr Opin Cell Biol* 2005;17:559–64.
 45. Taylor DD, Gercel-Taylor C. Tumor-derived exosomes and their role in cancer-associated T-cell signaling defects. *Br J Cancer* 2005;92:305–11.
 46. Sansom DM, Manzotti CN, Zheng Y. What's the difference between CD80 and CD86? *Trends Immunol* 2003;24:314–9.
 47. Salomon B, Lenschow DJ, Rhee L, et al. B7/CD28 costimulation is essential for the homeostasis of the CD4+CD25+ immunoregulatory T cells that control autoimmune diabetes. *Immunity* 2000;12:431–40.
 48. Moseman EA, Liang X, Dawson AJ, et al. Human plasmacytoid dendritic cells activated by CpG oligodeoxynucleotides induce the generation of CD4+CD25+ regulatory T cells. *J Immunol* 2004;173:4433–42.
 49. Mellor AL, Munn DH. IDO expression by dendritic cells: tolerance and tryptophan catabolism. *Nat Rev Immunol* 2004;4:762–74.
 50. Bauer TM, Jiga LP, Chuang JJ, et al. Studying the immunosuppressive role of indoleamine 2,3-dioxygenase: tryptophan metabolites suppress rat allogeneic T-cell responses *in vitro* and *in vivo*. *Transpl Int* 2005;18:95–100.

Expert Opinion

1. Introduction
2. Immunotherapy of cervical cancer
3. Immunotherapy of ovarian cancer
4. Expert opinion and conclusions

For reprint orders, please
contact:
reprints@ashley-pub.com

Ashley Publications
www.ashley-pub.com



Vaccines & Antibodies

Immunotherapy for gynaecological malignancies

George Coukos[†], Jose R Conejo-Garcia, Richard BS Roden & T-C Wu

[†]*University of Pennsylvania, Abramson Cancer Research Institute, and Center for Research on Reproduction and Women's Health, Philadelphia, PA 19104, USA*

Gynaecological malignancies, excluding breast cancer, cause ~ 25,000 deaths yearly among women in the US. Therefore, novel approaches for the prevention or treatment of these diseases are urgently required. In the case of cervical cancer, human papillomavirus (HPV) xenoantigens are readily recognised by the immune system, and their targeting has shown great promise in preclinical models of therapeutic vaccination and in clinical studies of preventative vaccination. A growing body of evidence indicates that ovarian cancer is also immunogenic and can thus be targeted through immunotherapy. This review outlines the principles and problems of immunotherapy for cervical and ovarian cancer, including the authors' personal assessment.

Keywords: cervical cancer, cytokine, HPV, immunotherapy, lymphocyte, ovarian cancer, tumour-infiltrating, vaccine development

Expert Opin. Biol. Ther. (2005) 5(9):1193-1210

1. Introduction

Gynaecological malignancies, excluding breast cancer, claim ~ 25,000 deaths yearly among women in the US. Approximately 15,000 of them are due to epithelial ovarian cancer (EOC) and another 5000 due to invasive cervical cancer. Similar figures apply to European countries, while worldwide cervical cancer remains a premier health issue for women. In fact, ~ 500,000 new cases of cervical cancer and 200,000 deaths occur each year worldwide, with nearly 80% of cases arising in less developed countries [1]. Aggressive surgery and combination chemotherapy have had little impact on the long-term survival of patients with advanced EOC. Furthermore, multimodality therapy, including chemotherapy and radiation, are destined to fail in a large number of patients with advanced cervical cancer. These numbers create a pressing need to develop novel approaches for the prevention or treatment of these diseases.

It is now generally accepted that tumour cells express unique antigens or over-express antigens that are recognised by the immune system [2-4]. Identifying these antigens provides the opportunity for developing potentially successful immunotherapy. In the case of cervical cancer, the therapeutic targets are easily identified: human papillomavirus (HPV) xenoantigens are readily recognised by the immune system, and their targeting has shown great promise in preclinical models of therapeutic vaccination and in clinical studies of preventative vaccination. These advances would also be applicable to vulvar or vaginal cancers caused by HPV. For other gynaecological malignancies, the field of immunotherapy is at its infancy. With few exceptions [5], most work has been done in ovarian cancer. Tumour-associated antigens (TAAs) have not undergone rigorous scrutiny, and systematic characterisation of immune surveillance mechanisms has not been undertaken to date. However, mounting evidence indicates that ovarian cancer is also immunogenic and can thus be targeted through immunotherapy. This review will summarise the current status of immunotherapy for cervical and ovarian cancer.

2. Immunotherapy of cervical cancer

Approximately 90 – 98% of cervical cancers are associated with HPV infection, which is common and is acquired mainly through sexual contact (for review see [6]). There are > 100 known genotypes of HPV, but only some are associated with infection of the genital mucosa. Genital HPV types can be classified into 'high-risk' and 'low-risk' varieties, based on the frequency of their identification in cervical cancers. 'Low-risk' types (i.e., HPV-6 and -11) are associated with benign proliferative growths, such as genital warts. 'High-risk' HPVs can cause cervical intraepithelial neoplasia (CIN) and, if left untreated, may lead to cervical cancer (for review see [7]). Thus, numerous studies have indicated that HPV infection is necessary for the development of cervical cancer.

All HPV types have a circular, double-stranded DNA genome containing ~ 8000 base pairs and encoding two classes of proteins: 'early' proteins, which regulate viral DNA replication (E1, E2), RNA transcription (E2) and cell transformation (E5, E6, E7); and 'late' proteins (L1, L2), the structural components of the viral capsid. The viral DNA ordinarily replicates extrachromosomally. In HPV-associated malignant transformation, viral DNA may be integrated into the cellular DNA, and integration often results in deletion of large sectors of the viral genome. Late genes (L1 and L2) and some early genes (such as E2 and E5) are usually lost, leaving E6 and E7 as the principal open reading frames found in carcinomas (for review see [7]).

Several studies demonstrate that virus-neutralising antibodies mediate protection of animals from experimental papillomavirus infection [8-10]. Although antibody-mediated neutralisation of virus has important preventative utility, several lines of evidence suggest that cell-mediated immune responses are important in controlling established HPV infections as well as HPV-associated neoplasms (for review see [11]). First, the prevalence of HPV-related diseases (infections and neoplasms) is increased in patients with impaired cell-mediated immunity, including transplant recipients [12] and HIV-infected patients [13,14]. Second, animals immunised with non-structural viral proteins are protected from papillomavirus infection or the development of neoplasia. Immunisation also facilitates the regression of existing lesions [15,16]. Third, infiltrating CD4⁺ (T helper cells) and CD8⁺ (cytotoxic T cells) T cells have been observed in spontaneously regressing warts [17]. Finally, warts in patients who are on immunosuppressive therapy often disappear when treatment is discontinued (for review see [18]).

The well-characterised foreign (viral) antigens and the well-defined virologic, genetic and pathological progression of HPV have provided a unique opportunity to evaluate interventions with antigen-specific immunotherapy. Conceptually, two different types of HPV vaccines can be designed: prophylactic (preventative) vaccines that prevent HPV infection, and therapeutic (curative) vaccines that would induce regression of established HPV infection and its sequelae.

2.1 Preventative HPV vaccines

Preventative HPV vaccine development has been complicated by the lack of animal models for the genital mucosa-tropic HPV types and by difficulty in propagating the virus in culture. These problems have been partially overcome using cutaneous and mucosal animal papillomaviruses as models, and by the development of virus-like particles (VLPs) and pseudovirions.

The papillomavirus major capsid protein L1 – over-expressed in mammalian [19,20], insect [21], yeast [22] or bacterial cells [23] – spontaneously assembles to form VLPs that are devoid of the oncogenic viral genome. Parenteral injection of these VLPs, or even the pentameric L1 capsomer [24], elicits high titres of serum neutralising antibodies and protection from experimental challenge with infectious virus in several animal papillomavirus models [8,9,25]. Genetic vaccination with an L1 expression vector also protects from experimental viral challenge [26-28].

Although VLP vaccination provides immunity from experimental inoculation, protection against sexual transmission of HPV requires neutralising antibodies acting at mucosal surfaces. Serum neutralising IgG induced by parenteral VLP vaccination may enter via transudation into the genital tract and maintain a sufficient level to provide sterilising immunity across the menstrual cycle. Neutralising antibodies may either transudate from plasma into genital secretions and/or be synthesised by local plasma cells. Induction of plasma cells requires direct immunisation of the mucosa-associated lymphoid tissue [29,30], but nasal instillation of VLPs was found to be efficient in generating specific antibodies, including serum IgG, and IgG and IgA in mucosal secretions of mice [23,31]. More recently, oral vaccination with HPV VLPs in mice has been shown to induce systemic virus-neutralising antibodies, suggesting that HPV VLPs may be antigenically stable in the environment of the gastrointestinal tract. These studies provide the possibility of vaccinating large populations with HPV VLP without using syringes [32].

In recent clinical data, intramuscular vaccination of women with HPV-16 VLPs was found to induce significant antibody titres in cervical secretions [33]. A comparison by the same researchers of nasal spray or aerosol for mucosal delivery of 50 µg of HPV-16 VLPs to humans revealed that aerosol was effective at inducing an antibody response, with IgG found predominantly in serum and both IgG and IgA found in cervical secretions.

Early Phase I/II clinical trials using HPV L1 VLP delivered intramuscularly have demonstrated the immunogenicity and safety of this vaccine [34,35]. Importantly, Koutsky *et al.* have reported data from a clinical trial of HPV-16 L1 VLPs indicating for the first time that a vaccine strategy can be implemented in humans to prevent HPV-16 infections and HPV-16-associated premalignant lesions [36]. A similar vaccine strategy is being tested with HPV-11 VLPs [37] and VLP vaccination may also be extended to other oncogenic HPV types. Vaccination of a single animal with multiple

HPV VLP types does not detract from the response to the individual types [38]. A quadrivalent HPV VLP vaccine (types 6, 11, 16 and 18) from Merck is in a clinical trial at present; preliminary results found that the vaccine was well-tolerated and generated neutralising antibody titres. These HPV VLP vaccines may be useful not only for the prevention of cervical cancer, but also for the prevention of other HPV-associated malignancies, including a subset of head and neck squamous cell carcinomas, vulvar cancers and other anogenital cancers.

A clearer picture of the long-term effects, including duration of antibody titres and side effects, will likely emerge several years after this study and other parallel studies of HPV VLP vaccines have matured. Concern has been raised that widespread HPV-16 vaccination may eventually exert evolutionary pressure, selecting outgrowth of other types of HPV and/or some HPV-16 variants that carry mutation(s) on the L1 gene and, thus, are unaffected by the vaccine. However, this is improbable given the slow evolution of HPV and evidence of cross-neutralisation of variants by immune sera [38,39].

Although the VLP vaccine shows great promise for HPV control in industrialised nations, it is probably not ready for use in developing countries due to its cost. Many developing countries do not have sufficient resources for routine Pap smear testing, let alone preparation and parenteral administration of VLPs. Another difficulty is the instability of the preventative HPV VLP vaccine at room temperature over long periods of time. The VLP vaccine requires sophisticated equipment for production and refrigerated storage facilities. Future vaccine research should work toward a new generation of HPV vaccines that are cheaper, more easily administered, and more stable in order to be applicable worldwide (for a review of prophylactic HPV vaccines and associated issues see [40]). Naked DNA vaccines that express L1 are effective in animals and may be cheaper than using purified VLP, particularly in the formulation of polymeric vaccines based on multiple HPV genotypes.

There are at least 15 oncogenic HPV genotypes, and *in vitro* neutralisation studies suggest that they may represent an equivalent number of serotypes [38], although limited cross-reactivity can occur between L1s of different genotypes with > 85% sequence identity [38]. Therefore, protection against infection by all of these types with a VLP-based vaccine would probably require a highly polymeric vaccine that would be difficult to generate. Another potential alternative for comprehensive protection is to vaccinate against L2.

L2 is immunologically subdominant to L1, as immunisation with virions or capsids comprising L1 and L2 elicits almost exclusively L1-specific antibody [41]. However, induction of *in vitro* neutralising antibody [41,42] and protection of animals from experimental infection by vaccination with recombinant L2 alone [43-45] demonstrates the promise of L2 as a prophylactic vaccine. Indeed, L2-specific cross-neutralising polyclonal sera and monoclonal antibodies have been demonstrated [41,46,47]. A recent study by Embers *et al.* indicates that protection by

L2 peptide vaccination is probably mediated by neutralising antibody [10]. Vaccination of patients with fusion proteins containing L2 has proven safe. As seen in animal models, the humoral immune responses of patients to L2 are much weaker than to L1 VLP [48-50]. Therefore, if the relatively weak immunogenicity of L2 can be overcome, vaccination against L2 holds great potential for prophylaxis against infection by a broad range of HPV types and their associated cancers.

2.2 Therapeutic HPV vaccines

Although vaccination with preventative HPV vaccines is able to generate high titres of serum neutralising antibodies in animals and in humans, such immunisation may not be able to generate significant therapeutic effects for established or breakthrough HPV infections that have escaped antibody-mediated neutralisation. Therapeutic vaccines should induce specific cell-mediated immunity that prevents the development of lesions and eliminates pre-existing lesions or even malignant tumours. Among early viral antigens, neither E1 nor E2 are consistently expressed in carcinoma, while E5 shows limited immunogenicity and has not been extensively studied as a vaccine antigen. Likewise, E4 and the L1 and L2 capsid proteins are unlikely to be suitable targets for therapeutic vaccine development because these proteins are not detectably expressed in basal epithelial cells of benign lesions or in abnormal proliferative cells of premalignant and malignant lesions [51,52]. Although recent studies indicate that vaccination with VLPs may generate a capsid protein-specific cytotoxic T lymphocyte (CTL) response [53,54], such a response against L1 or L1/L2 VLPs alone may not be able to generate a significant therapeutic effect.

E6 and E7 are completely foreign viral proteins and may, therefore, harbour more antigenic peptides/epitopes than a mutant cellular protein. Furthermore, as E6 and E7 are required for the induction and maintenance of the malignant phenotype [55], cervical cancer cells are unlikely to evade an immune response through antigen loss. Thus, although care must be taken, given the oncogenic nature of these genes, E6 and E7 proteins represent good targets for developing antigen-specific immunotherapies or vaccines for cervical cancer. As E6 and E7 are virus-encoded oncogenic proteins, for clinical translation the E6/E7 genes have to be mutated to alleviate concerns about their oncogenic potential.

Various forms of HPV vaccines, such as vector-, peptide-, protein-, DNA-, chimeric VLP- and cell-based vaccines, have been described in experimental systems targeting HPV-16 E6 and/or E7 proteins. The following sections provide a brief description of several therapeutic HPV vaccines that have been tested in the early phases of clinical trials.

2.2.1 Live vector vaccines

Live vector vaccines have been evaluated in clinical trials. Results of Phase I/II clinical trials using recombinant vaccinia

virus encoding HPV-16 and HPV-18 E6/E7 (called TA-HPV) indicated that the vaccine was well-tolerated and that some patients with CIN-3, early invasive cervical cancer or advanced cervical cancer developed T cell immune responses after vaccination [56-58]. TA-HPV was also able to generate specific immune responses in some patients with HPV-associated vulval or vaginal intraepithelial neoplasia [59,60]. In a study conducted by Baldwin and colleagues, 5 of 12 patients had at least a 50% reduction in lesion diameter over 24 weeks, and one patient showed complete regression after vaccination [59]. Recombinant *Listeria monocytogenes* has also shown promise in preclinical models and will be undergoing clinical testing in the near future [61,62].

2.2.2 Peptide/protein vaccines

Phase I/II clinical trials have demonstrated that peptide vaccines are both safe and well-tolerated in humans. In one study, women were vaccinated with HPV-16 E7 peptides, either amino acids (aa) 12 – 20 alone, or aa 12 – 20 mixed with aa 86 – 93 covalently linked to a T helper stimulating peptide. Dysplasia was cleared in 3 of 18 patients with high-grade cervical or vulvar intraepithelial neoplasia, and measured regression of lesions was observed in 6 of 18 of the same patients [63]. Lipopeptides have also been used in clinical trials. Although regression of cancer was not noted, vaccination with lipidated HPV-16 E7 peptide was found to generate CTL responses in some patients with HPV-associated cancer [64].

Several of the strategies employed in preclinical protein vaccine studies have been translated into clinical trials. Some approaches have used a fusion of HPV capsid proteins with HPV early proteins, possibly providing prophylactic as well as therapeutic benefit. Clinical trials demonstrated that a fusion of HPV-6 L2 and E7 adsorbed onto Alhydrogel (called TA-GW) was well-tolerated and could clear HPV genital warts in some patients [48]. A fusion of HPV-16 L2, E6 and E7 (called TA-CIN) was well-tolerated by patients, it elicited antibodies in all women tested and produced T cell immunity in a subset of women tested [50]. TA-CIN vaccination has also been combined with TA-HPV vaccination in a 'prime-boost' clinical trial in patients with high-grade vulval intraepithelial neoplasia (VIN). In a recent study, ten women with HPV-16-positive high-grade VIN were immunised with TA-HPV and boosted three times with TA-CIN. Nine of ten women demonstrated HPV-16-specific proliferative T cell and/or serological responses following vaccination. In addition, three women showed lesion shrinkage or symptom relief, although there was no direct correlation between clinical and immunological responses [65]. Other fusion strategies have also been used to make proteins for HPV vaccination. In a small, Phase I/II clinical trial, a fusion of *Haemophilus influenzae* lipoprotein D and HPV-16 E7 (called PD-E7 or D16E7) administered with adjuvant induced potent E7-specific CD8⁺ T cell responses and regression of lesions in some patients with CIN-1 or CIN-3 [66]. HspE7 (Stressgen Biotechnologies Corp., Victoria, BC, Canada), a fusion of BCG Hsp65 and

HPV-16 E7, is another vaccine now in clinical trials for the treatment of patients with HPV-associated anal dysplasia [67].

These therapeutic vaccines may be appealing in high-risk populations where compliance and long-term follow-up can be a problem for all types of treatments. It is important to note that the results from most of the therapeutic vaccine clinical studies are quite preliminary. Only a few patients were included in these studies. Furthermore, a relatively small proportion of the lesions have been cleared. It is difficult to rule out the possibility that the observed lesion has been biopsied off or that adjacent CIN lesions could undergo regression related to the inflammatory response of the biopsy. In addition, it has been reported that CIN lesions can undergo spontaneous regression [68]. At this point, the relative cost of treatment of CIN with local ablative measures versus vaccine approaches is not clear as there is no therapeutic HPV vaccine in the market at present.

2.2.3 DNA vaccines

At present, a plasmid DNA vaccine encoding multiple human leukocyte antigen (HLA)-A2-restricted epitopes derived from the HPV-16 E7 protein has been evaluated in a Phase I clinical trial in patients with high-grade anal intraepithelial lesions [69] and in a Phase I clinical trial in patients with CIN-2/3 [70]. The vaccine, ZYC-101 (ZYCOS Inc., now acquired by MGI Pharma, MA, USA), is composed of plasmid DNA encapsulated in biodegradable polymer micro-particles. The initial results of these trials suggest that the DNA vaccine was well-tolerated in all individuals at all dose levels tested. Furthermore, 10 of 12 individuals with anal dysplasia demonstrated an increased immune response to the peptide epitopes encoded within the DNA vaccine [69]; 5 of 15 women with CIN-2/3 had complete histological responses and 11 of 15 women with CIN-2/3 had HPV-specific T cell responses [70]. A Phase II trial of ZYC-101a, a next-generation ZYC-101 vaccine that contains plasmid DNA encoding both HPV-16 and HPV-18 E6 and E7 epitopes, has also been reported recently. Although there was no overall significant difference in clearance of CIN-2/3 between the placebo and ZYC-101a treatment groups, data from a prospectively defined subgroup of younger women demonstrated a significantly higher rate of disease resolution for individuals treated with ZYC-101a [71]. In addition to ZYC-101 vaccines, a DNA vaccine encoding E7 linked to *Mycobacterium tuberculosis* Hsp70 (pNGVL4a-Sig/E7(detox)/Hsp70) has entered clinical trials at Johns Hopkins Hospital. Initial results indicate that the vaccine is well-tolerated (Timble C, pers. commun.).

2.2.4 Dendritic cell-based vaccines

Greater understanding about the origin of dendritic cells (DCs), their antigen uptake mechanisms, and the signals that stimulate their migration and maturation into immunostimulatory antigen-presenting cells (APCs) has aided the development of DC-based vaccines (for review

see [72]). HPV-specific DC-based vaccines can be generated using the following methods:

- DCs pulsed with E6 and/or E7 peptides/proteins
- DCs transduced with DNA, RNA or viral vectors encoding E6 and/or E7

Genes encoding costimulatory molecules or cytokines can also be introduced into DCs to enhance their ability to stimulate the immune system via enhanced T cell interactions. Despite the versatility in preparing DCs, the production of DCs is labour-intensive. DCs must be cultured *ex vivo* on an individualised basis. DC vaccines can also potentially vary in quality because of the wide variety of methods for culturing DCs, loading antigen and administering vaccines. In addition, some concerns have been raised that immature DCs may potentially result in antigen tolerance (for review see [73]). Although promising preclinically, DC-based vaccines for HPV have had limited clinical testing. One clinical study monitored a woman with metastatic cervical cancer who received a vaccine made of DCs pulsed with HPV-18 E7 protein. Although vaccination did not result in permanent remission, it inhibited tumour progression and greatly improved the patient's performance without significant side effects [74]. DCs pulsed with tumour lysate have also been used in some clinical trials [75]. In general, DC-based vaccines may be more useful for tumour cells without well-defined tumour-specific antigens because they are quite labour-intensive, HPV antigen-specific, DC-based vaccines.

3. Immunotherapy of ovarian cancer

The case of immunotherapy for ovarian cancer is not so well-established as for cervical cancer. As for most other non-virally induced solid tumours, tumour rejection antigens have not been well characterised. The lack of obvious success in Phase I/II trials to date has cast doubts on the rationale and potential of immunotherapy in EOC. However, accumulating evidence shows that ovarian tumours are recognised and attacked by the immune system. EOCs may display a brisk lymphocyte infiltrate [78-81], while tumour-derived lymphocytes exhibit oligoclonal expansion [82,83], recognise tumour antigens [84-88] and display tumour-specific cytolytic activity *ex vivo* [89-93]. *Ex vivo* expanded T cell clones recognise different antigenic determinants within the same patients, indicating heterogeneity of the response within individuals [92]. Evidence of spontaneous antitumour immune response activation in ovarian carcinoma was recently provided. Tumour-specific peripheral blood T cell precursors were detected in ~ 50% of patients with advanced ovarian carcinoma [94]. The authors recently characterised tumour-infiltrating lymphocytes (TILs) in 176 advanced ovarian cancers. It was shown that, whereas TILs could be detected in the stroma surrounding tumour islets in the majority of tumours, T cells infiltrating tumour islets (intratumoural T cells) were detected only in 55% of the

patients [95]. Intratumoural T cells were associated with significantly longer clinical remission after chemotherapy as well as improved overall survival. Therefore, ovarian carcinoma belongs to the list of tumours that could greatly benefit from the strengthening of tumour–host interactions through immunotherapy; this list now includes vertical-growth-phase melanoma and breast, prostate, renal cell, oesophageal and colorectal carcinomas [96-101].

Results reported recently with cancer vaccines in other solid tumours are encouraging, especially in the adjuvant setting [102-105]. In addition, adoptive lymphocyte therapy has yielded dramatic results in melanoma [76]. Up to 50% of treated patients that have been published to date in one trial demonstrated objective durable responses, with a > 50% reduction at all tumour sites [76]. The best results of this group were achieved with a combination of adoptive therapy, which included polyclonal T cells, IL-2 and lymphodepletion. Analysis of the TCR V β gene products demonstrated that there was a significant correlation between tumour regression and the degree of persistence in peripheral blood of adoptively transferred T cell clones. In fact, persistence of multiple tumour-reactive T cell clones following adoptive transfer was associated with sustained complete regression of all metastatic lesions in lungs and soft tissues [76,106,107]. Thus, efforts at developing immunotherapy for ovarian cancer should be intensified rather than abandoned. This review will recapitulate previous and ongoing clinical trials as well as future directions about four different immunotherapy approaches: therapeutic vaccines; adoptive T cell therapy strategies; cytokine therapies; and antiregulatory T cell treatments.

3.1 Tumour vaccines

Tumour vaccines represent one of the most common immunotherapy approaches against ovarian cancer, although only a handful of trials have reported clinically measurable benefits. Earlier clinical trials have been designed empirically without fundamental knowledge of the immune biology of solid tumours and resulted in poor clinical responses. As advancements in molecular and cellular immunology continue to grow rapidly, significant progress has been made in our understanding of immune dysfunction caused by tumours and in our ability to manipulate the immune system in an effort to circumvent such dysfunction.

3.1.1 Antigen-based vaccination

3.1.1.1 Tumour-associated antigens

The induction of T cell-specific responses in a reproducible and controlled clinical setting would ideally require the identification of ovarian-specific tumour antigens. Lessons learned from other tumours, mainly melanoma, indicate that tumour cells do express unique antigens that are recognisable by the immune system [2-4]. These can be differentiation antigens, also expressed by embryonal cells, but not by adult normal cells; overexpression/amplification antigens, also expressed by normal cells, but at levels that are too low to induce an

immune response under physiological conditions; and newly acquired mutational antigens, resulting from mutations associated with the oncogenic process. The best differentiation tumour rejection antigen identified to date is the HLA-A2-restricted onconeural protein antigen cdr2 [108,109], based on the high frequencies of CTLs in patients with EOC and the syndrome of paraneoplastic cerebellar degeneration (PCD). However, due to the shared expression of cdr2 in epithelial tumour and cerebellar Purkinje cells that results in PCD, cdr2 is not a promising candidate for vaccines.

HER-2/neu (c-erbB-2) is an attractive overexpression/amplification antigen for breast and ovarian cancer vaccines [110,111]. Although overexpressed in only 10–15% of primary ovarian cancers [112], a large proportion of recurrent tumours may be positive for HER-2, based on the examination of cells that have been placed in culture [113]. HER-2 is immunogenic in patients with ovarian cancer. A protein vaccine consisting of a high dose (900 µg) of a HER-2/neu intracellular domain peptide elicited rapid, specific, T cell-mediated immunity in most ovarian cancer patients treated [114]. Interestingly, a third of patients developed IgG immunity to the native HER-2/neu protein after peptide immunisation, while intermolecular epitope spreading to p53 was evident in 20% of vaccinated patients [115].

Few other tumour antigens have been identified in ovarian cancer; among them are amino enhancer of split protein [116], the folate binding protein [87], sialylated TN (sTN), a mucin antigen [117-119], MUC-1 [120], NY-ESO-1, a testis differentiation antigen [121,122], and mesothelin [123]. In a recent study, a synthetic analogue of sTN was administered to patients with advanced ovarian carcinoma. No acute toxicities as well as a documented immune response were reported, with several patients maintaining stable disease for extended time [124]. p53 overexpression as a result of mutations is highly prevalent in late as well as early stage sporadic serous carcinomas [125], and has been observed in all early invasive serous carcinomas and the adjacent dysplastic ovarian surface epithelium in ovaries removed prophylactically from BRCA heterozygous women [126]. In addition, p53 loss is important for ovarian carcinogenesis in genetically engineered mouse models [127,128]. Thus, vaccination against p53 is a logical approach. A trial of p53 vaccination is ongoing at present at the National Cancer Institute (NCI).

Another tumour antigen expressed by a high proportion of ovarian tumours that calls for more investigation is CA-125. Two independent studies showed that immunotargeting of CA-125 yields tangible clinical results. A recent Phase I/IIb study proved the safety and immunogenicity of anti-idiotypic antibody vaccine ACA125, which functionally imitates CA-125, in 119 patients with advanced ovarian carcinoma. Development of CA-125-specific antibodies and antibody-dependent cell-mediated cytotoxicity of CA-125-positive tumour cells was observed in 50.4 and 26.9% of patients, respectively. Antiantidiotypic antibody (Ab3)-positive patients showed a significantly longer survival (median

23.4 months) as compared with Ab3-negative patients (median 4.9 months; $p < 0.0001$) [129]. Furthermore, treatment with the high-affinity murine monoclonal antibody oregovomab (OvaRex[®], AltaRex, MA, USA), which results in formation of circulating immune complexes that can trigger a cellular immune response targeting CA-125, shows promise in ovarian cancer [130]. In a recent Phase III trial of upfront therapy, addition of OvaRex consolidation following carboplatin–paclitaxel chemotherapy resulted in 2.3-fold increase in median time to progression in a preliminary report (adjusted hazard ratio 0.474; $p = 0.0261$; 95% confidence interval: 0.246–0.915). This was observed only in the subset of patients ($n = 67$) with < 2 cm residual disease after primary surgical debulking and favourable response to chemotherapy, as assessed by serum CA-125 < 65 U/ml before the third cycle and normalised but measurable CA-125 at study entry (CA-125 > 5 and ≤ 35 U/ml) [131].

Universal antigens are expressed by a variety of tumour cells, but not normal cells, as their expression is necessary to maintain the transformed phenotype [132]. The human telomerase reverse transcriptase (hTERT) is one such promising TAA for therapeutic vaccination as it is expressed in $> 85\%$ of EOCs [133,134]. Unlike other TAAs, telomerase is absent in most normal cells. CTLs recognise peptides derived from hTERT and kill hTERT-positive carcinoma cells *in vitro* [135]. hTERT is immunogenic in patients with solid tumours.

Other universal antigens tested include cytochrome P450 CYP1B1 and survivin. CYP1B1 is a member of the CYP1 P450 enzyme family that is overexpressed in a variety of solid tumours. Preclinical work has shown that human CYP1B1-encoding plasmid DNA formulated in poly(lactide-co-glycolide) microparticles (ZYCOS, Inc.) is well-tolerated and elicits durable immune responses that are dependent on repeat immunisation [136]. Survivin expression has been described during embryonic development and in adult cancerous tissues, with greatly reduced expression in adult normal differentiated tissues, particularly if their proliferation index is low. Survivin has been defined as a universal tumour antigen and as the fourth most significant transcriptosome expressed in human tumours [137,138].

3.1.1.2 Mode of delivery

A variety of methodologies have been developed and tested for the delivery of antigen vaccines. Recombinant proteins or synthetic peptides may be injected directly to patients, but require coadministration of adjuvants to enhance recruitment and/or activation of DCs at the site of injection. Classical adjuvants used in vaccine trials have included keyhole limpet haemocyanin [139], Montanide ISA-51, bacillus Calmette–Guérin (BCG) or cytokines such as granulocyte-macrophage colony-stimulating factor (GM-CSF) and IL-2 [140]. Other strategies include DNA-based vaccines in which DNA encoding for tumour-specific antigens may be inserted into recombinant viruses and transduced into DCs [141-143]. The use of CpG oligonucleotides or heat-shock protein adjuvants is very promising in this setting [144].

DCs have shown great promise in tumour vaccination, as they are professionally endowed with the ability to present antigen. Different methodologies to generate clinically meaningful quantities of DCs from peripheral blood precursors have been developed [145-147]. DCs can now be pulsed successfully *in vitro* with recombinant proteins, synthetic peptides, mRNA or cDNA of known antigens. The first lesson painfully learned from clinical trials is that mature DCs are superior to immature DCs in the induction of immunological responses. A direct comparison of peptide-loaded immature and mature DCs in patients with metastatic melanoma has shown that only mature DCs induce antigen-specific cytolytic effector responses [148] and correlate with favourable clinical outcomes [149]. In fact, immature DCs might rather induce tolerance to presented antigens in the context of therapeutic vaccination [148,150]. It has also become progressively clear that DCs exhibit a tolerogenic and pro-angiogenic phenotype within ovarian cancer [151-154] and that tumour-derived factors induce not only intratumoural, but also systemic suppression of DC differentiation and/or maturation [155-157]. The level and stability of DC maturation are thus critical factors that may affect the efficacy of vaccine therapy [158]. DCs with partial but irreversible maturation might be best positioned to achieve efficient vaccination. For example, genetic manipulation of DCs *ex vivo* to confer expression of cytokine transgenes or CD40 ligand has been shown to maintain the therapeutic potency of DC vaccines. Promising protocols have explored the use of CD40/Toll-like receptor 7 stimulation [159,160]. Alternatively, blockade of systemic immunosuppressive factors might permit proper maturation of DCs *in vivo* [161].

3.1.2 Whole tumour antigen vaccines

In the absence of known tumour antigens, whole-cell vaccines offer relative simplicity of preparation and the theoretical advantage of a broad tumour antigen repertoire from which to draw an immune response. Ovarian cancer lends itself to this approach because tumour cells can be easily recovered through the collection of ascites or cytoreductive surgery. However, difficulty in establishing autologous tumour cell cultures, especially from solid tumour nodules, and issues of cost may be important shortcomings.

Preparation of whole tumour cell vaccines is critical for determining immunogenicity. In order to increase the immunogenicity of whole-cell tumour vaccines, cells have been associated with specific adjuvant haptens, such as dinitrophenyl (DNP), which can trigger a strong inflammatory response. A recent clinical Phase I trial using DNP-modified autologous ovarian tumour cells in stage III patients reported no acute toxicities. Some patients developed a measurable immune response, although no clinically meaningful responses were observed [162]. A promising approach is being tested at present at Dana Farber, where patients receive autologous tumour cells transfected with recombinant replication-restricted adenovirus encoding

GM-CSF. A similar trial in early and advanced stage non-small cell lung cancer showed a 10% complete response rate lasting 6 – 22 months and overall longer survival in patients receiving vaccines secreting higher amounts of GM-CSF [163]. Promising results were also reported in melanoma with this approach [164].

An alternative approach proposed entails the use of 'exosomes', membranous material released by tumours and abundantly found in ascites. Exosomes express class I MHC and TAAs, and may be suitable for tumour vaccination [165]. However, exosomes were recently shown to also express FasL and a 26-kDa factor inducing T cell suppression, resulting in CD3-zeta and JAK-3 downregulation, and induction of apoptosis in cytotoxic T cells [166].

A viable alternative is offered by DC vaccines, prepared by pulsing autologous DCs with dead tumour cells. DCs are efficient at presenting antigens captured from apoptotic or necrotic cells [167], although apoptotic cells may provide less potent maturation-inducing signals than necrotic cells [168]. Thus, the method of preparation of tumour cells is also critical in this context, and addition of inflammatory molecules or moieties derived from pathogens may enhance DC performance. A promising variation for the design of cancer vaccines involves the fusion of whole tumour cells with DCs. The DC-tumour fusion presents a variety of TAAs to T cells in the presence of costimulatory signals. Some encouraging results have been obtained in ovarian cancer [160] and other tumours [169].

Yet another approach to whole tumour vaccination has used virus extracts to increase whole-cell vaccine immunogenicity, based on the observation that viruses can be highly inflammatory. This led to the development of a variety of viral oncolysates for use in clinical trials for many different cancers, including ovarian cancer [170-172]. Clinical experimentation with viral oncolysate vaccines has shown that antitumour immune responses may be elicited in select patients. Freedman *et al.* have studied the use of UV-irradiated influenza-A virus to produce oncolysate vaccine prepared with established EOC cell lines [173]. Treatment consisted of several courses of intraperitoneal or intrapleural oncolysate administration. Some patients experienced several months of unexpected progression-free survival and few exhibited a significant clinical response [174]. Other important work with viral oncolysates has been carried out by the Heidelberg group utilising the Newcastle disease virus (NDV), which is non-pathogenic in humans [175]. Remarkably, they found that use of live inactivated low-dose NDV with intact tumour cells had superior results compared with tumour lysates and led to the generation of specific CTLs with antitumour but no antiviral activity. A 50% 2-year survival was reported in a Phase II trial using repeated doses of NDV-modified autologous tumour cells in 31 patients with advanced EOC [176]. Several mechanisms have been proposed to explain the induction of antitumour immune response. Virally induced inflammatory cytokines or chemokines may activate immune cells; viral/tumour antigen interactions may increase

the uptake of tumour antigens by DCs; helper T cells may be activated by recall immune mechanisms against viral antigens; and tumour cells may acquire increased immunogenicity owing to the activation of danger signals [177-179].

3.2 Adoptive therapies with antitumour T cells

The power of adoptively transferred TILs has been brilliantly demonstrated in some patients with melanoma. Adoptive immunotherapy with autologous tumour-reactive T cells expanded *ex vivo* from TILs, immediately following a conditioning non-myeloablative chemotherapy regimen, resulted in significant clinical response rate in patients with metastatic disease [76]. Although the variety of treatments previously received by enrolled patients makes it difficult to extrapolate the results to a particular clinical situation, adoptive transfer of TILs emerges as a powerful approach against advanced cancers. In that context, lymphoablative chemotherapy appears to be critical for the expansion of antitumour CD8⁺ T cells, owing to the release of haematopoietic cytokines and, probably, to the depletion of regulatory T cells (Treg).

In ovarian carcinoma there is a robust rationale for the implementation of adoptive T cell therapy. Tumour-specific T cells have been detected in peripheral blood from 50% of patients [94]. In addition, it was found that approximately half of patients with advanced ovarian cancer exhibit T cells infiltrating tumour islets (intratumoural T cells). The detection of intratumoural T cells correlated strongly with dramatically improved overall survival [95]. A significant correlation was found between the presence of intratumoural T cells and the detection of peripheral blood T cells recognising tumour antigens in 10 consecutive patients with ovarian cancer studied (manuscript submitted). Relevant also is evidence that tumour-specific T cell lines can be generated from tumour-associated T cells in ~ 50% of patients [180]. These findings suggest that the adoptive transfer of autologous lymphocytes may represent a powerful therapeutic tool in ovarian carcinoma.

Earlier strategies utilised peripheral blood lymphocytes, tumour-associated lymphocytes (e.g., from ascites) or TILs, which were expanded and activated *ex vivo*. Typically, T cell expansion was achieved with IL-2 stimulation. In an Italian study, following cytoreductive surgery 28 patients with advanced ovarian cancer received two cycles of five daily intraperitoneal infusions of autologous *in vitro* activated peripheral blood T lymphocytes retargeted with bispecific monoclonal antibody OC/TR, which is directed against CD3 and the folate receptor, plus recombinant IL-2. A 27% overall response rate and 10% complete response rate were seen which lasted 18 – 26 months [181]. There was evidence of intraperitoneal immune response, but no systemic immune response [182]. Although results in terms of clinical responses thus far have not been impressive and the IL-2 effect could not be clearly separated from the immunisation effect in terms of the response rate described, adverse reactions were quite mild in this and other trials [183].

Clearly, numerous parameters call for optimisation. For example, the ideal procedure for the expansion of tumour-derived lymphocytes requires extensive investigation. Our current understanding on the critical importance of T cell costimulation for proper T cell activation and effector function may partially explain failures of past trials. In fact, evidence suggests that in the absence of costimulatory signals, such as those provided through the CD28 receptor pathway [184,185], antigen presentation leads to T cell anergy or apoptotic clonal deletion [186]. Costimulatory signalling to T cells may be provided artificially through monoclonal antibodies directed against the CD28 receptor [187]. Magnetic beads coated with anti-CD3/anti-CD28 antibodies represent a much more efficient strategy [188], although the starting repertoire of CD8⁺ cells may not be preserved during culture. Artificial APCs coated with OKT3/anti-CD28 antibodies and expressing 4-1BB ligand [189] represent a promising advance, as they prevent apoptosis in CD8⁺ T cells. However, a significant proportion of tumour-infiltrating CD8⁺ T cells do not express CD28. These can be still expanded by artificial APCs expressing the NKG2D ligand *Letal* and coated with OKT3/CD28 antibodies or even OKT3 alone, as the authors recently reported [190].

Selection of input lymphocyte subsets for *ex vivo* expansion may be of critical importance with respect to feasibility and efficacy. TILs presumably contain a higher frequency of TAA-specific T cells than peripheral blood T cells. If tumour-associated lymphocytes isolated from ascites exhibited similar antitumour cytotoxic properties to TILs derived from solid tumour nodules, they would provide a convenient source for the rapid expansion of effector cells, as cells would be ready for transfer in clinically significant amounts (ideally hundreds of millions) shortly following debulking. Similarly, the optimal stage of differentiation of adoptively transferred lymphocytes requires careful evaluation. Preliminary studies suggest that differentiated T cells are less effective against *in vivo* models of cancer than naive and early effector CD8⁺ T cells, due to downregulation of costimulatory molecules and entry into a senescence state (Gattinoni *et al.*, pers. commun.). This paradoxical observation provides new criteria for the selection of ideal lymphocyte subsets for adoptive transfer. The use of specific tumour antigens to expand efficient clones might also improve the reproducibility of treatments, allowing the establishment of standard protocols. Finally, the identification of CD4⁺CD25⁺ Treg infiltrating ovarian cancer by two studies [191,192] raises important questions on the requirement to deplete tumour-derived Treg prior to the expansion of T cells for adoptive transfer.

Selection of patients for adoptive lymphocyte therapy also requires careful evaluation. At this point it is not known whether all patients are eligible for adoptive lymphocyte therapy. For example, is there a difference between patients whose tumours exhibit intratumoural T cells (~ 50% of patients in the authors' study) and those whose tumours exhibit T cells only in the stroma surrounding islets (peritumoural T cells)?

Significant differences may exist in lymphocyte clonality, phenotype and potential for adoptive therapy. Certainly, the results from the NCI melanoma trial do indicate that significant differences may exist among patients. These need to be understood in order to optimise this approach [76,106,107].

3.3 Therapies targeting regulatory T cells

A critical mechanism of peripheral immune tolerance is mediated by CD4⁺CD25⁺ Treg, a T cell subset endowed with powerful suppressor activity. Treg prevent specific T cell immunity by suppressing CD8⁺ T cell activation and secretion of IL-2 and interferon (IFN)- γ . Treg inhibit specific cytotoxicity in a contact-dependent fashion and/or through contact-independent, paracrine mechanisms [193-195]. Ovarian cancer has been the tumour model in which Treg were demonstrated to play an important immunopathogenetic role in the human. The first evidence for the contribution of Treg to immune dysfunction in cancer in humans was in fact provided in patients with ovarian cancer and lung tumours, where increased frequency of transforming growth factor- β -secreting Treg with potent immunosuppressive functions were identified in tumour, ascites and peripheral blood [192]. Tumour-infiltrating Treg profoundly suppressed the function of effector and cytotoxic antitumour T cells [196]. Furthermore, Treg in human ovarian cancer were recently shown to defeat tumour antigen-specific immunity, foster tumour growth and predict poor patient survival [191].

At present, several clinical trials are testing the efficacy of targeting Treg. Approaches involve the use of an anti-CTLA4 monoclonal antibody [197,198] or DAB₃₈₉IL-2 diphtheria toxin fusion protein (denileukin diftitox, ONTAK[®], Ligand Pharmaceuticals, CA, USA) directed against IL-2 receptor/CD25 [199]. Patients with recurrent, multi-drug resistant ovarian cancer have been treated in these trials. If initial data are encouraging, suppression of Treg will certainly become an important component of tumour immunotherapy strategies.

3.4 Cytokine therapy

Cytokines such as IFN- α , - β or - γ , IL-2 and IL-12 are believed to contribute to the proliferation of specific populations of leukocytes involved in antitumour immunity. These have been used in numerous clinical trials with inconsistent results. Type I IFNs have demonstrated complex antitumour properties, including direct induction of cancer cell apoptosis and potent enhancement of antitumour immune responses through the stimulation of DCs [200,201]. An early trial in which recombinant human (rh)IFN- β protein was administered intraperitoneally twice-weekly to eight patients with advanced ovarian carcinomas refractory to conventional chemotherapy yielded largely negative results, with the growth of solid tumour lesions unaffected in all but one patient who had stable disease. However, IFN- β treatment induced regression of ascites in four of seven patients with effusions [202]. Phase I/II trials show that intraperitoneal therapy with recombinant IFN- α alone or combined with cisplatin as salvage for persistent ovarian cancer

after primary chemotherapy may achieve clinical efficacy in small volume disease [203,204], but has no significant effect on recurrent, platinum-resistant disease [205]. Failures may be partly attributed to the short half-life of recombinant IFN proteins *in vivo* and to the narrow therapeutic window requiring delivery of low doses of cytokine [206].

In a Gynecologic Oncology Group Phase II study, intravenous rhIL-12 was administered to patients with recurrent or refractory epithelial ovarian cancer at 250 ng/kg bolus as a single dose on day 1 followed by a 2-week rest period, with subsequent cycles administered daily for 5 days followed by a 16-day rest period per cycle. No significant response was observed, but > 50% of the patients experienced disease stabilisation [207]. In a Phase I study of weekly intraperitoneal rhIL-12, a 10% complete response and ~ 40% disease stabilisation were observed in patients with peritoneal carcinomatosis from Müllerian carcinomas, gastrointestinal tract carcinomas and peritoneal mesothelioma. More frequent toxicities included fever, fatigue, abdominal pain, nausea and catheter-related infections [208]. Unfortunately, the Phase II clinical trial has only seen prolonged stability in several patients, but not objective responses.

More encouraging results have been reported with IFN- γ and IL-2. Intraperitoneal administration of rhIFN- γ has shown a promising increase in survival with low toxicity [209]. Importantly, a threefold prolongation of progression-free survival was observed in a Phase III multi-centre study from Europe with subcutaneous administration of rhIFN- γ (100 μ g every other day, every other week) combined with upfront cisplatin and cyclophosphamide chemotherapy, with minimal added toxicity [210]. A Phase I/II study of intraperitoneal rhIL-2 in 41 patients with laparotomy-confirmed persistent or recurrent ovarian cancer showed that weekly IL-2 infusion is well-tolerated and demonstrates evidence of possible long-term efficacy in a modest number of patients. A pathological complete response rate of 20% was seen [211]. IL-2 enhances the cytotoxicity of T cells, but it can also stimulate Treg, monocytes and macrophages that produce immunosuppressive cytokines in mice [212]. In fact, a study reported an increase in IL-10 production following the administration of two concentrations of IL-2 in sequence with IFN- γ [213].

Optimisation of intraperitoneal cytokine immune therapy for epithelial ovarian cancer obviously requires maintaining intratumoural cytokine levels sufficient to induce antitumour responses. Recombinant cytokine therapy is limited by the inability to achieve high intratumoural/intraperitoneal doses without eliciting systemic toxicity and by the short half-life of recombinant proteins. Cytokine gene therapy using recombinant viral vectors can achieve higher and sustained cytokine levels at the tumour site than those resulting from systemic or regional administration of recombinant cytokine proteins without engendering systemic toxicity [214]. Intraperitoneal administration of recombinant adenovirus delivering mouse IFN- β (Ad.IFN- β) has demonstrated

marked efficacy in preclinical models [215]. A trial of intrapleural adenovirus delivering human IFN- β is being completed at present at the University of Pennsylvania. Toxicity has been minimal. One patient with measurable, recurrent, platinum-resistant ovarian carcinoma achieved complete response of both pleural and intraperitoneal disease in this trial (Sterman DH, unpublished observation).

4. Expert opinion and conclusions

In summary, significant progress has been made in the field of HPV vaccine development. The recognition of high-risk HPV as the primary aetiological agent for cervical cancer and its precursor lesions has paved the way for the development of preventative and therapeutic HPV vaccines that may lead to the control of cervical cancer and other HPV-associated malignancies. HPV VLPs show promise as a protective vaccine capable of generating neutralising antibodies to prevent HPV infection in patients. However, such a preventative vaccine would not benefit those with established oncogenic HPV infections. Given the prevalence of HPV infection, it is therefore critical to continue in parallel the development of therapeutic vaccine approaches. Many experimental HPV vaccine strategies, including vector-, peptide-, protein-, nucleic acid-, chimeric VLP- and cell-based vaccines, pseudovirions and RNA replicons, have been shown to enhance HPV antigen-specific immune cell activity and antitumour responses in murine tumour systems. Several clinical trials are underway at present, based on encouraging preclinical results from these therapeutic HPV vaccines. A head-to-head comparison of these vaccines will help identify the most potent therapeutic HPV vaccine with minimal negative side effects.

While the cervical cancer vaccines discussed in this review are mainly focused on targeting HPV encoded antigens, cervical cancer vaccines can also target non-HPV endogenous antigens that are uniquely expressed or over expressed in cervical cancers. Quite different from vaccines targeting HPV antigens, which are foreign antigens, cancer vaccines targeting endogenous antigens have specific issues such as tolerance. In general, the response to human cancer vaccines targeting endogenous antigens alone was poor, and it was only when vaccine treatment was combined with interleukin (IL)-2, adoptive therapy and lymphodepletion that beneficial results were observed in some cancer systems, such as malignant melanoma [76]. In general, most tested cancer vaccines are well-tolerated, and some of them were observed to induce

specific immune responses by quantitative T cell assays such as enzyme-linked immunospot using peripheral blood mononuclear cells. However, the objective clinical response rate was low [77]. Thus, continuous exploration of new strategies to enhance cancer vaccine potency may facilitate the generation of better cancer vaccines targeting endogenous antigens.

Clinical HPV vaccine trials provide a unique opportunity to identify the characteristics and mechanisms of the immune response that best correlate with clinical vaccine potency. Such immunological parameters will help define protective and therapeutic immune mechanisms for controlling HPV infections and HPV-related disease. Rational development of more effective vaccines for HPV infections would be greatly facilitated by comprehensive information on these protective immune mechanisms in humans. With continued endeavours in HPV vaccine development, we may soon be able to implement a variety of safe and effective strategies for the eventual control of HPV-associated cervical cancer.

Promising results in ovarian cancer immunotherapy compel us to continue efforts in order to optimise immunotherapy methodologies, define and validate patient selection criteria and test combinatorial therapy approaches. A major effort must be dedicated towards defining and validating T cell tumour antigens that are suitable for vaccine therapy. The combination of vaccination with immunomodulation through depletion of Treg is a very promising approach that warrants further investigation. Given the overall poor performance of therapeutic vaccination in patients with advanced, bulky tumours [77], this approach is probably best applied in the adjuvant setting, in patients with advanced stage tumours following complete response to chemotherapy, and/or in patients with early disease at high risk for recurrence. Adoptive cell therapy should be more successful at treating measurable disease. Significant efforts have to focus on optimising the recovery, selection and *ex vivo* expansion of lymphocytes for adoptive transfer. Development of combinatorial approaches incorporating cytotoxic and/or lymphodepleting chemotherapy, cytokines, vaccination, Treg-depleting therapy and adoptive lymphocyte therapy is likely to maximise our therapeutic success against ovarian cancer.

Acknowledgements

This work was supported by NCI SPORE P01-CA83638 and the Ovarian Cancer Research Foundation (GC), and NCI SPORE P01-CA98252 (TCW).

Bibliography

Papers of special note have been highlighted as either of interest (*) or of considerable interest (***) to readers.

1. JEMAL A, THOMAS A, MURRAY T, THUN M: Cancer statistics, 2002. *CA Cancer J. Clin.* (2002) **52**:23-47.
2. ROSENBERG SA: The identification of cancer antigens: impact on the development of cancer vaccines. *Cancer J.* (2000) **6**(Suppl. 2):S142-S149.
3. ZENG G: MHC class II-restricted tumor antigens recognized by CD4+ T cells: new strategies for cancer vaccine design. *J. Immunother.* (2001) **24**:195-204.
4. NOVELLINO L, CASTELLI C, PARMIANI G: A listing of human tumor antigens recognized by T cells: March 2004 update. *Cancer Immunol. Immunother.* (2005) **54**(3):187-207.
5. SANTIN AD: HER2/neu overexpression: has the Achilles' heel of uterine serous papillary carcinoma been exposed? *Gynecol. Oncol.* (2003) **88**:263-265.
6. WAGGONER SE: Cervical cancer. *Lancet* (2003) **361**:2217-2225.
7. ZUR HAUSEN H: Papillomaviruses and cancer: from basic studies to clinical application. *Nat. Rev. Cancer* (2002) **2**:342-350.
8. BREITBURD F, KIRNBAUER R, HUBBERT NL *et al.*: Immunization with viruslike particles from cottontail rabbit papillomavirus (CRPV) can protect against experimental CRPV infection. *J. Virol.* (1995) **69**:3959-3963.
- **This article reports that neutralising IgG mediate protection after rabbit VLP vaccination.**
9. SUZICH JA, GHIM SJ, PALMER-HILL FJ *et al.*: Systemic immunization with papillomavirus L1 protein completely prevents the development of viral mucosal papillomas. *Proc. Natl. Acad. Sci. USA* (1995) **92**:11553-11557.
- **This article reports that neutralising IgG mediate protection after canine VLP vaccination.**
10. EMBERS ME, BUDGEON LR, PICKEL M, CHRISTENSEN ND: Protective immunity to rabbit oral and cutaneous papillomaviruses by immunization with short peptides of L2, the minor capsid protein. *J. Virol.* (2002) **76**:9798-9805.
11. WU TC: Immunology of the human papilloma virus in relation to cancer. *Curr. Opin. Immunol.* (1994) **6**:746-754.
12. HALPERT R, FRUCHTER RG, SEDLIS A, BUTT K, BOYCE JG, SILLMAN FH: Human papillomavirus and lower genital neoplasia in renal transplant patients. *Obstet. Gynecol.* (1986) **68**:251-258.
13. LAGA M, ICENOGLE JP, MARSELLA R *et al.*: Genital papillomavirus infection and cervical dysplasia-opportunistic complications of HIV infection. *Int. J. Cancer* (1992) **50**:45-48.
14. SCHAFER A, FRIEDMANN W, MIELKE M, SCHWARTLANDER B, KOCH MA: The increased frequency of cervical dysplasia-neoplasia in women infected with the human immunodeficiency virus is related to the degree of immunosuppression. *Am. J. Obstet. Gynecol.* (1991) **164**:593-599.
15. BRANDSMA JL: Animal models for HPV vaccine development. *Papillomavirus Rep.* (1994) **5**:105-111.
16. SELVAKUMAR R, BORENSTEIN LA, LIN YL, AHMED R, WETTSTEIN FO: Immunization with nonstructural proteins E1 and E2 of cottontail rabbit papillomavirus stimulates regression of virus-induced papillomas. *J. Virol.* (1995) **69**:602-605.
17. TAGAMI H: Regression phenomenon of numerous flat warts-an experiment on the nature of tumor immunity in man. *Int. J. Dermatol.* (1983) **22**:570-571.
18. BENTON C, SHAHIDULLAH H, HUNTER JA: Human papillomavirus in the immunosuppressed. *Papillomavirus Rep.* (1992) **3**:23-26.
19. HAGENSEE M, GALLOWAY D: Growing human papillomaviruses and virus-like particles in the laboratory. *Papillomavirus Rep.* (1993) **4**:121-124.
20. ZHOU J, SUN XY, DAVIES H, CRAWFORD L, PARK D, FRAZER IH: Definition of linear antigenic regions of the HPV16 L1 capsid protein using synthetic virion-like particles. *Virology* (1992) **189**:592-599.
21. KIRNBAUER R, BOOY F, CHENG N, LOWY DR, SCHILLER JT: Papillomavirus L1 major capsid protein self-assembles into virus-like particles that are highly immunogenic. *Proc. Natl. Acad. Sci. USA* (1992) **89**:12180-12184.
- **This study demonstrates that L1 has an intrinsic capacity to assemble into empty capsid-like structures with immunogenicity similar to that of infectious virions. It provides a foundation for considering L1 preparations as candidates for a serological test for measuring antibodies to conformational virion epitopes and for a vaccine to prevent papillomavirus infection.**
22. SASAGAWA T, PUSHKO P, STEERS G *et al.*: Synthesis and assembly of virus-like particles of human papillomaviruses Type 6 and Type 16 in fission yeast *Schizosaccharomyces pombe*. *Virology* (1995) **206**:126-135.
23. NARDELLI-HAEFLIGER D, RODEN RB, BENYACOUB J *et al.*: Human papillomavirus Type 16 virus-like particles expressed in attenuated *Salmonella typhimurium* elicit mucosal and systemic neutralizing antibodies in mice. *Infect. Immun.* (1997) **65**:3328-3336.
24. CHEN BP, LI YS, ZHAO Y *et al.*: DNA microarray analysis of gene expression in endothelial cells in response to 24-h shear stress. *Physiol. Genomics* (2001) **7**:55-63.
25. KIRNBAUER R: Papillomavirus-like particles for serology and vaccine development. *Intervirology* (1996) **39**:54-61.
26. DONNELLY JJ, MARTINEZ D, JANSEN KU, ELLIS RW, MONTGOMERY DL, LIU MA: Protection against papillomavirus with a polynucleotide vaccine. *J. Infect. Dis.* (1996) **173**:314-320.
27. SOMASUNDARUM K, ZHANG H, ZENG YX *et al.*: Arrest of the cell cycle by the tumour-suppressor BRCA1 requires the CDK-inhibitor p21WAF1/CIP1. *Nature* (1997) **389**:187-190.
28. STANLEY MA, MOORE RA, NICHOLLS PK *et al.*: Intra-epithelial vaccination with COPV L1 DNA by particle-mediated DNA delivery protects against mucosal challenge with infectious COPV in beagle dogs. *Vaccine* (2001) **19**:2783-2792.
29. RUSSELL MW, MOLDOVEANU Z, WHITE PL, SIBERT GJ, MESTECKY J, MICHALEK SM: Salivary, nasal, genital, and systemic antibody responses in monkeys immunized intranasally with a bacterial protein antigen and the cholera toxin b subunit. *Infect. Immun.* (1996) **64**:1272-1283.
30. LOWE RS, BROWN DR, BRYAN JT *et al.*: Human papillomavirus Type 11 (HPV-11) neutralizing antibodies in the serum and genital mucosal secretions of African green monkeys immunized with

- HPV-11 virus-like particles expressed in yeast. *J. Infect. Dis.* (1997) 176:1141-1145.
31. BALMELLI C, RODEN R, POTTS A, SCHILLER J, DE GRANDI P, NARDELLI-HAEFLIGER D: Nasal immunization of mice with human papillomavirus Type 16 virus-like particles elicits neutralizing antibodies in mucosal secretions. *J. Virol.* (1998) 72:8220-8229.
 32. MASIAKOS PT, MACLAUGHLIN DT, MAHESWARAN S *et al.*: Human ovarian cancer, cell lines, and primary ascites cells express the human Mullerian inhibiting substance (MIS) Type II receptor, bind, and are responsive to MIS. *Clin. Cancer Res.* (1999) 5:3488-3499.
 33. NARDELLI-HAEFLIGER D, WIRTHNER D, SCHILLER JT *et al.*: Specific antibody levels at the cervix during the menstrual cycle of women vaccinated with human papillomavirus 16 virus-like particles. *J. Natl. Cancer Inst.* (2003) 95:1128-1137.
 - **This study reports the influence of the menstrual cycle and oral contraceptive use on the levels of total and specific antibodies in the cervical secretions of women who had been immunised with HPV-VLPs. Although such vaccination generated relatively high titres of anti-HPV-16 antibodies in the cervix, a decrease in neutralising antibody titres was observed around ovulation.**
 34. HARRO CD, PANG YY, RODEN RB *et al.*: Safety and immunogenicity trial in adult volunteers of a human papillomavirus 16 L1 virus-like particle vaccine. *J. Natl. Cancer Inst.* (2001) 93:284-292.
 35. EVANS TG, BONNEZ W, ROSE RC *et al.*: A Phase I study of a recombinant viruslike particle vaccine against human papillomavirus Type 11 in healthy adult volunteers. *J. Infect. Dis.* (2001) 183:1485-1493.
 36. KOUTSKY LA, AULT KA, WHEELER CM *et al.*: A controlled trial of a human papillomavirus Type 16 vaccine. *N. Engl. J. Med.* (2002) 347:1645-1651.
 - **This paper describes a HPV-L1 VLP trial that produced 100% effective protection from persistent HPV infection. This trial was the first to demonstrate protection against natural transmission of oncogenic HPV after vaccination with L1 VLPs.**
 37. BROWN DR, BRYAN JT, SCHROEDER JM *et al.*: Neutralization of human papillomavirus Type 11 (HPV-11) by serum from women vaccinated with yeast-derived HPV-11 L1 virus-like particles: correlation with competitive radioimmunoassay titer. *J. Infect. Dis.* (2001) 184:1183-1186.
 38. RODEN RB, GREENSTONE HL, KIRNBAUER R *et al.*: *In vitro* generation and type-specific neutralization of a human papillomavirus Type 16 virion pseudotype. *J. Virol.* (1996) 70:5875-5883.
 39. PASTRANA DV, VASS WC, LOWY DR, SCHILLER JT: NHPV16 VLP vaccine induces human antibodies that neutralize divergent variants of HPV16. *Virology* (2001) 279:361-369.
 40. LOWY DR, FRAZER IH: Chapter 16: Prophylactic human papillomavirus vaccines. *J. Natl. Cancer Inst. Monogr.* 2003:111-116.
 41. RODEN RB, YUTZY WH 4TH, FALLON R, INGLIS S, LOWY DR, SCHILLER JT: Minor capsid protein of human genital papillomaviruses contains subdominant, cross-neutralizing epitopes. *Virology* (2000) 270:254-257.
 - **This study presents evidence of crossreactive neutralising epitopes in L2, providing a rationale for developing L2-specific vaccines.**
 42. RODEN RB, KIRNBAUER R, JENSON AB, LOWY DR, SCHILLER JT: Interaction of papillomaviruses with the cell surface. *J. Virol.* (1994) 68:7260-7266.
 43. CAMPO MS, GRINDLAY GJ, O'NEIL BW, CHANDRACHUD LM, MCGARVIE GM, JARRETT WF: Prophylactic and therapeutic vaccination against a mucosal papillomavirus. *J. Gen. Virol.* (1993) 74:945-953.
 44. CHRISTENSEN ND, KREIDER JW, KAN NC, DIANGELO SL: The open reading frame L2 of cottontail rabbit papillomavirus contains antibody-inducing neutralizing epitopes. *Virology* (1991) 181:572-579.
 - **This paper and [45] report an early demonstration of the protective efficacy of L2 vaccination in animal models.**
 45. LIN YL, BORENSTEIN LA, SELVAKUMAR R, AHMED R, WETTSTEIN FO: Effective vaccination against papilloma development by immunization with L1 or L2 structural protein of cottontail rabbit papillomavirus. *Virology* (1992) 187:612-619.
 - **See [44].**
 46. KAWANA K, YOSHIKAWA H, TAKETANI Y, YOSHIKAWA K, KANDA T: Common neutralization epitope in minor capsid protein L2 of human papillomavirus types 16 and 6. *J. Virol.* (1999) 73:6188-6190.
 - **This paper reports a common cross-neutralisation epitope for HPV-6 and -16 (located within amino acids 108 – 120 of L2 in HPV-16), suggesting that this epitope may be shared by other genital HPVs. Thus, this paper provides evidence of crossreactive neutralising epitopes in L2.**
 47. KAWANA Y, KAWANA K, YOSHIKAWA H, TAKETANI Y, YOSHIKAWA K, KANDA T: Human papillomavirus Type 16 minor capsid protein L2 N-terminal region containing a common neutralization epitope binds to the cell surface and enters the cytoplasm. *J. Virol.* (2001) 75:2331-2336.
 48. LACEY CJ, THOMPSON HS, MONTEIRO EF *et al.*: Phase IIa safety and immunogenicity of a therapeutic vaccine, TA-GW, in persons with genital warts. *J. Infect. Dis.* (1999) 179:612-618.
 49. THOMPSON HS, DAVIES ML, WATTS MJ *et al.*: Enhanced immunogenicity of a recombinant genital warts vaccine adjuvanted with monophosphoryl lipid A. *Vaccine* (1998) 16:1993-1999.
 50. DE JONG A, O'NEILL T, KHAN AY *et al.*: Enhancement of human papillomavirus (HPV) Type 16 E6 and E7-specific T-cell immunity in healthy volunteers through vaccination with TA-CIN, an HPV16 L2E7E6 fusion protein vaccine. *Vaccine* (2002) 20:3456-3464.
 51. STOLER MH, RHODES CR, WHITBECK A, WOLINSKY SM, CHOW LT, BROKER TR: Human papillomavirus Type 16 and 18 gene expression in cervical neoplasias. *Hum. Pathol.* (1992) 23:117-128.
 52. STOLER MH, WOLINSKY SM, WHITBECK A, BROKER TR, CHOW LT: Differentiation-linked human papillomavirus types 6 and 11 transcription in genital condylomata revealed by *in situ* hybridization with message-specific RNA probes. *Virology* (1989) 172:331-340.
 53. RUDOLF MP, NIELAND JD, DASILVA DM *et al.*: Induction of HPV16 capsid protein-specific human T cell responses by virus-like particles. *Biol. Chem.* (1999) 380:335-340.
 54. OHLSCHLAGER P, OSEN W, DELL K *et al.*: Human papillomavirus Type 16 L1

- capsomeres induce L1-specific cytotoxic T lymphocytes and tumor regression in C57BL/6 mice. *J. Virol.* (2003) 77:4635-4645.
55. CROOK T, MORGENSTERN JP, CRAWFORD L, BANKS L: Continued expression of HPV-16 E7 protein is required for maintenance of the transformed phenotype of cells co-transformed by HPV-16 plus EJ-ras. *EMBO J.* (1989) 8:513-519.
56. KAUFMANN AM, STERN PL, RANKIN EM *et al.*: Safety and immunogenicity of TA-HPV, a recombinant vaccinia virus expressing modified human papillomavirus (HPV)-16 and HPV-18 E6 and E7 genes, in women with progressive cervical cancer. *Clin. Cancer Res.* (2002) 8:3676-3685.
57. ADAMS M, BORYSIEWICZ L, FIANDER A *et al.*: Clinical studies of human papilloma vaccines in pre-invasive and invasive cancer. *Vaccine* (2001) 19:2549-2556.
58. BORYSIEWICZ LK, FIANDER A, FIANDER A, NIMAKO M *et al.*: A recombinant vaccinia virus encoding human papillomavirus types 16 and 18, E6 and E7 proteins as immunotherapy for cervical cancer. *Lancet* (1996) 347:1523-1527.
- **This is the first paper to describe a clinical trial of an HPV vaccine utilising a vaccinia virus vector.**
59. BALDWIN PJ, VAN DER BURG SH, BOSWELL CM *et al.*: Vaccinia-expressed human papillomavirus 16 and 18 e6 and e7 as a therapeutic vaccination for vulval and vaginal intraepithelial neoplasia. *Clin. Cancer Res.* (2003) 9:5205-5213.
60. DAVIDSON EJ, DAVIDSON JA, STERLING JC, BALDWIN PJ, KITCHENER HC, STERN PL: Association between human leukocyte antigen polymorphism and human papillomavirus 16-positive vulval intraepithelial neoplasia in British women. *Cancer Res.* (2003) 63:400-403.
61. WEISKIRCH LM, PATERSON Y: *Listeria monocytogenes*: a potent vaccine vector for neoplastic and infectious disease. *Immunol. Rev.* (1997) 158:159-169.
62. HUSSAIN SF, PATERSON Y: What is needed for effective antitumor immunotherapy? Lessons learned using *Listeria monocytogenes* as a live vector for HPV-associated tumors. *Cancer Immunol. Immunother.* (2005) 54(6):577-586.
63. MUDERSPACH L, WILCZYNSKI S, ROMAN L *et al.*: A Phase I trial of a human papillomavirus (HPV) peptide vaccine for women with high-grade cervical and vulvar intraepithelial neoplasia who are HPV 16 positive. *Clin. Cancer Res.* (2000) 6:3406-3416.
64. STELLER MA, GURSKI KJ, MURAKAMI M *et al.*: Cell-mediated immunological responses in cervical and vaginal cancer patients immunized with a lipidated epitope of human papillomavirus Type 16 E7. *Clin. Cancer Res.* (1998) 4:2103-2109.
65. DAVIDSON EJ, FAULKNER RL, SEHR P *et al.*: Effect of TA-CIN (HPV 16 L2E6E7) booster immunisation in vulval intraepithelial neoplasia patients previously vaccinated with TA-HPV (vaccinia virus encoding HPV 16/18 E6E7). *Vaccine* (2004) 22:2722-2729.
66. HALLEZ S, SIMON P, MAUDOUX F *et al.*: Phase I/II trial of immunogenicity of a human papillomavirus (HPV) Type 16 E7 protein-based vaccine in women with oncogenic HPV-positive cervical intraepithelial neoplasia. *Cancer Immunol. Immunother.* (2004) 53:642-650.
67. CHU NR: Therapeutic vaccination for the treatment of mucosotropic human papillomavirus-associated disease. *Expert Opin. Biol. Ther.* (2003) 3:477-486.
68. HOPFL R, HEIM K, CHRISTENSEN N *et al.*: Spontaneous regression of CIN and delayed-type hypersensitivity to HPV-16 oncoprotein E7. *Lancet* (2000) 356:1985-1986.
69. KLENCKE B, MATIJEVIC M, URBAN RG *et al.*: Encapsulated plasmid DNA treatment for human papillomavirus 16-associated anal dysplasia: a Phase I study of ZYC101. *Clin. Cancer Res.* (2002) 8:1028-1037.
- **This study represents the first therapeutic HPV DNA vaccine clinical trial in patients with anal dysplasia. Ten out of twelve patients demonstrated an increased immune response to the peptide epitopes encoded by the DNA vaccine, and three patients experienced partial histological responses. The DNA vaccine was well-tolerated in all of the patients.**
70. SHEETS EE, URBAN RG, CRUM CP *et al.*: Immunotherapy of human cervical high-grade cervical intraepithelial neoplasia with microparticle-delivered human papillomavirus 16 E7 plasmid DNA. *Am. J. Obstet. Gynecol.* (2003) 188:916-926.
71. GARCIA F, PETRY KU, MUDERSPACH L *et al.*: ZYC101a for treatment of high-grade cervical intraepithelial neoplasia: a randomized controlled trial. *Obstet. Gynecol.* (2004) 103:317-326.
72. LANZAVECCHIA A, SALLUSTO F: Regulation of T cell immunity by dendritic cells. *Cell* (2001) 106:263-266.
73. FIGDOR CG, DE VRIES IJ, LESTERHUIS WJ, MELIEF CJ: Dendritic cell immunotherapy: mapping the way. *Nat. Med.* (2004) 10:475-480.
74. SANTIN AD, BELLONE S, GOKDEN M, CANNON MJ, PARHAM GP: Vaccination with HPV-18 E7-pulsed dendritic cells in a patient with metastatic cervical cancer. *N. Engl. J. Med.* (2002) 346:1752-1753.
75. ADAMS M, NAVABI H, JASANI B *et al.*: Dendritic cell (DC) based therapy for cervical cancer: use of DC pulsed with tumour lysate and matured with a novel synthetic clinically non-toxic double stranded RNA analogue poly [I]:poly [C(12)U] (Ampligen®). *Vaccine* (2003) 21:787-790.
76. DUDLEY ME, WUNDERLICH JR, ROBBINS PF *et al.*: Cancer regression and autoimmunity in patients after clonal repopulation with antitumor lymphocytes. *Science* (2002) 298:850-854.
- **This influential report represents the first successful use of adoptive cell transfer with TILs following non-myeloablative chemotherapy for the treatment of patients with melanoma.**
77. ROSENBERG SA, YANG JC, RESTIFO NP: Cancer immunotherapy: moving beyond current vaccines. *Nat. Med.* (2004) 10:909-915.
- **A critical evaluation of cancer vaccine approaches available at present, which emphasise alternative strategies that mediate cancer regression in clinical models.**
78. SANTIN AD, HERMONAT PL, RAVAGGI A *et al.*: Phenotypic and functional analysis of tumor-infiltrating lymphocytes compared with tumor-associated lymphocytes from ascitic fluid and peripheral blood lymphocytes in patients with advanced ovarian cancer. *Gynecol. Obstet. Invest.* (2001) 51:254-261.
79. NEGUS RP, STAMP GW, HADLEY J, BALKWILL FR: Quantitative assessment of the leukocyte infiltrate in ovarian cancer and its relationship to the expression of C-C

- chemokines. *Am. J. Pathol.* (1997) 150:1723-1734.
80. SCHONDORF T, ENGEL H, KURBACHER CM *et al.*: Immunologic features of tumor-infiltrating lymphocytes and peripheral blood lymphocytes in ovarian cancer patients. *J. Soc. Gynecol. Investig.* (1998) 5:102-107.
 81. KOOI S, ZHANG HZ, PATENIA R, EDWARDS CL, PLATSOUKAS CD, FREEDMAN RS: HLA class I expression on human ovarian carcinoma cells correlates with T-cell infiltration *in vivo* and T-cell expansion *in vitro* in low concentrations of recombinant interleukin-2. *Cell. Immunol.* (1996) 174:116-128.
 82. HAYASHI K, YONAMINE K, MASUKO-HONGO K *et al.*: Clonal expansion of T cells that are specific for autologous ovarian tumor among tumor-infiltrating T cells in humans. *Gynecol. Oncol.* (1999) 74:86-92.
 83. HALAPI E, YAMAMOTO Y, JUHLIN C *et al.*: Restricted T cell receptor V-beta and J-beta usage in T cells from interleukin-2-cultured lymphocytes of ovarian and renal carcinomas. *Cancer Immunol. Immunother.* (1993) 36:191-197.
 84. FISK B, BLEVINS TL, WHARTON JT, IOANNIDES CG: Identification of an immunodominant peptide of HER-2/neu protooncogene recognized by ovarian tumor-specific cytotoxic T lymphocyte lines. *J. Exp. Med.* (1995) 181:2109-2117.
 85. KOOI S, FREEDMAN RS, RODRIGUEZ-VILLANUEVA J, PLATSOUKAS CD: Cytokine production by T-cell lines derived from tumor-infiltrating lymphocytes from patients with ovarian carcinoma: tumor-specific immune responses and inhibition of antigen-independent cytokine production by ovarian tumor cells. *Lymphokine Cytokine Res.* (1993) 12:429-437.
 86. PEOPLES GE, GOEDEGEBUURE PS, SMITH R, LINEHAN DC, YOSHINO I, EBERLEIN TJ: Breast and ovarian cancer-specific cytotoxic T lymphocytes recognize the same HER2/neu-derived peptide. *Proc. Natl. Acad. Sci. USA* (1995) 92:432-436.
 87. PEOPLES GE, ANDERSON BW, FISK B, KUDELKA AP, WHARTON JT, IOANNIDES CG: Ovarian cancer-associated lymphocyte recognition of folate binding protein peptides. *Ann. Surg. Oncol.* (1998) 5:743-750.
 88. DADMARZ RD, ORDOUBADI A, MIXON A *et al.*: Tumor-infiltrating lymphocytes from human ovarian cancer patients recognize autologous tumor in an MHC class II-restricted fashion. *Cancer J. Sci. Am.* (1996) 2:263.
 89. SANTIN AD, BELLONE S, RAVAGGI A, PECORELLI S, CANNON MJ, PARHAM GP: Induction of ovarian tumor-specific CD8+ cytotoxic T lymphocytes by acid-eluted peptide-pulsed autologous dendritic cells. *Obstet. Gynecol.* (2000) 96:422-430.
 90. PEOPLES GE, SCHOOF DD, ANDREWS JV, GOEDEGEBUURE PS, EBERLEIN TJ: T-cell recognition of ovarian cancer. *Surgery* (1993) 114:227-234.
 91. IOANNIDES CG, FREEDMAN RS, PLATSOUKAS CD, RASHED S, KIM YP: Cytotoxic T cell clones isolated from ovarian tumor-infiltrating lymphocytes recognize multiple antigenic epitopes on autologous tumor cells. *J. Immunol.* (1991) 146:1700-1707.
 92. IOANNIDES CG, PLATSOUKAS CD, RASHED S, WHARTON JT, EDWARDS CL, FREEDMAN RS: Tumor cytotoxicity by lymphocytes infiltrating ovarian malignant ascites. *Cancer Res.* (1991) 51:4257-4265.
 93. FREEDMAN RS, TOMASOVIC B, TEMPLIN S *et al.*: Large-scale expansion in interleukin-2 of tumor-infiltrating lymphocytes from patients with ovarian carcinoma for adoptive immunotherapy. *J. Immunol. Methods* (1994) 167:145-160.
 94. SCHLIENGER K, CHU CS, WOO EY *et al.*: TRANCE- and CD40 ligand-matured dendritic cells reveal MHC class I-restricted T cells specific for autologous tumor in late-stage ovarian cancer patients. *Clin. Cancer Res.* (2003) 9:1517-1527.
 95. ZHANG L, CONEJO-GARCIA JR, KATSAROS D *et al.*: Intratumoral T cells, recurrence, and survival in epithelial ovarian cancer. *N. Engl. J. Med.* (2003) 348:203-213.
 96. SCHUMACHER K, HAENSCH W, ROEFZAAD C, SCHLAG PM: Prognostic significance of activated CD8(+) T cell infiltrations within esophageal carcinomas. *Cancer Res.* (2001) 61:3932-3936.
 97. VESALAINEN S, LIPPONEN P, TALJA M, SYRJANEN K: Histological grade, perineural infiltration, tumour-infiltrating lymphocytes and apoptosis as determinants of long-term prognosis in prostatic adenocarcinoma. *Eur. J. Cancer* (1994) 30A:1797-1803.
 98. MARROGI AJ, MUNSHI A, MEROGI AJ *et al.*: Study of tumor infiltrating lymphocytes and transforming growth factor-beta as prognostic factors in breast carcinoma. *Int. J. Cancer* (1997) 74:492-501.
 99. NAITO Y, SAITO K, SHIIBA K *et al.*: CD8+ T cells infiltrated within cancer cell nests as a prognostic factor in human colorectal cancer. *Cancer Res.* (1998) 58:3491-3494.
 100. NAKANO O, SATO M, NAITO Y *et al.*: Proliferative activity of intratumoral CD8(+) T-lymphocytes as a prognostic factor in human renal cell carcinoma: clinicopathologic demonstration of antitumor immunity. *Cancer Res.* (2001) 61:5132-5136.
 101. HALPERN AC, SCHUCHTER LM: Prognostic models in melanoma. *Semin. Oncol.* (1997) 24:S2-S7.
 102. THURNER B, HAENDLE I, RODER C *et al.*: Vaccination with mage-3A1 peptide-pulsed mature, monocyte-derived dendritic cells expands specific cytotoxic T cells and induces regression of some metastases in advanced stage IV melanoma. *J. Exp. Med.* (1999) 190:1669-1678.
 103. KUGLER A, STUHLER G, WALDEN P *et al.*: Regression of human metastatic renal cell carcinoma after vaccination with tumor cell-dendritic cell hybrids. *Nat. Med.* (2000) 6:332-336.
 104. JOCHAM D, RICHTER A, HOFFMANN L *et al.*: Adjuvant autologous renal tumour cell vaccine and risk of tumour progression in patients with renal-cell carcinoma after radical nephrectomy: Phase III, randomised controlled trial. *Lancet* (2004) 363:594-599.
 105. SOSMAN JA, UNGER JM, LIU PY *et al.*: Adjuvant immunotherapy of resected, intermediate-thickness, node-negative melanoma with an allogeneic tumor vaccine: impact of HLA class I antigen expression on outcome. *J. Clin. Oncol.* (2002) 20:2067-2075.
 106. ZHOU J, DUDLEY ME, ROSENBERG SA, ROBBINS PF: Persistence of multiple tumor-specific T-cell clones is associated with complete tumor regression in a melanoma patient receiving adoptive cell transfer therapy. *J. Immunother.* (2005) 28:53-62.

107. ROBBINS PF, DUDLEY ME, WUNDERLICH J *et al.*: Cutting edge: Persistence of transferred lymphocyte clonotypes correlates with cancer regression in patients receiving cell transfer therapy. *J. Immunol.* (2004) **173**:7125-7130.
108. ALBERT ML, DARNELL JC, BENDER A, FRANCISCO LM, BHARDWAJ N, DARNELL RB: Tumor-specific killer cells in paraneoplastic cerebellar degeneration. *Nat. Med.* (1998) **4**:1321-1324.
109. DARNELL RB: The importance of defining the paraneoplastic neurologic disorders. *N. Engl. J. Med.* (1999) **340**:1831-1833.
110. MURRAY JL, PRZEPIORKA D, IOANNIDES CG: Clinical trials of HER-2/neu-specific vaccines. *Semin. Oncol.* (2000) **27**:71-75; discussion 92-100.
111. DISIS ML, SCHIFFMAN K: Cancer vaccines targeting the HER2/neu oncogenic protein. *Semin. Oncol.* (2001) **28**:12-20.
112. BOOKMAN MA, DARCY KM, CLARKE-PEARSON D, BOOTHBY RA, HOROWITZ IR: Evaluation of monoclonal humanized anti-HER2 antibody, trastuzumab, in patients with recurrent or refractory ovarian or primary peritoneal carcinoma with overexpression of HER2: a Phase II trial of the Gynecologic Oncology Group. *J. Clin. Oncol.* (2003) **21**:283-290.
113. HELLSTROM I, GOODMAN G, PULLMAN J, YANG Y, HELLSTROM KE: Overexpression of HER-2 in ovarian carcinomas. *Cancer Res.* (2001) **61**:2420-2423.
114. DISIS ML, SCHIFFMAN K, GUTHRIE K *et al.*: Effect of dose on immune response in patients vaccinated with an her-2/neu intracellular domain protein-based vaccine. *J. Clin. Oncol.* (2004) **22**:1916-1925.
- **This report shows that a HER-2/neu ICD protein vaccine was effective in eliciting HER-2/neu-specific T cell immunity in the majority of ovarian cancer patients who completed the vaccine regimen.**
115. DISIS ML, GOODELL V, SCHIFFMAN K, KNUTSON KL: Humoral epitope-spreading following immunization with a HER-2/neu peptide based vaccine in cancer patients. *J. Clin. Immunol.* (2004) **24**:571-578.
116. BABCOCK B, ANDERSON BW, PAPAYANNOPOULOS I *et al.*: Ovarian and breast cytotoxic T lymphocytes can recognize peptides from the amino enhancer of split protein of the Notch complex. *Mol. Immunol.* (1998) **35**:1121-1133.
117. MILES D, PAPAZISIS K: Rationale for the clinical development of STn-KLH (Theratope(R)) and anti-MUC-1 vaccines in breast cancer. *Clin. Breast Cancer* (2003) **3**(Suppl. 4):S134-S138.
118. HOLMBERG LA, OPARIN DV, GOOLEY T *et al.*: Clinical outcome of breast and ovarian cancer patients treated with high-dose chemotherapy, autologous stem cell rescue and THERATOPE STn-KLH cancer vaccine. *Bone Marrow Transplant.* (2000) **25**:1233-1241.
119. GHAZIZADEH M, OGAWA H, SASAKI Y, ARAKI T, AIHARA K: Mucin carbohydrate antigens (T, Tn, and sialyl-Tn) in human ovarian carcinomas: relationship with histopathology and prognosis. *Hum. Pathol.* (1997) **28**:960-966.
120. TAYLOR-PAPADIMITRIOU J, BURCHELL J, MILES DW, DALZIEL M: MUC1 and cancer. *Biochim. Biophys. Acta* (1999) **1455**:301-313.
121. JUNGBLUTH AA, JUNGBLUTH AA, STOCKERT E *et al.*: NY-ESO-1 and LAGE-1 cancer-testis antigens are potential targets for immunotherapy in epithelial ovarian cancer. *Cancer Res.* (2003) **63**:6076-6083.
122. STOCKERT E, JAGER E, CHEN YT *et al.*: A survey of the humoral immune response of cancer patients to a panel of human tumor antigens. *J. Exp. Med.* (1998) **187**:1349-1354.
123. CHEN YT, SCANLAN MJ, SAHIN U *et al.*: A testicular antigen aberrantly expressed in human cancers detected by autologous antibody screening. *Proc. Natl. Acad. Sci. USA* (1997) **94**:1914-1918.
124. VANDERKWAAK TJ, ALVAREZ RD: Immune directed therapy for ovarian carcinoma. *Curr. Opin. Obstet. Gynecol.* (1999) **11**:29-34.
125. SHIH IEM, KURMAN RJ: Ovarian tumorigenesis: a proposed model based on morphological and molecular genetic analysis. *Am. J. Pathol.* (2004) **164**:1511-1518.
126. POTHURI B, LEITAO M, BARAKAT R *et al.*: Genetic analysis of ovarian carcinoma histogenesis. *Society of Gynecologic Oncologists 32nd Annual Meeting.* Nashville, TN, USA (3 - 7 March 2001).
127. ORSULIC S, LI Y, SOSLOW RA, VITALE-CROSS LA, GUTKIND JS, VARMUS HE: Induction of ovarian cancer by defined multiple genetic changes in a mouse model system. *Cancer Cell* (2002) **1**:53-62.
128. FLESKEN-NIKITIN A, CHOI KC, ENG JP, SHMIDT EN, NIKITIN AY: Induction of carcinogenesis by concurrent inactivation of p53 and Rb1 in the mouse ovarian surface epithelium. *Cancer Res.* (2003) **63**:3459-3463.
129. REINARTZ S, KOHLER S, SCHLEBUSCH H *et al.*: Vaccination of patients with advanced ovarian carcinoma with the anti-idiotype ACA125: immunological response and survival (Phase Ib/II). *Clin. Cancer Res.* (2004) **10**:1580-1587.
130. BEREK JS: Immunotherapy of ovarian cancer with antibodies: a focus on oregovomab. *Expert Opin. Biol. Ther.* (2004) **4**:1159-1165.
131. BEREK JS, TAYLOR PT, GORDON A *et al.*: Randomized, placebo-controlled study of oregovomab for consolidation of clinical remission in patients with advanced ovarian cancer. *J. Clin. Oncol.* (2004) **22**:3507-3516.
132. GORDAN JD, VONDERHEIDE RH: Universal tumor antigens as targets for immunotherapy. *Cytotherapy* (2002) **4**:317-327.
133. VONDERHEIDE RH, HAHN WC, SCHULTZE JL, NADLER LM: The telomerase catalytic subunit is a widely expressed tumor-associated antigen recognized by cytotoxic T lymphocytes. *Immunity* (1999) **10**:673-679.
134. COUNTER CM, HIRTE HW, BACCHETTI S, HARLEY CB: Telomerase activity in human ovarian carcinoma. *Proc. Natl. Acad. Sci. USA* (1994) **91**:2900-2904.
135. SCARDINO A, GROSS DA, ALVES P *et al.*: HER-2/neu and hTERT cryptic epitopes as novel targets for broad spectrum tumor immunotherapy. *J. Immunol.* (2002) **168**:5900-5906.
136. LUBY TM, COLE G, BAKER L, KORNHER JS, RAMSTEDT U, HEDLEY ML: Repeated immunization with plasmid DNA formulated in poly(lactide-co-glycolide) microparticles is well tolerated and stimulates durable T cell responses to the tumor-associated antigen cytochrome P450 1B1. *Clin. Immunol.* (2004) **112**:45-53.

137. OTTO K, ANDERSEN MH, EGGERT A *et al.*: Lack of toxicity of therapy-induced T cell responses against the universal tumour antigen survivin. *Vaccine* (2005) **23**:884-889.
138. ANDERSEN MH, THOR SP: Survivin-a universal tumor antigen. *Histol. Histopathol.* (2002) **17**:669-675.
139. HARRIS JR, MARKL J: Keyhole limpet hemocyanin (KLH): a biomedical review. *Micron* (1999) **30**:597-623.
140. RIBAS A, BUTTERFIELD LH, GLASPY JA, ECONOMOU JS: Current developments in cancer vaccines and cellular immunotherapy. *J. Clin. Oncol.* (2003) **21**:2415-2423.
141. TODRYK S, MCLEAN C, ALI S *et al.*: Disabled infectious single-cycle herpes simplex virus as an oncolytic vector for immunotherapy of colorectal cancer. *Hum. Gene Ther.* (1999) **10**:2757-2768.
142. ISHIDA T, CHADA S, STIPANOV M *et al.*: Dendritic cells transduced with wild-type p53 gene elicit potent anti-tumour immune responses. *Clin. Exp. Immunol.* (1999) **117**:244-251.
143. DIAO J, SMYTHE JA, SMYTH C, ROWE PB, ALEXANDER IE: Human PBMC-derived dendritic cells transduced with an adenovirus vector induce cytotoxic T-lymphocyte responses against a vector-encoded antigen *in vitro*. *Gene Ther.* (1999) **6**:845-853.
144. BELARDELLI F, FERRANTINI M, PARMIANI G, SCHLOM J, GARACI E: International meeting on cancer vaccines: how can we enhance efficacy of therapeutic vaccines? *Cancer Res.* (2004) **64**:6827-6830.
145. INABA K, TURLEY S, YAMAIDE F *et al.*: Efficient presentation of phagocytosed cellular fragments on the major histocompatibility complex class II products of dendritic cells. *J. Exp. Med.* (1998) **188**:2163-2173.
146. MACKENSON A, HERBST B, CHEN JL *et al.*: Phase I study in melanoma patients of a vaccine with peptide-pulsed dendritic cells generated *in vitro* from CD34(+) hematopoietic progenitor cells. *Int. J. Cancer* (2000) **86**:385-392.
147. THURNER B, RODER C, DIECKMANN D *et al.*: Generation of large numbers of fully mature and stable dendritic cells from leukapheresis products for clinical application. *J. Immunol. Methods* (1999) **223**:1-15.
148. JONULEIT H, GIESECKE-TUETTENBERG A, TUTING T *et al.*: A comparison of two types of dendritic cell as adjuvants for the induction of melanoma-specific T-cell responses in humans following intranodal injection. *Int. J. Cancer* (2001) **93**:243-251.
149. MCILROY D, GREGOIRE M: Optimizing dendritic cell-based anticancer immunotherapy: maturation state does have clinical impact. *Cancer Immunol. Immunother.* (2003) **52**:583-591.
150. DHODAPKAR MV, STEINMAN RM, KRASOVSKY J, MUNZ C, BHARDWAJ N: Antigen-specific inhibition of effector T cell function in humans after injection of immature dendritic cells. *J. Exp. Med.* (2001) **193**:233-238.
- **This article describes how immature DCs can inhibit the effector T cell function *in vivo* in humans, and urges caution with the use of immature DCs when trying to enhance tumour or microbial immunity.**
151. CONEJO-GARCIA JR, BENENCIA F, COURREGES MC *et al.*: Tumor-infiltrating dendritic cell precursors recruited by a beta-defensin contribute to vasculogenesis under the influence of Vegf-A. *Nat. Med.* (2004) **10**:950-958.
- **This seminal work describes the identification of a new population of myeloid DCs that turn into endothelial-like cells in the tumour microenvironment, thus contributing to tumour vascularisation. This subset, named vascular leukocytes, represents novel therapeutic targets.**
152. CONEJO-GARCIA JR, BUCKANOVICH RJ, BENENCIA F *et al.*: Vascular leukocytes contribute to tumor vascularization. *Blood* (2005) **105**:679-681.
- **This paper reports the identification of a high frequency of vascular leukocytes in human ovarian carcinoma specimens.**
153. CURIEL TJ, CHENG P, MOTTRAM P *et al.*: Dendritic cell subsets differentially regulate angiogenesis in human ovarian cancer. *Cancer Res.* (2004) **64**:5535-5538.
154. CURIEL TJ, WEI S, DONG H *et al.*: Blockade of B7-H1 improves myeloid dendritic cell-mediated antitumor immunity. *Nat. Med.* (2003) **9**:562-567.
155. CHOMARAT P, BANCHEREAU J, DAVOUST J, PALUCKA AK: IL-6 switches the differentiation of monocytes from dendritic cells to macrophages. *Nat. Immunol.* (2000) **1**:510-514.
156. GABRILOVICH D, ISHIDA T, OYAMA T *et al.*: Vascular endothelial growth factor inhibits the development of dendritic cells and dramatically affects the differentiation of multiple hematopoietic lineages *in vivo*. *Blood* (1998) **92**:4150-4166.
- **This work depicts the mechanism by which VEGF is responsible for the defective function of DCs in the tumour microenvironment.**
157. GABRILOVICH DI, ISHIDA T, NADAF S, OHM JE, CARBONE DP: Antibodies to vascular endothelial growth factor enhance the efficacy of cancer immunotherapy by improving endogenous dendritic cell function. *Clin. Cancer Res.* (1999) **5**:2963-2970.
158. CHOMARAT P, BANCHEREAU J: Interleukin-4 and interleukin-13: their similarities and discrepancies. *Int. Rev. Immunol.* (1998) **17**:1-52.
159. AHONEN CL, DOXSEE CL, MCGURRAN SM *et al.*: Combined TLR and CD40 triggering induces potent CD8+ T cell expansion with variable dependence on Type I IFN. *J. Exp. Med.* (2004) **199**:775-784.
160. GONG J, NIKRUI N, CHEN D *et al.*: Fusions of human ovarian carcinoma cells with autologous or allogeneic dendritic cells induce antitumor immunity. *J. Immunol.* (2000) **165**:1705-1711.
161. NAIR S, BOCZKOWSKI D, MOELLER B, DEWHIRST M, VIEWEG J, GILBOA E: Synergy between tumor immunotherapy and antiangiogenic therapy. *Blood* (2003) **102**:964-971.
- **This study shows that there is a strong synergy of antiangiogenic therapy combined with tumour immunotherapy of cancer.**
162. BERD D, KAIRYS J, DUNTON C *et al.*: Autologous, hapten-modified vaccine as a treatment for human cancers. *Semin. Oncol.* (1998) **25**:646-653.
163. NEMUNAITIS J, STERMAN D, JABLONS D *et al.*: Granulocyte-macrophage colony-stimulating factor gene-modified autologous tumor vaccines in non-small-cell lung cancer. *J. Natl. Cancer Inst.* (2004) **96**:326-331.
164. SOIFFER R, HODI FS, HALUSKA F *et al.*: Vaccination with irradiated, autologous melanoma cells engineered to secrete granulocyte-macrophage

- colony-stimulating factor by adenoviral-mediated gene transfer augments antitumor immunity in patients with metastatic melanoma. *J. Clin. Oncol.* (2003) 21:3343-3350.
165. ZITVOGEL L, REGNAULT A, LOZIER A *et al.*: Eradication of established murine tumors using a novel cell-free vaccine: dendritic cell-derived exosomes. *Nat. Med.* (1998) 4:594-600.
- **This study shows how exosome-based cell-free vaccines represent a promising alternative to DC adoptive therapy for suppressing tumour growth.**
166. TAYLOR DD, GERCEL-TAYLOR C: Tumour-derived exosomes and their role in cancer-associated T-cell signalling defects. *Br. J. Cancer* (2005) 92(2):305-311.
167. ALBERT ML, PEARCE SF, FRANCISCO LM *et al.*: Immature dendritic cells phagocytose apoptotic cells via alphavbeta5 and CD36, and cross-present antigens to cytotoxic T lymphocytes. *J. Exp. Med.* (1998) 188:1359-1368.
168. SAUTER B, ALBERT ML, FRANCISCO L, LARSSON M, SOMERSAN S, BHARDWAJ N: Consequences of cell death: exposure to necrotic tumor cells, but not primary tissue cells or apoptotic cells, induces the maturation of immunostimulatory dendritic cells. *J. Exp. Med.* (2000) 191:423-434.
169. AVIGAN D: Dendritic cell-tumor fusion vaccines for renal cell carcinoma. *Clin. Cancer Res.* (2004) 10:6347S-6352S.
170. ARROYO PJ, BASH JA, WALLACK MK: Active specific immunotherapy with vaccinia colon oncolysate enhances the immunomodulatory and antitumor effects of interleukin-2 and interferon alpha in a murine hepatic metastasis model. *Cancer Immunol. Immunother.* (1990) 31:305-311.
171. BASH JA, WALLACK MK: Vaccinia virus oncolysates in the treatment of malignant melanoma. *Cancer Treat. Res.* (1988) 43:177-190.
172. SINKOVICS JG: Viral oncolysates as human tumor vaccines. *Int. Rev. Immunol.* (1991) 7:259-287.
173. FREEDMAN RS, IOANNIDES CG, MATHIOUDAKIS G, PLATSOUKAS CD: Novel immunologic strategies in ovarian carcinoma. *Am. J. Obstet. Gynecol.* (1992) 167:1470-1478.
174. IOANNIDES CG, DEN OTTER W: Concepts in immunotherapy of cancer: introduction. *In Vivo* (1991) 5:551-552.
175. SCHIRRMACHER V: Clinical trials of antitumor vaccination with an autologous tumor cell vaccine modified by virus infection: improvement of patient survival based on improved antitumor immune memory. *Cancer Immunol. Immunother.* (2004) 54(6):587-598.
176. MOBUS V, HORN S, STOCK M, SCHIRRMACHER V: Tumor cell vaccination for gynecological tumors. *Hybridoma* (1993) 12:543-547.
177. AUSTIN FC, BOONE CW: Virus augmentation of the antigenicity of tumor cell extracts. *Adv. Cancer Res.* (1979) 30:301-345.
178. MELCHER A, TODRYK S, HARDWICK N, FORD M, JACOBSON M, VILE RG: Tumor immunogenicity is determined by the mechanism of cell death via induction of heat shock protein expression. *Nat. Med.* (1998) 4:581-587.
179. SCHIRRMACHER V, AHLERT T, PROBSTLE T *et al.*: Immunization with virus-modified tumor cells. *Semin. Oncol.* (1998) 25:677-696.
180. FREEDMAN RS, PLATSOUKAS CD: Immunotherapy for peritoneal ovarian carcinoma metastasis using *ex vivo* expanded tumor infiltrating lymphocytes. *Cancer Treat. Res.* (1996) 82:115-146.
181. CANEVARI S, STOTER G, ARIENTI F *et al.*: Regression of advanced ovarian carcinoma by intraperitoneal treatment with autologous T lymphocytes retargeted by a bispecific monoclonal antibody. *J. Natl. Cancer Inst.* (1995) 87:1463-1469.
182. LAMERS CH, BOLHUIS RL, WARNAAR SO, STOTER G, GRATAMA JW: Local but no systemic immunomodulation by intraperitoneal treatment of advanced ovarian cancer with autologous T lymphocytes re-targeted by a bi-specific monoclonal antibody. *Int. J. Cancer* (1997) 73:211-219.
183. YAMAGUCHI T, BAMBA K, KITAYAMA A *et al.*: Long-term intravenous administration of activated autologous lymphocytes for cancer patients does not induce antinuclear antibody and rheumatoid factor. *Anticancer Res.* (2004) 24:2423-2429.
184. GREENFIELD EA, NGUYEN KA, KUCHROO VK: CD28/B7 costimulation: a review. *Crit. Rev. Immunol.* (1998) 18:389-418.
185. ALLISON JP, KRUMMEL MF: The Yin and Yang of T cell costimulation. *Science* (1995) 270:932-933.
186. BECKER JC, BRABLETZ T, CZERNY C, TERMEER C, BROCKER EB: Tumor escape mechanisms from immunosurveillance: induction of unresponsiveness in a specific MHC-restricted CD4+ human T cell clone by the autologous MHC class II+ melanoma. *Int. Immunol.* (1993) 5:1501-1508.
187. LEVINE BL, BERNSTEIN WB, CONNORS M *et al.*: Effects of CD28 costimulation on long-term proliferation of CD4+ T cells in the absence of exogenous feeder cells. *J. Immunol.* (1997) 159:5921-5930.
188. LEVINE BL, COTTE J, SMALL CC *et al.*: Large-scale production of CD4+ T cells from HIV-1-infected donors after CD3/CD28 costimulation. *J. Hematother.* (1998) 7:437-448.
189. MAUS MV, THOMAS AK, LEONARD DG *et al.*: *Ex vivo* expansion of polyclonal and antigen-specific cytotoxic T lymphocytes by artificial APCs expressing ligands for the T-cell receptor, CD28 and 4-1BB. *Nat. Biotechnol.* (2002) 20:143-148.
190. CONEJO-GARCIA JR, BENENCIA F, COURREGES MC *et al.*: Ovarian carcinoma expresses the NKG2D ligand *Letal* and promotes the survival and expansion of CD28(-) antitumor T cells. *Cancer Res.* (2004) 64:2175-2182.
191. CURIEL TJ, COUKOS G, ZOU L *et al.*: Specific recruitment of regulatory T cells in ovarian carcinoma fosters immune privilege and predicts reduced survival. *Nat. Med.* (2004) 10:942-949.
- **This paper conclusively demonstrates for the first time that tumour-associated regulatory T cells impair the function of T effector cells in tumour-bearing patients.**
192. WOO EY, CHU CS, GOLETZ TJ *et al.*: Regulatory CD4(+)CD25(+) T cells in tumors from patients with early-stage non-small cell lung cancer and late-stage ovarian cancer. *Cancer Res.* (2001) 61:4766-4772.
193. BLUESTONE JA, ABBAS AK: Natural versus adaptive regulatory T cells. *Nat. Rev. Immunol.* (2003) 3:253-257.
194. SAKAGUCHI S: Naturally arising CD4+ regulatory t cells for immunologic

- self-tolerance and negative control of immune responses. *Annu. Rev. Immunol.* (2004) **22**:531-562.
195. READ S, POWRIE F: CD4(+) regulatory T cells. *Curr. Opin. Immunol.* (2001) **13**:644-649.
196. WOO EY, YEH H, CHU CS *et al.*: Cutting edge: Regulatory T cells from lung cancer patients directly inhibit autologous T cell proliferation. *J. Immunol.* (2002) **168**:4272-4276.
197. PHAN GQ, YANG JC, SHERRY RM *et al.*: Cancer regression and autoimmunity induced by cytotoxic T lymphocyte-associated antigen 4 blockade in patients with metastatic melanoma. *Proc. Natl. Acad. Sci. USA* (2003) **100**:8372-8377.
198. HODI FS, MIHM MC, SOIFFER RJ *et al.*: Biologic activity of cytotoxic T lymphocyte-associated antigen 4 antibody blockade in previously vaccinated metastatic melanoma and ovarian carcinoma patients. *Proc. Natl. Acad. Sci. USA* (2003) **100**:4712-4717.
199. FRANKEL AE, FLEMING DR, HALL PD *et al.*: A Phase II study of DT fusion protein denileukin difitox in patients with fludarabine-refractory chronic lymphocytic leukemia. *Clin. Cancer Res.* (2003) **9**:3555-3561.
200. LE BON A, TOUGH DF: Links between innate and adaptive immunity via Type I interferon. *Curr. Opin. Immunol.* (2002) **14**:432-436.
201. TAKAOKA A, HAYAKAWA S, YANAI H *et al.*: Integration of interferon-alpha/beta signalling to p53 responses in tumour suppression and antiviral defence. *Nature* (2003) **424**:516-523.
202. RAMBALDI A, INTRONA M, COLOTTA F *et al.*: Intraperitoneal administration of interferon beta in ovarian cancer patients. *Cancer* (1985) **56**:294-301.
203. FUJIWARA K, MARKMAN M, STONEBRAKER B *et al.*: Intraperitoneal interferon-alpha in residual ovarian carcinoma: a Phase II gynecologic oncology group study. *Gynecol. Oncol.* (1999) **75**:10-14.
204. BEREK JS, WELANDER C, SCHINK JC, GROSSBERG H, MONTZ FJ, ZIGELBOIM J: A Phase I-II trial of intraperitoneal cisplatin and alpha-interferon in patients with persistent epithelial ovarian cancer. *Gynecol. Oncol.* (1991) **40**:237-243.
205. MARKMAN M, BELINSON J, WEBSTER K *et al.*: Phase II trial of interferon-beta as second-line treatment of ovarian cancer, fallopian tube cancer, or primary carcinoma of the peritoneum. *Oncology* (2004) **66**:343-346.
206. WEISS K: Safety profile of interferon-alpha therapy. *Semin. Oncol.* (1998) **25**:9-13.
207. HURTEAU JA, BLESSING JA, DECESARE SL, CREASMAN WT: Evaluation of recombinant human interleukin-12 in patients with recurrent or refractory ovarian cancer: a gynecologic oncology group study. *Gynecol. Oncol.* (2001) **82**:7-10.
208. LENZI R, ROSENBLUM M, VERSCHRAEGEN C *et al.*: Phase I study of intraperitoneal recombinant human interleukin 12 in patients with Mullerian carcinoma, gastrointestinal primary malignancies, and mesothelioma. *Clin. Cancer Res.* (2002) **8**:3686-3695.
209. PUJADE-LAURINE E, GUASTALLA JP, COLOMBO N *et al.*: Intraperitoneal recombinant interferon gamma in ovarian cancer patients with residual disease at second-look laparotomy. *J. Clin. Oncol.* (1996) **14**:343-350.
210. WINDBICHLER GH, HAUSMANINGER H, STUMMVOLL W *et al.*: Interferon-gamma in the first-line therapy of ovarian cancer: a randomized Phase III trial. *Br. J. Cancer* (2000) **82**:1138-1144.
211. EDWARDS RP, GOODING W, LEMBERSKY BC *et al.*: Comparison of toxicity and survival following intraperitoneal recombinant interleukin-2 for persistent ovarian cancer after platinum: twenty-four-hour versus 7-day infusion. *J. Clin. Oncol.* (1997) **15**:3399-3407.
212. OHTA M, MITOMI T, KIMURA M, HABU S, KATSUKI M: Anomalies in transgenic mice carrying the human interleukin-2 gene. *Tokai J. Exp. Clin. Med.* (1990) **15**:307-315.
213. FREEDMAN RS, KUDELKA AP, KAVANAGH JJ *et al.*: Clinical and biological effects of intraperitoneal injections of recombinant interferon-gamma and recombinant interleukin 2 with or without tumor-infiltrating lymphocytes in patients with ovarian or peritoneal carcinoma. *Clin. Cancer Res.* (2000) **6**:2268-2278.
214. LIU M, ACRES B, BALLOUL JM *et al.*: Gene-based vaccines and immunotherapeutics. *Proc. Natl. Acad. Sci. USA* (2004) **101**(Suppl. 2):14567-14571.
215. ODAKA M, STERMAN DH, WIEWRODT R *et al.*: Eradication of intraperitoneal and distant tumor by adenovirus-mediated interferon-beta gene therapy is attributable to induction of systemic immunity. *Cancer Res.* (2001) **61**:6201-6212.

Affiliation

George Coukos^{†1}, Jose R Conejo-Garcia¹, Richard BS Roden² & T-C Wu²

[†]Author for correspondence

¹University of Pennsylvania, Abramson Cancer Research Institute, and Center for Research on Reproduction and Women's Health, Philadelphia, PA 19104, USA

²Johns Hopkins Medical Institutions, Departments of Pathology, Oncology, Molecular Microbiology and Immunology, Obstetrics and Gynecology, Baltimore, MD 21287, USA

Award Number: OC010017

TITLE:

PATHOGENESIS OF OVARIAN SEROUS CARCINOMA AS THE BASIS FOR IMMUNOLOGIC DIRECTED DIAGNOSIS AND TREATMENT: PROJECT 3: Development of Antigen-Specific Cancer Vaccines for the Control of Ovarian Cancer

PRINCIPAL INVESTIGATOR:

T.-C. Wu, M.D., Ph.D.

CONTRACTING ORGANIZATION:

The Johns Hopkins School of Medicine
720 Rutland Avenue,
Baltimore, MD 21205

REPORT DATE: March 12, 2006

TYPE OF REPORT:

Final progress report

PREPARED FOR: U.S. Army Medical Research and Materiel Command
Fort Detrick, Maryland 21702-5012

DISTRIBUTION STATEMENT: Approved for Public Release;
Distribution Unlimited

The views, opinions and/or findings contained in this report are those of the author(s) and should not be construed as an official Department of the Army position, policy or decision unless so designated by other documentation.

REPORT DOCUMENTATION PAGE			<i>Form Approved</i> <i>OMB No. 074-0188</i>	
Public reporting burden for this collection of information is estimated to average 1 hour per response, including the time for reviewing instructions, searching existing data sources, gathering and maintaining the data needed, and completing and reviewing this collection of information. Send comments regarding this burden estimate or any other aspect of this collection of information, including suggestions for reducing this burden to Washington Headquarters Services, Directorate for Information Operations and Reports, 1215 Jefferson Davis Highway, Suite 1204, Arlington, VA 22202-4302, and to the Office of Management and Budget, Paperwork Reduction Project (0704-0188), Washington, DC 20503				
1. AGENCY USE ONLY (Leave blank)	2. REPORT DATE March 12, 2006	3. REPORT TYPE AND DATES COVERED Final (07/01/02-06/30/05 and no cost		
4. TITLE AND SUBTITLE PATHOGENESIS OF OVARIAN SEROUS CARCINOMA AS THE BASIS FOR IMMUNOLOGIC DIRECTED DIAGNOSIS AND TREATMENT: PROJECT 3 Development of Antigen-Specific Cancer Vaccines for the Control of Ovarian Cancer			5. FUNDING NUMBERS OC010017	
6. AUTHOR(S) T.-C. Wu, M.D., Ph.D.				
7. PERFORMING ORGANIZATION NAME(S) AND ADDRESS(ES) Department of Pathology, The Johns Hopkins School of Medicine E-Mail:wutc@jhmi.edu			8. PERFORMING ORGANIZATION REPORT NUMBER	
9. SPONSORING / MONITORING AGENCY NAME(S) AND ADDRESS(ES) U.S. Army Medical Research and Materiel Command Fort Detrick, Maryland 21702-5012			10. SPONSORING / MONITORING AGENCY REPORT NUMBER	
11. SUPPLEMENTARY NOTES				
12a. DISTRIBUTION / AVAILABILITY STATEMENT Approved for Public Release; Distribution Unlimited			12b. DISTRIBUTION CODE	
13. ABSTRACT (Maximum 200 Words) Mesothelin is highly expressed in a majority of ovarian cancer cells and is expressed at low levels in normal cells. Therefore, mesothelin represents an ideal target antigen for ovarian cancer vaccine development. DNA vaccines employing a single-chain trimers (SCT) targeting a human mesothelin CTL epitope can bypass antigen processing and presentation and result in significant enhancement of DNA vaccine potency. In the current study, we created a DNA vaccine employing the SCT technology targeting human mesothelin and characterized the ensuing antigen-specific CD8 ⁺ T cell-mediated immune responses and anti-tumor effects against human mesothelin-expressing tumors in HLA-A2 transgenic mice. Our results showed that vaccination with DNA employing the SCT of HLA-A2 linked to human mesothelin epitope aa540-549 (pcDNA3-Hmeso540-β2m-A2) generated strong human mesothelin peptide (aa540-549)-specific CD8 ⁺ T cell immune responses in HLA-A2 transgenic mice. Furthermore, vaccination with pcDNA3-Hmeso540-β2m-A2 prevented the growth of HLA-A2 positive, human mesothelin-expressing tumor cell lines in HLA-A2 transgenic mice compared to vaccination with DNA encoding SCT linked to the OVA CTL epitope. Thus, the employment of SCT of HLA-A2 linked to the human mesothelin epitope aa540-549 represents a potential opportunity for the clinical translation of DNA vaccines against human mesothelin-expressing tumors, particularly ovarian cancer cells.				
14. SUBJECT TERMS			15. NUMBER OF PAGES 11	
			16. PRICE CODE	
17. SECURITY CLASSIFICATION OF REPORT Unclassified	18. SECURITY CLASSIFICATION OF THIS PAGE Unclassified	19. SECURITY CLASSIFICATION OF ABSTRACT Unclassified	20. LIMITATION OF ABSTRACT	

Table of Contents

Cover..... 1

SF 298..... 2

Table of Contents..... 3

Introduction..... 4

Body..... 5

Key Research Accomplishments..... 10

Reportable Outcomes..... 11

Conclusions..... 11

References..... 11

Appendices.....

C.-F. Hung, R. Calizo, Y.-C. Tsai, L. He, and T.-C. Wu (2006) A DNA vaccine encoding a single-chain trimer of HLA-A2 linked to human mesothelin peptide generates anti-tumor effects against human mesothelin-expressing tumors. *Vaccine* (in press)

C.-F. Hung, Y.-C. Tsai, L. He, and T.-C. Wu (2006) Control of mesothelin-expressing ovarian cancer using adoptive transfer of mesothelin peptide-specific CD8+ T cells. *Gene Therapy* (in press)

INTRODUCTION

Metastatic ovarian cancer is almost an incurable disease and is responsible for the highest mortality rate (20%) among patients with gynecologic malignancies. Current efforts to reduce this mortality rate, including improvement of early detection and treatment, have been relatively unsuccessful. Existing therapies for advanced disease, such as chemotherapy and radiation therapy, rarely result in long-term benefits in patients with locally advanced and metastatic disease.¹⁻³ Immunotherapy provides a promising alternative approach for the control of ovarian cancer.

The ideal cancer therapy should have the potency to eradicate systemic tumors and control metastases, as well as the specificity to discriminate between malignant and normal cells. In both of these respects, the immune system is an attractive candidate. The immune system has multiple complementary effector mechanisms capable of killing target cells, including T cells, macrophages, granulocytes, and natural killer cells. T cells can generate tumor-specific immune responses via a vast array of clonally distributed antigen receptors, which can recognize tumor-specific antigens. It is well established that T cells recognize peptide fragments of cellular proteins bound to major histocompatibility complex (MHC) molecules on the surfaces of cells, and any cellular protein (including those from which tumor antigens derive) can be presented to T cells in this way. Thus, identification of tumor-associated antigens uniquely expressed in ovarian cancer is important for the development of antigen-specific cancer immunotherapy. Mesothelin represents an ideal target antigen for the control of ovarian cancers since it is expressed in over 95% of ovarian cancers and is absent or expressed at low levels in normal tissues.⁴

DNA vaccines targeting human mesothelin provide a potentially effective approach for the control of mesothelin-expressing ovarian cancer. DNA vaccines are considered to be a potentially promising form of vaccine for the control of infectious diseases and cancers since they offer many advantages over other conventional vaccines such as peptide or attenuated live pathogens. For instance, DNA vaccines are relatively safe and can be administered repeatedly without adverse effects. In addition, DNA vaccines are relatively easy to produce on a large scale and are able to yield products with high purity and stability. Most importantly, effective DNA vaccine delivery systems, such as the direct intradermal administration of DNA vaccines via gene gun to professional antigen presenting cells (APCs), have been well established. Using this delivery method, we have previously developed several innovative strategies to enhance DNA vaccine potency by modifying the properties of DNA-transfected APCs (for reviews, see ^{5,6}).

One of the strategies that we have recently developed to enhance DNA vaccine potency is the employment of single-chain trimer (SCT) technology to bypass antigen processing and ensure stable MHC class I presentation of the antigenic peptide by transfected APCs. We have previously constructed a DNA vaccine encoding an SCT composed of an immunodominant CTL epitope of human papillomavirus type 16 (HPV-16) E6 antigen, $\beta 2m$, and H-2K^b MHC class I heavy chain (pIRES-E6- $\beta 2m$ -K^b). Transfection of human embryonic kidney cells (293 cells) with pIRES-E6- $\beta 2m$ -K^b DNA has been shown to bypass antigen processing and lead to stable presentation of E6 peptide. Furthermore, C57BL/6 mice vaccinated with pIRES-E6- $\beta 2m$ -K^b exhibited significantly increased E6 peptide-specific CD8⁺ T cell immune responses and more potent anti-tumor effects against E6-expressing tumors compared to mice vaccinated with DNA encoding wild-type E6.⁷ These findings indicate that a DNA vaccine encoding a SCT may potentially improve DNA vaccine potency and elicit antigen-specific immune responses capable of controlling tumors or infectious diseases.

In the current study, we have evaluated the efficacy of a DNA vaccine employing an SCT targeting a human mesothelin-specific CTL epitope (aa540-549) using HLA-A2 transgenic mice. HLA-A2 transgenic mice have extensively been used to identify functional, human CTL epitopes and to evaluate the efficacy of candidate vaccines, since these transgenic mice may have CTL repertoires similar to those of humans. We demonstrated that HLA-A2 transgenic mice vaccinated with DNA employing an SCT of HLA-A2 linked to the human mesothelin epitope aa540-549 (pcDNA3-Hmeso540- β 2m-A2) were capable of generating strong human mesothelin peptide (aa540-549)-specific CD8⁺ T cell immune responses. Furthermore, mice vaccinated with pcDNA3-Hmeso540- β 2m-A2 were able to more effectively prevent the growth of HLA-A2 positive, human mesothelin-expressing tumor cell lines compared to vaccination with control DNA. The implications of this approach for clinical application were discussed.

BODY

Cells transfected with DNA encoding human mesothelin (pcDNA3-Hmeso) or infected with vaccinia encoding human mesothelin (Vac-Hmeso) express human mesothelin

To characterize human mesothelin expression of cells transfected with DNA or infected with vaccinia, TK- cells were either transfected with pcDNA3-Hmeso or infected with Vac-Hmeso vaccinia. Transfected or infected cells were characterized by staining with human mesothelin-specific antibodies followed by flow cytometry analysis. TK- cells transfected with pcDNA3-Hmeso expressed human mesothelin, as shown in **Figure 1A**. In contrast, TK- cells transfected with pcDNA3 vector did not express human mesothelin. Similarly, TK- cells infected with Vac-Hmeso expressed human mesothelin, while TK- cells infected with wild type vaccinia did not express human mesothelin (**Figure 1B**). These results confirm that we have successfully generated a human mesothelin-expressing DNA construct and vaccinia virus.

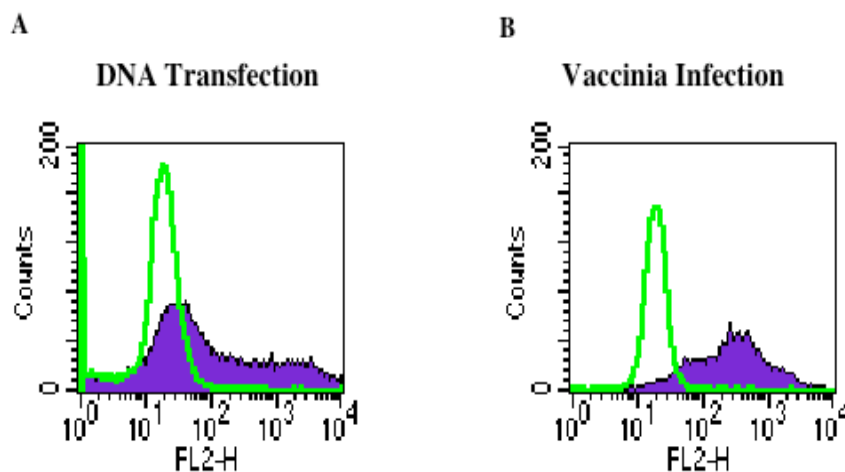


Figure 1. Flow cytometry analysis to characterize human mesothelin expression of cells transfected with DNA or infected with vaccinia. (A) TK- cells transfected with pcDNA3-Hmeso (filled histogram) or pcDNA3 vector (clear histogram). **(B)** TK- cells infected with Vac-Hmeso (filled histogram) or wild-type vaccinia (clear histogram). Transfected or infected TK- cells were stained with human mesothelin-specific antibodies and characterized by flow cytometry analysis.

Identification of human mesothelin epitopes aa116-125 and aa540-549 as HLA-A2-restricted human mesothelin-specific CTL epitopes

The availability of a human mesothelin-expressing DNA construct and vaccinia virus allows us to design prime and boost vaccination regimens in order to generate high numbers of human mesothelin-specific CD8⁺ T cells in vaccinated mice. Using splenocytes derived from HLA-A2 transgenic mice vaccinated with pcDNA3-Hmeso and boosted with Vac-Hmeso, we were able to develop quantitative human mesothelin-specific CD8⁺ T cell immunological assays. In order to identify candidate HLA-A2-restricted human mesothelin-specific CTL epitopes, we used the BioInformatics & Molecular Analysis Section (BIMAS) database for HLA-A2 peptide binding predictions. We identified several candidate 9- or 10-residue peptides for human mesothelin. Their positions, MHC restrictions, sequences and scores are presented in **Table 1**.

Table 1. Candidate HLA-A2 restricted human mesothelin-specific CTL epitopes predicted by BIMAS

Peptide name Start position	MHC class I	Peptide sequence	BIMAS score
Peptide-20	HLA2	SLLFLLFSL	1054
Peptide-17	HLA2	ALGSLLFLL	284
Peptide-64	HLA2	QLLGFPCEAV	257
Peptide-116	HLA2	ALPLDLLLFL	270
Peptide-530	HLA2	VLPLTVAEV	271
Peptide-540	HLA2	KLLGPHVEGL	311
Peptide-602	HLA2	LLGPGPVLTV	271

Bioinformatics & Molecular Analysis Section (BIMAS) was used to analyze various 9-residue peptides from mesothelin for H-2 binding predictions. The sequences, positions, MHC restrictions, and scores (according to the numbers of mesothelin-specific, IFN- γ -expressing CTLs generated by the candidate peptide) of the potential human mesothelin epitopes were determined.

To determine which candidate peptides represent true HLA-A2-restricted human mesothelin-specific CTL epitopes, we used the candidate peptides identified by BIMAS to stimulate splenocytes from vaccinated HLA-A2 transgenic mice. As shown in **Figure 2**, splenocytes from vaccinated mice pulsed with human mesothelin peptides aa116-125 or aa540-549 generated significantly greater numbers of human mesothelin-specific, IFN- γ -expressing CTLs than splenocytes pulsed with the other human mesothelin peptides ($p < 0.001$). These data indicate that the human mesothelin peptides aa116-125 and aa540-549 can be recognized by CD8⁺ T cells generated by HLA-A2 transgenic mice primed with pcDNA3-Hmeso and boosted with Vac-Hmeso. Furthermore, there are no CD8-specific T cell responses to these epitopes when using the same vaccines to vaccinate C57BL/6 mice (data not shown). Thus, these data confirm that aa116-125 and aa540-549 human mesothelin epitopes are HLA-A2-restricted

human mesothelin-specific CTL epitopes but not H-2 D^b, K^b-restricted CTL epitopes. Furthermore, between these two identified peptides, aa540-549 generated greater numbers of IFN- γ -expressing CTLs than aa116-125.

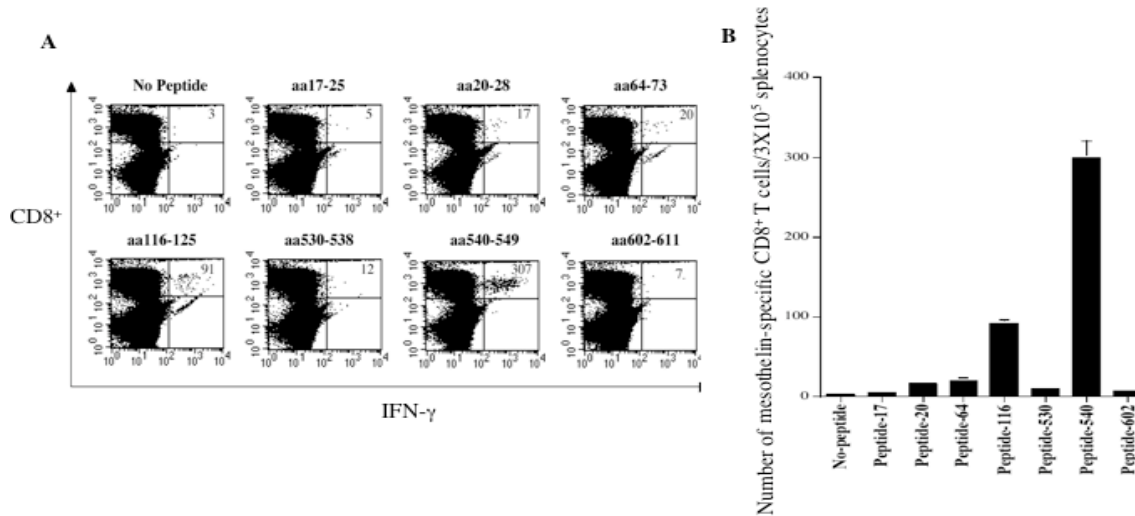


Figure 2. Intracellular cytokine staining followed by flow cytometry analysis to characterize HLA-A2-restricted human mesothelin-specific CTL epitopes. HLA-A2 transgenic mice were vaccinated with 2 μ g/mouse of pCDNA3-Hmeso followed by an intraperitoneal booster with Vac-Hmeso (1×10^7 pfu/mouse). Splenocytes were harvested one week after the last vaccination and stimulated with various candidate human mesothelin epitopes (see Table 1) for 16 hours. Activation of human mesothelin-specific CD8⁺ T cells was determined by intracellular cytokine staining for CD8 and IFN- γ expression. **(A)** Representative figure of flow cytometry data. **(B)** Bar graph depicting number of IFN- γ -expressing human mesothelin-specific CD8⁺ T cells out of 3×10^5 splenocytes isolated from vaccinated mice.

Vaccination with pcDNA3-Hmeso540- β 2m-A2 enhances the human mesothelin-specific CD8⁺ T cell responses in vaccinated HLA-A2 transgenic mice

The identification of aa540-549 as a strong HLA-A2-restricted human mesothelin-specific CTL epitope allowed us to generate a DNA vaccine encoding a SCT of HLA-A2 linked to this epitope (pcDNA3-Hmeso540- β 2m-A2) (**Figure 3**). We also generated a DNA vaccine encoding an SCT of HLA-A2 linked to OVA (pcDNA3-OVA- β 2m-A2) as a negative control.

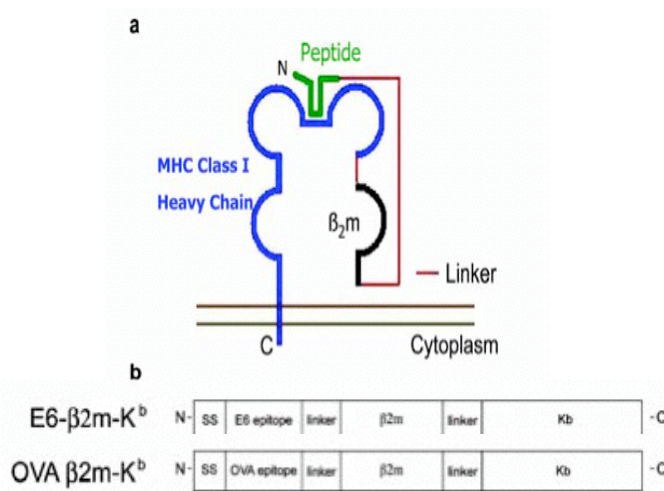


Figure 3. Diagrams depicting structure of our SCT and structures of chimeric DNA constructs. (A) Diagram of a peptide:β2m:MHC SCT on cell surface. **(B)** Diagram of an SCT encoding human mesothelin aa540-549 linked to β2m and an HLA-A2-restricted MHC Class I molecule, and a SCT encoding OVA linked to β2m and an HLA-A2-restricted MHC Class I molecule. Each was cloned into the pcDNA3 vector to make the DNA vaccines used in the study.

To assess the immunogenicity of our DNA vaccine, we vaccinated mice with pcDNA3-Hmeso540-β2m-A2 or pcDNA3-OVA-β2m-A2 and then performed intracellular cytokine staining with flow cytometry analysis to characterize human mesothelin-specific CD8⁺ T cell precursors using human mesothelin aa540-549 peptide as a stimulant. HLA-A2 transgenic mice vaccinated with pcDNA3-Hmeso540-β2m-A2 generated a significantly higher frequency of human mesothelin-specific IFN-γ-secreting CD8⁺ T cell precursors compared to mice immunized with pcDNA3-OVA-β2m-A2 (**Figure 4**). These data indicate that vaccination with DNA encoding an SCT of HLA-A2 linked to a human mesothelin-specific CTL epitope is capable of generating strong human mesothelin-specific CD8⁺ T cell immune responses in HLA-A2 transgenic mice.

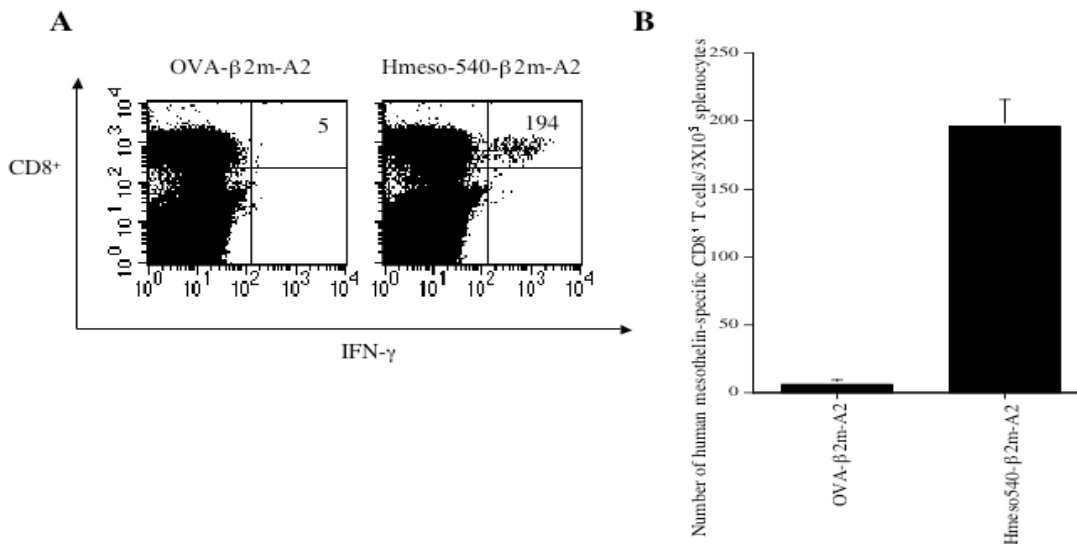


Figure 4. Characterization of human mesothelin-specific CD8⁺ T cells in vaccinated HLA-A2 transgenic mice. Mice (5 per group) were immunized with pcDNA3-OVA-β2m-A2 or pcDNA3-Hmeso540-β2m-A2. Splenocytes from vaccinated mice were collected and stimulated with human mesothelin-specific peptides (aa540-549). Intracellular cytokine staining followed by flow cytometry analysis was performed. **(A)** Representative figure of the flow cytometry data. **(B)** Bar graph depicting the number of human mesothelin peptide (aa540-549)-specific IFN-γ-secreting CD8⁺ T cell precursors/3 × 10⁵ splenocytes (mean±SD). The data presented in this figure are from one representative experiment of two performed.

A syngeneic tumor cell line that expresses human mesothelin and HLA-A2

In order to generate a tumor cell line expressing human mesothelin and HLA-A2 for use in tumor prevention experiments in HLA-A2 transgenic mice, we have transduced TC-1/A2 cell lines with a retrovirus containing human mesothelin to generate TC-1/A2/Hmeso. We have previously generated an HLA-A2-expressing murine tumor model, TC-1/A2, that is capable of growing consistently in HLA-A2 transgenic mice through subcutaneous injection⁸. We have further characterized the expression of HLA-A2 and human mesothelin in TC-1/A2/Hmeso cells using flow cytometry analyses. TC-1 cells were used as negative controls. As shown in **Figure 5**, TC-1/A2/Hmeso cells (filled histogram) showed significantly higher expression of both HLA-A2 and human mesothelin compared to TC-1 cell lines (clear histogram). These data indicate that the TC-1/A2/Hmeso tumor cell line is successfully engineered to express significant levels of both HLA-A2 and human mesothelin proteins. Furthermore, TC-1/A2/Hmeso was able to successfully grow in HLA-A2 transgenic mice when subcutaneously challenged after DNA vaccination.

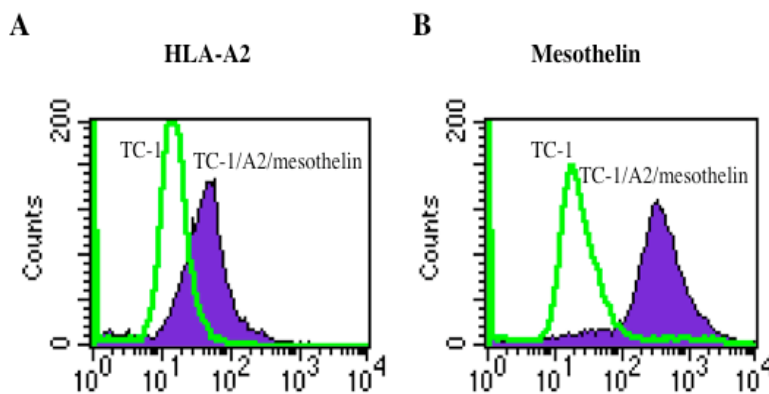


Figure 5. Flow cytometry analysis to demonstrate the expression of HLA-A2 and human mesothelin in TC-1/A2/Hmeso cell line. TC-1/A2/Hmeso was generated by transducing TC-1/A2 with a retrovirus containing human mesothelin as described in the Materials and Methods. **(A)** Characterization of HLA-A2 expression in TC-1/A2/Hmeso (filled histogram) and TC-1 (clear histogram). The cell lines were stained with HLA-A2-specific monoclonal antibody followed by flow cytometry analysis. **(B)** Characterization of human mesothelin expression in TC-1 TC-1/A2/Hmeso (filled histogram) and TC-1 (clear histogram). The cell lines were stained with human mesothelin-specific antibody followed by flow cytometry analysis.

pcDNA3-Hmeso540-β2m-A2 vaccination prevents the growth of human mesothelin-expressing TC-1/A2/Hmeso tumors in mice

Given the immunogenicity of pcDNA3-Hmeso540-β2m-A2 (see **Figure 4**), we next explored whether it could elicit effective protective anti-tumor effects against the HLA-A2 positive, human mesothelin-expressing tumor cell line, TC-1/A2/Hmeso. Tumor cells were injected subcutaneously one week after DNA vaccination. During a 6-week follow-up period, 60% of mice receiving pcDNA3-Hmeso540-β2m-A2 remained tumor free. All of the pcDNA3-OVA-β2m-A2-immunized mice exhibited tumor growth by the second week (**Figure 6**). This suggests that vaccination with pcDNA3-Hmeso540-β2m-A2 can generate significant protective effects against human mesothelin-expressing tumors. Thus, our data indicate that a DNA vaccine encoding an SCT of a human MHC class I molecule linked to a CTL epitope from human mesothelin antigen is capable of generating a strong antigen-specific CD8⁺ T cell immune response and antitumor effects in vaccinated HLA-A2 transgenic mice.

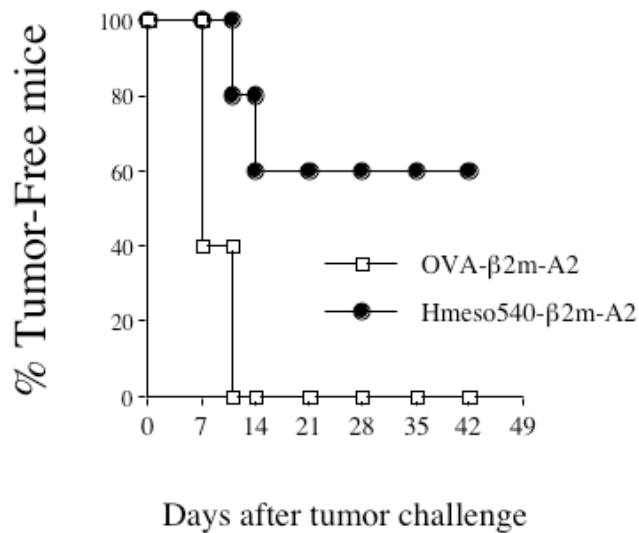


Figure 6. *In vivo* tumor protection experiment to demonstrate the antitumor effect generated by pcDNA3-Hmeso540-β2m-A2 against human mesothelin-expressing TC-1/A2/Hmeso tumors in HLA-A2 transgenic mice. Mice (5 per group) were immunized with OVA-β2m-A2 or Hmeso540-β2m-A2 four times at one-week interval. At 1 week after the last vaccination, mice were challenged subcutaneously with 5×10^4 TC-1/A2/Hmeso cells/mouse and monitored for evidence of tumor growth by palpation and inspection thrice a week.

KEY RESEARCH ACCOMPLISHMENTS

- ◆ We have identified human mesothelin epitopes aa116-125 and aa540-549 as HLA-A2-restricted human mesothelin-specific CTL epitopes.
- ◆ We have shown that vaccination with pcDNA3-Hmeso540-β2m-A2 DNA enhances the human mesothelin-specific CD8⁺ T cell responses in vaccinated HLA-A2 transgenic mice.
- ◆ We have generated a syngeneic tumor cell line expresses human mesothelin and HLA-A2.
- ◆ We have shown that pcDNA3-Hmeso540-β2m-A2 vaccination prevents the growth of human mesothelin-expressing TC-1/A2/Hmeso tumors in HLA-A2 transgenic mice.

REPORTABLE OUTCOMES

C.-F. Hung, R. Calizo, Y.-C. Tsai, L. He, and T.-C. Wu (2006) A DNA vaccine encoding a single-chain trimer of HLA-A2 linked to human mesothelin peptide generates anti-tumor effects against human mesothelin-expressing tumors. *Vaccine* (in press)

C. -F. Hung, Y.-C. Tsai, L. He, and T.-C. Wu (2006) Control of mesothelin-expressing ovarian cancer using adoptive transfer of mesothelin peptide-specific CD8+ T cells. *Gene Therapy* (in press)

CONCLUSIONS

The employment of single-chain trimers (SCT) of HLA-A2 linked to the human mesothelin epitope aa540-549 represents a potential opportunity for the clinical translation of DNA vaccines against human mesothelin-expressing tumors, particularly ovarian cancer cells.

REFERENCES

- 1 Systemic treatment of early breast cancer by hormonal, cytotoxic, or immune therapy. 133 randomised trials involving 31,000 recurrences and 24,000 deaths among 75,000 women. Early Breast Cancer Trialists' Collaborative Group [see comments]. *Lancet* 1992; **339**: 1-15.
- 2 Baum M, Ebb S, Brooks M. Biological fall out from trials of adjuvant tamoxifen in early ovarian cancer. . In: Salmon SE, ed. Adjuvant therapy of cancer V1. Philadelphia: WB. *Saunders*, 1990: 269-274.
- 3 Swain SM. Selection of therapy for stage III breast cancer. *Surg Clin North Am* 1990; **70**: 1061-1080.
- 4 Scholler N *et al*. Soluble member(s) of the mesothelin/megakaryocyte potentiating factor family are detectable in sera from patients with ovarian carcinoma. *Proc Natl Acad Sci U S A* 1999; **96**: 11531-11536.
- 5 Hung CF, Wu TC. Improving DNA vaccine potency via modification of professional antigen presenting cells. *Curr Opin Mol Ther* 2003; **5**: 20-24.
- 6 Boyd D, Hung CF, Wu TC. DNA vaccines for cancer. *IDrugs* 2003; **6**: 1155-1164.
- 7 Huang CH *et al*. Cancer Immunotherapy Using a DNA Vaccine Encoding a Single-Chain Trimer of MHC class I Linked to an HPV-16 E6 Immunodominant CTL Epitope. *Cancer Res* (submitted) 2004.
- 8 Peng S *et al*. Characterization of HLA-A2-restricted HPV-16 E7-specific CD8(+) T-cell immune responses induced by DNA vaccines in HLA-A2 transgenic mice. *Gene Ther* 2005.

Project 3 Publications:

1. C.-F. Hung, R. Calizo, Y.-C. Tsai, L. He, and T.-C. Wu (2006) A DNA vaccine encoding a single-chain trimer of HLA-A2 linked to human mesothelin peptide generates anti-tumor effects against human mesothelin-expressing tumors. *Vaccine* (in press)
2. C.-F. Hung, Y.-C. Tsai, L. He, and T.-C. Wu (2006) Control of mesothelin-expressing ovarian cancer using adoptive transfer of mesothelin peptide-specific CD8⁺ T cells. *Gene Therapy* (in press)



A DNA vaccine encoding a single-chain trimer of HLA-A2 linked to human mesothelin peptide generates anti-tumor effects against human mesothelin-expressing tumors

Chien-Fu Hung^{a,*}, Roanne Calizo^a, Ya-Chea Tsai^a,
Liangmei He^a, T.-C. Wu^{a,b,c,d}

^a Department of Pathology, Johns Hopkins Medical Institutions, Baltimore, MD, USA

^b Department of Obstetrics and Gynecology, Johns Hopkins Medical Institutions, Baltimore, MD, USA

^c Department of Molecular Microbiology and Immunology, Johns Hopkins Medical Institutions, Baltimore, MD, USA

^d Department of Oncology, Johns Hopkins Medical Institutions, Baltimore, MD, USA

Received 3 May 2006; received in revised form 16 June 2006; accepted 20 June 2006

Abstract

Mesothelin is highly expressed in a majority of ovarian cancer cells and is expressed at low levels in normal cells. Therefore, mesothelin represents a potential target antigen for ovarian cancer vaccine development. DNA vaccines employing single-chain trimers (SCT) have been shown to bypass antigen processing and presentation and result in significant enhancement of DNA vaccine potency. In the current study, we created a DNA vaccine employing an SCT targeting human mesothelin and characterized the ensuing antigen-specific CD8⁺ T cell-mediated immune responses and anti-tumor effects against human mesothelin-expressing tumors in HLA-A2 transgenic mice. Our results showed that vaccination with DNA employing an SCT of HLA-A2 linked to human mesothelin epitope aa540–549 (pcDNA3–Hmeso540–β2m–A2) generated strong human mesothelin peptide (aa540–549)-specific CD8⁺ T cell immune responses in HLA-A2 transgenic mice. Vaccination with pcDNA3–Hmeso540–β2m–A2 prevented the growth of HLA-A2 positive human mesothelin-expressing tumor cell lines in HLA-A2 transgenic mice in contrast to vaccination with DNA encoding SCT linked to OVA CTL epitope. Thus, the employment of SCT of HLA-A2 linked to the human mesothelin epitope aa540–549 represents a potential opportunity for the clinical translation of DNA vaccines against human mesothelin-expressing tumors, particularly ovarian cancer cells.

© 2006 Elsevier Ltd. All rights reserved.

Keywords: DNA vaccine; Immunotherapy; Human mesothelin; Single-chain trimer

1. Introduction

Metastatic ovarian cancer is almost an incurable disease and is responsible for the highest mortality rate among patients with gynecologic malignancies. Current efforts to reduce this mortality rate, including improvement of early

detection and treatment, have been relatively unsuccessful. Existing therapies for advanced disease, such as chemotherapy and radiation therapy, rarely result in long-term benefits in patients with locally advanced and metastatic disease [1–3].

The ideal cancer therapy should have the potency to eradicate systemic tumors and control metastases as well as the specificity to discriminate between malignant and normal cells. In both of these respects, the immune system is an attractive therapeutic pathway. The immune system has multiple complementary effector mechanisms capable of killing

* Corresponding author at: Department of Pathology, The Johns Hopkins University School of Medicine, CRB II Room 307, 1550 Orleans Street, Baltimore, MD 21231, USA. Tel.: +1 410 614 3899; fax: +1 443 287 4295.

E-mail address: chung2@jhmi.edu (C.-F. Hung).

target cells. These mechanisms may be mediated by T cells, macrophages, granulocytes, and natural killer cells. T cells can generate tumor-specific immune responses via a vast array of clonally distributed antigen receptors, which can recognize tumor-specific antigens. It is well established that T cells recognize peptide fragments of cellular proteins bound to major histocompatibility complex (MHC) molecules on the surfaces of cells, and any cellular protein (including those from which tumor antigens derive) can be presented to T cells in this way. Thus, identification of tumor-associated antigens uniquely expressed in ovarian cancer is important for the development of antigen-specific cancer immunotherapy. Mesothelin represents a potential target antigen for the control of ovarian cancers since it is expressed in over 95% of ovarian cancers and is absent or expressed at low levels in normal tissues [4].

DNA vaccines targeting human mesothelin offer a potentially effective approach to the control of mesothelin-expressing ovarian cancer. DNA vaccines are considered to be a promising form of vaccine for the control of infectious diseases and cancers since they offer many advantages over other conventional vaccines such as peptide or attenuated live pathogens. For instance, DNA vaccines are relatively safe and can be administered repeatedly without adverse effects. In addition, DNA vaccines are comparatively easy to produce on a large scale and are able to yield products with high purity and stability. Most importantly, effective DNA vaccine delivery systems, such as direct intradermal administration of DNA vaccines via gene gun to professional antigen presenting cells (APCs), have been well established. Using this delivery method, we have previously developed several innovative strategies to enhance DNA vaccine potency by modifying the properties of DNA-transfected APCs (for reviews, see [5,6]).

One of the strategies that we have recently developed to enhance DNA vaccine potency is the employment of single-chain trimer (SCT) technology to bypass antigen processing and ensure stable MHC class I presentation of the antigenic peptide by transfected APCs. We have previously constructed a DNA vaccine encoding an SCT composed of an immunodominant CTL epitope of human papillomavirus type 16 (HPV-16) E6 antigen, $\beta 2m$, and H-2K^b MHC class I heavy chain (pIRES-E6- $\beta 2m$ -K^b). Transfection of human embryonic kidney cells (293 cells) with pIRES-E6- $\beta 2m$ -K^b has been shown to bypass antigen processing and lead to the stable presentation of E6 peptide. Furthermore, C57BL/6 mice vaccinated with pIRES-E6- $\beta 2m$ -K^b exhibited significantly increased E6 peptide-specific CD8⁺ T cell immune responses and more potent anti-tumor effects against E6-expressing tumors compared to mice vaccinated with DNA encoding wild-type E6 [7]. These findings indicate that a DNA vaccine encoding an SCT may potentially improve DNA vaccine potency and elicit antigen-specific immune responses capable of controlling tumors or infectious diseases.

In the current study, we evaluated the efficacy of a DNA vaccine employing an SCT targeting a human mesothelin-

specific CTL epitope (aa540–549) using HLA-A2 transgenic mice. HLA-A2 transgenic mice have extensively been used to identify functional, human CTL epitopes and to evaluate the efficacy of candidate vaccines, since these transgenic mice may have CTL repertoires similar to those of humans. We demonstrated that HLA-A2 transgenic mice vaccinated with DNA employing an SCT of HLA-A2 linked to the human mesothelin epitope aa540–549 (pcDNA3–Hmeso540- $\beta 2m$ -A2) were capable of generating strong human mesothelin peptide (aa540–549)-specific CD8⁺ T cell immune responses. Furthermore, mice vaccinated with pcDNA3–Hmeso540- $\beta 2m$ -A2 were able to more effectively prevent the growth of HLA-A2 positive, human mesothelin-expressing tumor cell lines compared to vaccination with control DNA. The implications of this approach for clinical application were discussed.

2. Materials and methods

2.1. Plasmid DNA constructs and DNA preparation

To clone pcDNA3–Hmeso, human mesothelin was PCR amplified by primers (5′-aaagaattcccctccctgggatctacagacc-3′ and 5′-tttagatctggccagggtggaggctaggag-3′) and full-length human mesothelin clone (622 amino acids, GenBank accession NM.005823) from incite (Wilmington, Delaware) as a template. The PCR product of human mesothelin was cloned into the *EcoRI/BamHI* sites of pcDNA3.1 mychis (Invitrogen). To generate pMSCV(n)-Hmeso, human mesothelin was cut at *NotI/AflIII* from pcDNA3–Hmeso and cloned into the *NotI/EcoRI* sites of pMSCV(n).

To make the vaccinia construct PSC11-Hmeso, human mesothelin was cut from pcDNA3–Hmeso by *NotI/AflIII* and cloned into the *NotI/SamI* sites of PSCII. To construct pIRES–Hmeso540- $\beta 2m$ -K^b, an insert containing the immunodominant mesothelin aa540–549 epitope and flanking *AgeI/NheI* restriction enzyme sites was made by annealing two single-stranded oligo-nucleotides (5′-ccggtttgatgctaaactctgggacccacgtggaggcctggaggaggtg-3′ and 5′-ctagcacctctcccaggccctccacgtgggtgccagaaagtttagcatacaaaa-3′). It was then cloned into pIRES–OVA–K^b (pIRES–OVA- $\beta 2m$ -K^b gifted from T.H. Hansen (Department of Genetics, Washington University School of Medicine, St. Louis, MO)). To construct the single-chain trimer pcDNA3–Hmeso540- $\beta 2m$ -A2, HLA-A2 was RT-PCR amplified by primers (5′-GGTAGATCTggtggtggtgtagtgctctactccatgagga3-3′ and 5′-GGGAAGCTTtcacgctttacaatctcgag-3′) and RNA from HLA-A*0201/D^d transgenic mice as a template. A2 PCR product was cut at *BglIII/HindIII* and Hmeso540- $\beta 2m$ was cut at *NotI/BamHI* from pIRES–Hmeso540- $\beta 2m$ -K^b. Both fragments were cloned into the *NotI/HindIII* sites of pcDNA3.1 (–) (Invitrogen). To generate pcDNA3–OVA- $\beta 2m$ -A2, Hmeso540- $\beta 2m$ was isolated from pcDNA3–Hmeso540- $\beta 2m$ -A2 and replaced by OVA- $\beta 2m$ from pIRES–OVA- $\beta 2m$ -K^b.

2.2. Cells

The HPV-16 E6-expressing murine tumor model, TC-1, has been described previously [8]. Briefly, TC-1 cells were obtained by co-transformation of primary C57BL/6 mice lung epithelial cells by HPV-16 E6, E7 and an activated *ras* oncogene. TK-was purchased from ATCC.

To generate TC-1/A2/Hmeso cell line, TC-1/A2 cells [9] were transduced with a retrovirus containing HLA-A2 and human mesothelin. Briefly, pMSCV(n)-Hmeso was transfected into Phoenix packaging cell line and the virion-containing supernatant was collected 48 h after transfection. The supernatant was immediately clarified using a 0.45-mm cellulose acetate syringe filter (Nalgene, Rochester, NY) and used to infect TC-1/A2 cells in the presence of 8 µg/mL Polybrene (Sigma, St. Louis, MO). TC-1/A2/Hmeso cells were isolated by preparative flow cytometry of stained cells with human mesothelin antibody (Signet laboratories Dedham, MA).

2.3. Mice

HLA-A*0201/D^d (AAD) transgenic female C57BL/6 mice, 6–8 weeks of age, were kindly provided by Dr. Victor Engelhard at the University of Virginia Health Sciences Center [10]. These transgenic mice express a chimeric HLA-A2 class I molecule comprising the α-1 and -2 domains of HLA-A*0201, and the α-3 transmembrane and cytoplasmic domain of H-2D^d. This allows the murine CD8 molecule on the murine CD8⁺ T cells to interact with the syngeneic α-3 domain of the chimeric MHC class I molecule. Wild-type C57BL/6 female mice (6–8 weeks old) were also purchased from the National Cancer Institute. All animals were maintained under specific pathogen-free conditions, and all procedures were performed according to approved protocols and in accordance with recommendations for the proper use and care of laboratory animals.

2.4. Generation of recombinant vaccinia

The recombinant vaccinia virus was generated by following the protocol of Earl and Moss [11]. Briefly, PSC11-Hmeso was transfected into the wild-type vaccinia-infected CV-1 using Lipofectamine 2000 in order to facilitate heterologous recombination. The recombinant vaccinia viruses were isolated as described previously [12]. Plaque-purified recombinant vaccinia viruses were checked for the expression of mesothelin protein by Western blot analysis.

2.5. In vitro characterization of mesothelin expression

TK-cells were transfected with pcDNA3–Hmeso or pcDNA3 vector by Lipofectamine 2000 (Invitrogen) for 24 h. TK-cells were infected with Vac-Hmeso or wild-type vaccinia with Vac-luciferase at titres of 1 MOI (Mutiplicity of

Infection) for 24 h. Transfected or infected TK-cells were stained with mouse anti-human mesothelin antibody (CAK1, Signet Laboratories Inc., Dedham, MA) and anti-mouse IgG-FITC (Jackson ImmunoResearch).

2.6. Vaccination and tumor challenge

DNA-coated gold particles were prepared according to a previously described protocol [13]. DNA-coated gold particles were delivered to the shaved abdominal region of mice using a helium-driven gene gun (BioRad, Hercules, CA) with a discharge pressure of 400 p.s.i. For the identification of human mesothelin-specific CTL epitope, HLA-A2 mice were vaccinated three times with 2 µg of pcDNA3–Hmeso DNA vaccines and boosted with 1×10^7 PFU vaccinia encoding human mesothelin. For the characterization of anti-tumor effects and immune responses generated by DNA vaccine encoding an SCT technology, HLA-A2 transgenic mice were immunized with 2 µg of pcDNA3–Hmeso540–β2m–A2 or pcDNA-OVA–β2m–A2. For *in vivo* tumor protection experiments, the mice received three boost vaccinations with the same dose at 1-week intervals. Then these mice were subcutaneously challenged with 5×10^4 TC-1/A2/Hmeso tumor cells in the right leg and then monitored once a week.

2.7. Intracellular cytokine staining and flow cytometry analysis

Splenocytes were harvested from mice 1 week after the last vaccination. Cell surface CD8 marker staining, intracellular IFN-γ staining and flow cytometry analysis were performed as described previously [13]. Briefly, 4×10^6 pooled splenocytes from each vaccination group were incubated with 1 µg/ml of specific peptide in the presence of 1 µl/ml of GolgiPlug (BD Pharmingen) at 37 °C overnight. Cells are then washed with FACScan buffer and stained with phycoerythrin-conjugated monoclonal rat anti-mouse CD8 antibody, followed by intracellular cytokine staining with FITC-conjugated IFN-γ using the Cytofix/Cytoperm kit according to the manufacturer's instruction (BD Pharmingen, San Diego, CA). Analysis was performed on a Becton-Dickinson FACScan with CELLQuest software (Becton Dickinson Immunocytometry System, Mountain View, CA).

2.8. Statistical analysis

All data expressed as means ± S.E.M. are representative of at least two different experiments. Data for intracellular cytokine staining with flow cytometry analysis were evaluated by ANOVA. Comparisons between individual data points were made using a Student's *t*-test. For statistical analysis of the tumor protection experiment, we used Kaplan–Meier analysis.

3. Results

3.1. Cells transfected with DNA encoding human mesothelin (pcDNA3–Hmeso) or infected with vaccinia encoding human mesothelin (Vac–Hmeso) express human mesothelin

To characterize human mesothelin expression of cells transfected with DNA or infected with vaccinia, TK-cells were either transfected with pcDNA3–Hmeso or infected with Vac–Hmeso vaccinia. Transfected or infected cells were characterized by staining with human mesothelin-specific antibodies followed by flow cytometry analysis. As shown in Fig. 1A, TK-cells transfected with pcDNA3–Hmeso expressed human mesothelin (filled histogram). In contrast, TK-cells transfected with pcDNA3 vector did not express human mesothelin (clear histogram). Similarly, as seen in Fig. 1B, TK-cells infected with Vac–Hmeso expressed human mesothelin (filled histogram), while TK-cells infected with wild-type vaccinia did not express human mesothelin (clear histogram). These results confirm that we have successfully generated human mesothelin-expressing DNA construct and vaccinia virus.

3.2. Identification of human mesothelin epitopes aa116–125 and aa540–549 as HLA-A2-restricted human mesothelin-specific CTL epitopes

The availability of human mesothelin-expressing DNA construct and vaccinia virus allows us to design prime and boost vaccination regimens in order to generate high numbers of human mesothelin-specific CD8⁺ T cells in vaccinated mice. Using splenocytes derived from HLA-A2 transgenic mice vaccinated with pcDNA3–Hmeso and boosted with Vac–Hmeso, we were able to develop quantitative human mesothelin-specific CD8⁺ T cell immunological assays. In order to identify candidate HLA-A2-restricted human mesothelin-specific CTL epitopes, we used the BioInformat-

Table 1

Candidate HLA-A2-restricted human mesothelin-specific CTL epitopes predicted by BIMAS

Peptide name start position	MHC class I	Peptide sequence	BIMAS score
Peptide-20	HLA2	SLLFLLFSL	1054
Peptide-17	HLA2	ALGSLLFLL	284
Peptide-64	HLA2	QLLGfPCA EV	257
Peptide-116	HLA2	ALPLdLLLFL	270
Peptide-530	HLA2	VLPLTVAEV	271
Peptide-540	HLA2	KLLGpHVEGL	311
Peptide-602	HLA2	LLGpPVLTV	271

Bioinformatics & Molecular Analysis Section (BIMAS) was used to analyze various nine-residue peptides from mesothelin for H-2 binding predictions. The sequences, positions, MHC restrictions, and scores of the potential human mesothelin epitopes were determined.

ics & Molecular Analysis Section (BIMAS) database for HLA-A2 peptide binding predictions. We identified several candidate 9- or 10-residue peptides for human mesothelin. Their positions, MHC restrictions, sequences and scores are presented in Table 1. To determine which candidate peptides represent the true HLA-A2-restricted human mesothelin-specific CTL epitopes, we used the candidate peptides identified by BIMAS to stimulate splenocytes from vaccinated HLA-A2 transgenic mice. As shown in Fig. 2, splenocytes from vaccinated mice pulsed with human mesothelin peptides aa116–125 or aa540–549 generated significantly greater numbers of human mesothelin-specific, IFN- γ -expressing CTLs than splenocytes pulsed with the other human mesothelin peptides ($p < 0.001$). These data indicate that the human mesothelin peptides aa116–125 and aa540–549 can be recognized by CD8⁺ T cells generated by HLA-A2 transgenic mice primed with pcDNA3–Hmeso and boosted with Vac–Hmeso. Furthermore, there are no CD8-specific T cell responses to these epitopes when using the same vaccines to vaccinate C57BL/6 mice (data not shown). Thus, these data confirm that aa116–125 and aa540–549 human mesothelin epitopes are HLA-A2-restricted human mesothelin-specific CTL epitopes

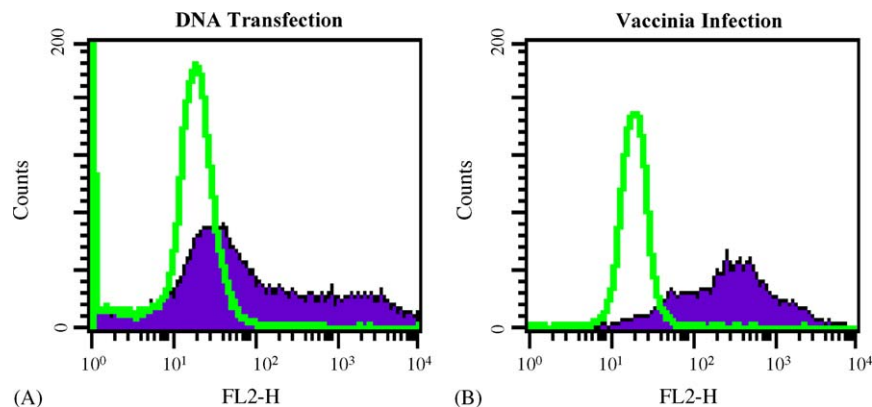


Fig. 1. Flow cytometry analysis to characterize human mesothelin expression of cells transfected with DNA or infected with vaccinia. (A) TK-cells transfected with pcDNA3–Hmeso (filled histogram) or pcDNA3 vector (clear histogram). (B) TK-cells infected with Vac–Hmeso (filled histogram) or wild-type vaccinia (clear histogram). Transfected or infected TK-cells were stained with human mesothelin-specific antibodies and characterized by flow cytometry analysis as described in Section 2.

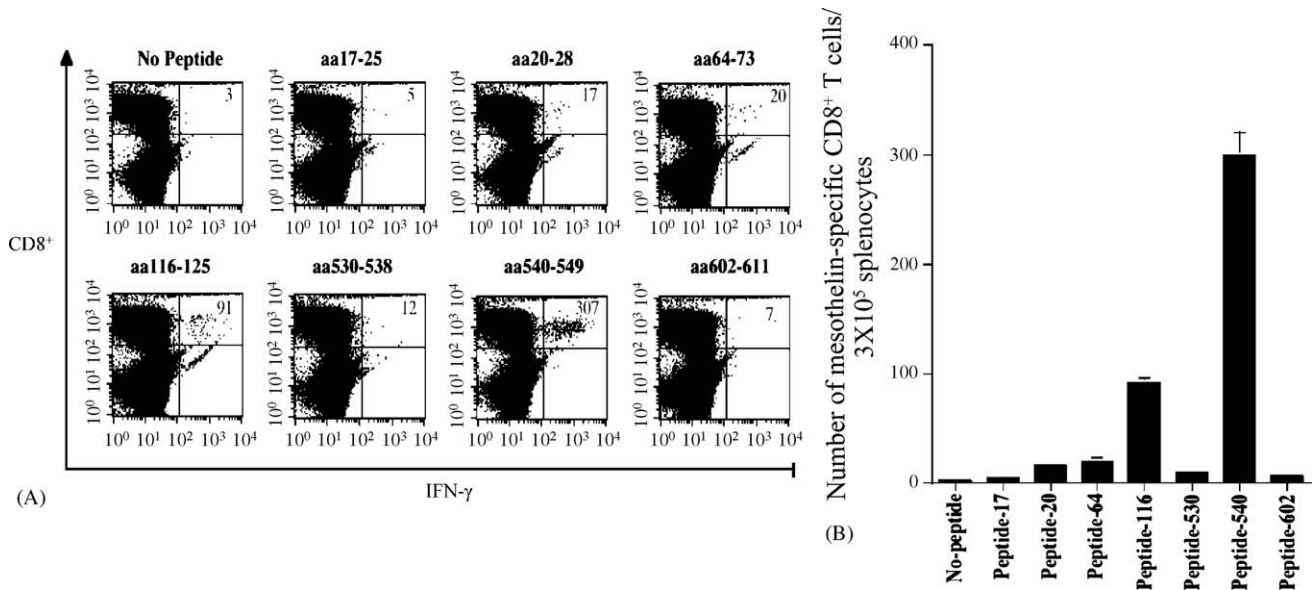


Fig. 2. Intracellular cytokine staining followed by flow cytometry analysis to characterize HLA-A2-restricted human mesothelin-specific CTL epitopes. HLA-A2 transgenic mice were vaccinated with 2 μg/mouse of pcDNA3-Hmeso followed by an intraperitoneal booster with Vac-Hmeso (1 × 10⁷ PFU/mouse). Splenocytes were harvested 1 week after the last vaccination and stimulated with various candidate human mesothelin epitopes (see Table 1) for 16 h. The activation of human mesothelin-specific CD8⁺ T cells was determined by intracellular cytokine staining for CD8 and IFN-γ expression. (A) Representative figure of flow cytometry data. (B) Bar graph depicting number of IFN-γ-expressing human mesothelin-specific CD8⁺ T cells out of 3 × 10⁵ splenocytes isolated from vaccinated mice.

but not H-2 D^b, K^b-restricted CTL epitopes. Furthermore, between these two identified peptides, aa540–549 generated greater numbers of IFN-γ-expressing CTLs than aa116–125.

3.3. Vaccination with pcDNA3-Hmeso540-β2m-A2 enhances human mesothelin-specific CD8⁺ T cell responses in vaccinated HLA-A2 transgenic mice

The identification of aa540–549 as a strong HLA-A2-restricted human mesothelin-specific CTL epitope allowed us to generate a DNA vaccine encoding an SCT of HLA-

A2 linked to this epitope (pcDNA3-Hmeso540-β2m-A2) (Fig. 3). We also generated a DNA vaccine encoding an SCT of HLA-A2 linked to OVA (pcDNA3-OVA-β2m-A2) as a negative control. To assess the immunogenicity of our DNA vaccine, we vaccinated mice with pcDNA3-Hmeso540-β2m-A2 or pcDNA3-OVA-β2m-A2 and then performed intracellular cytokine staining with flow cytometry analysis to characterize human mesothelin-specific CD8⁺ T cell precursors using human mesothelin aa540–549 peptide as a stimulant. HLA-A2 transgenic mice vaccinated with pcDNA3-Hmeso540-β2m-A2 generated a

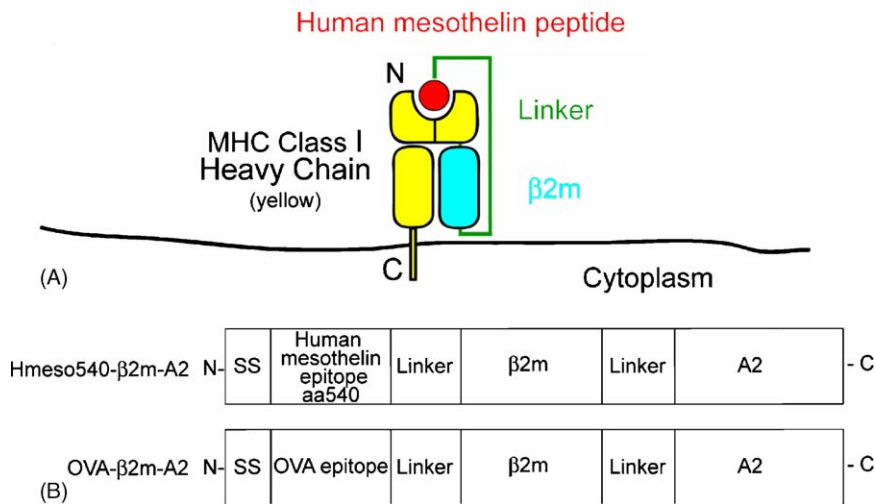


Fig. 3. Diagrams depicting the structure of our SCT and structures of chimeric DNA constructs. (A) Diagram of a peptide:β2m:MHC SCT on cell surface. (B) Diagram of an SCT encoding human mesothelin aa540–549 linked to β2m and an HLA-A2-restricted MHC class I molecule, and a SCT encoding OVA linked to β2m and an HLA-A2-restricted MHC class I molecule. Each was cloned into the pcDNA3 vector to make the DNA vaccines used in the study.

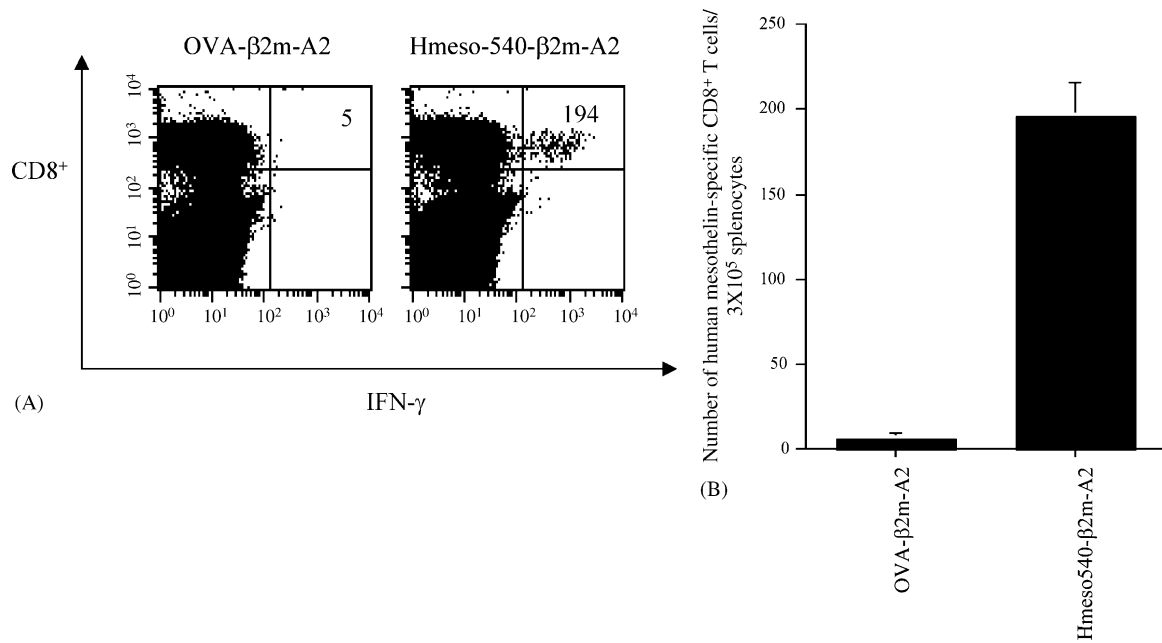


Fig. 4. Characterization of human mesothelin-specific CD8⁺ T cells in vaccinated HLA-A2 transgenic mice. Mice (five per group) were immunized with pcDNA3–OVA-β2m–A2 or pcDNA3–Hmeso540–β2m–A2. Splenocytes from vaccinated mice were collected and stimulated with human mesothelin-specific peptides (aa540–549). Intracellular cytokine staining followed by flow cytometry analysis was performed. (A) Representative figure of the flow cytometry data. (B) Bar graph depicting the number of human mesothelin peptide (aa540–549)-specific IFN-γ-secreting CD8⁺ T cell precursors/3 × 10⁵ splenocytes (mean ± S.D.). The data presented in this figure are representative from one of two experiments performed.

significantly higher frequency of human mesothelin-specific IFN-γ-secreting CD8⁺ T cell precursors compared to mice immunized with pcDNA3–OVA-β2m–A2 (Fig. 4). These data indicate that vaccination with DNA encoding an SCT of HLA-A2 linked to a human mesothelin-specific CTL epitope is capable of generating strong human mesothelin-specific CD8⁺ T cell immune responses in HLA-A2 transgenic mice.

3.4. A syngeneic tumor cell line expresses human mesothelin and HLA-A2

In order to generate a tumor cell line expressing human mesothelin and HLA-A2 for use in tumor prevention experiments in HLA-A2 transgenic mice, we have transduced TC-

1/A2 cell lines with a retrovirus containing human mesothelin to generate TC-1/A2/Hmeso. We have previously generated an HLA-A2-expressing murine tumor model, TC-1/A2, that is capable of growing consistently in HLA-A2 transgenic mice through subcutaneous injection [9]. We have further characterized the expression of HLA-A2 and human mesothelin in TC-1/A2/Hmeso cells using flow cytometry analysis. TC-1 cells were used as negative controls. As shown in Fig. 5, TC-1/A2/Hmeso cells (filled histogram) showed significantly higher expression of both HLA-A2 and human mesothelin compared to TC-1 cell lines (clear histogram). These data indicate that the TC-1/A2/Hmeso tumor cell line is successfully engineered to express significant levels of both HLA-A2 and human mesothelin proteins.

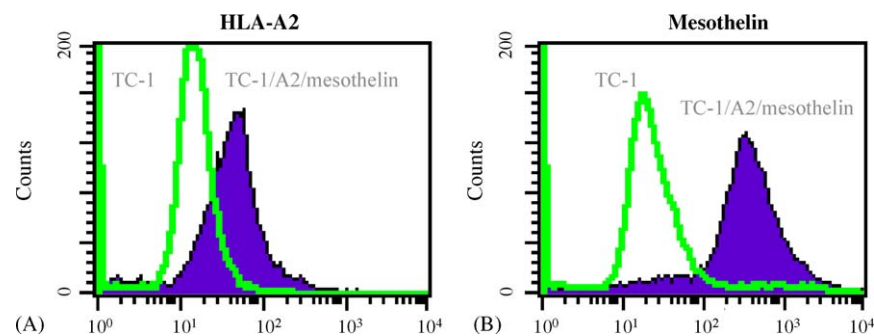


Fig. 5. Flow cytometry analysis to demonstrate the expression of HLA-A2 and human mesothelin in TC-1/A2/Hmeso cell line. TC-1/A2/Hmeso was generated by transducing TC-1/A2 with a retrovirus containing human mesothelin as described in Section 2. (A) Characterization of HLA-A2 expression in TC-1/A2/Hmeso (filled histogram) and TC-1 (clear histogram). The cell lines were stained with HLA-A2-specific monoclonal antibody followed by flow cytometry analysis. (B) Characterization of human mesothelin expression in TC-1 TC-1/A2/Hmeso (filled histogram) and TC-1 (clear histogram). The cell lines were stained with human mesothelin-specific antibody followed by flow cytometry analysis.

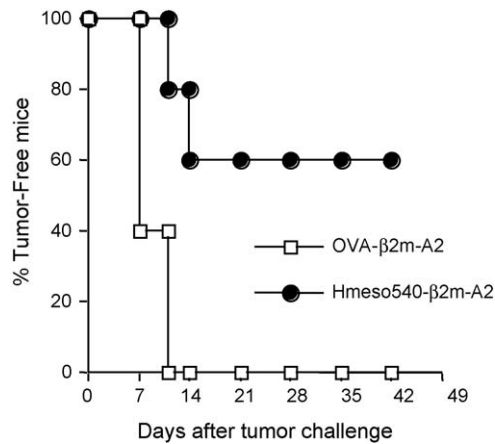


Fig. 6. *In vivo* tumor protection experiment to demonstrate the anti-tumor effects generated by pcDNA3–Hmeso540–β2m–A2 against human mesothelin-expressing TC-1/A2/Hmeso tumors in HLA-A2 transgenic mice. Mice (five per group) were immunized with OVA–β2m–A2 or Hmeso540–β2m–A2 four times at 1-week interval. At 1 week after the last vaccination, mice were challenged subcutaneously with 5×10^4 TC-1/A2/Hmeso cells/mouse and monitored for evidence of tumor growth by palpation and inspection once a week.

3.5. pcDNA3–Hmeso540–β2m–A2 vaccination prevents the growth of human mesothelin-expressing TC-1/A2/Hmeso tumors in mice

Given the immunogenicity of pcDNA3–Hmeso540–β2m–A2 (see Fig. 4), we next explored whether it could elicit effective protective anti-tumor effects against the HLA-A2 positive, human mesothelin-expressing tumor cell line, TC-1/A2/Hmeso. Tumor cells were injected subcutaneously 1 week after DNA vaccination. During a 6-week follow-up period, 60% of mice receiving pcDNA3–Hmeso540–β2m–A2 remained tumor-free. All of the pcDNA3–OVA–β2m–A2-immunized mice exhibited tumor growth by the second week (Fig. 6). These results are statistically significant ($p < 0.01$), indicating that vaccination with pcDNA3–Hmeso540–β2m–A2 can generate significant protective effects against human mesothelin-expressing tumors. Thus, our data indicate that a DNA vaccine encoding an SCT of a human MHC class I molecule linked to a CTL epitope from human mesothelin antigen is capable of generating a strong antigen-specific CD8⁺ T cell immune response and anti-tumor effects in vaccinated HLA-A2 transgenic mice.

4. Discussion

In the current study, we have identified an HLA-A2-restricted human mesothelin-specific CD8⁺ T cell epitope using HLA-A2 transgenic mice. We found that HLA-A2 transgenic mice vaccinated with a DNA vaccine encoding an SCT linked to human mesothelin CTL epitope was able to generate potent human mesothelin peptide-specific CD8⁺ T cell immune responses as well as anti-tumor effects against

human mesothelin-expressing tumors in HLA-A2 transgenic mice. Our results are consistent with our previous study using a DNA vaccine employing SCT technology targeting the HPV-16 E6 immunodominant CTL epitope [7]. Thus, DNA vaccines employing the SCT technology have been shown to enhance antigenic peptide-specific CD8⁺ T cell immune responses in different antigenic systems. It is therefore likely that DNA vaccines employing the SCT technology may also be applicable to other antigenic systems related to viral infections or other cancers.

Intradermal administration of DNA vaccines encoding a single-chain trimer has several advantages over peptide vaccines administered exogenously. First, intradermal administration of DNA vaccines allows for direct targeting of DNA to dendritic cells *in vivo*. In comparison, exogenously administered peptides may not be directly targeted to dendritic cells. Second, DNA vaccines encoding a single-chain trimer can lead to a more stable presentation of encoded antigenic peptides compared to conventional peptide vaccines. Third, peptides administered exogenously are more susceptible to degradation compared to peptides presented through the single-chain trimer encoded by the DNA vaccine. All these features lead to a more persistent activation of antigen-specific CD8⁺ T cells by DNA vaccines encoding the SCT technology compared to peptide vaccines.

The SCT technology is particularly useful for generating HLA-A2-restricted antigen-specific CD8⁺ T cell immune responses in HLA-A2 (AAD) transgenic mice. Because HLA-A2 (AAD) transgenic mice express both murine MHC class I molecules and HLA-A2, it is possible that vaccination with DNA vaccines encoding a full-length antigen may also present the antigens through the murine MHC class I molecule in vaccinated mice. This may render it difficult to determine if the antigen-specific CD8⁺ T cell immune responses are truly HLA-A2-restricted. For instance, we have previously demonstrated that DNA encoding calreticulin (CRT) linked to full-length HPV-16 E7 antigen generated strong H-2D^b-restricted E7(aa49–57)-specific CD8⁺ T cell immune responses but not HLA-A2-restricted E7(aa11–20)-specific CD8⁺ T cell immune responses in HLA-A2 (AAD) transgenic mice [9]. By bypassing the typical class I antigen processing pathway, vaccination with a DNA vaccine encoding an SCT of HLA-A2 linked to a CTL epitope ensures cell surface presentation of the HLA-A2 MHC I molecule:antigenic peptide complex by a transfected APC, allowing for the generation of only HLA-A2-restricted, peptide-specific CD8⁺ T cell immune responses in HLA-A2 (AAD) transgenic mice.

In the current study, we used BIMAS to identify several candidate HLA-A2-restricted human mesothelin-specific CTL epitopes that may be used for our SCT technology. However, predictive algorithms used to predict for potential CTL epitopes may not always be 100% accurate, and the highest scoring peptides may not actually trigger the optimal CTL responses. Hence, in order to identify the true HLA-A2-restricted human mesothelin-specific epitopes, we tested

several of the candidate human mesothelin epitopes for their ability to generate CD8⁺ T cell immune responses. We have identified two HLA-A2-restricted human mesothelin-specific CD8⁺ T cell epitopes using HLA-A2 transgenic mice. One of these CTL epitopes, aa540–549, was also recently identified using PBMCs derived from ovarian or pancreatic cancer patients [14]. In that study, it was shown that the HLA-A2-restricted P547–556 peptide (KLLGPHVEGL, equivalent to the amino acid sequence of aa540–549 in our study) was able to activate mesothelin-specific CD8⁺ T cells and lyse mesothelin-expressing pancreatic and ovarian cells [14].

In another study, HLA-A2-restricted mesothelin-derived peptides 20–28 and 530–538 were identified as CTL epitopes [15]. These CTL epitopes are quite different from what we described in our current study. This discrepancy may be due to the different vaccination as well as experimental approaches used for these studies. Thomas et al. used PBMCs from patients vaccinated with GMCSF-transduced, mesothelin-expressing allogeneic pancreatic cancer cells as a source of T cells [15]. In comparison, we used T cells derived from HLA-A2 transgenic mice vaccinated with human mesothelin-expressing DNA followed by vaccinia. Thus, in our model, it is likely that we are able to identify human mesothelin-specific CTL epitopes with potentially high avidity since tolerance is not a concern in our mouse model. In comparison, human mesothelin-specific T cells derived from patients vaccinated with GMCSF-transduced allogeneic pancreatic cancer cells may belong to the category of low avidity T cells because of tolerance to human mesothelin in patients.

The identification of human mesothelin CTL epitopes will facilitate the development of quantitative CD8⁺ T cell immunological assays, including peptide-loaded HLA-A2-restricted tetramer assays. These assays will be important for the characterization of mesothelin-specific CD8⁺ T cell immune responses in patients with mesothelin-expressing ovarian or pancreatic cancer. Furthermore, these assays will be particularly useful for characterizing human mesothelin-specific immune responses before and after vaccination with mesothelin-specific cancer vaccines.

Although the SCT technology can be used to elicit robust peptide-specific CD8⁺ T cell immune responses, it is not effective in activating CD4⁺ T helper cells. Because it is now clear that CD4⁺ T helper cells are important for generating memory T cells, it will be desirable to design an immunization regimen that utilizes DNA vaccines employing the SCT technology in conjunction with DNA vaccines capable of activating CD4⁺ T helper cells. A previous study has developed a DNA vaccine carrying an invariant chain (Ii) gene in which the class II-associated invariant chain peptide (CLIP) region was replaced by a T helper epitope. Immunization of mice with this DNA plasmid induced antigen-specific IFN- γ and interleukin 2-producing helper T cells [16]. Thus, co-administration of a DNA vaccine encoding a CD4⁺ helper T cell epitope and a DNA vaccine encoding the SCT technology may provide an opportunity to generate both CD8⁺ T cell and CD4⁺ helper T cell immune responses, enhancing

the long-term protective immunity by developing a reservoir of antigen-specific memory T cells.

Another possible concern for the employment of a DNA vaccine encoding an SCT is that tumor cells may evade antigen-specific CD8⁺ T cell immune attack by the mutation of the mesothelin gene at the CTL epitope, so called “antigenic drift” [17]. If such a mutation occurs on the mesothelin CTL epitope in mesothelin-expressing tumors, the DNA vaccines employing the SCT technology may be unable to elicit an effective immune response. One possible approach to avoid such a pitfall is to consider DNA vaccines employing an SCT targeting a combination of different mesothelin CTL epitopes to more effectively control tumors. For instance, in the current study, we have identified two mesothelin CTL epitopes, aa116–125 and aa540–549 (Fig. 1). A combination DNA vaccine targeting both of these epitopes may circumvent the potential problem of “antigenic drift” of CTL epitopes. With continued identification of other human mesothelin CTL epitopes, we may be able to develop a better regimen of mesothelin-specific DNA vaccines to avoid the undesirable effects of mutations on the CTL epitope of the tumor antigens. In addition, such an approach can be used to enhance anti-tumor effects by creating DNA vaccines targeting ovarian cancer tumor-associated antigens other than human mesothelin and administering these vaccines in conjunction with our mesothelin-specific SCT vaccine.

In summary, we have identified HLA-A2-restricted human mesothelin-specific CD8⁺ T cell epitopes. In addition, we have developed a DNA vaccine employing SCT technology targeting an identified CTL epitope. Our data suggest that DNA vaccines employing the SCT can generate potent human mesothelin-specific immune responses as well as anti-tumor effects against human mesothelin-expressing tumors in HLA-A2 transgenic mice. Our study in the preclinical transgenic mouse model will likely serve as a solid foundation for future clinical translation of DNA vaccines for immunotherapy of gynecologic cancers.

Acknowledgments

We thank Richard Roden for helpful discussions. We would also like to thank Ralph Hruban and David Boyd for critical review of this paper. This work was supported by ovarian cancer grants from Department of Defense and the Alliance for Cancer Gene Therapy (ACGT).

References

- [1] Systemic treatment of early breast cancer by hormonal, cytotoxic, or immune therapy. 133 randomised trials involving 31,000 recurrences and 24,000 deaths among 75,000 women. Early Breast Cancer Trialists' Collaborative Group [see comments]. *Lancet* 1992;339(8784): 1–15.
- [2] Baum M, Ebb S, Brooks M. Biological fall out from trials of adjuvant tamoxifen in early ovarian cancer. In: Salmon SE, editor. Adju-

- vant therapy of cancer, vol V1. Philadelphia: WB Saunders; 1990. p. 269–74.
- [3] Swain SM. Selection of therapy for stage III breast cancer. *Surg Clin N Am* 1990;70(5):1061–80.
- [4] Scholler N, Fu N, Yang Y, Ye Z, Goodman GE, Hellstrom KE, et al. Soluble member(s) of the mesothelin/megakaryocyte potentiating factor family are detectable in sera from patients with ovarian carcinoma. *Proc Natl Acad Sci USA* 1999;96(20):11531–6.
- [5] Hung CF, Wu TC. Improving DNA vaccine potency via modification of professional antigen presenting cells. *Curr Opin Mol Ther* 2003;5(1):20–4.
- [6] Boyd D, Hung CF, Wu TC. DNA vaccines for cancer. *IDrugs* 2003;6(12):1155–64.
- [7] Huang CH, Peng S, He L, Tsai YC, Boyd DA, Hansen TH, et al. Cancer immunotherapy using a DNA vaccine encoding a single-chain trimer of MHC class I linked to an HPV-16 E6 immunodominant CTL epitope. *Gene Ther* 2005;12(15):1180–6.
- [8] Lin K-Y, Guarnieri FG, Staveley-O'Carroll KF, Levitsky HI, August T, Pardoll DM, et al. Treatment of established tumors with a novel vaccine that enhances major histocompatibility class II presentation of tumor antigen. *Cancer Res* 1996;56:21–6.
- [9] Peng S, Trimble C, He L, Tsai YC, Lin CT, Boyd DA, et al. Characterization of HLA-A2-restricted HPV-16 E7-specific CD8(+) T-cell immune responses induced by DNA vaccines in HLA-A2 transgenic mice. *Gene Ther* 2006;13(1):67–77.
- [10] Newberg MH, Smith DH, Haertel SB, Vining DR, Lacy E, Engelhard VH. Importance of MHC class I alpha2 and alpha3 domains in the recognition of self and non-self MHC molecules. *J Immunol* 1996;156(7):2473–80.
- [11] Earl PL, Moss B. Mutational analysis of the assembly domain of the HIV-1 envelope glycoprotein. *AIDS Res Hum Retroviruses* 1993;9(7):589–94.
- [12] Wu T-C, Guarnieri FG, Staveley-O'Carroll KF, Viscidi RP, Levitsky HI, Hedrick L, et al. Engineering an intracellular pathway for MHC class II presentation of HPV-16 E7. *Proc Natl Acad Sci* 1995;92:11671–5.
- [13] Chen CH, Wang TL, Hung CF, Yang Y, Young RA, Pardoll DM, et al. Enhancement of DNA vaccine potency by linkage of antigen gene to an HSP70 gene. *Cancer Res* 2000;60(4):1035–42.
- [14] Yokokawa J, Palena C, Arlen P, Hassan R, Ho M, Pastan I, et al. Identification of novel human CTL epitopes and their agonist epitopes of mesothelin. *Clin Cancer Res* 2005;11(17):6342–51.
- [15] Thomas AM, Santarsiero LM, Lutz ER, Armstrong TD, Chen YC, Huang LQ, et al. Mesothelin-specific CD8(+) T cell responses provide evidence of in vivo cross-priming by antigen-presenting cells in vaccinated pancreatic cancer patients. *J Exp Med* 2004;200(3):297–306.
- [16] Nagata T, Aoshi T, Suzuki M, Uchijima M, Kim Y-H, Yang Z, et al. Induction of protective immunity to *Listeria monocytogenes* by immunization with plasmid DNA expressing a helper T-cell epitope that replaces the class II-associated invariant chain peptide of the invariant chain. *Infect Immun* 2002;70(5):2676–80.
- [17] Bai XF, Liu J, Li O, Zheng P, Liu Y. Antigenic drift as a mechanism for tumor evasion of destruction by cytolytic T lymphocytes. *J Clin Invest* 2003;111(10):1487–96.

**Control of mesothelin-expressing ovarian cancer using adoptive
transfer of mesothelin peptide-specific CD8⁺ T cells**

Chien-Fu Hung¹, Ya-Chea Tsai¹, Liangmei He¹, and T.-C. Wu^{1,2,3,4}

Departments of Pathology¹, Obstetrics and Gynecology², Molecular Microbiology and
Immunology³, Oncology⁴, Johns Hopkins Medical Institutions, Baltimore, Maryland,
USA

Running title: Mesothelin-specific ovarian cancer immunotherapy

Final word count: 7,448

Address correspondence to Dr. C-F Hung, Department of Pathology, The Johns Hopkins
University School of Medicine, CRB II Room 307, 1550 Orleans Street, Baltimore,
Maryland 21231, USA. Phone: (410) 614-3899; Fax: (443) 287-4295; E-Mail:
chung2@jhmi.edu

Abstract

Cancer immunotherapy targeting mesothelin represents a potentially plausible approach for the control of ovarian cancer since most ovarian cancers express high levels of mesothelin. In the current study, we created a mesothelin-positive luciferase-expressing ovarian cancer model, MOSEC/luc. This luciferase-expressing tumor model allowed us to quantitate tumor distribution and tumor load in tumor-challenged mice using a non-invasive bioluminescence imaging system. In addition, we identified an H-2D^b-restricted mesothelin peptide-specific CTL epitope (aa406-414) that was endogenously processed and presented by MOSEC/luc tumor cells. We showed that adoptive transfer of mesothelin peptide (aa406-414)-specific CD8⁺ T cells led to the control of MOSEC/luc tumor cells. The MOSEC/luc tumor model and the newly identified H-2D^b-restricted murine mesothelin-specific CTL epitope (aa406-414) will be very useful for the development of immunotherapy for ovarian cancer as well as for the development of quantitative CD8⁺ T cell-mediated immunological assays.

Keywords: immunotherapy; mesothelin; ovarian cancer, adoptive T cells

Introduction

Metastatic ovarian cancer is extremely difficult to cure and is responsible for the highest mortality rate among patients with gynecologic malignancies. Current efforts to reduce this mortality rate, including improvement of early detection and treatment, have been relatively unsuccessful. **Existing standard therapies for advanced disease such as primary cytoreductive surgery followed by chemotherapy rarely result in long-term benefits for patients with locally advanced and metastatic disease.**¹⁻³ Thus, identification of alternative approach to control ovarian cancer represents an urgent concern.

Immunotherapy represents a potentially plausible approach for the control of ovarian cancer. The ideal cancer therapy should have the potency to eradicate systemic tumors and control metastases as well as the specificity to discriminate between malignant and normal cells. In both of these respects, the immune system is an attractive therapeutic approach. The immune system has multiple complementary effector mechanisms capable of killing target cells. Of these effector mechanisms, T cells can generate tumor antigen-specific immune responses because they have a vast array of clonally distributed antigen receptors, which can recognize tumor-specific antigens. It is well established that T cells recognize peptide fragments of cellular proteins bound to major histocompatibility complex (MHC) molecules on the surfaces of cells, and any cellular protein (including those from which tumor antigens are derived) can be presented to T cells in this way. **Antigen-specific immunotherapy has been implemented in ovarian cancer treatment in human clinical trials such as HER-2/neu, MUC-1, NY-**

ESO-1 and CA-125.⁴ Thus, cancer immunotherapy aimed at enhancing the function of antigen-specific T cells represents a rational treatment approach.

The identification of tumor-associated antigens uniquely expressed in ovarian cancer is also an important step for the development of effective immunotherapeutic strategies to control ovarian cancer. Mesothelin has been identified as an antigen that is highly expressed in a majority of ovarian cancers,⁵ but has low expression in **mesothelial cells lining the pleura, pericardium, and peritoneum,⁶** making it a potentially valuable target for the development of ovarian cancer vaccines and immunotherapeutic strategies. **The mesothelin gene encodes a 69-kDa precursor protein that is processed to a 40-kDa membrane-bound protein called mesothelin and a 31-kDa shed fragment termed megakaryocyte-potentiating factor (MPF) that is secreted from the cell.⁶**

The development of ovarian cancer vaccines and immunotherapeutic strategies requires a suitable **preclinical model**. The ovarian cancer tumor model, MOSEC, which is derived from mouse ovarian surface epithelial cells, has previously been shown to be capable of generating ascites and tumor growth in C57BL/6 mice receiving intraperitoneal tumor challenge.⁷ Furthermore, the morphology of MOSEC tumor cells resembles ovarian serous carcinoma. Thus, the MOSEC ovarian cancer model serves as a **potentially suitable preclinical model for testing ovarian cancer vaccines.**

In the current study, we have created a luciferase-expressing MOSEC (MOSEC/luc) tumor model that has allowed us to quantitate the distribution and tumor load in tumor-challenged mice using the non-invasive bioluminescence imaging system. In addition, we characterized the expression of murine mesothelin in the MOSEC/luc

tumor model. We also determined that MOSEC/luc is endogenously processed and presented the murine mesothelin CTL epitope (aa406-414). Furthermore, we showed that adoptive transfer of mesothelin peptide (aa406-414)-specific CD8⁺ T cells led to the control of MOSEC/luc tumor cells. The generation of MOSEC/luc and the identification of murine mesothelin peptide aa406-414 as a H-2D^b-restricted CTL epitope serve as a good foundation for the development of antigen-specific immunotherapies for ovarian cancer as well as quantitative mesothelin-specific CD8⁺ T cell immunological assays.

Results

Generation and characterization of an ascitogenic luciferase-expressing ovarian cancer cell line, MOSEC/luc

One of the major challenges for the development of preclinical ovarian cancer models is the quantitative measurement of tumor growth in the peritoneal cavity. In order to create a suitable preclinical ovarian cancer model that is capable of forming ascites and expressing luciferase, we transduced an ovarian cancer cell line, MOSEC, with a retrovirus expressing firefly luciferase (MOSEC/luc). This would enable us to quantitate the tumor load using luciferase imaging. To determine if mice challenged with MOSEC/luc would generate ascites and sufficient luciferase activity for bioluminescence imaging, we challenged C57BL/6 mice, intraperitoneally, with MOSEC/luc tumor cells (5×10^6 cells/mouse). The luciferase expression was characterized using the non-invasive bioluminescence imaging system. As demonstrated in **Figure 1A**, mice intraperitoneally challenged with MOSEC/luc tumor cells were capable of developing significant ascites 8 weeks after the tumor challenge. In addition, the mice showed detectable luciferase

expression in the peritoneal cavity 8 weeks after the tumor challenge (**Figure 1C**). In contrast, C57BL/6 mice without MOSEC/luc tumor challenge did not show increased abdominal girth (**Figure 1B**) or luciferase expression (**Figure 1D**) in the peritoneal cavity. Thus, our data indicated that we successfully generated an ascitogenic luciferase-expressing MOSEC tumor cell line (MOSEC/luc) that would allow us to quantitate tumor load and distribution of MOSEC tumor cells in tumor-challenged mice using non-invasive bioluminescence imaging.

Murine mesothelin is highly expressed in MOSEC/luc tumor cells

Mesothelin has become a potentially ideal target for developing cancer vaccines against ovarian cancer(s) because it is highly expressed in ovarian cancer cells and is absent or expressed at low levels in normal cells. In order to determine whether MOSEC/luc tumor cells also express murine mesothelin, we characterized mesothelin expression in MOSEC/luc tumor cell line by RT-PCR and flow cytometry analysis. As shown in **Figure 2A**, mRNA expression of murine mesothelin was detected in MOSEC/luc tumors but not in dendritic cells (DCs).⁸ **In addition, we performed quantitative real-time RT-PCR. As shown in Table 1, gene expression of mesothelin is undetectable in DCs. In contrast, a significant high level of murine mesothelin expression was detected in MOSEC/luc. The mRNA expression ratio of mesothelin:beta-actin was 0.01342.** We also performed flow cytometry analysis using rat sera acquired from rats vaccinated with effective DNA vaccine encoding murine mesothelin. **Since there are no commercial mouse mesothelin antibodies available, we have created mesothelin-specific antibody using sera from rat vaccinated with**

DNA encoding murine mesothelin as described in the Materials and Methods. As demonstrated in **Figure 2B**, mesothelin expression was detected in MOSEC/luc cells but not in DCs. These data indicated that murine mesothelin is highly expressed in MOSEC/luc tumor cells.

The murine mesothelin peptide aa406-414 contains a CD8⁺ CTL epitope.

To identify murine mesothelin-specific CD8⁺ T cell epitopes, we initially used the Bioinformatics & Molecular Analysis Section (BIMAS)⁹ to predict for candidate murine MHC class I-restricted murine mesothelin-specific CTL epitopes (see **Figure 3A**). We next determined which of these epitopes represented the true mesothelin-specific CD8⁺ T cell epitopes using synthetic peptides and splenocytes that contained murine mesothelin-specific CD8⁺ T cells. C57BL/6 mice were vaccinated with a murine mesothelin-expressing DNA vaccine (pcDNA3-Meso) in conjunction with the anti-apoptotic BAK and BAX siRNA to generate mesothelin-specific CD8⁺ T cells. **We have previously shown the co-administration of DNA vaccines encoding human papillomavirus type 16 (HPV-16) E7 with siRNA targeting key pro-apoptotic proteins Bak and Bax prolongs the lives of antigen-expressing dendritic cells in the draining lymph nodes, enhances antigen-specific CD8⁺ T cell responses, and elicits potent antitumor effects against an E7-expressing tumor model in vaccinated mice.**¹⁰ Splenocytes from vaccinated mice were harvested one week after the last vaccination and were stimulated with each of the various candidate mesothelin CTL peptides (**Figure 3A**). As shown in **Figure 3B**, splenocytes stimulated with mesothelin peptide aa406-414 generated the highest number of IFN- γ -secreting CD8⁺ T cells compared to those stimulated with the

other candidate peptides. These data indicate that the murine mesothelin peptide aa406-414 is a mesothelin-specific CD8⁺ T cell epitope.

Generation and characterization of a murine mesothelin peptide(aa406-414)-specific CD8⁺ T cell line

We generated a murine mesothelin (aa406-414)-specific CD8⁺ T cell line by repeatedly stimulating splenocytes from the mesothelin DNA-vaccinated mice with mesothelin aa406-414 peptide. To determine whether the CD8⁺ T cell line is indeed mesothelin (aa406-414)-specific, the CD8⁺ T cell line was incubated with either mesothelin peptide aa406-414 or irrelevant E7 peptide aa49-57. As shown in **Figure 4A**, murine mesothelin aa406-414 peptide was able to activate the CD8⁺ T cells to release IFN- γ . In contrast, the control E7 aa49-57 failed to activate the CD8⁺ T cells. These data suggest that the CD8⁺ T cell line was murine mesothelin (aa406-414)-specific. We also confirmed that the CD8⁺ T cell line is a murine mesothelin-specific CD8⁺ T cell line using peptide-loaded MHC class I tetramer staining. As shown in **Figure 4B**, while the CD8⁺ T cells can be specifically detected by peptide-loaded H-2D^b tetramer, the CD8⁺ T cells can not be detected by E7 peptide-loaded H-2D^b tetramer. Taken together, these findings indicate that we have successfully generated a H-2D^b-restricted murine mesothelin peptide (aa406-414)-specific CD8⁺ T cell line.

Murine mesothelin(aa406-414)-specific CD8⁺ T cells can effectively kill MOSEC/luc tumor cells *in vitro*

The generation of a murine mesothelin (aa406-414)-specific CD8⁺ T cell line will allow us to determine whether the identified murine mesothelin-specific CD8⁺ T cell epitope (mesothelin aa406-414) is naturally processed and presented by cells expressing mesothelin. In order to quantitatively analyze if the mesothelin peptide-specific CD8⁺ T cells can specifically lyse the target cells loaded with mesothelin peptide, we transduced DCs with a retrovirus expressing firefly luciferase (DC/luc). This cell line allowed us to characterize CTL activity using non-radioactive bioluminescence imaging. The specific lysis of DC/luc would lead to the loss of luciferase activity. To demonstrate that murine mesothelin(aa406-414)-specific CD8⁺ T cells can specifically lyse mesothelin peptide-loaded DC/luc, we incubated the T cells with DC/luc pulsed with or without murine mesothelin aa406-414 peptide at different E/T ratios. As shown in **Figure 5A**, while the murine mesothelin (aa406-414)-specific CD8⁺ T cell line was able to kill DC/luc pulsed with murine mesothelin peptide aa406-414, the CD8⁺ T cell line was not able to lyse the DC/luc without peptide **or DC/luc pulsed with irrelevant E7 peptide aa49-57 (data not shown)**. Furthermore, when the T cell line was incubated with the MOSEC/luc tumor cells, they were able to specifically lyse the MOSEC/luc tumor cells (**Figure 5B**). These data indicate that murine mesothelin-specific CTL epitope (mesothelin aa406-414) is naturally processed and presented by the mesothelin-expressing tumor cells.

Adoptive transfer of murine mesothelin(aa406-414)-specific CD8⁺ T cells led to the control of MOSEC/luc tumor cells *in vivo*

We further assessed whether adoptive transfer of mesothelin (aa406-414)-specific CD8⁺ T cells could lead to the control MOSEC/luc tumors *in vivo*. C57BL/6 mice were

challenged with MOSEC/luc tumors and then treated by injection with mesothelin(aa406-414)-specific CD8⁺ T cells intraperitoneally. Mice without CD8⁺ T cell treatment were used as a control. Luciferase imaging was performed following the tumor challenge. As shown in **Figure 6**, while mice without treatment with mesothelin peptide-specific CD8⁺ T cells continued to show tumor growth as indicated by luciferase expression, mice treated with murine mesothelin (aa406-414)-specific CD8⁺ T cells showed a significant reduction of tumor growth as demonstrated by the decrease in luciferase activity.

Furthermore, tumor challenged mice treated with mesothelin-specific T cells survived much longer than tumor challenged mice without mesothelin specific T cell treatment (P<0.05) (Figure 6C). These data indicate that the adoptive transfer of murine mesothelin (aa406-414)-specific CD8⁺ T cells is able to control the MOSEC/luc tumors *in vivo*.

Discussion

In the current study, we have created a mesothelin-positive luciferase-expressing murine ovarian cancer model, MOSEC/luc. We demonstrated that MOSEC/luc endogenously processed and presented the murine mesothelin CTL epitope (aa406-414) and serves as a suitable preclinical ovarian cancer model for the characterization of therapeutic effects using non-invasive bioluminescence imaging. Additionally, this MOSEC/luc tumor model and the identified murine mesothelin CTL epitope will facilitate the development of immunotherapy for ovarian cancer and quantitative CD8⁺ T cell-mediated immunological assays.

There are several quantitative CD8⁺ T cell-mediated immunological assays that are commonly used for the characterization of antigen-specific immune responses. These assays include intracellular cytokine staining, ELISPOT, and peptide-loaded MHC class I tetramer staining. Among these assays, tetramer staining requires the identification of an MHC class I-restricted CTL epitope. Our newly identified H-2D^b-restricted murine mesothelin-specific CTL epitope (aa406-414) has allowed us to generate a mesothelin peptide-loaded H-2D^b tetramer, which we used to characterize a mesothelin peptide-specific CD8⁺ T cell line (**Figure 4**). These assays will be very useful for the characterization of mesothelin-specific immune responses generated by various antigen-specific vaccines targeting mesothelin.

One of the major limitations to ovarian cancer immunotherapy is the difficulty of generating ovarian cancer mouse models. Without suitable ovarian cancer models in immune intact mice, it will be difficult to test new therapies for ovarian cancers. Mouse ovarian surface epithelial cells (MOSEC), in immune intact mice were developed by Roby et al.⁷ MOSEC ovarian cancer cells were created by isolation of mouse ovarian surface epithelial cells and in vitro culture for more than 20 passages. Injection of these cells into the peritoneal cavity of immune intact mice resulted in the formation of ascitic fluid and multiple tumor implants. In addition, a more aggressive ovarian cancer line, Defb29Vegf was generated by stable transfection of VEGF and defensin in the MOSEC cell line¹¹. Furthermore, primary mouse ovarian surface epithelial cells which are deficient in p53 and any two of the oncogenes *c-myc*, *K-ras*, and *Akt* were sufficient to induce ovarian tumor formation when these cells were injected into mice.¹² Similarly, primary mouse

ovarian surface epithelial cells which are deficient in p53 and Brca1 with Myc were also sufficient to induce transformation of ovarian cells.¹³

A spontaneously occurring ovarian cancer mouse model, the Mullerian Inhibitory Substance type II Receptor (*MISIIR*) transgenic mice, has recently been generated.¹⁴ The *MISIIR* transgenic mice that express the transforming region of SV40 under the control of the Mullerian inhibitory substance type II receptor gene promoter are capable of developing bilateral ovarian tumors. The *MISIIR* transgenic mice have been shown to develop ovarian carcinomas spontaneously within 6-13 weeks after birth.¹⁴ Another transgenic mouse which expresses oncogenic K-ras and conditional Pten deletion within the ovarian surface epithelium has been shown to lead to the induction of invasive and widely metastatic endometrioid ovarian adenocarcinomas.¹⁵

The newly created MOSEC/luc tumor model will serve as an important model for the characterization of tumor load and distribution in tumor-challenged mice using non-invasive bioluminescence imaging. Previous studies also validate the use of luminescence imaging system for quantitatively measuring tumor load *in vivo*.¹⁶⁻¹⁹ Thus, the bioluminescence imaging used in this study represents a plausible non-invasive approach to measure tumor load and distribution in mice. **However, a potential concern related to retrovirus transduction is the difference in expression of MHC class I molecules between MOSEC and MOSEC/luc cells. This may influence the interpretation of the data. We found that both the cell lines express comparable levels of MHC class I molecules (data not shown). Another potential issue is that MOSEC/luc cells may generate immune responses against luciferase because luciferase is a foreign protein**

to the mice. This may lead to regression of MOSEC/luc tumors when injected in mice. However, this is probably unlikely because the growth rates of MOSEC and MOSEC/luc in C57BL6 mice are comparable (data not shown).

While we have demonstrated that the murine mesothelin aa406-414 represents a mesothelin-specific CTL epitope, we do not know if it is an immunodominant CTL epitope. Thus, it will be crucial for us to further characterize additional mesothelin-specific CTL epitopes and to determine the immunodominant epitopes for murine mesothelin. This information is important for the future development of effective mesothelin-specific vaccines. Further characterization of mesothelin-specific CTL epitopes using overlapping peptides covering the full length of murine mesothelin protein may allow us to identify additional mesothelin-specific CTL epitope/s. Several studies have employed this approach to successfully identify antigen-specific CTL epitopes.^{20,21}

Our study describes the identification of a murine mesothelin-specific CTL epitope. This is the first time a murine mesothelin-specific CTL epitope was identified in mouse ovarian cancer. Previous studies by us and others have identified several human mesothelin CD8⁺ T cell epitopes. For instance, we have recently identified two HLA-A2-restricted human mesothelin-specific CD8⁺ T cell epitopes using HLA-A2 transgenic mice.²² One of these CTL epitopes, aa540-549, was also recently identified using PBMCs derived from ovarian or pancreatic cancer patients.²³ In another study, HLA-A2-restricted mesothelin-derived peptides 20-28 and 530-538 were identified as CTL epitopes.²⁴ These human mesothelin CTL epitopes will be useful for the development of quantitative T cell immunological assays that are important for the

characterization of mesothelin-specific CD8⁺ T cell immune responses in patients with mesothelin-expressing ovarian cancer.

Materials and Methods

Mice

C57BL/6 mice were acquired from the National Cancer Institute. All animals were maintained under specific pathogen-free conditions, and all procedures were performed according to approved protocols and in accordance with recommendations for the proper use and care of laboratory animals.

Cell lines

The MOSEC cell line ⁷ and dendritic cell line (DC) ^{8 25} were prepared as described previously. **The dendritic cell line has been shown to express all phenotypic markers of dendritic cells.** ^{8 25} MOSEC-luciferase (MOSEC/luc) and dendritic cell-luciferase (DC/luc) were generated by transducing MOSEC and DCs with a retrovirus containing luciferase. In order to generate a retrovirus containing luciferase, a pLuci-thy1.1 construct expressing both luciferase and thy1.1 was made. Firefly luciferase was amplified by PCR from pGL3-basic (Promega) using the 5' primer CGGAGATCTATGGAAGACGCCAAAAC and the 3' primer CGGGTAACTTACACGGCGATCTTCC. The amplified luciferase cDNA was inserted into the BglII and HpaI sites of the bicistronic vector pMIG-thy1.1. Both luciferase and thy1.1 cDNA are under the control of a single promoter element and separated by an internal ribosomal entry site (IRES). The pLuci-thy1.1 was transfected

into Phoenix packaging cell line and the virion-containing supernatant was collected 48 h after transfection. The supernatant was immediately treated using a 0.45-mm cellulose acetate syringe filter (Nalgene, Rochester, NY) and used to infect MOSEC and DCs in the presence of 8 mg/mL Polybrene (Sigma, St. Louis, MO). MOSEC/luc and DC/luc cells were **sorted** using preparative flow cytometry of stained cells with Thy1.1 antibody (BD, Franklin Lakes, NJ).

Plasmid DNA Constructs and DNA Preparation

For the generation of plasmid encoding murine mesothelin, pcDNA3-meso, the DNA fragment encoding mesothelin, was first amplified in RT-PCR. RNA was extracted from the MOSEC cell line by TRIZOL (Invitrogen, Carlsbad, CA). RT-PCR was performed using the Superscript One-Step RT-PCR Kit (Invitrogen) and a set of primers: 5'-cccgaattcatggccttgccaacagctcga-3' and 5'-tatggatccgctcagccttaaagctgggag-3'. The amplified product was then digested with *EcoRI* and *HindIII* and further cloned into the vector pcDNA3.1/myc-His(-) (Invitrogen, Carlsbad, CA). The DNA was amplified in *Escherichia coli* DH5 and purified as described previously.²⁶

Quantitative real-time RT-PCR

Before first-strand cDNA synthesis, RNA samples were treated with Deoxyribonuclease I (Invitrogen, Carlsbad, CA) to eliminate DNA contamination. Reverse Transcription Polymerase Chain Reaction (PCR) was performed with Oligo(dT) primer and M-MLV Reverse Transcriptase (Invitrogen) according to manufacturer's protocol. Then, we used the first-strand cDNA for real-time PCR,

which was performed with iQ SYBR Green Supermix (Bio-Rad, Hercules, CA, USA) on MyiQ real-time PCR detection system (Bio-Rad) according manufacture's protocol. The forward primer for mouse mesothelin is TTGGGTGGATACCACGTCTG; the reverse primer is CGGAGTGTAATGTTCTTCTGTC. We used beta-actin as the reference gene. The forward primer for beta-actin is CCCTAAGGCCAACCGTGAA and the reverse primer is GAGCATAGCCCTCGTAGAT

DNA/siRNA Vaccination

Gene gun particle-mediated DNA/siRNA vaccination was done using a helium-driven gene gun (Bio-Rad, Hercules, CA) according to the protocol for RNA vaccination provided by the manufacturer, with a slight modification. Briefly, DNA/siRNA-coated gold particles were prepared by combining 25 mg of 1.6 μm gold microcarriers (Bio-Rad), 50 μg of plasmid DNA (50 μL), 5 μg of siRNA (50 μL), and 10 μL of 3 mol/L sodium acetate. Isopropyl alcohol (200 μL) was added to the mixture dropwise while mixing by vortex. This mixture was allowed to precipitate at room temperature for 10 min. The microcarrier/DNA/siRNA suspension was then centrifuged (10,000 rpm for 30 sec) and washed thrice in fresh absolute ethanol before resuspending in 3 mL polyvinylpyrrolidone (0.1 mg/mL, Bio-Rad) in absolute ethanol. The solution was then loaded into 2.5 ft of gold-coated tube (Bio-Rad) and allowed to settle for 10 minutes. The ethanol was gently removed, and the microcarrier/DNA/siRNA suspension was evenly attached to the inside surface of the tube by rotation. The tube was then dried by 0.4 L/min of flowing nitrogen gas. The dried tube coated with microcarrier/DNA/siRNA was

then cut to 0.5 in. cartridges and stored in a capped dry bottle at 4°C. The DNA/siRNA-coated gold particles (1 µg DNA and 0.1 µg siRNA per bullet) were delivered to the shaved abdominal region of the mice using a helium-driven gene gun (Bio-Rad) with a discharge pressure of 400 p.s.i. C57BL/6 mice were immunized with 2 µg of the pcDNA3 plasmid encoding murine mesothelin and mixed with 0.2 µg BAK + BAX siRNA or control siRNA. The mice received three boosters with the same dose 1 week later. siRNAs were synthesized using 2'-*O*-ACE-RNAphosphoramides (Dharmacon, Lafayette, CO). The sequences of BAK, BAX, and control RNAi were described previously.¹⁰

Generation of an E7mesothelin-specific CTL cell line

We used methods described previously to generate the mesothelin specific CTL cell line²⁷. Six-week-old female C57BL/6 mice were immunized four times by 2 µg of the pcDNA3 plasmid encoding murine mesothelin and mixed with 0.2 µg BAK + BAX siRNA. Splenocytes were harvested on day 7 after the last vaccination. For initial *in vitro* stimulation, 5x10⁶ splenocytes were pulsed with IL-2 at a concentration of 20 U/ml and 1 µg of mesothelin peptide (amino acids 406–414) for 7 days. Propagation of the mesothelin-specific CTL cell line was performed in 24-well plates by mixing (2 ml/well) 1x10⁶ splenocytes containing mesothelin-specific CTLs with 3x10⁶ irradiated splenocytes and pulsing them with IL-2 at a concentration of 20 U/ml and 1 µg of mesothelin peptide (amino acids 406–414). This procedure was repeated every 7 days.

Intracellular Cytokine Staining and Flow Cytometry Analysis

Cell surface marker staining for CD8 and intracellular cytokine staining for IFN- γ as well as flow cytometry analysis were performed under conditions described previously.²⁶ Splenocytes were harvested from mice 1 week after the last vaccination. For detecting mesothelin-specific CD8⁺ T-cell precursors, 5x10⁶ pooled splenocytes from each vaccination group were incubated for 16 h with either 1 μ g/ml mesothelin peptide 406-414(GQKMNAQA1) or other peptides containing an MHC class I epitope **based on Bioinformatics & Molecular Analysis Section (BIMAS)⁹** (in **Figure 3A**). Analysis was performed on a Becton-Dickinson FACSCalibur with CELLQuest software (Becton Dickinson Immunocytometry System, Mountain View, CA). For tetramer staining of a murine mesothelin-specific CD8⁺ T cell line, the murine mesothelin peptide (aa406-414)-loaded H-2D^b tetramer (purchased from Beckman Coulter, San Diego, CA) was used to stain for murine mesothelin peptide (aa406-414)-specific CD8⁺ T cells (from NIH). The E7-peptide-loaded H-2D^b tetramer was used as a negative control.

Cytolytic activity assay

A non-radioactive method for cytolytic activity assay that utilizes luciferase to measure target cell viability was performed.²⁸ Target cells were luciferase-expressing dendritic cell line (DC/luc) with or without pulsing with mesothelin-specific peptide aa406-414, or luciferase-expressing MOSEC cell line (MOSEC/luc). The target cells were plated at a concentration of 10,000 cells per 0.1 mL/well in 96-well microplates. The cells were then co-cultured with increasing amounts of mesothelin-specific CD8⁺ T cells (in a final volume of 0.2 mL/well) at 37⁰C for 6h. A final concentration of 0.14 mg/mL luciferin (Promega) was added to each well, the plate was dark adapted for 10

min at 37⁰C, and luminescence was read on the IVIS Imaging System Series 200 (Xenogen). Cytolytic activity was determined by measuring the number of viable luciferase positive cells remaining following incubation with effectors. The percentage of lysis was calculated from the following equation:

$100 - [100 \times (A - B) / (C - B)]$, where *A* is the reading of photon counts for experimental cells, *B* is the background photon counts determined by plating target cells in media with a final concentration of 1% SDS, *C* is maximum photon counts determined by plating target cells in media without effector cells.

Treatment of mice with mesothelin-specific CD8⁺ T cells

For determination of the direct effects of mesothelin-specific CD8⁺ T cells on the growth of MOSEC/luc tumors, two groups of mice were challenged with 2x10⁵ MOSEC/luc tumors by intraperitoneal injection. One group (**5 mice**) was intraperitoneally treated with 2x10⁶ mesothelin (aa406-414)-specific CD8⁺ T cells and the other group (**5 mice**) was treated with 1X PBS one day after MOSEC/luc challenge intraperitoneally. Tumor image was then measured using IVIS Imaging System Series 200 (Xenogen). Bioluminescence tumor image was taken one day after MOSEC/luc challenge and four days after the transfer of mesothelin(aa406-414)-specific CD8⁺ T cells. For detection of bioluminescence signals, mice were injected with 300µl of 15mg/ml luciferin (Promega) intraperitoneally. Mice were imaged using the IVIS Imaging System Series 200 (Xenogen) 10 min after luciferin injection. Bioluminescence signals were acquired for three minutes. **The survival of the tumor challenged mice with or without T cell treatment was also followed.**

Statistical Analysis

All data expressed as means \pm standard deviation (s.d.) are representative of at least two different experiments. Data for intracellular cytokine staining with flow cytometry analysis were evaluated by ANOVA. Comparisons between individual data points were made using a Student's *t*-test. **For the survival analysis of tumor challenged mice receiving T cell treatment, Kaplan and Meier method and the log-rank statistic were used. All *p* values < 0.05 were considered significant.**

Acknowledgements

We thank Dr. Richard Roden for helpful discussions. We gratefully acknowledge Roanne Calizo and Archana Monie for the preparation of the manuscript. This work was supported by ovarian cancer grants from the Alliance for Cancer Gene Therapy (ACGT) and the NCDGG (1U19 CA113341-01).

References

- 1 Ozols RF. Systemic therapy for ovarian cancer: current status and new treatments. *Semin Oncol* 2006; **33**: S3-11.
- 2 Pfisterer J, Ledermann JA. Management of platinum-sensitive recurrent ovarian cancer. *Semin Oncol* 2006; **33**: S12-16.
- 3 Bhoola S, Hoskins WJ. Diagnosis and management of epithelial ovarian cancer. *Obstet Gynecol* 2006; **107**: 1399-1410.

- 4 Coukos G, Conejo-Garcia JR, Roden RB, Wu TC. Immunotherapy for gynaecological malignancies. *Expert Opin Biol Ther* 2005; **5**: 1193-1210.
- 5 Scholler N, Fu N, Yang Y, Ye Z, Goodman GE, Hellstrom KE *et al*. Soluble member(s) of the mesothelin/megakaryocyte potentiating factor family are detectable in sera from patients with ovarian carcinoma. *Proc Natl Acad Sci U S A* 1999; **96**: 11531-11536.
- 6 Hassan R, Bera T, Pastan I. Mesothelin: a new target for immunotherapy. *Clin Cancer Res* 2004; **10**: 3937-3942.
- 7 Roby KF, Taylor CC, Sweetwood JP, Cheng Y, Pace JL, Tawfik O *et al*. Development of a syngeneic mouse model for events related to ovarian cancer. *Carcinogenesis* 2000; **21**: 585-591.
- 8 Shen Z, Reznikoff G, Dranoff G, Rock KL. Cloned dendritic cells can present exogenous antigens on both MHC class I and class II molecules. *J Immunol* 1997; **158**: 2723-2730.
- 9 Parker KC, Bednarek MA, Coligan JE. Scheme for ranking potential HLA-A2 binding peptides based on independent binding of individual peptide side-chains. *J Immunol* 1994; **152**: 163-175.
- 10 Kim TW, Lee JH, He L, Boyd DA, Hardwick JM, Hung CF *et al*. Modification of professional antigen-presenting cells with small interfering RNA in vivo to enhance cancer vaccine potency. *Cancer Res* 2005; **65**: 309-316.
- 11 Conejo-Garcia JR, Benencia F, Courreges MC, Kang E, Mohamed-Hadley A, Buckanovich RJ *et al*. Tumor-infiltrating dendritic cell precursors recruited by a

- beta-defensin contribute to vasculogenesis under the influence of Vegf-A. *Nat Med* 2004; **10**: 950-958.
- 12 Orsulic S, Li Y, Soslow RA, Vitale-Cross LA, Gutkind JS, Varmus HE. Induction of ovarian cancer by defined multiple genetic changes in a mouse model system. *Cancer Cell* 2002; **1**: 53-62.
- 13 Xing D, Orsulic S. A mouse model for the molecular characterization of brca1-associated ovarian carcinoma. *Cancer Res* 2006; **66**: 8949-8953.
- 14 Connolly DC, Bao R, Nikitin AY, Stephens KC, Poole TW, Hua X *et al.* Female mice chimeric for expression of the simian virus 40 TAg under control of the MISIR promoter develop epithelial ovarian cancer. *Cancer Res* 2003; **63**: 1389-1397.
- 15 Dinulescu DM, Ince TA, Quade BJ, Shafer SA, Crowley D, Jacks T. Role of K-ras and Pten in the development of mouse models of endometriosis and endometrioid ovarian cancer. *Nat Med* 2005; **11**: 63-70.
- 16 Tseng JC, Levin B, Hurtado A, Yee H, Perez de Castro I, Jimenez M *et al.* Systemic tumor targeting and killing by Sindbis viral vectors. *Nat Biotechnol* 2004; **22**: 70-77.
- 17 Tseng JC, Hurtado A, Yee H, Levin B, Boivin C, Benet M *et al.* Using sindbis viral vectors for specific detection and suppression of advanced ovarian cancer in animal models. *Cancer Res* 2004; **64**: 6684-6692.
- 18 Jenkins DE, Oei Y, Hornig YS, Yu SF, Dusich J, Purchio T *et al.* Bioluminescent imaging (BLI) to improve and refine traditional murine models of tumor growth and metastasis. *Clin Exp Metastasis* 2003; **20**: 733-744.

- 19 Drake JM, Gabriel CL, Henry MD. Assessing Tumor Growth and Distribution in a Model of Prostate Cancer Metastasis using Bioluminescence Imaging. *Clin Exp Metastasis* 2006.
- 20 Harrer T, Harrer E, Barbosa P, Kaufmann F, Wagner R, Bruggemann S *et al.* Recognition of two overlapping CTL epitopes in HIV-1 p17 by CTL from a long-term nonprogressing HIV-1-infected individual. *J Immunol* 1998; **161**: 4875-4881.
- 21 Currier JR, deSouza M, Chanbancherd P, Bernstein W, Birx DL, Cox JH. Comprehensive screening for human immunodeficiency virus type 1 subtype-specific CD8 cytotoxic T lymphocytes and definition of degenerate epitopes restricted by HLA-A0207 and -C(W)0304 alleles. *J Virol* 2002; **76**: 4971-4986.
- 22 Hung CF, Calizo R, Tsai YC, He L, Wu TC. DNA vaccine encoding a single-chain trimer of HLA-A2 linked to human mesothelin peptide generates anti-tumor effects against human mesothelin-expressing tumors *Vaccine* 2006; (**in press**).
- 23 Yokokawa J, Palena C, Arlen P, Hassan R, Ho M, Pastan I *et al.* Identification of novel human CTL epitopes and their agonist epitopes of mesothelin. *Clin Cancer Res* 2005; **11**: 6342-6351.
- 24 Thomas AM, Santarsiero LM, Lutz ER, Armstrong TD, Chen YC, Huang LQ *et al.* Mesothelin-specific CD8(+) T cell responses provide evidence of in vivo cross-priming by antigen-presenting cells in vaccinated pancreatic cancer patients. *J Exp Med* 2004; **200**: 297-306.

- 25 Wang TL, Ling M, Shih IM, Pham T, Pai SI, Lu Z *et al.* Intramuscular administration of E7-transfected dendritic cells generates the most potent E7-specific anti-tumor immunity. *Gene Ther* 2000; **7**: 726-733.
- 26 Chen CH, Wang TL, Hung CF, Yang Y, Young RA, Pardoll DM *et al.* Enhancement of DNA vaccine potency by linkage of antigen gene to an HSP70 gene. *Cancer Res* 2000; **60**: 1035-1042.
- 27 Ji H, Wang TL, Chen CH, Pai SI, Hung CF, Lin KY *et al.* Targeting human papillomavirus type 16 E7 to the endosomal/lysosomal compartment enhances the antitumor immunity of DNA vaccines against murine human papillomavirus type 16 E7-expressing tumors. *Hum Gene Ther* 1999; **10**: 2727-2740.
- 28 Brown CE, Wright CL, Naranjo A, Vishwanath RP, Chang WC, Olivares S *et al.* Biophotonic cytotoxicity assay for high-throughput screening of cytolytic killing. *J Immunol Methods* 2005; **297**: 39-52.

Figure Legends

Figure 1. Characterization of ascites formation and luciferase expression in mice challenged with MOSEC/luc tumor cells. C57BL/6 mice were intraperitoneally challenged with 5×10^6 cells/mouse of MOSEC/luc tumor cells. **(A)** Representative gross picture to demonstrate ascites formation in mice 8 weeks after MOSEC/luc tumor challenge. The arrow indicates growth of abdominal girth. **(B)** Representative gross picture of non-tumor-challenged control mice. **(C)** Representative luminescence image of MOSEC/luc-challenged mice 8 weeks after tumor challenge. **(D)** Representative luminescence image of control mice without tumor challenge. **For detection of bioluminescence signals, mice were injected with luciferin intraperitoneally. Mice were imaged using the IVIS Imaging System Series 200.** Bioluminescence signals were acquired for one minute.

Figure 2. RT-PCR and flow cytometry analysis to characterize murine mesothelin expression in MOSEC/luc tumor cells. **(A)** Gel electrophoresis to characterize the amplified product from RT-PCR. Lane 1, size marker. Lane 2, RNA from MOSEC/luc tumor cells. Lane 3, RNA from murine mesothelin-negative DCs used as a negative control. Note: Specific amplification was observed in Lane 2 (MOSEC/luc cells) but not in Lane 3 (DCs), as indicated by an arrow. **(B)** Flow cytometry analysis to characterize murine mesothelin expression in MOSEC/luc cells (left panel) or DCs (right panel). The filled histogram represents cells stained with rat sera containing polyclonal antibodies against murine mesothelin. **The sera were derived from rats vaccinated with DNA**

encoding murine mesothelin. The clear histogram represents cells stained with rat sera acquired before vaccination (negative control). PE-labeled goat anti-rat IgG was used as a secondary antibody for the flow cytometry analyses.

Figure 3. Identification of mesothelin-specific CTL epitopes. (A) Potential H-2-restricted mesothelin CTL epitopes predicted by the BIMAS Program. (B) Bar graph depicting the number of IFN- γ -expressing mesothelin-specific CD8⁺ T cells in splenocytes stimulated with various candidate mesothelin peptides. **The splenocytes were derived from C57BL/6 mice vaccinated with pcDNA3-Meso combined with BAK+BAX siRNA.** The splenocytes were harvested one week after the last vaccination and stimulated with each of the peptides listed in **Figure 3A** for 16 hours. Murine mesothelin-specific CD8⁺ T cell immune responses were determined by intracellular cytokine staining for IFN- γ and CD8.

Fig 4. Characterization of a murine mesothelin(aa406-414)-specific H2k^b-restricted CD8⁺ T cell line. (A) Intracellular cytokine staining followed by flow cytometry analysis to characterize a murine mesothelin (aa406-414)-specific CD8⁺ T cell line. **The CD8⁺ T cells were incubated overnight with H-2D^b-restricted mesothelin (aa406-414)-specific peptide or irrelevant peptide (E7 aa 49-57) in the presence of GolgiPlug.** Cells were washed once with FACS wash buffer and stained with PE-conjugated monoclonal rat antimouse CD8a. Cells were then permeabilized, fixed and stained with FITC-conjugated rat anti-mouse IFN- γ . Flow cytometry analysis was performed using **FACSCalibur** with CELLQuest software. (B) Tetramer staining of a murine mesothelin-

specific CD8⁺ T cell line. The murine mesothelin peptide (aa406-414)-loaded H-2D^b tetramer was used to stain for murine mesothelin peptide (aa406-414)-specific CD8⁺ T cells. The E7-peptide-loaded H-2D^b tetramer was used as a negative control.

Fig 5. Bioluminescence imaging assay to demonstrate the specific lysis of murine mesothelin-expressing tumor cells by murine mesothelin peptide-specific CD8⁺ T cells. The target cells were luciferase-expressing dendritic cell line (DC/luc) with or without pulsing with mesothelin-specific peptide aa406-414, or luciferase-expressing MOSEC cell line (MOSEC/luc). **The target cells were co-cultured with increasing numbers of murine mesothelin peptide-specific CD8⁺ T cells (10^4 , 5×10^4 , 2.5×10^5 cells/well for DC/luc cell lines with or without pulsing with peptide; 10^4 , 3×10^4 , 9×10^4 , 2.7×10^5 cells/well for MOSEC/luc cell line) in a final volume of 0.2 mL/well at 37^oC for 6h.** Luciferin was added to each well and luminescence was read on the IVIS Imaging System Series 200. **(A)** Bioluminescence images of the DC/luc cell line or DC/luc+406peptide cell line. **Note: Significant lysis was observed in DC/luc + 406 peptide but not in DC/luc (P < 0.001).** **(B)** Bioluminescence imaging assay for the MOSEC/luc cell line.

Fig 6. Characterization of luciferase expression in tumor-challenged mice injected with mesothelin-specific(aa406-414) CD8⁺ T cells. C57BL/6 mice (**5 mice per group**) were challenged intraperitoneally with MOSEC/luc tumor cells. One day after tumor challenge, the mice were intraperitoneally administered with either mesothelin (aa406-414)-specific CD8⁺ T cells/mouse or 1X PBS. For detection of bioluminescence signals,

the mice were injected with luciferin intraperitoneally. **Mice were imaged using the IVIS Imaging System Series 200, 10 min after luciferin injection.** (A) Bioluminescence images of the **representative** tumor-challenged mice at days 1, 4, and 31 after MOSEC/luc tumor cell injection. (B) Bar graph depicting the photon counts from mice (**5 per group**) at days 1, 4, and 31 after MOSEC/luc tumor challenge. **Note: There is a significant difference between tumor challenged mice with or without T cell transfer ($P < 0.05$)** (C) **Kaplan-Meier survival analysis for MOSEC/luc tumor challenged mice with T cell transfer (closed circles) or without T cell transfer (open circles).**

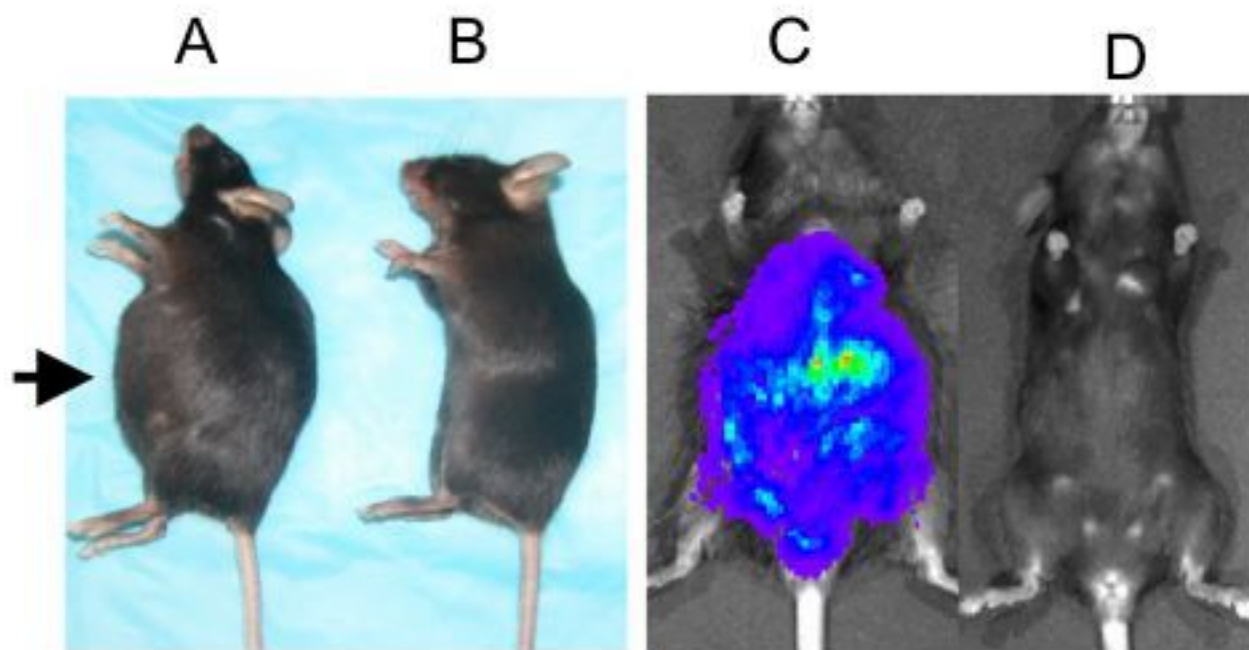


Figure 1

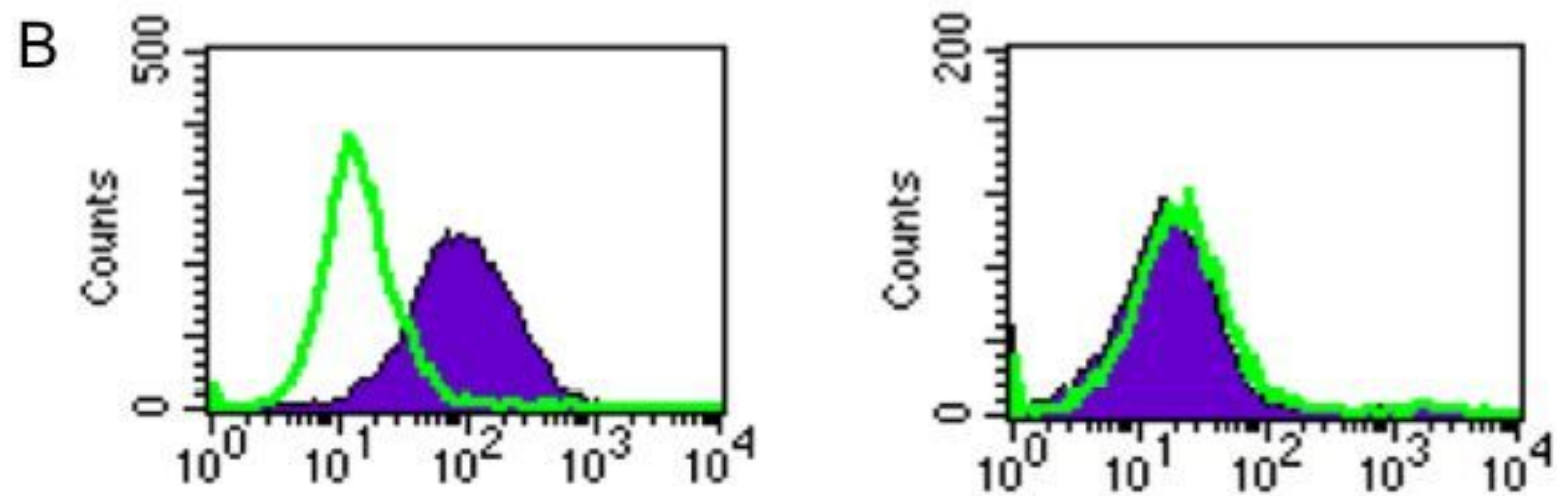
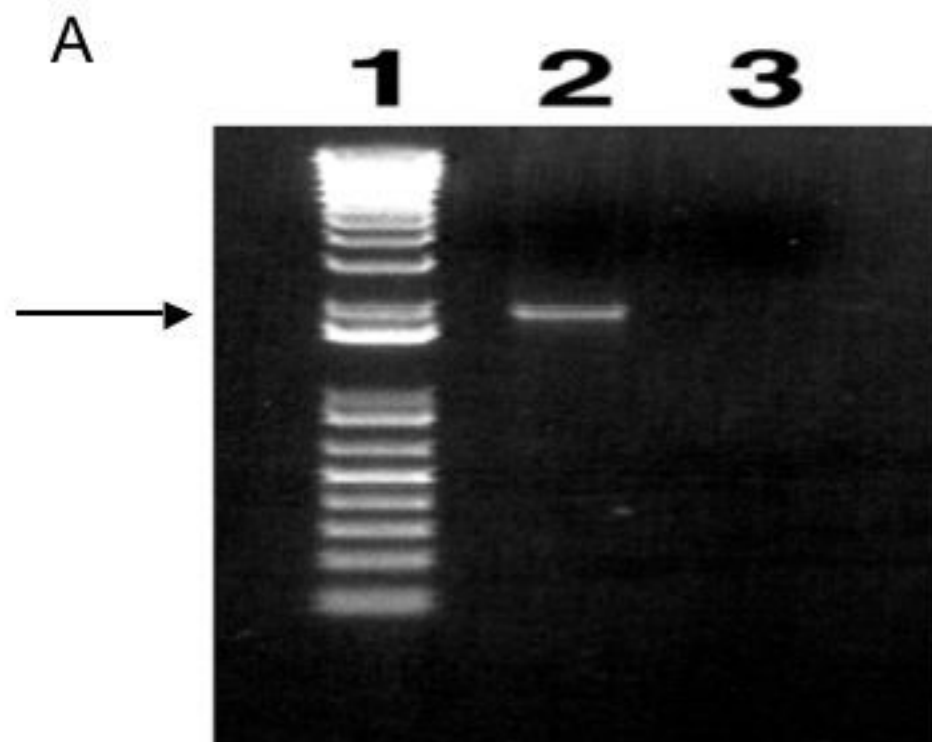


Figure 2

A

Peptide name Start position	MHC class I	Peptide sequence	BIMAS score
Peptide- 146	H-2D ^b	ISKANVDVL	1119
Peptide- 343	H-2K ^b	EIPFTYEQI	72
Peptide- 406	H-2D ^b	GQKMNAQAI	210
Peptide- 484	H-2D ^b	SAFQNVSGI	2217
Peptide- 544	H-2D ^b	LLGPNIVDL	119
Peptide- 583	H-2K ^b	GIPNGYLVL	72

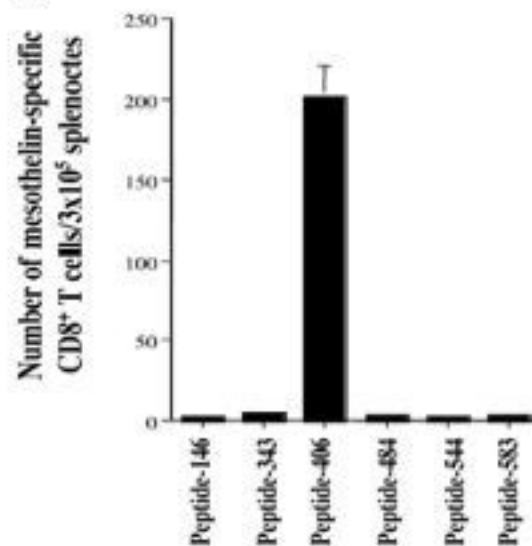
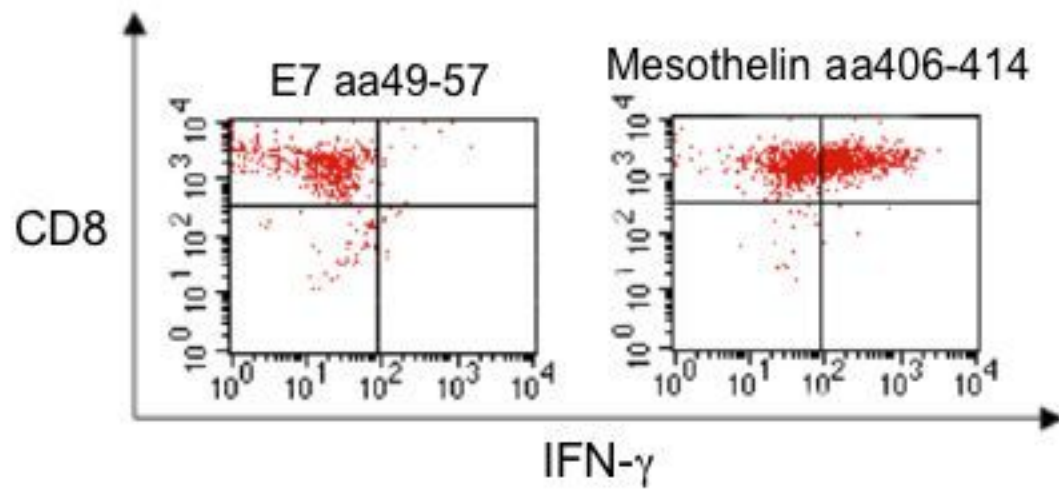
B

Figure 3

A



B

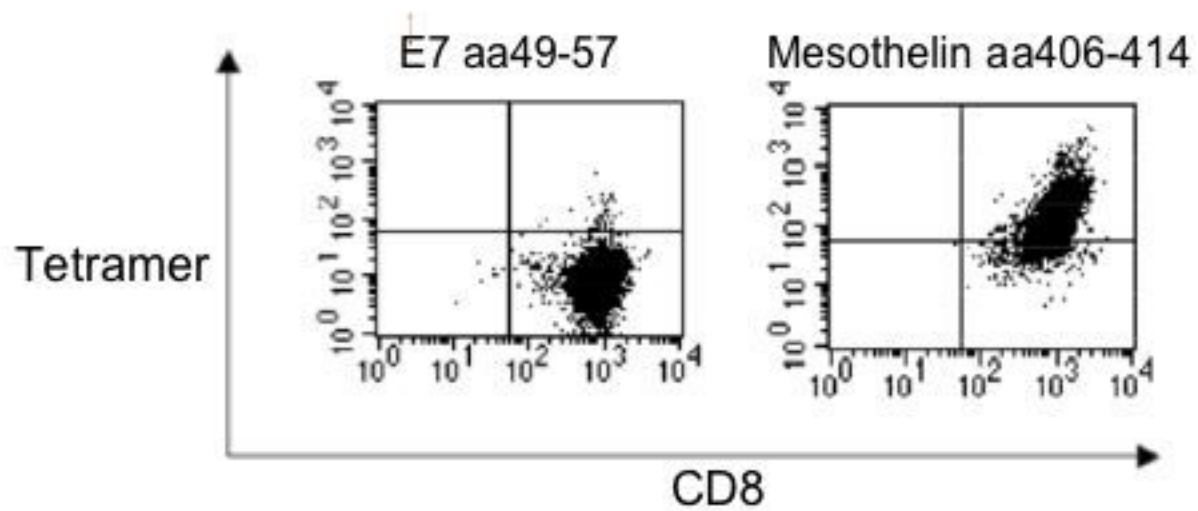


Figure 4

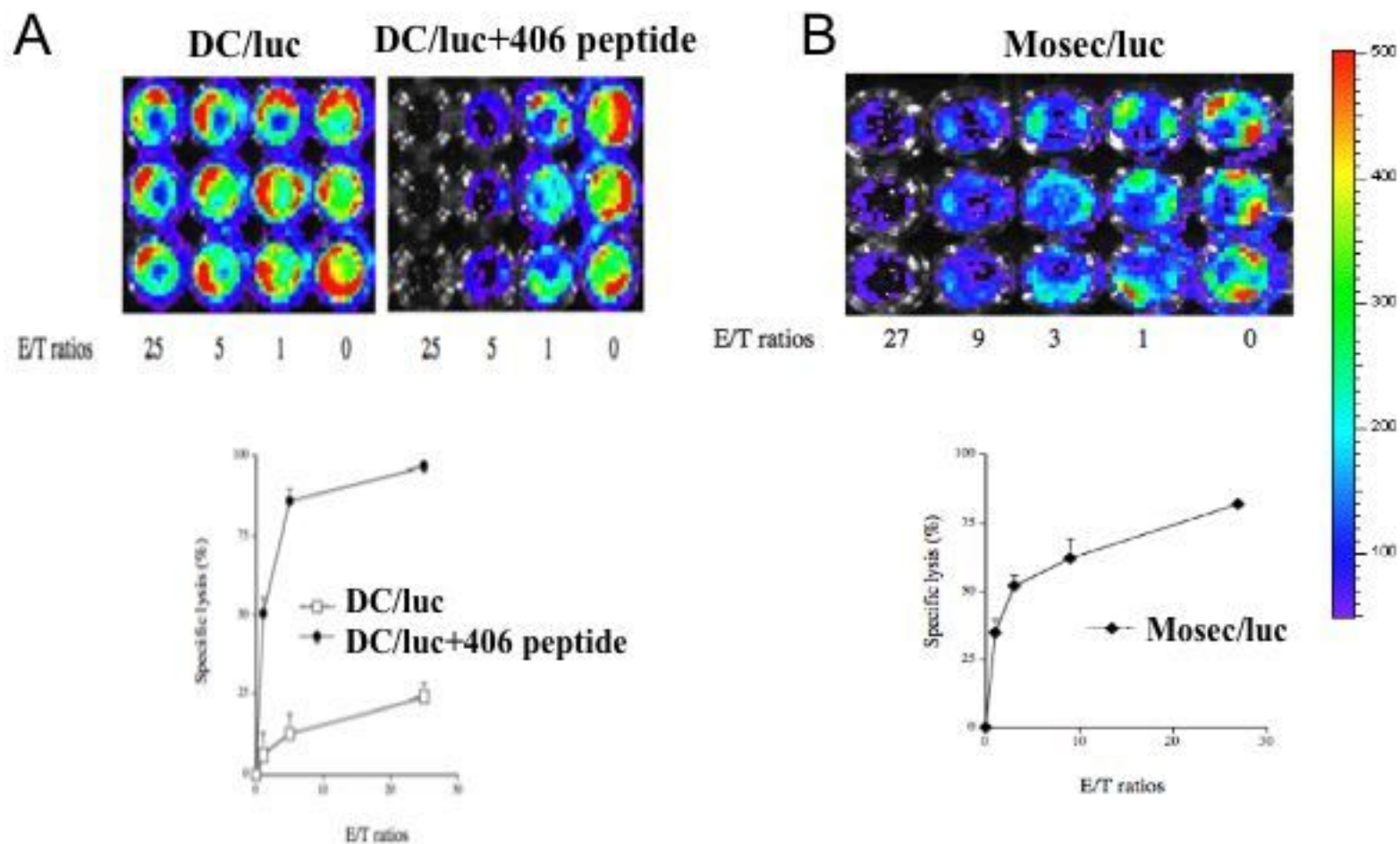


Figure 5

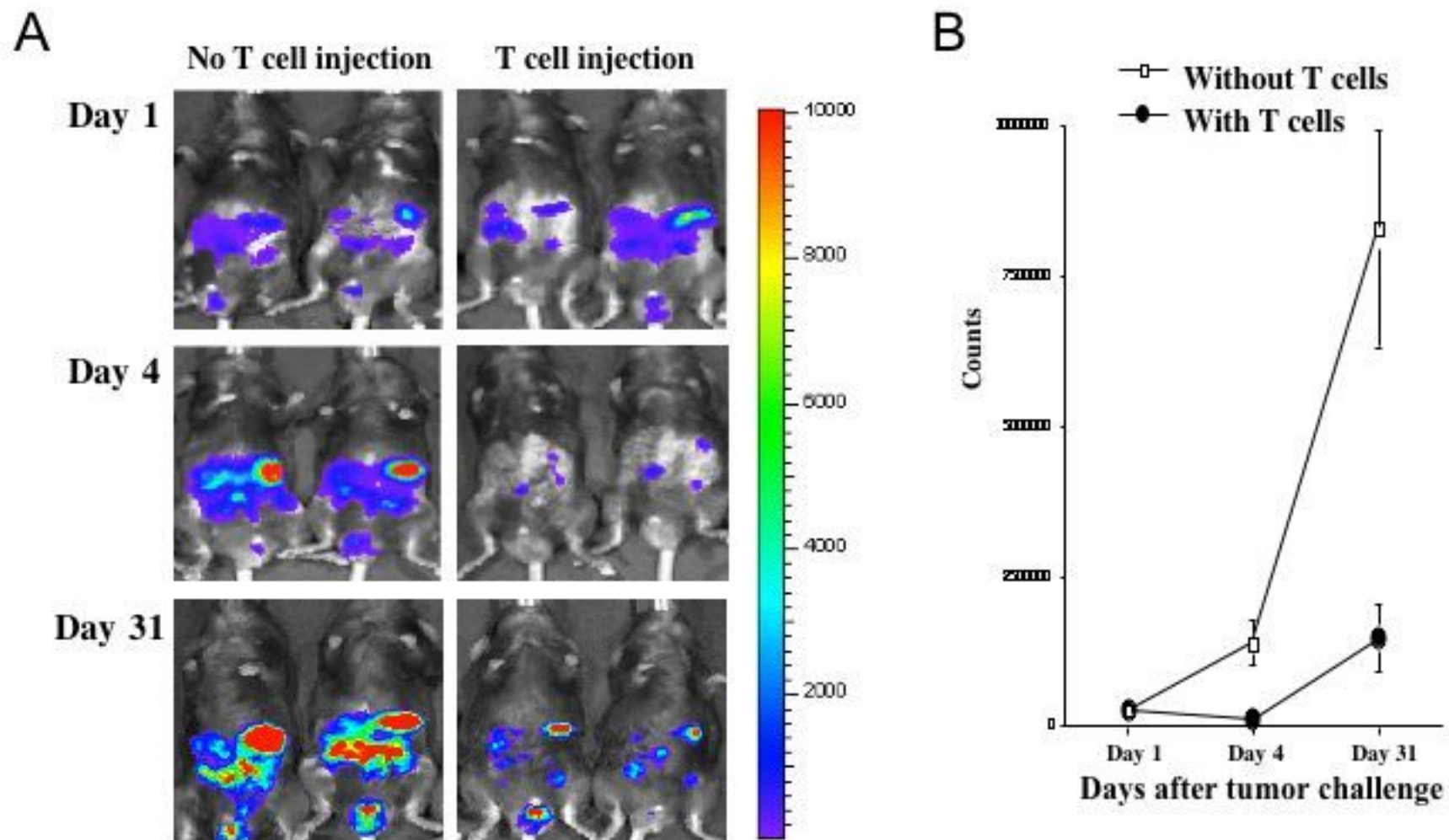


Figure 6

C

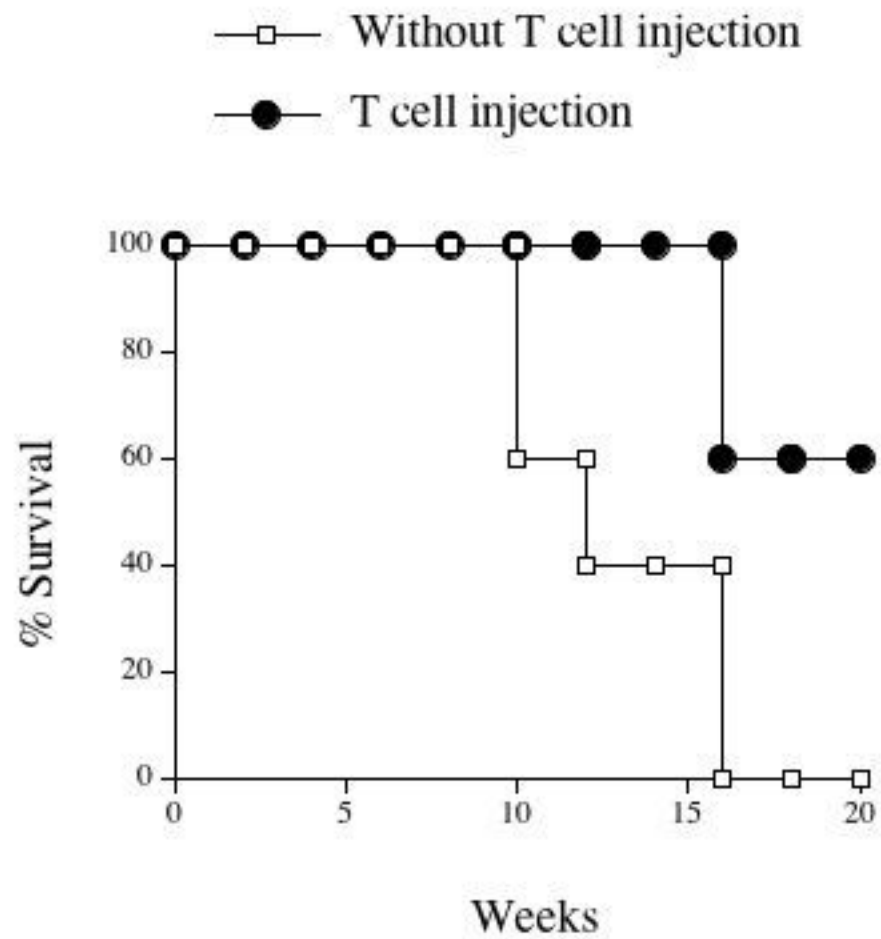


Figure 6

Table 1: Characterization of murine mesothelin expression by quantitative RT-PCR

Cell	Gene	Repeat	Mean Ct Value	Standard Deviation	mRNA Expression Ratio Mesothelin:beta-actin
DCs	beta_actin	4	20.54	0.061	
DCs	mesothelin	4	0	N/A	0
MOSEC/luc	beta_actin	4	20.18	0.195	
MOSEC/luc	mesothelin	4	26.4	0.188	0.01342

DCs: dendritic cells

MOSEC: mouse ovarian surface epithelial tumor